



University of Miguel Hernandez

PhD Program in Molecular and Cell Biology

International Doctorate Mention

**The stress-mediated antiproliferative
effects of marine invertebrate extracts in
human colon cancer cell models**

PhD Student

Verónica Ruiz Torres

PhD supervisors

Vicente Micol Molina

Enrique Barraión Catalán

Elche, 2019



Universidad Miguel Hernández

Programa de Biología Molecular y Celular

Mención Doctorado Internacional 2019

**Efecto antiproliferativo de extractos
procedente de invertebrados marinos
mediado por estrés en modelos celulares
humanos de cáncer de colon**

Estudiante de doctorado

Verónica Ruiz Torres

Directores de tesis

Vicente Micol Molina

Enrique Barraión Catalán

Elche, 2019



La presente tesis se presenta en la modalidad de Compendio de Publicaciones con Mención Internacional formada por el conjunto de trabajos previamente publicados:

- **An Updated Review on Marine Anticancer Compounds: The Use of Virtual Screening for the Discovery of Small-Molecule Cancer Drugs.**

Verónica Ruiz-Torres, José Antonio Encinar, Maria Herranz-López, Almudena Pérez-Sánchez, Vicente Galiano, Enrique Barrajon-Catalán and Vicente Micol.

Molecules. 2017 Jun 23;22(7). pii: E1037. **Impact Factor: 3.060** (2018); 5-Year Impact Factor: 3.380 (2018). **Q2**. doi: 10.3390/molecules22071037. Review. PubMed PMID: 28644406; PubMed Central PMCID: PMC6152364.

- **New Mammalian Target of Rapamycin (mTOR) Modulators Derived from Natural Product Databases and Marine Extracts by Using Molecular Docking Techniques.**

Verónica Ruiz-Torres, Maria Losada-Echeberría, Maria Herranz-López, Enrique Barrajon-Catalán, Vicente Galiano, Vicente Micol and José Antonio Encinar.

Marine Drugs. 2018 Oct; 16(10): 385. **Impact Factor: 3.772** (2018), 5-Year Impact Factor: 4.446 (2018). **Q1**. doi: 10.3390/md16100385. PMCID: PMC6213183; PMID: 30326670.



Dr. Vicente Micol Molina, catedrático de la Universidad Miguel Hernández en Bioquímica y Biología Molecular y el Dr. Enrique Barraión Catalán, profesor Ayudante Doctor de la Universidad Miguel Hernández del Departamento de Ingeniería, Área de Farmacia y Tecnología Farmacéutica,

CERTIFICAN

Que el trabajo de investigación que conduce a la obtención del grado de Doctora: **“Efecto antiproliferativo mediado por estrés de extractos de invertebrados marinos en modelos humanos de cáncer de colon”** que es autora Dña. Verónica Ruiz Torres, ha sido realizado bajo nuestra dirección en el Instituto de Investigación, Desarrollo e Innovación en Biotecnología Sanitaria de Elche (IDIBE) y se desarrolla en modalidad por Compendio de Publicaciones con Mención de Doctorado Internacional.

Para que consten los efectos oportunos, firman el presente certificado en Elche (Alicante), a de septiembre de 2019.

Dr. Vicente Micol Molina

Dr. Enrique Barraión Catalán



El Dr. Ricardo Mallavía Marín, Catedrático del Departamento de Química Inorgánica y coordinador del Programa de Doctorado en Biología Molecular y Celular del Instituto de Investigación, Desarrollo e Innovación en Biotecnología Sanitaria de Elche (IDIBE) de la Universidad Miguel Hernández (UMH) de Elche,

CERTIFICA

Que la doctoranda Verónica Ruiz Torres, ha completado el Programa de formación Doctoral en Biología Molecular y Celular, alcanzando los objetivos establecidos en el mismo. Y que la tesis titulada: **“Efecto antiproliferativo mediado por estrés de extractos de invertebrados marinos en modelos humanos de cáncer de colon”** reúne los indicios de calidad exigidos para el campo de evaluación. La estudiante es la primera firmante de los siguientes artículos:

- **An Updated Review on Marine Anticancer Compounds: The Use of Virtual Screening for the Discovery of Small-Molecule Cancer Drugs.** Verónica Ruiz-Torres, José Antonio Encinar, Maria Herranz-López, Almudena Pérez-Sánchez, Vicente Galiano, Enrique Barraión-Catalán and Vicente Micol. *Molecules*. 2017 Jun 23;22(7). pii: E1037. **Impact Factor: 3.060** (2018); 5-Year Impact Factor: 3.380 (2018). **Q2**. doi: 10.3390/molecules22071037. Review. PubMed PMID: 28644406; PubMed Central PMCID: PMC6152364.

- **New Mammalian Target of Rapamycin (mTOR) Modulators Derived from Natural Product Databases and Marine Extracts by Using Molecular Docking Techniques.** Verónica Ruiz-Torres, Maria Losada-Echeberría, Maria Herranz-López, Enrique Barrajón-Catalán, Vicente Galiano, Vicente Micol and José Antonio Encinar. *Marine Drugs*. 2018 Oct; 16(10): 385. **Impact Factor: 3.772** (2018), 5-Year Impact Factor: 4.446 (2018). **Q1**. doi: 10.3390/md16100385. PMID: 30326670.

Por ello, **DA SU CONFORMIDAD** para la defensa por Compendio de Publicaciones con Mención Internacional y para que consten los efectos oportunos, firman el presente certificado en Elche (Alicante), a de septiembre de 2019.



Fdo.: Dr. Ricardo Mallavía Marín



Esta tesis doctoral ha sido realizada gracias a la beca predoctoral (ACIF/2015/158) del programa de subvenciones para la contratación de personal investigador de carácter predoctoral concedida por la Conselleria de Educación, Cultura y Deporte de la Generalitat Valenciana y el Fondo Social Europeo en el 2015. También fueron recibidas dos ayudas para la movilidad bajo el programa de subvenciones para estancias de contratados predoctorales en centros de investigación fuera de la Comunitat Valenciana con referencias BEFPI/2017/031 de tres meses y BEFPI/2018/050 de 6 meses en la Universidad de Queen's en Belfast (Irlanda del Norte).



La presente tesis doctoral está enmarcada dentro del proyecto **Nuevos compuestos antitumorales para tratar el cáncer de colón**, el cual está reconocido como proyecto de interés social por el Consell Assesor del Mecenatge de la Generalitat Valenciana con fecha 14 de mayo de 2019.





*Para Fran, el mejor compañero de viaje,
a mis padres, hermano y su familia*

Biblioteca
UNIVERSIDAD Miguel Hernández

Agradecimientos



Doctoral Student:
Verónica Ruiz Torres

Son muchos las personas e instituciones que han contribuido a la finalización de este trabajo.

En primer lugar me gustaría agradecer a **la Universidad Miguel Hernández de Elche**, al Instituto de Investigación, Desarrollo e Innovación en Biotecnología Sanitaria de Elche (IDIBE) y a su director **Dr. Antonio Ferrer Montiel** por brindarme la oportunidad de formarme y adquirir el desarrollo profesional obtenido. También me gustaría agradecer a la **Universidad de Queen's** de Belfast por permitirme realizar dos estancias en el Centre for Cancer Research & Cell Biology (CCRCB).

Agradezco al personal administrativo, **Maite, Pepi, Eva, Vicente** y especialmente a **Ricardo** por su excelente labor, paciencia y profesionalidad.

Me gustaría mostrar mi total gratitud a mis directores de tesis a los doctores **Vicente Micol Molina** y **Enrique Barraión Catalán** por su apoyo y confianza en mi trabajo que han permitido mi formación como investigadora. Su inestimable ayuda y esfuerzo han contribuido enormemente al desarrollo de esta tesis.

Deseo agradecer a mis compañeros del grupo de **Compuestos Bioactivos Naturales**. A **Almudena** (mi muero de amor) por ayudarme en todo, especialmente por facilitarme el camino y a **Luz María** (Lucecilla) especialista en tirar cafés y por entender mis chistes malos. Las tres formamos el Equipo Romero. Muchas gracias por todo (infinitas cosas que no puedo enumerar) porque sin vosotras no habría sido lo mismo. También a **María Losada** por los buenos momentos vividos, por su compañerismo y por haberme ayudado con los insufribles papeleos de la tesis. Millones de gracias a las tres. Gracias a **Mariló**, compañera de VALi+d, por compartir los procesos burocráticos de esta

ayuda y por tu compañía durante estos años. Gracias a **Noelia** por hacer el esfuerzo de venir a visitarme cuando estaba de estancia, por tu ayuda con el HPLC y por tu alegría. Gracias a **María Herranz** por la ayuda ofrecida y por formar parte de esta experiencia. A **Jesica, Eminee, Maribel, Javi y Sara Gea** por todos los buenos momentos. También me gustaría agradecer a **Maite** por ser como una madre en el laboratorio, por tu ayuda y dedicación. Gracias al servicio técnico, especialmente a **Eva e Irene**.

Gracias al **Dr. Miguel Saceda** y al **Dr. José Antonio Encinar** por sus inestimables contribuciones a este trabajo y por su amabilidad.

Gracias al grupo de Ingredientes Bioactivos, dirigido por el **Dr. Antonio Segura Carretero**, por su contribución a la identificación de compuestos bioactivos de los extractos utilizados en este trabajo.

Me gustaría también agradecer a la **Dr. Sandra Van Schaeybröeck** por acogerme en su laboratorio, por tratarme como a una más de su grupo y por enseñarme a interpretar rutas metabólicas. Al **Dr. Nicholas Forsythe** por su hospitalidad y por enseñarme la fascinante técnica del Western blot.

Gracias a **Cristiaan Echegoyen** por su generosidad y asesoramiento con las especies marinas.

Mi reconocimiento a todos los profesores que han influenciado en mi forma de pensar. Gracias a todo el profesorado de Ciencias del Mar, especialmente a **Paqui Giménez** por ser una referencia a seguir.

Gracias a tod@s los amigos de Callosa, por comportarse como una auténtica familia y por motivarme a seguir en todo momento. Gracias a aquellos que contribuyeron directamente, con la maquetación de esta tesis. Gracias

especialmente a **Inma, Rosendo, Víctor y Aroa**, por venir a verme a Belfast y por regalarme una noche increíble e inolvidable con brindis de champán y por dejarme incrustada en mi cabeza la canción del donut.

A **Conchi, José Francisco, Manolo y Jose**, gracias por su apoyo y compañía.

A mi hermano **Jose**, a mi cuñada **Elena** y a mis sobrinos **Álvaro y Claudia**, gracias por compartir muy buenos momentos en familia.

Mi infinita gratitud a **mis padres** por ser un modelo a seguir, por ser las mejores personas del mundo, generosas, amables y divertidos. Gracias por enseñarme que nunca hay que dejar de luchar. Gracias por apoyarme y dármelo todo.

Por último, aunque en el pádel eres un paquete, gracias **Fran** por ser el ingrediente perfecto de todo este proceso, porque has sido un apoyo incondicional incluso en los momentos más difíciles y por ofrecerme de forma generosa toda tu ayuda. Gracias por creer siempre en mi y por ser un modelo a seguir. Mil gracias por ser el mejor compañero de vida (*You are my wonderwall too*).

~ Muchas gracias ~

“La naturaleza no hace nada incompleto ni nada en vano”

Aristóteles



Abbreviations and acronyms

7-AAD	7-Aminoactinomycin D
ANOVA	Analysis of Variance
APC	Adenomatous Polyposis Coli
ATCC	American Type Culture Collection
ATF4	Activating Transcription Factor 4
ATF6	Activating Transcription Factor 6
ATP	Adenosine Triphosphate
BIP/GRP78	Binding immunoglobulin protein
C3/7/8/9	Caspase 3/ Caspase 7/ Caspase 8/ Caspase 9
CE	Complete Extract
Chlo	Chloroquine
CHOP	C/EBP Homologous Protein
CI	Cell Index
CII	Cell Index of Invasion
CIM	Cell Index of Migration
CIP	Cell Index of Proliferation
CR	<i>Carotacyon</i> sp
CRC	Colorectal Cancer
DCFH-DA	2',7'-Dichlorodihydrofluorescein diacetate
DMEM	Dulbecco's Modified Eagle's Medium
DMSO	Dimethyl Sulphoxide
DNA	Deoxyribonucleic Acid
EDTA	Ethylenediaminetetraacetic acid
eIF2 α	Eukaryotic translation initiation factor 2 alpha
EMA	European Medicines Agency
EMEM	Eagle's Minimum Essential Medium
ER	Endoplasmic Reticulum
ERS	Endoplasmic Reticulum Stress
ESI	Electrospray Ionisation
F	Fraction
FBS	Fetal Bovine Serum
FCS	Fetal Calf Serum
FDA	U.S. Food and Drug Administration (USA)
H2AX	Histone H2AX
HEPES	4-(2-hydroxyethyl)-1-piperazineethanesulfonic acid
HGUE-C-1	Hospital General Universitario de Elche Colon cancer cell line
HPLC	High Performance Liquid Chromatography
HRP	Horseradish Peroxidase
I4	HCT-116 Invasive population 4
I9	HCT-116 Invasive population 9
IC ₅₀	The half maximal inhibitory concentration
IRE1 α	Inositol Requiring Enzyme 1 alpha
JNK	c-Jun N-terminal kinase

LDH	Lactate Dehydrogenase
MMP	Mitochondrial Membrane Permeabilization
MNPs	Marine Natural Products
MS	Mass Spectrometer
mTOR	mammalian Target of Rapamycin
MTT	3-(4,5-dimethylthiazol-2-yl)-2,5-diphenyltetrazolium bromide
NA	<i>Phyllidia varicosa</i>
NAC	N-acetyl cysteine
NB	<i>Dolabella auricularia</i>
Nec-1	Necrostatin-1
NPs	Natural Products
Nsa	Necrosulfonamide
P	Parentals
4-PBA	Phenylbutyric acid
PERK	Protein kinase RNA-like endoplasmic reticulum kinase
PI	Propidium Iodide
PS	<i>Pseudocolochirus violaceus</i>
QTOF	Q-Time-of-Flight system
RNA	Ribonucleic Acid
ROS	Reactive Oxygen Species
rpm	Revolutions per minute
RTCA	Real Time Cell Analyzer
siRNA	Small interfering RNA
UV-Vis	Ultraviolet-Visible
XBP1	X-Box Binding Protein
zVAD	z-VAD-fkm caspases inhibitor

ABSTRACT/RESUMEN	1
01 INTRODUCTION.....	11
CANCER AND HALLMARKS OF CANCER.....	13
1.1. <i>Epidemiology of cancer</i>	15
COLORECTAL CANCER (CRC).....	17
1.2. <i>Epidemiology of CRC</i>	17
1.3. <i>Anatomy of the Gastrointestinal System and CRC</i>	18
1.4. <i>Risk Factors</i>	20
1.5. <i>CRC screening tests</i>	20
1.6. <i>Staging CRC</i>	22
1.7. <i>Genetic changes in CRC</i>	25
1.8. <i>Biomarkers in CRC</i>	28
1.9. <i>Treatment of CRC</i>	31
REPROGRAMMING METABOLISM IN CANCER.....	35
1.10. <i>The PI3K/Akt/mTOR pathway</i>	36
1.11. <i>Endoplasmic Reticulum Stress</i>	37
1.12. <i>Oxidative Stress</i>	41
TUMOR INVASION AND METASTASIS.....	47
1.13. <i>The invasion-metastasis cascade</i>	47
1.14. <i>Tumor migration modalities</i>	48
1.15. <i>Endothelial transmigration</i>	50
1.16. <i>Migratory promoters</i>	51
1.17. <i>ROS/ERS effector in migration, invasion and metastasis</i>	51
MARINE DRUG DISCOVERY.....	54
1.18. <i>Marine ecosystem and potential</i>	54
1.19. <i>Marine Natural Products (MNPs) classification</i>	55
1.20. <i>MNPs biological activity</i>	58
1.21. <i>MNPs producers</i>	62
1.22. <i>Methodologies of Screening MNPs</i>	63
02 OBJECTIVES.....	67
03 METHODOLOGY.....	71
PROCEDURE SCHEME AND SELECTION OF MARINE EXTRACTS.....	73
CHEMICALS AND REAGENTS.....	75
EXTRACTS AND FRACTIONS PREPARATION.....	75

3.1.	<i>Marine invertebrate material</i>	75
3.2.	<i>Complete extraction and fractionation</i>	76
	CELL CULTURE MAINTENANCE.....	77
	CELLULAR AND MOLECULAR BASED ASSAYS.....	77
3.3.	<i>Cell viability assay by MTT assay</i>	77
3.4.	<i>Proliferation assay by RTCA</i>	78
3.5.	<i>Survival assay by clonogenic test</i>	79
3.6.	<i>Cell cycle analysis</i>	79
3.7.	<i>Apoptosis tests</i>	80
3.8.	<i>Necrosis assays</i>	81
3.9.	<i>Mitochondrial state</i>	83
3.10.	<i>Oxidative status</i>	83
3.11.	<i>DNA Damage</i>	84
3.12.	<i>Migration and invasion assay by RTCA</i>	84
3.13.	<i>Superinvasive populations isolation</i>	85
3.14.	<i>Reverse transfection</i>	86
3.15.	<i>Western blot analysis</i>	87
	DETERMINATION OF SECONDARY METABOLITES BY HPLC-ESI-TOF-MS	88
	STATISTICAL PROCEDURE	89
04	RESULTS	91
	THE SUMMARIZED RESULTS OF CHAPTER 1	93
	THE SUMMARIZED RESULTS OF CHAPTER 2	97
	THE SUMMARIZED RESULTS OF CHAPTER 3	103
	THE SUMMARIZED RESULTS OF CHAPTER 4	107
05	DISCUSSION	113
06	CONCLUSIONS	135
07	REFERENCES	139
08	SCIENTIFIC PRODUCTION	159
	CHAPTER 1	161
	<i>An Updated Review on Marine Anticancer Compounds: The Use of Virtual Screening for the Discovery of Small-Molecule Cancer Drugs</i>	
	CHAPTER 2	215
	<i>Marine invertebrate extracts induce colon cancer cell death via ROS-mediated DNA oxidative damage and mitochondrial impairment</i>	

CHAPTER 3.....	287
<i>New Mammalian Target of Rapamycin (mTOR) Modulators Derived from Natural Product Databases and Marine Extracts by Using Molecular Docking Technique</i>	
CHAPTER 4.....	367
<i>A nudibranch marine extract chemosensitizes selectively colorectal cancer cells inducing endoplasmic reticulum stress mediated by ROS</i>	
09 ANEXES	399





Figure Index

FIGURE 1. THE TUMOR MICROENVIRONMENT AND TYPE OF CELLS.....	13
FIGURE 2. THERAPEUTIC TARGETING OF THE HALLMARKS OF CANCER.	14
FIGURE 3. EPIDEMIOLOGY OF CANCER	16
FIGURE 4. TOP CANCER PER COUNTRY, ESTIMATED NUMBER OF NEW CASES IN 2018	17
FIGURE 5. LARGE INTESTINE ANATOMY AND GASTROINTESTINAL WALL	19
FIGURE 6. CRC DEVELOPMENT, SCREENING METHODS AND TREATMENT	21
FIGURE 7. DIFFERENT STAGES OF CRC	23
FIGURE 8. CHEMICAL STRUCTURES OF CRC DRUGS.	33
FIGURE 9. THE PI3K/AKT/MTOR PATHWAY	37
FIGURE 10. ENDOPLASMIC RETICULUM	38
FIGURE 11. ER STRESS AND UPR	40
FIGURE 12. ROS AND RESPIRATION CHAIN IN THE MITOCHONDRIA	42
FIGURE 13. THE DOUBLE-FACED ROLE OF REACTIVE OXYGEN SPECIES (ROS) IN CANCER.....	43
FIGURE 14. SOLID TUMOR PROGRESSION AND ROS INFLUENCE.....	45
FIGURE 15. METASTASIS AS A MULTI-STEP PROCESS.	48
FIGURE 16. STRESS SIGNALING AND THE MESTASTATIC CASCADE.....	52
FIGURE 17. OCEAN ZONES AND MARINE ECOSYSTEM.....	54
FIGURE 18. MAJOR PATHWAYS OF MARINE SECONDARY METABOLITES.....	56
FIGURE 19. MARINE INVERTEBRATES.....	63
FIGURE 20. PHENOTYPIC VS TARGET-BASED SCREENING SYSTEMS	64
FIGURE 21. THE MARINE EXTRACTS SCREENING.	73
FIGURE 22. SUPERINVASIVE POPULATION ISOLATION PROCEDURE.....	86
FIGURE 23. MARINE SELECTED INVERTEBRATES.....	97
FIGURE 24. GRAPHICAL ABSTRACT CHAPTER 3.	104
FIGURE 25. SCHEMATIC MECHANISM OF ACTION OF NB EXTRACT.....	134



Table Index

TABLE 1. CRC BIOMARKERS AND THEIR PREDICTIVE VALUE	27
TABLE 2. LIST OF APPROVED MARINE ANTICANCER DRUGS FROM AN INVERTEBRATE	57
TABLE 3. LIST OF MARINE DRUGS IN CLINICAL TRIALS (PHASES III AND II).....	58
TABLE 4. LIST OF MARINE DRUGS IN CLINICAL TRIALS (PHASES II-1 AND I).	59
TABLE 5. PHENOTYPIC VS TARGET-BASED SCREENING SYSTEMS.....	64
TABLE 6. SCREENING OF MARINE INVERTEBRATE SPECIES.	74



Abstract / Resumen



Doctoral Student:
Verónica Ruiz Torres

Cancer is one of the leading causes of death worldwide and requires the attention and effort of the scientific community for the development of new strategies and the discovery of drugs that help fight the disease [1]. It is necessary to discover novel effective therapies focused on avoiding cancer cell proliferation and reducing side effects.

Marine compounds, produced to survive in response to harsh and competitive environmental conditions, are postulated as a potential anticancer source. In the last decades, marine metabolites have shown novel wide chemical structures, which have been attributed to interesting biological activities and this fact has been registered by the increasing numbers of drugs approved by the U.S. Food and Drug Administration (FDA) and the European Medicines Agency (EMA). In particular, marine invertebrates are considered one of the richest biodiverse groups. To date, a large number of natural products extracted or synthesized based on marine compounds from invertebrates have been established as antineoplastic drugs.

In chapter 1, the current marine natural products (MNPs) that have been established as antineoplastic drugs were reviewed and their putative mechanisms of action in the different hallmarks of cancer described, giving an overview of the richness of the chemical structures that they offer and introducing the use of virtual screening for drug discovery.

This thesis, in chapter 2, focuses on the search of the antiproliferative effect of several invertebrate marine extracts in human colon cancer cell models. The first part of the project focuses on the search for marine organisms that have intra and interspecific competence through the production of bioactive compounds. A selection of 20 organisms was made based on bibliographic sources and relayed on observations of competence in experimental aquariums. The next part consisted in to screen the *in vitro* antiproliferative effect on a panel of colon cancer cell models. Four extracts were selected due to their potential cytotoxic effect: *Phyllidia varicosa* (NA extract) and *Dolabella auricularia* (NB extract), obtained from two nudibranchs, *Carotalcyon* sp (CR extract) obtained

from a soft coral and *Pseudocolochirus violaceus* (PS extract) from a holothurian. The main bioactive compounds (98 compounds) represented in these four extracts were identified using an HPLC-ESI-TOF-MS analysis. Among the most abundant compounds characterized in each extract, terpenes and diterpenes, and steroids (CR); cembranolides (PS); diterpenes, polyketides and indole terpenes (NA); and porphyrin, drimenyl cyclohexanone and polar steroids (NB), were proposed to be the candidates for the observed activity.

CR, PS, NA, and NB showed strong antiproliferative ability and a cytostatic effect arresting the cell cycle in the G2/M phase. Likewise, CR, NA and NB extracts induced early apoptosis and PS extract exerted necrotic cell death. The four extracts showed a remarkable effect consisting on a dramatic intracellular reactive oxygen species (ROS) accumulation and mitochondrial depolarization, caspase activation and DNA damage.

In Chapter 3, the effect of marine natural products as inhibitors of rapamycin target (mTOR) in mammals was studied. This kinase is a master regulator of cell growth and metabolism and is deregulated in many types of cancer. Our results showed evidence of 11 pure compounds (selected by molecular coupling and calculated ADMET parameters) and two marine extracts to inhibit mTOR with the same effectiveness.

Finally, in Chapter 4, we explored in depth the antiproliferative effect of NB extract mediated by an induction of oxidative and endoplasmic reticulum stress in the human colon cancer cell model HCT-116. First, we found an overexpression of endoplasmic reticulum (ER) stress markers and an overproduction of reactive oxygen species (ROS) basally in the colon cancer cell model compared to the normal colon cells. This difference in the basal stress level made the tumor cells more sensitive to the NB extract. The results suggest that NB extract significantly increases cellular stress by inducing ROS and overexpressing proteins related to ER stress through the response to unfolding proteins.

In addition to the antiproliferative capacity, the ability of NB to inhibit one of the most dangerous characteristics of tumor cells, the migration and

invasion qualities of superinvasive models from HCT-116 was studied. The results were promising in showing that NB significantly reduced the migration and invasion rate of the most superinvasive populations with a smaller effect on the non-tumor line.

This thesis, therefore, demonstrates that marine compounds are a potential source of anti-cancer drugs due to the chemical diversity and broad biological activity that they offer. This fact is reflected in the increase in the number of drugs of marine origin that have been approved to date and the large number of scientific studies related to the field that are underway. In addition, this thesis offers interesting results about potential antitumor activity from marine invertebrate extracts and reveals some strengths of its mechanism of action. Likewise, the present study offers results of how the new strategies of computational screening that allow the search of regulatory compounds of key targets against cancer increase the effectiveness in the search of antitumor compounds.





El cáncer es una de las principales causas de muerte en todo el mundo y requiere la atención y el esfuerzo de la comunidad científica para el desarrollo de nuevas estrategias en el descubrimiento de fármacos que ayuden a combatir la enfermedad [1]. Es necesario descubrir nuevas terapias efectivas que se centren en evitar la proliferación de células cancerosas y evitar los efectos secundarios. Los compuestos marinos, producidos como consecuencia de un intento de supervivencia ante condiciones adversas y de competencia, se presentan como una fuente potencial contra el cáncer. En las últimas décadas, los metabolitos marinos han mostrado una oferta de estructuras químicas novedosas a las que se le han atribuido actividades biológicas interesantes. Este hecho que queda registrado por el creciente número de medicamentos aprobados por la Administración de Drogas y Alimentos de los Estados Unidos (FDA) y la Agencia Europea de Medicamentos (EMA) de origen marino. En particular, los invertebrados marinos se proponen como fuente potencial de moléculas bioactivas por representar uno de los grupos más biodiversos. Hasta la fecha, una gran cantidad de productos naturales han sido extraídos o sintetizados en base a compuestos marinos de invertebrados y se han establecido como fármacos antineoplásicos.

En el capítulo 1 de esta tesis, se revisaron los actuales productos naturales marinos (MNP) que se establecieron como medicamentos antineoplásicos, describiendo sus posibles mecanismos de acción contra dianas moleculares específicas contra el cáncer, brindando una visión general de la riqueza de las estructuras químicas que ofrecen e introduciendo el uso de la detección virtual para el descubrimiento de fármacos. Esta tesis, en el capítulo 2, se incluyen resultados sobre la búsqueda del efecto antiproliferativo de extractos marinos procedentes de invertebrados en modelos de células de cáncer de colon humano. La primera parte del proyecto se centró en la búsqueda de organismos marinos que tienen competencia intra e interespecífica a través de la producción de compuestos bioactivos. Se realizó una selección de 20 organismos en base a fuentes bibliográficas y se hizo una

selección de aquellos organismos que presentaron competencia en acuarios experimentales. Una vez seleccionados los organismos de interés, se analizó el efecto antiproliferativo *in vitro* en tres modelos celulares humanos de cáncer de colon (HGUE-C-1, HT-29 y SW-480).

Los cuatros extractos con mayor efecto citotóxico fueron de los nudibránquios *Phyllidia varicosa* (extracto NA) y *Dolabella auricularia* (extracto NB), del coral blando *Carotalcyon* sp (extracto CR) y uno de la holoturia *Pseudocolochirus violaceus* (extracto PS). Los principales compuestos bioactivos (98 compuestos) representados en estos cuatro extractos se identificaron utilizando un análisis HPLC-ESI-TOF-MS. Entre los compuestos más abundantes caracterizados en cada extracto se encontraron: diterpenos, esteroides, sesqui y sester-terpenos en el extracto CR; cembranólidos en PS; diterpenos, policétidos e indol terpenos en NA; y se propone que la porfirina, la drimenol ciclohexanona y los esteroides polares de NB, todos ellos fueron los responsables de la actividad observada.

Los cuatro extractos mostraron una fuerte capacidad antiproliferativa, mediante un efecto citostático a través de la parada del ciclo celular en la fase G2/M. Mientras que CR, NA y NB indujeron la activación de caspasas y apoptosis, PS promovió la muerte por necrosis sumada a la apoptótica. Además, los extractos marinos aumentaron las especies reactivas del oxígeno e indujeron estrés oxidativo, desestabilizaron la membrana mitocondrial y dañaron el ADN.

En el capítulo 3, se estudió el efecto de los productos naturales marinos como inhibidores de la diana de rapamicina (mTOR) en mamíferos. Esta quinasa es clave en el crecimiento y el metabolismo celular y se encuentra desregulada en muchos tipos de cáncer. Nuestros resultados mostraron evidencias de 11 compuestos puros (seleccionados por acoplamiento molecular y parámetros ADMET calculados) y de dos extractos marinos para inhibir mTOR. Además, extractos marinos y compuestos puros mostraron similitud en los resultados de inhibición con esta diana.

Finalmente, en el capítulo 4, la tesis aborda el estudio en profundidad del efecto antiproliferativo del extracto NB mediado por una inducción del estrés oxidativo y endoplásmico en el modelo celular de cáncer de colon humano HCT-116. En primer lugar, encontramos una sobreexpresión de marcadores del estrés del retículo endoplasmático (ER) y una sobreproducción de especies reactivas del oxígeno (del inglés reactive oxygen species, ROS) de forma basal en el modelo de células de cáncer de colon en comparación con las células de colon normales. Esta diferencia en el nivel de estrés basal hizo que las células tumorales fueran más sensibles al extracto NB. Los resultados sugieren que el extracto de NB consigue aumentar considerablemente el estrés celular mediante la inducción de ROS y la sobreexpresión de proteínas relacionadas con el estrés del RE a través de la respuesta a proteínas desplegadas.

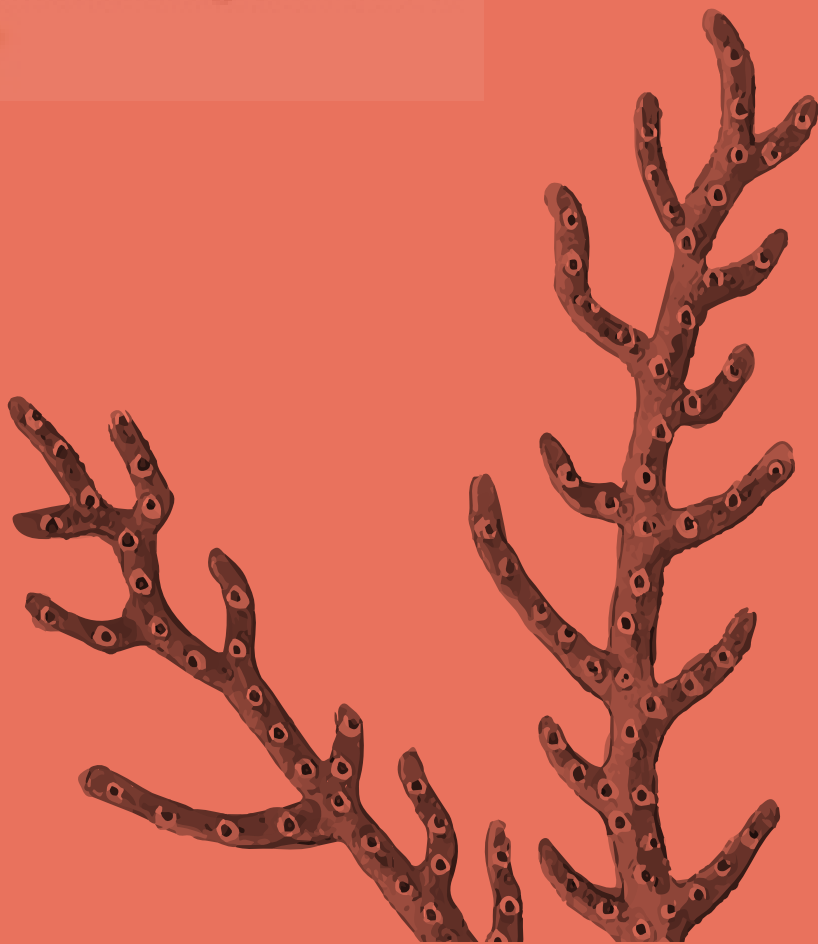
Además de la capacidad antiproliferativa, se estudió la capacidad de NB para inhibir una de las características más peligrosas de las células tumorales, la capacidad de migración e invasión de modelos superinvasivos procedentes de HCT-116. Los resultados fueron prometedores al mostrar que NB redujo considerablemente la tasa de migración e invasión de las poblaciones más superinvasivas y además se observó que ejercía un menor efecto en la línea no tumoral.

Esta tesis, por tanto, demuestra que los compuestos marinos son una fuente potencial de fármacos contra el cáncer ya que ofrecen una diversidad química y actividad biológica amplia. El incremento del número de fármacos de origen marino aprobados, así como el número de estudios científicos en este ámbito corroboran el impacto de este campo en la sociedad actual. Además, esta tesis ofrece resultados interesantes acerca de potenciales antitumorales procedentes de extractos de invertebrados marinos y desvela algunos puntos fuertes de su mecanismo de acción. Asimismo, el presente estudio ofrece resultados de como las nuevas estrategias de cribado computacional que permiten la búsqueda de compuestos reguladores de dianas claves contra el cáncer aumentan la efectividad en la búsqueda de compuestos antitumorales.



01

Introduction



Doctoral Student:
Verónica Ruiz Torres

CANCER AND HALLMARKS OF CANCER

Normal cells multiply and proliferate to keep a healthy condition and die when they are damaged or old. When cells suffered genetic damage, which is not correctly repaired, failures accumulate and uncontrolled processes start. In this scenario, cells do not die when they should and continue proliferating accumulating errors. The process by which a normal cell change to a tumor is called carcinogenesis.

A solid tumor consists of a complex aggregation of different types of cells (including stromal cells), the extracellular matrix (ECM), and molecules involved such as chemokines, cytokines, microRNAs, and growth factors. Among the cells that form a solid tumor, several cellular types are included as cancer stem cells and progenitors, tumor vessels (blood and lymphatic), immune cells (tumor-associated macrophages, TAMs and T-cells), myeloid-derived suppressors cells (MDSC), natural killer cells (NK cells), tumor-associated neutrophils (TANs), cancer-associated adipocytes (CAAs) and cancer-associated fibroblasts (CAFs) (**figure 1**).

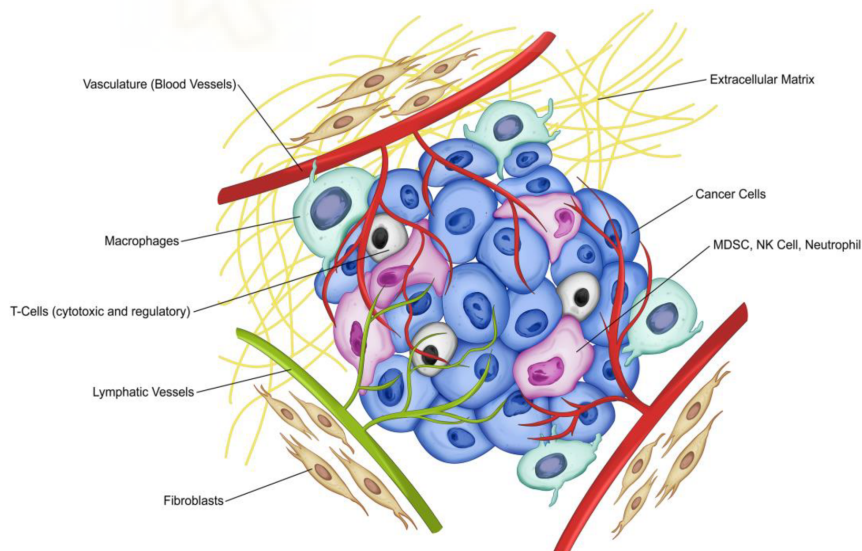


Figure 1. The tumor microenvironment and type of cells (from Norton K. et al. 2019 [2]).

Cancer means different clinical entities grouped as a complex disease where there are multiple variables interacting. Hanahan and Weinberg in the work called The hallmarks of Cancer in 2000 [3] proposed six properties that comprised malignant tumors i) a self-sufficiency in growth signals; ii) insensitivity to growth-inhibitory signals; iii) evasion of modes of programmed cell death (including apoptosis); iv) limitless replicative potential; v) sustained angiogenesis; and vi) tissue invasion and metastasis. In 2011, were added the ability to vii) reprogramming of energy metabolism; and viii) evasion of immune destruction (**figure 2**) [4]. They also suggested another dimension of complexity, which is related to the ability to contain a repertoire of recruited normal cells that help to generate a tumor microenvironment. Cancer shows these common characteristics that allow us to understand this complex disease and let the development of new clinical strategies for its management.

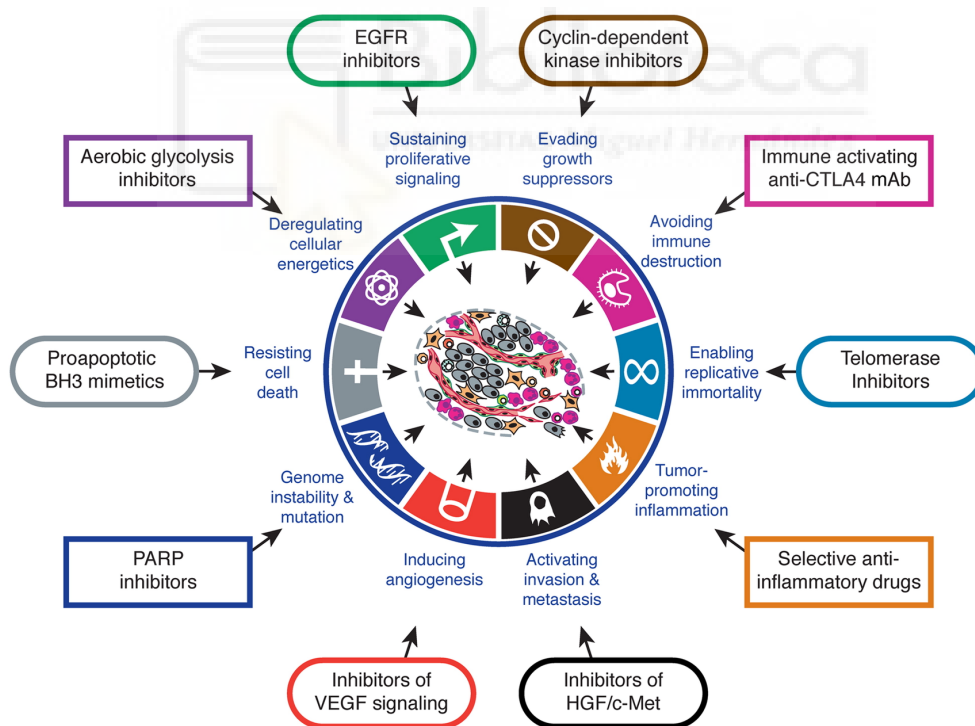


Figure 2. Therapeutic Targeting of the Hallmarks of Cancer (adapted from Hanahan D. et al. 2011 [4]).

1.1. Epidemiology of cancer

Cancer can appear in almost any organ or tissue, is heterogeneous and include over two-hundred of neoplastic diseases. GLOBOCAN estimated 18.1 million new cancer cases, and 9.6 million deaths occurred worldwide in 2018. It is calculated that over 29.5 millions of new cases will be in 2040, both sexes, all ages worldwide, a 70% higher in the next decades. The most common new types of cancer worldwide in 2018 were lung (11.6%), breast (11.6%), colorectum (10.2%), prostate (7.1%) and stomach (5.7%) and the highest shares of deaths in 2018 were lung (18.4%), colorectum (9.2%), stomach (8.2%) and liver (8.2%). Most affected areas at the global level are Asia (48.4%), Europe (23.4%), North America (13.2%) and Latin America and the Caribbean (7.8%) (**figure 3**) [5].

In Spain, SEOM (Sociedad Española de Oncología Médica) published an average of 215,500 cases in 2012, 228,482 in 2017 and 315,413 cases will be expected for 2035. Colorectum, prostate, lung, breast, bladder, and stomach [6] cancer were the most diagnosed ones in Spain in 2017.

Risk factors for cancer include growing older, lifestyle (such as type of diet and obesity), alcohol, tobacco, low physical activity, exposure to cancer-causing substances, chronic inflammation, hormones, infectious agents, radiation and sunlight. Some of these can be avoided changing lifestyle, however other such as age cannot.

Most cancers are named as the organ where they begin or cell they are made and by its ability to spread to other areas of the body. In general, the different types of cancer are:

- **Sarcoma** is originated in connective tissues for example bones, muscles, cartilage, fat, blood vessels or soft tissues. The frequency of this type of cancer is uncommon.
- **Leukemia** is cancer originated from bone marrow or blood cells and causes large amounts of abnormal blood cells. This type of cancer does not form solid tumors.

- **Lymphoma and myeloma** are originated from lymphocytes or cells from the immune system.
- **Melanomas** are cancer originated in melanocytes from the skin.
- **Carcinoma** is the most commonly diagnosed cancer and starts in the skin or tissues that cover organs and glandules. The most typical are lung, breast, colon, pancreas or prostate.

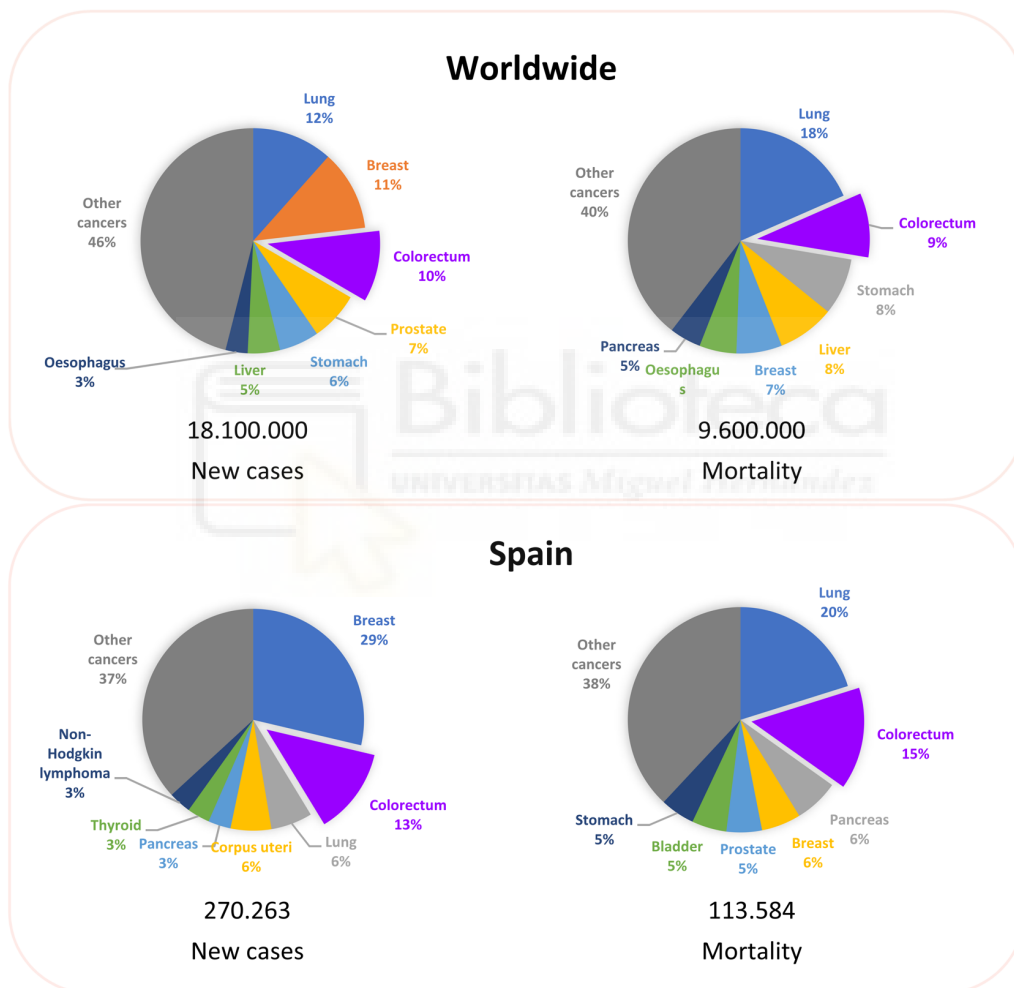


Figure 3. Epidemiology of Cancer (source GLOBOCAN 2018 [5]).

COLORECTAL CANCER (CRC)

Colorectal Cancer is a malignant abnormal cell proliferation arising in the colon and/or the rectum.

1.2.Epidemiology of CRC

According to GLOBOCAN, CRC is the third most prevalent cancer with 1.8 million new cases in 2018 in both sexes from all ages (**figure 4**). By sex, CRC is the third most prevalent in males and the second in females, accounting for 18.7% and 12.8% of worldwide incidence in men and women respectively. The CRC contributes to 9.2% of death due to cancer in 2018, estimating 11.4% in men and 7.2% in women [5] (**figure 3 and 4**).

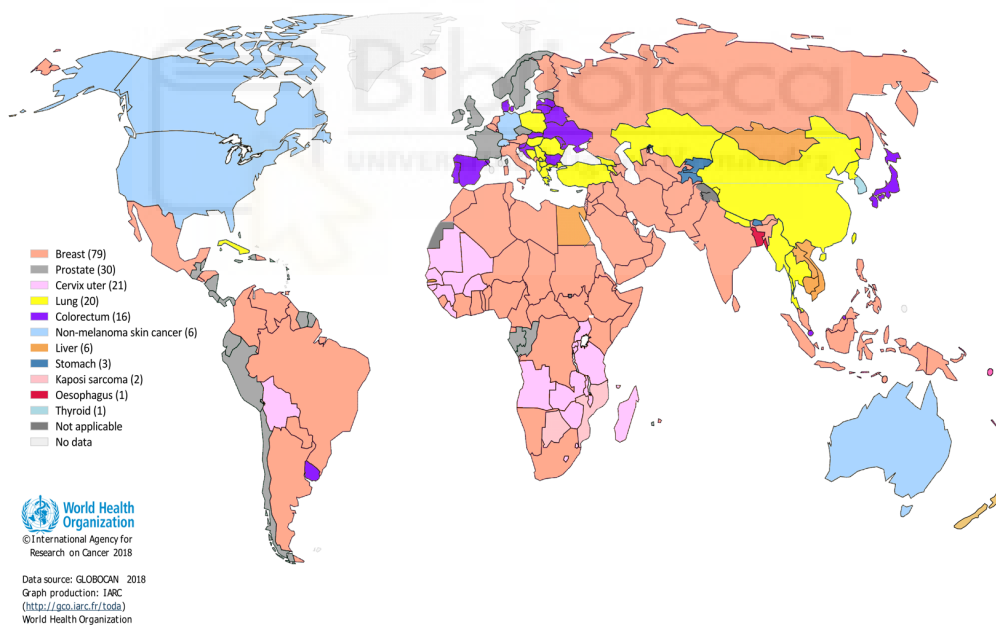


Figure 4. Top cancer per country, estimated number of new cases in 2018, both sexes, all ages (CRC) (source GLOBOCAN 2018 [5]).

In Spain, CRC is one of the most diagnosed cancer in 2019, among prostate, breast, lung, and bladder. CRC represented 31,172 cases in 2018, affecting men and women almost equally. In the last decades, Spain has registered a decrease in gastric cancer and it is related to dietary modifications, a decrease in the consumption of tobacco and alcohol. Although less CRC has been registered in Spain by Red Española de Registros de Cáncer (REDECAN) in 2015, and the same trend has been observed in the rest of Western countries, at a global level the CRC is still one of the most frequent [7].

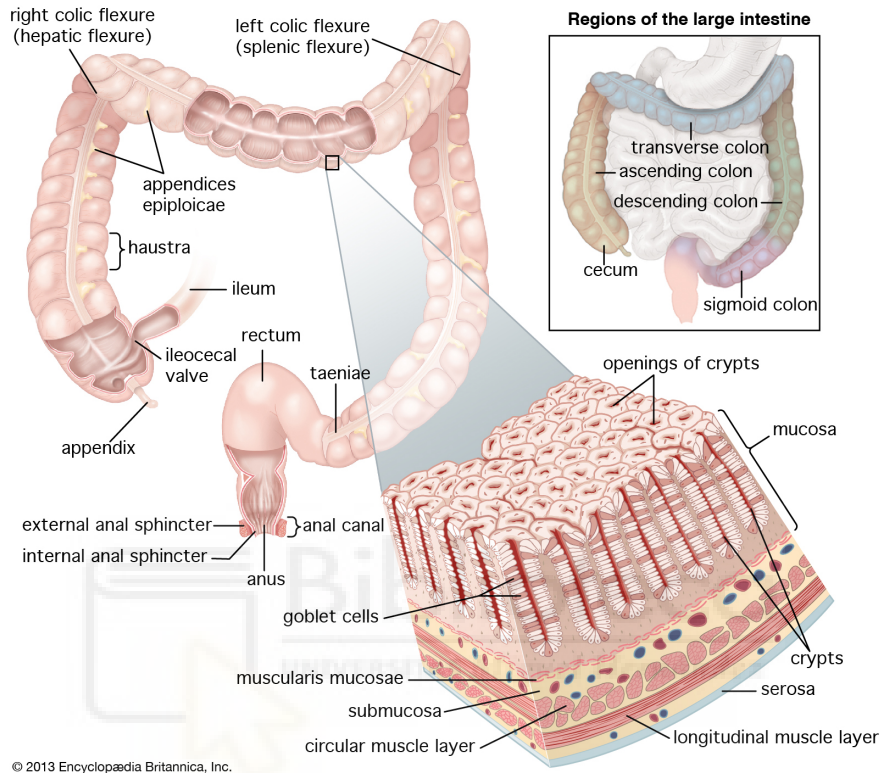
1.3. Anatomy of the Gastrointestinal System and CRC

The gastrointestinal system (GI) consists of organs connected from the mouth to the anus. The last part is formed by the small intestine, large intestine, and anus. The small intestine presents the duodenum, the jejunum, and ileum at the end of the digestive tract. The large intestine shows the appendix, cecum, colon, and rectum. The colon and rectum (colorectum) is the last part of GI where food is processed to obtain energy and where fecal matter is separated. The colon is a tube of 1.5 meters long and 5 centimeters in diameter formed by 4 parts (**figure 5**):

- **The Ascending colon** where it is found the cecum in which undigested food is kept, and it is located on the right part of the abdomen.
- **The transverse colon** that crosses the body from the right to the left side. The term proximal colon is also used to refer to ascending and transverse colon.
- **The descending colon** that is the part that descends through the left side.
- And the final part of the colon that is prior to the rectum and presents an S shape, which receives the name **sigmoid colon** or **distal colon**.

The specific function of the ascending and transverse colon is based on absorbing water, nutrients, and electrolytes, while the descending and rectum colon function is to expel fecal matter through the sigmoid colon into the rectum and finally through the anus. It is necessary to distinguish between anus cancer

and CRC because they are originated from different cell types and present different characteristics [8, 9].



© 2013 Encyclopædia Britannica, Inc.

Figure 5. Large intestine anatomy and gastrointestinal wall (source [10]).

CRC starts with a slow proliferation of abnormal cells on the inner or mucosal layer of the large intestine and protrudes into the intestinal lumen lining of the colon or rectum. This accumulation of cells is called polyp and the most common is the adenomatous polyp or adenoma, produced from a glandular cell, which is responsible to lubricate colorectum producing mucus. Above 10% of adenomas become cancerous and then is called adenocarcinoma, becoming in most cases of all CRCs [11]. CRC often develops slowly and might not cause symptoms right away, but histological, morphological and genetics changes are produced (**figure 6**). When an adenocarcinoma has been originated in the colon or rectum, it can spread to the distant parts of the body from where

originated (a process called metastasis). The first step of metastasis is to get into are nearby lymph nodes and also blood vessels, from there metastatic cells expanded along liver, lungs, or peritoneum [12].

1.4.Risk Factors

Anyone can suffer CRC, however, there are some risk factors associated with this type of disease. First of all, modifiable risk factors associated mainly with lifestyle will be discussed. Among them are diet, obesity, lack of physical activity, smoking and alcohol [13]. In contrast, it is known that a healthy diet rich in fiber, green leafy vegetables, folic acid and, calcium are factors that reduce the risk of CRC [14]. Unlike the previous ones, there are non-modifiable risk factors such as the aging, to present a personal history and the presence of colorectal polyps in family members, hereditary disorders such as Lynch syndrome, inflammatory bowel disease in familiar history, racial and ethnic background and diabetes type 2 [15].

Studies show that aging and hereditary predisposition are the most important factors in the development of CRC. The probability of developing CRC increases markedly after 50 years old, monitoring and screening people who are 50 years old or closely and high-risk individuals is the best prevention and detection of CRC [16].

1.5.CRC screening tests

CRC screening is the way of looking for a tumor in people who can suffer cancer. CRC screening can detect cancer and promote the removal of growing cancers at an early stage, reducing CRC mortality by decreasing incidence and disease. It is recommended to start at age of 50 for people who present risk of CRC and also people without risk showing a family history or certain medical conditions.

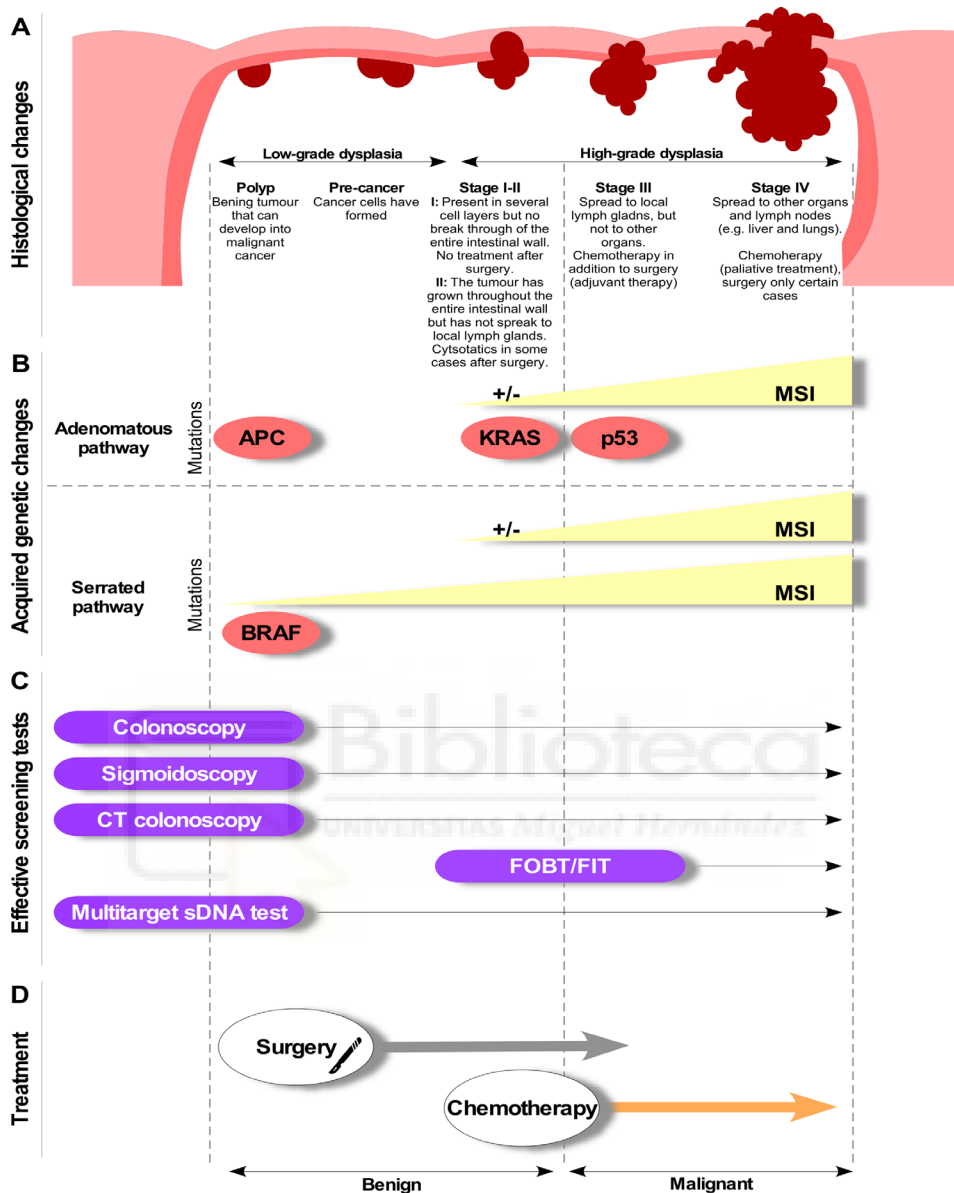


Figure 6. CRC development, screening methods and treatment (adapted from Simon K, 2016 [12]). (A) Histological changes of CRC; (B) acquired genetic changes of CRC; (C) effective screening tests for CRC. The temporal development of CRC is indicated from left to right in each panel. Includes methylation of BRAF, KRAS, BMP3, and NDRG4 genes. (D) Treatment of CRC. **Abbreviations** CRC, colorectal cancer; CIMP, CpG island methylator phenotype; CT, computed tomography; FOBT, fecal occult blood test; FIT, fecal immunochemical test; MSI, microsatellite instability; sDNA, stool DNA.

There are several varied screening tests (**figure 6 C**) that presents different advantages and limitations. The differences lie in the sensitivity of the test (percentage of people with cancer who really get a positive result with the test, the true-positive rate) and the specificity (percentage of patients without disease who receive a negative result or true-negative rate). Together, sensitivity and specificity define accuracy. All tests can avoid CRC death when being used in an appropriate time interval and with the recommended follow-up. The choice of one or the other method can affect subsequent decisions made by the doctor. The CRC screening include visual and stool-based tests. The **visual tests** are: colonoscopy, computed tomographic colonography (CTC), double-contrast barium enema and flexible sigmoidoscopy. The **stool-based tests** are the fecal immunochemical test (FIT), high-sensitivity guaiac-based fecal occult blood test (gFOBT) and FIT-DNA test (Cologuard®) (**figure 6 C**).

1.6. Staging CRC

Early CRC often has no symptoms, however, when a CRC is developed, general signs can be detected and include:

- Increased bowel dysfunction, such as diarrhea, constipation, and abdominal discomfort,
- Rectal and annum bleeding,
- Abdominal pain,
- Weakness, fatigue, and anemia due to blood loss,
- Weight loss

Screening and Staging of CRC is essential for determining the treatment and prognosis and is the best predictor for patient survival [17].

In 1926 Lockhart-Mummery proposed a CRC staging system based on the depth of invasion and lymph node from surgeries [18]. In 1932, Dukes summarized into 3 stages: **A** for limited carcinoma in the wall of the rectum, **B** for cancer has spread to the rectal tissue and **C** for metastasis presented in lymph nodes [19]. Duke's classification was modified by Kirklin, Dockerty, and

Waugh in 1949 and later by Astler and Collier in 1954 [20] adding 2 states. The modified Astler-Collier (MAC) classification is listed below (**figure 7**):

- **Type A**—Lesions limited to the mucosa and negative nodes.
- **Type B₁**—Lesions into the muscularis propria, but not penetrating it, with negative nodes.
- **Type B₂**—Lesions penetrating the muscularis propria, showing negative nodes.
- **Type C₁**—Lesions into the muscularis propria, but not penetrating it, with positive nodes.
- **Type C₂**—Lesions penetrating the muscularis propria with positive nodes.
- Later, Turnbull *et al.* in 1967 added the **stage D** to refer metastasized tumors to another part of the body such as the liver, lung, bones, and adjacent organs [21].

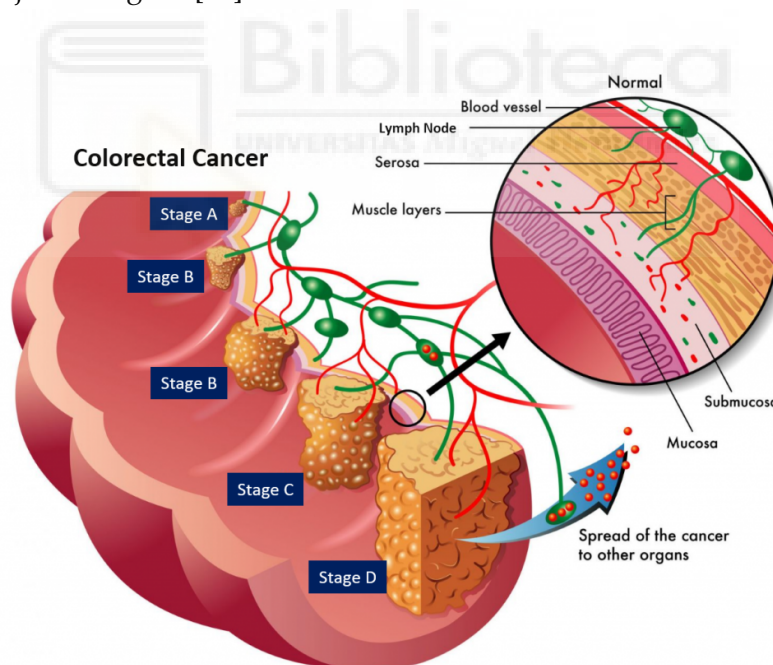


Figure 7. Different stages of CRC (from the Mcquarie University website [22]).

The widely accepted international method for CRC is the Tumour, Node, Metastasis (TNM) system of the American Joint Committee of Cancer (AJCC), proposed in 1987 [23]. This system is based on how deeply has the primary tumor grow plus a letter or number to describe it in more detail. It also describes the lymph nodes (N) state and which is the level of spread (metastasis) (M) [24].

➤ **T-Primary tumor**

Tx, Primary tumor cannot be evaluated.

T0, There is no evidence of primary tumor in colon or rectum.

Tis, Carcinoma *in situ*: intraepithelial or invasion of lamina propria.

T1, Tumor invades submucosa.

T2, Tumor invades muscularis propria.

T3, Tumor invades through muscularis propria into subserosa or into non-peritonealized pericolic or perirectal tissues.

T4, Tumor directly invades other organs or structures and/or perforates visceral peritoneum.

➤ **N-Regional lymph nodes**

NX, Regional lymph nodes cannot be assessed.

N0, No regional lymph node metastasis.

N1, Metastasis in one to three regional lymph nodes.

N2, Metastasis in four or more regional lymph nodes.

➤ **M-Distant metastasis**

MX, Distant metastasis cannot be assessed.

M0, No distant metastasis.

M1, Distant metastasis.

Doctors also add information about the type of cancer and its grade (G). G is evaluated based on the number of healthy cells from a tumor in comparison with a healthy tissue under a microscope. When cells are similar and low different cells grouping, Doctors call them “differentiated” or “low-grade tumor”. When there are big differences in cells, they call “poorly differentiated” or “high-grade tumor”.

GX, the tumor grade cannot be identified.

GX, the tumor grade cannot be identified.

G1, the cells are more like healthy cells (called well-differentiated).

G2, the cells are somewhat like healthy cells (called moderately differentiated).

G3, the cells look less like healthy cells (called poorly differentiated).

G4, the cells barely look like healthy cells (called undifferentiated).

1.7. Genetic changes in CRC

CRC development is the result of a combination of accumulated genetic mutations and epigenetic modifications of the human genome resulting in the transformation of the normal glandular epithelium into adenocarcinoma [25]. CRC patients present a wide molecular heterogeneity and it is believed to be responsible for the high variability in treatment response among patients with the same CRC stage [26]. Based on a genetic perspective CRC can be classified into sporadic (about 75% of cases), familial (20% of cases) and hereditary (10% of cases) [27].

In 1988, Vogelstein and colleagues hypothesized about CRC occurs from a multi-step malignant genetic alterations in certain oncogenes and tumor suppressor genes, which lead the transformation from tubular and tubulovillous adenomas into highly invasive adenocarcinomas. This identification would provide an important way to characterizing CRC [28]. However, recent research has reveal several main genetic pathways that lead the development colorectal carcinogenesis: the chromosomal instability pathway, Microsatellite Instability (MSI) and defective mismatch repair (dMMR), although other less established pathways have also been described [29] (**figure 6 B**).

1.7.1. Inherited CRC syndromes

It is estimated that a 5 – 10% of CRC patients present an inherited mutation, and their variants are known as the Lynch Syndrome (LS) or also

referred to as hereditary nonpolyposis colon cancer (HNPCC), Familial Adenomatous Polyposis (FAP), MYH-associated polyposis, and hamartomatous polyposis syndromes [27].

➤ **Hereditary nonpolyposis colon cancer (HNPCC)**

HNPCC is the most common autosomal dominant cancer predisposition syndrome responsible for about 3% of all cancer cases. This mutation is related to modify genes involved in DNA mismatch repair such as MLH1, MSH2, PMS1, PMS2 or MSH6. The mismatch mechanism involves the identification and reparation of different forms of DNA damage. Patients with HNPCC present an elevated risk to suffer other cancers [27, 30].

➤ **Familial adenomatous polyposis (FAP)**

FAP is the second most inherited CRC syndrome and occurs at a frequency of 1 - 2%. It is caused by an autosomal dominant inheritance of one allele of the Adenomatous Polyposis Coli (APC) gene tumor suppressor. FAP is characteristic to lead the development of colonic adenomas beginning in early adolescence [31] (**figure 6 B**).

➤ **MYH-associated polyposis**

This inherited CRC syndrome is a milder form of FAP and it is characterized by the development of multiple adenomatous colon polyps. MYH-associated polyposis is an autosomal recessive polyposis syndrome, caused by mutations in the MYH. This disorder causes cells to not correct mistakes in DNA copies when cell are dividing. About 1 – 2% of the population possess a mutated copy of the MYH gene and less than 1% of people have MYH-associated polyposis. People with MYH-associated polyposis has increased risk of several additional cancers.

➤ **Hamartomatous polyposis syndromes**

This hereditary autosomal dominant syndrome includes a rare group of hereditary autosomal dominant disorder such as Juvenile Polyposis Syndrome (JPS), PTEN hamartoma tumor syndrome, Cowden Syndrome (CS), Bannayan-Riley-Ruvalcaba Syndrome (BRRS), and Peutz-Jeghers Syndrome (PJS). It comprises less than 1% of all hereditary CRCs.

1.7.2. The Chromosomal instability (CIN) pathway

The CIN pathway is associated with traditional adenomas, observed in 65% – 70% of all sporadic cancers. This pathway resembles Volgestein's adenoma-carcinoma theory and is characterized by the accumulation of genetic and chromosomal defects, including mutation and aneuploidy [32].

CIN tumors display common mutations in the APC gene, which affects chromosome segregation in cell division. KRAS and BRAF proto-oncogene, which controls cell growth, differentiation, motility and survival, are mutated in colon tumors [33, 34]. KRAS mutations occur in 40 - 45% of CRCs while BRAF is found in 8 – 15% of CRC. Other genes such as SMAD2, SMAD 4 and also p53 gene (master regulator of transcription and apoptosis) can be affected by losing their functions [35] (**figure 6 B**).

1.7.3. The defective mismatch repair (MMR) pathway

The process of DNA synthesis generally produces incorrect base-pairing (base-base mismatches) or unmatched DNA loops (insertion-deletion loops). The Mismatch Repair (MMR) system controls these errors to maintain genomic stability. Alterations in MMR system have been characterized by MSI contributing to a 15 - 20% of CRCs. Microsatellites are short, repetitive 2-6 base-pair stretches of DNA scattered throughout the entire genome which displays particular vulnerability to insertions and deletions. MSI is the result of a defective MMR system [36].

1.7.4. Epigenetic pathways

Recently, sequencing has demonstrated unexpected genetic mutations associated with epigenetic alterations in CRC. Epigenetic mechanisms often involve DNA methylation and chromatin remodeling through histone modifications and non-coding RNAs (such as microRNAs) [37].

1.8. Biomarkers in CRC

CRC is a disease associated with high mortality. A good prognosis is crucial for early diagnosis and the implementation of efficient treatments. The molecular analysis and the search of biomarkers for CRC are making great progress. The inclusion of the study of reliable CRC biomarkers into clinical routine practices could improve the comprehension of genetic mutations in CRC and lead an efficient classification of phenotypes and genotype, and also can significantly accelerate patient prognosis, to predict the treatment response, and the possible recurrence risk (**table 1** and **figure 5**) [38].



Table 1. CRC biomarkers and their predictive value (source from [39]).

Biomarkers		Molecular basis	Predictive value	Detection method
Category	Type			
Pathological characteristics	Tumor stage			
	Lymph node status		D, P, PM	Diagnostic radiology and pathological/cytological examination
	Grade of differentiation			
Proliferation markers	Anatomy of invasion			
	Ki67	Nuclear antigen associated with proliferation	D, PM	IHC
	Cyclins	Regulation of cell cycle phase transition	D, PM	IHC
Chromosome abnormalities	p53	Tumor suppressor gene which shows loss of function	D, P, PM	IHC, RT-PCR, FISH
	H-ras, K-ras, N-ras	Membrane-associated GTPase integral to signal transduction cascade, if mutated, causes increased cellular proliferation	D, P, PM	IHC, RT-PCR, FISH
	Telomere length	Pathologic telomere length dynamics	D, PM	RT-PCR, Flow cytometry
Hypoxia-regulated genes	Telomerase activity	Maintenance of telomeres and therefore chromosomal length	D, P, PM	TRAP assay
	HIF-1	enables progression through successive cell cycles		
	Glut-1	HIF-1 transcription factor complex stabilized in hypoxic conditions, leading to transcription of hypoxia-regulated genes	D, P, PM	IHC
		Increased Glut-1 expression caused by malignant transformation and upregulated by hypoxia. Promotes switch to anaerobic glycolysis to support hypoxic tumor	D, P, PM	IHC

Cont.

Biomarkers		Molecular basis	Predictive value	Detection method
Category	Type			
Angiogenesis	VEGF	Angiogenic growth factor	P, PM	IHC, FISH, immunoassay
	PD-ECGF	Angiogenic growth factor with thymidine phosphorylase activity	P, PM	IHC
	Vascularity	New vasculature supports tumor growth	P, PM	IHC staining for endothelial receptors e.g. CD31, CD34, von Willebrand (factor VIII) combined with measurement of ICD or MVD using digital image analysis techniques
Epigenetics	Aberrant DNA hypermethylation	Inactivation of key tumor suppressor genes including APC, ATM, BMP3, CDKN2A, SFRP2, GATA4, GSTP1, HLF, MLH1, MGMT, NDRG4, RASSF2A, SFRP2, TFP12, VIM, and WIF1	D, P, PM	PCR-based methods and Pyrosequencing
	Aberrant DNA hypomethylation	Lids to chromosomal instability and global loss of imprinting	D, PM	PCR based methods and Pyrosequencing
	Gene expression patterns	Unique signature of the dysregulated genes/pathways at different forms and stages of CRC	D, P, PM	Array-based methods, NGS, RT-PCR
Tumor specific expression patterns	MicroRNA expression patterns	Unique signature of the dysregulated microRNAs at different forms and stages of CRC	D, P, PM	Array-based methods, NGS, RT-PCR

FISH: Fluorescent in-situ hybridization; HIF-1: Hypoxia inducible factor-1; HPLC: High pressure liquid chromatography; ICD: Inter-capillary distance; IGF-1: Insulin growth factor-1; IHC: Immunohistochemistry; MVD: Microvessel density; NGS: Next generation sequencing; PD-ECGF: Platelet-derived endothelial cell growth factor; RT-PCR: Reverse transcription–polymerase chain reaction; RIA: Radioimmunoassay; VEGF: Vascular endothelial growth factor; D: Diagnostic, P: Prognostic, PM: Predictive Markers.

1.9. Treatment of CRC

The CRC treatment has advanced rapidly due to the improvements in imaging, surgical techniques and chemotherapy. The CRC treatment plan is usually elaborated by doctors who work in different areas of cancer through multidisciplinary approaches. They consider the best options available for the stage, location and other tumor facts and making decisions finally on the basis of the risks against the benefits of each one of them (**figure 6 D**).

➤ Stage I CRC

If cancer has not spread to distant sites usually surgery to remove the tumor is the main treatment.

➤ Stage II CRC

When the tumor has grown through the wall and may extend into nearby tissue, however, it has not to reach lymph nodes, adjuvant chemotherapy could be complemented after surgery.

➤ Stage III CRC

In this stage, tumor has spread to nearby lymph nodes but did not spread to other parts of the body. The treatment is surgery to remove the section of the colon that contains the tumor along with the nearby lymph nodes (partial colectomy) and adjuvant chemotherapy. Radiotherapy can also be applied according to the medical evaluation.

➤ Stage IV CRC

Cancer has spread widely from the colon to distant organs and tissues such as lungs, brain, peritoneum or to distant lymph nodes. In most cases, surgery is not sufficient, and chemotherapy is the main treatment. Then, if the size of the tumors is reduced, the treatment consists of removing the section of the colon that contains the tumor along with the nearby lymph nodes.

1.9.1. Conventional chemotherapy and mechanism of action

The treatment of cancer using a chemical compound at a time or different compounds at one time combined with radiotherapy, surgery is

known as conventional chemotherapy. In general, chemotherapeutic drugs are (figure 8):

➤ **5-Fluorouracil (5-FU)**

The fluoropyrimidine 5-Fluorouracil (5-FU) is a member of the antimetabolite family of drugs. 5-FU is transformed through in the pyrimidine metabolism into active metabolites such as fluorodeoxyuridine monophosphate (FdUMP), fluorodeoxyuridine triphosphate (FdUTP), or fluorouridine triphosphate (FUTP). The main activities are the inhibition of thymidylate synthase and the misincorporation of active metabolites into DNA and RNA. Its effect is attributed to an increase in DNA damage, producing cell growth arrest and apoptosis. This drug is highly used in the treatment of cancer, however, research in recent years shows 5-FU has limitations in cancer resistance [40].

➤ **Capecitabine**

Capecitabine is a fluoropyrimidines (N-4 pentyloxycarbonyl 5-deoxy-5-fluorocytidine) which is metabolized to 5-FU through 3 metabolic steps. Capecitabine is first metabolized by the carboxylesterase of the liver to 5'-deoxy-5-fluorocytidine (5'-DFCR). 5'-DFCR is transformed by cytidine deaminase in the liver, plasma and tumor tissue to 5'-deoxy-5-fluorouridine (5'-DFUR). The last transformations render the active drug 5-FU by thymidine phosphorylase which interferes with the growth of the cancer cells as described above. Some research demonstrated Capecitabine showed the same effectiveness as 5-FU and fewer side effects as stomatitis, nausea, and alopecia [41].

➤ **Oxaliplatin**

Oxaliplatin is a third-generation platinum-based drug utilized as a chemotherapeutic agent in CRC. Oxaliplatin (trans-1-diaminocyclohexane oxalatoplatinum, L-OHP) is modified from first-generation platinum drugs. The amine groups of cisplatin (first-generation platinum drugs) are changed by diaminocyclohexane (DACH) ligand moieties [42]. Oxiplatin exerts its cytotoxic and apoptotic effect inducing DNA damage through interference with the N7

nitrogen on guanine in GC-rich DNA loci, forming DNA mono- and di-adducts [43].

➤ **Irinotecan**

Irinotecan or 7-ethyl-10-piperidino-piperidino-carboxyloxy derivative, is an analog of the alkaloid camptothecin which is transformed by carboxylesterases present in the liver to the active metabolite SN-38 [44]. Irinotecan has shown strong antitumor activity in wide preclinical models as well as clinically. SN-38 is a potent inhibitor of topoisomerase-I (topo-I). Topo-I plays a pivotal role in the process of DNA replication, transcription and recombination. SN-38 forms Topo I-SN-38-DNA complexes leading to the irreversible arrest of DNA replication, cell cycle arrest/delay via S-phase checkpoint stalling, and eventually apoptosis [45-47].

Limitations on chemotherapy reside in side effects that depend on the type of drug, the dosage, and length of treatment. Side effects sometimes are temporary, however, others are persistent. Most common are fatigue, memory problems and other mental deficits, nausea and vomiting, diarrhea, loss of appetite, hair loss, swelling and rashes, mouth sores, numbness, tingling, and cold intolerance. Another remarkable side effect is damage in blood-producing cells of the bone marrow, increasing the risk of infection and bleeding [48].

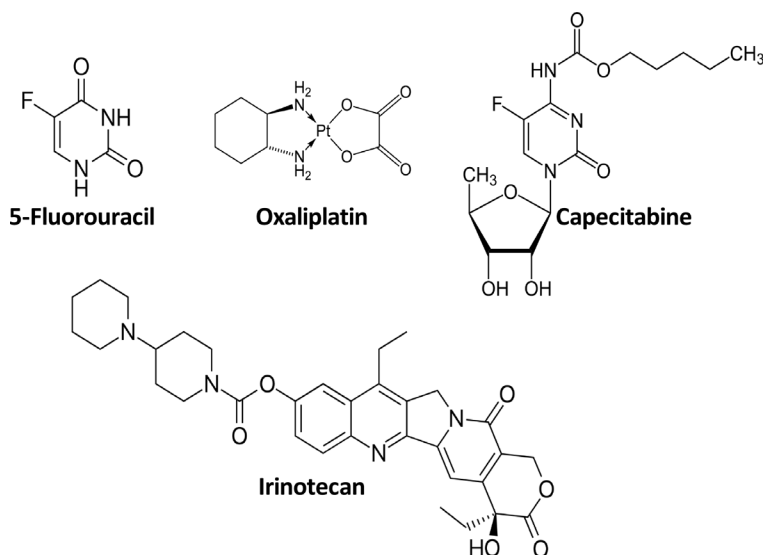


Figure 8. Chemical structures of CRC drugs.

1.9.2. Targeted chemotherapy and mechanism of action

Targeted therapy is increasing the attention in the treatment of cancer. This newer area focuses on understanding the molecular pathways involved in anticancer chemotherapy and targeting specific molecules that controls tumor progression. Targeted therapy often produces less severe side effects than conventional chemotherapy treatments and is used at the same time of chemotherapy or alone if traditional chemotherapy is no working [49]. Targeted chemotherapy for CRC has focused on angiogenesis through the vascular endothelial growth factor (VEGF) with bevacizumab, aflibercept, ramucirumab, and regorafenib, and modulating the epidermal growth factor receptor (EGFR) treated with cetuximab and panitumumab [50]. Angiogenesis is the process to form new vessels and connecting with the pre-existing blood vessels and plays a key role in CRC progression, invasion and metastasis to other organs. VEGF is the main regulator of the angiogenesis process. Targeting VEGF with anti-angiogenic agents has become a key strategy in cancer treatment [51]. EGFR is a transmembrane glycoprotein belonging to the epidermal growth factor receptor (HER)-erbB family of tyrosine kinase receptors. EGFR is an upstream activator of RAS/RAF/MAPK, STAT, and PI3K/AKT pathway related to cell proliferation, adhesion, angiogenesis, migration, and metastasis [52-55]. Thus, agents able to targeting VEGF/VEGFR contributed generally to improve the survival rate of patients in recent years [56].

REPROGRAMMING METABOLISM IN CANCER

In the 1920s, Otto Warburg reported the cancer anomaly metabolic stage and described the high rates of glucose uptake and lactate release in tumor conditions compared with normal tissues where oxygen was present [57]. Traditionally, it was thought that reprogramming of cancer metabolism was originated as part of a conserved evolutionary process derived from oncogenic changes and loss of functionality of tumor suppressors [58]. Over time, scientific community is assuming increasingly the metabolism and signaling pathway metabolic-derived as main responsible for the cellular identity in oncogenic process [59] and therefore, the existence of metabolites that promote oncogenesis (oncometabolites) which induce carcinogenesis [60]. Reprogrammed metabolic pathways in cancer cells keep the anabolic processes that support enhanced growth, proliferation, migration, and invasiveness, coined as *metabostemnes* by Mendez J.A and Alarcon T. [61].

Numerous oncogenes are involved in the metabolic switch such as Activated Protein Kinase (AMPK) [62], Hypoxia-Inducible Factor 1 α (HIF-1 α) [63], Myc [64], PI3K/Akt/mTOR [65] and rat sarcoma viral oncogene homolog (RAS) [66]. For example, It has been detected a pattern in glucose demand, a decrease in the oxidative phosphorylation complemented by an aerobic glycolysis and lactate production, fatty acid and protein biosynthesis [67] related to genetic alterations in the PI3K/AKT/mTOR/HIF pathway and the p53 tumor suppressor system.

Thus, altered metabolism can offer a distinctive mark to guide the development of anticancer precision drugs [68].

1.10. The PI3K/Akt/mTOR pathway

One of the most frequently hyperactivated metabolic pathways in human cancer is the PI3K/Akt/mTOR due to its contribution to different aspects of cellular function including nutrient uptake, anabolic reactions, cell growth and survival (**figure 9**) [69].

The phosphoinositide 3-kinases (PI3Ks) are a family of enzymes, which phosphorylates the 3'-hydroxyl group of the inositol ring of Phosphatidylinositides (PtdIns). The PI3Ks are classified in Class I, II, III and IV based on primary structure, regulation pathway, and *in vitro* lipid substrate specificity [70]. The most studied is class I PI3K which catalyzes the conversion of membrane-bound phosphatidylinositol-(4,5)-bisphosphate (PI(4,5)P₂) into phosphatidylinositol (3,4,5)-trisphosphate(PI(3,4,5)P₃) (also known as PIP3) *in vivo* [71]. PIP3 acts as a secondary messenger, binding to the Pleckstrin Homology (PH) domain of various signaling proteins, such as PI3K-dependent kinase-1 (PDK1) and the serine/threonine kinase AKT (in T308 residue) that derive ultimately cell proliferation, growth, survival, and resistance to apoptosis. Akt activation lead to the phosphorylation of tuberous sclerosis 2 (TSC2) and inhibits the rheb GTPase activity of the TSC1/TSC2 dimer [72]. Activated rheb stimulates the mammalian target of rapamycin (mTOR) which present two cellular complexes (mTORC1 and mTORC2). The mTORC1 complex is extremely sensitive to rapamycin. mTORC1 activates p70S06 kinase activity leading to the increase in protein synthesis and cell growth [73]. The mTORC2 complex is less sensitive to rapamycin and its related to the regulation of the actin in the cytoskeleton and controls diverse cellular processes involved in metabolisms, such as survival, apoptosis, and growth, through the phosphorylation of various effectors (**figure 9**) [74].

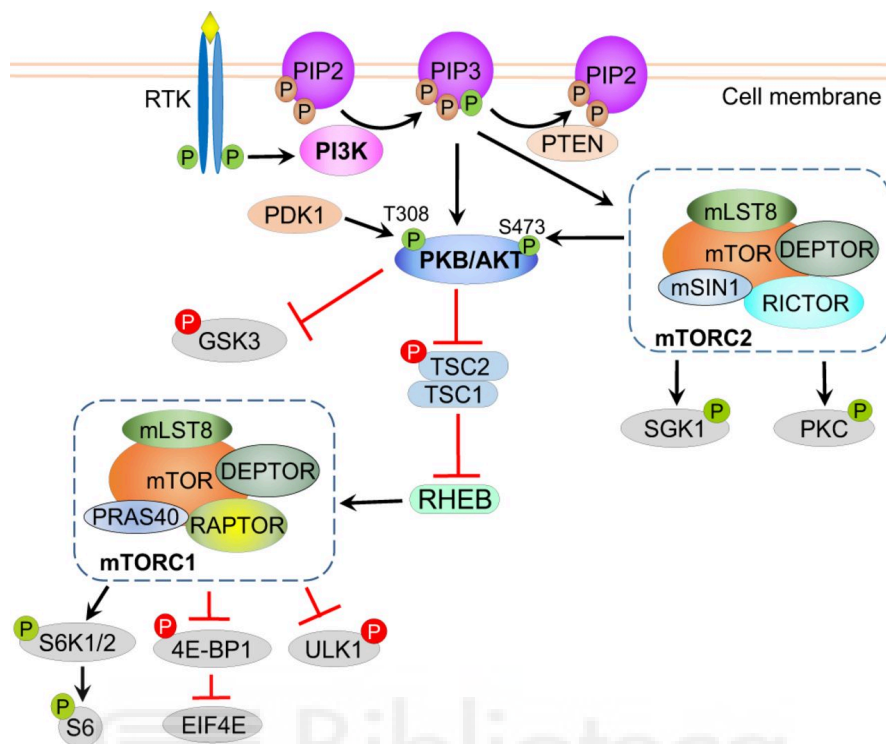


Figure 9. The PI3K/Akt/mTOR pathway and its main downstream effectors (from Yu J.S. et al. 2016 [75])

1.11. Endoplasmic Reticulum Stress

The largest organelle in the cell is the Endoplasmic reticulum (ER) which is composed of multiple different structural domains, each of which is associated with a specific function. ER size depends on the type of cell and activity and is divided into different parts (subdomains) such as tubule network and a series of flattened sacs that give rise to the smooth endoplasmic reticulum (SER) and the Rough Endoplasmic Reticulum (RER) with attached ribosomes to the external side. The space enclosed by the endoplasmic reticulum membrane, network, vesicles, and flattened sacs is known as lumen [76] (**figure 10**).

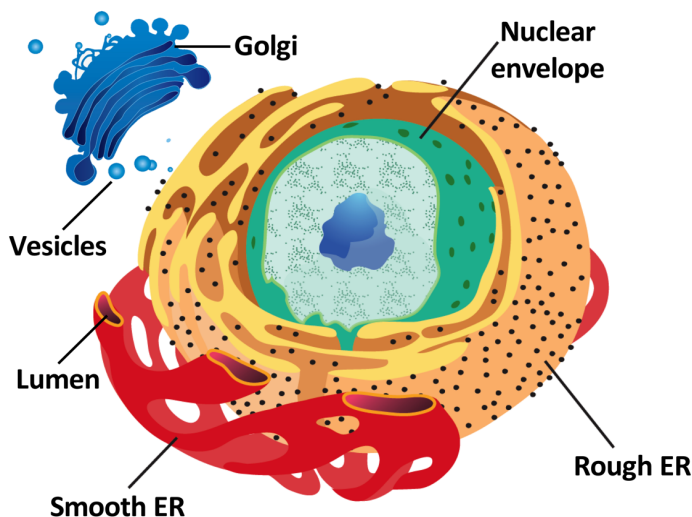


Figure 10. Endoplasmic reticulum (source from [77]).

The SER presents a wide range of functions including lipids, phospholipids and steroids synthesis or carrying out the metabolism of carbohydrates. It is also the place for transitional area of vesicles (with lipids and proteins) to be transported to the Golgi apparatus. Depending on the type of the cell, SER presents different functions. For example in muscles, SER assists in the contraction of muscle cells and in brain, contributes to hormones synthesis [78].

The RER plays the central role of protein synthesis and is studded with ribosomes. The translation is the process in which a new protein is assembled from an mRNA sequence that serves as a template. In the process of protein synthesis, at the signal sequence of its amino-terminal end, a signal recognition particle will be attached to the ribosome of the RER membrane and then dissociated. The new protein will be embedded in the RER membrane whether it is a transmembrane protein or transmitted to the lumen whether it is a water-soluble protein, via translocon channel. In the lumen, proteins are modified in their signal sequences or acquire their three-dimensional conformation.

Perturbations in the ER environment such as biochemical, physiological and pathologic causes like nutrient deprivation, oxidative stress, DNA damage,

and energy disturbance causes a malfunction of the ER which result in the accumulation of unfolded or misfolded proteins in the ER. This situation is known as **ER stress** and triggers the Unfolded Protein Response (UPR) which tries primarily to restore the ER organelle homeostasis in a pro-survival process [79]. However, when stress is sustained and/or prolonged, UPR activates cell death [80].

The UPR is based on three ER-transmembrane stress sensors (ER stress sensors): Inositol Requiring Enzyme 1 (IRE1), protein kinase RNA-activated (PKR)-like ER kinase (PERK) and Activating Transcription Factor 6 (ATF6). Under physiological conditions, ER stress sensors are inhibited by the binding of their luminal domains with the ER-resident chaperone called heat shock protein family A (Hsp70) member 5, also known as glucose-regulated protein 78 (GRP78) or BIP. BIP is in charge of controlling the flow between unfolded proteins to be folded. When there is a massive accumulation of unfolded or misfolded proteins, BIP determines an impaired equilibrium, leading the dissociation from ER stress sensors and activating the UPR [81] (**figure 11**).

➤ **PERK**

Is a ubiquitously transmembrane protein kinase type I with a cytosolic serine/threonine kinase domain. BIP detachment from the PERK leads to its oligomerization and trans-autophosphorylation. PERK activates eukaryotic initiation translation factor 2 α (eIF2 α) by phosphorylation which inhibits the protein synthesis reducing the protein load on the ER folding machinery and upregulate the Activating Transcription Factor 4 (ATF4). On the one hand, ATF4 promotes the expression of antioxidant response, amino acid biosynthesis and transport genes to keep cell survival. On the other hand, ATF4 can induce the expression of C/EBP Homologous Protein (CHOP) to mediate ER stress-induced apoptosis. According this, PERK has the duality of being involved in both survival and cell death [82].

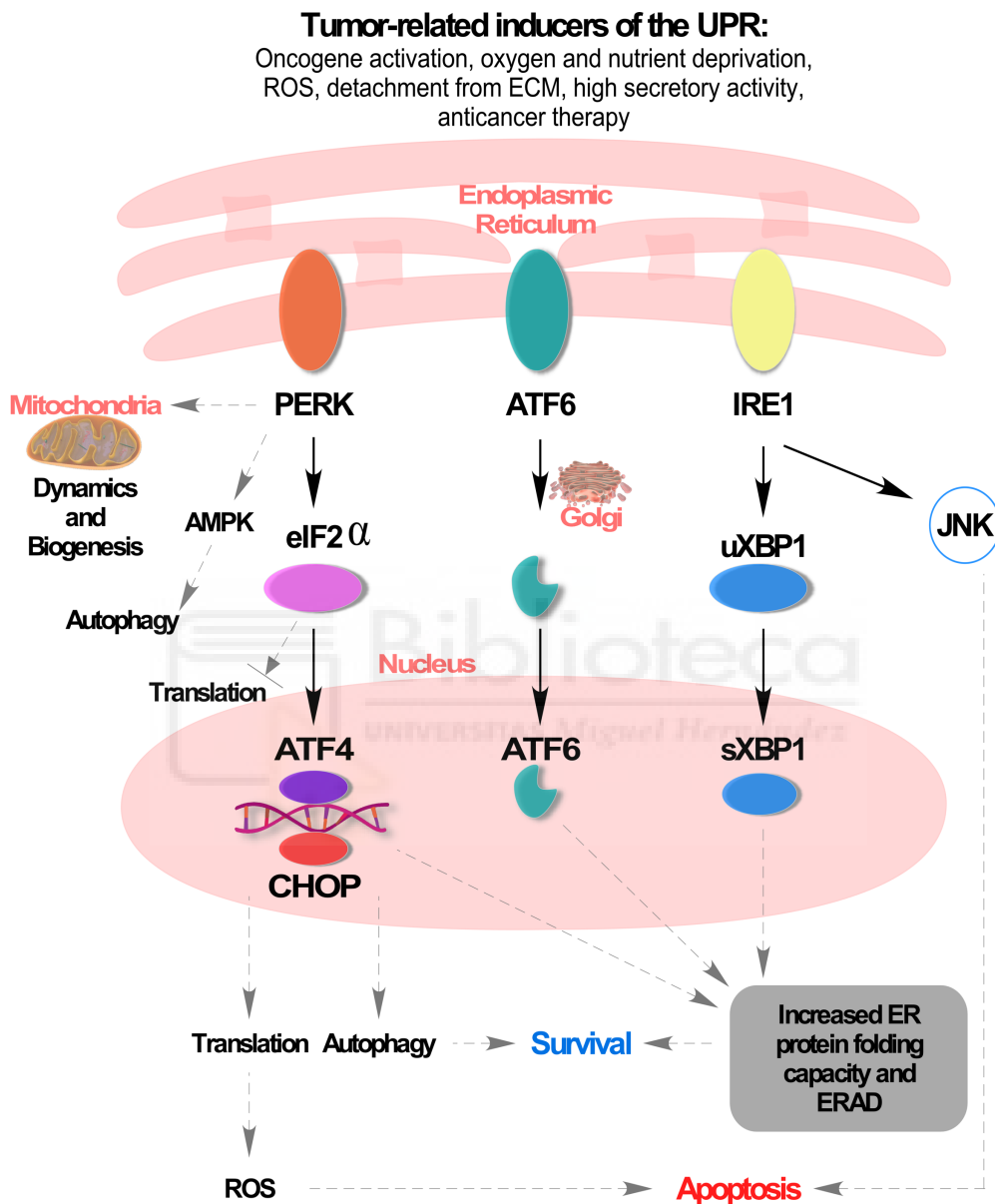


Figure 11. ER stress and UPR (adapted from Novoa, I., et al. [83])

➤ **ATF6**

The Activating Transcription Factor 6 (ATF6) is a type II transmembrane protein that belongs to an extensive family of leucine zipper proteins. BIP dissociation leads ATF6 to translocate to the Golgi apparatus where is cleaved by the two Golgi-resident proteases S1P and S2P, producing two cytosolic active transcription factors (ATF6 α and ATF6 β). Meanwhile, ATF6 α regulates the expression of ER genes and XBP1, ATF6 β is a very poor activator of UPR genes [84].

In cancer cells with uncontrolled proliferation and altered metabolism many of the factors that disturb homeostasis are present. Therefore, it is not surprising that ER stress is highly induced during tumor growth and progression. Thus, UPR components are deregulated in different tumor types making the adjacent environment hospitable for tumor development [85].

➤ **IRE1 α**

This ER stress sensor is a type I ubiquitously transmembrane with a cytosolic serine/threonine kinase domain. Its activation by BIP dissociation, induce IRE1 α oligomerization enabling trans-autophosphorylation and leads to an endoribonuclease activity, which splices X-box-binding protein (XBP1) mRNA (spliced mRNA called XBP1s is the active form). XBP1s can penetrate the nucleus and regulate the expression of genes implicated in protein folding, trafficking, and ER-associated Protein Degradation (ERAD) process. Another function of XBP1s is to promote cell survival inhibiting CHOP expression.

IRE1 α can induce cell death apoptosis binding to TNF Receptor-Associated Factor 2 (TRAF2) regulating JUN N-Terminal Kinase (JNK), which activates pro-apoptotic BIM and inhibits anti-apoptotic BCL-2 proteins [86].

1.12. Oxidative Stress

To survive and growth, cells need energy which is obtained from nutrients. Aerobic respiration or cell respiration is characteristic of eukaryotic cells in the presence of oxygen. This event involves catabolic reactions consisted of breaking large molecules (through the breaking of chemical bonds) into

smaller ones obtaining energy stored as Adenosine Triphosphate (ATP), which is used to drive steps requiring energy such as synthesis of biomolecules, locomotion or transport of molecules.

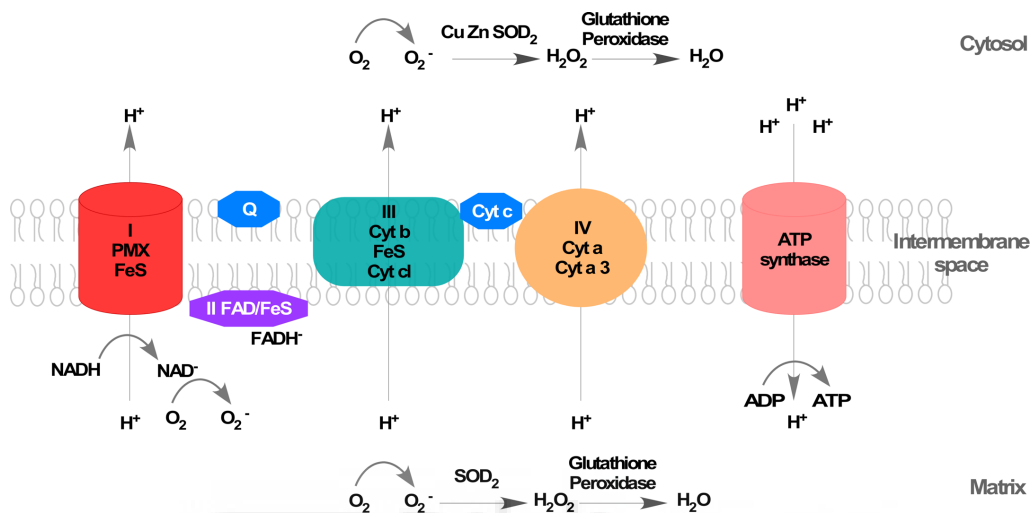


Figure 12. ROS and respiration chain in the mitochondria (adapted from Kumari, S., et al. [87])

Aerobic respiration takes place in the mitochondria of eukaryotic cells and uses oxygen as a reactant to break chemical bonds, known as respiratory chain or Electron Transport Chain (ETC, **figure 12**) [88]. This process is carried out through a series of complexes that lead to the transference of electrons from electron donors to electron acceptors in a redox reaction that drives the synthesis of ATP. Reactive Oxygen Species (ROS) are a byproduct from ETC and include the superoxide anion (O_2^-), hydrogen peroxide (H_2O_2), hydroxyl radicals ($OH\cdot$), singlet oxygen (1O_2), and ozone (O_3) which present different reactivities to different biological targets [89]. There are others reactive molecules originated from other elements such as nitrogen (reactive nitrogen species or RNS), sulfur (reactive sulfur species, RSS) and chloride (reactive chloride species, RCS) [90]. ROS in physiological conditions (low than 5%) are necessary for certain cellular events such as enzyme activation, gene

expression, the formation of disulfide bonds in protein synthesis or the caspase activity during the apoptosis cell death. However, high concentrations could induce pathology inducing damage in DNA, lipids and proteins [91] (**figure 13**). ROS are the most abundant species from oxidative metabolism. They can be induced internally by peroxisomes and enzymes such as detoxifying enzymes P_{450} , xanthine oxidase and the Nicotinamide Adenine Dinucleotide (NADPH) oxidase and NOX family and external factors like UV radiation, pollutants, smoking, alcohol, exercise or obesity. ROS induce DNA damage producing nicks in DNA, malfunctions in DNA repair system and DNA oxidation which generates 8-hydroxy-2'-deoxyguanosine, a mutagenic compound which enhances aging and carcinogenesis [92]. Also, lipids (such as polyunsaturated lipids in the cell membrane) are damaged through the oxidation process increasing permeability of the cell membrane [93]. Finally, proteins are altered by the formation of carbonyl and thiol groups that are converted into sulfur reactive radicals and leading to the loss of protein function [94].

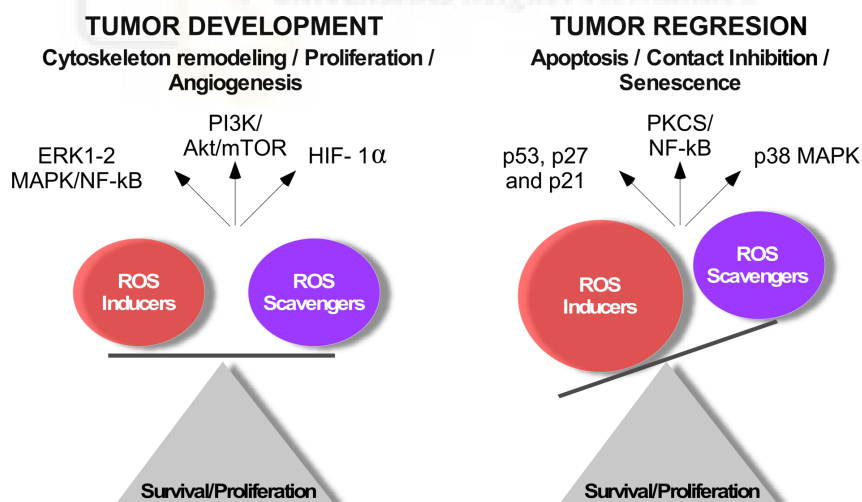


Figure 13. The double-faced role of reactive oxygen species (ROS) in cancer (adapted from Assi, M., et al. [95]). High balanced ROS level is determinant for abnormal cancer cell metabolism to ensure tumor development through altered pathways, while an excessive unbalance of ROS induce tumor regression, senescence and apoptosis.

As indicated above, a physiological level of ROS contributes to normal cellular maintenance, however, an increased oxidative state can trigger harmful processes. The increase in ROS is a direct consequence of the imbalance between pro-oxidant/anti-oxidant equilibrium. The endogenous antioxidant system is classified into enzymatic and non-enzymatic. The enzymatic scavengers are formed by the Superoxide Dismutase (SOD), Catalase (CAT), Glutathione Peroxidases (GPX), Thioredoxins (TRXs), Peroxiredoxins (PRXs) and Glutathione Transferase (GST). The non-enzymatic scavengers are vitamin A, C and E, carotene. Exogenous antioxidants are usually natural antioxidant compounds obtained from the diet (ascorbic acid or Vitamin C), tocopherol (Vitamin E), β -carotene (Vitamin A), lipoic acid, uric acid, glutathione and polyphenol metabolites and synthetic antioxidants (N-acetyl cysteine (NAC), tiron, pyruvate, selenium, butylated hydroxytoluene, butylated hydroxyanisole, and propyl gallate) [96, 97].

1.12.1. ROS in cancer survival

Already in the 90s, it was postulated that high amount of ROS was a driving factor for tumorigenesis because they induce cellular proliferation, evasion of programmed cell death, promote invasion and metastasis and angiogenesis [98]. The reason why ROS drives altered tumorigenic pathways is that cells (in a high ROS context) have acquired mechanisms to counteract the toxicity of elevated ROS.

Oxidative stress is involved in the promotion of pro-tumorigenic signaling. One of the effects of ROS is its ability to drive mitogenic signaling cascades. It is documented that ROS inhibits the tumor suppressor Phosphatase and Tensin homolog (PTEN), protein tyrosine phosphatase (PTP) and MAPK phosphatases leading growth factor activations, which induce sustained H₂O₂-dependent hyper-activation of the growth and survival PI3K/AKT/mTOR and MAPK/ERK signaling cascades [99].

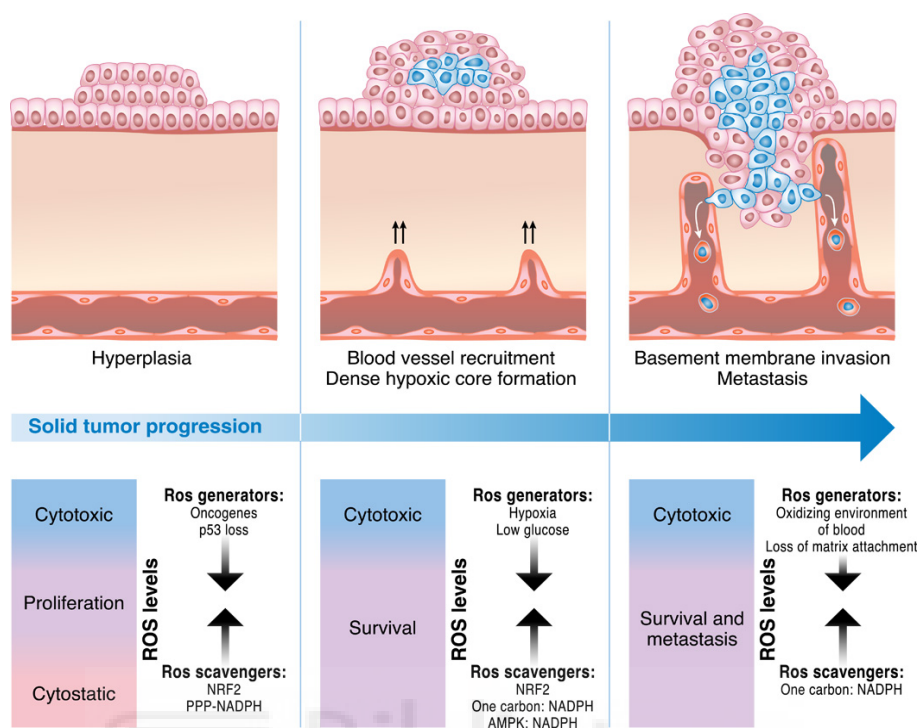


Figure 14. Solid tumor progression and ROS influence (DeBerardinis, R.J. and N.S. [100])

Accumulating evidence indicates that the intracellular ROS also promotes cell migration and invasion [101]. Epithelial cell acquires the condition of a mesenchymal cell phenotype through the Epithelial-Mesenchymal Transition (EMT). EMT in physiological conditions is an important process that modulates morphogenesis, embryonic development, and stem cell differentiation, induction of pluripotency, tissue repair, wound healing and stem cell behavior [102, 103]. In this dynamic process interplay extracellular signals and soluble factors such as Transforming Growth Factor- β (TGF- β), Epidermal Growth Factor (EGF), Fibroblast Growth Factor (FGF and different isoforms of Wnt proteins (proteins which transduce signals from cell surface receptors into the cell) or Matrix Metalloproteinases (MMP) and Nuclear Factors (NF- κ B). However, EMT is altered in a pathological condition such as fibrosis, cancer stem cells and progression [104] and ROS are involved directly in EMT disruption. Modified EMT by ROS promotes the alteration of

cell-cell adhesion in epithelial cells facilitating metastasis [105]. TGF- β 1 (one of the inducers of EMT) induce urokinase-type Plasminogen Activator (uPA) and MMP9 to facilitate cell migration and invasion via the activation of NF- κ B through the Rac1-NOXs-ROS-dependent mechanism [106]. Another effect of ROS is the increase of integrins (transmembrane receptors that facilitate cell-Extracellular Matrix (ECM) adhesion) and accelerate EMT [107] (**figure 14**).

Angiogenesis covers all the processes that promote new blood vessels to connect preexisting vasculature and is essential for many physiological processes, such as embryogenesis, tissue and organ regeneration and skeletal remodeling [108]. Oxidative stress drives vasculature and angiogenesis, whereas low levels of ROS promotes regeneration and growth, high or chronically ROS drives new vessels in tumor conditions [109]. The vascular endothelial growth factor (VEGF) is the main specific angiogenic growth factor, which control angiogenesis. VEGF, induced by ROS, stimulates VEGF receptor 2 (Flk/KDR) through a tyrosine phosphorylation that results in a downstream activation of ERK1/2, Akt and eNOS, which contributes to endothelial cell angiogenic process [110].

In addition to modifying key metabolic pathways that guarantee tumor development, tumor cells can modify the surrounding microenvironment and creating the conditions that ensure their development. A common feature in tumors is creating an oxygen-poor environment (hypoxia) due to a dramatic surge of oxygen demand [108]. It has been seen that tumor cells in a hypoxic environment are more resistant to apoptotic processes, becoming more invasive [111]. The capability of oxidative stress to promote angiogenesis is due to its associated hypoxia and the directly affected Hypoxia Inducible Factor (HIF). HIF-1 heterodimer is formed by subunits α and β . The subunit β is constitutively expressed in cells, whereas α is undetectable in normoxia and is induced fastly by different pathways involved when hypoxia conditions happens [112]. HIF1- α seems to regulate genes implicated in activating VEGF and Platelet-Derived Growth Factor (PDGF) increasing angiogenesis and it was correlated with poor clinical prognosis in many cancers [113, 114].

TUMOR INVASION AND METASTASIS

One of the most remarkable hallmarks of cancer is its ability to activate invasion and metastasis. Metastasis is the development of secondary malignant growths at a distance from a primary site of cancer. Primary tumors are generally removed with surgical techniques and adjuvant treatments and represent 10% of cancer-related mortalities. The remaining 90% of deaths is attributed directly to secondary tumors that present a greater resistance to existing therapies [115].

1.13. The invasion-metastasis cascade

The metastatic process can be divided in different steps [116, 117] (**figure 16**), listed below:

- 1) Primary tumor growth,
- 2) Blood vessel growth (angiogenesis),
- 3) Dissemination of cells from the primary tumor. Tumor cells that have acquired the ability to initiate the invasion-metastasis cascade.
- 4) Migration to the surrounding ECM and stromal layers and intravasation,
- 5) Evade cell detachment induced apoptosis (anoikis),
- 6) Transendothelial migration into blood or lymphatic vessels (intravasation) and arrest in new organ,
- 7) Extravasation the vessel,
- 8) Colonize the parenchyma of new tissues to form micrometastases and reinitiate their proliferative programs to develop new secondary tumors.

For this feature, tumor cells have to lose their epithelial cell-cell contacts, acquire migratory and invasive abilities, change the cytoskeletal reorganization, be able to form new cell-matrix adhesions and pursue a chemoattractant gradient through the ECM [118]. This process can be

modulated by molecular signaling pathways orchestrated by genetic and epigenetic alterations and tumor microenvironment modifications in which the EMT plays an essential role for most cancer types [119].

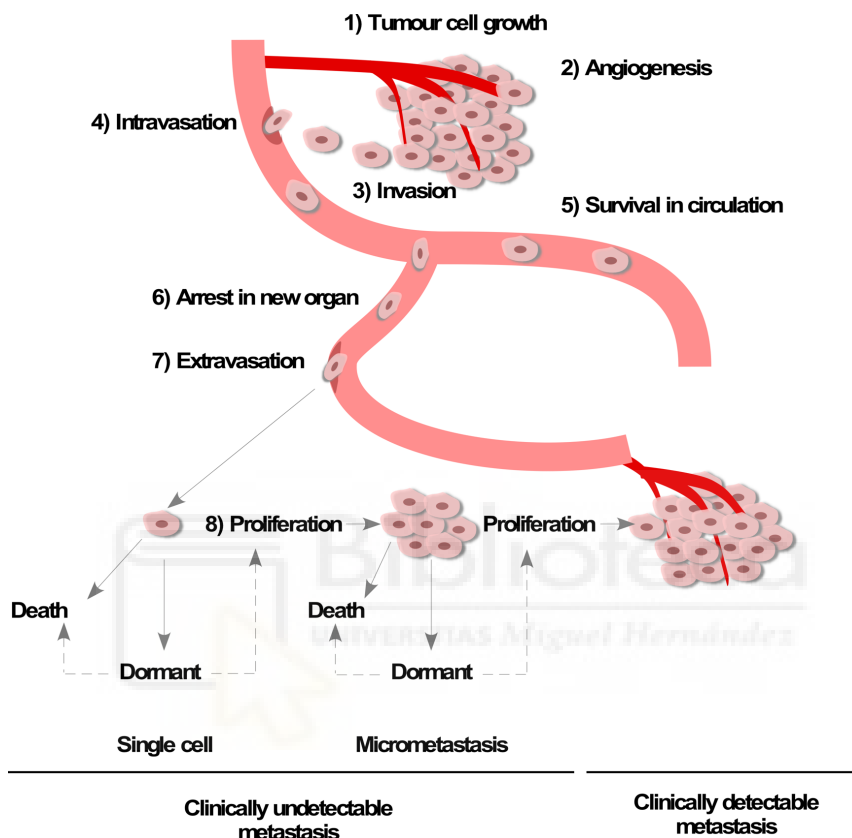


Figure 15. Metastasis as a multi-step process (adapted from McGee, S.F., et al. [120]).

1.14. Tumor migration modalities

There are different types of invasion. Cancer cells can invade new tissues as a single cell via mesenchymal or amoeboid motility or by moving collectively as epithelial sheets or detached cluster. Plasticity of invading cells leads to another modalities of invasion such as the Epithelial to Mesenchymal Transition (EMT), Mesenchymal to Amoeboid Transition (MAT) and Collective to Amoeboid Transition (CAT) [121].

EMT is the process by which epithelial cells can convert into a mesenchymal phenotype, being able to lead to connective tissue and bone [122]. Some EMT-promoter factors have been identified including integrins, Hepatocyte Growth Factor (HGF), Fibroblast Growth Factor (FGF), Vascular Endothelial Growth Factor (VEGF) and Platelet Derived Growth Factor (PDGF) [123]. For an EMT to occur, a loss of the epithelial characteristic and a gain of the gene expression that regulates the mesenchymal character must take place at the molecular level. One of the markers affected would be the epithelial marker E-cadherin, characteristic of the adhesion junctions. E-cadherin is responsible of stabilizing the contact of cell-to-cell and is linked to α , β , and p120-catenin connecting with actin of the cytoskeleton [124]. The inhibition of E-cadherin leads to the disassembly of adherence junctions [125]. Another hallmark of EMT is the change in the expression from E-cadherin to N-cadherin which is called cadherin-switch and promotes motility of EMT-transformed cells [126]. The EMT opposite process (mesenchymal to epithelial transition (MET), which leads the reorganization and the gain of cell-to-cell junctions has been identified in the process of metastasis and colonization of new tissues [127].

An independent cancer cell that detaches from the primary tumor is considered as a single cell migration. It can occur under mesenchymal migration when cells have displayed loss of cell-to-cell adhesion and have acquired fibroblast-like morphology. This type of migration is dependent on the formation of integrin-mediated cell ECM adhesions and cytoskeletal contractility. Cells under mesenchymal migration have elongated their morphology and degrade ECM by proteases.

Another single cell migration is amoeboid [128, 129]. This type of single migration is integrin independent and cell-ECM adhesions are weak. Amoeboid migratory cells are highly deformable and move faster than in mesenchymal migration mode allowing them to squeeze through gaps in the ECM barrier without ECM proteolysis [130, 131].

CAT is referred to a collective amoeboid transition originated from the detachment of individual cells from a cluster [132]. CAT has been observed in melanoma and fibrosarcoma cells [132].

MAT refers to the transition of mesenchymal cells to amoeboid cells and depends on Rac and Rho/ROCK signaling involved in cell cytoskeleton organization, migration, transcription and proliferation [133]. MAT has been detected in fibrosarcoma, breast carcinoma and melanoma [134, 135]. In CRC the most frequent ways of migration are EMT dependent in a collective way [136-138].

1.15. Endothelial transmigration

As commented before, endothelial transmigration is the part of the migratory process when cells reach vessels to spread to fur tissues or organs. The blood system is considered the main via, however lymphatic system plays an important role in dissemination. Before transmigration, tumor cells have to cross vessel wall, known as extravasation and intravasation. When tumor cells reach the vessel capillary the first step is to adhere to endothelial cells and underlay the basement membrane [139]. Some of migrating tumor cells are able to pass the endothelial barrier and transmigrate to other sites, nevertheless it is possible that some tumor cells never extravasate [140]. Experimental models suggested metastasis as an inefficient process since they estimated about 80% of intravenously injected cancer cells survived and extravasate, whereas 90% die within 24 h when targeted the organ [141].

The endothelial cell function in the metastasis formation process is crucial because can allow or block the secondary tumor development. Another aspect to consider is the ability of migratory cells to surpass physical limitations of blood vessels and immune system. Some studies showed different strategies of cancer cells to avoid setbacks in the process such as the ability to activate platelets, which protect them in the blood vessel migratory step [142].

1.16. Migratory promoters

If cancer cells are actively migrating through blood and lymph vessels is still unknown. Some researchers believe in a passively creep into the vasculature without an active migratory program. On the contrary, other studies propose different factor (growth factors, oncogene activators, oxygen or nutrients supply, oxidative stress, anticancer therapy or microenvironmental changes) as activators of the metastatic process [143].

One of the major considered factors in tumor progression as a metastatic inductor is stress and adaptive stress response. Cells are exposed to different stresses such as genetic mutations, physiological and environmental changes and also therapeutic drugs.

Cells under stress conditions, try to restore homeostasis by modifying their stress tolerance and changing the surrounding microenvironment (**figure 16**). These modifications contribute to an increase in the heterogeneity of tumoral phenotypes and could favor the dominance of more aggressive and metastatic phenotypes on a set of cancer cells. Thus, high stress levels could induce apoptosis in some tumor cells meanwhile others with activated adaptative pathways could survive to hostile environment [144].

1.17. ROS/ERS effector in migration, invasion and metastasis

Cancer cells produce more ROS than normal cells. This hypothesis has been difficult to demonstrate by the fact that normal cells (control cells) show less metabolic activity than tumor and have important genetic differences. However, different studies support this hypothesis. The transformation of an immortalized cell line (T72 cells) to an oncogenic version, by transfection-mediated silencing of RAS, showed that the most aggressive cell line exhibited a higher level of ROS [145].

In the other hand, Endoplasmic Reticulum (ER) stress has been also associated with tumor development and poor prognosis in some cancers [146] and there is a direct cellular response to ROS. ER, mitochondria (the major source of ROS) and peroxisomes are the three important redox-sensitive organelles forming the redox triangle. ROS accumulation in this model affects the correct functioning of ER-mitochondria Ca^{2+} exchange, oxidative phosphorylation and oxidative protein folding in the ER [147]. Some evidences propose the redox homeostasis as a condition for proper function of ER [148]. The UPR, which is activated by ER, induce apoptotic and adaptive response in tumor cells.

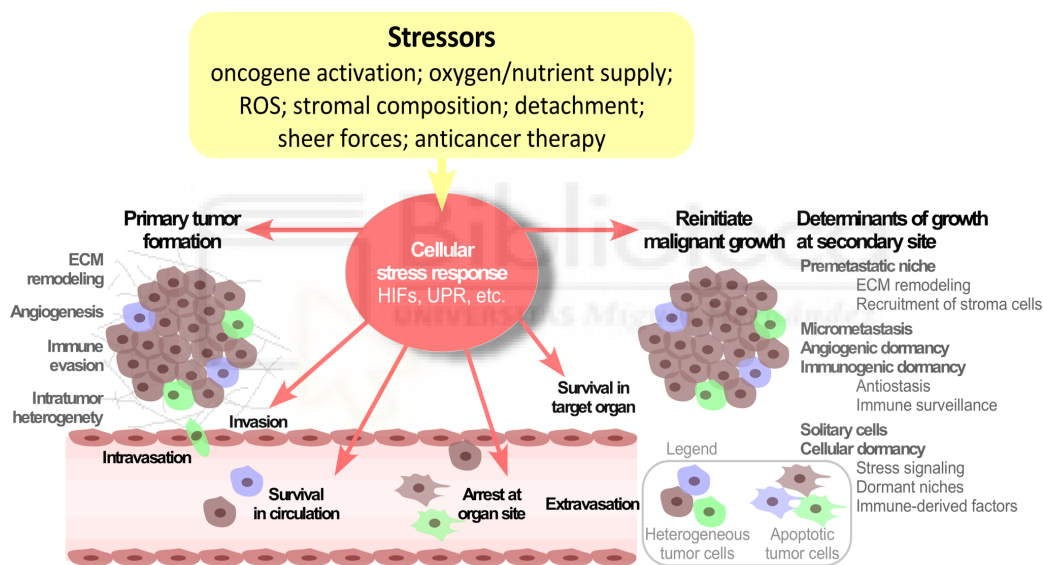


Figure 16. Stress signaling and the metastatic cascade (adapted from Senft, D. and Z.E.A. Ronai [144])

As mentioned before, ROS induce direct damage in biomolecules oxidizing DNA and compromising the DNA repair system, as well as generating mutagenic compounds, also oxidizing lipids and damaging carbonyls and thiols of protein when they are being synthesized [92-94]. These damaged proteins generate ER stress that leads to activation of the UPR as a

direct consequence. On the other hand, ROS stimulate metastasis processes through the activation of the PI3K/Akt/RAS/MAPK, modifying integrins synthesis and disrupting EMT [105, 106, 111]. Therefore, ROS and ER stress are closely related and both may activate signaling events leading metastatic processes involving migration, invasion and angiogenesis.



MARINE DRUG DISCOVERY

1.18. Marine ecosystem and potential

The term marine ecosystem refers to Earth's aquatic natural environment with high salt content including the non-living and living elements. Marine media is the largest in the Earth and covers more than 70% of the surface, being a 97% of Earth's water supply and a 90% of habitable space on Earth. The marine environment include coast, shore, nearshore (salt marshes, mudflats, seagrass meadows, mangroves, rocky intertidal systems and coral reefs) and offshore systems (epipelagic zone or surface ocean and deeper zones such as mesopelagic, bathypelagic, abyssopelagic, deep sea floor, hydrothermal vents and hadal zone) (**figure 17**) [149].

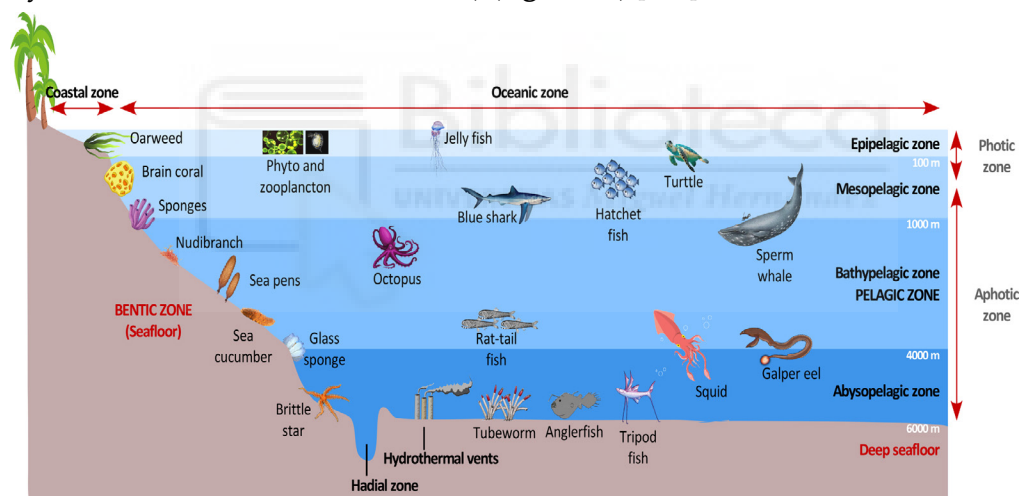


Figure 17. Ocean zones and marine ecosystem (adapted from Pendahuluan [150])

The marine environment is a very varied ecosystem in which marine organisms must survive to adverse conditions (e.g. high pressure, low light, salinity, competence). As a result of evolution, marine life constitutes one of the major domains of life represented by 36 phyla. Diverse marine life has become to adapt to different harsh conditions and develop complex system to avoid

rivalry for resources. The competition among species is one of the determining factors in the structuring of many communities [151]. For instance, sessile organisms such as coral reefs compete for space and light with neighboring colonies. Sometimes these organisms have the ability to grow fast and occupy the maximum possible area, however, others cannot compete with rapid growth and have developed other strategies such as the production of compounds that kill or inhibit (by direct or indirect contact) the growth of its opponents [152, 153]. These bioactive compounds are known as allelochemical or secondary metabolites because they are not needed for basic (primary) metabolism and this strategy is called allelopathy [154].

The use of secondary metabolites, traditionally from terrestrial plants and microbes, have been described throughout history in the form of traditional treatments by humans. These Natural Products (NP) have led to an improvement of human quality of life (e.g. penicillin, streptomycin, morphine) and constitute a potential source for biomedical research [155] being considered as much as 60% of total pharmaceutical drugs [156].

1.19. Marine Natural Products (MNPs) classification

Marine Natural Products (MNPs) provide a rich source of nutraceuticals and potential candidates for the treatment of several human diseases [157]. MNP are produced by two main biosynthetic routes: i) pyruvic and acetic acid and ii) shikimic acid (**figure 18**) and are generally classified as alkaloids, polyketides, terpenes, peptides and carbohydrates.

The main MNPs classes are as follows:

➤ **Alkaloids**

This class of compounds are referred to amino acids derived compounds with a broad spectrum of solubility. Alkaloid are classified as pyridoacrine alkaloids, indole alkaloid, pyrrole alkaloids, isoquinoline alkaloids, guanine alkaloids, aminoimidazole alkaloids, and sterol alkaloids [159] and have been isolated from sponges, tunicates, anemones and mollusks and have shown a wide range of bioactivities [160-162].

➤ **Polyketides**

Polyketides are a large group of secondary metabolites synthesized by the decarboxylative condensation of malonyl-CoA and other acyl-CoAs and more than one monomer type may be used to construct different sized aromatic groups or reduced chain. To polyketide class are included macrolides, polyethers, polyols and aromatic compounds. These class of compounds have been isolated from sponges, ascidians, soft corals, bryozoans [163] although it is thought that its main producers are bacteria or symbiotic fungi.

➤ **Terpenes**

Terpenes are derived from isopentenyl pyrophosphate units producing a five-carbon isoprene structure and are classified based on the number of units as monoterpenes, sesquiterpenes, diterpenes, sesterterpenes, triterpenes (steroids), and tetraterpenes (carotenoids) [164]. Some of the marine terpene producers are actinomycetes, soft coral, mollusk, and sponges [165].

➤ **Peptides**

Peptides consist of amino acid monomers (2 to 20) linked by peptide or amine bonds. Sixty percent of MNPs described belongs to peptide family and are identified most often in sponges and nudibranchs but also in mollusk, algae and tunicates. As polyketides, peptides are associated to be produced by commensal or symbiotic bacteria or fungi [166].

➤ **Carbohydrates and derivatives**

Carbohydrates are molecules formed by carbon, hydrogen, and oxygen usually with a hydrogen–oxygen atom ratio of 2:1 (as in water) and with the

empirical formula $C_m(H_2O)_n$. The most common carbohydrates isolated from marine organisms are polysaccharides (polymers of monosaccharides or sugars bonded with glycosidic residues and exhibiting a wide structural diversity). Another common group of carbohydrate is glycosides, consisted in two parts, the sugar aglycone group bounded to a functional group (terpene, flavonoid, coumarine or other group) through a glycosidic bond.

Glycosaminoglycans are a kind of linear and complex carbohydrate presented on animal cell surfaces. Marine carbohydrates have been isolated principally from sponges, algae, bacteria, and fungi [167].

1.20. MNPs biological activity

The most common uses of MNPs are in therapeutics providing useful antibacterial, anti-inflammatory, neuroprotective, antiparasitic, antiviral, analgesic, antimicrobial, antimalarial and anticancer agents [168]. One of the most interesting and demanded activity for MNPs is as anticancer effect. Current chemotherapy combines one or more cytotoxic antineoplastic drugs in a standardized regimen and the efficacy depend on the stage and type of cancer. However, chemotherapy effectiveness is restricted due to the recurrence of drug resistance (intrinsic or acquired) [169]. Furthermore, cancer as a multifactorial and multi-targeting disease that cannot be prevented by mono-targeted therapies and makes it necessary to search for more effective treatments. Given that marine compounds present novel chemical structures, they are considered as potential producers of marine anticancer agents. In recent years the number of drugs coming from marine origin or synthesized from them have increased considerable [170]. By the end of 2017, seven marine-derived compounds have been approved by the FDA organization for clinical use being 4 for cancer treatment [171] (**table 2**) and other marine-derived compounds were undergoing clinical trials (**table 3** and **4**).

Table 2. List of approved marine anticancer drugs from an invertebrate source (from [172]).

Compound Name	Organization and Year	Organism	Chemical Class	Disease Area	Mode of Action	Company	Refs
Cytarabine (Cytosar-U®)	FDA 1969	Sponge	Nucleoside	Anticancer	DNA polymerase inhibitor	Bedford, Enzon	[37]
Trabectedin (Yondelis®)	EMA 2007	Tunicate	Alkaloid	Anticancer	Inhibits cancer cell growth and affects the tumor microenvironment	PharmaMar	[39]
Eribulin mesylate (Havalen®)	FDA 2010	Sponge	Macrolide	Anti-breast cancer	Microtubule interfering agent	Eisai Inc.	[40]
Brentuximab vedotin (Adcetris®)	FDA 2011	Mollusk	Antibody-drug conjugate	Lymphoma	CD30-directed antibody-cytotoxic drug conjugate	Seattle Genetics Inc.	[41]

Table 3. List of marine drugs in clinical trials (phases III and II) (from [172]).

Clinical Status	Compound Name	Marine Organism	Chemical Class	Disease Area	Mode of Action	Company	Ref
Phase III	Plitidepsin	Tunicate	Depsipetide	Anti-cancer	Induces cell cycle arrest or apoptosis	PharmaMar	[76]
	Gemcitabine (GEM) (Gemzar)	Sponge	Nucleoside	Anti-cancer	Ribonucleotide reductase inhibitor Replaces cytidine during DNA replication	Eli Lilly and Company	[77]
	Glembatumumab vedotin	Mollusk	Antibody drug conjugate	Breast cancer and melanoma	Targets glycoprotein NMB (a protein overexpressed by multiple tumor types)	Celldex Therapeutics	[78]
Phase II	Elisidepsin	Mollusk	Depsipetide	Anti-cancer	Antineoplastic agent, modifying lipids from cell membrane	PharmaMar	[79]
	PM1004	Nudibranch	Alkaloid	Anti-cancer	DNA-binding	PharmaMar	[80]
	Pseudopterosins	Soft coral	Diterpen glycoside	Wound healing	Eicosanoid metabolism	The Regents Of The University Of California	[81]
	IPL576.092 (Contignasterol derivative)	Sponge	Miscellaneous	Anti-inflammatory	Inhibition of leucocyte infiltration and hypersensitivity during allergy	Aventis Pharma	[82]

Table 4. List of marine drugs in clinical trials (phases II-1 and D) (from [172]).

Clinical Status	Compound Name	Marine Organism	Chemical Class	Disease Area	Mode of Action	Company	Ref
Phase I/II	PM-10450 (Zalypsis®)	Sponge	Alkaloid	Anti-cancer drug	Transcription inhibitor	PharmaMar	[83]
	Discodermolide	Sponge	Polyketide	Anti-cancer drug	Microtubule interfering agent	Novartis	[84]
	Bryostatins-1	Bryozoa	Polyketide	Anti-cancer drug	Protein kinase C	National Cancer Institute	[85]
	Pinatuzumab vedotin	Mollusk	Antibody drug conjugate	Non-Hodgkin lymphoma, leukemia	Apoptosis stimulant; Mitosis inhibitor and Tubulin inhibitor	Genentech, Inc.	[86]
	Tisotumab Vedotin (HuMax®-TF-ADC)	Mollusk	Antibody drug conjugate	Ovarian, endometrium, cervix and prostate cancer	Antineoplastic, Drug conjugate, Immunotoxin and monoclonal antibodies	Genmab and Seattle Genetics	[87]
Phase I	HT1286 (Hemiasterlin derivative)	Sponge	Tripeptide	Anti-cancer drug	Microtubule interfering agent	Wyeth	[84]
	LAF389 (Bengamide B derivative)	Sponge	Peptide	Anti-cancer drug	Methionine aminopeptidase inhibitor	Novartis	[84]
	Hemiasterlin (E7974)	Sponge	Tripeptide	Anti-cancer drug	Microtubule interfering agent	Eisai Inc.	[84]
	PM-060184	Sponge	Polyketide	Anti-cancer drug	Microtubule interfering agent	PharmaMar	[88]
	NVP-LAQ824 (Psammnaplin derivative, Dacinostat)	Sponge	Miscellaneous	Anti-cancer drug	Histone deacetylase (HDAC) inhibitors or DNA methyltransferases (DNMT) inhibitor	Novartis Pharma	[89]

1.21. MNPs producers

Marine ecosystem provide higher diversity of living organism in comparison to terrestrial one [173]. The rate of registered marine species is 2000/year and it is expected to increase considerable this number with new technologies (e.g. scuba diving prospection, new analytical technologies and high-throughput screening methods) [174, 175].

Within the marine animal kingdom, the phyla invertebrate is the major group showing high richness in diversity and distribution. Invertebrates are characterized for lacking backbone and some of them have hard outer coverings that provide structure and protection. Six common phyla of invertebrates found in oceans are porifera (sponges), cnidaria (corals, jellyfish, and sea anemones), annelida (segmented worms), mollusca (snails, clams, mussels, scallops, squid and octopus), arthropoda (crabs, shrimp, barnacles, copepods and euphausiids) and echinodermata (sea stars, sea urchins and sea cucumbers) (**figure 18**) [176]. Marine invertebrates and associated microorganisms are identified as the major group of bioactive compound producers supplying around a 75% of MNPs [177].

The diverse group of metabolites provided by invertebrates belong to terpenoid, steroid, alkaloid, ethers, phenols, and peptide classes [177] and cytotoxicity related to cancer therapy is one of the most interesting activity [178, 179]. From marine anticancer compounds approved or in clinical trial by FDA, most of them were isolated or derived from sponges and molluscs [172].

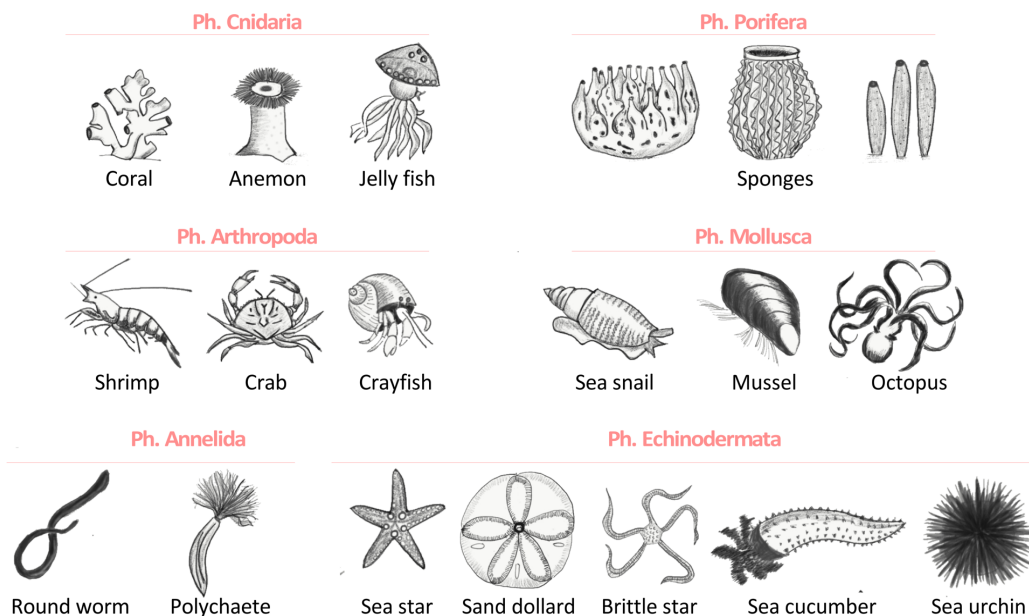


Figure 19. Marine Invertebrates.

1.22. Methodologies of Screening MNPs

The process of discovering bioactive compounds (natural products, modified natural products or synthetic) involve a large number of analytical and biological steps to assess the potential of biological extracts or molecules. There are two different and complementary approaches to discover new drugs: i) classical pharmacology or phenotypic drug discovery and ii) reverse pharmacology or target-based drug discovery [180]. Phenotypic screening system use cell lines or animal assays to measure a parameter on a quantitative manner. On the contrary, the target-based drug discovery checks isolated targets based on specific formulation or specific molecular hypothesis using computing platforms (the PC or *in silico*) which led to contrast rapidly if molecular targets (proteins or enzymes) interact with the compound in an automated system. The big difference between both methods is the first focus. In phenotypic screening the first consideration is to set the biological function and try to find if a selection of compounds can alter it. In the target-based system, the first objective is to find the molecular target involved in the disease

(gene, protein, or pathway) and compounds are screened to find high-affinity binding [181]. Both strategies show advantages and drawbacks, however, drug discovery requires both approaches when possible to provide efficient identification of safe and effective new drugs, as well as an effective launch to clinical success (**figure 20** and **table 5**).

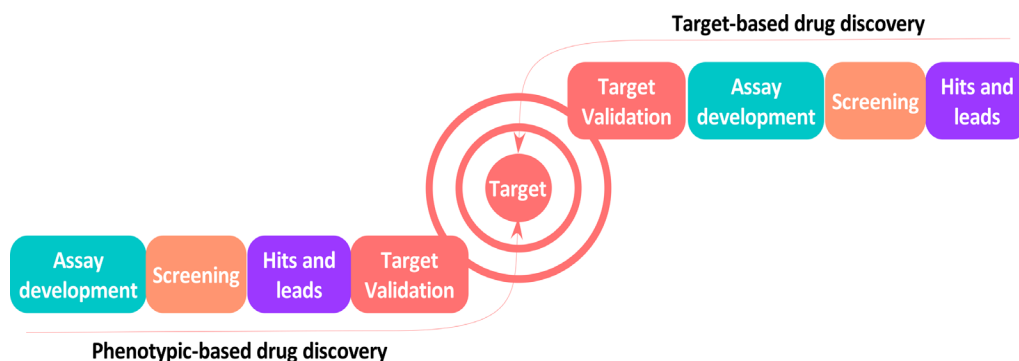


Figure 20. Phenotypic vs Target-based screening systems (Adapted from Cypotex [182]).

The phenotypic screening assays is usually performed *in vitro*, using cell lines and monitoring single parameters such as cellular death or expression of a particular protein. However, recently the high-content technology phenotypic approach has evolved and is possible to monitor several targets simultaneously. Phenotypic screening can be approached also *in vivo*, which the advantage that a compound or extract can be evaluated in the whole animal model. The success of this approach usually include serendipitous findings [183].

The target-based screening is typically selected for protein receptors or enzymes targets. This type of screening use three classes of computational or *in silico* methods according to their principle:

- **Shape screening:** when the structure and shape of a known compound bind to a target, this approach identify new compounds which show similar shape to the known binder [184].

- **Pharmacophore:** each type of atom has molecular patterns or chemical properties that are used to identify and characterize 2D or 3D molecules and are used to analyze the similarity between a small molecule library and identify the key features that contribute to biological function [185].
- **Docking and Reverse docking:** a database of proteins is compared with an active compound under study and docking is used to find the correct binding modes for the ligand-target complexes. In the reverse docking, target proteins are classified according to the ligand or active compound, using the coupling properties to the correct binding modes for their classification [186].

As discussed above, MNPs are a great source of antineoplastic drugs that should be explored, however, it is not feasible economically to test libraries of millions of bioactive compounds. A guided search is required to limit the enormous number of usable compounds. In this respect, molecular docking is widely used for the study of protein interactions using AutoDock/vina software to check the Gibbs free energy variation (ΔG , Kcal/mol). When the Gibbs free energy variation is less than (≤ -10 kcal/mol, compounds are potential modulators [156, 157]. This approach can be complemented with the estimation of the ADMET properties (absorption, distribution, metabolism, excretion and toxicity) that is very helpful to reduce the number of candidate compounds in a significant manner.

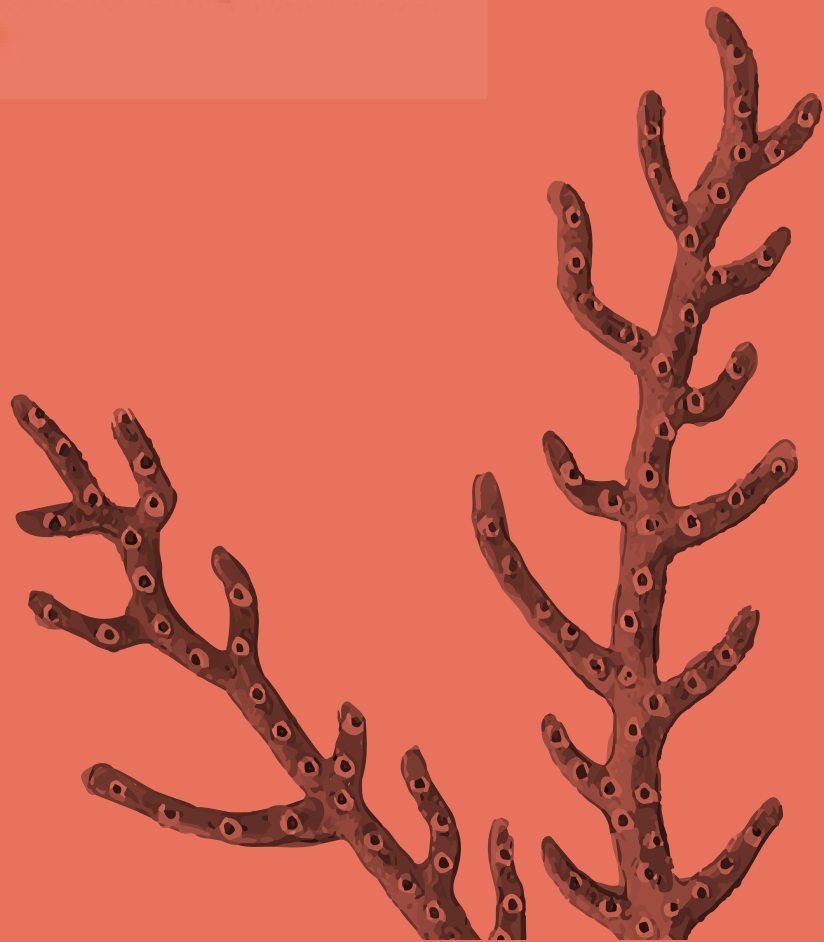
Table 5. Phenotypic vs Target-based screening systems.

Phenotypic approach	
Advantages	Disadvantages
Target linked to disease-relevant biological response	Mechanism of action/target unknown at onset
Antibodies bind to native target on cells	Target identification can be challenging
Multiple targets and/or mechanisms of action can be discovered	Substantial target validation can be required
More novelty, less competition	
Target-based approach	
Advantages	Disadvantages
Molecular target known	Target might not be important in disease
Mechanism of action known	Literature data on target might not be reproducible
Simple design of screening	Biochemical and functional assays might not correlate
History of delivering clinical therapeutics	Single, known mechanism of action
	More competition, less novelty



02

Objectives



Doctoral Student:
Verónica Ruiz Torres

The initial hypothesis of the present work is that the vast biological diversity of marine microorganisms can be translated into a vast diversity of unknown or unexplored chemical structures that may represent a source of new drugs with anticancer properties. Therefore, the objective of this work is to **study the antiproliferative capacity of extracts, obtained from marine invertebrates using *in vitro* colorectal cell models and to explore its putative mechanism of action in order to establish the basis for further preclinical assays for cancer research.**

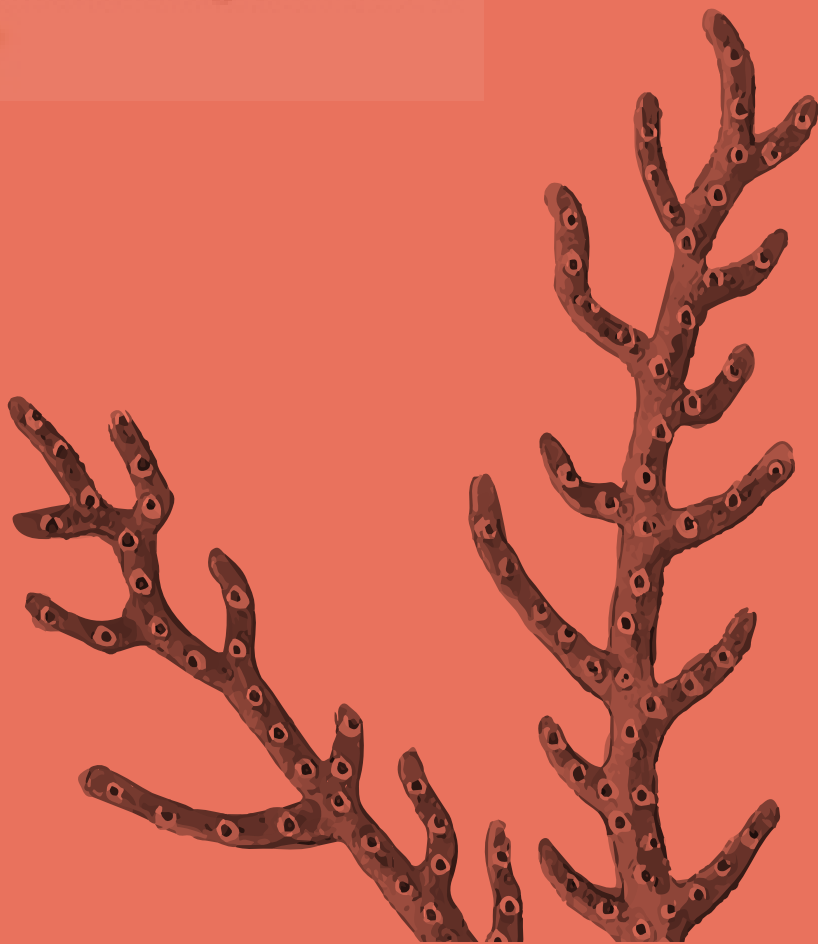
In order to achieve the general aim of this doctoral thesis the following specific aims arise:

- To identify the main marine invertebrate species with potential anticancer compounds derived from their antiproliferative capacity among a set of them available.
- Screening the cytotoxic and the antiproliferative effect of a selected group of marine invertebrate extracts and fractions using *in vitro* colorectal cancer cell models and to select the most active ones.
- Identify the main bioactive compounds derived from the most active extracts and fractions by High-Performance Liquid Chromatography coupled to mass spectrometry (HPLC-ESI-TOF-MS).
- To evaluate the antiproliferative capacity of the most active extracts through the study of cell proliferation, migration and invasion, cell cycle and stress balance.
- To explore the putative antitumor mechanism on cell proliferation of the marine extracts through the regulation of the PI3K/Akt/mTOR pathway.
- Study the capacity of the most active extract (derived from *Dolabella auricularia*) to modulate oxidative stress and endoplasmic reticulum stress in relation to the invasive phenotype of colorectal cancer cells.



03

Methodology



Doctoral Student:
Verónica Ruiz Torres

PROCEDURE SCHEME AND SELECTION OF MARINE EXTRACTS

The purpose of this point is to explain the steps followed in the procedure of this thesis (**figure 21**). The first step consisted in to select marine invertebrates with potential antitumor compounds. For that purpose, a search in scientific bibliographic bases to look for the most interesting families which show strong competitive behavior was made. In order to choose the most interesting species (distributed by the company TODO PEZ S.L.), different organisms were set in experimental aquariums and observed to register competitive situations between them. 20 marine species of marine invertebrates were chosen consisted of 12 soft corals, 4 hard corals, 2 nudibranchs, 1 anemone and 1 holothurian. For more details see **table 6**.

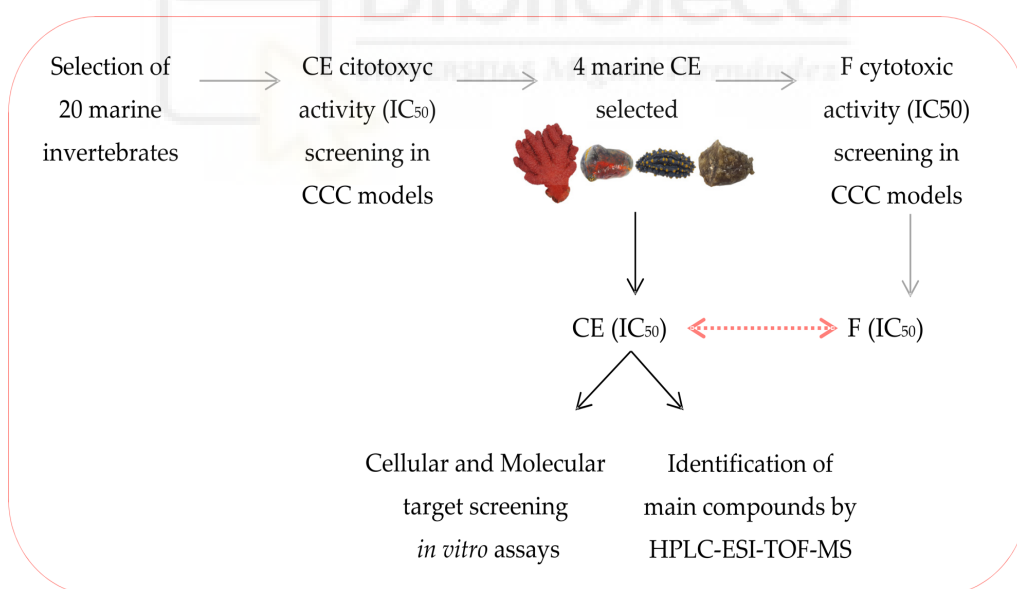


Figure 21. The schematic representation of the procedure for marine extracts screening and elucidation of cellular and molecular target modulation capability.

Cytotoxic activity of 20 marine complete extracts (CE) were screened by the MTT assay in a panel of three colon cancer cell lines HGUE-C-1, HT-29 and SW-480 (see more details in cellular and molecular based assay section). Different concentrations of marine extracts (0–100 $\mu\text{g}/\text{mL}$) were prepared to treat CRC cell lines for 24, 48 and 72 h, and the inhibition curves were obtained to calculate the concentration that produced 50% cell growth inhibition (IC_{50}). The selection criterion was based on IC_{50} values less than 30 $\mu\text{g}/\text{mL}$ at 48 h in at least 2 of the cell lines used, or 15 $\mu\text{g}/\text{mL}$ or less in at least one of the cell lines used. Comparing IC_{50} values let us to determine the 4 most active extract (CR, PS, NA and NB).

The next step consisted in making a fractionation based on three polarity ranges of each one of the selected extracts in order to isolate the most active compounds. Considering this premise, selected extracts were fractionated (see details in extracts and fractions preparation section) and re-screening by MTT assay in the same CRC cell lines and finally IC_{50} values from fractions (F) were compared to IC_{50} values from CE. Even though Fs were more active than CEs, the difference was not as higher as to assume the production effort and therefore it was decided to continue working with the complete extracts. Next approach consisted in to identify the main compounds in CE by HPLC-ESI-TOF-MS and to study cellular and molecular targets that affect the CE.

CHEMICALS AND REAGENTS

Reagents to extract bioactive compounds from marine organisms such as dichloromethane, methanol, n-butanol, ethyl acetate, n-hexane, and for chemical analysis by HPLC including acetonitrile, acetic acid and dimethylsulphoxide (DMSO) were purchased from Sigma-Aldrich (Europe). Distilled water was purified using a Milli-Q system (Millipore, Bedford, MA, USA).

Reagents for cellular and molecular assays like Thiazolyl Blue Tetrazolium Bromide (MTT), Hoechst 33342, propidium iodide (PI), 2',7'-Dichlorodihydrofluorescein diacetate (DCFH-DA) were purchased from Sigma-Aldrich (Europe).

EXTRACTS AND FRACTIONS PREPARATION

3.1. Marine invertebrate material

A list of marine invertebrate species was done after a specific search on bibliographic bases [187]. Once selected the most attractive for us, the distributor marine species company TODO PEZ S.L. allow us to stablish experimental aquariums for study the inter and intra-specific competence between selected organisms. 20 invertebrates were chosen for their potential ability to inhibit growth or kill other adjacent or distant organisms through the release of compounds that induce death.

The selected species were 12 soft corals, 4 hard corals, 2 nudibranchs, 1 anemone and 1 holothurian (**table 6**).

Table 6. Screening of marine invertebrate species.

Class	Scientific name	Code	Photo	Class	Scientific name	Code	Photo
Soft Coral	<i>Parazoanthus</i> sp.	P		Soft	<i>Euphyllia ancora</i>	Eu	
	<i>Discosoma</i> sp.	D		Coral	<i>Carotalcyon</i> sp.	CR	
	<i>Lemmalia</i> sp.	L		Anemone	<i>Aiptasia</i> sp.	A	
	<i>Capnella</i> sp.	C		Hard Coral	<i>Wellsohyllia</i> sp.	W	
	<i>Nepthea</i> sp.	N			<i>Echynophyllia</i> sp.	E	
	<i>Sarcophyton</i> sp.	SII			<i>Fungia</i> sp.	F	
	<i>Sinularia</i> sp.	Si			<i>Duncanopsamia</i> sp.	Du	
	<i>Cataphyllia</i> sp.	Cy		Nudibranch	<i>Phyllidia varicosa</i>	NA	
	<i>Xenia</i> sp.	X			<i>Dolabella auricularia</i>	NB	
	<i>Palythoa</i> sp.	Py		Holothurian	<i>Pseudocolochirus violaceus</i>	PS	

3.2. Complete extraction and fractionation

Selected organisms were cleaned and cut into small pieces. To extraction, the whole mass was macerated with dichloromethane:methanol (D:M) (1:1, v:v) at 4 °C for 24 h. After that, the solution was filtered and concentrated by a rotatory vacuum evaporator producing the crude extract or complete extract (CE). CE was divided in two parts. One half was saved as CE, while the second was partitioned subsequently with n-hexane (Hexane fraction, HF), ethyl acetate (Ethyl fraction, EF) and n-butanol (Butanol fraction, BF) to obtain non-polar, semi-polar and polar fractions respectively.

CEs and Fs were dried by speed vac, weighted and stored at -80 °C until used. For *in vitro* culture, extracts were dissolved in DMSO (50 mg/mL) and further diluted in culture medium yielding a final DMSO maximum

concentration of 0.2%. This concentration of DMSO did not affect cell viability. This methodology was extracted from Beedessee G *et. al* [188].

CELL CULTURE MAINTENANCE

The human colorectal carcinoma cell lines HT-29, SW-480 and HCT-116 were purchase from the American Type Culture Collection (ATCC, MN, USA) and HGUE-C-1 (an established cell line from primary human colon carcinoma) provided by Dr. Miguel Saceda (Hospital General Universitario de Elche, Spain). The normal colon cell line CCD18-Co was purchased from the American Type Culture Collection (ATCC, MN, USA).

Colorectal cancer cell lines were maintained in Dulbecco's Modified Eagle's Medium (DMEM), while normal colon cell line was growth using Eagle's Minimum Essential Medium (EMEM). Both media were supplemented with 10% heat inactivated fetal bovine serum (FBS) and 100 U/mL penicillin and 100 g/mL streptomycin. Cells were incubated at 37 °C in a humidified atmosphere containing 5%/95% of CO₂/air. Subculturing was done each 2-3 days using trypsin/ethylene diamine tetra-acetic acid at 0.05X according to the manufacturer's instructions. Cell culture reagents were purchased from Invitrogen Life Technologies (Carlsbad, CA, USA).

CELLULAR AND MOLECULAR BASED ASSAYS

3.3. Cell viability assay by MTT assay

The main purpose of this assay is to asses cell viability based on the activity of Nicotinamide Adenine Dinucleotide Phosphate (NADPH)-dependent cellular oxidoreductase enzymes to reduce the tetrazolium dye MTT ((3-(4, 5-dimethylthiazolyl-2)-2, 5-diphenyltetrazolium bromide) to water

insoluble formazan crystals, which has a purple color. This reaction occurs in the mitochondria of living cells although other reducing agents such as endoplasmic reticulum are also involved.

This assay starts seeding cells in a 96-multiwell culture plates at a density of 5×10^3 cells/well. After 24, 48 and 72 h of marine extracts and fractions treatment, MTT was added at a final concentration of 0.5 mg/mL and incubated for 3 h. When formazan crystals were synthesized, the medium was removed and DMSO was added to solve the formazan crystals. The absorbance of this coloured solution was quantified by measuring at 570 nm by a spectrophotometer microplate reader (SPECTROstar Omega, BMG Labtech, Germany). The IC_{50} values were determined using GraphPad Prism v5.0 software (GraphPad Software, La Jolla, CA, USA). The results are expressed as the percentage of cell viability/proliferation relative to control (untreated cells).

3.4.Proliferation assay by RTCA

The main goal of this test is to obtain real-time values of a cell line proliferation feature. In this assay is used the real-time using the xCELLigence system E-Plate Real Time Cell Analyzer (RTCA) (Roche Diagnostics GmbH, Germany) which is placed into the incubator. This technique registers changes in impedance values of each well where cells are growing and translate it to a cell index value (CI).

Colorectal cancer cells are seeded from 7.5×10^3 to 2.0×10^4 cells/well depending on the cell line. It is required by the manufacturer's, to reach a CI over 1 unit after 24 h from the seed. At this point cell are ready for the treatment, which is added at 10, 25, 50 and 100 $\mu\text{g/mL}$ for 96 h. CI was automatically monitored every 10 minutes, producing a kinetic curve. Data were normalized with CI from 24 h (when the treatment started).

3.5. Survival assay by clonogenic test

The main aim of this assay is to study the survive ability of cancer cells through the capability of cells to form a colony from a single.

Colon cancer cells are seeded in a 6-well plates at low density (5×10^2 cells per well) and treated the day after with different concentrations of marine extracts (CR, PS, NA and NB) for 24 h. After treatment, media is removed and fresh media is added. Cells are incubated for 6 days to allow colony formation.

Cell nucleus were stained with Hoechst 33342 and fixed with 70% ethanol for 5 minutes for determination of number of cells and diameter of colonies by the Cell Imaging Multi-Mode Reader Cytation 3 (BioTek, Germany). Finally, cells were stained with 0.05% crystal violet for 10 minutes to take photos of plates.

3.6. Cell cycle analysis

The cell cycle analysis is employed to distinguish cells in different phases of the cell cycle measuring DNA content using flow cytometry technique. Cells are permeabilised with a fluorescent dye which stains DNA and fluorescence intensity correlate with the amount of DNA contain. In this way cells in G1 gap have two copies of each chromosome, while in S phase have started to replicate DNA and have more DNA than cells in G1. In G2 cells have growth and each cell contains four copies of each chromosome. They will take proportionally more fluorescence dye the more DNA content.

For this assay cells at 1.5×10^5 cells per well were seeded into 6-well plates and treated with marine extracts at different concentrations for 24. Cells were harvested, washed with phosphate buffered saline (PBS) 1X and fixed with 70% ethanol. Cell cycle phases were determined using the intercalant DNA staining agent propidium iodide (PI). This measure was made according to the manufacturer's instruction by the Muse® Cell Analyzer (Merck KGaA, Darmstadt, Germany).

3.7. Apoptosis tests

These assays let us to study the apoptotic state or programmed cell death under marine extract treatment through the Phosphatidyl Serine (PhS) protein and mitochondrial membrane potential (MMP) disruption.

Annexin V assay

One of the earlier events of apoptosis is the externalization of PhS produced in the apoptotic bodies formation which provide a binding site for the anionic lipid binding protein annexin V. Cells were seeded at 1.5×10^5 cells per well into 6-well plates and let their adherence for 24 h. Cells were treated with marine extracts at different concentrations for 24 h and then harvested and washed with PBS 1X. Apoptosis was determined using The Muse® Annexin V and Dead Cell kit based on the detection of PhS on the surface of apoptotic cells, using the fluorescent label Annexin V.

Mitopotential assay

Changes in MMP is a hallmark of permeabilization of cellular plasma membrane in the apoptotic process. To measure MMP changes, MitoPotential Dye (a cationic and lipophilic dye) was used, combined with the DNA staining dye 7-Aminoactinomycin D (7-AAD) as indicator of cell death. The measure was made according to the manufacturer's instruction by the Muse® Mitopotential Assay Kit (Merck KGaA, Darmstadt, Germany). Cell seeding procedure was the same as for Annexin V.

Caspases assay

This assay provides data about the caspases, main executioners of apoptosis. It is a chemoluminescent assay which uses a proluminescent caspase 3/7 and caspase 8 DEVD-aminoluciferin substrate which when is combined with a thermostable luciferase reagent produces cell lysis and casapase cleavage

of the substrate. Aminoluciferin is consumed by the luciferase generating proportional luminescent to caspase 3/7 and 8.

The procedure for this assay, cells are seeded at (2×10^5 cells) into a 6-wells plate. After 24 h for adherence, cells were treated with marine extracts at different concentrations. Next step consisted on lysate cells using RIPA buffer and determine protein concentration by BCA Pierce Method. Caspase-3/7 and Caspase-8 were measured using a Caspase-Glo 3/7 and Caspase-Glo 8 assay kit (both from Promega, Madison, WI, USA) following the manufacturer's instruction. Total cell lysates containing equal amounts of proteins were gently mixed with Caspase-Glo 3/7 and 8 kit (ratio 1:1) and incubated for 30 – 40 min at room temperature in the dark. Luminiscence was measured using the Cell Imaging Multi-Mode Reader Cytation (BioTek Instruments, Inc., USA).

3.8.Necrosis assays

These tests are intended to demonstrate the necrosis as principal induced death by some marine extracts.

Lactate Dehydrogenase assay

Lactate Dehydrogenase (LDH) is a soluble enzyme released into extracellular space when the plasma membrane is permeabilized, constituting a key signature for necrotic process. To detect LDH release after marine extract treatment, the colorimetric LDH assay kit (Roche Diagnostics, Mannheim, Germany) was employed. Cells were treated with different concentrations of CR, PS, NA and NB extract for 24 h. After treatment, the supernatant was used according to the manufacturer's instruction (Roche Diagnostic Systems, Montclair, NJ, USA) adding LDH detection reagent, incubating for 15 min in the dark. In this reaction LDH reduces NAD to NADH, which interact with kit reagents producing colour and which was measured with a microplate reader (SPECTROstar Omega, BMG Labtech, Germany) at wavelength of 492 nm. LDH leakage (% cytotoxicity) was calculated as follows:

$$\text{Cytotoxicity (\%)} = \frac{\text{exp. value} - \text{low control}}{\text{high control} - \text{low control}} \times 100$$

Low control is the value of LDH activity from the untreated normal cells (basal LDH release) and high control is the maximum releasable LDH activity in the cells (100% LDH release).

Necrosis and Apoptosis

The main objective of this assay is to differentiate live and dead cells and within the classification death to distinguish necrotic from apoptotic. This assay combines a double nuclear fluorescent staining (Hoechst 33342 and Propidium Iodide (PI)). Hoechst 33342 dyes live and death cells, whereas PI need plasma cellular membrane be defective (dead cells). When cells showed blue (Hoechst 33342) round nucleus are considered as live. By contrast, necrotic cells (Hoechst 33342 plus PI) show round purple nuclei. Cells in the apoptotic state showed apoptotic bodies in pink when the membrane was damaged but also in blue when membrane remained intact.

Colon cancer cells were seeded at 5×10^5 /well into 96-well plates and treated with different concentrations of marine extracts for 24 h. Cells were washed and stained with Hoechst 33342 at 5 $\mu\text{g}/\text{mL}$ and PI at 50 $\mu\text{g}/\text{mL}$ for 15 minutes at 37 °C and then were washed once in PBS 1X. Fluorescence intensity was registered and cells were photographed using a Cell Imaging Multi-Mode Reader Cytation (BioTek Instruments, Inc., USA) equipped with 40X objective and fluorescent cubes (DAPI ex. 377-447 nm and TEXAS ex. 586-647 nm). Results represented are means \pm S.D. of three independent experiments.

3.9. Mitochondrial state

The aim of this assay is to study the state of mitochondria through their membrane potential. This test uses a combination of two fluorescent labels. MitoTracker Red CMXRos which react to the highly negative mitochondrial membrane potential and MitoTracker Green which has been widely utilized to represent the mitochondrial mass.

Both MitoTracker dyes are cationic fluorophores that react to the highly negative mitochondrial membrane potential. When mitochondrial membrane is damaged and pores became to appear, Mitochondrial Membrane Polarization (MMP) begins to be reduced and the relation red/green decrease.

For this assay cells were seeded at 5×10^5 /well into 96-well plates and treated with marine extracts at different concentrations. After treatment, cells were washed twice in PBS 1X and incubated with 0.5 $\mu\text{g}/\text{mL}$ MitoTracker Red CMXRos and 15 ng/mL MitoTracker Green (Molecular Probes) at 37 °C for 45 min. Cells were then washed twice in PBS and analyzed by the fluorescent wavelength value using the Cell Imaging Multi-Mode Reader Cytation (BioTek Instruments, Inc., USA). Photographies were taken using a Cell Imaging Multi-Mode Reader Cytation (BioTek Instruments, Inc., USA) equipped with 20 X objective and fluorescent cubes (GFP ex-em. λ 469-525 nm and TEXAS ex-em. λ 586-647 nm). Data were compared to untreated cells and represented as means \pm S.D. of three independent experiments.

3.10. Oxidative status

This high throughput assay was performance to asses intracellular Reactive Oxygen Species (ROS). Cells were seed at 5×10^5 cells/well into 96-well plates. After 24 h for adherence, treatment of marine extracts was added and incubated for 24 h. The intracellular ROS was determined using 2',7'-Dichlorodihydrofluorescein Diacetate (DCFH-DA, Sigma-Aldrich) (10 μM) and compared with cell viability using DNA fluorescence staining Hoechst 33342 (Sigma-Aldrich) (10 $\mu\text{g}/\text{mL}$) which were incubated for 30 min. Fluorescence

was registered using the Cell Imaging Multi-Mode Reader Cytation (BioTek Instruments, Inc., USA) (DCFH-DA ex-em at 495-529 nm and Hoechst 33342 ex-em 350-461 nm). Data were compared to untreated cells and represented as means \pm S.D. of three independent experiments.

3.11. DNA Damage

This cytometric assay let us to study if a treatment produces DNA damage through formation of γ -H2AX in response to DNA double stranded breaks (DSBs).

Colon cancer cells were seeded at 1.5×10^5 cells per well into 6-well plates and treated with marine extracts at different concentrations for 24 h. Cells were harvested and washed with PBS 1X. To asses DNA damage, was combined a phospho-specific anti-phospho-Histone H2A.X (Ser139)-Alexa Fluor®555 and an anti-Histone H2A.XPECy5 conjugated antibody to measure total levels of Histone H2A.X according to the manufacturer's instruction by the Muse® Cell Analyzer (Merck KGaA, Darmstadt, Germany). Data were compared to the total cell amount and given as % activated. Data were shown as mean \pm S.D. of three independent experiments.

3.12. Migration and invasion assay by RTCA

The objective of this assay is to evaluate the migration and invasion features in a real time. The xCELLigence system Real Time Cell Analyzer (Roche Diagnostics GmbH, Germany) using CIM-Plates registers changes in impedance which are translates to a Cell Index (CI) of migration (CIM) and invasion (CII). RTCA also register cell index of proliferation (CIP) using E-Plates (see more details in point 5.7).

For this assay was required to starve SFB from the HCT-116 media 6 h prior to the conducting the experiment because this enhance the migration and invasion ability of this colon cancer cell line. In this assay special CIM-Plates are used. CIM-Plates consisted in two chambers separated by a Polyethylene

Terephthalate (PET) membrane with microporus of 8 μm containing gold electrode arrays on the bottom side of the membrane. In the upper chamber, where cells will be added, the media should have no SFB (0% SFB), whereas in the bottom chamber the media contain 10% SFB, which is a chemoattractant of migrating and invasive HCT-116 cells. In the bottom chamber is added the study samples such as marine extracts and controls (0% SFB is C- or 0% migration and invasion and 10% SFB like C+ or 100% migration and invasion). When CIM-Plate is prepared, it is allowed to equilibrate into the incubator for 1 h. Next step consists in to add 4×10^4 HCT-116 cells in each upper chamber in serum-free media. When cells go through pores and add to the bottom side, impedance will change and RTCA will register these changes. The CI was monitored for 48 h and expressed as CIM or CIP.

It is important to note that invasion differs to migration assay because is added a layer of Matrigel™ (BD Biosciences) in the upper chamber which simulates the invasive process through the extracellular matrix. To coat CIM-Plate is used a solution of 1:40 of Matrigel™ (BD Biosciences)) according to the manufacturer's instruction. The impedance value was monitored for 48 h and expressed as Cell Index of invasion (CII) following the same procedure as migration. Data were compared to untreated cells and represented as means \pm S.D. of three independent experiments.

3.13. Superinvasive populations isolation

The main goal of this assay is to isolate the most invasive subpopulations of HCT-116 cell line. For that purpose, HCT-116 populations were growth and forced to invade using Corning® BioCoat™ Matrigel® Invasion Chamber, 8.0 μm PET membrane 6-wells plates. This special plate is similar to CIM-Plate used in RTCA system. In each well there is an insert coated with Corning® BioCoat™ Matrigel® which generate 2 chambers. The upper chamber where cells will be seeded (media 0% SFB) and the bottom chamber (media 10% SFB, chemoattractant). Cells at 1.25×10^5 HCT-116 cells/mL were seeded in the upper chamber and allowed to invade bottom chamber for 48 h.

After that time, invasive cells (in the bottom chamber) were collected and re-seeded in a 25 cm² flask to get confluence. The process was repeated for 4 times to obtain invasive subpopulation 4 (I4) and 9 times to isolate invasive 9 (I9) (figure 22).

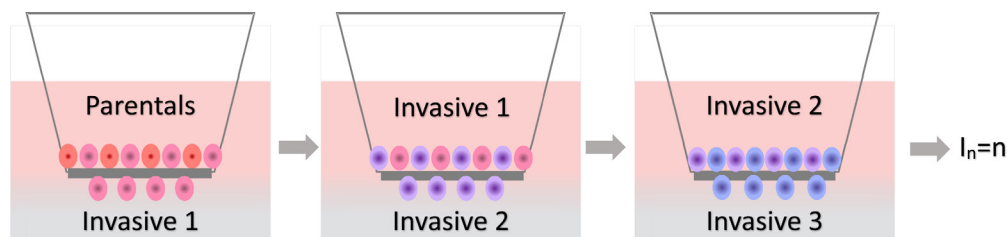


Figure 22. Superinvasive population isolation procedure

3.14. Reverse transfection

This assay let us to silence some of caspases 8 and 9 protein expression in HCT-116.

HCT-116 cells were transfected with C8, C9 and control scrambled siRNA using Hiperfect (Quiagen) following the manufacturer's reverse-transfection protocol. SiRNAs were prepared at 10 nM in RNase-free water (Quiagen) in a 90 dishes. Hiperfect and Optimem (transfectant agents) were incubated for 30 min at room temperature. Next step was to add cells were to the mastermix prepared before at 1.5×10^6 cells per dish. After 24 h, the culture medium was switched to a medium containing 10 µg/mL of NB extract and incubated for a further 24 h.

Theses C8 and C9 silenced HCT-116 cells were lysated to obtain protein for Western blot assay and Caspases measurement.

3.15. Western blot analysis

Colon cell lines were treated with marine extracts for 24 h. Protein lysates were obtained using RIPA lysis buffer-radioimmunoprecipitation (RIPA Buffer) (BioRad Laboratories Inc.), for 60 min at -20°C and then supernatant was collected after centrifugation at 13,200 rpm for 20 min. To measure protein amount, a spectrophotometrically determination was done using the Thermo Scientific Pierce Kit (BCA Protein assay kit), at 562 nm.

To prepare Western blot samples, 30 $\mu\text{g}/\text{lane}$ of protein were prepared with 0.5 M Tris HCl at pH 6.8, 10% glycerol, 10% w/v SDS, 5% β -mercaptoethanol and 0.05% (w/v) bromophenol blue. Protein samples and a prestained ladder molecular weight marker (Thermo Fisher Scientific, Waltham, MA, USA) were separated by electrophoresis using SDS-PAGE and transferred from the gel to nitrocellulose membranes (Bio-Rad). Transferred proteins were blocked with 5% non-fat milk in Tris buffered saline containing 0.05% Tween 20 (TBST) at room temperature for 1 h.

The next step was to incubate blots with primary antibodies overnight (PARP Rabbit mAb Antibody #9532, ATF4 mAb Rabbit (D4B8) #1815, ATF-6 (D4Z8V) mAb Rabbit #65880, IRE1 α (14C10) mAb Rabbit #3294, phospho-JNK (Thr183/Tyr185) mAb Mouse antibody #9255, CHOP (L63F7) mAb Mouse antibody #2895, BiP (C50B12) mAb Rabbit #3177, XBP-1s (D2C1F) mAb Rabbit #12782, Phospho-eIF2 α (Ser51) (D9G8) mAb Rabbit #3398, eIF2 α (D7D3) mAb Rabbit #5324, Caspase-3 Antibody #9662, Caspase-9 #9502 from Cell Signaling Technology Inc. Beverly, MA, USA. Caspase-8 (human) monoclonal antibody (12F5) was obtained from Enzo Life Sciences, Inc. and phosphor-IRE1 α (S724) #ab124945 (Abcam) and anti- β -actin antibody was obtained from Sigma-Aldrich, St. Louis, MO, USA. After incubation with primary antibodies, the second step was to wash blots with TBST 3 times for 5 min and then incubated with secondary antibodies for 1 to 3 h. ChemiDocTM XRS+ System (Bio-Rad) with Image LabTM software was used to detect chemoluminescence of relevant bands.

DETERMINATION OF SECONDARY METABOLITES BY HPLC-ESI-TOF-MS

A Agilent 1200 series Rapid Resolution Liquid Chromatograph (Agilent Technologies, CA, USA), which was comprised of a binary pump, degasser, and auto sampler was used for the qualitative analysis of bioactive compounds from the CR, PS, NA and NB marine extracts. To separate main compounds, was used a Poroshell 120 EC-C18 (3.6 x 100 mm, 2.7 mm) analytical column (Agilent Technologies, Palo Alto, CA, USA) at room temperature. Then, the chromatographic separation was performance using two different methods based on the ionization mode. 1% of acetic acid in water (phase A) and acetonitrile (phase B) formed the mobile phases. The flow rate was set at 0.5 mL/min at 25 °C.

The analysis parameters in the first method, were arranged using a negative-ion mode with a scan range from m/z 50 to 1000 and the following multi-step linear gradient was employed: 0 min, 5% B; 5 min, 15% B; 20 min, 30% B; 35 min, 95% B; 40 min, 5% B. In the method carried out in positive ionization mode the scan ranged from m/z 50 to 1500 and the conditions of the solvent multi-step linear gradient were the following: 0 min, 10% B; 5 min, 65% B; 15 min, 100% B; 19 min, 100% B.

The HPLC system was coupled to a microTOF (Bruker Daltonics, Bremen, Germany), an orthogonal- accelerated TOF mass spectrometer, using an electrospray interface (ESI) (model G1607A from Agilent Technologies, Palo Alto, CA) operating in both, negative and positive-ion modes. The effluent from the HPLC column was splitted using a T-type phase separator before being introduced into the mass spectrometer (split ratio = 1:3). The optimum values for the ESI-MS parameters were as follows: capillary voltage, +4.0 kV; drying gas temperature, 200 °C; drying gas flow, 9.0 L/min; and nebulizing gas pressure, 2.0 bars.

Peak identification was performed by generation of the candidate formula with a mass accuracy limit of 10 ppm. The characterization strategy was based on the interpretation of their mass spectra provided by the TOF-MS and by using previously reported information in the literature for marine invertebrates. For the acquisition of chemical structure information the following databases were consulted:

- SciFinder Scholar (<http://scifinder.cas.org>),
- MassBank (<http://massbank.jp>), and
- METLIN Metabolite Database (<http://metlin.scripps.edu>).

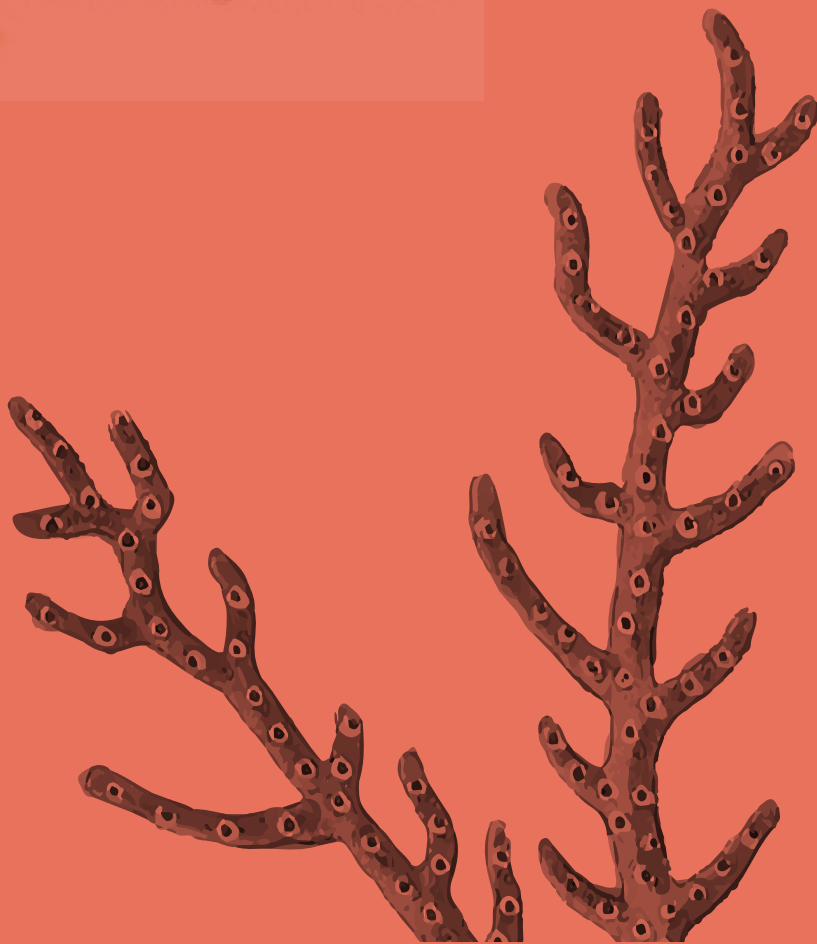
Furthermore, a recent published database of marine natural compounds (<http://docking.umh.es/chemlib/mnplib>) has been employed.

STATISTICAL PROCEDURE

Data were shown as the mean \pm standard deviation (SD) of 3 independent assays. Data from treatment were compared to controls and significant differences were tested by one-way analysis of variance (ANOVA), followed by Tukey's post hoc test for multiple comparisons using GraphPad Prism 6, Windows 10, CA. Statistically, significant differences were assumed at $*p < 0.05$, $**p < 0.01$, $***p < 0.001$ or $****p < 0.0001$.



Results



Doctoral Student:
Verónica Ruiz Torres

THE SUMMARIZED RESULTS OF CHAPTER 1

An Updated Review on Marine Anticancer Compounds: The Use of Virtual Screening for the Discovery of Small-Molecule Cancer Drugs

Marine compounds are presented as unlimited source of new isolable compounds which offer novel chemical structures. In fact, general studies revealed molecular scaffolds derived from marine organisms showed high novel structures in comparison to terrestrial [170]. The interest in marine compounds as sources of drugs has considerably increased and its reflects of the rising number of scientific publications related to marine research in the field of health in recent years (**figure 1, chapter 1**) [172]. By 2017, eight drugs (plitidpesin, trabectedin, brentuximab, eribulin mesylate, omega-3 acid ethyl ester, ziconotide, vidarabine and cytarabine) derived by marine organism were approved by the European Union or by the Food and Drug Administration for different diseases being a 63% of the approvals for cancer treatment and a 63% were derived by marine invertebrates. This biodiverse classification encompasses a wide range of phyla such as Porifera, Cnidaria, Annelida, Bryozoa, Mollusca, Arthropoda and Echinodermata and representing approximately a 75% of the 20.000 MNPs described to date [177]. Marine invertebrates are reported to produce alkaloids, polyketides, terpenes, peptides, carbohydrates and carbohydrates variants [189, 190].

In addition to approved MNPs, many compounds with marine origin by 2017 were ongoing in clinical trials. For instance, plitidpesin and gemcitabine were in phase III, whereas, glembatumumab vedotin, elisidepsin, PM-1004, pseuopterosins and contignasterol derivative were in phase II. Between phase I and II, were found PM-10450 and Discodermolide and compounds bryostatin-1, pinatuzumab vedotin, tisotumab vedotin, hemiasterlin derivative, bengamide B derivative, hemiasterlin, PM-060184 and psammaplin derivative remained in phase I. Of those registered in clinical phases, 97% came from invertebrates, belonging above a 53% to the Phorifera phylum or more commonly known as marine sponges [172].

One of the interesting approach of this review is the classification of MNPs under research or preclinical uses according to their ability to modulate different cancer hallmarks based on proposed by Hanahan and Weinberg [3]. Based on this targets the review lists the most current MNPs as i) growth inhibitors and anti-tubulin agents, ii) apoptosis and autophagy inductors, migration, invasion, iii) metastatic and angiogenic inhibitors and iv) Mitogen-Activated Protein Kinases (MAPKs) inhibitors, its main mechanism of action, as well as the marine species from which they were obtained.

Cancer is a heterogeneous disease which needs efficient therapies that attack the direct molecular agents responsible for the disease and avoid secondary side effects. Related to this purpose, *in silico* methods in general and particularly virtual screening are useful tools which lead the discovery of MNPs as anticancer compounds. This technique, presented in the Introduction section, estimates different properties via computational methods which indicates the eligibility of a proposed compound to act against the specific targets and reduce the vast cost of testing millions of compounds.

The first step of molecular docking was to use AutoDock/vina Software based on the Gibbs free energy variation and the Absorption, Distribution, Metabolism, Excretion and Toxicity (ADMET) criteria.

A MNPs database was built and compared to an anticancer compounds database containing the main 168 anticancer drugs included in Genomics of Drug Sensitivity in Cancer" project (their data are available at <http://www.cancerrxgene.org/>). This research show that 82% of MNPs in our database showed a molecular weight of 500 Da or lower. When cLogP was analyzed, a 95% of the compounds have a cLogP equal to or less than 9 and considering the cLogS value, we found a 93% of MNPs are within the range of the anticancer compounds. Molecular flexibility of the number of rotatable bonds as an indicator of oral bioavailability of drug candidates was studied. When MNPs were compared to anticancer compounds, we found 77% and 93%, respectively, satisfy that condition. Furthermore, the H-bond donors (HBDs) analyses revealed a 86% (marine compounds) and 83% (anticancer compounds)

have 5 or fewer HBDs and 10 or fewer H-bond acceptors. Taking docking results into account, these data reveal a high potential of MNPs as anticancer drugs.





THE SUMMARIZED RESULTS OF CHAPTER 2

Marine Invertebrate Extracts induce Colon Cancer Cell Death via ROS-mediated DNA Oxidative Damage and Mitochondrial Impairment

CH2_1. Marine extracts derived from selected invertebrates inhibit the proliferation of colon cancer cells.

We first selected 20 marine organisms based on their ability to injure (coral bleaching by direct or indirect contact) or kill other reef species that they cohabit. The selected specimens were obtained from experiments performed in the facilities of a collaborating company dedicated to the cultivation of marine species (TODOPEZ, SL, Alicante, Spain). The selected organisms (**table 6, Methodology section**) include 12 soft corals, 4 hard corals, 2 nudibranchs, 1 anemone and 1 holothurian were used to obtain the complete extracts (CE).

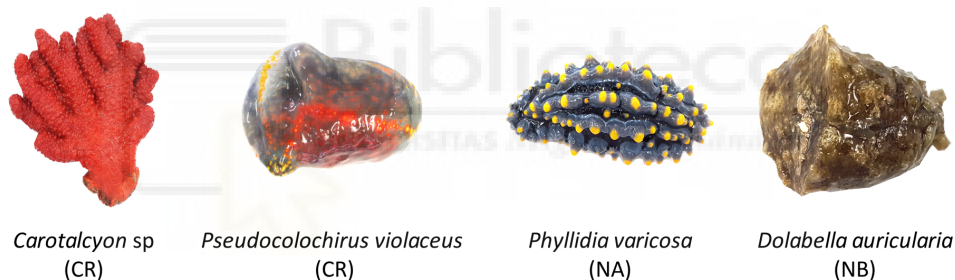


Figure 23. Marine selected invertebrates for further characterization and antiproliferative study.

CEs cytotoxicity were tested using eight concentrations (0–100 $\mu\text{g}/\text{mL}$) for 24, 48 and 72 h in a panel of three human colon cancer cell lines using MTT assay. Inhibition curves were represented to calculate IC_{50} values to be compared between cell lines. The most active CEs were selected by presenting IC_{50} values less than 30 $\mu\text{g}/\text{mL}$ at 48 h in at least 2 of the cell lines used or ≤ 15 $\mu\text{g}/\text{mL}$ in at least one of the cell lines used. Based on this criteria, the most active extracts were CR from red coral, PS from a holothurian, NA and NB (from

nudibranchs) (**figure 23**) and were promoted for further characterization (**table 2, chapter 2**).

Among the 4 chosen extracts, NB and PS CEs exhibited the lowest IC₅₀ values, indicating to have the most potential antiproliferative ability. Data obtained by proliferation assay by Real Time Cellular Assay (RTCA) confirmed the results obtained by MTT and allowed us to classify the extracts from the most to the least active, i.e., NB, PS, NA and CR.

The ability of a single cell to grow into a colony by the clonogenic *in vitro* assay was also studied. After marine extracts treatment at different concentrations, a general reduction in the average and the size of colonies were registered, however, PS and NB produced a drastic inhibition in comparison to CR and NA which reduced gradually.

CH2_2. Marine extracts modified cell cycle and induce cell death in human colon cell models.

The cell cycle profile after marine extracts treatment after 24 h on HGUE-C-1, HT-29 and SW-480 was analyzed by flow cytometry (**figure 2 A-D, chapter 2**). Different patterns of phases in the cell cycle were observed, however, the most significant result produced in general by marine extracts was a considerable increase in cells arrested in the G2/M phase in all cell lines used mainly by NB, NA and CR extract. By contrast, PS although produced a significant increase in the cell arrest in G2/M it was not as significant in comparison to the other extracts.

Apoptosis induction in the three human colon cancer cell models was also studied using the Annexin V detection method (**figure 2 E-F, chapter 2**). In this assay, the increase of cells in early apoptosis is a clear indicator of the induction of apoptosis. After the treatment of cells with marine extracts at different concentrations for 24 h, it was observed that CR, NA and NB showed a similar effect. An increase dose dependent in the total number of apoptotic cells with a higher proportion of early apoptotic cells than late apoptotic. On

the contrary, PS increased late apoptotic cells higher than early apoptotic suggesting a necrotic mechanism.

In order to confirm results obtained from the type of cell death produced by marine extracts, an assay was performed to determine the enzyme lactate dehydrogenase (LDH) activity (**figure 3 A-D, chapter 2**). Data obtained from LDH assay showed PS was the only extract which released LDH compared with the negative control indicating to mediate the necrotic cell death and confirming the data obtained from apoptosis studies.

In addition to LDH, Hoechst 33342/PI assay which let to monitor morphological changes into the nucleus was performed. In this test, cells are co-stained with the exclusion dye propidium iodide, which does not cross the intact plasma membrane, and the nuclear dye Hoechst 33342, which always stain DNA content (**figure 3 E-G, chapter 2**). Using a high content image fluorescent cell analyzer, fluorescent ration and photographs were taken. Results confirmed apoptotic body formation after NB, NA and CR extract treatment for 24 h, whereas PS induced the formation of round pink nuclei in all cells, indicating a fast permeabilization and disruption of the cell membrane, which is characteristic of the necrosis process, confirming once again the previously obtained results on this extract.

Cell death study was finally completed analyzing the activation of caspases (the specific proteases activated in the apoptosis mechanism). Caspase 3/7 executioners and the initiator caspase 8 levels were measured in protein lysates of colon cancer cells after marine treatment for 24 h and were compared to untreated controls. Among the four extracts, CR, PS and NB were able to increase considerably caspases 3/7 and 8. Differences between them were observed, exhibiting NB the greatest ability to activate caspase 8. However, PS increased considerable higher executioner caspases 3/7 levels than NB and CR indicating a different mechanism of cell death (**figure 5 A-B, chapter 2**).

CH2_3. Marine extracts stimulate intracellular ROS and mitochondrial membrane depolarization.

In this study, we determined whether marine extracts modify oxidative stress through ROS increase [191]. Using 2',7'-dihydrodichlorofluorescein diacetate (DCFH-DA) assay, intracellular ROS levels were measured. ROS were found consistently increased in a dose-dependent manner after CR, PS, NA and NB treatment for 24 h (**figure 4 A-D, chapter 2**). Among the four extracts, NB exhibited the highest levels, increasing to 4.5-, 12.6- and 10.1-fold in HGUE-C-1, HT-29 and SW-480 cells, respectively, compared to the control at the maximum concentration tested, i.e., 10 µg/mL

Metabolic stress triggered by intracellular ROS is a factor related to compromise mitochondrial function, therefore it was considered to study changes in the mitochondrial membrane potential (MMP) after marine extracts treatment of colon cancer cell models (**figure 4 E-H, chapter 2**). Changes in MMP were measured by flow cytometry using the MUSE cell analyzer which indicates the number of depolarized live cells (Dep_Live) and depolarized dead cells (Dep_Dead). A high ratio of Dep_Live to Dep_Dead cells suggests an apoptotic-mediated mechanism, and a low ratio of Dep_Live to Dep_Dead cells would represent a necrotic process. In general, our data showed CR, NA and NB increased the proportion of depolarized cells in a dose-dependent manner compared to untreated cells. These results would indicate a progressive disruption in the mitochondrial membrane associated to an apoptotic way. On the contrary, PS decreased the ratio Dep_Live/Dep_Dead cells indicating a sharp mitochondrial membrane depolarization and the induction of a different mechanism of cell death like necrosis.

Changes of MMP were confirmed using an alternative technique, such as the measurement of the ratio between two mitochondrial fluorescence probes, i.e., MitoTracker Red, which identifies viable mitochondria, and MitoTracker Green, which labels all mitochondria, as described in the **supplementary information of chapter 2**.

CH2_4. Marine extracts stimulate damage DNA in human colon cancer cell lines.

ROS imbalance produce oxidative stress and disrupt homeostasis of a variety intracellular processes. One of the direct consequences of an uncontrolled ROS increase is DNA damage which can be detected through the H2A.X protein activation. After marine extracts treatment, H2A.X was activated substantially by the four marine extracts (**figure 6, chapter 2**).

CH2_5. Characterization of marine invertebrate extracts using HPLC-ESI-TOF-MS.

CR, PS, NA and NB extracts were analytically characterized using HPLC-ESI-TOF-MS in both positive and negative modes, as described in determination of secondary metabolites by HPLC-ESI-TOF-MS in the Methodology section. Their Base Peak Chromatograms (BPCs) are depicted in **supplementary information of article 2 in scientific production section**, and peaks were identified using the approach described in the Materials and Methods section.

This nontargeted approach allowed us to identify 24 compounds in PS, 25 compounds in NA, 31 compounds in NB and 21 compounds in the CR extract. These compounds belonged to different chemical classes, i.e., terpenes, peptides, fatty acids, alkaloids and polyketides, among others and accounted for 98 different metabolites (**tables 3, 4, 5 and 6 of chapter 2**)



THE SUMMARIZED RESULTS OF CHAPTER 3

New Mammalian Target of Rapamycin (mTOR) Modulators Derived from Natural Product Databases and Marine Extracts by Using Molecular Docking Techniques

CH3_1. Screening of compounds based on the docking to ATP and the Rapamycin Binding site of the mTOR Catalytic Domain.

As described in the introduction, mTOR is a molecular target involved in cell metabolism, growth, proliferation and survival that is directly related to cancer, obesity and aging. mTOR functions via two multiprotein complexes, mTORC1 and mTORC2. mTORC1 is characterized by be regulated by PI3-K/Akt and to be sensitive to rapamycin. mTORC2 is sensitive to growth factors and is characterized to be no sensitive to rapamycin. First step was to create a library containing 484,527 compounds. Among these substances, 14,442 were from Marine Natural Products [187], 144,766 were obtained from ZINC natural products [192] and 325,319 from the Super Natural II [193] databases respectively. Then, candidates for further studies were selected using a selection criteria based on a low variation of the Gibbs free energy ($\Delta G \leq -11$ kcal/mol) by the ATP and rapamycin binding sites of mTORC. When rapamycin binding site was analyzed, 692 compounds from Marine Natural Product, 22,635 from the Super Natural II and 142 from the ZINC natural product database were selected. When ATP binding site was analyzed only 23 compounds from the marine natural product database and a 107 from the Super Natural database were found.

After this first selection, suitable ADMET (absorption, distribution, metabolism, excretion, and toxicity) parameters were analyzed by a gaussian distribution: the total surface area (A), topological polar surface area (B), calculated LogS (C), molecular weight (D), calculated logP (E), hydrogen-bond acceptors (F), violations of Lipinski's rule of five (G), hydrogen-bond donors (H), drug likeness (I), drug score (J), calculated Caco-2 permeability (K), calculated rat acute toxicity (L), calculated *Tetrahyena pyrifomis* toxicity (M),

and calculated fish toxicity (N). Only compounds that comply the fourteen parameters were selected (**figure 2, chapter 3**). After applying all these parameters, 6 compounds were selected for ATP binding site of mTOR from the Marine Natural Product database and 45 from the Super Natural II database. In the other hand, for rapamycin binding site, 137 compounds were selected from the marine natural product database, 99 from ZINC natural products and 209 from the Super Natural II database.

Among selected, high structural diversity was found and were grouped in twenty-six compounds for the ATP binding site and a hundred and six for rapamycin binding site. Gibbs free energy variation was calculated for chosen compounds and two conclusions were obtained compounds had an almost identical affinity to the ATP binding site of mTOR and PI3K (related to mTOR pathway) and also affinity was relatively low. So we decided to use compounds against rapamycin binding site.

The third filter was commercial availability (adequate quantity and affordable price) to develop *in vitro* experiments. To select the compounds, the definition of clusters of compounds (with up to 70% identity in their structure) was the criteria followed and let us to choose at least one representative compound for its chemical structure. Taking everything into account, molecular docking analysis led us to select 11 compounds against the allosteric rapamycin binding site of mTOR (**figure 24**).

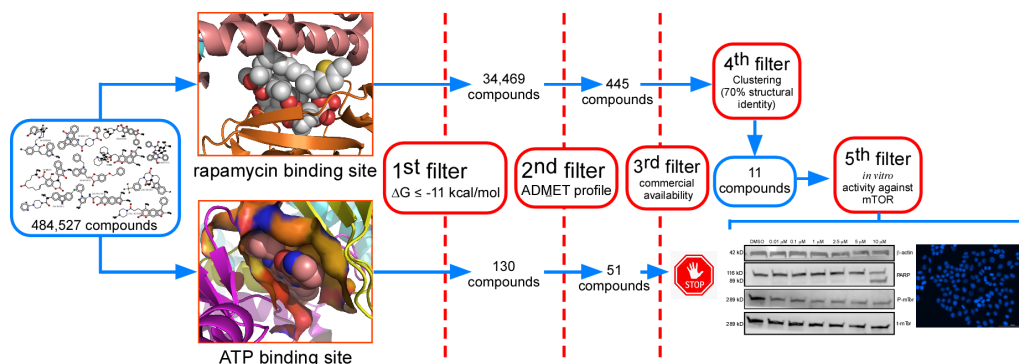


Figure 24. Graphical abstract Chapter 3.

CH3_2. Cytotoxic activity of selected compounds based on the docking to ATP and the Rapamycin Binding site of the mTOR Catalytic Domain in the human colon cancer cell model HCT-116.

HCT-116 cells were treated with selected compounds at different concentrations (0-20 μM) for 24 h and cytotoxic was evaluated using the MTT assay and counting nuclei using the fluorescent stain Hoechst 33342. 20 μM of compounds and rapamycin were toxic for all compounds. Based on non-toxic concentrations, compounds were classified different groups. SN00078968 compound which showed the maximum non-toxic concentration at 0.1 μM , SN00097418 at 1 μM , compounds ZINC09531209, ZINC08918463, SN00081767, ZINC13623590, and ZINC09530812 at 5 μM , and finally, compounds SN00111586, SN00150533, SN00082651, and SN00113250, concentrations at 10 μM (**figure 6, chapter 3**).

CH3_3. Modulating effect by selected compounds in mTOR.

Screening of up-regulation or down-regulation of mTOR by selected compounds was studied by the Western blot assay using phospho-mTOR (Ser2448) rabbit monoclonal antibody which detects P-Ser2848 in mTOR. The 11 selected compounds were able to inhibit the expression of mTOR between 20 to 40% in comparison to the control (**figure 7, chapter 3**).

CH3_4. Modulating effect of three marine invertebrate extracts on the activity of mTOR.

We studied the ability of three marine invertebrate complete extracts (CEs) modulating mTOR and were compared to docking selected compounds by the Western blot assay. Marine extracts were composed by a soft coral (CR), an holothurian (PS) and a nudibranch (NA) described in previous sections of this thesis. Concentrations were adjusted by MTT assay to be effective without being toxic to 10 $\mu\text{g/mL}$ (CR extract), 1 $\mu\text{g/mL}$ (PS extract), and 5 $\mu\text{g/mL}$ (NA extract).

mTOR modulating activity by marine extracts was analyzed by Western blot. Surprisingly, CR and PS extracts activated mTOR activity more than 50%, whereas NA reduced activation of phospho-mTOR a 40% (**figure 8, chapter 3**).



THE SUMMARIZED RESULTS OF CHAPTER 4

A Nudibranch Marine Extract Chemosensitizes Selectively Colorectal Cancer Cells inducing Endoplasmic Reticulum Stress mediated by ROS.

In the previous study (chapter 2: Marine invertebrate extracts induce colon cancer cell death via ROS-mediated DNA oxidative damage and mitochondrial impairment) results of marine invertebrate screening by its cytotoxic activity were shown. Data obtained from this project revealed the extract from the nudibranch (*Dolabella auricularia*, NB) showed a potent antiproliferative effect through oxidative stress (intracellular ROS increase), generating DNA damage, mitochondrial depolarization and cell cycle arrest in G2/M phase. These results showed the interesting anticancer potential of the NB extract and rise the need to study in depth the mechanism of action of this extract.

CH4_1. NB extract inhibits selectively the human colon cell line HCT-116 and less the fibroblast colon cell line.

The first point to study was to elucidate if NB exerted the same effect in the human colon cancer cell model HCT-116 and non-tumoral human colon fibroblast cell model CCD-18Co. After treatment of both cell lines with NB extract at different concentrations for 24 h, MTT assay was performance to calculate IC₅₀ values. Data showed interesting results because NB was able to inhibit cancer cell line proliferation at lower doses than the normal (HCT-116 IC₅₀: 1.01 ± 0.19 µg/mL versus CCD-18Co: 15.04 ± 1.38 µg/mL). To complete antiproliferative NB information, survival or clonogenic assay and RTCA proliferation assay in the human colon cancer cell line (HCT-116) were performance. NB at the lowest concentration of 0.5 µg/mL was able to reduce the average size to a 92% and a 62% the number of colonies of HCT-116. In turn, NB also plummeted the proliferation profile of HCT-116 obtained by RTCA proliferation assay at 0.5 µg/mL (**figure 1, chapter 4**).

CH4_2. NB extract increased intracellular ROS and activated Endoplasmic Reticulum (ER) stress related proteins in colon cancer cell lines.

Intracellular ROS level was increased in a dose- and in a time-dependent manner in HCT-116 cancer cell line. Whereas in colon cancer cell lines increased to a 2.3 fold at 5 µg/mL of NB respect to the untreated HCT-116 cells only a 1.1 fold was done in normal cell line CCD-18Co.

Endoplasmic Reticulum (ER) stress was also measured after NB treatment for 24 h by Western blot in colon cancer cell lines. Results indicated NB after 1-3 h of treatment increase the expression of the ER stress related proteins such as phospho-IRE1 α , phospho-JNK, phospho-eIF2 α , ATF4 and CHOP compared total and β -actin and persisted to 24 h (**figure 2, chapter 4**).

CH4_3. Analysis of NB extract effect in cell cycle distribution and apoptotic cell death in colon cancer cell lines and its relation to ER stress.

Cell cycle distribution of the human colon cancer cell line HCT-116 was compared to normal colon cell line CCD-18Co after NB treatment for 24 h. Data revealed NB at 10 µg/mL possess a strong ability to accumulate cells in G2/M phase to $89.12 \pm 0.52\%$ in treated cells versus $28.91 \pm 1.29\%$ in untreated HCT-116, whereas in CCD-18Co the increase was to $33.49 \pm 3.68\%$ at 10 µg/mL versus $18.91 \pm 2.72\%$ in untreated cells. These data suggest that the ability of NB to induce G2/M was higher in colon cancer cells than in normal cells. In addition to G2/M arrest, NB caused an increase in subG1 phase (cell death) in HCT-116 and CCD-18Co, however, the highest percentage was low not overcoming the 5% (**figure 3 a, c and d, chapter 4**).

To study the relationship between ER stress and the apoptotic cell death induced by NB, the cell permeable caspase inhibitor that blocks the activity of caspase proteases and inhibits apoptosis, z-VAD-fmk (z-VAD) was used. This assay let us to know that caspases orchestrate a part of cell death induced by NB but it not seems to be related to ER stress induced. Among caspases studied, 3/7 and 8 intervened in the process of apoptosis promoted by NB at 24 and 48 h. SiRNA silencing C8 and C9 assay confirmed C8 (extrinsic apoptosis) was

activated by NB inducing cell death and modulating phospho-IRE1 α and phospho-JNK ER stress markers however ATF4 and CHOP (highly activated by NB) did not respond to C8 activation. Additionally, it was studied the possible relation between cell cycle arrest in G2/M with caspases activation. Results showed G2/M arrest was non-dependent of caspases activation. Meaning, the cell cycle arrest in G2/M is not directly related to apoptosis induced by NB (**figure 3 e-f, chapter 4**).

CH4_4. Analysis of NB extract effect in non-apoptotic death in colon cancer cell lines.

We studied the contribution of non-caspases dependent cell deaths such as necrosis, necroptosis and autophagy induced by NB to tumor cell lines. Results showed any of these kind of cell deaths were not contributing to the cell death and the cell cycle arrest in G2/M observed was not influenced by this kind of cell death after NB treatment (**figure 4 a-e, chapter 4**).

CH4_5. Relation of ER stress and oxidative stress. What is the first effect of NB: the ER stress or the oxidative stress?

To study ER stress and oxidative stress involvement in NB effect the ROS scavenger N-acetyl cysteine (NAC, 5 mM) and the ER stress inhibitor 4-Phenylbutyric acid (4-PBA, 5 mM) and its combination were used. If ER stress was a direct effect of NB and occurred before the increase in ROS, by inhibiting ER stress produced by NB with 4-PBA, it should be noted that intracellular ROS does not accumulate after treatment and G2/M, H2A.X and early apoptosis would be diminished after NB treatment exposure. On the other hand, if ROS were the main cause of NB effect, by using NAC it would be expected to see a reduction of altered parameters. Finally, if both stresses (ROS and ER stress) have an important role, the combination of NAC and 4-PBA would show the best results resetting altered parameters. Data obtained revealed the antioxidant NAC reduced cell death and the expression of phospho-JNK and the transcription factors ATF4 and CHOP, suggesting that ROS are directly

related to this ER-stress markers. By contrast, although the ER stress inhibitor (4-PBA) or the combination 4-PBA plus NAC did not reduce cell death, the inhibition of ER stress markers such as phospho-IRE1 α and phospho-JNK was produced. Therefore, these results suggest that ROS are the main quasantes of the effect of NB, through the induction of phopho-JNK, ATF4 and CHOP and as a consequence they could induce the activation of other targets of the stress of the reticulum as phospho-IRE1 α (**figure 5 a-e, chapter 5**).

CH4_6. Relation between ER stress and ROS response in superinvasive HCT-116 populations.

When ER stress and oxidative stress levels are high they can orchestrate cell death, by contrast tolerable levels paradoxically can promote tumor progression [194, 195] as described in introduction. In this part of the study, the effect of NB in the invasive HCT-116 populations was analyzed trying to correlate ROS level and invasive properties.

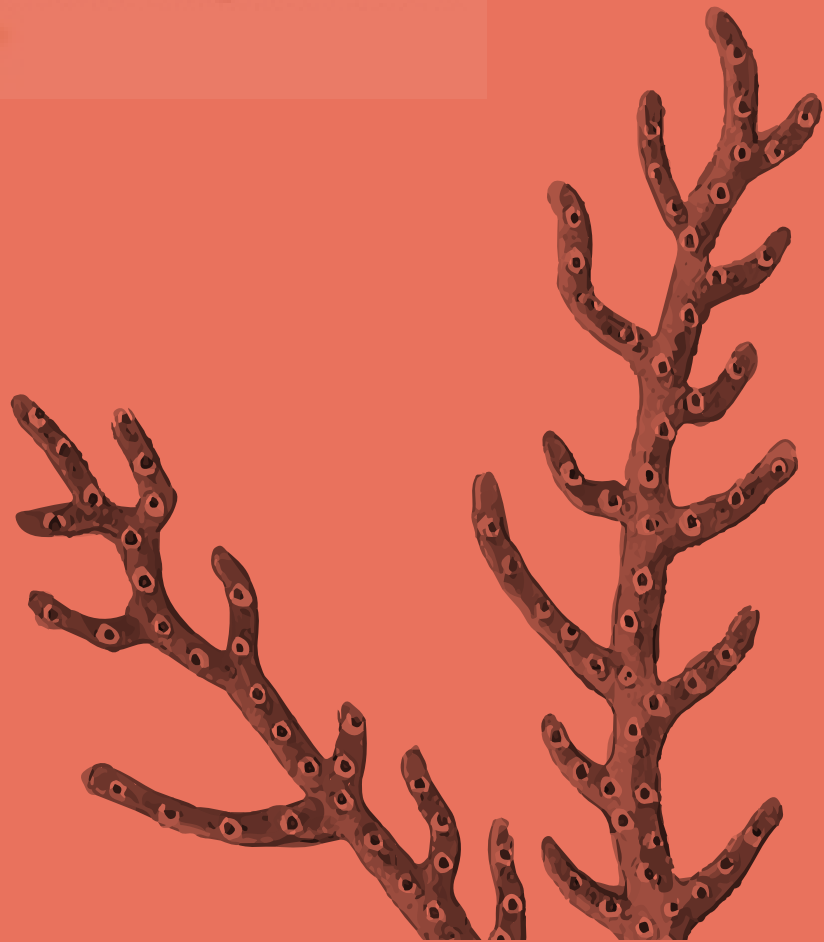
First step consisted in isolating superinvasive populations using Boyden chambers (CorningTM BioCoatTM MatrigelTM Invasion Chamber with BD Matrigel Matrix 6 plates) (for more details see material and methods section). In this sense, HCT-116 superinvasive populations I4 and I9 cells were isolated. Proliferation, migration and invasion rate was compared for I4, I9 and Parentals (P, wild type HCT-116). Results showed the higher level of differentiation of cells, the more Cell Index of Proliferation (CIP), Migration (CIM) and Invasiveness (CII) presented. Next step consisted of to compare ROS and ER stress levels in superinvasive populations. As expected, the ER stress-related proteins (checked by Western blot) and ROS levels (by DCFH-DA fluorescent label) were up-regulated as the higher degree of invasiveness. After characterizing the basal parameters of the superinvasive populations, the next objective was to study the effect of NB in the new cellular models. RTCA assay let us to register a considerably reduction of CIP, CIM and CII of superinvasives and parentals HCT-116 cell lines after NB treatment for 48 h at 0.001 $\mu\text{g}/\text{mL}$ (**figure 6 a-f, chapter 5**).

Takin into account the more invasiveness the more intracellular ROS levels and the more ER stress is shown, the final point was to study how affects NB to these differentiated superinvasive populations. What happens to the cells which show a higher stress level when is more increased for example with NB extract? To answer this question, the effect of NB combined with NAC and 4-PBA in the invasiveness of HCT-116 superinvasive populations was studied. When ROS was inhibited by NAC, the CII was reset by 18.6% in P, 59.3% in I4 and 82.4% in I9. When ER stress was inhibited by 4-PBA, the invasion rate was also recovered by 48.9% in P, 95.2 % in I4 and 85.0 % in I9. The combination of both stress inhibitors reversed more the inhibitory effect of NB extract by 49.3% in P, 83.6% in I4 and 122.6% in I9. Thus, these data suggest the anti-invasive effect of NB happens inducing mainly oxidative stress but also ER stress in superinvasive cell models (with high basal stress levels) and when scavenger stressors are used, highly metastatic cells recover its invasive ability (**figure 7 a-g, chapter 5**).





Discussion



Doctoral Student:
Verónica Ruiz Torres

Given the current need to find new molecules against cancer that enable the discovery of more effective treatments without side effects or cancer drug resistance, marine compounds are proposed as potential means to meet this challenge. In this context, the present thesis demonstrates the antiproliferative potential of marine extracts in colon cancer research by identifying the main bioactive compounds that compose the selected extracts, studying their antiproliferative ability by characterizing their effect on the cell cycle and the type of cell death they induce, exploring their role in the deregulation of the PI3K/Akt/mTOR metabolic pathway, their antiproliferative effect in highly metastatic colon cancer lines and their relationship to cellular stress.

Marine invertebrate compounds as potential antitumor drugs: what have they contributed thus far, and what could they provide?

In chapter 1: “**An Updated Review on Marine Anticancer Compounds: The Use of Virtual Screening for the Discovery of Small-Molecule Cancer Drugs**”, we analyzed the data available through 2017 on marine natural products (MNPs) that have been established and marketed as antineoplastic drugs and as new candidates for use in preclinical phases, their chemical structures and their related mode of action against cancer hallmarks.

In this review, we examine a wide variety of chemical marine compounds or derivatives with antiproliferative activity in cancer. Most MNPs have been classified into alkaloids, polyketides, terpenes, peptides, and carbohydrate chemical classes. One of the main chemical differences between marine and terrestrial natural products (TNPs) relates to the size and solubility of the molecules. Shang *et al.* [196] pointed out that MNPs, in general, have lower solubility due to the presence of longer chains and larger rings than are found in TNPs. They verified that MNPs feature 8- to 10-membered rings and have more nitrogen atoms and halogens, bromines, and fewer oxygen atoms; in contrast, many TNPs are smaller and have ring systems and bonds that are more stable. Another important MNP characteristic is their chemical novelty and complexity, which are superior to those of the TNPs. Kong DX. *et al.*

reported that 71% of molecular scaffolds in the Dictionary of Marine Natural Products were used only by marine organisms [170] and suggested that MNPs have complex pathways and synthesis processes that are more complex and diverse than those of the TNPs. These complex structures and chemical diversity, achieved through optimization of the bioactive molecules for survival through lengthy evolution, make MNPs attractive sources for drug discovery [197, 198].

Data obtained to generate this review reflect an increasing interest in MNPs in the fields of pharmacology, toxicology, biochemistry, genetics, molecular biology and medicine over the last twenty years. In particular, six of the eight clinically approved drugs and the vast majority of compounds in clinical and preclinical trials are applied in cancer therapy [187]. **Cytarabine** is a novel approved MNP. This antimetabolite drug combined with antileukemic agents was better able to attain high remission rates compared to other drugs used in children with different acute myeloid leukemia phenotypes, revolutionizing treatments that had been available since the 1960s [199]. **Trabectedin** shows a novel and complex mechanism because it interacts with the minor groove of the DNA double helix and allows the interaction with nuclear proteins. Trabectedin disrupts several transcription factors, DNA binding proteins and the DNA repair system in a novel way compared to the other DNA-interacting agents [200]. This compound was approved by the EMA for advanced soft tissue sarcoma in 2007, after the failure of anthracyclines and ifosfamide, and for the treatment of relapsed ovarian cancer. Some studies confirmed that trabectedin causes clinical benefits in some histological cancer subtypes, significantly increasing survival [201]. **Eribulin**, a synthetic analog of halichondrin B (from the sponge *Halichondria okadaï*), has been used as a monotherapy, known as Halaven[®], for the treatment of metastatic breast cancer. A novel aspect of this compound is that eribulin is the only anticancer drug used in the last decade to show increased overall survival with an acceptable toxicity profile in breast cancer patients who had been pretreated with extensive chemotherapy. Halaven[®] seems to depolymerize microtubules as its main

mechanism of action. In phase III trials, this compound demonstrated improved survival in different patient subgroups, including women with Human Epidermal Growth Factor receptor 2 (HER2)-negative and triple-negative breast cancer, creating a new paradigm for the treatment of breast cancer [202, 203]. **Dolastatin 10** from the sea hare *Dolabella auricularia* led to the development of brentuximab vedotin (Adcetris®). This compound was fast-tracked for approval by the FDA in 2011 based on its efficacy and safety as a single agent that led to complete remission in 33% and tumor reductions in 94% of Hodgkin lymphoma patients [204]. Adcetris® selectively targets malignant Hodgkin and Reed-Stenberg cells [205]. Many other marine-derived compounds in the clinical and preclinical pipelines offer interesting results for future drug development. The discovery of these new drugs offers an available arsenal to face the therapeutic challenges posed by cancer.

A significant contribution of our research has been the generation of a marine natural compounds database (<http://docking.umh.es/chemlib/mnplib>) performed by computational methods based on computational methods on protein-ligand interactions. Weight, cLogP, cLogS, rotatable bonds and other parameters, such as molecular flexibility and oral bioavailability, were compared among 14,442 MNP compounds and 168 anticancer compounds tested by the “Genomics of Drug Sensitivity in Cancer” project, with the results showing that MNPs have great potential as anticancer compound candidates. Fang *et al.* [206] developed a model to predict the interaction of natural products (NPs) with new drug targets, and the results showed 7314 interactions linked to 751 targets and 2388 NPs. This approach enabled them to identify drug target interactions and make drug safety predictions. Hongyi Zhou *et al.* [207] developed a model based on a proteome scale approach with related protein targets and side effects. This model identifies unexpected drug-protein interactions and provides a prefilter to the academic community to use in new drug development. Taking in mind all these advance, computational screening has the potential to prevent drug side effects [208], increase drug efficacy [209], repurpose drugs [210] and design multitarget molecules [211]. Given the state

of the art of MNPs, we can conclude that marine compounds are largely untapped sources for the generation of new anticancer drugs.

In vitro screening studies as essential tools in the search for new marine invertebrate extracts with antiproliferative activity to add to the drug discovery pipeline.

In chapter 2, “**Marine invertebrate extracts induce colon cancer cell death via ROS-mediated DNA oxidative damage and mitochondrial impairment**”, we showed the potential ROS-mediated antiproliferative activity and characterized the composition of 4 marine invertebrate extracts: two nudibranchs (*Phyllidia varicosa*, NA, and *Dolabella auricularia*, NB), a holothurian (*Pseudocolochirus violaceus*, PS) and a soft coral (*Carotalcyon* sp., CR). The objective of this study was to screen 20 marine invertebrates extracts with antiproliferative potential to select the most active ones and further characterize the mechanism(s) involved in their antiproliferative effect, to elucidate the molecular targets potentially affected in colon cancer cells and to find the main compounds involved in this mechanism.

CR, PS, NA and NB strongly inhibited cell viability, triggered pronounced induction of G2/M arrest and damaged DNA in colon cancer cell models at low doses. Girish Beedessee *et al.* [212] showed in their study that an ethyl acetate extract of the Mauritian invertebrate sponge *Jaspis* sp. had a very low IC₅₀ value, 0.06 µg/mL (72 h), in acute myeloid leukemia HL-60 cells, as well as mitochondrial membrane depolarization, DNA fragmentation and G2/M cell accumulation. The criterion for cytotoxicity considered in the research of Girish Beedessee *et al.* was in accordance with that of the National Cancer Institute, which has documented the activity of crude extracts with IC₅₀ value less than or equal to 20 µg/mL in the initial stages. Comparing these data to our results, the *Dolabella auricularia* extract showed the lowest IC₅₀ values among the four extracts examined (from 0.6 to 0.1 µg/mL). However, PS, NA and CR also displayed very interesting IC₅₀ values: PS from 37.4 to 0.7 µg/mL, NA from 61.8

to 10.0 µg/mL and CR from 82.0 to 9.4 µg/mL in different human colon cancer cell lines.

A wide variety of studies have shown the ability of MNPs, from the same chemical class as our extracts, to damage DNA, initiate p53-dependent and p53-independent blocking of the G2/M checkpoint, which prevents mitosis [213-218]. Sinularin is a cembranoid MNP isolated from the soft coral *Sinularia flexibilis* by Weinheimer *et al.* in 1977, which shows antiproliferative activity in epidermoid carcinoma, P388 lymphocytic leukemia, human gastric carcinoma and melanoma cells [219-221]. Sinularin exhibits antiproliferative activity by damaging DNA and arresting the cell cycle in the G2/M phase in association with an increase in the Ataxia Telangiectasia-Mutated (ATM)-checkpoint kinase 2 (Chk2)-Cdc25C axis. ATM is a well-conserved protein throughout the evolutionary pathway that controls the maintenance of genome integrity and cell cycle checkpoints by inducing cell cycle arrest and DNA repair. The cytotoxic activity of sinularin is also correlated with the induction of mitochondrial apoptosis through Bcl-2 and disruption of the mitochondrial membrane potential [222]. Our results showed that the soft coral *Carotalcyon* sp. contains the multioxygenated cembranoid sinulariaoid D, which seems to have the same mechanism of action as sinularin.

Dolabella auricularia is known for its cytotoxic effects and is composed of dolastatin peptides, which are involved in inhibited microtubule assembly and in the treatment of solid tumors. Dolastatins 10 and 15 are considered the most potent contributors to the antiproliferative activity of NB extract. Dolastatin 15 is known to induce G2/M cell cycle arrest in different human myeloma cell lines and to promote apoptosis [223]. Therefore, it is possible that some peptides of the NB extract contribute to its antiproliferative activity and lead to DNA damage and cell cycle arrest in G2/M.

Interestingly, CR, PS, NA and, more intensively, NB extracts induce much greater intracellular ROS production in tumoral cells than normal cells, and these high levels are produced concomitantly with cell cycle arrest and accumulated DNA damage. Several reports have suggested that marine

compounds and some derivatives, such as psammaphin A and bromophenol (phenolic compounds) or soblidotin (a peptide derived from dolastatin 10), obtained from invertebrates inhibit the proliferation of cancer cells by damaging DNA or blocking repair processes, subsequently inducing increased production of ROS and disrupting microtubule stability, making them promising anticancer agents [224-226]. In 2018, Liang-Mou Kuo *et al.* [227] discovered an extract from the marine gorgonian *Pinnigorgia* sp. with antiproliferative capacity that inhibits cell viability and induces apoptosis of HCS-T6 cells (rat hepatic stellate cell line), DNA fragmentation, caspase-3 activation and ROS production in a concentration-dependent manner. In this study, three pure secoosterol compounds (steroids) from the *Pinnigorgia* sp. were isolated: Pinnigorgiol A-C. Among these compounds, Pinnigorgiol A showed the strongest inhibitory effect on HSC-T6 cells and increased ROS, so it was proposed as the main responsible compounds that mimics the effect of the whole extract. Research in this area suggests that marine extracts and pure compounds such as steroids and peptides are the main inductors of ROS accumulation and agents of DNA double-strand breaks, which cause cell cycle arrest. NA and NB contain a high proportion of steroids among their identified compounds, which led us to propose this class of compounds as those responsible for the observed biological activity that is similar to the mechanism of action reported by the authors cited in the bibliography.

Our results demonstrated that NB, NA and CR marine extracts induce apoptotic mechanisms by increasing early apoptotic cell proportion, which depends on caspase activation and DNA fragmentation. Apoptosis is one of the targets in cancer research because it offers advantages over nonapoptotic cell deaths. In certain drug-curable malignancies, such as pediatric leukemia, apoptosis seems to be the prominent factor in tumor remission [228]. Interestingly, the expression of apoptotic activators in cancer cells seems to be correlated to cancer cells with a high sensitivity to apoptosis, as has been shown in many traditional cancer therapies. These results indicate that the ability of NB, NA and CR extracts to induce apoptotic cell death may deserve further

attention for anticancer strategies [230]. In contrast, the PS extract induces typical features of necrosis [231] but also activates caspases, as is typical in apoptosis. Although it has been traditionally believed that apoptosis is the preferred means for drug-induced cell death and a desired outcome criterion used for drug discovery, it has been increasingly accepted that other kinds of cell death may be useful in chemotherapy. It has been shown that, in some cancers with a defective apoptotic cell death pathway, cytostatic and cytotoxic agents induce alternative cell death, such as necrosis, mitotic catastrophe, senescence and autophagy, and thus play a relevant role in chemotherapy treatment [232-235]. Chew Hooi Wong *et al.* [236] reported the ability of compound 1,3-dibutyl-2-thiooxo-imidazolidin-4,5-dione to induce noncanonical autophagy and apoptosis in the human colorectal cancer cell line HCT-116 via ROS production and extracellular regulated kinase (ERK) and c-Jun N-terminal Kinase (JNK) activation. Several studies have demonstrated the ability of several natural compounds to generate ROS and induce different types of cell death [237-239]. For instance, research from our group showed that rosemary terpenes promoted the generation of the intracellular ROS that resulted in necrotic cell death in human colon cancer cell lines. It seems that ROS are the links between all these effects, making them the key factors in the mechanism of action of CR, PS, NA and NB extracts.

The chemical composition of the most active extracts was analyzed by using HPLC-ESI-TOF-MS. A complex variety of metabolites were found and classified as terpenes, peptides, fatty acids, alkaloids and polyketides, among others. A total of 99 compounds were identified. Among the identified compounds, several had been previously found in marine ecosystems, a few were identified for the first time, and others were also found in terrestrial habitats. Some compounds of the nudibranch *Dolabella auricularia*, the holothurian *Pseudocolochirus violaceus* [240-243] and the nudibranch *Phyllidia varicosa* [244, 245] have been chemically characterized. However, very little information has been found on the composition of the soft coral *Carotalcyon* sp. The most researched compounds from *Dolabella auricularia* are the

glycoproteins dolabellans A, C, E and P [246], the depsipeptides dolastatins (specially dolastatin 10 and 15) [247] and the protein hemocyanin [248]. Although the best-known compounds of this nudibranch were not characterized in our analysis, our research is one of the few that lists the various compositions of the whole extract of this organism, with fatty acids, steroids and terpenes identified as the main compounds of *Dolabella auricularia* extracts.

Previous research on *Pseudocolochirus violaceus* shows that this organism is rich in terpenes such as sulfated triterpene glycosides, i.e., violaceosides I, II, and III [249]. Our chemical analysis also revealed a high content of diterpenes; however, we provide a complete characterization of the whole extract of this organism in which fatty acids and alkaloids are also abundant.

Reports on *Phyllidia varicosa* show that the most abundant compounds are two 9-thiocyanatopupukeanane sesquiterpene isomers isolated from the methanolic extract of this organism [244]. Our research on the composition of *Dolabella auricularia*, *Pseudocolochirus violaceus* and *Phyllidia varicosa* is the first to be published on the characterization of the complete extracts of these organisms. Our data also show that *Phyllidia varicosa* is rich in fatty acids, phospholipids, macrolides and terpenes.

The analysis of the chemical composition of the four marine extracts reveals a high proportion of fatty acids for all four of them. These compounds are typically isolated from marine bacteria and green and red algae and are also found in marine invertebrates such as sponges and corals [250, 251]. It is common that corals and sponges have compounds typically found in algae because they filter water and contain symbionts that contribute to the synthesis of these compounds. Furthermore, nudibranchs and holothurians are predators of sponges and corals, so it is not unusual to find this type of compound in them [252].

Another large group of compounds found in the four marine extracts studied in this work consists of those that belong to the terpene and diterpene families, such as spongian-16-one, which is found in large quantities in the extract of soft coral CR and in the nudibranchs NA and NB. This compound has

been previously described in the Australian nudibranch and marine sponges of the orders *Dictyoceratida* and *Dendroceratida* [253].

Steroids such as punicinol D in *Carotalcyon* sp. and trofoside A in the *Dolabella auricularia* are also important constituents of these extracts. Punicinol D is an active compound isolated from a gorgonian octocoral, and it inhibits the proliferation of and induces cytotoxicity in A549 cells *in vitro* [254]. Trofoside A was previously isolated from starfish [255].

Phospholipids such as 1-O-hexadecyl-sn-glycero-3-phosphocholine (lyso-PAF) were also found in the coral extract CR and nudibranch NA. Lyso-PAF is a major compound of lipids with marine origins, and it has been found in relative abundance in the marine sponge *Spirastrella abata*. Its inhibitory activity against cholesterol biosynthesis in human cells has been reported [256].

The alkaloids were another of the main groups found in the analyzed marine extracts. Specifically, an analog of the compound ecteinascidin was found in the holothurian PS extract [257].

Amino alcohols were also found among the characterized compounds in the marine extracts. The 2-amino-1,3-hexadecanediol was identified in the holothurian PS extracts and was previously isolated in marine endophytes from the red sea algae *Acanthophora dendroides* and the brown alga *Sargassum sabrepandum* extracts [258].

Due to their significant abundance in the coral extract (CR), the phospholipid lyso-PAF and the diterpene spongian-16-one would be candidate compounds to contribute to the antiproliferative activity of the extract. The physiological lipid lyso-PAF has not exhibited anticancer effects before but is able to modulate cell membrane physical properties. In this regard, lyso-PAF has shown a stronger disruptive effect on promyelocytic leukemia HL-60 cell model membranes than the anticancer agent edelfosine [259], and it has an anti-angiogenic role in human breast cancer cells [260]. The anticancer effects of spongian-16-one will be discussed in more detail below.

In the holothurian PS extract, the natural cembrane lopholide and the ecteinascidin analog were the major identified compounds. The cytotoxic activity against the breast cancer cell model MDA-MB-231 through apoptosis induction has been reported for cembrane diterpenes isolated from the extract of the colonial cnidarian sea pen *Virgularia gustaviana* [261]. The cembrane diterpene lopholide analogs isolated from Gorgonian *Lophogorgia peruana* inhibited the growth of various cancer cells at different concentrations: from 14.5 to 2.7 μM for MDA-MB-231 breast cancer cells, from 17.9 to 2.9 μM for human epithelial carcinoma A-549 cells and from 14.7 to 2.4 μM for human colon cancer HT-29 cells [262]. Our results showed promising IC_{50} values using the CR extract in human colon cancer cell lines: 58.1 $\mu\text{g/mL}$ for HGUE-C-1 cells, 10.6 $\mu\text{g/mL}$ for HT-29 cells and 14.8 $\mu\text{g/mL}$ for SW-480 cells.

In the case of the NA extract, the compounds that are fairly abundant and may be responsible for the extract activity are the saturated fatty acid derivatives such as hexadecanoic acid, chlorophyll ethyl pheophorbide A and pentadecanoic acid. Fatty acids isolated from the Antarctic macroalgae *Adenocystis utricularis*, *Curdia racovitzae*, and *Georgiella confluens* were reported as inhibitors of the growth of human breast cancer MCF-7 and MDA-MB-231 cells [263]. The phospholipid 1-O-hexadecyl-sn-glycero-3-phosphocholine (lyso-PAF), also found in the CR extract, and the diterpene spongian-16-one [264], found in the NA extract, were previously shown to have antitumor potential [259, 260].

Finally, the most abundant compounds in the extract of nudibranch NB were the diterpene spongian-16-one (also found in the NA and CR extracts), the methyl ester pyropheophorbide A and the fatty acid 9,12-octadecadienoic acid, which have been reported to possess antiproliferative activity [264-266]. Spongian-16-one has been reported to show antiproliferative activity against a mouse lymphocytic leukemia cell line (L1210 cells, IC_{50} of 16.4 μM) and human HeLa contaminant carcinoma (KB cells, IC_{50} of 30.2 μM) but also in the human colorectal cancer cell line SW-620 (IC_{50} values $>30 \mu\text{M}$) [253]. In our study, the

NB extract showed relevant IC₅₀ values in human colon cancer cell lines: 0.1 µg/mL for HGUE-C-1, 0.1 µg/mL for HT-29 and 0.2 µg/mL for SW-480 cells. Considering that spongian-16-one is one compound in the complex mixture of the NB extract and that the IC₅₀ values obtained are low, other compounds of the extract must contribute to the observed strong antiproliferative effects of the extract.

Our results support the hypothesis that the antiproliferative activity of the four selected extracts takes place by inhibiting cell growth through G2/M cell cycle arrest, most likely because of the increase in intracellular ROS and the concomitant DNA damage, which leads to apoptosis in the case of the CR, NA and NB extracts and apoptosis and necrosis in the case of PS. Based on the abundance of the compounds in every extract, the observed antiproliferative activity of the NB extract could be attributed to the diterpene spongian-16-one, but the contribution of other minor compounds, either with synergic or additive effects, cannot be disregarded. This compound was also abundant in the CR and NA extracts and correlated with a strong antiproliferative effect and apoptotic cell death.

Another abundant compound was the diterpene lopholide in the PS extract, which could be responsible for the predominant necrotic effect of this extract. Finally, fatty acids such as tetracosapentanoic, heptadecenoic, stearic and 9,12-octadecadienoic acids and phospholipids, such as the lyso-PAF analogs in the case of the CR extract, in NA and NB might contribute to their antiproliferative effect most probably due to their capacity to modulate membrane properties. Nevertheless, further bioguided fractionation and isolation research should be conducted to confirm this hypothesis.

The importance of the development of targeted therapies against specific molecular hallmarks of cancer to reduce side effects, decrease resistance and enhance the effectiveness of treatments.

For appropriate progress in the development of anticancer drugs, treatments should be aimed at improving efficiency and preventing side effects and resistance development [267]. In chapter 3, we described the results obtained from the study, **“New Mammalian Target of Rapamycin (mTOR) Modulators Derived from Natural Product Databases and Marine Extracts by Using Molecular Docking Techniques”**. This study focused on identifying new compounds that target mTOR protein (master regulator of cellular growth and metabolism), which seems to be deregulated in many cancers. In this study, we used computational analysis (docking) to simulate the interaction between mTOR and natural compounds and then determined their effects using *in vitro* assays, comparing the results with complete extracts obtained from three different marine invertebrates.

Kinases constitute a large family of enzymes encoded by 518 genes in the human genome [268] that play important roles in a variety of cellular functions, such as proliferation, cell cycle, apoptosis, motility, growth, and differentiation, among others. Through misregulated expression, amplification, aberrant phosphorylation and mutations, altered kinases have a strong connection to different pathologies, including the survival and spread of cancer, aging and inflammatory disorders [269], making them important pharmacological targets for future drug discovery.

We analyzed the molecular docking sites for ATP and the rapamycin binding cave of mTOR with 484,527 compounds, taking into account Gibbs free energy variations (negative Gibbs free energy variation values are indicators of binding reaction spontaneity). Our results showed an interesting Gibbs free energy for 34,469 compounds with the rapamycin binding site and 130 with the ATP site. Analysis of the mTOR structure revealed that the common catalytic domain for the ATP binding site is smaller than that for rapamycin [270]; thus, the size of the binding site could explain the greater number of candidate

inhibitors for rapamycin than for ATP. Furthermore, an X-ray diffraction analysis of the kinase structure showed the existence of a catalytic domain for binding ATP and Mg^{2+} . Research showed that most kinase inhibitor drugs indiscriminately block ATP from the pockets of different kinases (low specificity), contributing to side effects [271, 272]. We compared the affinity of 40 FDA-approved drugs used for antineoplastic treatments by the ATP binding site of the catalytic domain of different kinases. We found that the affinity for the ATP binding sites of the kinase proteins was similar and quite low. These results corroborate that the ATP binding sites in kinases have low specificity [273] and suggest that the ATP binding site is not desirable for targeting specific kinases. Therefore, to inhibit mTOR kinase, candidates should target the rapamycin pocket [274].

Use of *in silico* analysis tools to find molecules with therapeutic value is an emerging method that enables us to screen thousands of compounds to find the most promising compounds at reduced costs compared with that of high-throughput experimental screening [275]. A total of 484,527 compounds were explored with this technology. The selection of appropriate cutoff filters is a critical step for the success of bioinformatics screening of optimal candidate molecules. A low Gibbs free energy variation value is commonly used as a filter for molecular docking [276-278]. An appropriate threshold of $\Delta G \leq -11$ kcal/mol enabled us to discard 89.4% of the initial compounds. Absorption, distribution, metabolism, excretion and toxicological parameters (ADMET) are also key factors in the selection of optimal molecules. Binding DB [279] is a valuable database that contains this valuable information. These statistical physicochemical and toxicological parameters are used in the second filter and reduced the number of suitable inhibitors mTOR candidates to 491 compounds (51 against the ATP binding site, which were discarded due to the abovementioned reasons, and 445 against the rapamycin binding site). The strict filters used in this study enabled us to select suitable marine compounds for *in vitro* tests, reducing the effort and achieving the expected results, validating our approach [280].

Despite the high number of emerging marine natural compounds, their restricted commercial availability limits the ability to test them. We clustered selected compounds with as much as 70% shared structural identity and tested at least one compound from each cluster. Among the final candidates, we chose eleven compounds to compare against the three marine invertebrate extracts using *in vitro* analysis. Of the eleven selected compounds, five presented strong capacity of inhibition. These compounds were characterized by a molecular weight between 400 to 500 g/mol, a high content of heterocyclic systems and high content of ketone groups and nitrogen elements in their chemical structure. On the one hand, the synthetic compounds ZINC9531209 and ZINC8918463, both with 5 rings, achieved a phospho-mTOR inhibition ranging between 35 and 45%. On the other hand, the natural compounds SN00078968, SN00111586 and SN00097418, all with 7 rings, achieved an inhibition capacity between 30 and 35%. This complex heterocyclic structure has been previously linked with mTOR inhibition by other authors. Schenone S. *et al.* [281] considered that dual PI3K/mTOR inhibitors bear pyrimidine ring combined with other heterocycles such as morpholino group in their chemical structure which is essential for enzymatic reactions. Apse B. *et al.* [282, 283] showed that two of the first selective mTOR inhibitors were pyrazolo[3,4-d] pyrimidine derivatives PP242 (torkinib) and PP30. They were characterized by having C4 – NH₂ group, a N1 isopropyl substituent and two different heterocyclic substituents on C3. These compounds exerted potent inhibition on mTORC1 and mTORC2 with IC₅₀ values of 8 nM and 80 nM, respectively and also inhibited other kinases. Despite the positive results obtained by these compounds, Hoang B *et al.* [284] reported the activation of ERK and resistance problem requires further research. This is the first study showing that *in silico* selection of potential mTOR inhibitors correlates with their inhibitory capacity in cell model.

Our results showed that the selected compounds were able to reduce mTOR activation *in vitro* by 20 and 40% and the marine extracts reduced it by 40%, while rapamycin reduced mTOR activation by 60% under the same

conditions. Of the three marine extracts studied in this work, two of them (CR and PS) showed to up-regulate mTOR activity and one (NA) to down-regulate. The inhibitory effect of the nudibranch extract (NA) achieved a difference of 40% with respect to the control. Although there are no reports of marine extracts from nudibranchs with mTOR inhibitory capacity, this activity has been reported for other marine organisms. Notoamides, alkaloids obtained from the coral-associated *Aspergillus ochraceus* fungus induced apoptosis and autophagy mediated by the P38/JNK pathway in HepG2 and Huh-7 liver cancer cell models [281]. Other compounds of marine origin such as SD118-xanthocillin X obtained from the fungus *Penicillium commune* in a sample of marine sediment [282] or the carotenoid pigment fucoxanthin obtained from brown algae [285] have been reported for presenting induction capacity of autophagy linked to mTOR modulation.

These results validate the *in silico* approach and support its use as an exceptional tool for more efficiently selecting compounds to target specific hallmark cancer proteins.

The marine invertebrate Dolabella auricularia extract chemosensitizes highly invasive colon cancer cells by inducing oxidative and endoplasmic reticulum stress.

In chapter 2, we selected the most active extracts (*Carotalcyon* sp. (CR), *Pseudocolochirus violaceus* (PS), *Phyllidia varicosa* (NA) and *Dolabella auricularia* (NB)) among twenty marine invertebrates based on their antiproliferative activity. This study gave us clues about the putative factors that induce antiproliferative activity, i.e., intracellular ROS generation, DNA damage, cell cycle arrest, apoptosis and/or necrosis, but the underlying molecular mechanism and the potential molecular targets were still unknown. To dissect and elucidate the molecular mechanism, we focused on the most active extract, i.e., *Dolabella auricularia* (NB).

In chapter 4, we showed the results obtained from the study: **“A nudibranch marine extract chemosensitizes selectively colorectal cancer cells by inducing endoplasmic reticulum stress mediated by ROS”**.

First, the NB extract was demonstrated to induce more cytotoxic effects in the colon cancer cell line than in the normal colon cells. Cellular energy metabolism bioenergetics are different when cancer and normal cells are compared. It is known that specific metabolites (oncometabolites [286]) induce specific metabolic pathways to generate enough ATP and to change energy metabolism conditions. This situation is considered as a metabolic reprogramming and is designed for improving proliferation and cancer spread [287]. Menendez JA *et al.* coined the term metabostemness to define the metabolic factors that control the genetic reprogramming from normal and non-tumor cancer stem cells to less differentiated cancer stem cells [61]. Accordingly, the transition from stemness in cancer tissues might not only be hardwired by genetic or epigenetic controllers but may also be caused by the pivotal regulatory role in the cellular metabolite. Our results from two cell lines may indicate that normal and colon cancer cell lines may express two quite different metabolites that are targeted by the marine extract, promoting a distinct response to cellular stress.

Our data showed that intracellular ROS induced by NB treatment was in accordance with the activation of ERS-related proteins in colon cancer cells, whereas these effects exhibited lower levels in normal cells. These results reaffirm that the metabolic machinery and the way by which normal and highly invasive cancer cells respond to oxidative damage induced by NB differ widely. NB damages DNA and protein molecules by increasing ROS levels, which results in G2/M phase arrest and activation of the ERS-related proteins that finally drive cells to predominantly caspase 8-dependent apoptosis.

Many studies have shown a consistent correlation between oxidative stress and direct damage to biomolecules such as DNA, proteins and lipids through oxidative and nitration processes, leading to ERS and apoptotic cell

death [288-295]. When cells accumulate unfolded protein due to the treatment with NB extract, the Unfolded Protein Response (UPR) is activated. UPR begins with the activation of the chaperone GRP78 (also known as BIP), which stimulates the Inositol-Requiring Enzyme 1 α (IRE1 α), Protein Kinase RNA (PKR)-like Kinase (PERK) and Activating Transcription Factor 6 (ATF6) as main ER stress sensors. This response maintains cell survival by limiting the entry of proteins into the ER and modifying the Endoplasmic Reticulum-Associated protein Degradation (ERAD) [296]. However, when ER stress is chronic or cannot be controlled, some transcription factors activate the cell death machinery that leads to apoptosis, autophagy or necrosis [294]. The NB extract did not activate GRP78 or PERK, and ATF6 was also reduced after 3 h of NB exposure. Furthermore, phospho-JNK and the transcription factors ATF4, sXBP1 and CHOP showed high levels of activation after a short exposure time. These results indicate that low doses and limited exposure to NB activate high levels of ER stress and induce the cell death mechanisms related to ER stress in the colorectal cancer HCT-116 cell line. Several studies have correlated oxidative stress with direct damage to crucial molecules, such as DNA, by the oxidation or nitration processes that cause ER stress [288, 289]. Interestingly, transgenic mice that overexpress antioxidant enzymes showed downregulated levels of transcription factors ATF4 and CHOP compared to the levels found in wild-type mice [297]. Yueliang Zhao *et al.* reported that brosimone I, an isoprenoid-substituted flavonoid isolated from the fruit *Artocarpus heterophyllus*, exhibited G1 cell cycle arrest and apoptosis in HCT-116 cells via induced ROS and Ca²⁺ imbalance, and a correlation between ER stress and the activation of the CaMKK β -AMPK signaling pathway was also discovered [298]. An extract derived from the *Agelas sp* sponge induced accumulation of ROS and unfolded proteins, which seemed to chemosensitize the Hepatocellular Carcinoma Cell line (HCC) prior to ionizing radiation [299].

Our results clearly demonstrate that NB induces accumulation of intracellular ROS and activates ER stress in the colon cancer cell line HCT-116 but not in the normal colon cell line. In addition, we used the colorectal cancer

HCT-116 cell line to produce super-invasive cells, i.e., I4 and I9, which had enhanced migration and invasive capacity that was several-fold greater than that of the parental HCT-116 cell line. These super-invasive cells exhibited an overstressed metabolic status with increased basal levels of ROS that correlated with a greater capacity for migration and invasiveness, most likely as an adaptive mechanism, which revealed metabolic mechanisms that strongly differed from those of the parental cell lines. Interestingly, our data showed that NB was able to prevent the proliferation, migration and invasion of these super-invasive populations, similar to its effect on the proliferation capacity of the parental HCT-116 colon cancer cells. Treatment of I4 and I9 super-invasive colon cancer cell populations with the NB extract showed even lower IC₅₀ values compared to those of parental cells and displayed higher levels of ROS, ER stress and DNA damage, indicating that the metabolic machinery of these cells is more sensitive to NB marine compounds than the parental cells.

Different studies have suggested that high levels of stress (oxidative and ER stress) are increased to a greater extent in tumor cells than in normal cells [195, 300, 301] and have indicated that this situation is an initiating point of tumor progression [36], which was explained as the development of enzymatic strategies that enable cancer cells to maintain homeostasis, for example, through an improved antioxidant capacity [302, 303]. It has been reported that human metastatic melanoma in an immunodeficient mouse model exhibited an increased capacity to withstand oxidative stress, including increased dependence on NADPH-generating enzymes in the folate pathway [302]. Moreover, the use of antioxidants stimulated distant metastasis in the same model, which suggests that oxidative stress limits distant metastasis in melanoma cells.

Our research indicates that NB induces greater stress in highly aggressive cancer cell models than in normal colon cells, as measured by ROS and ER stress-related protein levels. When specific inhibitors, such as the ROS scavenger N-acetyl cysteine or the ER stress inhibitor 4-phenylbutyric acid,

were used prior to NB treatment, HCT-116, normal, and super-invasive cells in particular, partially recovered their proliferative and invasiveness. This result clearly indicates that the effect of the NB extract mechanism of action is mediated through ROS and ER stress. Although ROS seem to be the cause of ER stress, our results have not allowed us to establish a direct cause-effect relationship, probably due to the high interaction between ROS and ERS. We propose that the main effect of NB extract on colon cancer cells is the generation of an oxidative imbalance, which causes ER stress through the activation of the c-JNK terminal kinase that generates mitochondrial damage and more ROS and activates the nuclear transcription factors ATF4 and CHOP responsible for cell death. On the other hand, the oxidative imbalance also seems to stop the cell cycle in G2/M avoiding cell progression in the presence of damaged DNA. Furthermore, we postulate that NB marine compounds exert drastically different effects in normal and colon cancer cells (**figure 24**). Whereas the level of ROS was not sufficient to trigger a strong stress cellular response in normal cells, NB promoted a high level of ROS in colon cancer cells. Although colon cancer cells seemed to exhibit an increased capacity to withstand oxidative stress, the NB extract promoted a level of cellular stress that extended beyond the threshold and triggered extensive cellular damage.

Our data provide reasonable evidence to conclude that the *Dolabella auricularia* extract and some of its compounds may be considered natural chemosensitizers of invasive colon cancer cell models through the induction of an overstressed metabolic state. Based on our results, the activity of the NB marine compounds seems to be strongly dependent on the cellular metabotype, which shows different effects on noncancerous, tumor or tumor-initiating cells (CSCs). Therefore, a possible role for these compounds in the modulation of the metabotype of cancer cells as part of their molecular mechanism that extends beyond that of genetic or epigenetic controllers deserve further research attention. The study of these marine extracts and compounds could provide an opportunity to discover new metabolo-epigenetic specific drugs aimed at targeting the metabostemness of cancer cells.

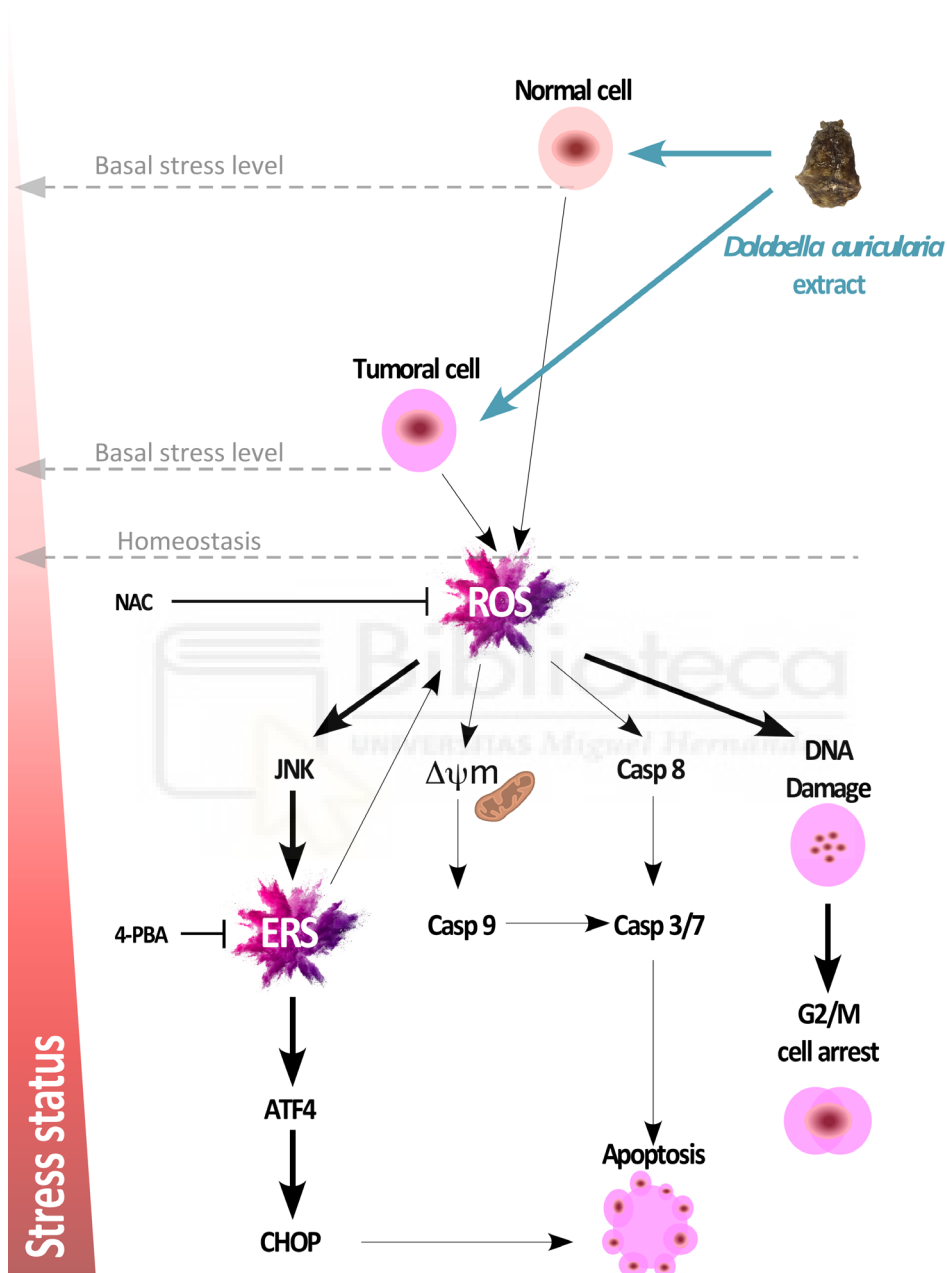
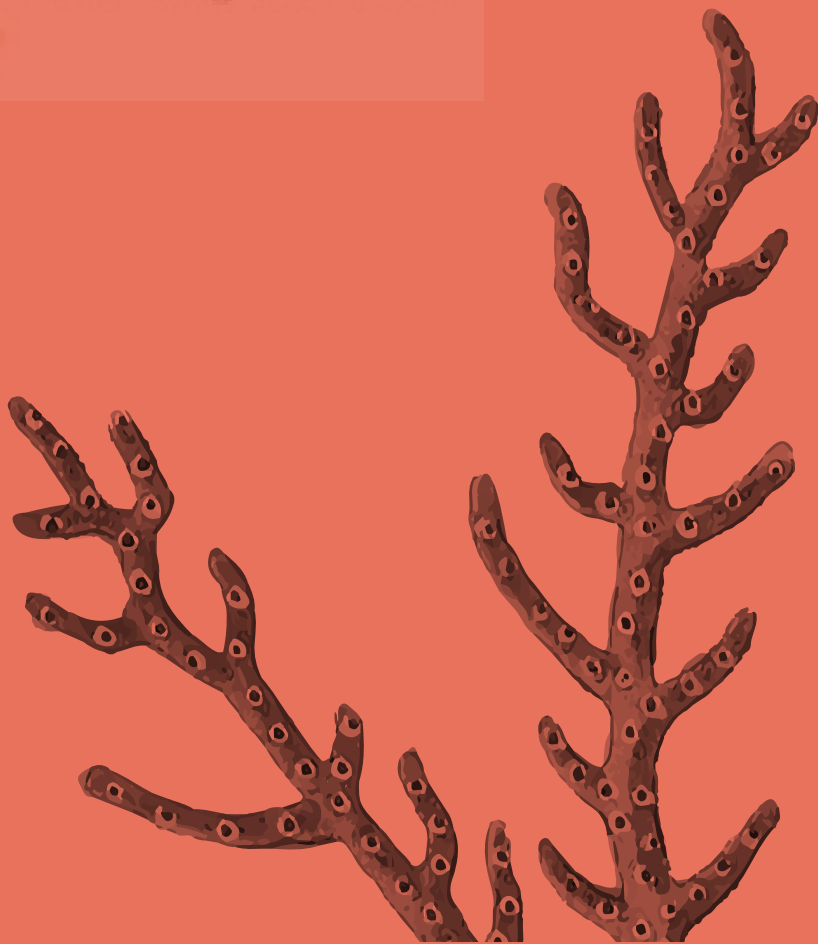


Figure 25. Schematic mechanism of action of NB extract.

Conclusions



Doctoral Student:
Verónica Ruiz Torres

1 Marine compounds, especially those from invertebrates, have a presumed advantage over terrestrial natural products as sources of potential anticancer molecules due to their wide diversity and their ability to target the different hallmarks of cancer.

2 The increased interest in marine drug discovery and the development of computational approaches enable screening for potential compounds based on specific target activities, which will enhance the development of more effective antitumor drugs.

3 Twenty marine invertebrate organisms were selected based on their ability to injure or kill other reef species. Among those, four marine organisms showed strong antiproliferative effects on colon cancer cells: the soft coral *Carotalcyon* sp., *Pseudocolochirus violaceus*, *Phyllida varicosa* and *Dolabella auricularia*.

4 The selected extracts showed antiproliferative activity on three human colon cancer cell lines by inducing oxidative stress, which led to a cytostatic effect that arrested the cell cycle, damaged DNA and induced different types of cell death. *Carotalcyon* sp., *Phyllida varicosa* and *Dolabella auricularia* induced cell death through an apoptotic pathway, whereas the *Pseudocolochirus violaceus* extract activated the necrosis pathway.

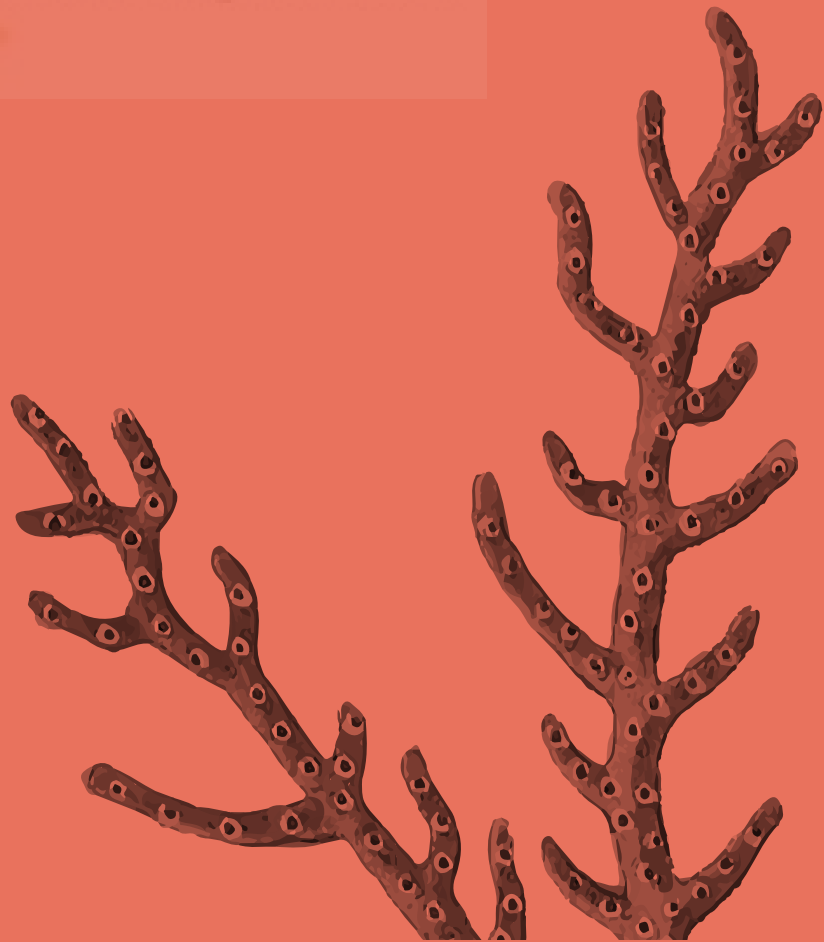
5 Based on their abundance in marine extracts, we propose that fatty acids and methyl esters such as tetracosapentanoic, heptadecenoic, stearic and 9,12-octadecadienoic acids, and phospholipids such as 1-O-hexadecyl-sn-glycero-3-phosphocholine may contribute to the antiproliferative activity most probably through cell membrane modulation. Nevertheless, diterpenes such as lopholide or spongian-16-one and some alkaloid analogs may exert stronger antiproliferative effects as previously reported.

6 The molecular docking of computer-aided drug design methods enabled us to select 11 marine compounds out of a library containing 484,527 compounds, which efficiently targeted the master regulator kinase of metabolism, mTOR, with relatively little effort and an increased rate of success for advancing to preclinical steps. This is the first study showing that *in silico* selection of potential mTOR inhibitors correlates with their inhibitory capacity in cell model.

7 The extract derived from *Dollabella auricularia* exerted antiproliferative, antimigratory and anti-invasive effects by inducing oxidative stress, overstressing the endoplasmic reticulum and efficiently sensitizing human colon cancer cells with respect to less sensitive normal colon cells.

8 We postulate that the compounds derived from *Dollabella auricularia* may be used to target the cellular metabotype, which differs among normal, tumoral and cancer stem cells. Thus, further research on the mechanism of action of these compounds, after their isolation, to discover new metabolo-epigenetic-specific anticancer drugs is fully justified.

References



Doctoral Student:
Verónica Ruiz Torres

1. Beedessee, G., et al., Cytotoxic activities of hexane, ethyl acetate and butanol extracts of marine sponges from Mauritian Waters on human cancer cell lines. *Environmental Toxicology and Pharmacology*, 2012. 34(2): p. 397-408.
2. Norton, K.-A., et al., Multiscale Agent-Based and Hybrid Modeling of the Tumor Immune Microenvironment. *Processes (Basel, Switzerland)*, 2019. 7(1): p. 37.
3. Hanahan, D. and R.A. Weinberg, The hallmarks of cancer. *Cell*, 2000. 100(1): p. 57-70.
4. Hanahan, D. and R.A. Weinberg, Hallmarks of cancer: the next generation. *Cell*, 2011. 144(5): p. 646-74.
5. Cancer, I.A.f.R.o., *Cancer Today - GLOBOCAN*. 2019.
6. Médica, S.E.d.O., *SEOM*. 2019.
7. Cáncer, R.E.d.R.d., *REDECAN*. 2019.
8. Irving, M.H. and B. Catchpole, ABC of colorectal diseases. *Anatomy and physiology of the colon, rectum, and anus. BMJ (Clinical research ed.)*, 1992. 304(6834): p. 1106-1108.
9. Jorge, J.M. and S.D. Wexner, *Anatomy and physiology of the rectum and anus. Eur J Surg*, 1997. 163(10): p. 723-31.
10. Britannica, E., *Regions of the large intestine*. 2019.
11. Kehoe, J. and V.P. Khatri, Staging and prognosis of colon cancer. *Surg Oncol Clin N Am*, 2006. 15(1): p. 129-46.
12. Simon, K., Colorectal cancer development and advances in screening. *Clinical interventions in aging*, 2016. 11: p. 967-976.
13. Johnson, C.M., et al., Meta-analyses of colorectal cancer risk factors. *Cancer Causes Control*, 2013. 24(6): p. 1207-22.
14. Society, A.C., *Facts and Figures*. 2015.
15. Carethers, J.M., Risk factors for colon location of cancer. *Transl Gastroenterol Hepatol*, 2018. 3: p. 76.
16. Carethers, J.M., The Increasing Incidence of Colorectal Cancers Diagnosed in Subjects Under Age 50 Among Races: CRaCking the Conundrum. *Digestive Diseases and Sciences*, 2016. 61(10): p. 2767-2769.
17. Hagggar, F.A. and R.P. Boushey, Colorectal cancer epidemiology: incidence, mortality, survival, and risk factors. *Clin Colon Rectal Surg*, 2009. 22(4): p. 191-7.
18. Lockhart-Mummery, J.P., Two hundred cases of cancer of the rectum treated by perineal excision. *BJS*, 1926. 14(53): p. 110-124.
19. Dukes, C.E., The classification of cancer of the rectum. *The Journal of Pathology and Bacteriology*, 1932. 35(3): p. 323-332.
20. Astler, V.B. and F.A. Collier, The prognostic significance of direct extension of carcinoma of the colon and rectum. *Annals of surgery*, 1954. 139(6): p. 846-852.
21. Turnbull, R.B., Jr., et al., Cancer of the colon: the influence of the no-touch isolation technic on survival rates. *Ann Surg*, 1967. 166(3): p. 420-7.
22. Australia, M.U.-S., *BIOMARKER DISCOVERY OFFERS CLEARER PROGNOSIS FOR BOWEL AND RECTAL CANCER PATIENTS*. 2015.

23. Hutter, R.V., At last--worldwide agreement on the staging of cancer. *Arch Surg*, 1987. 122(11): p. 1235-9.
24. Wu, J.S., Rectal cancer staging. *Clinics in colon and rectal surgery*, 2007. 20(3): p. 148-157.
25. Hanada, T., et al., IFN γ -dependent, spontaneous development of colorectal carcinomas in SOCS1-deficient mice. *J Exp Med*, 2006. 203(6): p. 1391-7.
26. Jemal, A., et al., Cancer statistics, 2006. *CA Cancer J Clin*, 2006. 56(2): p. 106-30.
27. Schluskel, A.T., et al., The evolution of colorectal cancer genetics-Part 1: from discovery to practice. *J Gastrointest Oncol*, 2014. 5(5): p. 326-35.
28. Vogelstein, B., et al., Genetic alterations during colorectal-tumor development. *N Engl J Med*, 1988. 319(9): p. 525-32.
29. Comprehensive molecular characterization of human colon and rectal cancer. *Nature*, 2012. 487(7407): p. 330-7.
30. Larrea, A.A., S.A. Lujan, and T.A. Kunkel, SnapShot: DNA mismatch repair. *Cell*, 2010. 141(4): p. 730 e1.
31. Fodde, R., The APC gene in colorectal cancer. *Eur J Cancer*, 2002. 38(7): p. 867-71.
32. Pino, M.S. and D.C. Chung, The chromosomal instability pathway in colon cancer. *Gastroenterology*, 2010. 138(6): p. 2059-72.
33. Kambara, T., et al., BRAF mutation is associated with DNA methylation in serrated polyps and cancers of the colorectum. *Gut*, 2004. 53(8): p. 1137-1144.
34. Garassino, M.C., et al., Should KRAS mutations be considered an independent prognostic factor in patients with advanced colorectal cancer treated with cetuximab? *J Clin Oncol*, 2008. 26(15): p. 2600; author reply 2601-2.
35. Walther, A., R. Houlston, and I. Tomlinson, Association between chromosomal instability and prognosis in colorectal cancer: a meta-analysis. *Gut*, 2008. 57(7): p. 941-50.
36. Kheirelseid, E.A., et al., Mismatch repair protein expression in colorectal cancer. *J Gastrointest Oncol*, 2013. 4(4): p. 397-408.
37. Hitchins, M.P., The role of epigenetics in Lynch syndrome. *Fam Cancer*, 2013. 12(2): p. 189-205.
38. Deschoolmeester, V., et al., A review of the most promising biomarkers in colorectal cancer: one step closer to targeted therapy. *The oncologist*, 2010. 15(7): p. 699-731.
39. Aghagolzadeh, P. and R. Radpour, New trends in molecular and cellular biomarker discovery for colorectal cancer. *World J Gastroenterol*, 2016. 22(25): p. 5678-93.
40. Longley, D.B., D.P. Harkin, and P.G. Johnston, 5-fluorouracil: mechanisms of action and clinical strategies. *Nat Rev Cancer*, 2003. 3(5): p. 330-8.
41. Comella, P., A review of the role of capecitabine in the treatment of colorectal cancer. *Ther Clin Risk Manag*, 2007. 3(3): p. 421-31.
42. Raymond, E., et al., Cellular and molecular pharmacology of oxaliplatin. *Mol Cancer Ther*, 2002. 1(3): p. 227-35.

43. Soulie, P., et al., Oxaliplatin/cisplatin (L-OHP/CDDP) combination in heavily pretreated ovarian cancer. *Eur J Cancer*, 1997. 33(9): p. 1400-6.
44. Illum, H., Irinotecan and radiosensitization in rectal cancer. *Anti-Cancer Drugs*, 2011. 22(4): p. 324-329.
45. Xu, Y. and M.A. Villalona-Calero, Irinotecan: mechanisms of tumor resistance and novel strategies for modulating its activity. *Ann Oncol*, 2002. 13(12): p. 1841-51.
46. Fuchs, C., E.P. Mitchell, and P.M. Hoff, Irinotecan in the treatment of colorectal cancer. *Cancer Treat Rev*, 2006. 32(7): p. 491-503.
47. Chen, A.Y. and L.F. Liu, DNA topoisomerases: essential enzymes and lethal targets. *Annu Rev Pharmacol Toxicol*, 1994. 34: p. 191-218.
48. Nurgali, K., R.T. Jagoe, and R. Abalo, Editorial: Adverse Effects of Cancer Chemotherapy: Anything New to Improve Tolerance and Reduce Sequelae? *Frontiers in pharmacology*, 2018. 9: p. 245-245.
49. Price, T.J., et al., Targeted therapy for metastatic colorectal cancer. *Expert Rev Anticancer Ther*, 2018. 18(10): p. 991-1006.
50. Peeters, M. and T. Price, Biologic therapies in the metastatic colorectal cancer treatment continuum--applying current evidence to clinical practice. *Cancer Treat Rev*, 2012. 38(5): p. 397-406.
51. Kim, K.J., et al., Inhibition of vascular endothelial growth factor-induced angiogenesis suppresses tumour growth in vivo. *Nature*, 1993. 362(6423): p. 841-4.
52. Mendelsohn, J. and J. Baselga, Epidermal growth factor receptor targeting in cancer. *Semin Oncol*, 2006. 33(4): p. 369-85.
53. Hynes, N.E. and H.A. Lane, ERBB receptors and cancer: the complexity of targeted inhibitors. *Nat Rev Cancer*, 2005. 5(5): p. 341-54.
54. Larki, P., et al., Coexistence of KRAS and BRAF Mutations in Colorectal Cancer: A Case Report Supporting The Concept of Tumoral Heterogeneity. *Cell journal*, 2017. 19(Suppl 1): p. 113-117.
55. Guo, F., et al., Mutation status and prognostic values of KRAS, NRAS, BRAF and PIK3CA in 353 Chinese colorectal cancer patients. *Scientific Reports*, 2018. 8(1): p. 6076.
56. Bennouna, J., et al., Continuation of bevacizumab after first progression in metastatic colorectal cancer (ML18147): a randomised phase 3 trial. *Lancet Oncol*, 2013. 14(1): p. 29-37.
57. Warburg, O., On the origin of cancer cells. *Science*, 1956. 123(3191): p. 309-14.
58. Kroemer, G. and J. Pouyssegur, Tumor Cell Metabolism: Cancer's Achilles' Heel. *Cancer Cell*, 2008. 13(6): p. 472-482.
59. Folmes, C.D., T.J. Nelson, and A. Terzic, Energy metabolism in nuclear reprogramming. *Biomark Med*, 2011. 5(6): p. 715-29.
60. Collins, R.R.J., et al., Oncometabolites: A New Paradigm for Oncology, Metabolism, and the Clinical Laboratory. *Clinical Chemistry*, 2017. 63(12): p. 1812.

61. Menendez, J.A. and T. Alarcón, Metabostemness: a new cancer hallmark. *Frontiers in oncology*, 2014. 4: p. 262-262.
62. Tan, W., et al., Deciphering the metabolic role of AMPK in cancer multi-drug resistance. *Seminars in Cancer Biology*, 2019. 56: p. 56-71.
63. Singh, D., et al., Overexpression of hypoxia-inducible factor and metabolic pathways: possible targets of cancer. *Cell & bioscience*, 2017. 7: p. 62-62.
64. Stine, Z.E., et al., MYC, Metabolism, and Cancer. *Cancer discovery*, 2015. 5(10): p. 1024-1039.
65. Koundouros, N. and G. Poulogiannis, Phosphoinositide 3-Kinase/Akt Signaling and Redox Metabolism in Cancer. *Frontiers in oncology*, 2018. 8: p. 160-160.
66. Kawada, K., K. Toda, and Y. Sakai, Targeting metabolic reprogramming in KRAS-driven cancers. *Int J Clin Oncol*, 2017. 22(4): p. 651-659.
67. Sreedhar, A. and Y. Zhao, Dysregulated metabolic enzymes and metabolic reprogramming in cancer cells. *Biomedical reports*, 2018. 8(1): p. 3-10.
68. Lien, E.C., C.A. Lyssiotis, and L.C. Cantley, Metabolic Reprogramming by the PI3K-Akt-mTOR Pathway in Cancer. *Recent Results Cancer Res*, 2016. 207: p. 39-72.
69. Mossmann, D., S. Park, and M.N. Hall, mTOR signalling and cellular metabolism are mutual determinants in cancer. *Nature Reviews Cancer*, 2018. 18(12): p. 744-757.
70. Spoerke, J.M., et al., Phosphoinositide 3-kinase (PI3K) pathway alterations are associated with histologic subtypes and are predictive of sensitivity to PI3K inhibitors in lung cancer preclinical models. *Clin Cancer Res*, 2012. 18(24): p. 6771-83.
71. Cui, W., Y. Cai, and X. Zhou, Advances in subunits of PI3K class I in cancer. *Pathology*, 2014. 46(3): p. 169-176.
72. Manning, B.D. and L.C. Cantley, AKT/PKB signaling: navigating downstream. *Cell*, 2007. 129(7): p. 1261-74.
73. Hay, N. and N. Sonenberg, Upstream and downstream of mTOR. *Genes Dev*, 2004. 18(16): p. 1926-45.
74. Li, X., et al., Efficacy of PI3K/AKT/mTOR pathway inhibitors for the treatment of advanced solid cancers: A literature-based meta-analysis of 46 randomised control trials. *PLoS One*, 2018. 13(2): p. e0192464.
75. Yu, J.S. and W. Cui, Proliferation, survival and metabolism: the role of PI3K/AKT/mTOR signalling in pluripotency and cell fate determination. *Development*, 2016. 143(17): p. 3050-60.
76. Schwarz, D.S. and M.D. Blower, The endoplasmic reticulum: structure, function and response to cellular signaling. *Cell Mol Life Sci*, 2016. 73(1): p. 79-94.
77. Ruiz, M., *The endomembrane system*. 2019.
78. English, A.R., N. Zurek, and G.K. Voeltz, Peripheral ER structure and function. *Curr Opin Cell Biol*, 2009. 21(4): p. 596-602.
79. Walter, P. and D. Ron, The unfolded protein response: from stress pathway to homeostatic regulation. *Science*, 2011. 334(6059): p. 1081-6.

80. Tabas, I. and D. Ron, Integrating the mechanisms of apoptosis induced by endoplasmic reticulum stress. *Nat Cell Biol*, 2011. 13(3): p. 184-90.
81. Corazzari, M., et al., Endoplasmic Reticulum Stress, Unfolded Protein Response, and Cancer Cell Fate. *Front Oncol*, 2017. 7: p. 78.
82. Novoa, I., et al., Feedback inhibition of the unfolded protein response by GADD34-mediated dephosphorylation of eIF2alpha. *J Cell Biol*, 2001. 153(5): p. 1011-22.
83. Wang, M. and R.J. Kaufman, The impact of the endoplasmic reticulum protein-folding environment on cancer development. *Nat Rev Cancer*, 2014. 14(9): p. 581-97.
84. Shen, J., et al., ER stress regulation of ATF6 localization by dissociation of BiP/GRP78 binding and unmasking of Golgi localization signals. *Dev Cell*, 2002. 3(1): p. 99-111.
85. Martinon, F., Targeting endoplasmic reticulum signaling pathways in cancer. *Acta Oncol*, 2012. 51(7): p. 822-30.
86. Ron, D. and S.R. Hubbard, How IRE1 reacts to ER stress. *Cell*, 2008. 132(1): p. 24-6.
87. Kumari, S., et al., Reactive Oxygen Species: A Key Constituent in Cancer Survival. *Biomark Insights*, 2018. 13: p. 1177271918755391.
88. Kumari, A., Chapter 3 - Electron Transport Chain, in *Sweet Biochemistry*, A. Kumari, Editor. 2018, Academic Press. p. 13-16.
89. Simic, M.G., D.S. Bergtold, and L.R. Karam, Generation of oxy radicals in biosystems. *Mutat Res*, 1989. 214(1): p. 3-12.
90. Griendling, K.K., et al., Measurement of Reactive Oxygen Species, Reactive Nitrogen Species, and Redox-Dependent Signaling in the Cardiovascular System. *Circulation Research*, 2016. 119(5): p. e39-e75.
91. Schieber, M. and N.S. Chandel, ROS function in redox signaling and oxidative stress. *Curr Biol*, 2014. 24(10): p. R453-62.
92. Cadet, J. and J.R. Wagner, DNA base damage by reactive oxygen species, oxidizing agents, and UV radiation. *Cold Spring Harb Perspect Biol*, 2013. 5(2).
93. Gaschler, M.M. and B.R. Stockwell, Lipid peroxidation in cell death. *Biochem Biophys Res Commun*, 2017. 482(3): p. 419-425.
94. Levine, R.L., Carbonyl modified proteins in cellular regulation, aging, and disease, 3 2Guest Editor: Earl Stadtman 3This article is part of a series of reviews on "Oxidatively Modified Proteins in Aging and Disease." The full list of papers may be found on the homepage of the journal. *Free Radical Biology and Medicine*, 2002. 32(9): p. 790-796.
95. Assi, M., The differential role of reactive oxygen species in early and late stages of cancer. *Am J Physiol Regul Integr Comp Physiol*, 2017. 313(6): p. R646-r653.
96. Birben, E., et al., Oxidative stress and antioxidant defense. *World Allergy Organ J*, 2012. 5(1): p. 9-19.

97. Lu, J.M., et al., Chemical and molecular mechanisms of antioxidants: experimental approaches and model systems. *J Cell Mol Med*, 2010. 14(4): p. 840-60.
98. St Clair, D.K., et al., Suppression of radiation-induced neoplastic transformation by overexpression of mitochondrial superoxide dismutase. *Mol Carcinog*, 1992. 6(4): p. 238-42.
99. Lee, S.R., et al., Reversible inactivation of the tumor suppressor PTEN by H₂O₂. *J Biol Chem*, 2002. 277(23): p. 20336-42.
100. DeBerardinis, R.J. and N.S. Chandel, Fundamentals of cancer metabolism. *Science Advances*, 2016. 2(5): p. e1600200.
101. Chiang, A.C. and J. Massague, Molecular basis of metastasis. *N Engl J Med*, 2008. 359(26): p. 2814-23.
102. Tzanakakis, G., et al., Role of the extracellular matrix in cancer-associated epithelial to mesenchymal transition phenomenon. *Dev Dyn*, 2018. 247(3): p. 368-381.
103. Lee, J.M., et al., The epithelial-mesenchymal transition: new insights in signaling, development, and disease. *J Cell Biol*, 2006. 172(7): p. 973-81.
104. Yang, J. and R.A. Weinberg, Epithelial-Mesenchymal Transition: At the Crossroads of Development and Tumor Metastasis. *Developmental Cell*, 2008. 14(6): p. 818-829.
105. Lamouille, S., J. Xu, and R. Derynck, Molecular mechanisms of epithelial-mesenchymal transition. *Nat Rev Mol Cell Biol*, 2014. 15(3): p. 178-96.
106. Tobar, N., V. Villar, and J.F. Santibanez, ROS-NFkappaB mediates TGF-beta1-induced expression of urokinase-type plasminogen activator, matrix metalloproteinase-9 and cell invasion. *Mol Cell Biochem*, 2010. 340(1-2): p. 195-202.
107. Lam, C.R., et al., Loss of TAK1 increases cell traction force in a ROS-dependent manner to drive epithelial-mesenchymal transition of cancer cells. *Cell Death Dis*, 2013. 4: p. e848.
108. Hoeben, A., et al., Vascular endothelial growth factor and angiogenesis. *Pharmacol Rev*, 2004. 56(4): p. 549-80.
109. Yun, J., et al., Redox-dependent mechanisms in coronary collateral growth: the "redox window" hypothesis. *Antioxid Redox Signal*, 2009. 11(8): p. 1961-74.
110. Ushio-Fukai, M. and R.W. Alexander, Reactive oxygen species as mediators of angiogenesis signaling: role of NAD(P)H oxidase. *Mol Cell Biochem*, 2004. 264(1-2): p. 85-97.
111. Muz, B., et al., The role of hypoxia in cancer progression, angiogenesis, metastasis, and resistance to therapy. *Hypoxia (Auckland, N.Z.)*, 2015. 3: p. 83-92.
112. Semenza, G.L., Hydroxylation of HIF-1: oxygen sensing at the molecular level. *Physiology (Bethesda)*, 2004. 19: p. 176-82.
113. Semenza, G.L., Evaluation of HIF-1 inhibitors as anticancer agents. *Drug Discov Today*, 2007. 12(19-20): p. 853-9.

114. Huang, X., et al., Hypoxia-inducible mir-210 regulates normoxic gene expression involved in tumor initiation. *Mol Cell*, 2009. 35(6): p. 856-67.
115. Chaffer, C.L. and R.A. Weinberg, A perspective on cancer cell metastasis. *Science*, 2011. 331(6024): p. 1559-64.
116. Sahai, E., Illuminating the metastatic process. *Nature Reviews Cancer*, 2007. 7: p. 737.
117. Valastyan, S. and R.A. Weinberg, Tumor metastasis: molecular insights and evolving paradigms. *Cell*, 2011. 147(2): p. 275-92.
118. Gupta, G.P. and J. Massague, Cancer metastasis: building a framework. *Cell*, 2006. 127(4): p. 679-95.
119. Zheng, H. and Y. Kang, Multilayer control of the EMT master regulators. *Oncogene*, 2014. 33(14): p. 1755-63.
120. McGee, S.F., et al., Mammary gland biology and breast cancer. Conference on Common Molecular Mechanisms of Mammary Gland Development and Breast Cancer Progression. *EMBO reports*, 2006. 7(11): p. 1084-1088.
121. van Zijl, F., G. Krupitza, and W. Mikulits, Initial steps of metastasis: cell invasion and endothelial transmigration. *Mutat Res*, 2011. 728(1-2): p. 23-34.
122. Kalluri, R. and R.A. Weinberg, The basics of epithelial-mesenchymal transition. *J Clin Invest*, 2009. 119(6): p. 1420-8.
123. Thiery, J.P., et al., Epithelial-mesenchymal transitions in development and disease. *Cell*, 2009. 139(5): p. 871-90.
124. Harris, T.J. and U. Tepass, Adherens junctions: from molecules to morphogenesis. *Nat Rev Mol Cell Biol*, 2010. 11(7): p. 502-14.
125. Batlle, E., et al., The transcription factor snail is a repressor of E-cadherin gene expression in epithelial tumour cells. *Nat Cell Biol*, 2000. 2(2): p. 84-9.
126. Liang, X., EMT: new signals from the invasive front. *Oral Oncol*, 2011. 47(8): p. 686-7.
127. Christiansen, J.J. and A.K. Rajasekaran, Reassessing epithelial to mesenchymal transition as a prerequisite for carcinoma invasion and metastasis. *Cancer Res*, 2006. 66(17): p. 8319-26.
128. Yilmaz, M. and G. Christofori, Mechanisms of motility in metastasizing cells. *Mol Cancer Res*, 2010. 8(5): p. 629-42.
129. Friedl, P. and K. Wolf, Plasticity of cell migration: a multiscale tuning model. *J Cell Biol*, 2010. 188(1): p. 11-9.
130. Pankova, K., et al., The molecular mechanisms of transition between mesenchymal and amoeboid invasiveness in tumor cells. *Cell Mol Life Sci*, 2010. 67(1): p. 63-71.
131. Hecht, I., et al., Tumor invasion optimization by mesenchymal-amoeboid heterogeneity. *Sci Rep*, 2015. 5: p. 10622.
132. Hegerfeldt, Y., et al., Collective cell movement in primary melanoma explants: plasticity of cell-cell interaction, beta1-integrin function, and migration strategies. *Cancer Res*, 2002. 62(7): p. 2125-30.

133. Parri, M. and P. Chiarugi, Rac and Rho GTPases in cancer cell motility control. *Cell communication and signaling : CCS*, 2010. 8: p. 23-23.
134. Parri, M., et al., EphA2 reexpression prompts invasion of melanoma cells shifting from mesenchymal to amoeboid-like motility style. *Cancer Res*, 2009. 69(5): p. 2072-81.
135. Zulehner, G., et al., Nuclear beta-catenin induces an early liver progenitor phenotype in hepatocellular carcinoma and promotes tumor recurrence. *Am J Pathol*, 2010. 176(1): p. 472-81.
136. Kitamura, T., et al., SMAD4-deficient intestinal tumors recruit CCR1+ myeloid cells that promote invasion. *Nat Genet*, 2007. 39(4): p. 467-75.
137. Nabeshima, K., et al., Cohort migration of carcinoma cells: differentiated colorectal carcinoma cells move as coherent cell clusters or sheets. *Histol Histopathol*, 1999. 14(4): p. 1183-97.
138. Feng, B., et al., Colorectal cancer migration and invasion initiated by microRNA-106a. *PLoS one*, 2012. 7(8): p. e43452-e43452.
139. Nicolson, G.L., Metastatic tumor cell interactions with endothelium, basement membrane and tissue. *Curr Opin Cell Biol*, 1989. 1(5): p. 1009-19.
140. Al-Mehdi, A.B., et al., Intravascular origin of metastasis from the proliferation of endothelium-attached tumor cells: a new model for metastasis. *Nat Med*, 2000. 6(1): p. 100-2.
141. Luzzi, K.J., et al., Multistep nature of metastatic inefficiency: dormancy of solitary cells after successful extravasation and limited survival of early micrometastases. *Am J Pathol*, 1998. 153(3): p. 865-73.
142. Im, J.H., et al., Coagulation facilitates tumor cell spreading in the pulmonary vasculature during early metastatic colony formation. *Cancer Res*, 2004. 64(23): p. 8613-9.
143. Bockhorn, M., R.K. Jain, and L.L. Munn, Active versus passive mechanisms in metastasis: do cancer cells crawl into vessels, or are they pushed? *Lancet Oncol*, 2007. 8(5): p. 444-8.
144. Senft, D. and Z.E.A. Ronai, Adaptive Stress Responses During Tumor Metastasis and Dormancy. *Trends in cancer*, 2016. 2(8): p. 429-442.
145. Trachootham, D., et al., Selective killing of oncogenically transformed cells through a ROS-mediated mechanism by beta-phenylethyl isothiocyanate. *Cancer Cell*, 2006. 10(3): p. 241-52.
146. Kwon, D., et al., Overexpression of endoplasmic reticulum stress-related proteins, XBP1s and GRP78, predicts poor prognosis in pulmonary adenocarcinoma. *Lung Cancer*, 2018. 122: p. 131-137.
147. Yoboue, E.D., R. Sitia, and T. Simmen, Redox crosstalk at endoplasmic reticulum (ER) membrane contact sites (MCS) uses toxic waste to deliver messages. *Cell Death & Disease*, 2018. 9(3): p. 331.
148. Banerjee, A., et al., Increased reactive oxygen species levels cause ER stress and cytotoxicity in andrographolide treated colon cancer cells. *Oncotarget*, 2017. 8(16): p. 26142-26153.

149. Ocean Institute. Aqua Facts. 2019, june 15; Available from: <https://www.oceanicinstitute.org/aboutoceans/aquafacts.html>.
150. Pendahuluan, EKOLOGI DAN ILMU LINGKUNGAN. 2017.
151. Barott, K.L. and F.L. Rohwer, Unseen players shape benthic competition on coral reefs. *Trends Microbiol*, 2012. 20(12): p. 621-8.
152. McClintock, J.B., et al., Ecology of antarctic marine sponges: an overview. *Integr Comp Biol*, 2005. 45(2): p. 359-68.
153. Loh, T.L. and J.R. Pawlik, Chemical defenses and resource trade-offs structure sponge communities on Caribbean coral reefs. *Proc Natl Acad Sci U S A*, 2014. 111(11): p. 4151-6.
154. Paul, V.J., M.P. Puglisi, and R. Ritson-Williams, Marine chemical ecology. *Nat Prod Rep*, 2006. 23(2): p. 153-80.
155. Dias, D.A., S. Urban, and U. Roessner, A historical overview of natural products in drug discovery. *Metabolites*, 2012. 2(2): p. 303-336.
156. Nobili, S., et al., Natural compounds for cancer treatment and prevention. *Pharmacol Res*, 2009. 59(6): p. 365-78.
157. Mayer, A.M., et al., The odyssey of marine pharmaceuticals: a current pipeline perspective. *Trends Pharmacol Sci*, 2010. 31(6): p. 255-65.
158. Isah, T., et al., Secondary metabolism of pharmaceuticals in the plant in vitro cultures: strategies, approaches, and limitations to achieving higher yield. *Plant Cell, Tissue and Organ Culture (PCTOC)*, 2018. 132(2): p. 239-265.
159. Seneca, CHAPTER 2 - Alkaloid Chemistry, in *Alkaloids - Secrets of Life*, T. Aniszewski, Editor. 2007, Elsevier: Amsterdam. p. 61-139.
160. Molinski, T.F., Marine pyridoacridine alkaloids: structure, synthesis, and biological chemistry. *Chemical Reviews*, 1993. 93(5): p. 1825-1838.
161. Hertiani, T., et al., From anti-fouling to biofilm inhibition: new cytotoxic secondary metabolites from two Indonesian Agelas sponges. *Bioorg Med Chem*, 2010. 18(3): p. 1297-311.
162. Bringmann, G., et al., Ancistectorine D, a naphthylisoquinoline alkaloid with antiprotozoal and antileukemic activities, and further 5,8'- and 7,1'-linked metabolites from the Chinese liana *Ancistrocladus tectorius*. *Fitoterapia*, 2016. 115: p. 1-8.
163. Della Sala, G., et al., Polyketide synthases in the microbiome of the marine sponge *Plakortis halichondrioides*: a metagenomic update. *Mar Drugs*, 2014. 12(11): p. 5425-40.
164. Gross, H. and G.M. König, Terpenoids from Marine Organisms: Unique Structures and their Pharmacological Potential. *Phytochemistry Reviews*, 2006. 5(1): p. 115-141.
165. Elissawy, A.M., et al., Bioactive terpenes from marine-derived fungi. *Mar Drugs*, 2015. 13(4): p. 1966-92.
166. Cheung, R.C., T.B. Ng, and J.H. Wong, Marine Peptides: Bioactivities and Applications. *Mar Drugs*, 2015. 13(7): p. 4006-43.

167. Kang, H.K., C.H. Seo, and Y. Park, The effects of marine carbohydrates and glycosylated compounds on human health. *Int J Mol Sci*, 2015. 16(3): p. 6018-56.
168. Malve, H., Exploring the ocean for new drug developments: Marine pharmacology. *Journal of pharmacy & bioallied sciences*, 2016. 8(2): p. 83-91.
169. Yuan, R., et al., Natural products to prevent drug resistance in cancer chemotherapy: a review. *Ann N Y Acad Sci*, 2017. 1401(1): p. 19-27.
170. Kong, D.X., Y.Y. Jiang, and H.Y. Zhang, Marine natural products as sources of novel scaffolds: achievement and concern. *Drug Discov Today*, 2010. 15(21-22): p. 884-6.
171. Abadines, I.B., et al., The Marine Pharmacology and Pharmaceuticals Pipeline in 2018. *The FASEB Journal*, 2019. 33(1_supplement): p. 504.1-504.1.
172. Ruiz-Torres, V., et al., An Updated Review on Marine Anticancer Compounds: The Use of Virtual Screening for the Discovery of Small-Molecule Cancer Drugs. *Molecules*, 2017. 22(7).
173. Hill, R.T. and W. Fenical, Pharmaceuticals from marine natural products: surge or ebb? *Curr Opin Biotechnol*, 2010. 21(6): p. 777-9.
174. Pimm, S.L., Biodiversity: not just lots of fish in the sea. *Curr Biol*, 2012. 22(23): p. R996-7.
175. Beesoo, R., et al., Apoptosis inducing lead compounds isolated from marine organisms of potential relevance in cancer treatment. *Mutat Res*, 2014. 768: p. 84-97.
176. De Zoysa, M., Chapter 9 - Medicinal Benefits of Marine Invertebrates: Sources for Discovering Natural Drug Candidates, in *Advances in Food and Nutrition Research*, S.-K. Kim, Editor. 2012, Academic Press. p. 153-169.
177. Hu, G.-P., et al., Statistical Research on Marine Natural Products Based on Data Obtained between 1985 and 2008. *Marine Drugs*, 2011. 9(4): p. 514-525.
178. Imperatore, C., et al., Alkaloids from marine invertebrates as important leads for anticancer drugs discovery and development. *Molecules*, 2014. 19(12): p. 20391-423.
179. Pejin, B., M. Mojovic, and A.G. Savic, Novel and highly potent antitumour natural products from cnidarians of marine origin. *Nat Prod Res*, 2014. 28(24): p. 2237-44.
180. Lee, J.A., et al., Modern Phenotypic Drug Discovery Is a Viable, Neoclassic Pharma Strategy. *Journal of Medicinal Chemistry*, 2012. 55(10): p. 4527-4538.
181. Lee, J.A., et al., Modern phenotypic drug discovery is a viable, neoclassic pharma strategy. *J Med Chem*, 2012. 55(10): p. 4527-38.
182. Cyprotex, 2019.
183. Plowright, A.T. and L. Drowley, Chapter Eight - Phenotypic Screening, in *Annual Reports in Medicinal Chemistry*, R.A. Goodnow, Editor. 2017, Academic Press. p. 263-299.
184. Huang, H., et al., Reverse Screening Methods to Search for the Protein Targets of Chemopreventive Compounds. *Frontiers in chemistry*, 2018. 6: p. 138-138.

185. Horvath, D., Pharmacophore-based virtual screening. *Methods Mol Biol*, 2011. 672: p. 261-98.
186. Kharkar, P.S., S. Warriar, and R.S. Gaud, Reverse docking: a powerful tool for drug repositioning and drug rescue. *Future Med Chem*, 2014. 6(3): p. 333-42.
187. Ruiz-Torres, V., et al., An Updated Review on Marine Anticancer Compounds: The Use of Virtual Screening for the Discovery of Small-Molecule Cancer Drugs. *Molecules*, 2017. 22(7).
188. Beedessee, G., et al., Cytotoxic activities of hexane, ethyl acetate and butanol extracts of marine sponges from Mauritian Waters on human cancer cell lines. *Environ Toxicol Pharmacol*, 2012. 34(2): p. 397-408.
189. Mayer, A.M., et al., Marine pharmacology in 2009-2011: marine compounds with antibacterial, antidiabetic, antifungal, anti-inflammatory, antiprotozoal, antituberculosis, and antiviral activities; affecting the immune and nervous systems, and other miscellaneous mechanisms of action. *Mar Drugs*, 2013. 11(7): p. 2510-73.
190. Hu, G.P., et al., Statistical research on marine natural products based on data obtained between 1985 and 2008. *Mar Drugs*, 2011. 9(4): p. 514-25.
191. Zhang, J., et al., ROS and ROS-Mediated Cellular Signaling. *Oxidative medicine and cellular longevity*, 2016. 2016: p. 4350965-4350965.
192. Sterling, T. and J.J. Irwin, ZINC 15--Ligand Discovery for Everyone. *J Chem Inf Model*, 2015. 55(11): p. 2324-37.
193. Banerjee, P., et al., Super Natural II--a database of natural products. *Nucleic Acids Res*, 2015. 43(Database issue): p. D935-9.
194. Clarke, H.J., et al., Endoplasmic reticulum stress in malignancy. *Cancer Cell*, 2014. 25(5): p. 563-73.
195. Dejeans, N., et al., Overexpression of GRP94 in breast cancer cells resistant to oxidative stress promotes high levels of cancer cell proliferation and migration: implications for tumor recurrence. *Free Radic Biol Med*, 2012. 52(6): p. 993-1002.
196. Shang, J., et al., Cheminformatic Insight into the Differences between Terrestrial and Marine Originated Natural Products. *J Chem Inf Model*, 2018. 58(6): p. 1182-1193.
197. Ziemert, N., et al., Diversity and evolution of secondary metabolism in the marine actinomycete genus *Salinispora*. *Proceedings of the National Academy of Sciences of the United States of America*, 2014. 111(12): p. E1130-E1139.
198. Giordano, D., et al., Chapter Four - Marine Microbial Secondary Metabolites: Pathways, Evolution and Physiological Roles, in *Advances in Microbial Physiology*, R.K. Poole, Editor. 2015, Academic Press. p. 357-428.
199. Howard, J.P., V. Albo, and W.A. Newton Jr, Cytosine arabinoside: Results of a cooperative study in acute childhood leukemia. *Cancer*, 1968. 21(3): p. 341-345.
200. D'Incalci, M. and C.M. Galmarini, A review of trabectedin (ET-743): a unique mechanism of action. *Mol Cancer Ther*, 2010. 9(8): p. 2157-63.
201. Demetri, G.D., et al., Efficacy and Safety of Trabectedin or Dacarbazine for Metastatic Liposarcoma or Leiomyosarcoma After Failure of Conventional

- Chemotherapy: Results of a Phase III Randomized Multicenter Clinical Trial. *J Clin Oncol*, 2016. 34(8): p. 786-93.
202. Aseyev, O., J.M. Ribeiro, and F. Cardoso, Review on the clinical use of eribulin mesylate for the treatment of breast cancer. *Expert Opin Pharmacother*, 2016. 17(4): p. 589-600.
203. Hu, X., W. Huang, and M. Fan, Emerging therapies for breast cancer. *J Hematol Oncol*, 2017. 10(1): p. 98.
204. Younes, A., et al., Results of a Pivotal Phase II Study of Brentuximab Vedotin for Patients With Relapsed or Refractory Hodgkin's Lymphoma. *Journal of Clinical Oncology*, 2012. 30(18): p. 2183-2189.
205. Illés, Á., Á. Jóna, and Z. Miltényi, Brentuximab vedotin for treating Hodgkin's lymphoma: an analysis of pharmacology and clinical efficacy. *Expert Opinion on Drug Metabolism & Toxicology*, 2015. 11(3): p. 451-459.
206. Fang, J., et al., Quantitative and Systems Pharmacology. 1. In Silico Prediction of Drug-Target Interactions of Natural Products Enables New Targeted Cancer Therapy. *Journal of chemical information and modeling*, 2017. 57(11): p. 2657-2671.
207. Zhou, H., M. Gao, and J. Skolnick, Comprehensive prediction of drug-protein interactions and side effects for the human proteome. *Scientific reports*, 2015. 5: p. 11090-11090.
208. Tatonetti, N.P., T. Liu, and R.B. Altman, Predicting drug side-effects by chemical systems biology. *Genome Biol*, 2009. 10(9): p. 238.
209. Hopkins, A.L., J.S. Mason, and J.P. Overington, Can we rationally design promiscuous drugs? *Current Opinion in Structural Biology*, 2006. 16(1): p. 127-136.
210. Vanhaelen, Q., et al., Design of efficient computational workflows for in silico drug repurposing. *Drug Discovery Today*, 2017. 22(2): p. 210-222.
211. Reker, D., et al., Identifying the macromolecular targets of de novo-designed chemical entities through self-organizing map consensus. *Proceedings of the National Academy of Sciences of the United States of America*, 2014. 111(11): p. 4067-4072.
212. Beedessee, G., et al., Ethyl acetate extract of the Mauritian sponge *Jaspis* sp. induces cell arrest in human promyelocytic leukemia cells. *Environmental Toxicology and Pharmacology*, 2013. 36(1): p. 58-65.
213. Yang, J.I., et al., Aqueous extracts of the edible *Gracilaria tenuistipitata* are protective against H₂O₂-induced DNA damage, growth inhibition, and cell cycle arrest. *Molecules*, 2012. 17(6): p. 7241-54.
214. Rajesh, R.P. and M. Annappan, Anticancer effects of brominated indole alkaloid Eudistomin H from marine ascidian *Eudistoma viride* against cervical cancer cells (HeLa). *Anticancer Res*, 2015. 35(1): p. 283-93.
215. Lin, Y.C., et al., A Soft Coral-Derived Compound, 11-Dehydrosinulariolide, Induces G₂/M Cell Cycle Arrest and Apoptosis in Small Cell Lung Cancer. *Mar Drugs*, 2018. 16(12).

216. Fu, C.W., et al., Anticancer efficacy of unique pyridine-based tetraindoles. *Eur J Med Chem*, 2015. 104: p. 165-76.
217. Chung, T.W., et al., Sinularin induces DNA damage, G2/M phase arrest, and apoptosis in human hepatocellular carcinoma cells. *BMC Complement Altern Med*, 2017. 17(1): p. 62.
218. Beedessee, G., et al., Ethyl acetate extract of the Mauritian sponge *Jaspis* sp. induces cell arrest in human promyelocytic leukemia cells. *Environ Toxicol Pharmacol*, 2013. 36(1): p. 58-65.
219. Weinheimer, A.J., et al., Marine anticancer agents: sinularin and dihydrosinularin, new cembranolides from the soft coral, *Sinularia flexibilis*. *Tetrahedron Letters*, 1977. 18(34): p. 2923-2926.
220. Su, T.R., et al., Proteomic investigation of anti-tumor activities exerted by sinularin against A2058 melanoma cells. *Electrophoresis*, 2012. 33(7): p. 1139-52.
221. Wu, Y.J., et al., Sinularin Induces Apoptosis through Mitochondria Dysfunction and Inactivation of the p13K/Akt/mTOR Pathway in Gastric Carcinoma Cells. *Mar Drugs*, 2016. 14(8).
222. Chung, T.-W., et al., Sinularin induces DNA damage, G2/M phase arrest, and apoptosis in human hepatocellular carcinoma cells. *BMC complementary and alternative medicine*, 2017. 17(1): p. 62-62.
223. Maderna, A. and C.A. Leverett, Recent advances in the development of new auristatins: structural modifications and application in antibody drug conjugates. *Mol Pharm*, 2015. 12(6): p. 1798-812.
224. Wang, L.J., et al., Design, synthesis and biological evaluation of novel bromophenol derivatives incorporating indolin-2-one moiety as potential anticancer agents. *Mar Drugs*, 2015. 13(2): p. 806-23.
225. Kim, D.H., J. Shin, and H.J. Kwon, Psammaphin A is a natural prodrug that inhibits class I histone deacetylase. *Experimental & Molecular Medicine*, 2007. 39: p. 47.
226. Ciavatta, M., et al., Marine Mollusk-Derived Agents with Antiproliferative Activity as Promising Anticancer Agents to Overcome Chemotherapy Resistance: MARINE MOLLUSK-DERIVED AGENTS WITH ANTIPROLIFERATIVE ACTIVITY. Vol. 37. 2016.
227. Kuo, L.-M., et al., The Bioactive Extract of *Pinnigorgia* sp. Induces Apoptosis of Hepatic Stellate Cells via ROS-ERK/JNK-Caspase-3 Signaling. *Marine Drugs*, 2018. 16(1).
228. Sellers, W.R. and D.E. Fisher, Apoptosis and cancer drug targeting. *The Journal of clinical investigation*, 1999. 104(12): p. 1655-1661.
229. Lopez, J. and S.W.G. Tait, Mitochondrial apoptosis: killing cancer using the enemy within. *British Journal Of Cancer*, 2015. 112: p. 957.
230. Taylor, R.C., S.P. Cullen, and S.J. Martin, Apoptosis: controlled demolition at the cellular level. *Nature Reviews Molecular Cell Biology*, 2008. 9: p. 231.
231. Kitanaka, C. and Y. Kuchino, Caspase-independent programmed cell death with necrotic morphology. *Cell Death Differ*, 1999. 6(6): p. 508-15.

232. Burney, I., *Cancer Chemotherapy and Biotherapy: Principles and Practice*. Sultan Qaboos University Medical Journal, 2011. 11(3): p. 424-425.
233. Brown, J.M. and L.D. Attardi, The role of apoptosis in cancer development and treatment response. *Nat Rev Cancer*, 2005. 5(3): p. 231-7.
234. Melino, G., R.A. Knight, and P. Nicotera, How many ways to die? How many different models of cell death? *Cell Death Differ*, 2005. 12 Suppl 2: p. 1457-62.
235. Mathew, R., V. Karantza-Wadsworth, and E. White, Role of autophagy in cancer. *Nat Rev Cancer*, 2007. 7(12): p. 961-7.
236. Wong, C.H., et al., Simultaneous Induction of Non-Canonical Autophagy and Apoptosis in Cancer Cells by ROS-Dependent ERK and JNK Activation. *PLOS ONE*, 2010. 5(4): p. e9996.
237. Valencia, A. and J. Morán, Reactive oxygen species induce different cell death mechanisms in cultured neurons. *Free Radical Biology and Medicine*, 2004. 36(9): p. 1112-1125.
238. Holze, C., et al., Oxceptosis, a ROS-induced caspase-independent apoptosis-like cell-death pathway. *Nature Immunology*, 2018. 19(2): p. 130-140.
239. Jia, Y., et al., Curcumol induces RIPK1/RIPK3 complex-dependent necroptosis via JNK1/2-ROS signaling in hepatic stellate cells. *Redox Biology*, 2018. 19: p. 375-387.
240. Zhang, S.Y., et al., Two new bioactive triterpene glycosides from the sea cucumber *Pseudocolochirus violaceus*. *J Asian Nat Prod Res*, 2006. 8(1-2): p. 1-8.
241. Zhang, S.Y., Y.H. Yi, and H.F. Tang, Cytotoxic sulfated triterpene glycosides from the sea cucumber *Pseudocolochirus violaceus*. *Chem Biodivers*, 2006. 3(7): p. 807-17.
242. Zhang, S.Y., H.F. Tang, and Y.H. Yi, Cytotoxic triterpene glycosides from the sea cucumber *Pseudocolochirus violaceus*. *Fitoterapia*, 2007. 78(4): p. 283-7.
243. Silchenko, A.S., et al., Structures of violaceosides C, D, E and G, sulfated triterpene glycosides from the sea cucumber *Pseudocolochirus violaceus* (Cucumariidae, Dendrochirotida). *Nat Prod Commun*, 2014. 9(3): p. 391-9.
244. Yasman, Y., et al., New 9-thiocyanatopupukeanane sesquiterpenes from the nudibranch *Phyllidia varicosa* and its sponge-prey *Axinyssa aculeata*. *J Nat Prod*, 2003. 66(11): p. 1512-4.
245. Stoffels, B.E., et al., Phylogenetic relationships within the Phyllidiidae (Opisthobranchia, Nudibranchia). *Zookeys*, 2016(605): p. 1-35.
246. Iijima, R., J. Kisugi, and M. Yamazaki, A novel antimicrobial peptide from the sea hare *Dolabella auricularia*. *Dev Comp Immunol*, 2003. 27(4): p. 305-11.
247. Poncet, J., The dolastatins, a family of promising antineoplastic agents. *Curr Pharm Des*, 1999. 5(3): p. 139-62.
248. MAKINO, N., Hemocyanin from *Dolabella auricularia*: I. Preparation and Properties. *The Journal of Biochemistry*, 1971. 70(1): p. 149-155.
249. Zhang, S.-Y., Y.-H. Yi, and H.-F. Tang, Cytotoxic Sulfated Triterpene Glycosides from the Sea Cucumber *Pseudocolochirus violaceus*. *Chemistry & Biodiversity*, 2006. 3(7): p. 807-817.

250. Berge, J.P. and G. Barnathan, Fatty acids from lipids of marine organisms: molecular biodiversity, roles as biomarkers, biologically active compounds, and economical aspects. *Adv Biochem Eng Biotechnol*, 2005. 96: p. 49-125.
251. Kumari, P., et al., 3 - Algal lipids, fatty acids and sterols, in *Functional Ingredients from Algae for Foods and Nutraceuticals*, H. Domínguez, Editor. 2013, Woodhead Publishing. p. 87-134.
252. Leal, C.M., et al., Marine Microorganism-Invertebrate Assemblages: Perspectives to Solve the "Supply Problem" in the Initial Steps of Drug Discovery. *Marine Drugs*, 2014. 12(7).
253. Forster, L.C., et al., Spongian-16-one Diterpenes and Their Anatomical Distribution in the Australian Nudibranch *Goniobranchus collingwoodi*. *Journal of Natural Products*, 2017. 80(3): p. 670-675.
254. Moritz, M.I., et al., Polyoxygenated steroids from the octocoral *Leptogorgia punicea* and in vitro evaluation of their cytotoxic activity. *Mar Drugs*, 2014. 12(12): p. 5864-80.
255. Levina, E.V., et al., Trofosides A and B and other cytostatic steroid-derived compounds from the far east starfish *Trofodiscus über*. *Russian Journal of Bioorganic Chemistry*, 2007. 33(3): p. 334-340.
256. Shin, B.A., et al., Lyso-PAF Analogues and Lysophosphatidylcholines from the Marine Sponge *Spirastrella abata* as Inhibitors of Cholesterol Biosynthesis. *Journal of Natural Products*, 1999. 62(11): p. 1554-1557.
257. Martinez, E.J., et al., Phthalascidin, a synthetic antitumor agent with potency and mode of action comparable to ecteinascidin 743. *Proc Natl Acad Sci U S A*, 1999. 96(7): p. 3496-501.
258. Ahmed, E.F., et al., A Comparative biochemical study on two marine endophytes, *Bacterium SRCnm* and *Bacillus sp. JS*, Isolated from red sea algae. *Pak J Pharm Sci*, 2016. 29(1): p. 17-26.
259. Flasiński, M., et al., Influence of platelet-activating factor, lyso-platelet-activating factor and edelfosine on Langmuir monolayers imitating plasma membranes of cell lines differing in susceptibility to anti-cancer treatment: the effect of plasmalogen level. *Journal of the Royal Society, Interface*. 11(95): p. 20131103-20131103.
260. Montrucchio, G., et al., Potential angiogenic role of platelet-activating factor in human breast cancer. *Am J Pathol*, 1998. 153(5): p. 1589-96.
261. Sharifi, S., et al., Inducing Apoptosis of Cancer Cells Using Sea Pen *Virgularia gustaviana* Extract Which is Comparable to Cembrane Diterpene Sarcophine. *Iranian journal of pharmaceutical research : IJPR*, 2018. 17(2): p. 640-652.
262. Sánchez, M.C., et al., Cembrane Diterpenes from the Gorgonian *Lophogorgia peruana*. *Journal of Natural Products*, 2006. 69(12): p. 1749-1755.
263. Pacheco, B.S., et al., Cytotoxic Activity of Fatty Acids From Antarctic Macroalgae on the Growth of Human Breast Cancer Cells. *Frontiers in bioengineering and biotechnology*, 2018. 6: p. 185-185.

264. Karuso, P. and P. Scheuer, Natural Products from Three Nudibranchs: *Nembrotha kubaryana*, *Hypselodoris infucata* and *Chromodoris petechialis*. *Molecules*, 2002. 7(1): p. 1.
265. Cheng, H.H., et al., Cytotoxic pheophorbide-related compounds from *Clerodendrum calamitosum* and *C. cyrtophyllum*. *Journal of Natural Products*, 2001. 64(7): p. 915-919.
266. Baudelet, P.-H., et al., Antiproliferative activity of *Cyanophora paradoxa* pigments in melanoma, breast and lung cancer cells. *Marine drugs*, 2013. 11(11): p. 4390-4406.
267. Nass, S.J., et al., Accelerating anticancer drug development – opportunities and trade-offs. *Nature Reviews Clinical Oncology*, 2018. 15(12): p. 777-786.
268. Hunter, T. and J.A. Cooper, Protein-tyrosine kinases. *Annu Rev Biochem*, 1985. 54: p. 897-930.
269. Cicenas, J., et al., Kinases and Cancer. *Cancers*, 2018. 10(3): p. 63.
270. Yang, H., et al., mTOR kinase structure, mechanism and regulation. *Nature*, 2013. 497(7448): p. 217-223.
271. Hasinoff, B.B., The cardiotoxicity and myocyte damage caused by small molecule anticancer tyrosine kinase inhibitors is correlated with lack of target specificity. *Toxicology and Applied Pharmacology*, 2010. 244(2): p. 190-195.
272. Force, T. and K.L. Kolaja, Cardiotoxicity of kinase inhibitors: the prediction and translation of preclinical models to clinical outcomes. *Nature Reviews Drug Discovery*, 2011. 10: p. 111.
273. Smyth, L.A. and I. Collins, Measuring and interpreting the selectivity of protein kinase inhibitors. *Journal of chemical biology*, 2009. 2(3): p. 131-151.
274. Yang, H., et al., mTOR kinase structure, mechanism and regulation. *Nature*, 2013. 497: p. 217.
275. Nantasenamat, C. and V. Prachayasittikul, Maximizing computational tools for successful drug discovery. *Expert Opin Drug Discov*, 2015. 10(4): p. 321-9.
276. Bello-Perez, M., et al., Discovery of nonnucleoside inhibitors of polymerase from infectious pancreatic necrosis virus (IPNV). *Drug Des Devel Ther*, 2018. 12: p. 2337-2359.
277. Encinar, J.A., et al., In silico approach for the discovery of new PPARgamma modulators among plant-derived polyphenols. *Drug Des Devel Ther*, 2015. 9: p. 5877-95.
278. Galiano, V., et al., Looking for inhibitors of the dengue virus NS5 RNA-dependent RNA-polymerase using a molecular docking approach. *Drug Des Devel Ther*, 2016. 10: p. 3163-3181.
279. Gilson, M.K., et al., BindingDB in 2015: A public database for medicinal chemistry, computational chemistry and systems pharmacology. *Nucleic Acids Research*, 2015. 44(D1): p. D1045-D1053.
280. Gilson, M.K., et al., BindingDB in 2015: A public database for medicinal chemistry, computational chemistry and systems pharmacology. *Nucleic Acids Res*, 2016. 44(D1): p. D1045-53.

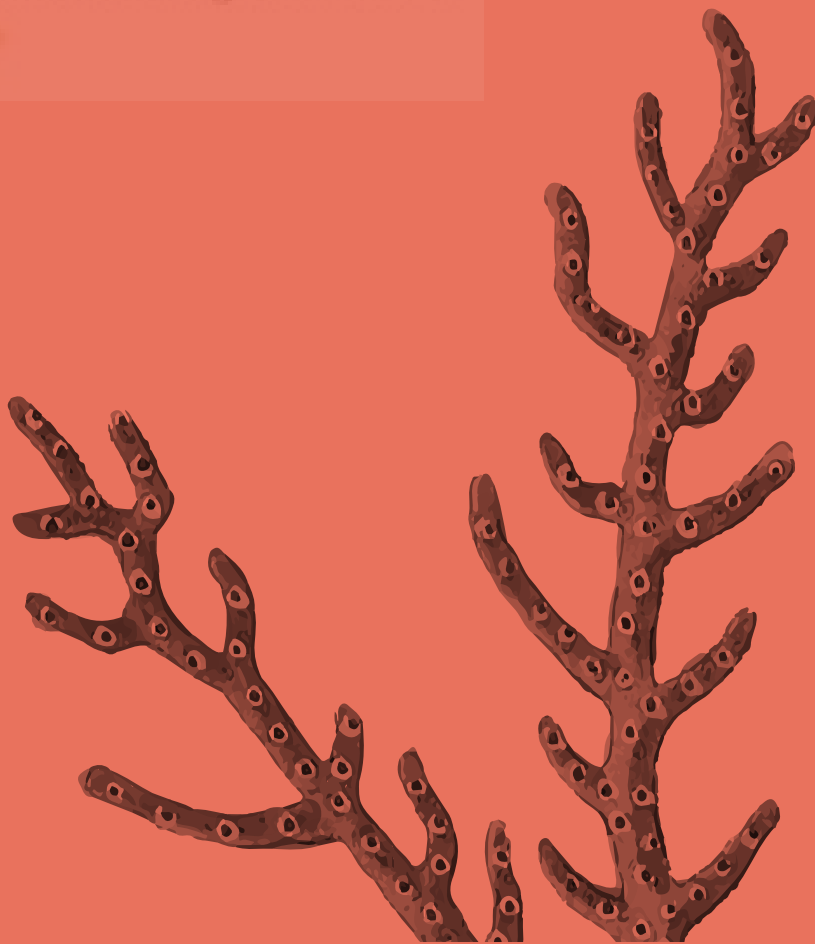
281. Schenone, S., et al., ATP-competitive inhibitors of mTOR: an update. *Curr Med Chem*, 2011. 18(20): p. 2995-3014.
282. Feldman, M.E., et al., Active-site inhibitors of mTOR target rapamycin-resistant outputs of mTORC1 and mTORC2. *PLoS Biol*, 2009. 7(2): p. e38.
283. Apsel, B., et al., Targeted polypharmacology: discovery of dual inhibitors of tyrosine and phosphoinositide kinases. *Nature chemical biology*, 2008. 4(11): p. 691-699.
284. Hoang, B., et al., The PP242 mammalian target of rapamycin (mTOR) inhibitor activates extracellular signal-regulated kinase (ERK) in multiple myeloma cells via a target of rapamycin complex 1 (TORC1)/eukaryotic translation initiation factor 4E (eIF-4E)/RAF pathway and activation is a mechanism of resistance. *The Journal of biological chemistry*, 2012. 287(26): p. 21796-21805.
285. Apsel, B., et al., Targeted polypharmacology: discovery of dual inhibitors of tyrosine and phosphoinositide kinases. *Nat Chem Biol*, 2008. 4(11): p. 691-9.
286. Menendez, Javier A., et al., Oncometabolic Nuclear Reprogramming of Cancer Stemness. *Stem Cell Reports*, 2016. 6(3): p. 273-283.
287. Kee, H.J. and J.-H. Cheong, Tumor bioenergetics: an emerging avenue for cancer metabolism targeted therapy. *BMB reports*, 2014. 47(3): p. 158-166.
288. Karpinska, A. and G. Gromadzka, [Oxidative stress and natural antioxidant mechanisms: the role in neurodegeneration. From molecular mechanisms to therapeutic strategies]. *Postepy Hig Med Dosw (Online)*, 2013. 67: p. 43-53.
289. Hasnain, S.Z., J.B. Prins, and M.A. McGuckin, Oxidative and endoplasmic reticulum stress in beta-cell dysfunction in diabetes. *J Mol Endocrinol*, 2016. 56(2): p. R33-54.
290. Saglar, E., et al., Assessment of ER Stress and autophagy induced by ionizing radiation in both radiotherapy patients and ex vivo irradiated samples. *J Biochem Mol Toxicol*, 2014. 28(9): p. 413-7.
291. Cai, Y., et al., Betulinic acid chemosensitizes breast cancer by triggering ER stress-mediated apoptosis by directly targeting GRP78. *Cell Death Dis*, 2018. 9(6): p. 636.
292. Kim, I., W. Xu, and J.C. Reed, Cell death and endoplasmic reticulum stress: disease relevance and therapeutic opportunities. *Nat Rev Drug Discov*, 2008. 7(12): p. 1013-30.
293. Sovolyova, N., et al., Stressed to death - mechanisms of ER stress-induced cell death. *Biol Chem*, 2014. 395(1): p. 1-13.
294. Sano, R. and J.C. Reed, ER stress-induced cell death mechanisms. *Biochim Biophys Acta*, 2013. 1833(12): p. 3460-3470.
295. Li, H.Y., et al., Celastrol induces apoptosis and autophagy via the ROS/JNK signaling pathway in human osteosarcoma cells: an in vitro and in vivo study. *Cell Death Dis*, 2015. 6: p. e1604.
296. Gardner, B.M. and P. Walter, Unfolded proteins are Ire1-activating ligands that directly induce the unfolded protein response. *Science*, 2011. 333(6051): p. 1891-4.

297. Hayashi, T., et al., Damage to the endoplasmic reticulum and activation of apoptotic machinery by oxidative stress in ischemic neurons. *J Cereb Blood Flow Metab*, 2005. 25(1): p. 41-53.
298. Zhao, Y., Y. Zhou, and M. Wang, Brosimone I, an isoprenoid-substituted flavonoid, induces cell cycle G1 phase arrest and apoptosis through ROS-dependent endoplasmic reticulum stress in HCT116 human colon cancer cells. *Food & Function*, 2019. 10(5): p. 2729-2738.
299. Choi, C., et al., Radiosensitization by Marine Sponge *Agelas* sp. Extracts in Hepatocellular Carcinoma Cells with Autophagy Induction. *Scientific Reports*, 2018. 8(1): p. 6317.
300. Pelicano, H., D. Carney, and P. Huang, ROS stress in cancer cells and therapeutic implications. *Drug Resist Updat*, 2004. 7(2): p. 97-110.
301. Wang, Q., et al., Overexpression of endoplasmic reticulum molecular chaperone GRP94 and GRP78 in human lung cancer tissues and its significance. *Cancer Detect Prev*, 2005. 29(6): p. 544-51.
302. Piskounova, E., et al., Oxidative stress inhibits distant metastasis by human melanoma cells. *Nature*, 2015. 527(7577): p. 186-91.
303. Gorrini, C., I.S. Harris, and T.W. Mak, Modulation of oxidative stress as an anticancer strategy. *Nat Rev Drug Discov*, 2013. 12(12): p. 931-47.



08

Scientific Production



Doctoral Student:
Verónica Ruiz Torres

An Updated Review on Marine Anticancer Compounds:

The use of Virtual Screening
for the discovery of Small-Molecule
Cancer Drugs

Doctoral Student:
Verónica Ruiz Torres

Review

An Updated Review on Marine Anticancer Compounds: The Use of Virtual Screening for the Discovery of Small-Molecule Cancer Drugs

Verónica Ruiz-Torres ¹, Jose Antonio Encinar ¹, María Herranz-López ¹, Almudena Pérez-Sánchez ¹, Vicente Galiano ², Enrique Barrañón-Catalán ^{1,*} and Vicente Micol ^{1,3}

¹ Institute of Molecular and Cell Biology (IBMC), Miguel Hernández University (UMH), Avda. Universidad s/n, Elche 03202, Spain; vruiz@umh.es (V.R.-T.); jant.encinar@umh.es (J.A.E.); mherranz@umh.es (M.H.-L.); almudena.perez@umh.es (A.P.-S.); vmicol@umh.es (V.M.)

² Physics and Computer Architecture Department, Miguel Hernández University, Avda. Universidad s/n, Elche 03202, Spain; vgaliano@umh.es

³ CIBER, Fisiopatología de la Obesidad y la Nutrición, CIBERobn, Instituto de Salud Carlos III. Palma de Mallorca 07122, Spain. (CB12/03/30038)

* Correspondence: e.barrajon@umh.es; Tel. +34 965222586

Molecules. 2017 Jun 23;22(7). pii: E1037. doi: 10.3390/molecules22071037.

Received: 22 May 2017; Accepted: 19 June 2017; Published: date

Abstract: Marine secondary metabolites are a promising source of unexploited drugs that have a wide structural diversity and have shown a variety of biological activities. These compounds are produced in response to the harsh and competitive conditions that occur in the marine environment. Invertebrates are considered to be among the groups with the richest biodiversity. To date, a significant number of marine natural products (MNPs) have been established as antineoplastic drugs. This review gives an overview of MNPs, both in research or clinical stages, from diverse organisms that were reported as being active or potentially active in cancer treatment in the past seventeen years (from January 2000 until April 2017) and describes their putative mechanisms of action. The structural diversity of MNPs is also highlighted and compared with the small-molecule anticancer drugs in clinical use. In addition, this review examines the use of virtual screening for MNP-based drug discovery and reveals that classical approaches for the selection of drug candidates based on ADMET (absorption, distribution, metabolism, excretion, and toxicity) filtering may miss potential anticancer lead compounds. Finally, we introduce a novel and publically accessible chemical library of MNPs for virtual screening purposes.

Keywords: marine natural product; invertebrate; cancer; virtual screening



1. Introduction

Cancer is defined as “a group of diseases characterized by the uncontrolled growth and spread of abnormal cells” and is one of the deadliest diseases globally. Cancer represents the second most common cause of death in Europe and USA after cardiovascular diseases according to *Cancer Facts and Figures of 2016*, a publication distributed by the American Cancer Society [1], and data extracted in October 2016 from Eurostat-Statistics Explained web. According to the same source, in the EU, the most frequent cancers are colorectal, breast, prostate and lung cancers. The predominant cancer type changes as a function of sex. American Cancer Society estimates that the cancer incidence rate is 20% higher in men than in women. Additionally, while breast cancer is the most common in women, lung cancer is more predominant in men. The second most frequent cancer in both men and women is colorectal cancer. Although significant advances are being made against cancer, this disease remains a key public health concern and a tremendous burden on European and American societies [2]. Every year, the American Cancer Society collects and compiles the most recent surveillance and epidemiology data about cancer (incidence, mortality and survival). In 2017, 1,688,780 new cancer cases will emerge, and 600,920 cancer deaths are projected to occur in the United States [3].

Recently, many advances have been made in the development of surgical procedures, radiotherapy and chemotherapeutic agents [4], including the case of combining chemotherapy and hormone therapy with immunotherapy [5]. One of the main problems that needs to be overcome in cancer treatment is that a tumor should be considered as a heterogeneous multiple cell subpopulation [6]. Another aspect to take into account is the development of resistant phenotypes, which include cytotoxic resistance to anticancer compounds and/or resistance to pro-apoptotic stimuli. All these factors must be considered to develop effective therapies for cancer. Despite all efforts to prevent oncological disorders and to develop new therapies, the cancer rate persists worldwide. Thus, there is an increasing emphasis on strategies to maximize tumor control, prolong survival, minimize chemotherapy side effects and improve quality of life for patients [7]. From a research point of view, this situation also demands the development of new drug discovery strategies and molecules.

Thirty years ago, the main approach of the pharmaceutical industry toward drug discovery was based on combinatorial chemistry (chemical synthetic methods to produce a large number of compounds in a simple process) [8]. By contrast, in the last few years, a new trend on drug discovery has been focused on natural products. Natural products are one of the main sources of compounds for drug discovery and have demonstrated considerable potential in the biomedical field. At least one-third of the current top twenty drugs on the market are derived from a natural source, mainly plants, and approximately 50% of the marketed drugs are classified as naturally derived or designed on the basis of natural compounds [9,10]. In contrast, only one of 5000–10,000 of the new synthetic molecules in development becomes a commercial pharmaceutical drug due to toxicity discovered in the clinical phases. Moreover, meta-

analyses have shown that studies sponsored by pharmaceutical companies are several times more likely to report positive results. All these factors are promoting an abundance of scientific studies focused on the putative beneficial effects of natural compounds on human health.

First, it is postulated that natural molecules have been evolutionarily selected to bind to biological macromolecules [11]. Second, these natural molecules, which exhibit unique structures, can serve as lead compounds for the development of new analogues. These factors may be the causes for the high dependence of drug discovery on the continuous supply of novel natural products. Recent advances in synthetic methodology and strategy are overcoming the barriers represented by the structural complexity of many natural products [12]. For example, in the field of antibiotics, resistant strains of pathogenic bacteria are increasing in number, and new compounds to combat these bacterial pathogens are needed. Only a few antibiotics have been developed in the past few decades after generations of synthetic tailoring, but in most cases, they share a common core structure, or scaffold. Multidrug resistance and the latest generation of pathogens suggest the necessity of discovering new chemical structures [11].

The production of metabolites occurs in all organisms as a result of the intrinsic reactions in the body induced by exogenous stimuli or substances [13]. Metabolites can be intermediate or end products of metabolism, and these molecules are transformed into new ones by cascades of enzymatic reactions, which include the processes involved in anabolism, catabolism and excretion of molecules from the body [14]. Because of all these reactions, a set of small molecules, such as metabolic intermediates, hormones and other signaling molecules, are produced, i.e., the metabolome. The general classification of these biomolecules considers two types of metabolites: primary metabolites, which are involved at the cellular level and are essential for life (embryogenesis, cell division, proliferation, differentiation, growth, development, and reproduction) and secondary metabolites, which participate in the homeostasis and natural defense of organisms [15,16].

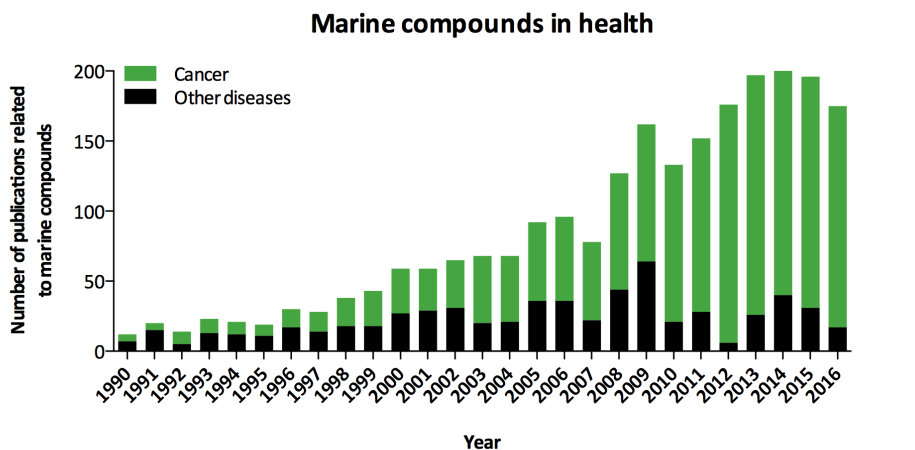
Natural products, especially secondary metabolites from terrestrial plants and microbes, have been a traditional source of drug molecules for many years (for example, the discoveries of aspirin, morphine and penicillin have led to an obvious “before” and “after” in terms of expectations and quality of life). Even in the area of cancer, products such as adriamycin or paclitaxel (Taxol) are used daily for the treatment of certain tumors [17]. The marine ecosystem offers unlimited sources of new isolable bioactive compounds with diversified chemical structures, which are considered potent sources for drug discovery [18]. Refinements in technologies (like scuba diving or marine prospection), along with the development of new analytical technologies, spectroscopy and high-throughput screening methods, have increased interest in unexplored MNPs.

Marine pharmacology is a new discipline that explores the marine environment searching for potential pharmaceuticals. In the last two decades, a large screening of marine compounds has been conducted, and a wide range of activities, such as antiviral [19] antibacterial [20], antifungal [21], antiparasitic [22], antitumor [23] and anti-

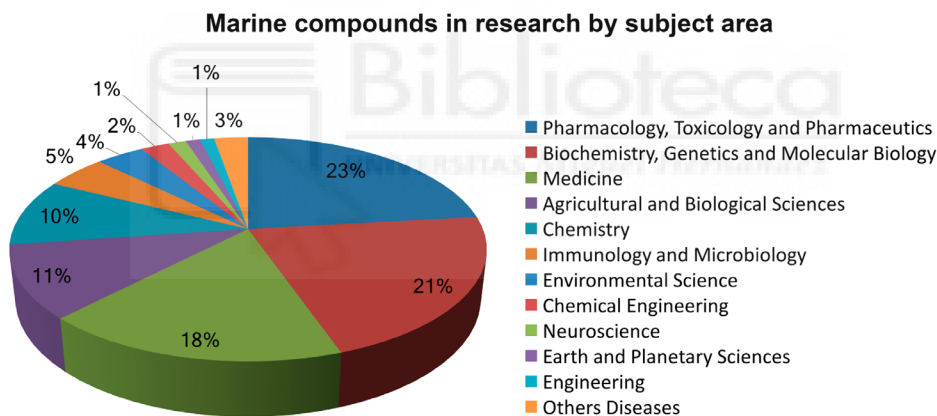
inflammatory [24], have been reported. Accordingly, marine compounds are becoming an option to be developed into ingredients for the cosmetic, pharmaceutical and food industries [25]. The marine chemical structures could also become an option for the treatment of drug-resistant infections [26] by offering new model structures. This hypothesis is also transferable to new anticancer drug development. Molecular scaffolds derived from marine organisms exhibit more novelty than terrestrial agents. A comparative analysis reported that 71.02% of molecular scaffolds in the Dictionary of MNPs were used only by marine organisms [27].

The marine environment represents approximately 70% of the earth's surface, and a huge biodiversity has been found, consisting of up to 36 phyla [28]. There is a hypothesis that high taxonomic diversity is correlated with a wide chemical diversity of natural products [29]. This great diversity of secondary metabolites affords marine organisms with a chance of survival in unfavorable conditions [30,31], and consequently, this diversity offers an abundant source of drugs that could be potential candidates for disease treatments. This is the reason why marine organisms represent a promising source of bioactive molecules [32]. Efforts to exploit this biochemical biodiversity have only just begun, and it is estimated that 18% of MNPs have been discovered so far compared with products of terrestrial origin [33].

In the history of the use of medicines, references to marine-based drugs are scarce. However, it is known that for thousands of years, ointments, concoctions and cataplasms of algae and marine muds have been used for treating endless diseases, especially in traditional Chinese and Japanese medicines [34]. In 1900, kainic acid, which was obtained from extracts of the seaweed *Digenea simplex*, was the first product of marine origin commercialized and was used as an insecticide and anthelmintic [35]. However, it was not until 1950 that the first drugs from sponges and marine microorganisms were identified. Spongothymidine and spongouridine, the first compounds isolated from the sponge *Cryptotheca crypta*, were obtained by chance [36]. An increasing number of documents about marine compounds with regard to human health have been published in the last twenty years (Figure 1A) in many different areas of knowledge (Figure 1B). To date, eight drugs isolated from marine organisms have been approved for different purposes (cytarabine, vidarabine, ziconotide, omega-3 acid ethyl esters, trabectedin, eribulin mesylate, brentuximab vedotin and iota-carrageenan) [2]. Five of these compounds are obtained from marine invertebrates and have been approved for use as pharmaceutical drugs in cancer treatment. These compounds are summarized in Table 1.



(A)



(B)

Figure 1. (A) The number of scientific publications about marine compounds displays an upward trend in the last twenty years, especially in the field of cancer. (B) Relevance of marine compounds by subject area. Data have been obtained from PubMed and Scopus for English language publications published without start date restrictions up to January 2017

Table 1. List of FDA- and EMEA-approved marine anticancer drugs from an invertebrate source.

Organization and Year	Compound Name	Marine Organism	Chemical Class	Disease Area	Mode of Action	Company or Institution	Refs
FDA 1969	Cytarabine (Ara-C)	Sponge	Nucleoside	Anticancer	DNA polymerase inhibitor	Bedford, Enzon	[37]
FDA 2004	Ziconotide	Cone snail	Peptide	Pain	Modulator of neuronal calcium channels	Neurex Corp	[38]
EMEA 2007	Trabectedin (E7389)	Tunicate	Alkaloid	Anticancer	Inhibits cancer cell growth of and affects the tumor microenvironment	PharmaMar	[39]
FDA 2010	Eribulin mesylate (E7389)	Sponge	Macrolide	Anti-breast cancer	Microtubule interfering agent	Eisai Inc.	[40]
FDA 2011	Brentuximab vedotin (SGN-35)	Mollusk	Antibody-drug conjugate	Lymphoma	CD30-directed antibody-cytotoxic drug conjugate	Seattle Genetics Inc.	[41]

The vast majority of animals living in the ocean fall into the category of invertebrates, and most of the scientific studies to date related to marine drug discovery are focused in these organisms. In fact, marine invertebrates, which lack a backbone (vertebral column), are identified as one of the foremost groups of biological organisms in terms of rich diversity and distribution [42]. Invertebrates are considered a ubiquitous and highly taxonomically diversified group since they can be found from the foreshore to the abyssal zone. Their major phyla include Porifera, Cnidaria, Annelida, Bryozoa, Mollusca, Arthropoda and Echinodermata [43]. Some invertebrate phyla have only one species, while others include more than 85% of all described animal species and consist of over a million species [43]. The most common marine invertebrates are from the Porifera, Cnidaria, Mollusca, Arthropoda and Echinodermata phyla and have provided a significant number of natural products with pharmacological properties, some of which are already in clinical trials [44]. In response to exposure to extreme and changing habitats, these organisms produce a wide variety of secondary metabolites that cannot be produced in other organisms. In addition to the number of unique natural products generated by invertebrates, the diversity of the group makes them a singular source of bioactive compounds [33]. At present, the various bioactive compounds from different invertebrates (cone snails, soft corals, sponges, sea squirts, marine worms, bryozoans, sea slugs and other marine organisms) have been recognized as an important source of antitumor compounds [45]. A study of 2011 by Hu et al. showed that approximately 75% of the 20,000 MNPs described to date are derived from marine invertebrates [46]. Therefore, it is expected that in the future, bioprospecting efforts will continue to target marine invertebrates. In 2012, Leal et al. [47] compiled scientific studies about existing MNPs and classified them according to phyla of their invertebrate source. They found that approximately 80% were into the phyla Porifera (47.1%) and Cnidaria (33.5%). The rest of them were in the phyla Echinodermata (7.4%), Chordata (6.0%), and Mollusca (5.0%). They also compared the MNPs by chemical group and demonstrated that in the Porifera or Cnidaria phyla, a particular chemical group was not always prevalent through the same phylum [47].

Typical compounds with health benefits obtained from invertebrates include polyunsaturated fatty acids, peptides, proteins, polysaccharides, polyphenols, saponins, sterols, minerals, and other bioactive compounds such as pigments (e.g., carotenoids) [48]. To date, more than 20,000 novel chemicals have been found from marine sources, and that number is rising every year [33]. In recent years, these marine secondary metabolites have yielded a considerable number of drug candidates, most of which are still in preclinical or early clinical development, with only a limited number already on the market [49]. Table 2 contains the most relevant examples of MNPs in clinical and preclinical phases.

The purpose of this article is to review the research literature published since 2000 in the field of marine antitumor pharmacology and propose new *in silico* strategies to accelerate drug discovery. In this sense, novel antitumor marine compounds from invertebrates grouped by their chemical structures, their putative mechanisms of action and their use in preclinical or clinical cancer studies are discussed. Moreover, we have

analyzed the discrepancy in the results from a comparison between the properties of drug candidates filtered *in silico* from a particular library that obeys ADMET rules and the properties of the 168 most promising anticancer compounds from the “Genomics of Drug Sensitivity in Cancer (GDSC) database”. A new library of MNPs for *in silico* and analytical purposes is also presented (<http://docking.umh.es/chemlib/mnplib>).

2. Chemical Classification of Marine Bioactive Compounds

Although several classifications have been made [46,50], taking into account their chemical structures, the most common chemical classes of MNPs are alkaloids, polyketides, terpenes, peptides, and carbohydrates. This section gives a brief description of the principal characteristics of the different classes of marine-sourced compounds.

2.1. Alkaloids

Alkaloids are a highly diverse group of widely distributed compounds. Pelletier et al. [48] defined alkaloids as “cyclic organic compounds containing nitrogen in a negative oxidation state which is of limited distribution among living organisms”. There are various classifications of alkaloids in terms of their chemical structure, biological activity, biosynthetic pathway, and composition as heterocyclic or nonheterocyclic compounds [51]. Kumar et al. [52] classified alkaloids into seven subclasses: pyridoacrine alkaloids, indole alkaloid, pyrrole alkaloids, isoquinoline alkaloids, guanine alkaloids, aminoimidazole alkaloids, and sterol alkaloids [53]. Alkaloids have been isolated from marine organisms such as sponges, tunicates, anemones, and mollusks, all of which are characterized bright colors and patterns, which are often related to alkaloids [54]. Alkaloids are attributed a wide range of biological activities, including antifouling [55], cytotoxic [56], antileukemic [57], antimalarial [58] and antimicrobial [59].

2.2. Polyketides

Polyketides are natural metabolites that comprise a highly diverse class of chemical structures. Compounds in this class include macrolides, polyethers, polyols and aromatic compounds. This class is often highly oxygenated [53] and contains multiple β -hydroxyketone or β -hydroxyaldehyde functional groups. Polyketides are complex organic compounds similar to fatty acids: first, because both are synthesized by the decarboxylative condensation of malonyl-CoA and other acyl-CoAs; however, in polyketides, more than one monomer type may be used to construct different sized aromatic groups or reduced chains. Second, polyketides and fatty acids are associated with a wide variety of essential cellular functions; however, polyketides are more complex in their biosynthetic routes [60]. These metabolites are isolated from sponges, ascidians, soft corals and bryozoans [33] and can be produced by commensal or

symbiotic bacteria [61]. Polyketides possess wide-ranging biological activities, including antibiotic, anticancer, antifungal, antiparasitic and neurotoxic effects [53].

2.3. Terpenes

Terpenes are the final products from biosyntheses involving a five-carbon isoprene structure. Depending on the number of units, they can be classified as monoterpenes, sesquiterpenes, diterpenes, sesterterpenes, triterpenes (steroids), and tetraterpenes (carotenoids) [53,62]. Several groups of marine organisms produce terpenes, which exhibit biological activities such as cytotoxic, antiproliferative, antifouling, antifungal, and antimicrobial activities [63].

2.4. Peptides

Peptides are sources of nitrogen and amino acids ranging in size from 2 to 20 amino acids residues and are related to numerous potential physiological functions. Bioactive peptides can be protein fragments that acquire functionality when liberated from the parent protein [64]. The first activity assigned to a peptide was neurotoxicity; however, at present, they are associated with other functions, such as cardiogenic, antiviral and antitumor, cardiotoxic and antimicrobial activity [65]. These functions, in addition to their excellent binding properties, low off-target toxicity, and high stability, make peptides promising molecules for the development of new therapeutics [66]. Approximately 60% of described natural products belong to peptide family [67]. Peptides are present in many marine species, and the extensive research that has been conducted on them has shown that they most often found in sponges [65], as occurred with polyketides, peptides can be also produced by commensal or symbiotic bacteria or fungi.

2.5. Carbohydrates, Glycosides and Others

The major class of carbohydrates that can be isolated from marine organisms are polysaccharides [53], but it is also possible to obtain low molecular weight glycosylated oligosaccharides, usually from sponges and tunicates [68]. Polysaccharides are a diverse class of macromolecules comprising polymers of monosaccharides bonded with glycosidic residues and exhibiting a wide structural diversity [69]. These versatile compounds are used extensively in pharmaceuticals, including in gel production, drug delivery systems, wound healing, tissue engineering, and blood dialysis membranes. In addition, they have displayed functions such as antimutagenic, antitumorogenic, hypocholesterolemic, and anticoagulant activities [70]. Marine oligosaccharides are generated by the hydrolysis of marine polysaccharides. Normally, oligosaccharides contain between 10 to 12 monosaccharide units, but certain oligosaccharides have 30 or more units, such as some rhamnogalacturonans [71]. Oligosaccharides have complex and heterogeneous chemical structures, and this is correlated with the diverse

biological actions in which they are involved [72]. Despite their biological relevance, there are no studies about the anticancer activity of carbohydrates of marine origin.

Glycosides are considered a class of carbohydrates. These molecules have a sugar bound to another functional group through a glycosidic bond. They have two parts, the sugar and the aglycone chemical group (a terpene, flavonoid, coumarine or other natural molecule) [73].

Glycosaminoglycans are molecules with a linear and complex carbohydrate structure [74]. These molecules are present on all animal cell surfaces and display considerable sequence heterogeneity, which is responsible for their highly specific interactions with other macromolecules [75].

Nucleoside analogues such as cytarabine and gemcitabine are compounds that have similar structures to cytosine and that inhibit DNA synthesis by being incorporated into nascent DNA chains, interfering with chain elongation and promoting abnormal fragment ligation.

3. MNP-Based Drugs that Are Approved or in Ongoing Clinical Trials

Some MNPs have already provided promising results in their preclinical phases and have been promoted to clinical trials or even approved by regulatory agencies. This section provides updated information on the most significant examples of currently approved drugs (summarized in Table 1) and those that are still in clinical trials (summarized in Table 2), grouping these compounds according to their chemical structure and giving details about their origins and their potential mechanisms of action.

Table 2. List of marine drugs in clinical trials.

Clinical Status	Compound Name	Marine Organism	Chemical Class	Disease Area	Mode of Action	Company or Institution	Refs
Phase III	Plitidepsin	Tunicate	Depsipetide	Anti-cancer	Induces cell cycle arrest or apoptosis	PharmaMar	[76]
	Gemcitabine (GEM) (Gemzar)	Sponge	Nucleoside	Anti-cancer	Ribonucleotide reductase inhibitor Replaces cytidine during DNA replication	Eli Lilly and Company	[77]
	Glembatumumab vedotin	Mollusk	Antibody drug conjugate	Breast cancer and melanoma	Targets glycoprotein NMB (a protein overexpressed by multiple tumor types)	Celldex Therapeutics	[78]
Phase II	Elisidepsin	Mollusk	Depsipetide	Anti-cancer	Antineoplastic agent, modifying lipids from cell membrane	PharmaMar	[79]
	PM1004	Nudibranch	Alkaloid	Anti-cancer	DNA-binding	PharmaMar	[80]
	Pseudopterosins	Soft coral	Diterpen glycoside	Wound healing	Eicosanoid metabolism	The Regents Of The University Of California	[81]
	IPL576,092 (Contignasterol derivative)	Sponge	Miscellaneous	Anti-inflammatory	Inhibition of leucocyte infiltration and hypersensitivity during allergy	Aventis Pharma	[82]

Cont.

Phase I/II	PM-10450 (Zalypsis®)	Sponge	Alkaloid	Anti-cancer drug	Transcription inhibitor	PharmaMar	[83]
	Discodermolide	Sponge	Polyketide	Anti-cancer drug	Microtubule interfering agent	Novartis	[84]
	Bryostatins-1	Bryozoa	Polyketide	Anti-cancer drug	Protein kinase C	National Cancer Institute	[85]
Phase I	Pinatuzumab vedotin	Mollusk	Antibody drug conjugate	Non-Hodgkin lymphoma, leukemia	Apoptosis stimulant; Mitosis inhibitor and Tubulin inhibitor	Genentech, Inc.	[86]
	Tisotumab Vedotin (HuMax®-TF-ADC)	Mollusk	Antibody drug conjugate	Ovarian, endometrium, cervix and prostate cancer	Antineoplastic, Drug conjugate, Immunotoxin and monoclonal antibodies	Genmab and Seattle Genetics	[87]
	HT1286 (Hemiasterlin derivative)	Sponge	Tripeptide	Anti-cancer drug	Microtubule interfering agent	Wyeth	[84]
Phase I	LAF389 (Bengamide B derivative)	Sponge	Peptide	Anti-cancer drug	Methionine aminopeptidase inhibitor	Novartis	[84]
	Hemiasterlin (E7974)	Sponge	Tripeptide	Anti-cancer drug	Microtubule interfering agent	Eisai Inc.	[84]
	PM-060184	Sponge	Polyketide	Anti-cancer drug	Microtubule interfering agent	PharmaMar	[88]
Phase I	NVP-LAQ824	Sponge	Miscellaneous	Anti-cancer drug	Histone deacetylase (HDAC) inhibitors or DNA methyltransferases (DNMT) inhibitor	Novartis Pharma	[89]
	(Psammaplin derivative, Dacinostat)	Sponge	Miscellaneous	Anti-cancer drug	Histone deacetylase (HDAC) inhibitors or DNA methyltransferases (DNMT) inhibitor	Novartis Pharma	[89]

Trabectedin (Yondelis[®], ET-743) (Figure 2), a semisynthetic tetrahydroisoquinoline alkaloid that was originally derived from the marine tunicate *Ecteinascidia turbinata*, was the first marine anticancer agent approved in the European Union for patients with soft tissue sarcoma (Table 1) [39,90]. PM1004, or Zalypsis[®], is related to jorumycin, a natural alkaloid isolated from the skin and mucus of the Pacific nudibranch *Jorunna funebris* [91,92] and also found in sponges and tunicates [92]. This compound is in phase II clinical studies (Table 2) because of its putative chemotherapeutic activity against solid human tumors and hematological malignancies (Ewing sarcoma, urothelial carcinoma, endometrial and cervical cancer and multiple myeloma) [83,93].

Among clinically approved polyketides, eribulin mesylate (E7389) (Table 1), which was originally extracted from the marine sponge *Halichondria okadai*, is an analogue of halichondrin B that acts as a non-taxane microtubule dynamics inhibitor. The FDA approved E7389 for the treatment of liposarcoma and breast cancer in 2010 [94]. Discodermolide (Table 2) is a polyketide in phase I/II trials isolated from the marine sponge *Discodermia dissoluta* that acts as a microtubule interfering agent, binding microtubule bundles, disrupting mitotic spindles and inducing cell cycle arrest at the G2/M phase [95]. Bryostatin 1 is a polyketide (Table 2 and Figure 2) isolated from the bryozoan *Bugula neritina* and derived from sponges and tunicates. This compound has been proven to be active against multiple carcinomas [96] and is currently undergoing two phase I trials for assessment as a treatment for Alzheimer's disease and cancer [37] (Table 2).

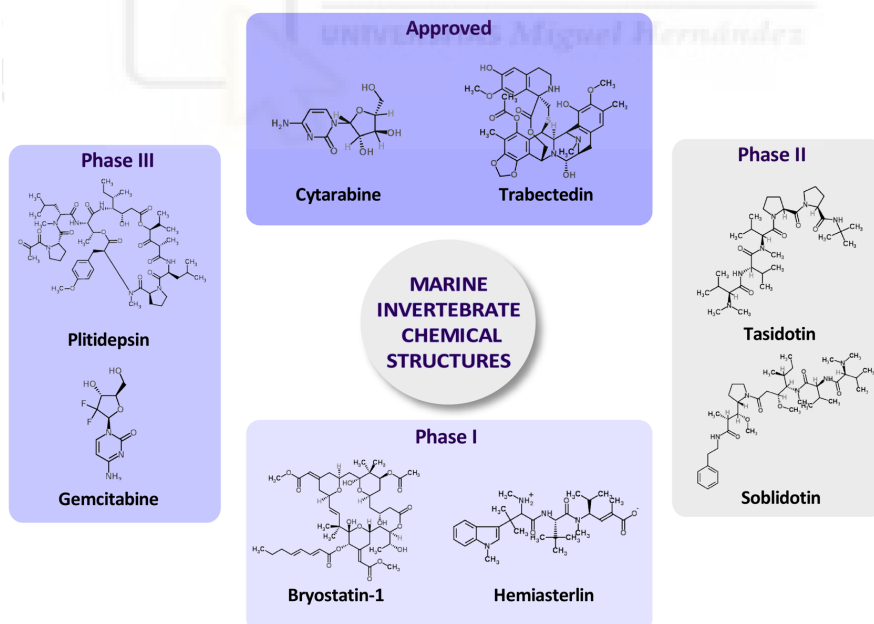


Figure 2. Chemical structures of selected marine invertebrate compounds that are either approved or in clinical trials.

Although there are no compounds from the terpene family in clinical trials related to their application in cancer treatment, there are data on the use of these compounds in other diseases. For example, the pseudopterosins (Table 2), which are diterpene glycosides from the soft coral *Pseudoptero-gorgia elisabethae*, showed potent activity as anti-inflammatory and wound-healing agent in a phase II clinical trial [97]. Moreover, Mayer et al. found that both pseudopterosin E and pseudopterosin A were effective at reducing edema when administered topically [98].

The most representative pharmaceutical products derived from marine peptides are ziconotide (Table 1) and brentuximab vedotin (SGN-35), which are a natural marine peptide and a peptide derivative, respectively, that have reached the market [99]. Brentuximab vedotin (Table 1) is an approved peptide derivative manufactured by chemical synthesis. This compound is an antibody-drug conjugate with a strong antimitotic capacity that targets the cell membrane protein CD30. It was approved by the FDA in 2011 for the treatment of Hodgkin and systemic anaplastic large-cell lymphoma [100].

Plitidepsin is a compound that features a peptide chemical structure (Table 2) and is currently in clinical phase III trials [101]. This marine cyclic depsipeptide (a polymeric compound with peptide and ester linkages), also known as Aplidin[®], (Figure 2) is isolated from the Mediterranean tunicate *Aplidium albicans* [102] and is now accessible via chemical synthesis. Plitidepsin is in phase III clinical development for several neoplasias, including breast, melanoma and non-small-cell lung cancers [103]. Plitidepsin induces dose-dependent cell cycle arrest in cultured cells from solid tumors and apoptotic process through the activation of c-Jun N-terminal kinase (JNK) [103]. In hematological cancer cells, plitidepsin activates the intrinsic and extrinsic apoptotic pathways [104,105] at nanomolar concentrations.

Soblidotin (TZT-1027) (Figure 2), which is in phase II trials, is an microtubule active drug derived from the antimitotic dolastatin-10, which was isolated from the sea hare *Dolabella auricularia*, that specifically damages tumor vasculatures by exerting a considerable antivascular effect along with an excellent cytotoxic effect [106]. Tasidotin (Table 2 and Figure 2), or synthadotin (ILX-651), is a water-soluble dolastatin pentapeptide derivate [107] with microtubule targeting activity in advanced solid tumors [107] and is also in phase II trials. Elisidepsin (PM02734, Irvalec[®]) and glembatumumab vedotin (Table 2) are also in phase II clinical trials. Elisidepsin, a synthetic cyclic depsipeptide belonging to the Kahalalide family of compounds [108], is derived from a sacoglossan sea slug species, *Elysia rufescens*. . Glembatumumab vedotin is a peptide in phase II (Table 2) that was isolated from mollusks and cyanobacteria and is currently synthesized to treat breast cancer and melanoma [109]. Pinatuzumab vedotin and Tisotumab vedotin, both of which were isolated from mollusks and cyanobacteria, are also in phase I trials. Pinatuzumab vedotin has activity against non-Hodgkin lymphoma and chronic lymphocytic leukemia [110]. Tisotumab vedotin (HuMax[®]-TF-ADC) is an antibody-drug conjugate that has inhibited tumor growth in preclinical experiments [111]. Hemiasterlin (E7974), which is also in phase I trials (Table 2 and Figure 2), is a cytotoxic tripeptide from the marine sponges

Hemiasterella minor, *Cymbastela* sp. and *Auletta* sp. [112] consisting of three sterically congested amino acids. The compound showed a potent antimetabolic effect related to the inhibition of tubulin polymerization by binding to the Vinca alkaloid binding site [113]. Marchetti et al. [114] have developed a hybrid drug by conjugating two tubulin inhibitors, one of which was hemiasterlin. This derivative possessed stronger and more potent anti-tubulin activity against human Caucasian ovary adenocarcinoma SKOV3 cells [114]. Taltobulin (HTI286), another hemiasterlin derivative, is also in phase I clinical trials [84].

Cytarabine (Ara-C) (Table 1, Figure 2) is a synthetic compound derived from spongothymidine, which was isolated from the marine sponge *Cryptotheca crypta*. This compound is a nucleoside that has already been approved and commercialized and that has mainly been used in leukemia [115]. Gemcitabine (Figure 2) is a nucleoside analogue (specifically, a fluorinated derivative of cytarabine) in phase II and III clinical development [77,116] and is used in various carcinomas, such as non-small cell lung cancer, pancreatic cancer, bladder cancer and breast cancer [117].

Finally, dacinostat (LAQ824) (Table 2 and Figure 2) is a synthetic hydroxamic acid derivative in phase I trials that inhibits histone deacetylases (which are validated targets for anticancer therapy) at nanomolar concentrations [118].

4. MNPs under Research or in Preclinical Stages Classified by Cancer Molecular Targets

In this part of the review, compounds under active research or in preclinical phases are summarized according to the ability of these natural products to modulate one or more hallmarks of cancer and become promising anticancer drug candidates. This section presents an overview of the most relevant compounds from 2010 to 2017. Before starting, it must be considered that normal cells become cancer cells through a wide range of genetic changes, and this process generates many different types of cancer [119]. However, most cancer types share similar characteristics, and these must be studied to progress anticancer drug discovery and cancer treatment. Hanahan and Weinberg identified six major targets in human tumors: self-sufficiency in growth signals, insensitivity to growth-inhibitory (antigrowth) signals, evasion of programmed cell death (apoptosis), limitless replicative potential, sustained angiogenesis, and tissue invasion and metastasis [120]. This part of the review focuses on marine compounds that play a role in some of the hallmarks described by Hanahan and Weinberg. Then, we have classified MNPs as growth inhibitors and anti-tubulin agents, inducers of apoptosis and autophagy, and anti-angiogenic, anti-migration, anti-invasion and anti-metastatic agents. In addition, due to their relevance in signal transduction pathways, a supplementary family that includes inhibitors of proliferation and of mitogen-activated protein kinases (MAPKs) are also included. All these categories are shown in Figure 3.

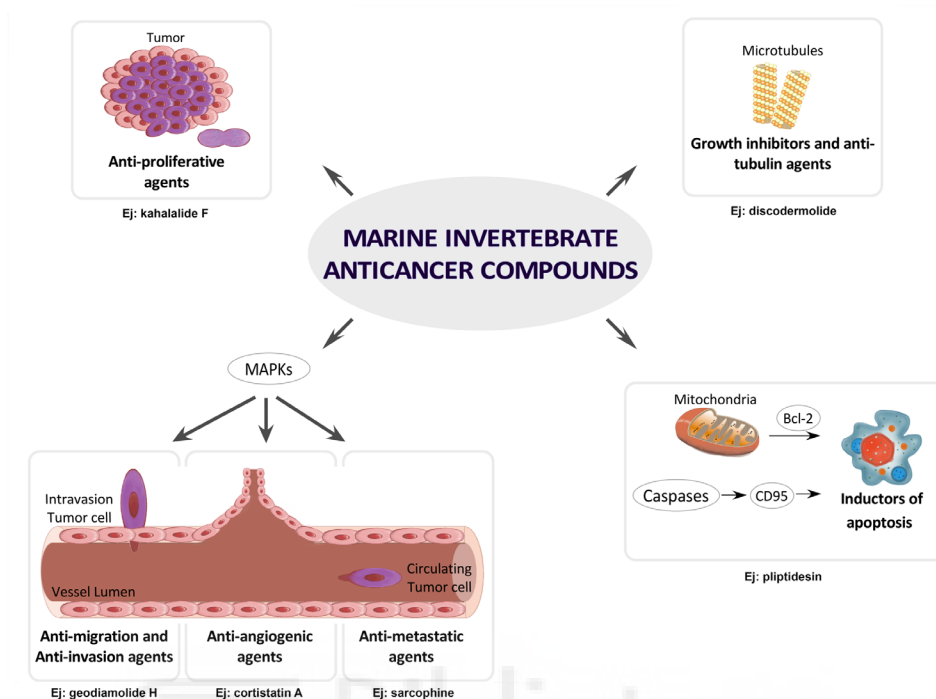


Figure 3. Major molecular targets of marine compounds known to modulate different hallmarks of cancer.

4.1. Growth Inhibitors and Anti-Tubulin Agents

Microtubules are cytoskeletal fibers composed of tubulin subunits. These structures are the key components of the cytoskeleton and are essential in all eukaryotic cells because of their functions, namely, the maintenance of cell shape, the transport of vesicles and cell signaling molecules, mitochondria homeostasis, motility and organelle distribution [121]. In addition, the microtubule system plays an important role in mitosis and cell division, making it an important target for anticancer drugs [122]. Microtubules are composed of heteropolymers of α -, γ - and β -tubulin in a head-to-tail arrangement that form dimers. These dimers polarize into 13 parallel protofilaments, which form a rigid hollow structure. Because both α - and β -tubulin dimers bind to GTP before assembling into microtubules, the equilibrium between the dimeric state and the polymeric state is regulated by dynamics that are dependent on the hydrolysis of the GTP nucleotide. GTP-bound heterodimers are more likely to polymerize, whereas those bound to GDP shift the equilibrium toward the free species. GTP is essential for the stability of the microtubules and the polymerization-depolymerization equilibrium. Microtubules and free tubulin dimers exist in a highly dynamic equilibrium, which is very sensitive to external factors [123]. Antitumor drugs can disrupt the microtubule equilibria, inhibiting the mitotic spindle and acting as antimetastatic agents by causing

mitotic arrest [124]. Microtubule-targeted antimetabolic drugs can be divided into microtubule-destabilizing agents and microtubule-stabilizing agents (Figure 3). The Vinca alkaloids (vinblastine, vincristine, vinorelbine, vindesine and vinflunine), cryptophycins, halichondrins, estramustine, colchicine and combretastatins are microtubule-destabilizing agents because they inhibit microtubule polymerization at high concentrations. The microtubule-stabilizing agents stimulate microtubule polymerization and include paclitaxel, docetaxel, the epothilones and discodermolide [125,126]. Microtubule-targeting agents are important anticancer drugs used in the treatment of breast, ovarian, and lung cancer [127]. The main MNPs associated with this category are listed below.

Dolastatin-10 was isolated from the marine mollusk *Dolabella auricularia* and the marine cyanobacterium *Symploca* sp. [128]. This compound is a linear pentapeptide containing several unique amino acid subunits and is one of the most potent members of a large class of peptides [129]. Dolastatin-10 was compared to other antimetabolic drugs (vinblastine, maytansine, rhizoxin, and phomopsin A) in terms of their ability to interfere with the binding of Vinca alkaloids to tubulin. The polymerization inhibition effect of dolastatin 10 was found to be even higher than that of vinblastine [129]. As mentioned above, there are two drugs based on dolastatin-10 in clinical trials: soblidotin and tasidotin (Table 2).

Vitilevuamide, a bicyclic 13 amino acid peptide isolated from two marine ascidians, *Didemnum cuculiferum* and *Polysyncranton lithostrotum* [130], had a cytotoxic effect at nanomolar concentrations on several human tumor cell lines. This compound exhibited potent inhibition of tubulin polymerization, displaying activity *in vivo* against P388 lymphocytic leukemia and showing an interaction with the GTP binding site, which was also weakly affected by the presence of vitilevuamide.

Some peptides from marine sources, such as diazomamide A [131] (isolated from the marine ascidian *Diazona angulata*) [132] and scleritodermin A [133] (isolated from the sponge *Scleritoderma nodosum*), have shown potent disruption of tubulin polymerization in different cancer cells and have a unique binding site on tubulin from the Vinca alkaloids [134].

Spongistatins, macrocyclic lactones containing six pyran rings that were isolated from sponges in the genus *Hytrios*, has exhibited a potent cytotoxic effect on solid tumors and thus are in phase I clinical trials. These compounds are also noncompetitive inhibitors of vinblastine and dolastatin binding [135]. At nanomolar concentrations, spongistatins exhibit potent activity by inhibiting microtubule organization and preventing mitotic spindle formation in human breast cancer cells [135].

Taltobulin (HTI-286) (Table 2) is a synthetic analogue of the naturally occurring tripeptide hemiasterlin (isolated from the sponge *Hemiasterella minor*) with potential antimetabolic and antineoplastic activities. This compound has advanced to clinical trials due to its ability to inhibit tubulin polymerization in a similar manner to colchicine and cause cell cycle arrest at the G2/M phase, blocking cell division and apoptosis [136].

Peloruside A, a macrolide (polyketide) isolated from the marine sponge *Mycale hentscheli*, binds to a distinct, non-taxoid binding site on tubulin. This compound was

tested in a human breast adenocarcinoma cell line (MCF7) stably expressing GFP- α -tubulin, and peloruside A at nanomolar concentrations was found to be able to inhibit the growth rate and change the length of microtubules [137] in a concentration-dependent manner. Zampanolide is another marine natural macrolide that belongs to the family of microtubule-stabilizing cytotoxic agents and was originally isolated in 1996 from the marine sponge *Fasciospongia rimosa* [138]. This compound has a highly unsaturated, 20-membered macrolide ring and an N-acyl hemiaminal side chain. Zampanolide was characterized as a cytotoxic agent that promoted tubulin assembly and blocked cells in G2/M phase of the cell cycle [139]. In recent studies, it has been confirmed as a microtubule-stabilizing agent that covalently reacts with the taxane luminal site in both tubulin α,β -heterodimers and microtubules [140].

Dictyostatin, an antimetabolic macrolide (polyketide) isolated from the sponge *Corallistidae* sp., demonstrated cytotoxic properties in human cancer cells at nanomolar concentrations with a Taxol-like mechanism of action, binding to tubulin and promoting microtubule assembly [141,142]. As mentioned above, Discodermolide (Table 2) is a polyketide already in clinical trials. In addition to its activity under study, this compound exerted antiproliferative action against paclitaxel-resistant human tumor cells that presented β -tubulin mutations [143]. Several hybrid compounds of discodermolide and dictyostatin have been developed and found to maintain their antiproliferative activity against several taxane-resistant cell lines [144,145]. Laulimalide is a macrolide isolated from the marine sponge *Cacospongia mycofijiensis* and has the ability to inhibit cell proliferation with anti-tubulin activity by promoting the assembly of the microtubules and stabilizing them in a Taxol-like way. However, this compound has a different binding site, which is placed on two adjacent β -tubulin units between the tubulin protofilaments of a microtubule [146].

4.2. Inductors of Apoptosis and Autophagy

In an organism, programmed cell death is a terminal point for cells and is involved in various processes, such as morphogenesis, maintenance of tissue homeostasis, and elimination of damaged cells. Dysfunction of programmed cell death and accumulation of errors can allow malignant cells to survive and disseminate. Many studies have categorized programmed cell death into three types: apoptosis, autophagy and a variant form of apoptosis called necroptosis [147,148]. This section of the review is focused on marine compounds that lead the apoptosis and autophagy of cancer cells.

Apoptosis involves the genetically programmed elimination of cells [149] and is a fundamental process associated with development, physiology and homeostasis. Any alteration in the balance of pro- and anti-apoptotic signals can lead to a variety of pathological conditions, including cancer [150].

In mammals, the most recent research indicates the existence of two major signaling systems that result in caspase activation and produce apoptosis (Figure 3). These pathways are the intrinsic or mitochondrial death [151] and the extrinsic or death receptor [152] pathways. Both are related to the cleavage of caspase-3 and produce

fragmentation of DNA, degradation of cytoskeletal and nuclear proteins, cross-linking of proteins, formation of apoptotic bodies, expression of ligands for phagocytic cell receptors and finally uptake by phagocytic cells [153]. The intrinsic pathway is stimulated by intracellular stress such as radiation, growth factor reduction, decreased cytokines and cytotoxic drugs. This pathway is controlled by the Bcl-2 family of proteins [154], which release cytochrome c (Cyt c) from the mitochondria to the cytosol and interact with APAF-1 to generate the apoptosome, a molecular platform for caspase 9 activation, which consequently activates caspases 3 and 7. The extrinsic pathway does not involve the mitochondria and is stimulated by cell-surface death receptors such as CD95 (Apo-1 or Fas), TRAIL, and tumor necrosis factor receptor 1.

Autophagy, an evolutionarily conserved catabolic process, is a cellular degradation pathway for the clearance of damaged or superfluous proteins and organelles [155]. Autophagy is often activated by reactive oxygen species (ROS) accumulation, hypoxia, nutrient deprivation, drug stimuli or endoplasmic reticulum stress (ERS). The main proteins involved in autophagy are the mammalian target of rapamycin complex 1 (mTORC1), phosphatidylinositol 3 kinase (PI3K), kinase AKT (AKT), Beclin-1 and p53 [156]. The PI3K/AKT pathway is the upstream target of the kinase mTOR. When PI3K and AKT are activated, autophagy is inhibited by the activation of mTOR. By contrast, inhibition of mTOR would activate autophagy [157].

Jasplakinolide (jaspamide), a cyclic depsipeptide isolated from the marine sponges *Jaspis johnstoni* and *J. splendens* [158,159], induces apoptosis in Jurkat T cells [33]. Jaspamide was found to induce apoptosis not only by activating caspase 3 and decreasing Bcl-2 protein expression but also by increasing Bax expression levels. Several new analogues have been isolated (B, C, V, etc.) from jasplakinolide, and all of them possess anticancer activity, as determined using NCI 60 cells [160]. Dolastatins 10 and 15 are potent linear pentapeptides isolated from the marine sea hare *Dolabella auricularia* [128,161]. Dolastatin 10 and bryostatin 1 (a polyketide isolated from the bryozoan *Bugula neritina*) can modulate the Bcl-2 and p53 oncoproteins in human diffuse large-cell lymphoma. In one study, the expression of Bcl-2 by human diffuse large cell lymphoma WSU-DLCL2 cells decreased when the cells were treated with bryostatin 1 and dolastatins 10 and 15 [162].

CS5931, a polypeptide isolated and purified from the sea squirt *Ciona savignyi*, has shown potent anticancer activity and induced apoptotic cell death in ileocecal colorectal adenocarcinoma (HCT-8) cells in a dose-dependent manner [163]. One study showed that in human carcinoma colorectal cells exposed to this compound, CS5931 exerted strong cell cycle arrest at the G2/M phase and a sub-G1 peak phase and induced release of Cyt C and activation of caspase 9 and 3. Mere 15 is a linear polypeptide isolated from the bivalve *Meretrix meretrix*. This compound exhibited *in vivo* activity against the growth of a human lung adenocarcinoma A549 xenograft in nude mice in a dose-dependent manner. This compound was also able to induce cell cycle arrest in G2/M phase followed by apoptosis. This apoptosis was characterized by the cleavage of procaspases 9 and 3, membrane blebbing, loss of mitochondrial membrane potential with subsequent Cyt C release, externalization of phosphatidylserine, condensation of

chromosomes and fragmentation of DNA [164]. The didemnins are a family of depsipeptides isolated from the tunicate *Trididemnum solidum* with antitumor, antiviral and immunosuppressive activities. The most characterized compound of this family is didemnin B, a branched N-methylated cyclic peptide, which selectively induces rapid and extensive apoptosis in a panel of breast cancer and colon cancer cell lines [165].

Monanchocidin A, a novel guanidine alkaloid isolated from the marine sponge *Monanchora pulchra* [166], features an unprecedented skeleton system derived from a polyketide precursor, (ω -3)-hydroxy fatty acid. This compound shows cytotoxicity against some cancer cell lines, such as human leukemia (THP-1), mouse epidermal (JB6 Cl41), and human cervix epithelioid carcinoma (HeLa) at micromolar levels. However, its mechanism of action has not been elucidated to date [166]. In a recent study, monochocidin A was tested in genitourinary cancer cell lines and showed the capability to affect malignant cell lines more intensively than non-malignant cell lines in a different way from classical apoptosis [167].

Tyrindoleninone, tyrindolinone, 6-bromoisatin and 6,6'-dibromindirubin are indole derivatives from the Muricidae family of marine gastropods with anticancer properties [168–170]. An *in vivo* study on a rodent model of colon cancer demonstrated the pro-apoptotic properties of crude extracts from the muricid gastropod *Dicathais orbita* [170]. Tyrindoleninone and 6-bromoisatin showed strong cytotoxicity against several colon cancer cells (HT29 and Caco-2) and were able to increase caspase 3/7 expression in both cell lines, inducing apoptosis [171].

The makaluvamines, a class of marine pyrroloiminoquinone alkaloids isolated from sponges in the genus *Zyzzya*, have been reported to possess potent *in vitro* and *in vivo* cytotoxicity against several human cancer cell lines. Their activity is related to topoisomerase II inhibition [172,173]. Chen et al. showed that a synthetic makaluvamine analogue (FBA-TPQ) had potent cytotoxic activity against human ovarian cancer A2780 and OVCAR-3 cells and induced apoptosis, G2/M cell cycle arrest and dose-dependent inhibition of OVCAR-3 xenograft tumor growth in female athymic nude mice (BALB/c, nu/nu) [174]. Analogues of the marine pyrrole-2-aminoimidazole alkaloids, i.e., oroidin, clathrodin, and hymenidin, isolated from Agelas sponges exhibited apoptotic-inducing activity in the HepG2 cell line with 25–38% apoptotic cells at 50 μ M [175].

Echinaside A and ds-echinaside A, which are glycosylated triterpenes isolated from the sea cucumber *Pearsonothuria graeffei*, showed cytotoxic activity against the P388, A549, MKN-28, HCT-116 and MCF-7 cancer cell lines. Both compounds displayed potent activity in blocking cell cycle progression and induced apoptosis through the intrinsic mitochondrial pathway, with ds-echinaside being the most potent one [176]. Stelletin A is a triterpenoid obtained from the marine sponge *Geodia japonica* that has a cytotoxic effect on murine melanoma B16F10 cells. Its effect is associated with inducing ERS and upregulating unfolded protein chaperone and glucose-regulated protein 78 in a dose-dependent manner. It was also shown to induce autophagy by increasing the levels of the membrane-bound form (LC3II) of autophagosome-associated protein light chain 3 (LC3). Wang et al. isolated the triterpene stelletin B from the marine sponge

Jaspis stellifera, and this compound caused G1 phase cycle arrest, apoptosis and autophagy in adenocarcinomic human lung adenocarcinoma cells (A549 cells), activity that was associated with a reduction in PI3K-p110 expression and the inhibition of the PI3K/Akt/mTOR pathway [177]. Frondoside A, a glycosylated triterpene isolated from the marine cucumber *Cucumaria frondosa*, has shown anti-migration and invasion activity [178]. In a recent study [179], frondoside A was able to induce cell cycle arrest in metastatic castration-resistant prostate cancer cells through caspase-dependent and caspase-independent apoptosis and to inhibit pro-survival autophagy. In animal trials, this compound inhibited the tumor growth of PC-3 and DU145 cells with a notable reduction in lung metastasis and in circulating tumor cells in the peripheral blood.

Ilimaquinone is a sesquiterpene quinone isolated from the Hawaiian sponge *Hippospongia metachromia* [180]. It is known to induce Golgi membrane fragmentation and is widely used to study the mechanism of vesicular trafficking [181]. This compound was able to promote hypoxia-inducible factor-1 (HIF-1) [182] and to induce G1 phase cycle arrest through upregulation of DNA damage-inducible gene 153 (CHOP/GADD153) in prostate cancer cells [183]. Another study on ilimaquinone and an ilimaquinone analogue (ethylsmenoquinone) showed that these compounds were able to induce G2/M cell cycle arrest and increase apoptosis by caspase-3 cleavage and autophagy; this mechanism was stimulated by both compounds through microtubule-associated protein 1 light chain 3 (LC3) in HCT116 colon cancer cells [184].

Nortopsentins A-C, which are indole imidazole alkaloids isolated from the marine sponge *Spongosorites ruetzleri*, exhibited *in vitro* cytotoxicity against leukemia P388 cells [185]. Two analogues of nortopsentin, 5-bromo-1-methyl-3-[2-(1*H*-pyrrolo[2,3-*b*]pyridin-3-yl)-1,3-thiazol-4-yl]-1*H*-pyrrolo[2,3-*b*]pyridine (T1) and 3-[2-(5-Bromo-1*H*-indol-3-yl)-1,3-thiazol-4-yl]-7-chloro-1*H*-pyrrolo[2,3-*c*]pyridine (T2) have shown selective cytotoxic effects on a broad spectrum of human cancer cell lines included in the NCI panel, whereas they did not affect normal intestinal cells. T1 was able to affect the apoptotic cell population by activating the mitochondria-mediated pathway in a dose-dependent manner, inducing cell cycle arrest at the G2/M phase, and inhibiting CDK-1 activity in HCT 116 colon cancer cells [186–188]. On the other hand, in the same cell model, T2 seemed to induce antiproliferative effects through apoptosis at high concentrations but effected a massive accumulation of autophagic vacuoles without apparent signs of apoptosis at low concentrations [189].

4.3. Inhibitors of Angiogenesis, Migration, Invasion or Metastasis

Angiogenesis is a normal physiological process that not only encompasses the proliferation, migration and morphogenesis of endothelial cells during the development of new blood vessels but also is responsible for providing oxygen and nutrients [190]. This process occurs during organogenesis or in a damaged organ and is involved in wound-healing activity, menstruation and placenta formation during pregnancy. In cancer, angiogenesis provides an opportunity for tumor growth and circulates tumor cells via the blood stream to other organs, inducing metastases [191].

Angiogenesis is controlled by a finely tuned balance of angiogenic inhibitors and stimulators. When angiogenesis is activated, first the established vessel is destabilized, followed by endothelial cell proliferation and migration and new tube formation [192].

The main actors of the angiogenic process are vascular endothelial growth factor (VEGF) and its receptor, VEGFR-2 (Flk-1/KDR). Angiogenesis is also associated with extracellular factors, including interleukin-8 (IL-8), tumor necrosis factor (TNF), fibroblast growth factor-2 (FGF-2), platelet-derived growth factor (PDGF), platelet-derived endothelial cell growth factor (PD-ECGF), angiopoietin-1, transforming growth factor beta-1 (TGF- β 1), transforming growth factor alpha (TGF- α) and epidermal growth factor (EGF) [193,194]. Blocking the VEGF-VEGFR-2 pathway and its downstream signaling is another strategy that leads to tumor growth inhibition. VEGF is overexpressed in some cancer cells and is a key factor in initiating the processes of angiogenesis, proliferation, migration, invasion and tube formation in endothelial cells [195].

Metastasis is probably the most serious feature of cancer, and it determinates clinical stages and prognosis [196]. Changes that cause tumor cells to become metastatic are complex and numerous, but some of the molecular targets are well identified. Matrix metalloproteinases (MMPs) are a family of zinc-dependent endopeptidases that play important roles in the degradation of the extracellular matrix and in the invasion and metastasis of tumors. MMPs, integrins, ICAM-1 and the extracellular matrix (ECM) are major factors involved in metastasis. MMP2 and MMP9, which are ECM degradation proteins, are the first actors on metastasis by locally degrading the ECM [197]. The next steps in the journey of a metastatic cancer cell are infiltration of the stroma and vascular tissue and extravasation and invasion of new tissue [198].

Research on the angiogenic and metastatic processes in cancer is mainly focused on compounds that block proteases, endothelial cell migration and proliferation, angiogenic growth factors or matrix proteins on the endothelial cell surface, such as integrins [199]. Compounds that can disrupt or normalize the processes of angiogenesis and/or metastasis are potential drugs for cancer treatment [200], and the main MNPs with these characteristics are listed below.

Geodiamolide H is a cyclodepsipeptide isolated from the Brazilian marine sponge *Geodia corticostylifera* [200]. This compound inhibited the invasion and migration activity of the human mammary Hs578T cell line in a dose-dependent manner (at nanomolar concentrations) in three types of assays: by time-lapse microscopy, in a Transwell® invasion assay and in a scratch-wound closure assay. This effect was attributed to its modification of the actin cytoskeleton of tumor cells; by contrast, normal cells were not affected. Stylissamide X is a proline-rich cyclic octapeptide isolated from an Indonesian marine sponge, *Stylissa* sp. [201]. Although this compound did not substantially modify cell viability at low micromolar concentrations (0.1 to 10 μ M), it was able to inhibit the migration of HeLa adenocarcinoma cells in both a wound-healing assay and a chemotaxicell chamber assay. A marine oligopeptide isolated and purified from the gastropod abalone (*Haliotis discus hannai*) had a specific inhibitory

effect on MMP-2/-9 and reduced the expression of proteins p50 and p65 in human fibrosarcoma (HT1080) cells in a dose-dependent manner [202].

Suberreamoline A, a bromotyrosine alkaloid isolated from the Red Sea sponges *Pseudoceratina arabica*, showed potent activity against the migration (in a wound-healing assay) and invasion (in the Cultrex® BME cell invasion assay) of MDA-MB-231 (a highly metastatic phenotype) human breast cancer cells at nanomolar concentrations [203]. Cortistatin A, a steroidal alkaloid isolated from the marine sponge *Corticium simplex*, showed anti-angiogenic properties in a migration assay using a chemotactic chamber and in the Matrigel tubular formation assay. Cortistatin A also inhibited the migration and tubular formation of HUVECs induced by VEGF or bFGF at 2 nM [204]. Aeroplysinin-1 is a brominated alkaloid from the marine sponge *Aplysina aerophoba*. This compound inhibited the growth of endothelial cells in culture through an apoptotic process. It was also able to cause a decrease in the expression of matrix MMP-2 and urokinase and exhibited a dose-dependent inhibitory effect in the *in vivo* chorioallantoic membrane assay (CAM), showing potent apoptosis-inducing activity in the developing endothelium [205].

Motuporamines A, B and C, which are macrocyclic alkaloids containing a spermidine-like substructure isolated from *Xestospongia exigua* extracts, inhibited the *in vitro* invasion of basement membranes by MDA-231 breast carcinoma and PC-3 prostate carcinoma cells. Motuporamine C was the most potent inhibitor of cell migration and angiogenesis. This compound also changed the cytoskeletal structure, decreased the activation of β 1-integrin (responsible for the adhesion and invasion of cancer cells) and inhibited cell migration and angiogenesis [206]. Bastadin 6, a macrocyclic tetramer alkaloid comprising brominated tyrosine derivatives that was isolated from the marine sponge *Lanthella* sp., showed an antiangiogenic effect through the inhibition of the vascular endothelial growth factor (VEGF)- or basic fibroblast growth factor (bFGF)-dependent proliferation of human umbilical vein endothelial cells (HUVECs), with 20- to 100-fold selectivity over normal fibroblasts. Another study showed that bastadins 9 and 16 (also isolated from the same sponge) together with bastadin 6 were able to display *in vitro* cytostatic, anti-angiogenic and antimigratory effects on mouse B16F10 melanoma cells [207]. It is proposed that these compounds exhibit selective induction activity against endothelial cells. Phidianidine A is an indole alkaloid isolated from the marine opisthobranch mollusk *Phidiana militaris* that significantly reduced CXCL12-induced migration in a rat pituitary adenoma cell line at 50 μ M [208]. Scepttrin, a natural bromopyrrole imidazole alkaloid produced by various marine sponges, inhibited cell motility in several cancer cell lines by reducing cell contractility and binding to monomeric actin [209].

Latrunculins A and B are marine-derived macrolides isolated from the Red Sea sponge *Negombata magnifica*. These compounds are associated with disrupting the organization of cell microfilaments [210] and have antimigratory activity against highly metastatic human prostate cancer PC-3M-CT⁺ cells and murine brain-metastatic melanoma B16B15b cells [211,212]. Laulimalide is another macrolide (polyketide) isolated from marine sponge *Cacospongia mycofijiensis* that has the ability to inhibit cell

proliferation with anti-tubulin activity (see Section 4.1). In addition, this compound exhibited cytotoxic activity at low doses and prevented blood vessel formation and VEGF-induced endothelial cell migration [213].

Among the terpenoids, the abovementioned triterpene glucoside ds-echinoside A (see Section 4.2), in addition to its effects on apoptosis regulation, inhibited the proliferation of human hepatocellular liver carcinoma cells (HepG2) with a IC_{50} value of 2.65 μ M, suppressing cell adhesion, migration and invasion in a dose-dependent manner. The putative mechanism involved a decrease in NF- κ B, VEGF and MMP-9 expression and an increase in tissue inhibitor of MMP-1 (TIMP-1) expression. Furthermore, this compound was able to reduce the tube formation of human endothelial cells and restrain neovascularization in the CAM assay [214]. Two sulfated triterpene glycosides (holothurin A and 24-dehydroechinoside A) isolated from *P. graeffei* significantly suppressed adhesion, invasion and migration in a HepG2 cellular model in a dose-dependent manner [215]. Another triterpene glucoside isolated from the marine cucumber *Cucumaria frondosa*, frondoside A, showed inhibition of migration and invasion at 0.1 to 1 μ M in the human estrogen receptor-negative breast cancer cell line MDA-MB-231 in a wound-healing model assay and in the Matrigel invasion assay [178]. In this assay, the effect of frondoside A was higher on MDA-MB-231 breast cancer cell than on the non-tumorigenic MCF 10-A cell line derived from normal human mammary epithelium. In addition, in a *in vivo* assay, frondoside A (100 μ g/kg/day *i.p.* for 24 days) strongly decreased the growth of MDA-MB-231 tumor xenografts in athymic mice without any manifest toxic side effects [216].

The sipholanes are triterpenes with a perhydrobenzoxepine (rings A and B) and bicyclodecane (rings C and D) conjugated ring system isolated from Red Sea sponge *Callyspongia siphonella* [217]. Three compounds of this family, sipholenol A, sipholenol E and sipholenone A, exhibited potent antimigratory activity in highly metastatic MDA-MB-231 breast cancer cells in a wound-healing assay [217]. Globostellatic acid X methyl esters (1–4) are triterpenes with an isomarabarican-type triterpenoidal skeleton isolated from the marine sponge *Rhabdastrella globostellata*. These compounds displayed potent inhibition of migration and tubular formation in human umbilical vein endothelial cells (HUVECs) induced by VEGF or bFGF [218].

Heteronemin, a natural sesterterpene isolated from the sponge *Heteronema erecta* [219], prevented tumor cell intravasation through the lymph-endothelial barrier in a three-dimensional (3D) cell culture model consisting of spheroids of the MCF-7 breast cancer cell [220].

The diterpenes pachycladins A and D, which were isolated from the Red Sea soft coral *Cladiella pachyclados* exhibited potent antimigratory activity when tested against prostate cancer PC-3 cells in a classical wound-healing assay. Sarcophines are marine-derived cembranoids (a class of diterpenes) with a 14-membered macrocyclic ring isolated from the soft coral *Sarcophytum glaucum* in the 1970s by Kashman and coworkers [221]. These complex compounds are described as one of the repellents that protect the coral against predators. Sarcophine exhibited potent anti-migration activity against highly metastatic mouse melanoma B16B15b cells [222] at micromolar

concentrations. Similar results were obtained when using a semisynthetic analogue of sarcophine against MDA-MB-231 breast cancer cells and PC-3 prostate cells in wound-healing assays [223]. The diterpenes sinulodurins A and B isolated from the Palau soft coral *Sinularia dura* inhibited the invasion of highly metastatic prostate cancer PC-3M-CT⁺ cells in a 3D-spheroid disaggregation assay model [224]. Strongylophorine-26 is a meroditerpenoid isolated from the marine sponge *Petrosia (Strongylophora) corticata* [225] that inhibits the invasion of TNBC MDA-MB-231 cells and has antimigratory activity, as determined in an *in vitro* wound-healing assay.

Smenospongine, a sesquiterpene aminoquinone isolated from the marine sponge *Dactylospongia elegans*, displayed potent inhibition of the proliferation, migration and tube formation of human endothelial cells, suggesting favorable anti-angiogenic activity [226].

WA-25 is a synthetic dihydroaustrasulfone alcohol compound with anti-inflammatory activity derived from the marine compound WE-2 (austrasulfone), which was isolated from the soft coral *Cladiella australis* [227]. WA-25 showed activity by suppressing microvessel sprouting in organotypic rat aortic rings, and in endothelial cells, this compound was able, in a dose-dependent manner, to inhibit MMP-2/MMP-9 expression, proliferation, migration and tube formation in HUVECs.

Finally, although they do not fit in any of the previously mentioned cancer hallmarks, callyspondiol and 14,15-dihydrosiphonodiol, which are polyacetylenediols isolated from marine sponges in the genus *Callyspongia* sp., are pharmacologically active substances that modulate immunity by the activation of human dendritic cells. These compounds might have effects on tumors or on autoimmune diseases [228].

4.4. Inhibitors of MAPKs

Mitogen-activated protein kinases (MAPKs) are a protein family that specifically phosphorylate the amino acids serine, threonine and tyrosine and are closely related to many cellular functions in cancer such as cell differentiation, proliferation and growth, cycle, apoptosis, migration, invasion and metastasis, energy metabolism and angiogenesis [229]. This family is activated by specific external factors and promotes the transduction of intracellular signals through the phosphorylation and activation of targets, which finally reach the nucleus and generate a cell response [230] (Figure 4). In many cases, MAPKs are considered as cellular amplifiers of biological signals, translating graded inputs into on or off outputs and filtering out low level noise [231]. MAPKs are frequently overexpressed or upregulated in cancer cells.

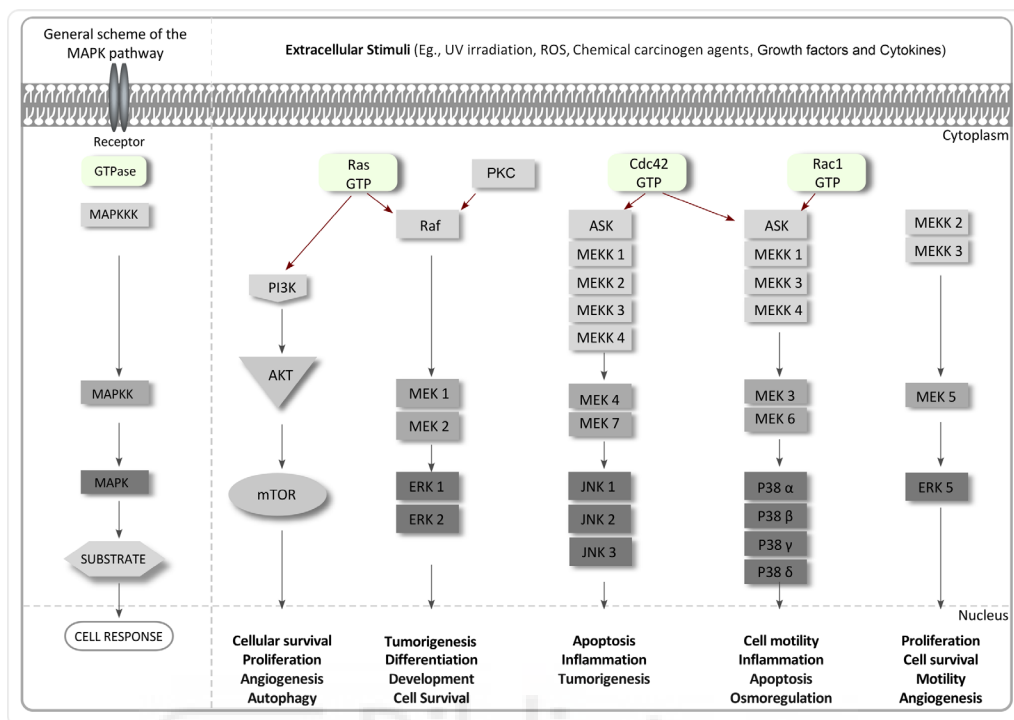


Figure 4. The relation between mammalian MAPK cascades and other kinases capable to induce cell responses involved in cancer. In MAPKs controlled signal transduction pathways after an extracellular stimuli transduced by a membrane receptor, the signal is conducted downstream by two kinases (MAPKKK and MAPKK) that finally arrives to a MAPK resulting in very functionally distinct responses (left part of the image). ERK is related to cellular survival, proliferation, angiogenesis and autophagy. JNK and p38 pathways are activated by MAPKKK (ASK) modulating tumorigenesis, cell motility, osmoregulation, inflammation and apoptosis. ERK 5 is a MAPK, which induces proliferation, cell survival, motility and angiogenesis. Finally, PI3K/AKT/mTOR axis is a serine-threonine protein kinases pathway induced by the GTPase Ras that plays an important role in cellular quiescence, proliferation and longevity and is an important regulator of oncogenesis and apoptosis in various types of cancers.

The most well-known MAPKs in mammals are MAPK/ERK kinase (MEK/ERK), protein kinase C (PKC), phosphoinositide 3-kinase (PI3K)/AKT, c-Jun N-terminal kinase (JNK), and p38 [232] (Figure 4). Cell proliferation and differentiation depend on epidermal growth factor (EGF), which induces the activation of receptor tyrosine kinase activity, of autophosphorylation and of the Ras/Raf/MEK/ERK signaling cascade [233]. Protein kinase C (PKC) is a family of phospholipid-dependent serine/threonine kinases involved in protein synthesis, gene expression, and cell proliferation, differentiation, and tumorigenesis. A wide range of distinct PKC enzymes have been found to be overexpressed in various cancers [234]. Phosphoinositide-3-kinase (PI3K)/AKT is a

mitogen-activated protein kinase and a serine-threonine-specific protein kinase that plays an important role in cellular survival signaling and is an important regulator of oncogenesis and apoptosis in various types of cancers (Figure 4). This pathway is activated by membrane receptors such as VEGFR and PDGFR and is considered an important target in cancer research [235]. c-Jun N-terminal kinase (JNK) is another member of the MAPK family that regulates a range of biological processes, such as tumorigenesis and neurodegenerative disorders (Figure 4). This family is sensitive to stress stimuli, including cytokines, UV and γ -irradiation, cytotoxic drugs, DNA-damaging agents, and reactive oxygen species [236]. The p38 mitogen-activated protein kinase (MAPK) plays a key role in cellular adaptation to external stimuli such as stress response and inflammation and mediates cellular responses to UV irradiation, osmotic shock, ischemia, and DNA damage [237] (Figure 4). Finally, ERK5 is the most recently identified member of the mitogen-activated protein kinase (MAPK) family and is phosphorylated and activated by MEK5 (Figure 4). This kinase plays a critical role in cardiovascular development and vascular integrity and also in pathological conditions such as cancer and tumour angiogenesis.

Misregulated kinases are strongly correlated with oncological diseases [238]. As a result, many efforts have been made to develop kinase inhibitors as anticancer treatments (some of them are reported to be in either phase I or phase II clinical trials [239]). Marine sponges are an excellent source of protein kinase inhibitors, with over 70 novel compounds isolated to date [240]. The most novel and relevant of these are detailed in this section.

Hymenialdisine and debromohymenialdisine from the marine sponge *Stylotella aurantium* showed significant inhibitory activity against MEK. They affected the Raf/MEK/ERK cascade through the inhibition of the phosphorylation of ERK by MEK-1 [241]. Segraves et al. found that a methanol fraction of the sponge *Batzella* sp. exhibited inhibition of Raf kinase [242].

11-hydroxystaurosporine from the marine tunicate *Eudistoma* sp. [17] and bryostatin-1 from the marine bryozoan *Bugula neritina* [240] showed notable activity against PKC [243,244]. Lasonolide A (isolated from the Caribbean sponge *Forcepia* sp.) [245], penazetidine A (isolated from the marine sponge *Penares sollasi*) [246] and corallidictyals A and B (isolated from the marine sponge *Aka coralliphaga*) also showed potent inhibitory activity against PKC.

Andersen et al., in 2006, reported the isolation of the previously unknown meroterpenoid liphagal 1 via extraction from the methanol fraction of the sponge *Aka coralliphaga*, which is found in Dominica [247]. Liphagal 1 has a novel structure consisting of a new 'liphagane' type of meroterpenoid carbon skeleton. Recently, the total chemical synthesis of liphagal and of other analogues [248] has been reported. Liphagal 1 has shown a cytotoxic effect on LoVo (Human colon cancer cells) and Caco (Human colon cancer cells) cells with an IC_{50} below 0.7 μ M and in MDA-468 (Human Breast cancer cells) with an IC_{50} of approximately 1.6 μ M [249]. This compound also presented inhibitory activity against PI3K [249].

Dolastatin (previously mentioned in Section 4.1), along with the cyclooxygenase-2 inhibitor celecoxib, was able to inhibit the development of colon cancer in a rat model by increasing apoptotic occurrence and rate. Molecular docking analysis showed that both compounds had the capacity to interact with the active sites of PI3-K/AKT. Additionally, these drugs inhibited the increased expression of PI3-K and AKT [250]. Kahalalide F (a cyclic depsipeptide), which was isolated from the marine mollusk *Elysia rufescens*, inhibited the PI3K–AKT signaling pathway in the breast cancer cell lines SKBR3 and BT474 [251]. Elisidepsin trifluoroacetate (PM02734, Irvalec), a marine-derived cyclic peptide that belongs to the previously mentioned Kahalalide family of compounds (see Section 3), showed cytotoxic activity, causing cell death through the inhibition of the AKT/mTOR pathway [252].

Aplidine (dehydrodidemnin B, DDB, Aplidin), a cyclic depsipeptide isolated from the Mediterranean tunicate *Aplidium albicans*, had an antiproliferative effect on breast, melanoma and non-small-cell lung cancers. Its activity involved increasing oxidative stress, thus causing the activation of JNK and p38 MAPK phosphorylation and inducing apoptosis [253]. The heterocyclic alkaloids onnamide A and theopederin B, which were isolated from the marine sponge *Theonella* sp., inhibited protein synthesis and induced stress-activated protein kinases p38 and JNK activation in a mink lung epithelial cell line [254].

5. New Perspectives on the Virtual Screening of MNPs for the Discovery of Anticancer Compounds

Different people who develop cancer with identical histopathological diagnoses and clinical stages may exhibit highly diverse epigenetic and genetic characteristics, and this may be the cause of their different response to the same therapy. We must also know the molecular taxonomy of different human cancers in order to implement personalized therapy. Genomics, proteomics and metabolomics are already contributing and will continue to contribute to the molecular classification of cancer. This classification will potentially facilitate the development of new biomarkers that may become cancer therapeutic targets [255]. High-throughput DNA sequencing techniques are enabling us to detect large numbers of gene mutations in different types of cancer. However, most of these mutations are biologically irrelevant and therefore have no clinical significance. Only certain mutations confer on cancerous cells aberrant growth, survival, and drug resistance; these are the drive mutations. Accordingly, the proteins resulting from the expression of these mutated genes will be the specific targets of “smart drugs” for cancer [255]. Where should we look for new compounds capable of modulating the biological activity of oncogenic biomarkers with these drive mutations? Let us look at nature, which has been the pharmacy from which man has obtained medicines since antiquity. In this regard, marine natural products represent an important potential source of molecules with antineoplastic activity that must be explored. It is not economically feasible to test libraries of millions of compounds while looking for bioactive molecules. For this reason, it is necessary to implement a guided

search via computational methods that reduces the vast chemical space to an experimentally approachable number of compounds. Molecular docking techniques are widely used for the study of protein-ligand interactions. After performing molecular docking experiments using AutoDock/vina software, the Gibbs free energy variation (ΔG , Kcal/mol) of a maximum of 20 poses/conformers is obtained for each ligand assayed. Compounds with lower calculated free energy variations (≤ -10 kcal/mol) are selected as putative biomarker modulators [256,257]. *In silico* prediction of the ADMET (absorption, distribution, metabolism, excretion, and toxicity) properties of a compound provides us with additional filters for our selection of antitumor drug candidate compounds.

Traditionally, most antineoplastic drugs are administered parenterally, and although the oral route is gaining interest since it is safer and better tolerated by the patient, the parenteral route possess some advantages: it avoids the discomfort of injections and can even be done by patients at home. The physicochemical properties of these drugs and the physiological barriers make oral administration a difficult challenge to overcome [258]. The “Genomics of Drug Sensitivity in Cancer” project characterized more than 1000 cell lines and 168 anticancer agents, and their data are available at <http://www.cancerrxgene.org/>. We have calculated the ADMET profile of these anticancer compounds and provided unrestricted access to them through the website[259]. Each record in our database includes up to 47 ADMET calculated parameters, and the molecular structure in MOL2 format is available for molecular docking purposes. A partial analysis of these data is shown in Figure 5. Interestingly, these data clearly demonstrate the above assertion that many anticancer agents have poor physicochemical properties. For example, Figure 5a shows that 28% of these compounds have a molecular weight greater than 500; additionally, approximately 10% have a cLogP greater than 5.0 (Figure 5b), and only 26% have a cLogS greater than 4 (Figure 5c).

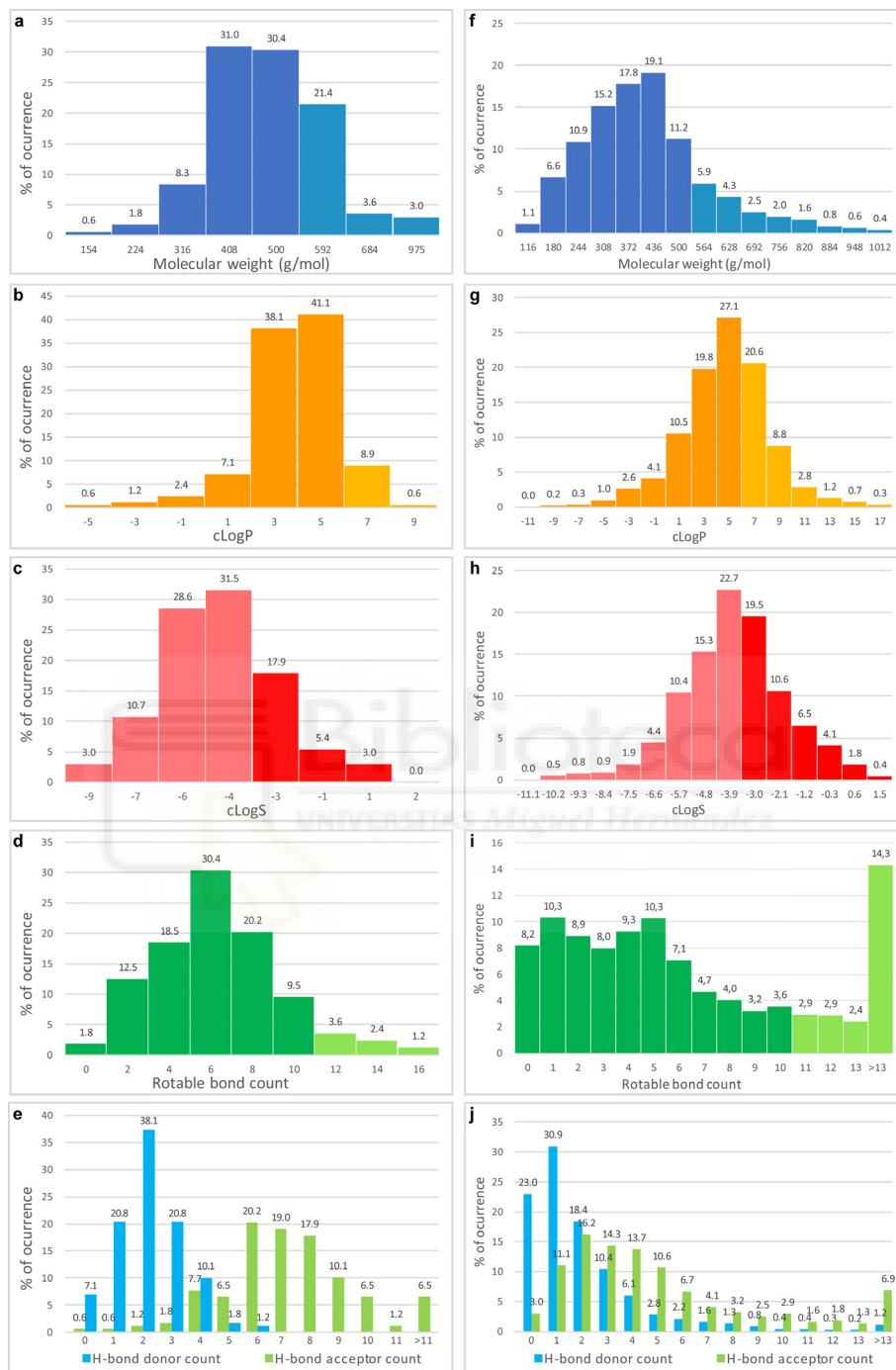


Figure 5. Distribution of the molecular weight (a,f), cLogP (b,g), cLogS (c,h), number of rotatable bonds (a,f) and number of hydrogen bond donors and acceptors (d,i) of the clinical oncologic drugs (a–e) and in the MNP database (f–j).

As an additional effort to improve the contribution of this paper, we have built a database of marine natural compounds by using data mining techniques to find the structural formulas of these compounds. The structures in MOL2 format and the ADMET profile of all compounds have been included in the database, which is available at the following address: [260]. It was reported that approximately 1% of the marine samples tested had potential antitumor activity compared to 0.1% of the terrestrial samples tested [261]. The systematic study of MNPs began almost 70 years ago with the pioneering works of Werner Bergmann and was continued by John Blunt and Murray Munro at the University of Canterbury, New Zealand, who created the MarinLit database [262]. From this work, we have extracted the CAS number of 20,451 molecules, of which 17,145 have been identified in the SciFinder database. To convert CAS numbers to chemical structures in an electronic format, we have used the NIH Chemical Identifier Resolution Service available at [263]. Using this service, we have managed to resolve 14,493 compounds with a molecular weight of less than 7000. These compounds are the ones that are currently included in the database of marine compounds fully accessible at the aforementioned address.

The right panels (f–j) in Figure 5 show analysis of selected physicochemical characteristics of the 14,442 marine compounds in our database, thus allowing us to compare them with the data shown in the left panels (a–e), which refer to the 168 compounds with anticancer activities tested by the “Genomics of Drug Sensitivity in Cancer” project. A few interesting observations should be made when the two databases, i.e., our own MNPs database and the anticancer compounds database, are compared. The frequency diagram shown in Figure 5f indicates that 82% of the MNPs in our database have a molecular weight lower than or equal to 500, and 99.6% of all compounds have a value similar to the maximum of the anticancer compounds (see Figure 5a); of the latter, 28% have an MW greater than 500. If we analyze the cLogP values of MNPs, we can observe that 95% of the compounds have a cLogP equal to or less than 9 (Figure 5g), which is the highest value found in the anticancer compounds (Figure 5a). Considering the cLogS value, we can see that 93% of MNPs (Figure 5h) are within the range of the anticancer compounds (Figure 5c).

The oral bioavailability of drug candidates can be correlated with molecular flexibility, as measured by the number of rotatable bonds, polar surface area and total hydrogen bond count, which is independent of molecular weight [264]. Compounds with 10 or less rotatable bonds, a polar surface area of less than 140 Å² and 12 or fewer H-bond donors and acceptors have a high probability of exhibiting good oral bioavailability. When we compare the data of the number of rotatable bonds of the marine compounds (Figure 5i) with that of the anticancer compounds (Figure 5d), we can observe that 77% and 93%, respectively, satisfy that condition. The comparison of the polar surface area values (data not shown) in both types of compounds yields similar values for the two groups, specifically, 84% (marine compounds) and 87% (anticancer compounds). Finally, the analysis of H-bond donors (HBDs) and acceptors for both sets of compounds also affords similar values: 86% (marine compounds) and

83% (anticancer compounds) have 5 or fewer HBDs and 10 or fewer H-bond acceptors. Taken together, these data show that most of the MNPs collected in our database have a high potential as lead compound candidates. Research focused on testing this library of compounds *in silico* against different targets of interest in cancer, in conjunction with *in vitro* verification in different cancer cell lines, is ongoing. Similarly, a recent paper on a database of natural compounds that have been tested in cancer cell lines will become a valuable tool to guide our search for target proteins in our *in silico* experiments [265]. We have analyzed the data presented in that database and showed a total of 127 proteins (data not shown), along with their UNIPROT code, that are targets for different compounds. In fact, we have abundant high-resolution structural information in the Protein Data Bank for many of these proteins, and therefore, it is very likely that the molecular docking data will soon provide us with several marine compounds that are good candidates for inhibiting some of these protein cancer biomarkers.

6. Limitations of Marine Invertebrates as Source for Anticancer Agents

Given the above, it has now been well established that the use of bioactive compounds of marine origin will bring increasing attraction in the following years as an alternative for the discovery of new drugs. Nevertheless, some limitations of the search for marine compounds from invertebrates must be considered, including the low amounts in which these products are produced by the organisms, the potential presence of toxins and inorganic salts derived from the organisms or environment, the wide diversity of chemical compounds produced by an organism, and the existence of nonspecific pharmacological targets.

To develop *in vitro* screening assays, small amounts are needed; however, in preclinical studies, hundreds of grams to kilograms are often required for testing purposes. Currently, this obstacle is overcome using a combination of novel techniques in chemical synthesis and improving harvest, aquaculture or isolation processes [266]. Another limiting factor in the use marine organisms is the potential presence of toxins from the organisms or of environmental origin and the presence of inorganic salts. These species may compromise the use of raw extracts for *in vitro* screening purposes. Often, the production of toxins by a marine invertebrate is an indicator that this organism is a candidate source of bioactive compounds. Therefore, an effort should be made to characterize the possible contaminants (inorganic salts and toxins) in order to make marine extracts compatible with *in vitro* testing. Many analytical techniques are currently available for the analysis, isolation, characterization and separation of active compounds in marine extracts [267,268]. The dependency of the variety of chemical compounds (chemotype) produced by an organism on environmental conditions might be solved using controlled aquaculture techniques. Controlled aquaculture not only could avoid the problem of exhausting the marine resources but also could be a feasible option to produce the required biomass for the high scale production needed in a drug discovery pipeline. Moreover, improvements in chemical synthesis techniques and combinatorial chemistry are providing satisfactory solutions for appropriate sourcing

[269,270]. Finally, the molecular targets for most of the newly discovered MNPs are unknown; therefore, high-throughput screening techniques, together with Omics and virtual screening, should be integrated to overcome the limitations of *in vitro* techniques.

7. Conclusions

This review summarizes the most recently isolated, derived or synthetically obtained compounds from marine invertebrates that have exhibited potential as cancer therapies within the last two decades. Undoubtedly, marine resources provide priceless and unexploited biochemical diversity and show a greater potential than plant resources for the discovery of new anticancer drugs, with approximately 18% of all MNPs discovered so far. The increasing number of publications on MNPs in the last few years reflects this fact.

A significant number of marine compounds have shown potential anticancer activities against the different hallmarks of cancer, such as cell growth inhibition, antimitotic activity (anti-tubulin effects), apoptosis and/or autophagy induction, and migration, invasion or metastasis inhibition. For most of the isolated compounds and their semisynthetic derivatives, the reported activities have been observed *in vitro*, but a significant number of these compounds, i.e., more than twenty, are either approved or in clinical phase. MNPs exhibit extensive chemical variability and complexity and include alkaloids, polyketides, terpenes, peptides and carbohydrates. Although marine resources are also limited, sourcing issues should be solved in the future by using aquaculture and biotechnology processes and the improvement of chemical synthesis in order to provide sufficient amounts of compounds for research purposes or pharmaceutical development.

Classical approaches based on the screening of extracts derived from marine organisms using *in vitro* techniques have limited applicability. The use of Omics has been extended to research on MNPs for anticancer drug discovery, offering new opportunities for the discovery of more specific cancer therapeutic targets or biomarkers. This will certainly enable the development of “precision medicine” in the near future. This large *in vitro* screening is generating a limitless number of compounds that require the use of virtual screening or computational methods to reduce the vast chemical space (thousands of compounds) to an experimentally approachable number of compounds. The combination of Omics techniques with virtual screening for the selection of compounds against particular cancer targets is becoming the method of choice in this area. Nevertheless, caution should be exercised in the selection of anticancer compounds for virtual screening. The comparison performed in this review, which includes the properties of the 168 most promising anticancer compounds from the GDSC database, demonstrates that using regular filtering techniques based on ADMET parameters may rule out many compounds with potential anticancer activity. Finally, a new public access MNPs library is reported for *in silico* purposes and is already being tested for different targets of interest in cancer [260].

Acknowledgments: Some of the investigations described in this review have been partially or fully supported by competitive public grants from the following institutions: AGL2011-29857-C03-03 and IDI-20120751 grants (Spanish Ministry of Science and Innovation), projects AGL2015-67995-C3-1-R, AGL2015-67995-C3-2-R and AGL2015-67995-C3-3-R from the Spanish Ministry of Economy and Competitiveness (MINECO); and PROMETEO/2012/007, PROMETEO/2016/006, ACOMP/2013/093, ACIF/2010/162, ACIF/2015/158 and ACIF/2016/230 grants from *Generalitat Valenciana* and CIBER (CB12/03/30038, Fisiopatología de la Obesidad y la Nutrición, CIBERobn, Instituto de Salud Carlos III). We are grateful to Research, Technological Innovation and Supercomputing Center of Extremadura (CenitS) for allowing us to use their supercomputing facilities (LUSITANIA II). Assistance with searches of the marine pharmaceutical literature in PubMed, Scopus and ScienceDirect is most gratefully acknowledged.

Conflicts of Interest: The authors declare no conflict of interest.

Abbreviations

ADMET	absorption, distribution, metabolism, excretion, and toxicity.
AMPK	AMP-activated protein kinase
CAM	chorioallantoic membrane assay
MNPs	marine natural products
MAPK	mitogen-activated protein kinase
VEGF	vascular endothelial growth factor
ERS	endoplasmic reticulum stress
MMP	matrix metalloproteinase

References

1. American Cancer Society. *Cancer Facts & Figures 2016*; American Cancer Society: Atlanta, GA, USA, 2016.
2. Mudit, M.; El Sayed, K.A. Cancer control potential of marine natural product scaffolds through inhibition of tumor cell migration and invasion. *Drug Discov. Today* **2016**, *21*, 1745–1760.
3. Siegel, R.L.; Miller, K.D.; Jemal, A. Cancer statistics, 2016. *CA Cancer J. Clin.* **2016**, *66*, 7–30.
4. Mullard, A. FDA approves first immunotherapy combo. *Nat. Rev. Drug Discov.* **2015**, *14*, 739–739.
5. Nicolini, A.; Carpi, A.; Ferrari, P.; Biava, P.M.; Rossi, G. Immunotherapy and hormone-therapy in metastatic breast cancer: A review and an update. *Curr. Drug Targets* **2016**, *17*, 1127–1139.
6. Khoo, B.L.; Chaudhuri, P.K.; Ramalingam, N.; Tan, D.S.; Lim, C.T.; Warkiani, M.E. Single-cell profiling approaches to probing tumor heterogeneity. *Int. J. Cancer* **2016**, *139*, 243–255.
7. Feinberg, A.P.; Ohlsson, R.; Henikoff, S. The epigenetic progenitor origin of human cancer. *Nat. Rev. Genet.* **2006**, *7*, 21–33.
8. Paterson, I.; Anderson, E.A. The renaissance of natural products as drug candidates. *Science* **2005**, *310*, 451.
9. Howitz, K.T.; Sinclair, D.A. Xenohormesis: Sensing the chemical cues of other species. *Cell* **2008**, *133*, 387–391.

10. Newman, D.J.; Cragg, G.M. Natural products as sources of new drugs over the last 25 years. *J. Nat. Prod.* **2007**, *70*, 461–477.
11. Fischbach, M.A.; Walsh, C.T. Antibiotics for emerging pathogens. *Science* **2009**, *325*, 1089–1093.
12. Cragg, G.M.; Grothaus, P.G.; Newman, D.J. Impact of natural products on developing new anti-cancer agents. *Chem. Rev.* **2009**, *109*, 3012–3043.
13. Pietra, F., *Secondary metabolites from marine microorganisms: bacteria, protozoa, algae and fungi. Achievements and prospects*. Natural Product Reports, 1997. **14**(5): p. 453-464.
14. Demain, A.L. Microbial production of primary metabolites. *Naturwissenschaften* **1980**, *67*, 582–587.
15. Harborne, J.B. Role of secondary metabolites in chemical defence mechanisms in plants. *Ciba Found. Symp.* **1990**, *154*, 126–134.
16. Bell, S.C.; Alford, R.A.; Garland, S.; Padilla, G.; Thomas, A.D. Screening bacterial metabolites for inhibitory effects against *Batrachochytrium dendrobatidis* using a spectrophotometric assay. *Dis. Aquat. Org.* **2013**, *103*, 77–85.
17. Elufioye, T.O.; Badal, S. Chapter 1—Background to pharmacognosy. In *Pharmacognosy*; Academic Press: Boston, MA, USA, 2017; pp. 3–13.
18. Molinski, T.F.; Dalisay, D.S.; Lievens, S.L.; Saludes, J.P. Drug development from marine natural products. *Nat. Rev. Drug Discov.* **2009**, *8*, 69–85.
19. Dang, V.T.; Benkendorff, K.; Green, T.; Speck, P. Marine snails and slugs: A great place to look for antiviral drugs. *J. Virol.* **2015**, *89*, 8114–8118.
20. Desbois, A.P.; Mearns-Spragg, A.; Smith, V.J. A fatty acid from the diatom *Phaeodactylum tricorutum* is antibacterial against diverse bacteria including multi-resistant *Staphylococcus aureus* (MRSA). *Mar. Biotechnol.* **2009**, *11*, 45–52.
21. Plaza, A.; Bifulco, G.; Keffer, J.L.; Lloyd, J.R.; Baker, H.L.; Bewley, C.A. Celebesides A-C and theopapuamides B-D, depsipeptides from an Indonesian sponge that inhibit HIV-1 entry. *J. Org. Chem.* **2009**, *74*, 504–512.
22. Wei, X.; Nieves, K.; Rodríguez, A.D. Neopetrosiamine A, biologically active bis-piperidine alkaloid from the caribbean sea sponge *neopetrosia proxima*. *Bioorg. Med. Chem. Lett.* **2010**, *20*, 5905–5908.
23. Nuijen, B.; Bouma, M.; Manada, C.; Jimeno, J.M.; Schellens, J.H.; Bult, A.; Beijnen, J.H. Pharmaceutical development of anticancer agents derived from marine sources. *Anticancer Drugs* **2000**, *11*, 793–811.
24. Asolkar, R.N.; Freel, K.C.; Jensen, P.R.; Fenical, W.; Kondratyuk, T.P.; Park, E.J.; Pezzuto, J.M. Arenamides A-C, cytotoxic NFκB inhibitors from the marine actinomycete *Salinispora arenicola*. *J. Nat. Prod.* **2009**, *72*, 396–402.
25. Lee, S.-M.; Lee, Y.-R.; Cho, K.-S.; Cho, Y.-N.; Lee, H.A.; Hwang, D.-Y.; Jung, Y.-J.; Son, H.-J. Stalked sea squirt (*Styela clava*) tunic waste as a valuable bioresource: Cosmetic and antioxidant activities. *Process Biochem.* **2015**, *50*, 1977–1984.
26. Abdelmohsen, U.R.; Balasubramanian, S.; Oelschlaeger, T.A.; Grkovic, T.; Pham, N.B.; Quinn, R.J.; Hentschel, U. Potential of marine natural products against drug-resistant fungal, viral, and parasitic infections. *Lancet Infect. Dis.* **2017**, *17*, e30–e41.
27. Kong, D.-X.; Jiang, Y.-Y.; Zhang, H.-Y. Marine natural products as sources of novel scaffolds: Achievement and concern. *Drug Discov. Today* **2010**, *15*, 884–886.

28. Pomponi, S.A. The bioprocess—Technological potential of the sea. *J. Biotechnol.* **1999**, *70*, 5–13.
29. Williams, P.G. Panning for chemical gold: Marine bacteria as a source of new therapeutics. *Trends Biotechnol.* **2009**, *27*, 45–52.
30. Jimeno, J.; Faircloth, G.; Sousa-Faro, F.J.; Scheuer, P.; Rinehart, K. New marine derived anticancer therapeutics—A journey from the sea to clinical trials. *Mar. Drugs* **2004**, *2*, 14–29.
31. Senthilkumar, K.; Kim, S.-K. Marine invertebrate natural products for anti-inflammatory and chronic diseases. *Evid.-Based Complement. Altern. Med.* **2013**, *2013*, 572859.
32. Nikapitiya, C. Chapter 24—Bioactive secondary metabolites from marine microbes for drug discovery. In *Advances in Food and Nutrition Research*; Se-Kwon, K., Ed.; Academic Press: New York, NY, USA, 2012; Volume 65, pp. 363–387.
33. Blunt, J.W.; Copp, B.R.; Keyzers, R.A.; Munro, M.H.G.; Prinsep, M.R. Marine natural products. *Nat. Prod. Rep.* **2015**, *32*, 116–211.
34. Kim, S.-K.; Pallela, R. Chapter 1—Medicinal foods from marine animals: Current status and prospects. In *Advances in Food and Nutrition Research*; Se-Kwon, K., Ed.; Academic Press: New York, NY, USA, 2012; Volume 65, pp. 1–9.
35. Ramsey, U.P.; Bird, C.J.; Shacklock, P.F.; Laycock, M.V.; Wright, J.L. Kainic acid and 1'-hydroxykainic acid from palmariales. *Nat. Toxins* **1994**, *2*, 286–292.
36. Landowne, R.A.; Bergmann, W. Contributions to the study of marine products. *L. Phospholipids of sponges*^{1,2}. *J. Org. Chem.* **1961**, *26*, 1257–1261.
37. Mayer, A.M.S.; Glaser, K.B.; Cuevas, C.; Jacobs, R.S.; Kem, W.; Little, R.D.; McIntosh, J.M.; Newman, D.J.; Potts, B.C.; Shuster, D.E. The odyssey of marine pharmaceuticals: A current pipeline perspective. *Trends Pharmacol. Sci.* **2010**, *31*, 255–265.
38. Olivera, B.M.; Cruz, L.J.; de Santos, V.; LeCheminant, G.W.; Griffin, D.; Zeikus, R.; McIntosh, J.M.; Galyean, R.; Varga, J.; Gray, W.R.; et al. Neuronal calcium channel antagonists. Discrimination between calcium channel subtypes using omega-conotoxin from *Conus magus* venom. *Biochemistry* **1987**, *26*, 2086–2090.
39. D'Incalci, M.; Badri, N.; Galmarini, C.M.; Allavena, P. Trabectedin, a drug acting on both cancer cells and the tumour microenvironment. *Br. J. Cancer* **2014**, *111*, 646–650.
40. Jordan, M.A.; Kamath, K.; Manna, T.; Okouneva, T.; Miller, H.P.; Davis, C.; Littlefield, B.A.; Wilson, L. The primary antimetabolic mechanism of action of the synthetic halichondrin e7389 is suppression of microtubule growth. *Mol. Cancer Ther.* **2005**, *4*, 1086–1095.
41. Newland, A.M.; Li, J.X.; Wasco, L.E.; Aziz, M.T.; Lowe, D.K. Brentuximab vedotin: A CD30-directed antibody-cytotoxic drug conjugate. *Pharmacotherapy* **2013**, *33*, 93–104.
42. De Zoysa, M. Medicinal benefits of marine invertebrates: Sources for discovering natural drug candidates. *Adv. Food Nutr. Res.* **2012**, *65*, 153–169.
43. Thorpe, J.P.; Solé-Cava, A.M.; Watts, P.C. Exploited marine invertebrates: Genetics and fisheries. *Hydrobiologia* **2000**, *420*, 165–184.
44. Gerwick, W.H.; Moore, B.S. Lessons from the past and charting the future of marine natural products drug discovery and chemical biology. *Chem. Biol.* **2012**, *19*, 85–98.
45. Saikia, S.; Kolita, B.; Dutta, P.P.; Dutta, D.J.; Neipihoi, Nath, S.; Bordoloi, M.; Quan, P.M.; Thuy, T.T.; Phuong, D.L.; et al. Marine steroids as potential anticancer drug candidates: *In silico* investigation in search of inhibitors of Bcl-2 and CDK-4/Cyclin D1. *Steroids* **2015**, *102*, 7–16.

46. Hu, G.-P.; Yuan, J.; Sun, L.; She, Z.-G.; Wu, J.-H.; Lan, X.-J.; Zhu, X.; Lin, Y.-C.; Chen, S.-P. Statistical research on marine natural products based on data obtained between 1985 and 2008. *Mar. Drugs* **2011**, *9*, 514–525.
47. Leal, M.C.; Madeira, C.; Brandao, C.A.; Puga, J.; Calado, R. Bioprospecting of marine invertebrates for new natural products—A chemical and zoogeographical perspective. *Molecules* **2012**, *17*, 9842–9854.
48. Voultziadou, E.; Vafidis, D. Marine invertebrate diversity in Aristotle’s zoology. *Contrib. Zool.* **2007**, *76*, 103–120.
49. Haefner, B. Drugs from the deep: Marine natural products as drug candidates. *Drug Discov. Today* **2003**, *8*, 536–544.
50. Mayer, A.M.S.; Rodríguez, A.D.; Tagliatalata-Scafati, O.; Fusetani, N. Marine pharmacology in 2009–2011: Marine compounds with antibacterial, antidiabetic, antifungal, anti-inflammatory, antiprotozoal, antituberculosis, and antiviral activities; affecting the immune and nervous systems, and other miscellaneous mechanisms of action. *Mar. Drugs* **2013**, *11*, 2510–2573.
51. Kukula-Koch, W.A.; Widelski, J. Chapter 9—Alkaloids A2—Badal, Simone. In *Pharmacognosy*; Delgoda, R., Ed.; Academic Press: Boston, MA, USA, 2017; pp. 163–198.
52. Zhang, Y.; Han, T.; Ming, Q.; Wu, L.; Rahman, K.; Qin, L. Alkaloids produced by endophytic fungi: A review. *Nat. Prod. Commun.* **2012**, *7*, 963–968.
53. Rocha-Santos, T.; Duarte, A.C. Introduction to the analysis of bioactive compounds in marine samples. In *Comprehensive Analytical Chemistry*; Elsevier: 2014; Volume 65, pp. 1–13.
54. Molinski, T.F. Marine pyridoacridine alkaloids: Structure, synthesis, and biological chemistry. *Chem. Rev.* **1993**, *93*, 1825–1838.
55. Hertiani, T.; Edrada-Ebel, R.; Ortlepp, S.; van Soest, R.W.M.; de Voogd, N.J.; Wray, V.; Hentschel, U.; Kozytska, S.; Müller, W.E.G.; Proksch, P. From anti-fouling to biofilm inhibition: New cytotoxic secondary metabolites from two Indonesian Agelas sponges. *Bioorg. Med. Chem.* **2010**, *18*, 1297–1311.
56. Vik, A.; Hedner, E.; Charnock, C.; Samuelsen, Ø.; Larsson, R.; Gundersen, L.L.; Bohlin, L. (+)-Agelasine D: Improved synthesis and evaluation of antibacterial and cytotoxic activities. *J. Nat. Prod.* **2006**, *69*, 381–386.
57. Bringmann, G.; Seupel, R.; Feineis, D.; Zhang, G.; Xu, M.; Wu, J.; Kaiser, M.; Brun, R.; Seo, E.-J.; Efferth, T. Ancistectorine D, a naphthylisoquinoline alkaloid with antiprotozoal and antileukemic activities, and further 5,8'- and 7,1'-linked metabolites from the Chinese liana *Ancistrocladus tectorius*. *Fitoterapia* **2016**, *115*, 1–8.
58. Appenzeller, J.; Mihci, G.; Martin, M.T.; Gallard, J.F.; Menou, J.L.; Boury-Esnault, N.; Hooper, J.; Petek, S.; Chevalley, S.; Valentin, A.; et al. Agelasines J, K, and L from the Solomon Islands marine sponge *Agelas cf. mauritiana*. *J. Nat. Prod.* **2008**, *71*, 1451–1454.
59. Chu, M.-J.; Tang, X.-L.; Qin, G.-F.; de Voogd, N.J.; Li, P.-L.; Li, G.-Q. Three new non-brominated pyrrole alkaloids from the South China Sea sponge *Agelas nakamurai*. *Chin. Chem. Lett.* **2017**, *28*, 1210–1213.
60. Hopwood, D.A. Complex enzymes in microbial natural product biosynthesis, part B: Polyketides, aminocoumarins and carbohydrates. Preface. *Methods Enzymol* **2009**, *459*, 4624–4625.

61. Hochmuth, T.; Piel, J. Polyketide synthases of bacterial symbionts in sponges—Evolution-based applications in natural products research. *Phytochemistry* **2009**, *70*, 1841–1849.
62. Tsukada, M.; Fukai, M.; Miki, K.; Shiraishi, T.; Suzuki, T.; Nishio, K.; Sugita, T.; Ishino, M.; Kinoshita, K.; Takahashi, K.; et al. Chemical constituents of a marine fungus, *Arthrinium sacchari*. *J. Nat. Prod.* **2011**, *74*, 1645–1649.
63. Ebel, R. Terpenes from marine-derived fungi. *Mar. Drugs* **2010**, *8*, 2340–2368.
64. Kim, S.-K.; Wijesekera, I. Development and biological activities of marine-derived bioactive peptides: A review. *J. Funct. Foods* **2010**, *2*, 1–9.
65. Cheung, R.C.; Ng, T.B.; Wong, J.H. Marine peptides: Bioactivities and applications. *Mar. Drugs* **2015**, *13*, 4006–4043.
66. Agrawal, S.; Adholeya, A.; Deshmukh, S.K. The pharmacological potential of non-ribosomal peptides from marine sponge and tunicates. *Front. Pharmacol.* **2016**, *7*, 333.
67. Mehbub, M.F.; Lei, J.; Franco, C.; Zhang, W. Marine sponge derived natural products between 2001 and 2010: Trends and opportunities for discovery of bioactives. *Mar. Drugs* **2014**, *12*, 4539–4577.
68. Kang, H.K.; Seo, C.H.; Park, Y. The effects of marine carbohydrates and glycosylated compounds on human health. *Int. J. Mol. Sci.* **2015**, *16*, 6018–6056.
69. Laurienzo, P. Marine polysaccharides in pharmaceutical applications: An overview. *Mar. Drugs* **2010**, *8*, 2435–2465.
70. Shi, L. Bioactivities, isolation and purification methods of polysaccharides from natural products: A review. *Int. J. Biol. Macromol.* **2016**, *92*, 37–48.
71. Safari, D.; Dekker, H.A.; Joosten, J.A.; Michalik, D.; de Souza, A.C.; Adamo, R.; Lahmann, M.; Sundgren, A.; Oscarson, S.; Kamerling, J.P.; et al. Identification of the smallest structure capable of evoking opsonophagocytic antibodies against *Streptococcus pneumoniae* type 14. *Infect. Immun.* **2008**, *76*, 4615–4623.
72. He, X.; Hwang, H.-m.; Aker, W.G.; Wang, P.; Lin, Y.; Jiang, X.; He, X. Synergistic combination of marine oligosaccharides and azithromycin against *Pseudomonas aeruginosa*. *Microbiol. Res.* **2014**, *169*, 759–767.
73. Kren, V.; Martinkova, L. Glycosides in medicine: “The role of glycosidic residue in biological activity”. *Curr. Med. Chem.* **2001**, *8*, 1303–1328.
74. Gandhi, N.S.; Mancera, R.L. The structure of glycosaminoglycans and their interactions with proteins. *Chem. Biol. Drug Des.* **2008**, *72*, 455–482.
75. Coombe, D.R.; Kett, W.C. Heparan sulfate-protein interactions: Therapeutic potential through structure-function insights. *Cell. Mol. Life Sci.* **2005**, *62*, 410–424.
76. Munoz-Alonso, M.J.; Gonzalez-Santiago, L.; Martinez, T.; Losada, A.; Galmarini, C.M.; Munoz, A. The mechanism of action of plitidepsin. *Curr. Opin. Investig. Drugs* **2009**, *10*, 536–542.
77. Krege, S.; Rexer, H.; vom Dorp, F.; de Geeter, P.; Klotz, T.; Retz, M.; Heidenreich, A.; Kuhn, M.; Kamradt, J.; Feyerabend, S.; et al. Prospective randomized double-blind multicentre phase II study comparing gemcitabine and cisplatin plus sorafenib chemotherapy with gemcitabine and cisplatin plus placebo in locally advanced and/or metastasized urothelial cancer: SUSE (AUO-AB 31/05). *BJU Int.* **2014**, *113*, 429–436.
78. Bendell, J.; Saleh, M.; Rose, A.A.N.; Siegel, P.M.; Hart, L.; Sirpal, S.; Jones, S.; Green, J.; Crowley, E.; Simantov, R.; et al. Phase I/II study of the antibody-drug conjugate

- glebatumumab vedotin in patients with locally advanced or metastatic breast cancer. *J. Clin. Oncol.* **2014**, *32*, 3619–3625.
79. Molina-Guijarro, J.M.; García, C.; Macías, Á.; García-Fernández, L.F.; Moreno, C.; Reyes, F.; Martínez-Leal, J.F.; Fernández, R.; Martínez, V.; Valenzuela, C.; et al. Elisidepsin interacts directly with glycosylceramides in the plasma membrane of tumor cells to induce necrotic cell death. *PLoS ONE* **2015**, *10*, e0140782.
80. Mandin, P.; Gottesman, S. A genetic approach for finding small rnas regulators of genes of interest identifies RybC as regulating the DpiA/DpiB two-component system. *Mol. Microbiol.* **2009**, *72*, 551–565.
81. Look, S.A.; Fenical, W.; Jacobs, R.S.; Clardy, J. The pseudopterisins: Anti-inflammatory and analgesic natural products from the sea whip pseudopterogorgia elisabethae. *Proc. Natl. Acad. Sci. USA* **1986**, *83*, 6238–6240.
82. Liu, J.; Huang, R.; Zhu, H. An improved and efficient synthesis for IPL576,092 and its analogues. *Monatshfte für Chemie – Chem. Mon.* **2013**, *144*, 1081–1085.
83. Petek, B.J.; Jones, R.L. PM00104 (Zalypsis®): A marine derived alkylating agent. *Molecules* **2014**, *19*, 12328–12335.
84. Bhatnagar, I.; Kim, S.-K. Marine antitumor drugs: Status, shortfalls and strategies. *Mar. Drugs* **2010**, *8*, 2702–2720.
85. Diaz, L.; Martinez-Bonet, M.; Sanchez, J.; Fernandez-Pineda, A.; Jimenez, J.L.; Munoz, E.; Moreno, S.; Alvarez, S.; Munoz-Fernandez, M.A. Bryostatin activates HIV-1 latent expression in human astrocytes through a PKC and NF-κB-dependent mechanism. *Sci. Rep.* **2015**, *5*, 12442.
86. Forero-Torres, A.; Kolibaba, K.S.; Lamy, T.; Jones, S.; Lee, C.; Sharman, J. Polatuzumab vedotin combined with obinutuzumab, cyclophosphamide, doxorubicin, and prednisone (G-CHP) for patients with previously untreated diffuse large B-cell lymphoma (DLBCL): Preliminary results of a phase Ib/II dose-escalation study. *Blood* **2016**, *128*, 1856.
87. Kim, Y.H.; Duvic, M.; Obitz, E.; Gniadecki, R.; Iversen, L.; Osterborg, A.; Whittaker, S.; Illidge, T.M.; Schwarz, T.; Kaufmann, R.; et al. Clinical efficacy of zanolimumab (HuMax-CD4): Two phase 2 studies in refractory cutaneous T-cell lymphoma. *Blood* **2007**, *109*, 4655–4662.
88. Newman, D.J.; Cragg, G.M. Marine-sourced anti-cancer and cancer pain control agents in clinical and late preclinical development (†). *Mar. Drugs* **2014**, *12*, 255–278.
89. Sleiman, S.F.; Olson, D.E.; Bourassa, M.W.; Karuppagounder, S.S.; Zhang, Y.L.; Gale, J.; Wagner, F.F.; Basso, M.; Coppola, G.; Pinto, J.T.; et al. Hydroxamic acid-based histone deacetylase (HDAC) inhibitors can mediate neuroprotection independent of hdac inhibition. *J. Neurosci.* **2014**, *34*, 14328–14337.
90. Atmaca, H.; Bozkurt, E.; Uzunoglu, S.; Uslu, R.; Karaca, B. A diverse induction of apoptosis by trabectedin in MCF-7 (HER2–/ER+) and MDA-MB-453 (HER2+/ER–) breast cancer cells. *Toxicol. Lett.* **2013**, *221*, 128–136.
91. Fontana, A.; Cavaliere, P.; Wahidulla, S.; Naik, C.G.; Cimino, G. A new antitumor isoquinoline alkaloid from the marine nudibranch *Jorunna funebris*. *Tetrahedron* **2000**, *56*, 7305–7308.

92. Oku, N.; Matsunaga, S.; Van Soest, R.W.M.; Fusetani, N. Renieramycin J, a highly cytotoxic tetrahydroisoquinoline alkaloid, from a marine sponge *Neopetrosia* sp. *J. Nat. Prod.* **2003**, *66*, 1136–1139.
93. Malve, H. Exploring the ocean for new drug developments: Marine pharmacology. *J. Pharm. Bioallied Sci.* **2016**, *8*, 83–91.
94. Scarpace, S.L. Eribulin mesylate (E7389): Review of efficacy and tolerability in breast, pancreatic, head and neck, and non-small cell lung cancer. *Clin. Ther.* **2012**, *34*, 1467–1473.
95. Shaw, S.J. The structure activity relationship of discodermolide analogues. *Mini Rev. Med. Chem.* **2008**, *8*, 276–284.
96. Zonder, J.A.; Shields, A.F.; Zalupski, M.; Chaplen, R.; Heilbrun, L.K.; Arlauskas, P.; Philip, P.A. A phase II trial of bryostatin 1 in the treatment of metastatic colorectal cancer. *Clin. Cancer Res.* **2001**, *7*, 38–42.
97. Caplan, S.L.; Zheng, B.; Dawson-Scully, K.; White, C.A.; West, L.M. Pseudopterosin A: Protection of synaptic function and potential as a neuromodulatory agent. *Mar. Drugs* **2016**, *14*, 55.
98. Mayer, A.M.; Jacobson, P.B.; Fenical, W.; Jacobs, R.S.; Glaser, K.B. Pharmacological characterization of the pseudopterosins: Novel anti-inflammatory natural products isolated from the caribbean soft coral, *Pseudopterogorgia elisabethae*. *Life Sci.* **1998**, *62*, L401–407.
99. Olivera, B.M. Conus Peptides: Biodiversity-based discovery and exogenomics. *J. Biol. Chem.* **2006**, *281*, 31173–31177.
100. Gopal, A.K.; Chen, R.; Smith, S.E.; Ansell, S.M.; Rosenblatt, J.D.; Savage, K.J.; Connors, J.M.; Engert, A.; Larsen, E.K.; Chi, X.; et al. Durable remissions in a pivotal phase 2 study of brentuximab vedotin in relapsed or refractory hodgkin lymphoma. *Blood* **2015**, *125*, 1236–1243.
101. Riely, G.J.; Gadgeel, S.; Rothman, I.; Saidman, B.; Sabbath, K.; Feit, K.; Kris, M.G.; Rizvi, N.A. A phase 2 study of TZT-1027, administered weekly to patients with advanced non-small cell lung cancer following treatment with platinum-based chemotherapy. *Lung Cancer* **2007**, *55*, 181–185.
102. Depenbrock, H.; Peter, R.; Faircloth, G.T.; Manzanares, I.; Jimeno, J.; Hanauske, A.R. *In vitro* activity of aplidine, a new marine-derived anti-cancer compound, on freshly explanted clonogenic human tumour cells and haematopoietic precursor cells. *Br. J. Cancer* **1998**, *78*, 739–744.
103. Munoz-Alonso, M.J.; Gonzalez-Santiago, L.; Zarich, N.; Martinez, T.; Alvarez, E.; Rojas, J.M.; Munoz, A. Plitidepsin has a dual effect inhibiting cell cycle and inducing apoptosis via Rac1/c-JUN NH2-terminal kinase activation in human melanoma cells. *J. Pharmacol. Exp. Ther.* **2008**, *324*, 1093–1101.
104. Mitsiades, C.S.; Ocio, E.M.; Pandiella, A.; Maiso, P.; Gajate, C.; Garayoa, M.; Vilanova, D.; Montero, J.C.; Mitsiades, N.; McMullan, C.J.; et al. Aplidin, a marine organism-derived compound with potent antimyeloma activity *in vitro* and *in vivo*. *Cancer Res.* **2008**, *68*, 5216–5225.
105. Morande, P.E.; Zanetti, S.R.; Borge, M.; Nannini, P.; Jancic, C.; Bezares, R.F.; Bitsmans, A.; Gonzalez, M.; Rodriguez, A.L.; Galmarini, C.M.; et al. The cytotoxic activity of Aplidin in chronic lymphocytic leukemia (CLL) is mediated by a direct effect on leukemic cells and an indirect effect on monocyte-derived cells. *Investig. New Drugs* **2012**, *30*, 1830–1840.

106. Natsume, T.; Watanabe, J.; Ogawa, K.; Yasumura, K.; Kobayashi, M. Tumor-specific antivasular effect of TZT-1027 (Soblidotin) elucidated by magnetic resonance imaging and confocal laser scanning microscopy. *Cancer Sci.* **2007**, *98*, 598–604.
107. Mita, A.C.; Hammond, L.A.; Bonate, P.L.; Weiss, G.; McCreery, H.; Syed, S.; Garrison, M.; Chu, Q.S.C.; DeBono, J.S.; Jones, C.B.; et al. Phase I and pharmacokinetic study of tasidotin hydrochloride (ILX651), a third-generation dolastatin-15 analogue, administered weekly for 3 weeks every 28 days in patients with advanced solid tumors. *Clin. Cancer Res.* **2006**, *12*, 5207.
108. Hamann, M.T.; Otto, C.S.; Scheuer, P.J.; Dunbar, D.C. Kahalalides: Bioactive peptides from a marine mollusk *Elysia rufescens* and its algal diet *Bryopsis* sp. *J. Org. Chem.* **1996**, *61*, 6594–6600.
109. Ott, P.A.; Pavlick, A.C.; Johnson, D.B.; Hart, L.L.; Infante, J.R.; Luke, J.J.; Lutzky, J.; Rothschild, N.; Spittle, L.; Cowey, C.L.; et al. A phase 2 study of glembatumumab vedotin (GV), an antibody-drug conjugate (ADC) targeting gpNMB, in advanced melanoma. *Ann. Oncol.* **2016**, *27*, 1147P–1147P.
110. Advani, R.H.; Lebovic, D.; Chen, A.; Brunvand, M.; Goy, A.; Chang, J.E.; Hochberg, E.; Yalamanchili, S.; Kahn, R.; Lu, D.; et al. Phase I study of the anti-CD22 antibody-drug conjugate pinatuzumab vedotin with/without rituximab in patients with relapsed/refractory B-cell non-Hodgkin's lymphoma. *Clin. Cancer Res.* **2016**, *6*, 1078–0432.
111. de Goeij, B.E.; Lambert, J.M. New developments for antibody-drug conjugate-based therapeutic approaches. *Curr. Opin. Immunol.* **2016**, *40*, 14–23.
112. Yamashita, A.; Norton, E.B.; Kaplan, J.A.; Niu, C.; Loganzo, F.; Hernandez, R.; Beyer, C.F.; Annable, T.; Musto, S.; Discafani, C.; et al. Synthesis and activity of novel analogs of hemiasterlin as inhibitors of tubulin polymerization: Modification of the a segment. *Bioorg. Med. Chem. Lett.* **2004**, *14*, 5317–5322.
113. Anderson, H.J.; Coleman, J.E.; Andersen, R.J.; Roberge, M. Cytotoxic peptides hemiasterlin, hemiasterlin A and hemiasterlin B induce mitotic arrest and abnormal spindle formation. *Cancer Chemother. Pharmacol.* **1997**, *39*, 223–226.
114. Marchetti, P.; Pavan, B.; Simoni, D.; Baruchello, R.; Rondanin, R.; Mischiati, C.; Feriotto, G.; Ferraro, L.; Hsu, L.-C.; Lee, R.M.; et al. A novel hybrid drug between two potent anti-tubulin agents as a potential prolonged anticancer approach. *Eur. J. Pharm. Sci.* **2016**, *91*, 50–63.
115. Liu, J.; Zhao, D.; He, W.; Zhang, H.; Li, Z.; Luan, Y. Nanoassemblies from amphiphilic cytarabine prodrug for leukemia targeted therapy. *J. Colloid Interface Sci.* **2017**, *487*, 239–249.
116. Akashi, Y.; Oda, T.; Ohara, Y.; Miyamoto, R.; Kurokawa, T.; Hashimoto, S.; Enomoto, T.; Yamada, K.; Satake, M.; Ohkohchi, N. Anticancer effects of gemcitabine are enhanced by co-administered iRGD peptide in murine pancreatic cancer models that overexpressed neuropilin-1. *Br. J. Cancer* **2014**, *110*, 1481–1487.
117. Kuo, W.-T.; Huang, J.-Y.; Chen, M.-H.; Chen, C.-Y.; Shyong, Y.-J.; Yen, K.-C.; Sun, Y.-J.; Ke, C.-J.; Cheng, Y.-H.; Lin, F.-H. Development of gelatin nanoparticles conjugated with phytohemagglutinin erythroagglutinating loaded with gemcitabine for inducing apoptosis in non-small cell lung cancer cells. *J. Mater. Chem. B* **2016**, *4*, 2444–2454.
118. de Bono, J.S.; Kristeleit, R.; Tolcher, A.; Fong, P.; Pacey, S.; Karavasilis, V.; Mita, M.; Shaw, H.; Workman, P.; Kaye, S.; et al. Phase I pharmacokinetic and pharmacodynamic study of LAQ824, a hydroxamate histone deacetylase inhibitor with a heat shock protein-90

- inhibitory profile, in patients with advanced solid tumors. *Clin. Cancer Res.* **2008**, *14*, 6663–6673.
119. Nowell, P.C. The clonal evolution of tumor cell populations. *Science* **1976**, *194*, 23–28.
 120. Hanahan, D.; Weinberg, R.A. The hallmarks of cancer. *Cell* **2000**, *100*, 57–70.
 121. Jordan, M.A.; Wilson, L. Microtubules as a target for anticancer drugs. *Nat. Rev. Cancer* **2004**, *4*, 253–265.
 122. Hadfield, J.A.; Ducki, S.; Hirst, N.; McGown, A.T. Tubulin and microtubules as targets for anticancer drugs. *Prog. Cell Cycle Res.* **2003**, *5*, 309–325.
 123. Avendaño, C.; Menéndez, J.C. Chapter 9—Anticancer drugs targeting tubulin and microtubules. In *Medicinal Chemistry of Anticancer Drugs*, 2nd ed.; Elsevier: Boston, MA, USA, 2015; pp. 359–390.
 124. Wood, K.W.; Cornwell, W.D.; Jackson, J.R. Past and future of the mitotic spindle as an oncology target. *Curr. Opin. Pharmacol.* **2001**, *1*, 370–377.
 125. Kaur, R.; Kaur, G.; Gill, R.K.; Soni, R.; Bariwal, J. Recent developments in tubulin polymerization inhibitors: An overview. *Eur. J. Med. Chem.* **2014**, *87*, 89–124.
 126. Mukhtar, E.; Adhami, V.M.; Mukhtar, H. Targeting microtubules by natural agents for cancer therapy. *Mol. Cancer Ther.* **2014**, *13*, 275–284.
 127. Jordan, M.A. Mechanism of action of antitumor drugs that interact with microtubules and tubulin. *Curr. Med. Chem. Anticancer Agents* **2002**, *2*, 1–17.
 128. Luesch, H.; Moore, R.E.; Paul, V.J.; Mooberry, S.L.; Corbett, T.H. Isolation of dolastatin 10 from the marine cyanobacterium *Symploca* species VP642 and total stereochemistry and biological evaluation of its analogue symplostatin 1. *J. Nat. Prod.* **2001**, *64*, 907–910.
 129. Bai, R.; Petit, G.R.; Hamel, E. Dolastatin 10, a powerful cytostatic peptide derived from a marine animal. *Biochem. Pharmacol.* **1990**, *39*, 1941–1949.
 130. Edler, M.C.; Fernandez, A.M.; Lassota, P.; Ireland, C.M.; Barrows, L.R. Inhibition of tubulin polymerization by vitilevuamide, a bicyclic marine peptide, at a site distinct from colchicine, the vinca alkaloids, and dolastatin 10. *Biochem. Pharmacol.* **2002**, *63*, 707–715.
 131. Lachia, M.; Moody, C.J. The synthetic challenge of diazonamide a, a macrocyclic indole bis-oxazole marine natural product. *Nat. Prod. Rep.* **2008**, *25*, 227–253.
 132. Cruz-Monserrate, Z.; Vervoort, H.C.; Bai, R.; Newman, D.J.; Howell, S.B.; Los, G.; Mullaney, J.T.; Williams, M.D.; Pettit, G.R.; Fenical, W.; et al. Diazonamide a and a synthetic structural analog: Disruptive effects on mitosis and cellular microtubules and analysis of their interactions with tubulin. *Mol. Pharmacol.* **2003**, *63*, 1273–1280.
 133. Nicolaou, K.C.; Guduru, R.; Sun, Y.P.; Banerji, B.; Chen, D.Y. Total synthesis of the originally proposed and revised structures of palmerolide A. *Angew Chem. Int. Ed. Engl.* **2007**, *46*, 5896–5900.
 134. Llorca, O.; Martin-Benito, J.; Gomez-Puertas, P.; Ritco-Vonsovici, M.; Willison, K.R.; Carrascosa, J.L.; Valpuesta, J.M. Analysis of the interaction between the eukaryotic chaperonin CCT and its substrates actin and tubulin. *J. Struct. Biol.* **2001**, *135*, 205–218.
 135. Uckun, F.M.; Mao, C.; Jan, S.T.; Huang, H.; Vassilev, A.O.; Navara, C.S.; Narla, R.K. Spongistatins as tubulin targeting agents. *Curr. Pharm. Des.* **2001**, *7*, 1291–1296.
 136. Zask, A.; Kaplan, J.; Musto, S.; Loganzo, F. Hybrids of the hemiasterlin analogue taltobulin and the dolastatins are potent antimicrotubule agents. *J. Am. Chem. Soc.* **2005**, *127*, 17667–17671.

137. Chan, A.; Andrae, P.M.; Northcote, P.T.; Miller, J.H. Peloruside A inhibits microtubule dynamics in a breast cancer cell line MCF7. *Investig. New Drugs* **2011**, *29*, 615–626.
138. Chen, Q.H.; Kingston, D.G. Zampanolide and dactylolide: Cytotoxic tubulin-assembly agents and promising anticancer leads. *Nat. Prod. Rep.* **2014**, *31*, 1202–1226.
139. Field, J.J.; Singh, A.J.; Kanakkanthara, A.; Halafihi, T.; Northcote, P.T.; Miller, J.H. Microtubule-stabilizing activity of zampanolide, a potent macrolide isolated from the tongan marine sponge *Cacospongia mycofijiensis*. *J. Med. Chem.* **2009**, *52*, 7328–7332.
140. Field, J.J.; Pera, B.; Calvo, E.; Canales, A.; Zurwerra, D.; Trigili, C.; Rodríguez-Salarichs, J.; Matesanz, R.; Kanakkanthara, A.; Wakefield, S.J.; et al. Zampanolide, a potent new microtubule stabilizing agent, covalently reacts with the taxane luminal site in both tubulin α,β -heterodimers and microtubules. *Chem. Biol.* **2012**, *19*, 686–698.
141. Isbrucker, R.A.; Cummins, J.; Pomponi, S.A.; Longley, R.E.; Wright, A.E. Tubulin polymerizing activity of dictyostatin-1, a polyketide of marine sponge origin. *Biochem. Pharmacol.* **2003**, *66*, 75–82.
142. Paterson, I.; Britton, R.; Delgado, O.; Wright, A.E. Stereochemical determination of dictyostatin, a novel microtubule-stabilising macrolide from the marine sponge *Corallistidae* sp. *Chem. Commun. (Camb.)* **2004**, 632–633.
143. Madiraju, C.; Edler, M.C.; Hamel, E.; Raccor, B.S.; Balachandran, R.; Zhu, G.; Giuliano, K.A.; Vogt, A.; Shin, Y.; Fournier, J.H.; et al. Tubulin assembly, taxoid site binding, and cellular effects of the microtubule-stabilizing agent dictyostatin. *Biochemistry* **2005**, *44*, 15053–15063.
144. Vollmer, L.L.; Jimenez, M.; Camarco, D.P.; Zhu, W.; Daghestani, H.N.; Balachandran, R.; Reese, C.E.; Lazo, J.S.; Hukriede, N.A.; Curran, D.P.; et al. A simplified synthesis of novel dictyostatin analogues with *in vitro* activity against epothilone b-resistant cells and antiangiogenic activity in zebrafish embryos. *Mol. Cancer Ther.* **2011**, *10*, 994–1006.
145. Brunden, K.R.; Gardner, N.M.; James, M.J.; Yao, Y.; Trojanowski, J.Q.; Lee, V.M.; Paterson, I.; Ballatore, C.; Smith, A.B., 3rd. Mt-stabilizer, dictyostatin, exhibits prolonged brain retention and activity: Potential therapeutic implications. *ACS Med. Chem. Lett.* **2013**, *4*, 886–889.
146. Churchill, C.D.; Klobukowski, M.; Tuszynski, J.A. The unique binding mode of laulimalide to two tubulin protofilaments. *Chem. Biol. Drug Des.* **2015**, *86*, 190–199.
147. Sun, Y.; Peng, Z.L. Programmed cell death and cancer. *Postgrad. Med. J.* **2009**, *85*, 134–140.
148. Su, Z.; Yang, Z.; Xu, Y.; Chen, Y.; Yu, Q. Apoptosis, autophagy, necroptosis, and cancer metastasis. *Mol. Cancer* **2015**, *14*, 48.
149. Debnath, J.; Baehrecke, E.H.; Kroemer, G. Does autophagy contribute to cell death? *Autophagy* **2005**, *1*, 66–74.
150. Fulda, S.; Pervaiz, S. Apoptosis signaling in cancer stem cells. *Int. J. Biochem. Cell Biol.* **2010**, *42*, 31–38.
151. Kroemer, G. Mitochondrial control of apoptosis: An introduction. *Biochem. Biophys. Res. Commun.* **2003**, *304*, 433–435.
152. Oliver, L.; Vallette, F.M. The role of caspases in cell death and differentiation. *Drug Resist. Updat.* **2005**, *8*, 163–170.
153. Elmore, S. Apoptosis: A review of programmed cell death. *Toxicol. Pathol.* **2007**, *35*, 495–516.
154. Cory, S.; Adams, J.M. The Bcl2 family: Regulators of the cellular life-or-death switch. *Nat. Rev. Cancer* **2002**, *2*, 647–656.

155. Mathew, R.; Karantza-Wadsworth, V.; White, E. Role of autophagy in cancer. *Nat. Rev. Cancer* **2007**, *7*, 961–967.
156. Mukhtar, E.; Adhami, V.M.; Khan, N.; Mukhtar, H. Apoptosis and autophagy induction as mechanism of cancer prevention by naturally occurring dietary agents. *Curr. Drug Targets* **2012**, *13*, 1831–1841.
157. Heras-Sandoval, D.; Perez-Rojas, J.M.; Hernandez-Damian, J.; Pedraza-Chaverri, J. The role of PI3K/AKT/mTOR pathway in the modulation of autophagy and the clearance of protein aggregates in neurodegeneration. *Cell Signal.* **2014**, *26*, 2694–2701.
158. Odaka, C.; Sanders, M.L.; Crews, P. Jaspilakinolide induces apoptosis in various transformed cell lines by a caspase-3-like protease-dependent pathway. *Clin. Diagn. Lab. Immunol.* **2000**, *7*, 947–952.
159. Ebada, S.S.; Wray, V.; De Voogd, N.J.; Deng, Z.; Lin, W.; Proksch, P. Two new jaspamide derivatives from the marine sponge *Jaspis splendens*. *Mar. Drugs* **2009**, *7*, 435–444.
160. Robinson, S.J.; Morinaka, B.I.; Amagata, T.; Tenney, K.; Bray, W.M.; Gassner, N.C.; Lokey, R.S.; Crews, P. New structures and bioactivity properties of jaspilakinolide (jaspamide) analogues from marine sponges. *J. Med. Chem.* **2010**, *53*, 1651–1661.
161. Aherne, G.W.; Hardcastle, A.; Valenti, M.; Bryant, A.; Rogers, P.; Pettit, G.R.; Srirangam, J.K.; Kelland, L.R. Antitumour evaluation of dolastatins 10 and 15 and their measurement in plasma by radioimmunoassay. *Cancer Chemother. Pharmacol.* **1996**, *38*, 225–232.
162. Maki, A.; Diwakaran, H.; Redman, B.; al-Asfar, S.; Pettit, G.R.; Mohammad, R.M.; al-Katib, A. The bcl-2 and p53 oncoproteins can be modulated by bryostatin 1 and dolastatins in human diffuse large cell lymphoma. *Anticancer Drugs* **1995**, *6*, 392–397.
163. Cheng, L.; Wang, C.; Liu, H.; Wang, F.; Zheng, L.; Zhao, J.; Chu, E.; Lin, X. A novel polypeptide extracted from *Ciona savignyi* induces apoptosis through a mitochondrial-mediated pathway in human colorectal carcinoma cells. *Clin. Colorectal Cancer* **2012**, *11*, 207–214.
164. Wang, C.; Liu, M.; Cheng, L.; Wei, J.; Wu, N.; Zheng, L.; Lin, X. A novel polypeptide from *Meretrix meretrix linnaeus* inhibits the growth of human lung adenocarcinoma. *Exp. Biol. Med.* **2012**, *237*, 442–450.
165. Potts, M.B.; McMillan, E.A.; Rosales, T.I.; Kim, H.S.; Ou, Y.-H.; Toombs, J.E.; Brekken, R.A.; Minden, M.D.; MacMillan, J.B.; White, M.A. Mode of action and pharmacogenomic biomarkers for exceptional responders to didemnin B. *Nat. Chem. Biol.* **2015**, *11*, 401–408.
166. Guzii, A.G.; Makarieva, T.N.; Denisenko, V.A.; Dmitrenok, P.S.; Kuzmich, A.S.; Dyshlovoy, S.A.; Krasokhin, V.B.; Stonik, V.A. Monanchocidin: A new apoptosis-inducing polycyclic guanidine alkaloid from the marine sponge *Monanchora pulchra*. *Org. Lett.* **2010**, *12*, 4292–4295.
167. Dyshlovoy, S.A.; Hauschild, J.; Amann, K.; Tabakmakher, K.M.; Venz, S.; Walther, R.; Guzii, A.G.; Makarieva, T.N.; Shubina, L.K.; Fedorov, S.N.; et al. Marine alkaloid monanchocidin overcomes drug resistance by induction of autophagy and lysosomal membrane permeabilization. *Oncotarget* **2015**, *6*, 17328–17341.
168. Benkendorff, K.; McIver, C.M.; Abbott, C.A. Bioactivity of the *Murex* Homeopathic Remedy and of Extracts from an Australian Muricid Mollusc against Human Cancer Cells. *Evid.-Based Complement. Altern. Med.* **2011**, *2011*, 879585.

169. Vine, K.L.; Locke, J.M.; Ranson, M.; Pyne, S.G.; Bremner, J.B. *In vitro* cytotoxicity evaluation of some substituted isatin derivatives. *Bioorg. Med. Chem.* **2007**, *15*, 931–938.
170. Westley, C.B.; McIver, C.M.; Abbott, C.A.; Le Leu, R.K.; Benkendorff, K. Enhanced acute apoptotic response to azoxymethane-induced DNA damage in the rodent colonic epithelium by tyrian purple precursors: A potential colorectal cancer chemopreventative. *Cancer Biol. Ther.* **2010**, *9*, 371–379.
171. Edwards, V.; Benkendorff, K.; Young, F. Marine compounds selectively induce apoptosis in female reproductive cancer cells but not in primary-derived human reproductive granulosa cells. *Mar. Drugs* **2012**, *10*, 64–83.
172. Casapullo, A.; Cutignano, A.; Bruno, I.; Bifulco, G.; Debitus, C.; Gomez-Paloma, L.; Riccio, R. Makaluvamine P, a new cytotoxic pyrroloiminoquinone from *Zyzyza cf. fuliginosa*. *J. Nat. Prod.* **2001**, *64*, 1354–1356.
173. Shinkre, B.A.; Raisch, K.P.; Fan, L.; Velu, S.E. Analogs of the marine alkaloid makaluvamines: Synthesis, topoisomerase II inhibition, and anticancer activity. *Bioorg. Med. Chem. Lett.* **2007**, *17*, 2890–2893.
174. Chen, T.; Xu, Y.; Guo, H.; Liu, Y.; Hu, P.; Yang, X.; Li, X.; Ge, S.; Velu, S.E.; Nadkarni, D.H.; et al. Experimental therapy of ovarian cancer with synthetic makaluvamine analog: *In vitro* and *in vivo* anticancer activity and molecular mechanisms of action. *PLoS ONE* **2011**, *6*, e20729.
175. Tomasic, T.; Nabergoj, D.; Vrbek, S.; Zidar, N.; Jakopin, Z.; Zula, A.; Hodnik, Z.; Jukic, M.; Anderluh, M.; Ilas, J.; et al. Analogues of the marine alkaloids oroidin, clathrodin, and hymenidin induce apoptosis in human HepG2 and THP-1 cancer cells. *MedChemComm* **2015**, *6*, 105–110.
176. Zhao, Q.; Xue, Y.; Wang, J.F.; Li, H.; Long, T.T.; Li, Z.; Wang, Y.M.; Dong, P.; Xue, C.H. *In vitro* and *in vivo* anti-tumour activities of echinoside A and ds-echinoside A from *Pearsonothuria graeffei*. *J. Sci. Food Agric.* **2012**, *92*, 965–974.
177. Wang, R.; Zhang, Q.; Peng, X.; Zhou, C.; Zhong, Y.; Chen, X.; Qiu, Y.; Jin, M.; Gong, M.; Kong, D. Stelletin B induces G1 arrest, apoptosis and autophagy in human non-small cell lung cancer A549 cells via blocking PI3K/Akt/mTOR pathway. *Sci. Rep.* **2016**, *6*, 27071.
178. Girard, M.; Bélanger, J.; ApSimon, J.W.; Garneau, F.-X.; Harvey, C.; Brisson, J.-R. Frondoside A. A novel triterpene glycoside from the holothurian *Cucumariafrondosa*. *Can. J. Chem.* **1990**, *68*, 11–18.
179. Dyshlovoy, S.A.; Menchinskaya, E.S.; Venz, S.; Rast, S.; Amann, K.; Hauschild, J.; Otte, K.; Kalinin, V.I.; Silchenko, A.S.; Avilov, S.A.; et al. The marine triterpene glycoside frondoside A exhibits activity *in vitro* and *in vivo* in prostate cancer. *Int. J. Cancer* **2016**, *138*, 2450–2465.
180. Do, M.T.; Na, M.; Kim, H.G.; Khanal, T.; Choi, J.H.; Jin, S.W.; Oh, S.H.; Hwang, I.H.; Chung, Y.C.; Kim, H.S.; et al. Ilimaquinone induces death receptor expression and sensitizes human colon cancer cells to TRAIL-induced apoptosis through activation of ROS-ERK/p38 MAPK-CHOP signaling pathways. *Food Chem. Toxicol.* **2014**, *71*, 51–59.
181. Sonoda, H.; Okada, T.; Jahangeer, S.; Nakamura, S. Requirement of phospholipase D for ilimaquinone-induced Golgi membrane fragmentation. *J. Biol. Chem.* **2007**, *282*, 34085–34092.
182. Du, L.; Zhou, Y.D.; Nagle, D.G. Inducers of hypoxic response: Marine sesquiterpene quinones activate HIF-1. *J. Nat. Prod.* **2013**, *76*, 1175–1181.

183. Chiu, S.C.; Huang, S.Y.; Chen, S.P.; Su, C.C.; Chiu, T.L.; Pang, C.Y. Tanshinone IIA inhibits human prostate cancer cells growth by induction of endoplasmic reticulum stress *in vitro* and *in vivo*. *Prostate Cancer Prostatic Dis.* **2013**, *16*, 315–322.
184. Lee, H.-Y.; Chung, J.K.; Hwang, H.I.; Gwak, J.; Park, S.; Ju, G.B.; Yun, E.; Kim, D.-E.; Chung, Y.-H.; Na, M.; et al. Activation of p53 with ilimaquinone and ethylsmenoquinone, marine sponge metabolites, induces apoptosis and autophagy in colon cancer cells. *Mar. Drugs* **2015**, *13*, 543–557.
185. Sakemi, S.; Sun, H.H. Nortopsentins A, B, and C. Cytotoxic and antifungal imidazolediybis[indoles] from the sponge *Spongisorites ruetzleri*. *J. Org. Chem.* **1991**, *56*, 4304–4307.
186. Diana, P.; Carbone, A.; Barraja, P.; Montalbano, A.; Parrino, B.; Lopergolo, A.; Pennati, M.; Zaffaroni, N.; Cirrincione, G. Synthesis and antitumor activity of 3-(2-phenyl-1,3-thiazol-4-yl)-1h-indoles and 3-(2-phenyl-1,3-thiazol-4-yl)-1h-7-azaindoles. *ChemMedChem* **2011**, *6*, 1300–1309.
187. Carbone, A.; Pennati, M.; Barraja, P.; Montalbano, A.; Parrino, B.; Spano, V.; Lopergolo, A.; Sbarra, S.; Doldi, V.; Zaffaroni, N.; et al. Synthesis and antiproliferative activity of substituted 3[2-(1h-indol-3-yl)-1,3-thiazol-4-yl]-1h-pyrrolo[3,2-b]pyridines, marine alkaloid nortopsentin analogues. *Curr. Med. Chem.* **2014**, *21*, 1654–1666.
188. Carbone, A.; Pennati, M.; Parrino, B.; Lopergolo, A.; Barraja, P.; Montalbano, A.; Spano, V.; Sbarra, S.; Doldi, V.; De Cesare, M.; et al. Novel 1h-pyrrolo[2,3-b]pyridine derivative nortopsentin analogues: Synthesis and antitumor activity in peritoneal mesothelioma experimental models. *J. Med. Chem.* **2013**, *56*, 7060–7072.
189. Carbone, A.; Parrino, B.; Di Vita, G.; Attanzio, A.; Spanò, V.; Montalbano, A.; Barraja, P.; Tesoriere, L.; Livrea, M.A.; Diana, P.; et al. Synthesis and antiproliferative activity of thiazolyl-bis-pyrrolo[2,3-b]pyridines and indolyl-thiazolyl-pyrrolo[2,3-c]pyridines, nortopsentin analogues. *Mar. Drugs* **2015**, *13*, 460–492.
190. Bielenberg, D.R.; Zetter, B.R. The contribution of angiogenesis to the process of metastasis. *Cancer J.* **2015**, *21*, 267–273.
191. Coultas, L.; Chawengsaksophak, K.; Rossant, J. Endothelial cells and VEGF in vascular development. *Nature* **2005**, *438*, 937–945.
192. Klagsbrun, M.; Moses, M.A. Molecular angiogenesis. *Chem. Biol.* **1999**, *6*, R217–R224.
193. Zhang, S.; Cao, Z.; Tian, H.; Shen, G.; Ma, Y.; Xie, H.; Liu, Y.; Zhao, C.; Deng, S.; Yang, Y.; et al. SKLB1002, a novel potent inhibitor of VEGF receptor 2 signaling, inhibits angiogenesis and tumor growth *in vivo*. *Clin. Cancer Res.* **2011**, *17*, 4439–4450.
194. Matsumoto, T.; Bohman, S.; Dixelius, J.; Berge, T.; Dimberg, A.; Magnusson, P.; Wang, L.; Wikner, C.; Qi, J.H.; Wernstedt, C.; et al. VEGF receptor-2 Y951 signaling and a role for the adapter molecule TSAd in tumor angiogenesis. *EMBO J.* **2005**, *24*, 2342–2353.
195. Nishi, M.; Abe, Y.; Tomii, Y.; Tsukamoto, H.; Kijima, H.; Yamazaki, H.; Ohnishi, Y.; Iwasaki, M.; Inoue, H.; Ueyama, Y.; et al. Cell binding isoforms of vascular endothelial growth factor-A (VEGF189) contribute to blood flow-distant metastasis of pulmonary adenocarcinoma. *Int. J. Oncol.* **2005**, *26*, 1517–1524.
196. Zetter, B.R. Angiogenesis and tumor metastasis. *Annu. Rev. Med.* **1998**, *49*, 407–424.

197. Noujaim, D.; van Golen, C.M.; van Golen, K.L.; Grauman, A.; Feldman, E.L. N-Myc and Bcl-2 coexpression induces MMP-2 secretion and activation in human neuroblastoma cells. *Oncogene* **2002**, *21*, 4549–4557.
198. Criscigliano, C.; Esposito, A.; Curigliano, G. Tumor-stroma crosstalk: Targeting stroma in breast cancer. *Curr. Opin. Oncol.* **2014**, *26*, 551–555.
199. Cobleigh, M.A.; Langmuir, V.K.; Sledge, G.W.; Miller, K.D.; Haney, L.; Novotny, W.F.; Reimann, J.D.; Vassel, A. A phase I/II dose-escalation trial of bevacizumab in previously treated metastatic breast cancer. *Semin. Oncol.* **2003**, *30*, 117–124.
200. Kubota, Y. Tumor angiogenesis and anti-angiogenic therapy. *Keio J. Med.* **2012**, *61*, 47–56.
201. Arai, M.; Yamano, Y.; Fujita, M.; Setiawan, A.; Kobayashi, M. Stylissamide X, a new proline-rich cyclic octapeptide as an inhibitor of cell migration, from an Indonesian marine sponge of *Stylissa* sp. *Bioorg. Med. Chem. Lett.* **2012**, *22*, 1818–1821.
202. Nguyen, V.T.; Qian, Z.J.; Ryu, B.; Kim, K.N.; Kim, D.; Kim, Y.M.; Jeon, Y.J.; Park, W.S.; Choi, I.W.; Kim, G.H.; et al. Matrix metalloproteinases (MMPs) inhibitory effects of an octameric oligopeptide isolated from abalone *Haliotis discus hannai*. *Food Chem.* **2013**, *141*, 503–509.
203. Shaala, L.A.; Youssef, D.T.A.; Sulaiman, M.; Behery, F.A.; Foudah, A.I.; Sayed, K.A.E. Subereamolline A as a potent breast cancer migration, invasion and proliferation inhibitor and bioactive dibrominated alkaloids from the red sea sponge *Pseudoceratina arabica*. *Mar. Drugs* **2012**, *10*, 2492–2508.
204. Aoki, S.; Watanabe, Y.; Sanagawa, M.; Setiawan, A.; Kotoku, N.; Kobayashi, M. Cortistatins A, B, C, and D, anti-angiogenic steroidal alkaloids, from the marine sponge *Corticium simplex*. *J. Am. Chem. Soc.* **2006**, *128*, 3148–3149.
205. Rodriguez-Nieto, S.; Gonzalez-Iriarte, M.; Carmona, R.; Munoz-Chapuli, R.; Medina, M.A.; Quesada, A.R. Antiangiogenic activity of aeroplysinin-1, a brominated compound isolated from a marine sponge. *FASEB J.* **2002**, *16*, 261–263.
206. Roskelley, C.D.; Williams, D.E.; McHardy, L.M.; Leong, K.G.; Troussard, A.; Karsan, A.; Andersen, R.J.; Dedhar, S.; Roberge, M. Inhibition of tumor cell invasion and angiogenesis by motuporamines. *Cancer Res.* **2001**, *61*, 6788–6794.
207. Mathieu, V.; Wauthoz, N.; Lefranc, F.; Niemann, H.; Amighi, K.; Kiss, R.; Proksch, P. Cyclic versus hemi-bastadins. Pleiotropic anti-cancer effects: From apoptosis to anti-angiogenic and anti-migratory effects. *Molecules* **2013**, *18*, 3543–3561.
208. Barbieri, F.; Thellung, S.; Wurth, R.; Gatto, F.; Corsaro, A.; Villa, V.; Nizzari, M.; Albertelli, M.; Ferone, D.; Florio, T. Emerging targets in pituitary adenomas: Role of the CXCL12/CXCR4-R7 system. *Int. J. Endocrinol.* **2014**, *2014*, 753524.
209. Cipres, A.; O'Malley, D.P.; Li, K.; Finlay, D.; Baran, P.S.; Vuori, K. Sceptrin, a marine natural compound, inhibits cell motility in a variety of cancer cell lines. *ACS Chem. Biol.* **2010**, *5*, 195–202.
210. Spector, I.; Shochet, N.R.; Blasberger, D.; Kashman, Y. Latrunculins--novel marine macrolides that disrupt microfilament organization and affect cell growth: I. Comparison with cytochalasin D. *Cell Motil. Cytoskeleton* **1989**, *13*, 127–144.
211. El Sayed, K.A.; Youssef, D.T.; Marchetti, D. Bioactive natural and semisynthetic latrunculins. *J. Nat. Prod.* **2006**, *69*, 219–223.
212. Sayed, K.A.; Khanfar, M.A.; Shallal, H.M.; Muralidharan, A.; Awate, B.; Youssef, D.T.; Liu, Y.; Zhou, Y.D.; Nagle, D.G.; Shah, G. Latrunculin A and its C-17-O-carbamates inhibit

- prostate tumor cell invasion and HIF-1 activation in breast tumor cells. *J. Nat. Prod.* **2008**, *71*, 396–402.
213. Lu, H.; Murtagh, J.; Schwartz, E.L. The microtubule binding drug laulimalide inhibits vascular endothelial growth factor-induced human endothelial cell migration and is synergistic when combined with docetaxel (taxotere). *Mol. Pharmacol.* **2006**, *69*, 1207–1215.
214. Zhao, Q.; Liu, Z.D.; Xue, Y.; Wang, J.F.; Li, H.; Tang, Q.J.; Wang, Y.M.; Dong, P.; Xue, C.H. Ds-echinoside A, a new triterpene glycoside derived from sea cucumber, exhibits antimetastatic activity via the inhibition of NF- κ B-dependent MMP-9 and VEGF expressions. *J. Zhejiang Univ. Sci. B* **2011**, *12*, 534–544.
215. Zhao, Q.; Xue, Y.; Liu, Z.D.; Li, H.; Wang, J.F.; Li, Z.J.; Wang, Y.M.; Dong, P.; Xue, C.H. Differential effects of sulfated triterpene glycosides, holothurin A1, and 24-dehydroechinoside A, on antimetastatic activity via regulation of the MMP-9 signal pathway. *J. Food Sci.* **2010**, *75*, H280–H288.
216. Al Marzouqi, N.; Iratni, R.; Nemmar, A.; Arafat, K.; Ahmed Al Sultan, M.; Yasin, J.; Collin, P.; Mester, J.; Adrian, T.E.; Attoub, S. Frondoside A inhibits human breast cancer cell survival, migration, invasion and the growth of breast tumor xenografts. *Eur. J. Pharmacol.* **2011**, *668*, 25–34.
217. Foudah, A.I.; Jain, S.; Busnena, B.A.; El Sayed, K.A. Optimization of marine triterpene siphonolols as inhibitors of breast cancer migration and invasion. *ChemMedChem* **2013**, *8*, 497–510.
218. Kotoku, N.; Tamada, N.; Hayashi, A.; Kobayashi, M. Synthesis of BC-ring model of globostellatic acid X methyl ester, an anti-angiogenic substance from marine sponge. *Bioorg. Med. Chem. Lett.* **2008**, *18*, 3532–3535.
219. Kazlauskas, R.; Murphy, P.T.; Quinn, R.J.; Wells, R.J. Heteronemin, a new scalarin type sesterterpene from the sponge *Heteronema Erecta*. *Tetrahedron Lett.* **1976**, *17*, 2631–2634.
220. Kopf, S.; Viola, K.; Atanasov, A.G.; Jarukamjorn, K.; Rarova, L.; Kretschy, N.; Teichmann, M.; Vonach, C.; Saiko, P.; Giessrigl, B.; et al. *In vitro* characterisation of the anti-intravasative properties of the marine product heteronemin. *Arch. Toxicol.* **2013**, *87*, 1851–1861.
221. Bernstein, J.; Shmeuli, U.; Zadock, E.; Kashman, Y.; Néeman, I. Sarcophine, a new epoxy cembranolide from marine origin. *Tetrahedron* **1974**, *30*, 2817–2824.
222. Sawant, S.S.; Youssef, D.T.; Reiland, J.; Ferniz, M.; Marchetti, D.; El Sayed, K.A. Biocatalytic and antimetastatic studies of the marine cembranoids sarcophine and 2-epi-16-deoxysarcophine. *J. Nat. Prod.* **2006**, *69*, 1010–1013.
223. Hassan, H.M.; Sallam, A.A.; Mohammed, R.; Hifnawy, M.S.; Youssef, D.T.A.; El Sayed, K.A. Semisynthetic analogues of the marine cembranoid sarcophine as prostate and breast cancer migration inhibitors. *Bioorg. Med. Chem.* **2011**, *19*, 4928–4934.
224. Radwan, M.M.; Manly, S.P.; El Sayed, K.A.; Wali, V.B.; Sylvester, P.W.; Awate, B.; Shah, G.; Ross, S.A. Sinulodurins A and B, antiproliferative and anti-invasive diterpenes from the soft coral *Simularia dura*. *J. Nat. Prod.* **2008**, *71*, 1468–1471.
225. Warabi, K.; McHardy, L.M.; Matainaho, L.; Van Soest, R.; Roskelley, C.D.; Roberge, M.; Andersen, R.J. Strongylophorine-26, a new meroditerpenoid isolated from the marine sponge *Petrosia* (*Strongylophora*) *corticata* that exhibits anti-invasion activity. *J. Nat. Prod.* **2004**, *67*, 1387–1389.

226. Kong, D.; Yamori, T.; Kobayashi, M.; Duan, H. Antiproliferative and antiangiogenic activities of smenospongine, a marine sponge sesquiterpene aminoquinone. *Mar. Drugs* **2011**, *9*, 154–161.
227. Wen, Z.-H.; Chao, C.-H.; Wu, M.-H.; Sheu, J.-H. A neuroprotective sulfone of marine origin and the *in vivo* anti-inflammatory activity of an analogue. *Eur. J. Med. Chem.* **2010**, *45*, 5998–6004.
228. Takei, M.; Umeyama, A.; Shoji, N.; Hashimoto, T. Polyacetylenediols regulate the function of human monocyte-derived dendritic cells. *Int. Immunopharmacol.* **2010**, *10*, 913–921.
229. Pearson, G.; Robinson, F.; Gibson, T.B.; Xu, B.E.; Karandikar, M.; Berman, K.; Cobb, M.H. Mitogen-activated protein (map) kinase pathways: Regulation and physiological functions. *Endocr. Rev.* **2001**, *22*, 153–183.
230. Brown, M.D.; Sacks, D.B. Protein scaffolds in map kinase signalling. *Cell Signal.* **2009**, *21*, 462–469.
231. Santen, R.J.; Song, R.X.; McPherson, R.; Kumar, R.; Adam, L.; Jeng, M.-H.; Yue, W. The role of mitogen-activated protein (map) kinase in breast cancer. *J. Steroid Biochem. Mol. Biol.* **2002**, *80*, 239–256.
232. Avruch, J. Map kinase pathways: The first twenty years. *Biochim. Biophys. Acta—Mol. Cell Res.* **2007**, *1773*, 1150–1160.
233. Downward, J. Targeting ras signalling pathways in cancer therapy. *Nat. Rev. Cancer* **2003**, *3*, 11–22.
234. Griner, E.M.; Kazanietz, M.G. Protein kinase c and other diacylglycerol effectors in cancer. *Nat. Rev. Cancer* **2007**, *7*, 281–294.
235. Slomovitz, B.M.; Coleman, R.L. The PI3K/AKT/mTOR pathway as a therapeutic target in endometrial cancer. *Clin. Cancer Res.* **2012**, *18*, 5856–5864.
236. Chambers, J.W.; LoGrasso, P.V. Mitochondrial c-Jun N-terminal kinase (JNK) signaling initiates physiological changes resulting in amplification of reactive oxygen species generation. *J. Biol. Chem.* **2011**, *286*, 16052–16062.
237. Cuadrado, A.; Nebreda, A.R. Mechanisms and functions of p38 MAPK signalling. *Biochem. J.* **2010**, *429*, 403–417.
238. Goldstein, D.M.; Gray, N.S.; Zarrinkar, P.P. High-throughput kinase profiling as a platform for drug discovery. *Nat. Rev. Drug Discov.* **2008**, *7*, 391–397.
239. Gross, S.; Rahal, R.; Stransky, N.; Lengauer, C.; Hoefflich, K.P. Targeting cancer with kinase inhibitors. *J. Clin. Investig.* **2015**, *125*, 1780–1789.
240. Skropeta, D.; Pastro, N.; Zivanovic, A. Kinase inhibitors from marine sponges. *Mar. Drugs* **2011**, *9*, 2131–2154.
241. Tasdemir, D.; Mallon, R.; Greenstein, M.; Feldberg, L.R.; Kim, S.C.; Collins, K.; Wojciechowicz, D.; Mangalindan, G.C.; Concepcion, G.P.; Harper, M.K.; et al. Aldisine alkaloids from the Philippine sponge *Stylissa massa* are potent inhibitors of mitogen-activated protein kinase kinase-1 (MEK-1). *J. Med. Chem.* **2002**, *45*, 529–532.
242. Segraves, N.L.; Crews, P. A madagascar sponge *Batzella* sp. As a source of alkylated iminosugars. *J. Nat. Prod.* **2005**, *68*, 118–121.
243. Kortmansky, J.; Schwartz, G.K. Bryostatin-1: A novel PKC inhibitor in clinical development. *Cancer Investig.* **2003**, *21*, 924–936.

244. Kinnel, R.B.; Scheuer, P.J. 11-hydroxystaurosporine: A highly cytotoxic, powerful protein kinase C inhibitor from a tunicate. *J. Org. Chem.* **1992**, *57*, 6327–6329.
245. Isbruckner, R.A.; Guzman, E.A.; Pitts, T.P.; Wright, A.E. Early effects of lasonolide A on pancreatic cancer cells. *J. Pharmacol. Exp. Ther.* **2009**, *331*, 733–739.
246. Alvi, K.A.; Jaspars, M.; Crews, P.; Strulovici, B.; Oto, E. Penazetidine A, an alkaloid inhibitor of protein kinase C. *Bioorg. Med. Chem. Lett.* **1994**, *4*, 2447–2450.
247. Marion, F.; Williams, D.E.; Patrick, B.O.; Hollander, I.; Mallon, R.; Kim, S.C.; Roll, D.M.; Feldberg, L.; Van Soest, R.; Andersen, R.J. Liphagal, a selective inhibitor of PI3 kinase α isolated from the sponge akacoralliphaga: Structure elucidation and biomimetic synthesis. *Org. Lett.* **2006**, *8*, 321–324.
248. Pereira, A.R.; Strangman, W.K.; Marion, F.; Feldberg, L.; Roll, D.; Mallon, R.; Hollander, I.; Andersen, R.J. Synthesis of phosphatidylinositol 3-kinase (PI3K) inhibitory analogues of the sponge meroterpenoid liphagal. *J. Med. Chem.* **2010**, *53*, 8523–8533.
249. Alvarez-Manzaneda, E.; Chahboun, R.; Alvarez, E.; José Cano, M.; Haidour, A.; Alvarez-Manzaneda, R. Enantioselective total synthesis of the selective PI3 kinase inhibitor liphagal. *Org. Lett.* **2010**, *12*, 4450–4453.
250. Piplani, H.; Rana, C.; Vaish, V.; Vaiphei, K.; Sanyal, S.N. Dolastatin, along with Celecoxib, stimulates apoptosis by a mechanism involving oxidative stress, membrane potential change and PI3-K/AKT pathway down regulation. *Biochim. Biophys. Acta—Gen. Subj.* **2013**, *1830*, 5142–5156.
251. Janmaat, M.L.; Rodriguez, J.A.; Jimeno, J.; Kruyt, F.A.E.; Giaccone, G. Kahalalide F induces necrosis-like cell death that involves depletion of ErbB3 and inhibition of Akt signaling. *Mol. Pharmacol.* **2005**, *68*, 502–510.
252. Ling, Y.H.; Miguel, A.; Zou, Y.; Yuan, Z.; Lu, B.; José, J.; Ana, M.C.; Perez-Soler, R. PM02734 (elisidepsin) induces caspase-independent cell death associated with features of autophagy, inhibition of the Akt/mTOR signaling pathway, and activation of death-associated protein kinase. *Clin. Cancer Res.* **2011**, *17*, 5353–5366.
253. García-Fernández, L.F.; Losada, A.; Alcaide, V.; Álvarez, A.M.; Cuadrado, A.; González, L.; Nakayama, K.; Nakayama, K.I.; Fernández-Sousa, J.M.; Muñoz, A.; et al. Aplidin™ induces the mitochondrial apoptotic pathway via oxidative stress-mediated JNK and p38 activation and protein kinase C δ . *Oncogene* **2002**, *21*, 7533–7544.
254. Lee, K.H.; Nishimura, S.; Matsunaga, S.; Fusetani, N.; Horinouchi, S.; Yoshida, M. Inhibition of protein synthesis and activation of stress-activated protein kinases by onnamide A and theopederin B, antitumor marine natural products. *Cancer Sci.* **2005**, *96*, 357–364.
255. Roychowdhury, S.; Chinnaiyan, A.M. Translating genomics for precision cancer medicine. *Annu. Rev. Genomics Hum. Genet.* **2014**, *15*, 395–415.
256. Encinar, J.A.; Fernandez-Ballester, G.; Galiano-Ibarra, V.; Micol, V. *In silico* approach for the discovery of new PPAR γ modulators among plant-derived polyphenols. *Drug Des. Devel. Ther.* **2015**, *9*, 5877–5895.
257. Galiano, V.; Garcia-Valtanen, P.; Micol, V.; Encinar, J.A. Looking for inhibitors of the dengue virus NS5 RNA-dependent RNA-polymerase using a molecular docking approach. *Drug Des. Devel. Ther.* **2016**, *10*, 3163–3181.
258. Thanki, K.; Gangwal, R.P.; Sangamwar, A.T.; Jain, S. Oral delivery of anticancer drugs: Challenges and opportunities. *J. Control. Release* **2013**, *170*, 15–40.

259. ADMET profile for antineoplastic drugs. Available online: http://dockingfiles.umh.es/anticancer-drugs/Anticancer_drugslist.asp (accessed on 22 June 2017).
260. Marine Natural Library Molecular Docking Site. Available online: <http://docking.umh.es/chemlib/mnplib> (accessed on 22 June 2017).
261. Montaser, R.; Luesch, H. Marine natural products: A new wave of drugs? *Future Med. Chem.* **2011**, *3*, 1475–1489.
262. Blunt, J.; Munro, M.H.G. *Dictionary of Marine Natural Products*, with CD-ROM; Chapman & Hall/CRC: Boca Raton, FL, USA, 2008.
263. National Institutes of Health (NIH) Chemical Identifier Resolution Service. Available online: <https://cactus.nci.nih.gov/chemical/structure> (accessed on 22 June 2017).
264. Veber, D.F.; Johnson, S.R.; Cheng, H.Y.; Smith, B.R.; Ward, K.W.; Kopple, K.D. Molecular properties that influence the oral bioavailability of drug candidates. *J. Med. Chem.* **2002**, *45*, 2615–2623.
265. Choi, H.; Cho, S.Y.; Pak, H.J.; Kim, Y.; Choi, J.Y.; Lee, Y.J.; Gong, B.H.; Kang, Y.S.; Han, T.; Choi, G.; et al. NPCARE: Database of natural products and fractional extracts for cancer regulation. *J. Cheminform.* **2017**, *9*, 2.
266. Newman, D.J. Developing natural product drugs: Supply problems and how they have been overcome. *Pharmacol. Ther.* **2016**, *162*, 1–9.
267. Grienke, U.; Silke, J.; Tasdemir, D. Bioactive compounds from marine mussels and their effects on human health. *Food Chem.* **2014**, *142*, 48–60.
268. Tornero, V.; Hanke, G. Chemical contaminants entering the marine environment from sea-based sources: A review with a focus on european seas. *Mar. Pollut. Bull.* **2016**, *112*, 17–38.
269. Leal, M.C.; Calado, R.; Sheridan, C.; Alimonti, A.; Osinga, R. Coral aquaculture to support drug discovery. *Trends Biotechnol.* **2013**, *31*, 555–561.
270. Cuevas, C.; Francesch, A. Development of yondelis® (trabectedin, ET-743). A semisynthetic process solves the supply problem. *Nat. Prod. Rep.* **2009**, *26*, 322–337.



© 2017 by the authors; licensee MDPI, Basel, Switzerland. This article is an open access article distributed under the terms and conditions of the Creative Commons Attribution (CC-BY) license (<http://creativecommons.org/licenses/by/4>)

**Marine Invertebrate Extracts
induce Colon Cancer Cell Death
via ROS-mediated DNA
Oxidative Damage and Mitochondrial
Impairment**

**Doctoral Student:
Verónica Ruiz Torres**

Article

Marine Invertebrate Extracts induce Colon Cancer Cell Death via ROS-mediated DNA Oxidative Damage and Mitochondrial Impairment.

Verónica Ruiz-Torres ¹, Celia Rodríguez-Pérez^{2,3}, María Herranz-López¹, Beatriz Martín-García^{2,3}, Ana-María Gómez-Caravaca³, David Arráez-Román^{2,3}, Antonio Segura-Carretero^{2,3}, Enrique Barrajón-Catalán^{1,*,#} and Vicente Micol ^{1,4,#}.

- 1 Instituto de Biología Molecular y Celular (IBMC) and Instituto de Investigación, Desarrollo e Innovación en Biotecnología Sanitaria de Elche (IDiBE), Universitas Miguel Hernández (UMH); 03202, Elche, Spain
- 2 Department of Analytical Chemistry, Faculty of Sciences, University of Granada, C/Fuentenueva s/n, Granada, Spain.
- 3 Research and Development of Functional Food Centre (CIDAF), PTS Granada, Avda. Del Conocimiento 37, Edificio BioRegion, 18016, Granada, Spain.
- 4 CIBER, Fisiopatología de la Obesidad y la Nutrición, CIBERobn, Instituto de Salud Carlos III, Palma de Mallorca 07122, Spain (CB12/03/30038).

* Correspondence: e.barrajon@umh.es; Tel.: +34-965-222-586

Both authors share senior co-authorship.

Under process of publishing

Abstract: Marine compounds are a potential source of new anticancer drugs. In this study, the antiproliferative effects of 20 invertebrate marine extracts on three colon cancer cell models (HGUE-C-1, HT-29 and SW-480) were evaluated. Extracts from two nudibranchs (*Phyllidia varicosa*, NA and *Dolabella auricularia*, NB), a holothurian (*Pseudocolochirus violaceus*, PS) and a soft coral (*Carotalcyon* sp., CR) were selected due to their potent cytotoxic capacities. The four marine extracts exerted strong antiproliferative capacity and induced cell cycle arrest in the G2/M phase, which evolved into early apoptosis in the case of the CR, NA and NB extracts and necrotic cell death for PS extract. All the extracts induced, to some extent, intracellular ROS accumulation and mitochondrial depolarization, caspase activation and DNA damage. The composition of the four extracts was fully characterized using an HPLC-ESI-TOF-MS analysis, identifying up to 98 compounds. Among the most abundant compounds identified in each extract, we propose that diterpenes, steroids, sesqui- and seterterpenes (CR); cembranolides (PS); diterpenes, polyketides and indole terpenes (NA); and porphyrin, drimenyl cyclohexanone and polar steroids (NB), might be the candidates for the observed activity. We postulate that ROS accumulation may be responsible for the subsequent DNA damage, mitochondrial depolarization and cell cycle arrest, ultimately inducing cell death either by apoptosis or necrosis.

Keywords: Marine invertebrate; soft Coral; holothurian; Nudibranch; antiproliferative; colon cancer; ROS; DNA damage; cell cycle; apoptosis; necrosis; HPLC-ESI-TOF-MS; cell death; natural compounds.



1. Introduction

Colorectal cancer (CRC) is a one of the most frequent causes of mortality worldwide, and approximately 95% cases consist of adenocarcinoma [1]. Conventional treatment methods, such as surgery, radiation and chemotherapy, usually fail to cure advanced stages of cancer development. For this reason, new drugs that may be suitable for the development of more active and specific treatments and are devoid of the side-effects associated with conventional methods must be identified [2].

Natural products are produced by the secondary metabolism of living organisms and present great chemical diversity [3]. These products represent an almost unlimited source for the identification of novel chemical structures that might serve as a basis for the development of new anticancer drugs [4]. In the last seventy years, approximately 49% of the molecules approved to treat cancer were originally natural products or were based directly on them [5]. Most of the natural products are derived from plants and terrestrial microorganisms [6, 7]; however, the marine environment has currently attracted increasing attention due to the potential druggability of marine compounds and the emerging technologies in bioprospection [8].

The biodiversity of the marine ecosystem has provided a wide number of new scaffolds with putative anticancer effects [9, 10]. A review of the most promising bioactive marine compounds discovered between 1985 to 2012 reported that considerable efforts have been focused on the discovery of anticancer drugs with applications in other diseases, such as cardiovascular, neuroprotective, antiviral, antifungal or antibacterial applications [11]. Our group has also recently published a comprehensive review of the most significant anticancer compounds derived from marine organisms that covers the period from January 2000 until April 2017 [10].

The marine and coastal ecosystems contain much harsher and diverse environmental conditions than terrestrial ecosystems due to the aquatic environment and the strong selective pressure, resulting in a much broader range of phyla and classes of organisms. For example, coral reef ecosystems are known by its intense biological competition for space, light and food. Secondary metabolites produced in response to competitive pressure, allow them to survive. Many scientific studies show the advantage of possessing these secondary metabolites to survive [12-15]. Of the more than 33 currently known phyla, 97% are present in and 45% are exclusive to the marine ecosystem [16]. Among marine organisms, invertebrates (animals without a backbone or spinal column) are the major source of bioactive compounds in the marine ecosystem and represent 60% of all marine animals. Marine invertebrates include phyla such as Porifera, Coelenterata, Mollusca, Tunicata, and Annelida, as well as bryozoans, and these invertebrates remain the major source of anticancer compounds being tested in the preclinical phase [10, 11, 17].

In the present study, the potential antitumor activities of twenty extracts obtained from marine invertebrates were tested to determine their antiproliferative capacities in human colon cancer cells. Four of the most promising extracts were

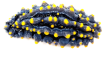
selected , two nudibranchs (*Phyllidia varicosa*, NA and *Dolabella auricularia*, NB), a holothurian (*Pseudocolochirus violaceus*, PS) and a soft coral (*Carotalcyon* sp., CR), and their compositions were characterized in depth using High-Performance Liquid Chromatography coupled to Electrospray Time-of-Flight Mass Spectrometry (HPLC-ESI-TOF-MS) analysis. The reported anticancer activity of the most abundant identified compounds was reviewed to proposed those that may explain the capacity of the extracts. The putative molecular mechanisms of these extracts were further dissected and discussed by studying the cell cycle, ROS generations and DNA damage, apoptosis, necrosis and mitochondrial function. The results support an antiproliferative mechanism that depends on the generation of free radical species at the intracellular level.

2. Results

2.1. Marine extracts derived from selected invertebrates inhibit the proliferation of colon cancer cells

First, 20 invertebrate marine species (Table 1) were selected as described in methods section. Then, the cytotoxic activity of their extracts toward cells in a panel of three human colon cancer cell lines was screened using the MTT assay. Solutions of each extract were prepared at eight concentrations (0–100 $\mu\text{g}/\text{mL}$) and were individually incubated with the HGUE-C-1, HT-29 and SW-480 cells for 24, 48 or 72 h, and the survival curves were obtained to calculate the concentration that inhibited the growth of 50% of cells (IC_{50}). These values are shown in Supplementary Table 2, and the cytotoxic curves are presented in Supplementary Figure 1. The most active extracts were selected when they presented IC_{50} values less than 30 $\mu\text{g}/\text{mL}$ at 48 h in at least 2 of the cell lines used or ≤ 15 $\mu\text{g}/\text{mL}$ in at least one of the cell lines used. According to these criteria, the four extracts that presented the lowest IC_{50} values (CR from red coral, PS from a holothurian, NA and NB from nudibranch marine organisms) were selected for further characterization. The most interesting result was obtained with NB CE, which showed IC_{50} (48 h) values of 0.3 $\mu\text{g}/\text{mL}$ (HGUE-C-1 cells), 0.1 $\mu\text{g}/\text{mL}$ (HT-29 cells) and 0.6 $\mu\text{g}/\text{mL}$ (SW-480 cells). Furthermore, the PS CE also showed high cytotoxicity, with IC_{50} values of 37.4 $\mu\text{g}/\text{mL}$ (HGUE-C-1 cells), 0.7 $\mu\text{g}/\text{mL}$ (HT-29 cells) and 18.6 $\mu\text{g}/\text{mL}$ (SW-480 cells). The NA extract also exhibited significant cytotoxic activity, with IC_{50} values of 137.3 $\mu\text{g}/\text{mL}$ (HGUE-C-1 cells), 10.0 $\mu\text{g}/\text{mL}$ (HT-29 cells) and 13.6 $\mu\text{g}/\text{mL}$ (SW-480 cells), and the CR CE exhibited IC_{50} values of 82.0 $\mu\text{g}/\text{mL}$ (HGUE-C-1 cells), 9.4 $\mu\text{g}/\text{mL}$ (HT-29 cells) and 27.6 $\mu\text{g}/\text{mL}$ (SW-480 cells) (Table 2).

Table 1. Marine species identification and codification

Class	Scientific name	Code	Photo	Class	Scientific name	Code	Photo
Soft Coral	<i>Parazoanthus</i> sp.	P		Soft Coral	<i>Euphyllia ancora</i>	Eu	
	<i>Discosoma</i> sp.	D			<i>Carotalcyon</i> sp.	CR	
	<i>Lemmalia</i> sp.	L		Anemone	<i>Aiptasia</i> sp.	A	
	<i>Capnella</i> sp.	C			<i>Wellsohyllia</i> sp.	W	
	<i>Nephtea</i> sp.	N		Hard Coral	<i>Echynophyllia</i> sp.	E	
	<i>Sarcophyton</i> sp.	SII			<i>Fungia</i> sp.	F	
	<i>Sinularia</i> sp.	Si			<i>Duncanopsamia</i> sp.	Du	
	<i>Cataphyllia</i> sp.	Cy		Nudibranch	<i>Phyllidia varicosa</i>	NA	
	<i>Xenia</i> sp.	X			<i>Dolabella auricularia</i>	NB	
	<i>Palythoa</i> sp.	Py		Holothurian	<i>Pseudocolochirus violaceus</i>	PS	

In order to confirm the results from MTT assays and to explore the antiproliferative and cytostatic effects of extracts, Real-Time Cell Analysis (RTCA) was conducted for 75 h. The RTCA assay facilitates the monitoring of the kinetics of cellular processes, such as changes in proliferation, migration and invasion, in contrast to labor-intensive label-based end-point assays [18]. This technique provides time-dependent cellular response profiles (TCRP) that are presented as cell indexes (CIs), which are measurements of changes in the growth rate, morphology and adhesive characteristics of the cell culture [19]. The proliferation profiles of HGUE-C-1, HT-29 and SW-480 cells after treatment with marine extracts was analyzed (Supplementary Figures 2 (CR), 3 (PS), 4 (NA) and 5 (NB)). The CIs were calculated from the kinetic profiles at 24, 48 and 72 h, and plotted in Fig 1 A-D. A significant effect on the inhibition of proliferation was observed in cells treated with marine extracts compared to the control. Overall, marine extracts noticeably decreased the CI in a dose-dependent manner in all cell models used; their strong activities at lower doses is worth noting, particularly for PS and NB extracts, which showed a dramatic decrease in the CI directly after treatment of all cell models with the lowest concentration (10 $\mu\text{g}/\text{mL}$). NB substantially decreased the CIs by 80.8% in HGUE-C-1 cells, 99.8% in HT-29 cells and 86.5% in SW-480 cells at 10 $\mu\text{g}/\text{mL}$ (48 h) and further enhanced that effect by 89.7% in HGUE-C-1 cells, 75.6% in HT-29 cells and 88.9% in SW-480 cells at 100 $\mu\text{g}/\text{mL}$ (48 h) (Fig 1 D). PS diminished the CI by 56.8% in HGUE-C-1 cells treated with 25 $\mu\text{g}/\text{mL}$ of the extract and reduced the CI by 81.6% at

100 µg/mL, 87.7% at 10 µg/mL and 99.4% at 100 µg/mL in HT-29 cells (48 h). Moreover, PS decreased the CI by 84.1% at 10 µg/mL and a 99.22% at 100 µg/mL in SW-480 cells (48 h) (Fig 1 B). CR and NA extracts decreased the proliferation and growth of all cell models examined in a dose-dependent manner, but their effects were less noticeable than NB and PS. After treatment with 25 or 100 µg/mL NA for 48 h, the HGUE-C-1 CI was decreased 11.5% and 37.9%, the HT-29 CI was reduced 5.5% and 88.7%, and the SW-480 CI decreased 25.4 % and 70.0%, respectively. A noticeable effect of NA on cells of all the cell lines tested was only observed at concentrations greater than 25 µg/mL (Fig 1 C). CR was the least potent of the four extracts in reducing proliferation. Treatments with 10 µg/mL and 100 µg/mL CR reduced the CI of HGUE-C-1 cells by 7.1% and 74.4%, respectively; a 16.9% decrease in the CI at 10 µg/mL and 59.7% decrease at 100 µg/mL were observed in HT-29 cells. Finally, decreases in the CI of 22.6 % and 82.6% were observed in SW-480 cells at 10 µg/mL and 100 µg/mL, respectively (Fig 1 A). The RTCA results from cells treated with the marine extracts were consistent with the findings from the MTT assay and allowed us to classify the extracts from the most to the least active, i.e., NB, PS, NA and CR.

Table 2. IC₅₀ µg/ml mean ± SD of three independent experiments. Values for the other marine extracts are showed in Supplementary Table 2.

Code	HGUE-C-1			HT-29			SW-480		
	24 h	48 h	72 h	24 h	48 h	72 h	24 h	48 h	72 h
CR	250.9 ± 92.1	82.0 ± 5.9	58.1 ± 3.4	15.0 ± 4.4	9.4 ± 1.4	10.6 ± 1.0	105.0 ± 10.9	27.6 ± 2.8	14.8 ± 1.6
PS	37.5 ± 3.0	37.4 ± 1.3	48.0 ± 1.8	3.3 ± 1.1	0.7 ± 0.4	2.1 ± 0.7	24.3 ± 2.0	18.6 ± 1.2	16.9 ± 0.6
NA	146.0 ± 29.0	61.8 ± 2.9	78.8 ± 3.4	13.0 ± 2.7	10.0 ± 0.7	9.3 ± 1.0	57.2 ± 6.9	13.6 ± 1.5	13.0 ± 2.0
NB	11.4 ± 3.4	0.3 ± 0.3	0.1 ± 0.2	5.0 ± 3.6	0.1 ± 0.1	0.1 ± 0.1	54.3 ± 24.2	0.6 ± 0.4	0.2 ± 0.1

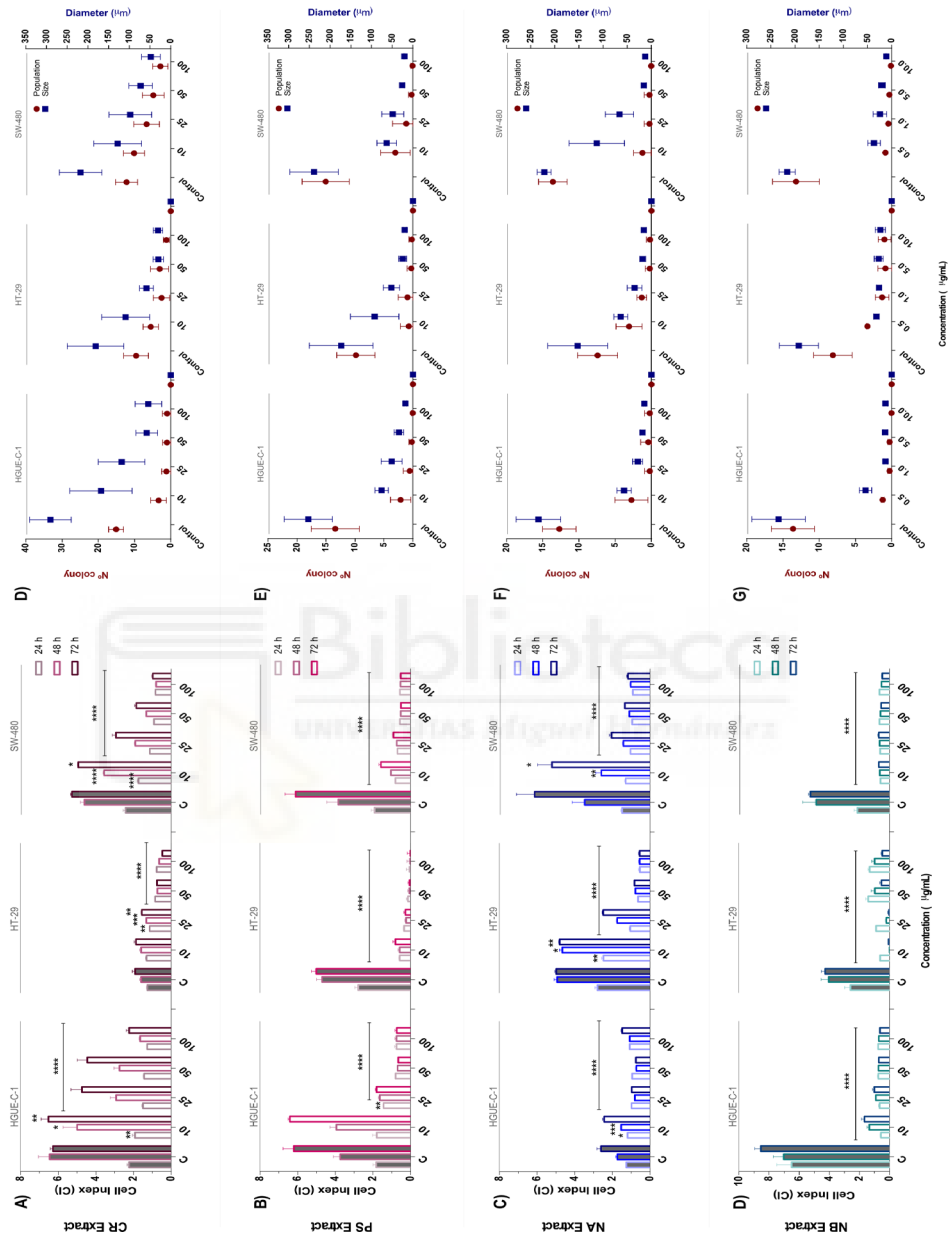


Figure 1. Assessments of the antiproliferative effects of invertebrate marine extracts on human colon carcinoma cell models using the Real Time Cell Analyzer System (RTCA) (A-H) or colony formation assay (E-H). Cell proliferation assays were performed using the Real Time Cell Analyzer (RTCA) Dual-Plate instrument and the colony formation assay was performed by measuring the size and number of colonies after seeding diluted cells into 6-well plates; both approaches are described in the Materials and Methods section. HGUE-C-1, HT-29 and SW-480 cells were treated with 10, 25, 50 or 100 $\mu\text{g}/\text{mL}$ of CR (A), PS (B), NA (C) and NB (D) for 24, 48 or 72 h for RTCA measurements, and for 24 h in the colony formation assays (CR (E), PS (F), NA (G) and NB (H)) and compared to untreated cells (Control cells plus dimethyl sulfoxide at 0.2%, C). The CIs measured at 24, 48 and 72 h are presented as the means \pm SD of three independent experiments. The population and size data from colony formation assays are presented as the means \pm SD of three independent experiments. p-values were calculated and compared to the same untreated cell line using ANOVAs. *p-value<0.05, **p-value<0.01, and ***p-value<0.001.

The antiproliferative activity of selected extracts were further characterized using the colony formation assay. This technique is used to test the ability of cancer cells to proliferate after a treatment, thereby retaining their ability to form a large colony or a clone [20]. Marine extracts markedly reduced the size and number of colonies formed by HGUE-C-1, HT-29 and SW-480 cells, as shown in Fig 1 E-H and Supplementary Figure 6. Marine extracts decreased the average size of the colonies and the number of cells present in each colony. CR gradually reduced the average colony size in a dose-dependent manner (Fig 1 E). Treatment with 100 $\mu\text{g}/\text{mL}$ CR reduced the size of HGUE-C-1 cells from 260 μm (14 cells per colony) to 36 μm , i.e., a 93% reduction; from 160 μm (9 cells per colony) to 24 μm (1 cell per colony) in HT-29 cells, i.e., an 87% reduction; and from 226 μm (14 cells per colony) to 38 μm (2 cells per colony) in SW-480 cells, i.e., a 76% decrease. Nevertheless, PS and NA were more active extracts than CR and produced a more drastic decrease in the colony size at the lowest concentrations tested in some of the cells lines and reaching an approximately 99% reduction in the colony size of all models at 100 $\mu\text{g}/\text{mL}$ (Fig 1 F and G). In contrast, NB produced the strongest effect on decreasing both colony size and cell population at the lowest concentration tested in all cell models (Fig 1 H). A general reduction in the average colony size of each colon cell model was induced by all marine extracts. Although the CR extract reduced size and number in a progressive manner, NA, PS and NB extracts produced drastic changes in these parameters at the lowest concentrations tested.

2.2. *Invertebrate marine extracts induce cell cycle arrest and apoptosis*

After confirming the antiproliferative activity of the four selected marine extracts, the next step was to study if these changes were mediated by a cytotoxic or cytostatic effect. Therefore, the cell cycle profiles were examined using flow cytometry. After the treatment of colon cancer cells (HGUE-C-1, HT-29 and SW-480) with different concentrations of marine extracts for 24 h, an altered cell cycle was found for all combinations of extracts and cell lines (Fig 2 A-D). Some differences in the pattern of phases of the cell cycle were observed depending on the extract and cell line, however

the most consistent effect was a considerable increase in the number of cells arrested in the G2/M phase in cells from all cell lines and, in some cases, a concomitant increase in the number of cells in the SubG1 phase.

NA and NB drastically increased the proportion of HT-29 and SW-480 cells in the G2/M phase at the expense of a reduction in the numbers of cells in the S and G0/G1 phases at the minimum dose tested (Fig 2 C and D). In particular, NB extract increased the proportion of HT-29 cells in the G2/M phase from $21.7 \pm 0.7\%$ to $80.4 \pm 0.8\%$ at $25 \mu\text{g/mL}$ and from $30.2 \pm 1.3\%$ to $84.6 \pm 0.8\%$ in SW-480 cells. In HGUE-C-1 cells, NB increased the proportion of cells in the G2/M phase in a dose-dependent manner, with a maximum percentage of 45.9 ± 0.8 observed in cells treated with $10 \mu\text{g/mL}$, but this treatment also increased the proportion of cells in the SubG1 phase (related to apoptotic cells) in a dose-dependent manner (maximum at $25 \mu\text{g/mL}$, reaching $43.9 \pm 1.5\%$). This increase in the proportion of cells in the SubG1 phase was also observed, to a lesser extent, in HT-29 and SW-480 cells (Fig 2 D).

The CR extract produced a gradual, dose-dependent change in the cell cycle of cells from all cell models. An increase in the proportion of cells in the G2/M phase was also observed, particularly in HT-29 and HGUE-C-1 cells, which occurred at the expense of the proportions of cells in the G0/1 and S phases (Fig 2 A). The proportion of cells in the G2/M phase increased from $20.8 \pm 0.6\%$ to $41.7 \pm 0.6\%$ in HGUE-C-1 cells, from $25.9 \pm 1.3\%$ to 81.7 ± 1.7 in HT-29 cells, and from $40.5 \pm 0.4\%$ to $48.2 \pm 0.6\%$ in SW-480 cells, all of which were treated with $100 \mu\text{g/mL}$ of the extract. Interestingly, a significant approximately 2-fold increase in the proportion of HGUE-C-1 cells in the SubG1 phase (cells in apoptosis) was observed following treatment with the CR extract, similar to the treatment with the NA and NB extracts. This increase was also observed, but to a lesser extent, in HT-29 cells.

The PS extract also induced G2/M arrest in cells from all cell lines; however, the change was not as prominent as those one observed for the NB, NA and CR extracts. The percentage of HGUE-C-1 cells and, to a lesser extent, SW-480 cells treated with PS extract in the SubG1 phase also increased (Fig 2 B).

To further study the effect of marine extracts in the induction of apoptosis of colon cancer cell models (HGUE-C-1, HT-29 and SW-480), the Annexin V detection method was used. This method allowed us to discriminate early apoptosis (cells expressing phosphatidylserine on the outer leaflet of the plasma membrane) from late apoptosis and necrosis (cells that have lost cell membrane integrity and are permeable to vital dyes). Nevertheless, this assay is not able to distinguish between cells in late apoptotic state from necrotic cells because they will be positive for both Annexin V and the vital dye. In order to distinguish necrotic cells from late apoptotic cells, a time course experiment monitoring a gradual increase of cells in early apoptosis to late apoptosis would be required [21, 22].

Fig 2 E-F shows the effects of marine extracts on apoptosis in the Annexin V assay and classifies them into two groups. CR, NA and NB extracts exerted a similar effect, i.e., an increase in the total number of apoptotic cells, along with a higher proportion of early apoptotic cells than late apoptotic cells. This effect was dose-

dependent, indicating that the apoptotic pathway was induced in these cells. In contrast, PS increased the percentage of late apoptotic cells compared with early apoptotic cells, suggesting a potential necrotic mechanism. In more detail, treatment with 100 $\mu\text{g/mL}$ of the CR extract increased the proportion of early apoptotic cells 2-fold compared to untreated HGUE-C-1, HT-29 and SW-480 cells. The CR extract also showed a 2-fold increase in the proportion of late apoptotic HT-29 and SW-480 cells and a 3-fold increase in the proportion of late apoptotic HGUE-C-1 cells. Only in the case of HGUE-C-1 the late apoptotic cell proportion was higher than that of early apoptotic cells (Fig 2 E). Treatment with 100 $\mu\text{g/mL}$ of the NA extract increased the proportions of early apoptotic HGUE-C-1, HT-29 and SW-480 cells by 6-fold, 4.5-fold and 4-fold, respectively. The proportions of late apoptotic HGUE-C-1, HT-29 and SW-480 cells were also increased 2.3-fold, 2.6 and 3.3-fold, respectively (Fig 2 G). At 100 $\mu\text{g/mL}$, NB increased the proportions of early apoptotic HGUE-C-1, HT-29 and SW-480 cells by 5.5-fold, 4.6-fold and 3.5-fold, respectively, compared to untreated cells. The proportions of late apoptotic HGUE-C-1, HT-29 and SW-480 cells increased 2.0-, 2.5- and 3.4-fold, respectively, following treatment with the NB extract (Fig 2 H). Finally, PS reduced the proportions of early apoptotic HGUE-C-1 and SW-480 cells and increased the proportion of early apoptotic HT-29 cells 3-fold compared to untreated cells. In contrast, the PS extract noticeably increased the proportions of late apoptotic HGUE-C-1, HT-29 and SW-480 cells by 5.2-, 8.6- and 18.8-fold, respectively (Fig 2 F).



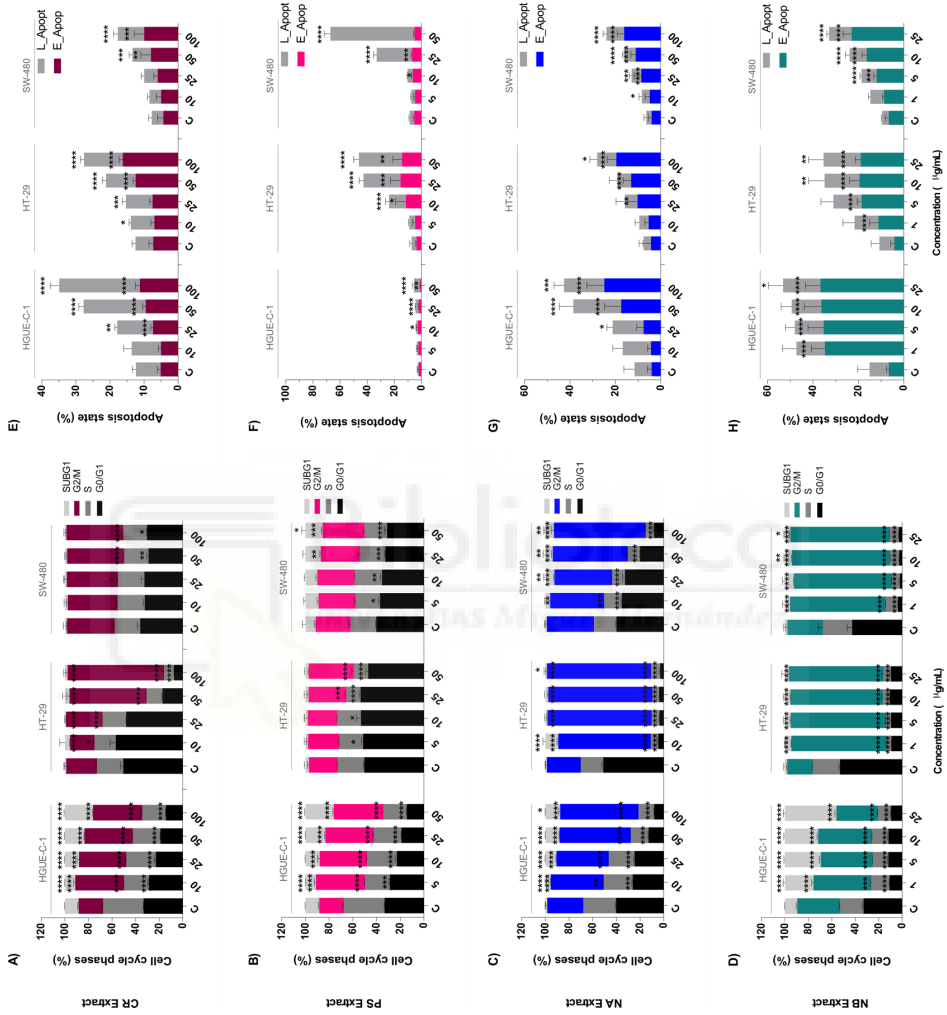


Fig. 2. Effects of the CR, PS, NA and NB marine extracts on the cell cycle (A-D) and apoptosis (E-H) of human colon carcinoma cell models using the Muse® Cell Analyzer and Annexin V assay. HGUE-C-1, HT-29 and SW-480 cells were plated at a density of 1×10^5 cells/well, treated with different concentrations of marine extracts for 24 h and harvested for each protocol, as described in the Materials section. The flow cytometry analysis and early (E_Apop) and late apoptotic cells (L_Apop) measurements were conducted using Muse® Cell Cycle and Muse® Annexin V & Dead Cell Kit (Merck Millipore), respectively, in the Muse® Cell Analyzer, according to the manufacturer's instructions. The results are presented as percentages (means \pm SD) from three independent experiments. p-values were calculated and compared to the same untreated cell line (Control cells plus dimethyl sulfoxide less than 0.2%, C) using ANOVAs. *p-value < 0.05, ** p-value < 0.01, *** p-value < 0.001 and **** p-value < 0.0001.

2.3. Effect of marine extracts on the non-apoptotic cell death of colon cancer cells

Lactate dehydrogenase (LDH) is one of the most abundant cytoplasmic enzymes that is released to the extracellular space when the plasma membrane is disrupted during necrotic cell death. LDH release was measured in the three colon cancer cell models (HGUE-C-1, HT-29 and SW-480) after treatment with different concentrations of the marine extracts (CR, PS, NA and NB) for 24 h and was compared to the positive control (C+, 100% LDH activity) and negative control (C-, 0% LDH activity) (Fig 3 A - D). Among the four marine extracts, the PS extract was the only extract that significantly increased LDH release compared with the negative control. PS increased LDH release in cells from all tested cell lines by > 24% compared to the negative control. The percentage of LDH release induced by 100 μ g/mL of the PS extract after 24 h of treatment was $24.71 \pm 3.16\%$ in HGUE-C-1 cells, $24.80 \pm 3.16\%$ in HT-29 cells and $24.14 \pm 3.54\%$ in SW-480 cells (Fig 3 B). Based on these results, PS seemed to induce cell death through a necrosis-related mechanism, as suggested by the late apoptosis results described above. In contrast, the cell death induced by the other extracts (CR, NB and NA) appeared to be mediated by the apoptotic pathway.

To further characterize the cell death process after the exposure of colon cancer cells to the marine extracts, Hoechst/Propidium iodide nuclear staining and fluorescence microscopy were performed. The cells were co-stained with the exclusion dye propidium iodide, which does not cross the intact plasma membrane, and the nuclear dye Hoechst 33342, and morphological changes were monitored using a high content image fluorescent cell analyzer. The cells were classified according to the shape of the nucleus and the ratio of propidium iodide (PI) (red) and Hoechst (blue) staining (Fig 3 F). The cells were considered viable cells if they presented a round blue nucleus. Necrotic cells exhibited round purple nuclei. Apoptotic cells showed characteristic apoptotic bodies in pink when the membrane was permeabilized and in blue when the membrane remained intact (Fig 3 F). Representative microscopy images were taken after cells were treated with marine extracts (Fig 3 E). The results showed significant and common phenomena, such as membrane blebbing, pyknosis and apoptotic bodies, after treatment with NB, NA and CR for 24 h. NB and NA induced the formation of well-characterized and evident apoptopodia (apoptotic membrane protrusions) in SW-

480 cells and apoptotic bodies with intact and permeable membranes were detected in cells from all cell lines examined (Fig 3 E). All these features were commonly observed during apoptosis. In contrast, PS induced the formation of round pink nuclei in all cells from each of the cell lines tested, indicating a fast permeabilization and disruption of the cell membrane, which is characteristic of the necrosis process.

The fluorescence intensity of PI and Hoechst 33342 were measured and normalized to untreated cells. A higher PI/Hoechst ratio indicates a greater degree of disruption of the plasma membrane and a higher probability of a necrotic process (Fig 3 G). The PS extract significantly increased the PI/Hoechst ratio by 2.6-fold in HGUE-C-1 cells, 2.1-fold in HT-29 cells and 2.1-fold in SW-480 cells. CR and NB extracts increased the intensity of PI at higher concentrations; however, the significance of the difference was less than the intensity produced by the PS extract. These results corroborate the observations from the LDH release assay. While NB, NA and CR appeared to induce cell death through an apoptotic mechanism, PS appeared to induce a necrotic process.

2.4. Marine extracts promote intracellular ROS generation and mitochondrial membrane depolarization

Due to their pleiotropic role in a large variety of cellular processes, radical oxygen species (ROS) may function either as mediators or triggers of the apoptotic or necrotic cell death pathways in cancer cells. We therefore sought to determine whether the marine extracts affected cellular ROS accumulation. For this purpose, cells were exposed to different concentrations of marine extracts for 24 h and then stained with 2,7-dihydrodichlorofluorescein diacetate (H₂DCF-DA) to detect intracellular ROS levels. ROS levels in HGUE-C-1, HT-29 and SW-480 cells were consistently and significantly increased in response to treatment with the marine extracts in a dose-dependent manner compared to untreated cells (Fig 4). Among all marine extracts, the NB extract exhibited the most potent effect on intracellular ROS accumulation, followed by PS, NA and CR. NB increased the ROS levels by 4.5-, 12.6- and 10.1-fold in HGUE-C-1, HT-29 and SW-480 cells, respectively, compared to the control at the maximum concentration tested, i.e., 10 µg/mL (Fig 4 D). PS increased ROS accumulation 4.3-, 7.0- and 8.9-fold in HGUE-C-1, HT-29 and SW-480 cells, respectively, at 100 µg/mL (Fig 4 B). The NA extract increased ROS levels 4.2-, 6.8- and 7.7-fold in HGUE-C-1, HT-29 and SW-480 cells, respectively, compared to untreated cells at the same concentration (Fig 4 C). Finally, the CR extract increased ROS levels 2.9-, 7.9- and 4.2-fold in HGUE-C-1, HT-29 and SW-480 cells, respectively, compared to the control at 100 µg/mL (Fig 4 A).

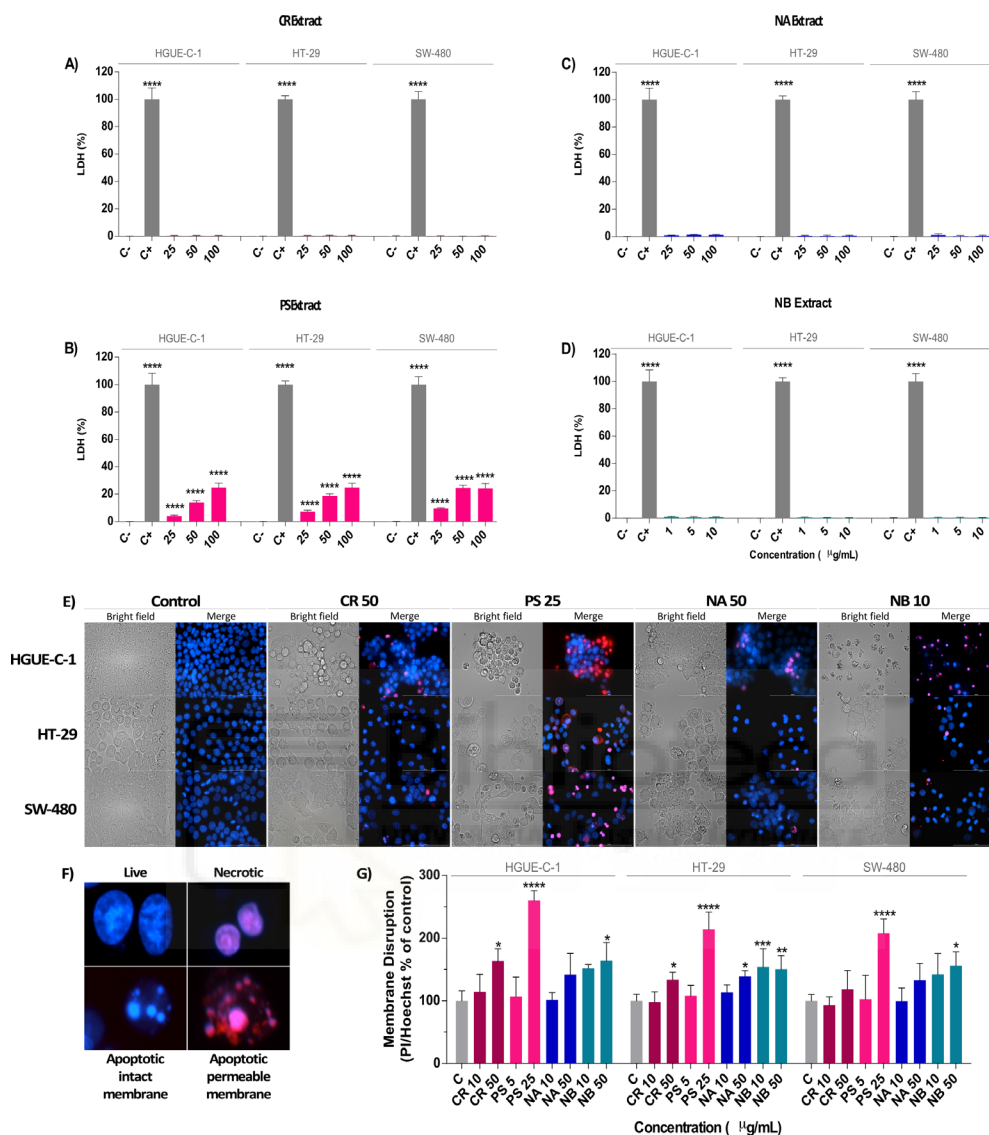


Fig. 3. Effects of the marine extracts on LDH release (A – D) and the formation of apoptotic bodies in colon cancer cells (E – G). The effects of several invertebrate marine extracts CR (A), PS (B), NA (C) and NB (D) on LDH release from colon cancer cells (24 h) were determined as described in the Materials and Methods section and compared to untreated cells (Control cells plus dimethyl sulfoxide less than 0.2%, C). The results are presented as the percentages (means \pm SD) from three independent experiments. p-values were calculated and compared to the same untreated cell line using ANOVAs. *p-value < 0.05, ** p-value < 0.01, *** p-value < 0.001 and **** p-value < 0.0001. The morphology of colon cancer cells was examined under a fluorescence microscope after treatment with the marine extracts for 24 h and staining with Hoechst 33342 and propidium iodide. Representative fluorescence microscopy images of HGUE-C-1, HT-29 and SW-480 cells treated with the different marine extracts shown in bright field, DAPI (Hoechst) and Texas red (PI)

channels at 20 X (E). Morphological classification of the nuclei in live cells, necrotic cells, and apoptotic cells with intact membranes and permeable membranes (F). Quantification of membrane disruption (PI/Hoechst ratio) as a measurement of necrosis after the treatment of colon cancer cells with various concentrations of the different marine extracts (G). The results are presented as the percentages (means \pm SD) from three independent experiments. p-values were calculated and compared to the same untreated cell line using ANOVAs. *p-value < 0.05, ** p-value < 0.01, *** p-value < 0.001 and **** p-value < 0.0001.

Changes in the mitochondrial membrane potential (MMP) that compromise mitochondrial function are related to metabolic stress triggered by ROS generation and inflammation. Moreover, variations in the MMP are also an indicator of irreversible checkpoints in the apoptotic process [23]. We analyzed the MMP using the cell analyzer Muse®, which allows us to measure the change in the mitochondrial membrane potential using a cationic, lipophilic dye and cellular plasma membrane permeabilization or cell death using 7-AAD. The effects of different concentrations of marine extracts on mitochondrial membrane depolarization (loss of $\Delta\psi_m$) were measured in HGUE-C-1, HT-29 and SW-480 cells that were exposed to the marine extracts for 24 h. Fig 4 (E - H) shows the effects of the marine extracts on the depolarization of mitochondrial membranes as follows: depolarized live cells (Dep_Live) and depolarized dead cells (Dep_Dead). High ratios of Dep_Live to Dep_Dead cells may suggest an apoptotic-mediated mechanism, and lower ratios represent a necrotic process; thus, this metric may be an indicator of the type of cell death caused by marine extracts. In general, CR, PS, NA and NB increased the proportions of depolarized cells in a dose-dependent manner compared to untreated cells (Fig 4). The results showed dissimilar behaviors of the NB, CR and NA marine extracts compared to the PS extract. NB, CR and NA extracts increased the proportion of Dep_Live cells compared to Dep_Dead cell population, which is characteristic of an apoptotic process, whereas PS increased the proportion of Dep_Dead cells compared to Dep_Live cells, which is typical of a non-apoptotic process.

Treatment with 100 $\mu\text{g/mL}$ of the CR extract increased the percentage of Dep_Live cells in a dose-dependent manner from $3.4 \pm 0.8\%$ in control cells to $8.7 \pm 2.0\%$ in HGUE-C-1 cells, from $3.4 \pm 1.8\%$ to $12.0 \pm 1.5\%$ in HT-29 cells and from $6.5 \pm 0.8\%$ to $11.8 \pm 2.0\%$ in SW-480 cells (Fig 4 E). The NA extract increased the percentage of Dep_Live cells to a greater extent than Dep_Dead cells in a dose-dependent manner, producing an effect that was 2 to 15 times stronger, depending on the cell line and the concentration of the extract. In HGUE-C-1 cells, the percentage of Dep_Live cells increased from $9.4 \pm 3.5\%$ in control cells to $24.3 \pm 4.4\%$ in cells treated with 100 $\mu\text{g/mL}$ NA, from $7.1 \pm 1.2\%$ to $24.4 \pm 4.5\%$ in treated HT-29 cells, and from $6.8 \pm 2.6\%$ to $16.1 \pm 3.9\%$ in SW-480 cells treated with the same concentration of the extract. NA also induced a significant but weaker increase in the percentage of Dep_Dead SW-480 cells at high concentrations (Fig 4 G). The NB extract increased the percentages of both types of depolarized cells in a dose-dependent manner, but the effect was much stronger on Dep_Live cells, i.e., 2- to 5-fold higher. NB increased the percentage of Dep_Live cells

from $6.4 \pm 3.6\%$ in control cells to $26.9 \pm 3.1\%$ in HGUE-C-1 cells treated with $25 \mu\text{g/mL}$ of the extract, from $11.4 \pm 6.0\%$ to $31.7 \pm 8.2\%$ in treated HT-29 cells, and from $10.8 \pm 2.2\%$ to $28.8 \pm 1.0\%$ in SW-480 cells treated with the same concentration of the extract (Fig 4 H). PS promoted a significant decrease in the percentage of Dep_Live cells in some cell lines and increased the proportion of Dep_Dead cells from 2- to 5-fold compared to control cells. PS increased the percentage of Dep_Live cells from $5.4 \pm 2.2\%$ to $13.2 \pm 5.7\%$ at $100 \mu\text{g/mL}$ in HGUE-C-1 cells, from $6.7 \pm 2.8\%$ to $20.2 \pm 8.0\%$ in HT-29 cells, and from $12.6 \pm 5.0\%$ in the control to $20.2 \pm 8.0\%$ in SW480 cells treated with the same concentration of the extract. However, a higher percentage of Dep_Dead cells was observed than Dep_Live in most cases, indicating a marked difference in the death mechanism. The data revealed substantial changes in the percentage of Dep_Dead HGUE-C-1 cells from $2.7 \pm 1.4\%$ in the control to $25.3 \pm 4.2\%$ at $100 \mu\text{g/mL}$, from $2.2 \pm 0.4\%$ to $55.3 \pm 15.4\%$ in HT-29 cells and from $2.3 \pm 0.4\%$ to $52.7 \pm 12.2\%$ in SW-480 cells treated with the same concentration of the extract (Fig 4 F).

These effects on the MMP were confirmed using alternative techniques, such as the measurement of the ratio between two mitochondrial fluorescence probes, i.e., MitoTracker Red (MitoRed), which identifies viable mitochondria, and MitoTracker Green (MitoGreen), which labels all mitochondria, as described in the Supplementary Information and Supplementary Figures 7 and 8.

2.5. Marine extracts induce cell death by activating caspases

Caspases are a highly specific proteases that are activated by cleavage in the apoptosis pathway and are responsible for initiating the death of mammalian cells. However, it is known that caspases are also involved in non-apoptotic pathways [24, 25]. To determine the marine extract-induced apoptosis effect and to confirm our previous results derived from the Annexin V and MitoPotential assays, the activation of the executioner caspases 3/7 and the initiator of extrinsic apoptosis caspase 8 [26, 27] were measured in colon cancer cells treated with different marine CE for 24 h. The results showed that CR, PS and NB were able to significantly increase the activity of caspases 3/7 and 8 when compared to control cells (Fig 5). However, the NA extract was not able to induce a noticeable activation of caspases 3/7 and 8.

The PS extract induced the most substantial increase in caspase 3/7 activity compared to the other extracts (Fig 5 A). The PS extract increased caspase 3/7 activity 3.5-fold in HGUE-C-1 cells, 3-fold in HT-29 cells and 2.5-fold in SW-480 cells, all of which were measured at an extract concentration of $10 \mu\text{g/mL}$. NB also significantly increased caspase activation 3-fold compared to the control in HGUE-C-1 cells, and up to 2.3-fold in HT-29 and SW-480 cells. CR was less active than PS and NB; however, a significant 2-fold increase in HGUE-C-1 cells and a 1.6-fold increase in SW-480 cells were observed when cells were treated with $25 \mu\text{g/mL}$ of the extract.

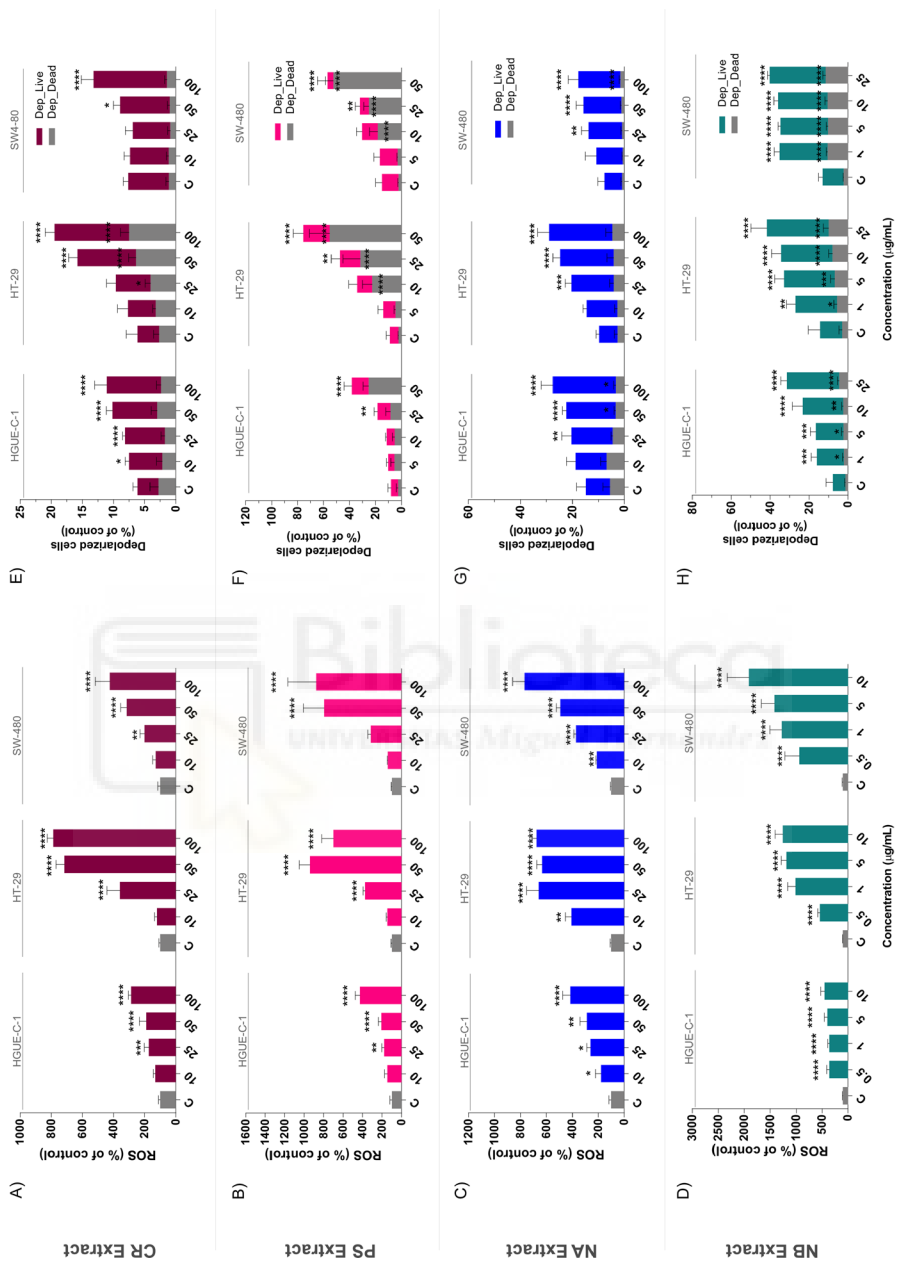


Fig. 4. Marine extracts cause intracellular ROS generation (A-D) and mitochondrial membrane depolarization (E-H) in human colon carcinoma cells. Intracellular ROS levels were assessed by measuring the intensity of dichloro-dihydro-fluorescein diacetate (H₂DCF-DA) fluorescence in HGUE-C-1, HT-29 and SW-480 cells after a 24 h treatment with the CR extract (A), PS extract (B), NA extract (C) and NB extract (D) and compared to untreated cells (Control cells plus dimethyl sulfoxide less than 0.2%, C). For the measurements of depolarized live cells (Dep_Live) and depolarized dead cells (Dep_Dead), cells were treated with different concentrations of marine extracts CR extract (E), PS extract (F), NA extract (G) and NB extract (H) for 24 h and harvested as indicated in the Materials and Methods section. Dep_Live cells and Dep_Dead cells were measured using the Muse® MitoPotential Assay Kit (Merck Millipore) according to the manufacturer's instructions. The results are presented as the percentages (means \pm SD) from three independent experiments. p-values were calculated and compared to the same untreated cell line using ANOVAs. *p -value < 0.05, ** p-value < 0.01, *** p-value < 0.001 and **** p-value < 0.0001.

Among all the marine extracts used, the NB extract exhibited the greatest ability to activate caspase 8, although CR and PS also activated this enzyme. NB increased caspase 8 activity by approximately 1.6-fold in HGUE-C1 cells compared to the control, approximately 2-fold in HT-29 cells and 1.7-fold in SW-480 cells. PS increased caspase 8 activation by 1.5-fold in HGUE-C-1 cells, 1.8-fold in HT-29 cells and 1.4-fold in SW-480 cells. CR again showed the weakest activation capacity, increasing caspase 9 activation by approximately 1.2-fold in all three cancer cell models (Fig 5 B). Finally, similar to the activation of caspases 3/7, the NA extract had no effect caspase 8 activity.

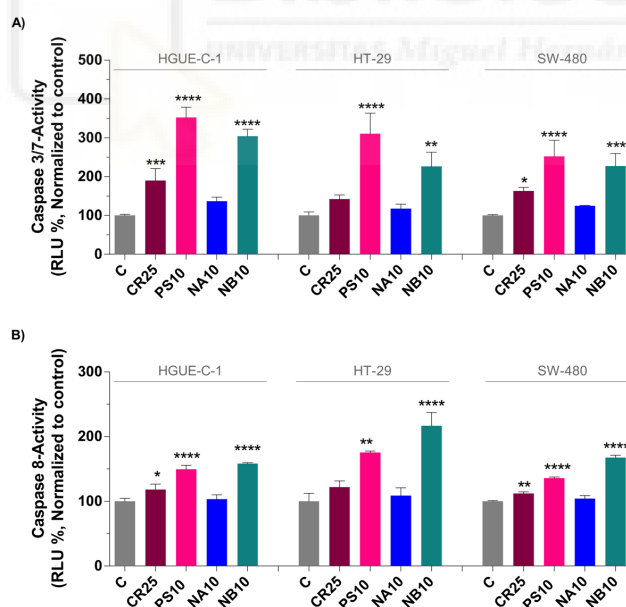


Fig. 5. Induction of apoptosis in colon cancer cells by CR, PS, NA and NB marine extracts via the activation of caspases. The activities of caspases 3/7 and 8 in colon cancer cells were determined using Caspase-Glo 3/7 (A) and Caspase-Glo 8 (B) assays after treatment with the marine extracts for 24 h. The results were compared to untreated cells (Control cells plus dimethyl sulfoxide less

than 0.2 %, C) and presented as the percentages (means \pm SD) from three independent experiments. p-values were calculated and compared to the same untreated cell line using ANOVAs. *p-value< 0.05, ** p-value< 0.01, *** p-value< 0.001 and **** p-value< 0.0001.

2.6. DNA Damage

A ROS imbalance triggers and alters a large variety of intracellular processes related to cell stress and the metabolic response, such as the MMP, mitochondrial function, endoplasmic reticulum stress and the unfolded protein response, or histone H2A.X activation and DNA damage. The putative activation of histone H2A.X by the marine extracts was assessed to investigate their effects on DNA damage. H2A.X is a histone variant of the H2A protein family that forms the octamer in nucleosomes. Factors that cause DNA double-strand breaks (DSBs) activate ataxia telangiectasia mutated (ATM) kinase through phosphorylation. Activated ATM is one of the mediators of histone H2A.X phosphorylation on Ser139, leading to the formation of γ -H2AX that is recruited to DSBs and initiates local DNA repair [28].

Treatments with marine extracts produced high levels of the active form γ -H2AX in most cases (Fig 6), suggesting that the increase in ROS levels described above may be related to this response by inducing significant DNA damage. Among the four marine extracts, NB promoted a substantial increase in H2A.X activation both at the lowest (1 μ g/mL) and highest concentrations (10 μ g/mL) tested, indicating extensive DNA damage. At 10 μ g/mL, NB increased the level of γ -H2AX from $5.5 \pm 0.8\%$ in control cells to $39.0 \pm 2.9\%$ in HGUE-C-1 cells, from $8.6 \pm 2.2\%$ to $56.1 \pm 2.3\%$ in HT-29 cells and from $6.9 \pm 1.1\%$ to $47.9 \pm 2.9\%$ in SW-480 cancer cells.

The CR, PS and NA extracts also significantly increased the phosphorylation of H2A.X at the highest concentrations tested. Treatment with 50 μ g/mL of the CR extract increased H2A.X phosphorylation from $5.5 \pm 0.8\%$ in control cells to $28.9 \pm 2.2\%$ in HGUE-C-1 cells, from $8.6 \pm 2.2\%$ to $25.6 \pm 0.9\%$ in HT-29 cells and from $6.9 \pm 1.1\%$ to $21.3 \pm 0.9\%$ in SW-480 cells. Likewise, 25 μ g/mL PS enhanced H2A.X activation from $5.5 \pm 0.8\%$ in control cells to $18.7 \pm 0.8\%$ in HGUE-C-1 cells, from $8.6 \pm 2.2\%$ to $35.1 \pm 2.4\%$ in HT-20 cells and from $6.9 \pm 1.1\%$ to $40.0 \pm 0.6\%$ in SW-480 cells. Lastly, 50 μ g/mL NA increased γ -H2AX levels from $5.5 \pm 0.8\%$ in control cells to $18.5 \pm 0.9\%$ in HGUE-C-1 cells, from $8.6 \pm 2.2\%$ to $31.5 \pm 2.8\%$ in HT-29 cells and from $6.9 \pm 1.1\%$ to $29.9 \pm 3.0\%$ in SW-480 cells.

2.7. Characterization of marine invertebrate extracts using HPLC-ESI-TOF-MS.

Substantial intraspecies variability in the production of secondary metabolites exists among marine invertebrates, which has not been well-defined [29]. This study is one of the most comprehensive investigations of the characterization of secondary metabolites from different marine sources (two nudibranchs, one holothurian and one a soft coral) using HPLC coupled to mass spectrometry to date.

The extracts of the four selected marine invertebrates were analytically characterized using HPLC-ESI-TOF-MS in both positive and negative modes, as described in the Materials and Methods section. Their base peak chromatograms (BPCs) are depicted in Supplementary Figures 9 and 10, and peaks were identified using the approach described in the Materials and Methods section. This nontargeted approach allowed us to identify 24 compounds in PS, 25 compounds in NA, 31 compounds in NB and 21 compounds in the CR extract. These compounds belonged to different chemical classes, i.e., terpenes, peptides, fatty acids, alkaloids and polyketides, among others and accounted for 98 different metabolites.

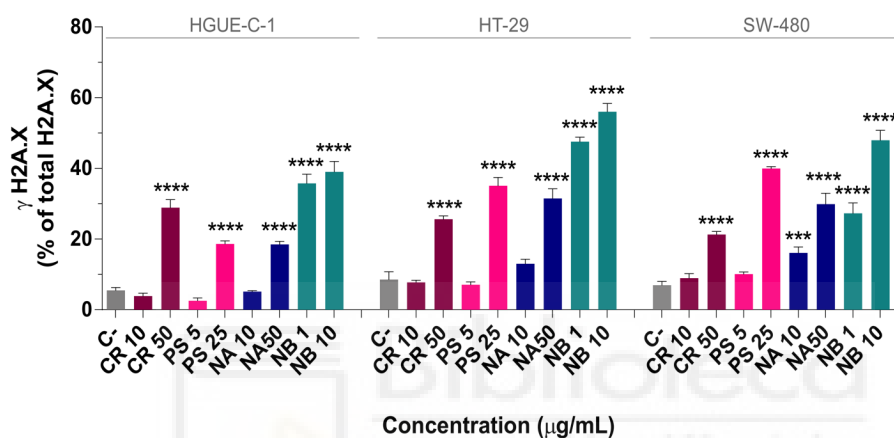


Fig. 6. Marine extracts induce histone H2A.X phosphorylation, an indicator of DNA damage, in colon cancer cells. The extent of DNA damage produced by marine extracts was assessed by measuring the levels of phosphorylated H2A.X histone (γ -H2A.X) (% of γ -H2A.X to total H2A.X) in HGUE-C-1, HT-29 and SW-480 cells after treatment with 10 and 50 μ g/mL CR or NA, 5 and 25 μ g/mL PS, and 1 and 10 μ g/mL NB for 24 h. The results were compared to untreated cells (Control cells plus dimethyl sulfoxide less than 0.2%, C) and presented as the percentages (mean \pm SD) from three independent experiments. p-values were calculated and compared to the same untreated cell line using ANOVAs. *p-value < 0.05, ** p-value < 0.01, *** p-value < 0.001 and **** p-value < 0.0001.

Tables 3, 4, 5 and 6 show the retention time (RT), experimental m/z of both negative ($[M-H]^-$) and positive ($[M-H]^+$) molecular ions, molecular formula, mass error, normalized area and the proposed identification of each compound. Compounds were numbered according to their elution order. Compounds reported for the first time in any marine organism investigated in the present study are marked with an asterisk (*). These tables also include the bibliographic references reporting the antiproliferative or anticancer activities of these compounds. Further data used for peak identification are extensively described in the Supplementary Information and commented in the Discussion section.

Table 3. HPLC-ESI-TOF-MS data of the compounds identified in CR extracts in negative and positive ionization mode. BPC is showed in Supplementary Figure 9A and 10A.

Peak	RT	m/z experimental	Molecular formula (M-H)	m/z calculated	error (ppm)	mSigma	Identified compound	Area ^a	Identification references	Antiproliferative activity
1	17.1	171.1017	C ₉ H ₁₅ O ₃	171.1027	5.4	29.2	Octenoic acid, -hydroxy-, methyl ester isomer 1*	0.16	[30]	
2	19.12	171.1017	C ₉ H ₁₅ O ₃	171.1027	5.4	25.5	Octenoic acid, -hydroxy-, methyl ester isomer 2*	0.08	[30]	
3	25.43	449.1448	C ₂₇ H ₂₅ O ₁₀	449.1453	1.3	32.9	Asebotin isomer 1*	0.11	[31]	[32]
4	25.66	153.1277	C ₁₀ H ₁₇ O	153.1285	4.9	62.5	Terpineol*	0.12	[33]	[34]
5	26.13	449.1457	C ₂₇ H ₂₅ O ₁₀	449.1453	-0.8	36.9	Asebotin isomer 2*	0.19	[31]	[32]
6	26.65	353.2311	C ₃₀ H ₄₃ O ₅	353.2333	6.3	29.3	Simulariaoid D	0.05	[35]	[35]
7	26.7	363.2502	C ₁₈ H ₃₁ N ₆ O ₂	363.2514	3.4	64.3	Sch 575948*	0.04	[36]	
8	28.36	439.3304	C ₃₂ H ₄₅ O ₄	439.3323	3.8	39.9	Actinoranone*	0.36	[37]	[37]
9	29.61	255.1588	C ₁₄ H ₂₃ O ₄	255.1602	5.4	87.2	Oxalic acid, allyl nonyl ester*	0.77	[38]	[38]
10	29.66	265.1461	C ₁₅ H ₂₁ O ₄	265.1445	-5.7	24.8	Dendronephthol C	1.73	[39]	[39]
11	33.43	429.2977	C ₂₇ H ₄₁ O ₄	429.3010	7.7	6.5	Deoxoscalarin*	1.65	[41]	[40]
12	36.18	303.2354	C ₂₀ H ₃₁ O ₂	303.2330	-7.9	35.8	spongian-16-one*	15.00	[43, 44]	[42]
13	37.02	283.2620	C ₁₈ H ₃₅ O ₂	283.2643	8.5	11.7	Stearic acid	3.45	[43, 44]	[45]
14	37.18	267.2312	C ₁₇ H ₃₁ O ₂	267.2330	6.7	3.1	Heptadecenoic acid	6.46	[43, 44]	[46]
15	37.7	327.2897	C ₂₀ H ₃₉ O ₃	327.2905	2.4	13	2-Hydroxyheicosanoic acid	4.59	[43, 44]	[47]
16	37.84	255.2317	C ₁₆ H ₃₁ O ₂	255.2330	5.3	11.7	Hexadecanoic acid	5.62	[43, 44]	[48]
17	38.05	281.2462	C ₁₈ H ₃₃ O ₂	281.2486	8.5	30.8	9-Octadecenoic acid	2.75	[43, 44]	[48, 49]
18	38.42	357.2772	C ₂₄ H ₃₇ O ₂	357.2799	7.6	8.3	Tetracosapentaenoic acid	6.54	[43, 44]	

Cont.

Peak	RT	m/z experimental	Molecular formula (M+H)	m/z calculated	error (ppm)	mSigma	Identified compound	Area ^a	Identification references	Antiproliferative activity
1	3.6	259.1768	C ₁₅ H ₂₄ NaO ₂	259.1669	-38.5	17.8	Scabralin A	0.50	[50]	[50]
2	8.70	482.3610	C ₂₄ H ₅₃ NO ₆ P	482.3605	-1.1	8.1	1-O-hexadecyl-sn-glycero-3-phosphocholine (lyso-PAF)*	27.74	[51]	[52, 53]
3	11.43	462.3596	C ₂₈ H ₄₈ NO ₄	462.3578	-3.9	23.4	Punicinol D*	2.35	[54]	[54]

^a RT: retention time (minutes). ^b Normalized area (%); *Described for the first time in a *soft coral*

Biblioteca
UNIVERSITAS Miguel Hernández

Table 4. HPLC-ESI-TOF-MS data of the compounds identified in PS extracts in negative and positive ionization mode. BPC is showed in Supplementary Figure 9B and 10B

Peak	RT	m/z experimental	Molecular formula (M+H)	m/z calculated	error (ppm)	mSigma	Identified compound	Area ^a	Identification references	Antiproliferative activity
1	9.81	280.1221	C ₁₅ H ₁₄ N ₃ O	280.1204	6.1	42.9	N-[(2E)-3-(2-Amino-1H-imidazo[5-y]-2-propen-1-yl)-1H-indole-2-carboxamide*	0.11	[55]	[55]
2	14.36	262.1113	C ₁₅ H ₁₂ N ₅	262.1098	-5.8	37.5	Acanthomine A isomer 1*	0.56	[56]	[57]
3	16.1	262.1105	C ₁₅ H ₁₂ N ₅	262.1098	-2.5	187.6	Acanthomine A isomer 2*	0.15	[58, 59]	[60]
4	22.36	651.2298	C ₃₁ H ₃₉ O ₁₅	651.2294	0.3	19	Juncenolide D*	0.61	[61]	
5	23.09	290.1416	C ₁₆ H ₂₀ NO ₄	290.1398	-6.3	19.8	Isopropyl-6-(4-methoxybenzyl)-4-methylmorpholine-2,5-dione*	0.13	[62]	
6	23.43	383.2072	C ₃₀ H ₃₁ O ₇	383.2075	0.8	24.4	Acetyl-methoxydeacetyl dihydrobotrydial isomer 1*	0.04	[62]	
7	23.84	383.2076	C ₃₀ H ₃₁ O ₇	383.2075	-0.1	20.2	Acetyl-methoxydeacetyl dihydrobotrydial isomer 2*	0.04	[63, 64]	[65, 66]
8	23.84	353.1972	C ₁₉ H ₂₉ O ₆	353.1970	-0.7	25.5	Gracilioether A*	0.04	[62]	
9	24.14	383.2067	C ₃₀ H ₃₁ O ₇	383.2075	2.2	35.7	Acetyl-methoxydeacetyl dihydrobotrydial isomer 3*	0.05		
10	25.4	455.1522	C ₂₆ H ₂₇ N ₄ O ₂ S	445.1547	5.6	50.1	Unknown	14.16	[58, 59]	[67, 68]
11	25.72	445.1491	C ₂₃ H ₂₅ O ₉	445.1504	3	24	Lopholide*	8.67	[69]	[69]
12	26.19	621.2349	C ₃₅ H ₃₃ N ₄ O ₇	621.2355	1	54.3	Eictenascidin analog*	5.59		
13	26.4	643.2497	C ₂₅ H ₃₉ N ₈ O ₁₀ S	643.2515	2.8	27.1	Unknown	26.67	[70]	[71, 72]

Cont.

14	34.93	301.2162	$C_{20}H_{29}O_2$	301.2173	3.7	1.1	Eicosapentaenoic acid	0.76	[70]	[73]
15	36.2	303.2328	$C_{20}H_{31}O_2$	303.2330	0.4	6.6	Arachidonic acid	1.13	[70]	[73]
16	37.04	283.2625	$C_{18}H_{35}O_2$	283.2643	6.2	20.6	Stearic acid	0.82	[70]	[45]
17	37.82	255.2319	$C_{16}H_{31}O_2$	255.2330	4.1	21.8	Hexadecanoic acid*	1.18	[70]	[48]
Peak	RT	m/z experimental	Molecular formula (M+H)	m/z calculated	error (ppm)	mSigma	Identified compound	Area ^a	Identification references	Antiproliferative activity
1	3.96	146.0598	C_9H_8NO	146.0600	1.7	15.3	3-Formylindole*	1.61	[74]	[75]
2	6.61	274.2730	$C_{16}H_{36}NO_2$	274.2741	3.7	8.4	2-Amino-1,3-hexadecanediol*	4.87	[76]	[77]
3	7.20	302.3039	$C_{18}H_{40}NO_2$	302.3054	4.9	11.2	Sphinganine 1*	3	[76]	[79]
4	14.84	597.3906	$C_{40}H_{53}O_4$	597.3938	5.4	29.7	Astaxanthin isomer 1*	0.5	[78]	[79]
5	16.68	597.3905	$C_{40}H_{53}O_4$	597.3938	5.6	27.1	Astaxanthin isomer 2*	0.43	[78]	[79]
6	18.64	565.4002	$C_{40}H_{53}O_2$	565.404	6.7	36.7	Canthaxanthin isomer 1*	0.76	[78]	[80]
7	19.48	565.4040	$C_{40}H_{53}O_2$	565.3999	7.3	12.9	Canthaxanthin isomer 2*	0.42	[78]	[80]

^a RT: retention time (minutes). ^b Normalized area (%); *Described for the first time in a sea holothurian.

Table 5. HPLC–ESI–TOF–MS data of the compounds identified in NA extracts in negative and positive ionization mode. BPC is showed in Supplementary Figure 9C and 10C.

Peak	RT	m/z experimental	Molecular formula (M-H)	m/z calculated	error (ppm)	mSigma	Identified compound	Area ^a	Identification references	Antiproliferative activity
1	8.03	255.0881	C ₁₃ H ₁₅ O ₆	255.0874	-2.8	22.8	Phenyl β-D-galactopyranoside*	0.21	[81]	[81]
2	12.68	241.0710	C ₁₁ H ₁₃ O ₆	241.0718	3.1	14.3	Tetillapyrone*	0.11	[82]	[83]
3	17.12	167.1067	C ₁₀ H ₁₃ O ₂	167.1078	0.5	17.6	Geranic acid*	0.24	[84]	[85]
4	18.04	420.2317	C ₂₅ H ₃₀ N ₃ O ₃	420.2293	-5.9	16.7	Ketopremarinosin A isomer 1*	1.92	[86]	[87]
5	20.43	420.2299	C ₂₅ H ₃₀ N ₃ O ₃	420.2293	-1.5	31.4	Ketopremarinosin A isomer 2*	1.44	[86]	[87]
6	27.19	353.2312	C ₃₀ H ₃₅ O ₃	353.2333	6.2	24	2-Furantridecanoic acid, 2,5-dihydro-2-hydroxy-3,4-dimethyl-5-oxo-, methyl ester*	0.22	[88]	
7	29.51	540.3280	C ₃₂ H ₄₆ NO ₆	540.3331	5.1	37.7	Palmerolide A derivative isomer 1*	1.87	[89, 90]	[89, 90]
8	29.75	619.2882	C ₃₇ H ₅₀ N ₄ O ₅	619.2926	7.1	44	Ethyl pheophorbide A*	5.87	[91]	[92, 93]
9	29.93	540.3295	C ₃₂ H ₄₆ NO ₆	540.3331	6.6	15.3	Palmerolide A derivative isomer 2*	3.93	[89, 90]	[89, 90]
10	30.22	602.3456	C ₃₂ H ₄₆ N ₃ O ₈	602.3487	4.5	37.2	Rhizovarin D*	2.26	[94]	[95]
11	34.95	301.2153	C ₂₀ H ₂₉ O ₂	301.2173	6.6	19.1	Eicosapentanoic acid isomer 1	0.46	[96]	[71, 72]
12	35.13	301.2162	C ₂₀ H ₂₉ O ₂	301.2173	3.5	10.5	Eicosapentanoic acid isomer 2	0.47	[96]	[71, 72]
13	35.6	227.2013	C ₁₄ H ₁₇ O ₂	227.2017	1.5	3.8	Tetradecanoic acid	1.88	[96]	

Cont.

14	36.02	253.2166	$C_{16}H_{29}O_2$	253.2173	2.6	33.4	9-Hexadecenoic acid	0.75	[96]	
15	36.22	303.2329	$C_{20}H_{31}O_2$	303.2330	0.1	14.4	Spongian-16-one	5.00	[96]	[42]
16	36.56	279.2323	$C_{18}H_{31}O_2$	279.2330	2.4	9.1	9,12-Octadecadienoic acid	3.84	[96]	[97]
17	36.74	241.2178	$C_{15}H_{29}O_2$	241.2173	-2.1	4.2	Pentadecanoic acid	5.24	[96]	[98]
18	37.04	283.2637	$C_{18}H_{35}O_2$	283.2643	2	9.6	Stearic acid	6.66	[96]	[45]
19	37.54	255.2319	$C_{16}H_{31}O_2$	255.2330	2.7	1.5	Hexadecanoic acid isomer 1	0.86	[96]	[48]
20	37.64	331.2640	$C_{22}H_{35}O_2$	331.2643	0.9	11.8	Docosatetraenoic acid isomer 1	3.60	[96]	
21	37.73	331.2646	$C_{22}H_{35}O_2$	331.2643	-1.1	5.1	Docosatetraenoic acid isomer 2	2.76	[96]	
22	37.83	255.2346	$C_{16}H_{31}O_2$	255.2330	-6.6	34	Hexadecanoic acid isomer 2	10.37	[96]	[48]
23	38.16	281.2483	$C_{18}H_{33}O_2$	281.2486	1.2	19.5	9-Octadecenoic acid	2.83	[96]	[48, 49]
Peak	RT	m/z experimental	Molecular formula (M+H)	m/z calculated	error (ppm)	mSigma	Identified compound	Area ^a	Identification references	Antiproliferative activity
1	7.21	302.3049	$C_{18}H_{40}NO_2$	302.3054	1.5	3.2	Sphinganine*	1.53	[99]	[75]
2	8.72	482.3604	$C_{24}H_{53}NO_6P$	482.3602	-0.4	31.4	1-O-hexadecyl-sn-glycero-3-phosphocholine (lyso-PAF)*	9.31	[100]	

^a RT: retention time (minutes). ^b Normalized area (%): *Described for the first time in *Phyllidia varicosata* (NA)

Table 6. HPLC-ESI-TOF-MS data of the compounds identified in NB extracts in negative and positive ionization mode. BPC is showed in Supplementary Figure 9D and 10D.

Peak	RT	m/z experimental	Molecular formula (M-H)	m/z calculated	error (ppm)	mSigma	Identified compound	Area ^a	Identification references	Antiproliferative activity
1	6.09	218.0820	C ₁₂ H ₁₂ NO ₃	218.0823	1.2	8.5	2,5-Morpholimedione, 3-methyl-6-(phenylmethyl)-*	0.48	[101]	
2	6.81	275.1408	C ₁₅ H ₁₉ N ₂ O ₃	275.1401	-2.4	15.8	piperazinedione, 3-[(4-hydroxyphenyl)methyl]-6-(2-methylpropyl)-*	0.32	[102]	[103]
3	8.01	255.0894	C ₁₂ H ₁₅ O ₆	255.0874	-7.9	13.3	Phenyl β-D-galactopyranoside*	0.10	[81]	
4	13.88	454.1905	C ₂₂ H ₃₂ NO ₇ S	454.1905	-0.1	23.5	Latrunculol A isomer 1*	0.55	[104]	[104]
5	14.87	438.1954	C ₂₀ H ₂₄ N ₅ O ₂	438.1935	-4.1	18.9	Indole, 3-[[3-[5-[4-(4-methyl-1-piperazinyl)phenyl]-2-furanyl]-1,2,4-oxadiazol-5-yl]methyl]-isomer 1	0.58	[105]	
6	15.64	454.1910	C ₂₂ H ₃₂ NO ₇ S	454.1905	3.4	37.7	Latrunculol A isomer 2*	0.15	[104]	[104]
7	15.94	438.1963	C ₂₀ H ₂₄ N ₅ O ₂	438.1935	-6.2	37	Indole, 3-[[3-[5-[4-(4-methyl-1-piperazinyl)phenyl]-2-furanyl]-1,2,4-oxadiazol-5-yl]methyl]-isomer 2*	0.24	[105]	
8	17.73	785.3622	C ₄₀ H ₄₉ N ₈ O ₉	785.3622	0.8	73.7	Kasumigamide	0.20	[106]	[107]

Cont.

9	20.15	352.9135	$C_9H_{11}Br_2N_2O_3$	352.9142	2	359.9	4,5-Dibromo-N-(2,2-dimethoxyethyl)-1H-pyrrole-2-carboxamide*	8.06	[108]	[108]
10	21.64	601.3731	$C_{35}H_{53}O_8$	601.3746	2.6	12.8	Agosterol E3*	0.16	[109]	[109]
11	23.8	417.1562	$C_{22}H_{25}O_8$	417.1555	-1.8	2.4	Unknown	0.11		
12	24.45	480.2132	$C_{23}H_{34}N_3O_6S$	480.2174	8.8	18.1	Carbamic acid, [(1R)-1-[[[(acetylamino)methyl]thio]methyl]-2-[[[(1S)-1-(acetyloxy)methyl]-2-phenylethyl]amino]-2-oxoethyl]methyl-, 1,1-dimethylethyl ester *	0.37	[110]	[110]
13	26.07	599.2904	$C_{34}H_{39}N_4O_6$	599.2862	4.9	5.9	Aplysiotoxin*	1.01	[110]	[111, 112]
14	29.92	540.3353	$C_{32}H_{46}NO_6$	540.3331	-2.1	30.3	Palmerolide A derivative* (7Z,10Z,13Z,16Z,19Z)-N-[2-(3,4-	0.70	[89, 90]	[89, 90]
15	34.08	464.3186	$C_{30}H_{42}NO_3$	464.3170	-3.4	27.9	Dihydroxyphenylethyl]-7,10,13,16,19-docosapentaenamide*	4.79	[113]	[113]
16	34.95	301.2195	$C_{20}H_{29}O_2$	301.2173	-7.4	10.8	Eicosapentanoic acid	2.59	[96]	[71, 72]
17	35.19	277.2195	$C_{18}H_{29}O_2$	277.2173	-8.1	7	Linolenic acid	1.72	[96, 114]	[115]
18	35.32	597.4049	$C_{33}H_{57}O_9$	597.4008	-6.9	23.1	Trofoside A	1.89	[116]	[116]
19	35.6	227.2039	$C_{14}H_{27}O_2$	227.2017	-9.8	22.5	Tetradecanoic acid	0.87	[96, 114]	[116]
20	35.82	327.2340	$C_{22}H_{31}O_2$	327.2330	-3.1	31.3	Docosahecanoic acid	0.43	[96, 114]	[117]
21	35.85	303.2342	$C_{20}H_{31}O_2$	303.2330	-4.1	24.8	Spongian-16-one isomer 1	0.43	[42]	[42]
22	35.97	253.2189	$C_{16}H_{29}O_2$	253.2173	-6.4	12.2	Palmitoleic acid	1.21	[96, 114]	[96, 114]

Cont.

23	36.22	303.2373	$C_{20}H_{31}O_2$	303.2350	-4.5	19.3	Spongian-16-one isomer 2	9.03	[42]	[42]
24	36.56	279.2353	$C_{18}H_{31}O_2$	279.2330	-8.3	1.1	9,12-Octadecadienoic acid	7.03	[96]	[97]
25	37.06	283.2663	$C_{18}H_{35}O_2$	283.2643	-7.3	3.7	Stearic acid	2.73	[96]	[45]
26	37.68	331.2670	$C_{22}H_{35}O_2$	331.2643	-8.2	3.6	Docosatetraenoic acid	5.69	[96]	
27	37.94	255.2350	$C_{16}H_{31}O_2$	255.2330	-8.2	16.5	Hexadecanoic acid	5.04	[96]	[48]
28	38.14	281.2508	$C_{18}H_{33}O_2$	281.2486	-8	9.1	9-Octadecenoic acid	4.77	[96]	[48, 49]
29	38.91	307.2650	$C_{20}H_{35}O_2$	307.2643	-2.3	6.9	Eicosadienoic acid	0.86	[96, 114]	[118]
Peak	RT	m/z experimental	Molecular formula (M+H)	m/z calculated	error (ppm)	mSigma	Identified compound	Area ^a	Identification references	Antiproliferative activity
1	6.89	436.2688	$C_{24}H_{38}NO_6$	436.2694	1.2	4.2	Purpurogummutantin*	3.84	[119]	[119]
2	14.98	535.2694	$C_{33}H_{53}N_4O_3$	535.2704	1.5	2.4	Pyropheophorbide_A*	8.11	[120]	[96]

^a RT: retention time (minutes). ^b Normalized area (%); *Described for the first time in *Dolabella auricularia* (NB)

3. Discussion

Anticancer research and the discovery of new drugs are continuously increasing the therapeutic arsenal available to face oncological challenges. Colorectal cancer is the third most prevalent cancer worldwide, and despite the great advances obtained in both treatment and survival rates, new therapeutic approaches are still needed, particularly for patients with the worst prognosis. Therefore, efforts aiming to identify new anticancer drugs, not only in the context of colorectal cancer but also for other types of cancer, are always worthwhile. Natural compounds have been traditionally used as an almost limitless source of new molecules that have been selected through evolution and, in many cases, have exerted an hermetic effect and multitarget activity in humans [122]. Among natural compounds, products from marine organisms have emerged more recently [10]. Marine organisms survive in a harsh microenvironmental ecosystem, leading to the generation of a sophisticated arsenal of metabolites with greater chemical novelty and diversity than terrestrial metabolites [10]. Thus, marine organisms, particularly marine invertebrates, are an excellent resource for the discovery of anticancer compounds [10, 123].

Among the 20 marine invertebrates screened in the present study for their antiproliferative activities toward cells in a panel of human colon cancer cell lines (Table 1, Supplementary Tables 2 and 3 and Supplementary Figure 1), four extracts from *Carotalcyon* sp. (CR, soft coral), *Pseudocolochirus violaceus* (PS, holothurian), *Phyllidia varicosa* (NA) and *Dolabella auricularia* (NB) both of which are nudibranchs, were selected by their strong antiproliferative effect.

The four selected extracts decreased cell viability at fairly low doses, in contrast to some previous reports [124, 125]. This antiproliferative effect was observed very soon after cells were treated (particularly with PS and NB extracts), as evidenced by the morphological alterations such as cell shrinkage, membrane blebbing and rounded or detached cells, which was observed via a Cell Imaging Multi-Mode Reader. The antiproliferative potential of the CR, PS, NA and NB extracts was further confirmed by their abilities to decrease the number of viable cells, and the cell proliferation rate was monitored via real time cell analysis to evaluate the inhibition of the capacity of the colon cancer cells to generate new colonies in the clonogenic assay (Fig 1).

The present study revealed a potent induction of G2/M arrest together with a concomitant decrease in the proportion of cells in the S phase by the extracts in a dose-dependent manner. One of the factors that could be contributing to the cell cycle arrest of colon cancer cells in the G2/M phase is the phosphorylation of H2A.X that was observed in cells from all cell lines treated with any of the extracts (NB in particular); H2A.X phosphorylation indicates the presence of DSBs and DNA damage (Fig 6). Cell cycle checkpoints are essential to maintain the genomic integrity of proliferating cells. After DNA damage, cells must detect and repair the damage and either transiently block cell cycle progression to allow time for repair or exit the cell cycle. The reversion of a DNA-damage-induced checkpoint requires the repair of these lesions, the prevention of a permanent exit from the cell cycle and the termination of checkpoint

signaling to allow the cell cycle to resume. The severity of the arrest and its reversal depend on the extent of the damage and the cellular repair capacity [126]. Our results show that the NB extract induced particularly extensive DNA damage (although the CR, PS and NA extracts also induced significant damage at high concentrations). This finding might explain the substantial increase in the percentage of cells in the G2/M phase, particularly after treatment with NA, NB and, to a lesser extent, CR. The arrested cells subsequently underwent early apoptosis and probably senescence due to their inability to properly repair the DNA (Fig 2). Compounds that inhibit the abnormal growth of cancer cells by inhibiting the DNA repair process or function as anti-microtubule agents are useful cancer treatments [127, 128]. Many compounds isolated from marine sponges, soblidotin and spongistatins, exhibit potent cytotoxic activities toward several cancer cell lines associated with their abilities to disturb microtubule homeostasis and to evade the DNA repair system [129-131].

ROS are pleiotropic and highly reactive molecules that are derived from incomplete oxidative phosphorylation during catabolism but are also produced by exogenous factors such as drugs, UV radiation and pollutants. The equilibrium of intracellular ROS levels plays an important role in regulating normal physiological cell functions, such as the cell cycle, proliferation, differentiation, migration and the activation of different cellular signaling pathways. When the ROS equilibrium is perturbed, these powerful molecules cause severe damage to macromolecules, leading to cell death [132, 133].

Interestingly, the four marine extracts selected in the present study induced intracellular ROS production (Fig 4 A - D) concomitant with cell cycle arrest and DNA damage accumulation. We postulate that this massive ROS accumulation may be responsible for the generation of DNA double-strand breaks and the subsequent activation of the DNA repair machinery, resulting in cell cycle arrest. In most cases, cell repair mechanisms are not sufficient and the cell cycle does not resume, which leads the cell to undergo senescence and cell death. The key factors and events that regulate the cellular decision to activate a specific cell death mechanism remain unknown and require further research.

As mentioned above, the NB, NA and CR extracts significantly increased the percentages of early apoptotic and depolarized live cells, which were strongly correlated with membrane blebbing, cellular shrinkage, pyknosis, caspase activation and DNA fragmentation that are typical features of an apoptotic cell death process (Fig 2, 3 and 5) [134]. This process was substantially accelerated in HGUE-C-1 cells, which are derived from a primary culture of colorectal adenocarcinoma cells and express wild-type p53, in contrast to the other two cell lines, which express the mutant p53 protein. This difference may explain why these cells exhibited higher apoptosis rates in the cell cycle analysis after treatment with the extracts (Fig 3), similar to the effects of other natural extracts [135]. In contrast, the PS extract showed a less prominent arrest in the G2/M phase and substantial increases in the proportions of late apoptotic and depolarized dead cells (Figs. 2 and 4). In addition, PS rapidly induced membrane permeabilization (PI/Hoechst staining) and LDH release, which are typical features of

the necrosis pathway, in which membrane rupture and rapid lysis of cells and organelles occurs (Fig. 3) [136].

In the present study, the different marine extracts appeared to induce cell death through different and complex mechanisms that may overlap to some extent. Our results show increased activation of caspase 3/7 and 8 cleavage activity by all extracts except NA. The maximum activation of caspase 3/7 was observed in cells treated with the PS and NB extracts, and the maximum activation of caspase 8 was observed in cells treated with the NB extract. The extrinsic apoptosis signaling pathway is usually activated by the binding of cell death ligands and results in caspase 8-mediated cell death with the subsequent activation of caspases 3/7. In contrast, the intrinsic pathway (mitochondrial or BCL-2-regulated pathway) is activated by cellular stress and chemotherapeutics and includes proapoptotic BCL-2 family protein activation, Cyt C release and the subsequent activation of caspases 3/7.

Because PS, which appeared to promote necrosis as the predominant death mechanism, as determined by LDH activity and fluorescence microscopy, also activated caspase 8 and caspases 3/7, we propose that the main cell death mechanism activated by this extract might be the extrinsic pathway. This option would also be compatible with a death mechanism that is less dependent on mitochondrial depolarization and promptly ends into necrosis. Moreover, the increase in caspase activity in necrotic processes has been previously described in other studies [137, 138] and was linked to the presence of ROS, as observed in the present study. Furthermore, at least for the PS extract, our results might indicate the activation of both apoptosis and necrosis to induce cell death; one pathway would predominate, depending on each single case. Since the marine extracts are very complex mixtures, a reasonable hypothesis is that the different compounds present in each extract simultaneously induce different death mechanisms [139]. Furthermore, even when a death mechanism prevails, crosstalk with another cell death mechanism may occur [140, 141].

In addition, cancer cell lines, which are usually fairly resistant to cell death, are highly diverse and heterogeneous and may present substantial alterations in their proliferation pathways and mechanisms that orchestrate cell death. Thus, the typical characteristics of a specific cell death process, such as apoptotic or non-apoptotic cell death, may vary appreciably [142-144]. Moreover, important events related to the control of cell cycle checkpoints or even defective apoptosis may result in cell death mechanisms, as evidenced in programmed cell death. In this context, the mitotic catastrophe (delayed mitosis-linked cell death), which occurs in cells displaying cell cycle arrest and a lack of doubling, shares characteristics with apoptosis and necrosis and manifests features typical of both processes [145]. Taken together, all these results describe a quite complex scenario that must be revisited in future studies.

Current anticancer treatments are accompanied by several undesired consequences, such as toxic effects. Therefore, new anticancer drugs must exert therapeutic effects and induce cell death in a controlled manner [146]. Cytotoxic compounds have been shown to induce cell death via necrosis, autophagy or apoptosis, which is desirable for a new candidate anticancer agent [147].

This study has also elucidated the chemical composition of the CR, PS, NA and NB extracts using HPLC-ESI-TOF-MS and revealed extremely diverse and complex compositions. The chemical characterization revealed a complex variety of metabolites that were mainly classified as terpenes, peptides, fatty acids, alkaloids and polyketides, among others, and 98 compounds were identified. The majority of the identified compounds were previously reported in the marine ecosystem; meanwhile, others were identified in terrestrial habitats. However, some of the compounds identified were found in a marine source for the first time. Some of the compounds identified in these marine extracts have previously been reported to inhibit a few hallmarks of cancer *in vivo* as discussed below.

The antiproliferative activities of up to 75 of the 98 identified compounds have been reported in the literature, accounting for 75.8% of the total identified compounds. Nevertheless, the semiquantitative analysis (as determined by the larger normalized area percentage) of the compounds contained in the marine extracts utilized reveals that the observed antiproliferative effects might be associated to particular families of compounds (Tables 3 – 6). For instance, main candidates to account for the antiproliferative effects in CR extract might be diterpenes such as spongian-16-one [42], polyoxygenated marine steroids such as punicinol D [54], or the sesquiterpene dendronephthol C [39] or the sesterterpene deoxoscalarin [40]. In PS extract, the furanocembranolide lopholide [67, 68] seem to be the most abundant compounds with reported antiproliferative capacity in cancer cells. Antibiotic TAN 547D is an antibiotic obtained from a microorganism [148], but its mechanism of action and antiproliferative activity toward cancer cells remain unknown.

Major compounds in the NA extract were long fatty acids and lyso-PAF, but other compounds with previously reported antiproliferative activity, such as the diterpene spongian-16-one [42], the chlorophyll ethyl pheophorbide A [92, 93], palmerolide A (a macrocyclic polyketide) [89, 90] and rhizovarin D (an indole diterpene) [95] were present in large amounts. Finally, the most abundant compounds in the NB extract were once again spongian-16-one and a porphyrin derivative, pyropheophorbide A, both of which have been reported to possess antiproliferative activity [42, 92, 93]. Moreover, purpurogemutantin (drimenyl cyclohexenone derivative) [119], trofoside A (polar steroids) [116] and aplysioviolin (a tetrapyrrolic chemodeterrent ink) [111, 112] were also fairly abundant in this extract. In any case, studies focused on the fractionation of these extracts may deserve further attention to identify the most active compounds/fractions to be utilized in animal trials.

In conclusion, the four invertebrate marine extracts selected and studied in this investigation may become suitable agents for the further development of anticancer agents against colorectal cancer. All the extracts studied here showed a strong antiproliferative capacity and induced G2/M cell cycle arrest that evolved to early apoptosis in the case of the CR, NA and NB extracts. However, PS exerted its antiproliferative effects by inducing necrosis cell death or a combination of necrosis and the extrinsic apoptotic pathway. We propose that intracellular ROS accumulation triggered by the extracts may be responsible for the subsequent DNA damage,

mitochondrial depolarization and cell cycle arrest, which ultimately induce cell death either by an apoptotic or necrotic mechanism, depending on the extract (Fig 7). Further studies focused on the extracts fractionation and isolation of the compounds responsible for the observed effects and obtaining additional information about the putative molecular mechanism may provide new insights into the development of new drug treatments for colon cancer.

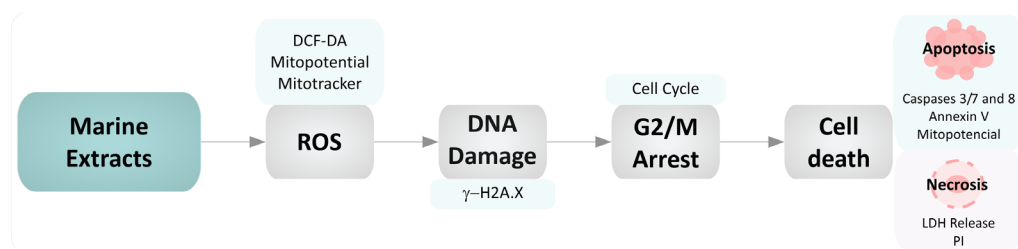


Fig. 7. Model depicting the putative mechanisms of action of invertebrate marine extracts in colon cancer cell models. Marine extracts trigger the intracellular accumulation of ROS that lead to a decreased MMP and mitochondria depolarization. Due to the presence of ROS, H2A.X is phosphorylated as a warning signal for DNA damage, leading to subsequent G2/M arrest. Afterwards, if metabolic stress exceeds the cell stress response, cells undergo either apoptotic or necrotic cell death, depending on the type of marine extract and the extent of damage.

4. Materials and Methods

4.1. Chemicals and Reagents

Organic solvents including dichloromethane, methanol, n-butanol, ethyl acetate, n-hexane were the reagents used for extracting the bioactive compounds from marine organisms, and HPLC-grade acetonitrile, acetic acid and dimethyl sulphoxide (DMSO) were purchased from Sigma-Aldrich (Europe). Water was purified using a Milli-Q system (Millipore, Bedford, MA, USA). Labels and reagents such as Thiazolyl Blue Tetrazolium Bromide (MTT), Hoechst 33342 propidium iodide (PI), 2',7'-Dichlorodihydrofluorescein diacetate (H₂DCF-DA) were purchased from Sigma-Aldrich (Europe).

4.2. Marine invertebrate material

Marine invertebrates were selected based on observations of inter and intra-specific competition in experimental aquariums and searches on bibliographic bases [149]. They were obtained from the distributor company of marine species TODO PEZ S.L. (Alicante, Spain). 20 species of marine invertebrates were chosen for their potential as producers of compounds with anticancer activity. The selected species were composed of 12 soft corals, 4 hard corals, 2 nudibranchs, 1 anemone and 1 holothurian. For more details see Table 1.

4.3. Extraction Method and Preparation of crude extracts

The freshly marine invertebrates were set free of any debris, cut into small pieces and weighted. The mass was macerated with dichloromethane:methanol (D:M) (1:1, v:v) at 4 °C for 24 h. After maceration, the solution was filtered and evaporated to dryness on a rotatory vacuum evaporator. The extracts were dried by speed vac, weighted and stored at -80 °C until used. The yield of solid extraction ranged from 1 to 11%, depending of the type of organism (Supplementary Table 1). For *in vitro* culture, extracts were dissolved in DMSO (50 mg/mL) and further diluted in culture medium yielding a final testing concentration of 100 µg/mL with a final DMSO concentration of 0.2%. This concentration of DMSO did not affect cell viability. This methodology was extracted from [150].

4.4. Cell culture

The human colorectal carcinoma cell lines HT-29 and SW-480 were purchase from the American Type Culture Collection (ATCC, MN, USA) and HGUE-C-1 (an established cell line from primary human colon carcinoma) provided by Dr. Miguel Saceda (Hospital General Universitario de Elche, Spain). In colorectal cancer disease

there are heterogeneous markers which have important implications for prognosis and clinical treatments. Some of the widely studied markers are the microsatellite instability (MSI), which supposes genetic hypermutability that results from impaired DNA mismatch repair in repetitive DNA sequences called microsatellites, and somatic mutations in BRAF and KRAS that represent a potential molecular marker for the risk of developing advanced neoplasia [151]. The cell lines used were chosen because of their capability to present some of these markers. The cell line HGUE-C-1 was produced by a primary culture in 2003, derived from ascitic effusion of a 76-year-old patient with colon cancer at the University General Hospital of Elche. This line supposes an interesting model for the study of chemoresistance due to is characterized by presenting resistance *in vivo* to the drugs 5-fluorouracil and Irinotecan. HGUE-C-1 is stable for microsatellite (MS) phenotype and showed wild type to KRAS and BRAF mutations [152]. HT-29, is an established cell line isolated from a primary tumor in 1964 from a 44-year-old caucasian female. HT-29 showed a phenotype of human colon adenocarcinoma moderately differentiated to grade II. This line presents epithelial morphology, is stable for MS, presents a wild type phenotype to KRAS and is mutated in BRAF (V600E) [153]. The SW480 cell line was isolated from a primary colon tumor of a 50-year-old Caucasian man. It presents epithelial morphology and mutation in the oncogene KRAS (G12V), is wild type to BRAF and is stable for MS [154].

All cell lines were maintained in Dulbecco's modified Eagle's medium (DMEM), supplemented with a 10% heat inactivated fetal bovine serum (FBS), 100 U/mL penicillin and 100 g/mL streptomycin. Cells were incubated at 37 °C in a humidified atmosphere containing 5%/95% of CO₂/air. Cells were trypsinized with 0.05 X trypsin/ethylene diamine tetra-acetic acid every three days according to the manufacturer's instructions. Cell culture reagents were purchased from Invitrogen Life Technologies (Carlsbad, CA, USA).

4.5. MTT Cell Viability Assay and IC₅₀ determination

HGUE-C-1, HT-29 and SW-480 cells were plated in 96-multiwell culture plates at a density of 5×10^3 cells/well. After 24, 48 and 72 h incubation with the crude extracts, MTT was added at a final concentration of 0.5 mg/mL and incubated for 3 h. Then, the medium was removed, and the formazan crystals were dissolved in DMSO. Absorbance was measured at 570 nm in a microplate reader (SPECTROstar Omega, BMG Labtech, Germany). The IC₅₀ values were determined using GraphPad Prism v5.0 software (GraphPad Software, La Jolla, CA, USA). The results are expressed as the percentage of cell viability/proliferation relative to the same untreated cell line (Control cells plus dimethyl sulfoxide at 0.2%, C).

4.6. RTCA Proliferation assay

The proliferation rate was monitored in real-time using the xCELLigence system E-Plate Real Time Cell Analyzer (RTCA) (Roche Diagnostics GmbH, Germany). This system collects impedance values of each well and translate to a cell index value (CI). Colon cancer cells were seeded at a density from 7.5×10^3 to 2.0×10^4 cells/well depending on the cell line, adjusted for after 24 h after the seed, the CI was near 1 as manufacturer's recommendations. HGUE-C-1, HT-29 and SW-480 cells were treated with marine extracts at 10, 25, 50 and 100 $\mu\text{g/mL}$ and CI was automatically monitored for duration of 75 h, which produced a kinetic curve. Data for cell proliferation was normalized at CI from 24 h (when the treatment was added).

4.7. Clonogenic assay

Colon cancer cells (HGUE-C-1, HT-29 and SW-480) were seeded in 6-well plates at a density of 5×10^3 cells per well and treated the day after with different concentrations of marine extracts (CR, PS, NA and NB) for a period of 24 h. After removing the treatment, fresh media was added and cells were kept in the tissue culture incubator for an additional 6 days without disturbance to allow colony formation (capacity of cells to produce progeny from a single cell to form a colony). Cell nucleus were stained with Hoechst 33342 and fixed with 70% ethanol for 5 minutes for determination of number and diameter of colonies by the Cell Imaging Multi-Mode Reader Cytation 3 (BioTek, Germany). Then cells were stained with 0.05% crystal violet for 10 minutes to take photos of plates.

4.8. Cell Cycle Analysis

1.5×10^5 cells per well were seeded into 6-well plates and treated with marine extracts at different concentrations for 24 h and then harvested and washed with phosphate buffered saline (PBS) 1X. The washed cells were fixed with 70% ethanol. The different stages of the cell cycle were determined based on differential DNA content using propidium iodide (PI) which is a nuclear DNA intercalating stain. This measure was made according to the manufacturer's instruction by the Muse® Cell Analyzer (Merck KGaA, Darmstadt, Germany).

4.9. Measurement of Apoptosis by Annexin V and Mitopotential

1.5×10^5 cells per well were seeded into 6-well plates and treated with marine extracts at different concentrations for 24 h and then harvested and washed with PBS 1X. The apoptosis was determined by using The Muse® Annexin V and Dead Cell kit based on the detection of phosphatidylserine (PS) on the surface of apoptotic cells, using the fluorescent label Annexin V.

Mitopotential assay utilizes the MitoPotential Dye (a cationic and lipophilic dye) to detect changes in the mitochondrial membrane potential (MMP) and is combined with 7-AAD as an indicator of cell death. Changes in MMP is a hallmark of permeabilization of cellular plasma membrane and the apoptotic process. The measure was made according to the manufacturer's instruction by the Muse® Cell Analyzer (Merck KGaA, Darmstadt, Germany).

4.10. *Caspase 3/7 and 8 activation*

For caspase 3/7 and 8 activity determination, HGUE-C-1, HT-29 and SW480 cells were seeded (2×10^5 cells) into a 6 well plate. After 24 h of incubation with marine extracts at different concentrations, cells were lysed with cell lysis buffer and the amount of protein were determined by BCA Pierce Method. Caspase-3 and 7 and Caspase-8 were measured using a Caspase-Glo 3/7 and Caspase-Glo 8 assay kit (both from Promega, Madison, WI, USA) following the manufacturer's instruction. Total cell lysates containing equal amounts of proteins were gently mixed with Caspase-Glo 3/7 and 8 kit (ratio 1:1) and incubated for 30 – 40 min at room temperature in the dark. Luminiscence was measured using the Cell Imaging Multi-Mode Reader Cytation (BioTek Instruments, Inc., USA).

4.11. *Lactate Dehydrogenase (LDH) measurement for necrosis assay*

LDH cytotoxicity assay kit (Roche Diagnostics, Mannheim, Germany) was employed to assess the cellular toxicity induced by compounds as a measure of permeabilization of plasma membrane like a key signature for necrotic process [155]. The measurement is based on the reduction of nicotinamide adenine dinucleotide (NADH) by LDH in the oxidation of lactate to pyruvate process, transforming the tetrazolium salt to a coloured formazan product. The amount of formazan product is determined by spectrophotometry and it is proportionally to LDH activity. HT-29, SW-480 and HGUE-C-1 cancer cells were treated with different concentrations of CR, PS, NA and NB extract for 24 h, then the supernatant was used to assay LDH activity, according to the manufacturer's instruction (Roche Diagnostic Systems, Montclair, NJ, USA). The concentration of LDH was measured with a microplate reader (SPECTROstar Omega, BMG Labtech, Germany) at wavelength of 490 nm.

4.12. *Nuclear staining with Hoechst 33342/Propidium iodide*

Colon cancer cells (5×10^5 /well) were seeded into 96-well plates treated with different concentrations of marine extracts (CR, PS, NA and NB) for a period of 24 h. Cells were washed and incubated with Hoechst 33342 at 5 µg/mL and propidium iodide (PI) at 50 µg/mL for 15 minutes at 37 °C, then were washed once in PBS (1X). Fluorescence intensity was measured and cells were photographed using a Cell Imaging Multi-Mode

Reader Cytation (BioTek Instruments, Inc., USA) equipped with 40 X objective and fluorescent cubes (DAPI $\lambda=377-447$ and TEXAS $\lambda=586-647$). Results presented are means \pm S.D. of three independent experiments.

4.13. *Mitochondrial Membrane Potential (MMP)*

Cells were seeded (5×10^5 /well) into 96-well plates and exposed with different concentrations of marine extracts. After treatment cells were washed twice in PBS 1X and incubated with 0.5 $\mu\text{g/ml}$ MitoTracker CMXRos and 15 ng/ml MitoTracker Green (Molecular Probes) at 37 °C for 45 min. Cells were then washed twice in PBS (1X) and analyzed by the fluorescent wavelength value using the Cell Imaging Multi-Mode Reader Cytation (BioTek Instruments, Inc., USA). Cells were photographed using a Cell Imaging Multi-Mode Reader Cytation (BioTek Instruments, Inc., USA) equipped with 20 X objective and fluorescent cubes (GFP $\lambda=469-525$ and TEXAS $\lambda=586-647$). Results presented are means \pm S.D. of three independent experiments.

4.14. *Detection of Reactive Oxygen Species (ROS)*

Cells were seeded (5×10^5 /well) into 96-well plates and treated with different concentrations of marine extracts. The intracellular generation of ROS was measured using 2',7'-Dichlorodihydrofluorescein diacetate (H₂DCF-DA, Sigma-Aldrich) (10 μM) and was compared with cell viability using DNA staining Hoechst 33342 (Sigma-Aldrich) (10 $\mu\text{g/mL}$). After treatment with marine extracts for 24 h cells were incubated with labels for 30 min in the cell incubator. The levels of intracellular ROS and nucleus number was determined by the fluorescent wavelength value using the Cell Imaging Multi-Mode Reader Cytation (BioTek Instruments, Inc., USA).

4.15. *Detection of phosphorylated H2A.X*

Cells were seeded at 1.5×10^5 cells per well into 6-well plates and treated with CR, PS, NA and NB at different concentrations for 24 h and then harvested and washed with PBS 1X. DNA damage was measured using at the same time a phospho-specific anti-phospho-Histone H2A.X (Ser139)-Alexa Fluor®555 and an anti-Histone H2A.XPECy5 conjugated antibody to measure total levels of Histone H2A.X according to the manufacturer's instruction by the Muse® Cell Analyzer (Merck KGaA, Darmstadt, Germany).

4.16. *Determination of secondary metabolites by HPLC-ESI-TOF-MS*

Analyses of bioactive compounds of these marine organisms were carried out using Agilent 1200 series rapid resolution liquid chromatograph (Agilent Technologies, CA, USA), which was comprised of a binary pump, degasser, and auto sampler.

Compounds were separated at room temperature using a Poroshell 120 EC-C18 (3.6 x 100 mm, 2.7 mm) analytical column (Agilent Technologies, Palo Alto, CA, USA). The chromatographic separation was carried out following two different methods depending on the ionization mode. The mobile phases consisted of 1% of acetic acid in water (phase A) and acetonitrile (phase B). The flow rate was set at 0.5 mL/min at 25 °C. The spectra in negative ionization mode was acquired over a mass range from m/z 50 to 1000 and the following multi-step linear gradient was employed: 0 min, 5% B; 5 min, 15% B; 20 min, 30% B; 35 min, 95% B; 40 min, 5 % B. In the method carried out in positive ionization mode the mass scan ranged from m/z 50 to 1500 and the conditions of the solvent multi-step linear gradient were the following: 0 min, 10% B; 5 min, 65% B; 15 min, 100% B; 19 min, 100% B.

The HPLC system was coupled to a micrOTOF (Bruker Daltonics, Bremen, Germany), an orthogonal- accelerated TOF mass spectrometer, using an electrospray interface (ESI) (model G1607A from Agilent Technologies, Palo Alto, CA) operating in both, negative and positive-ion modes. The effluent from the HPLC column was splitted using a T-type phase separator before being introduced into the mass spectrometer (split ratio = 1:3). The optimum values for the ESI-MS parameters were as follows: capillary voltage, +4.0 kV; drying gas temperature, 200 °C; drying gas flow, 9.0 L/min; and nebulizing gas pressure, 2.0 bars.

Peak identification was performed by the generation of the candidate formula with a mass accuracy limit of 10 ppm. considering RT, and experimental and theoretical masses. The mass score related to the contribution to mass accuracy, isotope abundance and isotope spacing for the generated molecular formula was set at ≥ 80 . The characterization strategy was based on the interpretation of their mass spectra provided by the TOF-MS and the comparison with previously reported information in the literature for marine invertebrates. For the acquisition of chemical structure information the following databases were consulted: SciFinder Scholar (<http://scifinder.cas.org>), MassBank (<http://massbank.jp>), and METLIN Metabolite Database (<http://metlin.scripps.edu>). Furthermore, a recent published database of marine natural compounds (<http://docking.umh.es/chemlib/mnplib>) has been employed.

4.17. Statistical analysis

Significant differences between the mean of control versus various doses were tested by one-way analysis of variance (ANOVA), followed by Tukey's post hoc test for multiple comparisons using GraphPad Prism 6, Windows 10, CA. Statistically, significant differences were assumed at $p < 0.05$ (* $p < 0.05$, ** $p < 0.01$, *** $p < 0.001$ or **** $p < 0.0001$).

Funding: This research was funded by projects AGL2015-67995-C3-1-R, AGL2015-67995-C3-2-R and AGL2015-67995-C3-3-R from the Spanish Ministry of Economy and Competitiveness (MINECO); Project P11-CTS-7625 from Andalusian Regional Government Council of Innovation and Science; projects PROMETEO/2012/007, PROMETEO/2016/006 and VALi+D fellowship

(ACIF/2015/158) from Generalitat Valenciana to VR-Tand CIBER (CB12/03/30038, Fisiopatología de la Obesidad y la Nutrición, CIBERObn). The author BMG gratefully acknowledges to the National Youth Guarantee System the grant for young research personnel. The funders had no role in study design, data collection and analysis, decision to publish, or preparation of the manuscript.

Acknowledgments: Authors want to thank to Chistian Echevogyen from Todopez S.L. (<http://www.todopez.es>) for his help providing marine specimens and his comments about marine invertebrates. Authors also want to thank to Dr. Miguel Saceda for HGUE-C-1 cells transfer and his invaluable comments about this complex cell line.

Conflicts of Interest: The authors declare no conflict of interest.

References

1. Ferlay, J., et al., Cancer incidence and mortality worldwide: sources, methods and major patterns in GLOBOCAN 2012. *Int J Cancer*, 2015. 136(5): p. E359-86.
2. Di Maio, M., et al., Symptomatic toxicities experienced during anticancer treatment: agreement between patient and physician reporting in three randomized trials. *J Clin Oncol*, 2015. 33(8): p. 910-5.
3. Herranz-López, M., M. Losada-Echeberria, and E. Barrajón-Catalán, The Multitarget Activity of Natural Extracts on Cancer: Synergy and Xenohormesis. *Medicines*, 2018. 6(1): p. 6.
4. Kong, D.X., Y.Y. Jiang, and H.Y. Zhang, Marine natural products as sources of novel scaffolds: achievement and concern, in *Drug Discov Today*. 2010: England. p. 884-6.
5. Newman, D.J. and G.M. Cragg, Natural Products as Sources of New Drugs from 1981 to 2014. *J Nat Prod*, 2016. 79(3): p. 629-61.
6. Pinto, A.S. and Diana, Plant Secondary Metabolites as Anticancer Agents: Successes in Clinical Trials and Therapeutic Application. *International Journal of Molecular Sciences*, 2018. 19(1): p. 263.
7. Nwodo, J.N., et al., Exploring Cancer Therapeutics with Natural Products from African Medicinal Plants, Part II: Alkaloids, Terpenoids and Flavonoids. *Anticancer Agents Med Chem*, 2016. 16(1): p. 108-27.
8. Leal, M.C., et al., Bioprospecting of marine invertebrates for new natural products - a chemical and zoogeographical perspective. *Molecules*, 2012. 17(8): p. 9842-54.
9. Martins, A., et al., Marketed marine natural products in the pharmaceutical and cosmeceutical industries: tips for success. *Mar Drugs*, 2014. 12(2): p. 1066-101.
10. Ruiz-Torres, V., et al., An Updated Review on Marine Anticancer Compounds: The Use of Virtual Screening for the Discovery of Small-Molecule Cancer Drugs. *Molecules*, 2017. 22(7): p. 1037.
11. Hu, Y., et al., Statistical Research on the Bioactivity of New Marine Natural Products Discovered during the 28 Years from 1985 to 2012, in *Mar Drugs*. 2015. p. 202-21.
12. Pawlik, J.R., et al., Chemical warfare on coral reefs: Sponge metabolites differentially affect coral symbiosis in situ. *Limnology and Oceanography*, 2007. 52(2): p. 907-911.
13. Chadwick, N.E. and K.M. Morrow, Competition among sessile organisms on coral reefs, in *Coral Reefs: An Ecosystem in Transition*. 2011. p. 347-371.
14. Ribeiro, F.V., et al., Long-term effects of competition and environmental drivers on the growth of the endangered coral *Mussismilia braziliensis* (Verrill, 1867). *PeerJ*, 2018. 2018(8).

15. Horwitz, R., M.O. Hoogenboom, and M. Fine, Spatial competition dynamics between reef corals under ocean acidification. *Scientific Reports*, 2017. 7: p. 40288.
16. Margulis, L. and M.J. Chapman, Chapter Three - ANIMALIA, in *Kingdoms and Domains*. 2009, Academic Press: London. p. 231-377.
17. Leal, M.C., et al., Trends in the discovery of new marine natural products from invertebrates over the last two decades--where and what are we bioprospecting? *PLoS One*, 2012. 7(1): p. e30580.
18. Limame, R., et al., Comparative analysis of dynamic cell viability, migration and invasion assessments by novel real-time technology and classic endpoint assays. *PLoS One*, 2012. 7(10): p. e46536.
19. Roshan Moniri, M., et al., Dynamic assessment of cell viability, proliferation and migration using real time cell analyzer system (RTCA). *Cytotechnology*, 2015. 67(2): p. 379-86.
20. Pérez-Sánchez, A., et al., Rosemary (*Rosmarinus officinalis*) extract causes ROS-induced necrotic cell death and inhibits tumor growth *in vivo*. *Scientific Reports*, 2018. Accepted, waiting for final publication. DOI 10.1038/s41598-018-37173-7.
21. Demchenko, A.P., Beyond annexin V: fluorescence response of cellular membranes to apoptosis. *Cytotechnology*, 2013. 65(2): p. 157-72.
22. Ravi Hingorani, R.H., Jun Deng, Jeanne Elia, Catherine McIntyre, and Dev Mittar, Detection of Apoptosis Using the BD Annexin V FITC Assay on the BD FACSVerserTM System. 2011: p. https://wwwbdbiosciences.com/documents/BD_FACSVerse_Apoptosis_Detection_AppNote.pdf.
23. Hearps, A.C., et al., Mitochondrial cytochrome c release precedes transmembrane depolarisation and caspase-3 activation during ceramide-induced apoptosis of Jurkat T cells. *Apoptosis*, 2002. 7(5): p. 387-94.
24. Lamkanfi, M., et al., Caspases in cell survival, proliferation and differentiation. *Cell Death Differ*, 2007. 14(1): p. 44-55.
25. Kuranaga, E. and M. Miura, Nonapoptotic functions of caspases: caspases as regulatory molecules for immunity and cell-fate determination. *Trends Cell Biol*, 2007. 17(3): p. 135-44.
26. Lakhani, S.A., et al., Caspases 3 and 7: key mediators of mitochondrial events of apoptosis. *Science*, 2006. 311(5762): p. 847-51.
27. Kumar, S., Mechanisms mediating caspase activation in cell death. *Cell Death Differ*, 1999. 6(11): p. 1060-6.
28. Sedelnikova, O.A., et al., Histone H2AX in DNA damage and repair. *Cancer Biol Ther*, 2003. 2(3): p. 233-5.
29. Gomes, N.G., et al., Marine Invertebrate Metabolites with Anticancer Activities: Solutions to the "Supply Problem". *Mar Drugs*, 2016. 14(5).
30. S. E. Abou-ElWafa, G., et al., ChemInform Abstract: Three New Unsaturated Fatty Acids from the Marine Green Alga *Ulva fasciata* Delile. Vol. 41. 2010.
31. A Hamdy, A.-H., et al., Bioactive Phenolic Compounds from the Egyptian Red Sea Seagrass *Thalassodendron ciliatum*. Vol. 67. 2012. 291-6.
32. Hamdy, A.H., et al., Bioactive phenolic compounds from the Egyptian Red Sea seagrass *Thalassodendron ciliatum*. *Z Naturforsch C*, 2012. 67(5-6): p. 291-6.
33. Vidal, N.P., et al., Farmed and wild sea bass (*Dicentrarchus labrax*) volatile metabolites: a comparative study by SPME-GC/MS. *J Sci Food Agric*, 2016. 96(4): p. 1181-93.

34. Villa-Ruano, N., et al., Volatile Profiling, Insecticidal, Antibacterial and Antiproliferative Properties of the Essential Oils of *Bursera glabrifolia* Leaves. *Chem Biodivers*, 2018. 15(11): p. e1800354.
35. Lei, L.-F., et al., Novel cytotoxic nine-membered macrocyclic polysulfur cembranoid lactones from the soft coral *Sinularia* sp. *Tetrahedron*, 2014. 70(38): p. 6851-6858.
36. Yang, S.-W., et al., A new sterol sulfate, Sch 572423, from a marine sponge, *Topsentia* sp. *Vol. 13*. 2003. 1791-4.
37. Nam, S.J., et al., Actinoranone, a cytotoxic meroterpenoid of unprecedented structure from a marine adapted *Streptomyces* sp. *Org Lett*, 2013. 15(21): p. 5400-3.
38. Selvin, J., et al., Optimization and production of novel antimicrobial agents from sponge associated marine actinomycetes *Nocardiopsis dassonvillei* MAD08. *Appl Microbiol Biotechnol*, 2009. 83(3): p. 435-45.
39. Elkhayat, E., et al., Dendronephthols A–C, new sesquiterpenoids from the Red Sea soft coral *Dendronephthya* sp. *Vol. 70*. 2014. 3822–3825.
40. Elhady, S.S., et al., Antiproliferative Scalarane-Based Metabolites from the Red Sea Sponge *Hyrtios erectus*. *Mar Drugs*, 2016. 14(7).
41. Molinski, T.F. and D.J. Faulkner, 6.alpha.,7.alpha.,17.beta.-Trihydroxy-15.beta.,17-oxidospongian-16-one 7-butyrate: a new diterpene lactone from an Australian *Aplysilla* species. *The Journal of Organic Chemistry*, 1986. 51(7): p. 1144-1146.
42. Karuso, P. and P. Scheuer, Natural Products from Three Nudibranchs: *Nembrotha kubaryana*, *Hypselodoris infucata* and *Chromodoris petechialis*. *Molecules*, 2002. 7(1): p. 1.
43. Imbs, A.B., O.A. Demina, and D.A. Demidkova, Lipid class and fatty acid composition of the boreal soft coral *Gersemia rubiformis*. *Lipids*, 2006. 41(7): p. 721-5.
44. Imbs, A.B., et al., Application of fatty acids for chemotaxonomy of reef-building corals. *Lipids*, 2007. 42(11): p. 1035-46.
45. Sudan, S. and H.V. Rupasinghe, Antiproliferative activity of long chain acylated esters of quercetin-3-O-glucoside in hepatocellular carcinoma HepG2 cells. *Exp Biol Med (Maywood)*, 2015. 240(11): p. 1452-64.
46. Rashid, Z., et al., Phenolics, fatty acids composition and biological activities of various extracts and fractions of Malaysian *Aaptos aaptos*. *Asian Pacific Journal of Tropical Biomedicine*, 2018. 8(11): p. 554-564.
47. Cateni, F., et al., Cerebrosides with antiproliferative activity from *Euphorbia peplis* L. *Fitoterapia*, 2010. 81(2): p. 97-103.
48. Kumari, M., et al., Antiproliferative and Antioxidative Bioactive Compounds in Extracts of Marine-Derived Endophytic Fungus *Talaromyces purpureogenus*. *Front Microbiol*, 2018. 9: p. 1777.
49. Isbilen, O., N. Rizaner, and E. Volkan, Anti-proliferative and cytotoxic activities of *Allium autumnale* P. H. Davis (Amaryllidaceae) on human breast cancer cell lines MCF-7 and MDA-MB-231. *BMC Complement Altern Med*, 2018. 18(1): p. 30.
50. Su, J.H., et al., Bioactive cadinane-type compounds from the soft coral *Sinularia scabra*. *Arch Pharm Res*, 2012. 35(5): p. 779-84.
51. Ivanisevic, J., et al., Lysophospholipids in the Mediterranean sponge *Oscarella tuberculata*: seasonal variability and putative biological role. *J Chem Ecol*, 2011. 37(5): p. 537-45.
52. da Costa, E., et al., Valorization of Lipids from *Gracilaria* sp. through Lipidomics and Decoding of Antiproliferative and Anti-Inflammatory Activity. *Mar Drugs*, 2017. 15(3).
53. Alam, N., et al., Additional bioactive Lyso-PAF congeners from the sponge *Spirastrella abata*. *J Nat Prod*, 2001. 64(4): p. 533-5.

54. Moritz, M.I., et al., Polyoxygenated steroids from the octocoral *Leptogorgia punicea* and *in vitro* evaluation of their cytotoxic activity. *Mar Drugs*, 2014. 12(12): p. 5864-80.
55. Zidar, N., et al., Antimicrobial activity of the marine alkaloids, clathrodin and oroidin, and their synthetic analogues. *Mar Drugs*, 2014. 12(2): p. 940-63.
56. Ibrahim, S.R. and G.A. Mohamed, Ingenine E, a new cytotoxic beta-carboline alkaloid from the Indonesian sponge *Acanthostrongylophora ingens*. *J Asian Nat Prod Res*, 2017. 19(5): p. 504-509.
57. Netz, N. and T. Opatz, Marine Indole Alkaloids. *Mar Drugs*, 2015. 13(8): p. 4814-914.
58. Sanchez, M.C., et al., Cembrane diterpenes from the gorgonian *Lophogorgia peruana*. *J Nat Prod*, 2006. 69(12): p. 1749-55.
59. Shen, Y.C., et al., New briaranes from the Taiwanese gorgonian *Junceella juncea*. *J Nat Prod*, 2003. 66(2): p. 302-5.
60. Li, C., et al., Bioactive (3Z,5E)-11,20-epoxybriara-3,5-dien-7,18-olide diterpenoids from the South China Sea gorgonian *Dichotella gemmacea*. *Mar Drugs*, 2011. 9(8): p. 1403-18.
61. Suntornchashwej, S., et al., Hectochlorin and morpholine derivatives from the Thai sea hare, *Bursatella leachii*. *J Nat Prod*, 2005. 68(6): p. 951-5.
62. Krohn, K., et al., Biologically active metabolites from fungi, 19: new isocoumarins and highly substituted benzoic acids from the endophytic fungus, *Scytalidium* sp. *Nat Prod Res*, 2004. 18(3): p. 277-85.
63. Festa, C., et al., Plakilactones from the marine sponge *Plakinastrella mamillaris*. Discovery of a new class of marine ligands of peroxisome proliferator-activated receptor gamma. *J Med Chem*, 2012. 55(19): p. 8303-17.
64. Ueoka, R., et al., Gracilioethers A-C, antimalarial metabolites from the marine sponge *Agelas gracilis*. *J Org Chem*, 2009. 74(11): p. 4203-7.
65. Ueoka, R., et al., Gracilioethers A-C, Antimalarial Metabolites from the Marine Sponge *Agelas gracilis*. *The Journal of Organic Chemistry*, 2009. 74(11): p. 4203-4207.
66. Festa, C., et al., Oxygenated polyketides from *Plakinastrella mamillaris* as a new chemotype of PXR agonists. *Mar Drugs*, 2013. 11(7): p. 2314-27.
67. Ortega, M.J., et al., Cembrane diterpenes from the Gorgonian *Leptogorgia laxa*. *Journal of Natural Products*, 2008. 71(9): p. 1637-1639.
68. Sánchez, M.C., et al., Cembrane diterpenes from the gorgonian *Lophogorgia peruana*. *Journal of Natural Products*, 2006. 69(12): p. 1749-1755.
69. Martinez, E.J., et al., Phthalascidin, a synthetic antitumor agent with potency and mode of action comparable to ecteinascidin 743. *Proc Natl Acad Sci U S A*, 1999. 96(7): p. 3496-501.
70. Zhang, X., et al., The sea cucumber genome provides insights into morphological evolution and visceral regeneration. *PLoS biology*, 2017. 15(10): p. e2003790-e2003790.
71. Castelli, S., et al., Conjugated eicosapentaenoic acid inhibits human topoisomerase IB with a mechanism different from camptothecin. *Arch Biochem Biophys*, 2009. 486(2): p. 103-10.
72. Yonezawa, Y., et al., Inhibitory effect of conjugated eicosapentaenoic acid on mammalian DNA polymerase and topoisomerase activities and human cancer cell proliferation. *Biochem Pharmacol*, 2005. 70(3): p. 453-60.
73. Berge, J.P., et al., *In vitro* anti-inflammatory and anti-proliferative activity of sulfolipids from the red alga *Porphyridium cruentum*. *J Agric Food Chem*, 2002. 50(21): p. 6227-32.
74. Martinez-Luis, S., et al., Antitrypanosomal alkaloids from the marine bacterium *Bacillus pumilus*. *Molecules*, 2012. 17(9): p. 11146-55.
75. Bharate, S.B., et al., Chemistry and biology of faspaplysin, a potent marine-derived CDK-4 inhibitor. *Mini Rev Med Chem*, 2012. 12(7): p. 650-64.

76. Kimura, K., et al., Structural elucidation of the neutral glycosphingolipids, mono-, di-, tri- and tetraglycosylceramides from the marine crab *Erimacrus isenbeckii*. *J Oleo Sci*, 2014. 63(3): p. 269-80.
77. Moon, S.H., et al., Altered levels of sphingosine and sphinganine in psoriatic epidermis. *Ann Dermatol*, 2013. 25(3): p. 321-6.
78. Bandaranayake, W.M. and A.D. Rocher, Role of secondary metabolites and pigments in the epidermal tissues, ripe ovaries, viscera, gut contents and diet of the sea cucumber *Holothuria atra*. *Marine Biology*, 1999. 133(1): p. 163-169.
79. Palozza, P., et al., Growth-inhibitory effects of the astaxanthin-rich alga *Haematococcus pluvialis* in human colon cancer cells. *Cancer Lett*, 2009. 283(1): p. 108-17.
80. Galasso, C., C. Corinaldesi, and C. Sansone, Carotenoids from Marine Organisms: Biological Functions and Industrial Applications. *Antioxidants (Basel)*, 2017. 6(4).
81. Wang, J.H., et al., A beta-galactose-specific lectin isolated from the marine worm *Chaetopterus variopedatus* possesses anti-HIV-1 activity. *Comp Biochem Physiol C Toxicol Pharmacol*, 2006. 142(1-2): p. 111-7.
82. Watanadilok, R., et al., Tetillapyrone and nortetillapyrone, two unusual hydroxypyran-2-ones from the marine sponge *Tetilla japonica*. *J Nat Prod*, 2001. 64(8): p. 1056-8.
83. El-Gamal, A.A., et al., Cytotoxic Compounds from the Saudi Red Sea Sponge *Xestospongia testudinaria*. *Mar Drugs*, 2016. 14(5).
84. Manzo, E., et al., Structure and synthesis of a unique isonitrile lipid isolated from the marine mollusk *Actinocyclus papillatus*. *Org Lett*, 2011. 13(8): p. 1897-9.
85. Preethy, C.P., et al., Antiproliferative property of n-hexane and chloroform extracts of *Anisomeles malabarica* (L). R. Br. in HPV16-positive human cervical cancer cells. *J Pharmacol Pharmacother*, 2012. 3(1): p. 26-34.
86. Salem, S.M., et al., Elucidation of final steps of the marineosins biosynthetic pathway through identification and characterization of the corresponding gene cluster. *J Am Chem Soc*, 2014. 136(12): p. 4565-74.
87. Blunt, J.W., et al., Marine natural products. *Nat Prod Rep*, 2016. 33(3): p. 382-431.
88. Chen, G., H.F. Wang, and Y.H. Pei, Secondary metabolites from marine-derived microorganisms. *J Asian Nat Prod Res*, 2014. 16(1): p. 105-22.
89. Diyabalanage, T., et al., Palmerolide A, a cytotoxic macrolide from the antarctic tunicate *Synoicum adareanum*. *J Am Chem Soc*, 2006. 128(17): p. 5630-1.
90. Noguez, J.H., et al., Palmerolide macrolides from the Antarctic tunicate *Synoicum adareanum*. *Bioorganic & Medicinal Chemistry*, 2011. 19(22): p. 6608-6614.
91. Chee, C.F., et al., Pheophorbide b ethyl ester from a *Chlorella vulgaris* dietary supplement. *Acta Crystallogr Sect E Struct Rep Online*, 2008. 64(Pt 10): p. o1986.
92. Baudelet, P.-H., et al., Antiproliferative activity of *Cyanophora paradoxa* pigments in melanoma, breast and lung cancer cells. *Marine drugs*, 2013. 11(11): p. 4390-4406.
93. Cheng, H.H., et al., Cytotoxic pheophorbide-related compounds from *Clerodendrum calamitosum* and *C. cyrtophyllum*. *Journal of Natural Products*, 2001. 64(7): p. 915-919.
94. Gao, S.S., et al., Rhizovarins A-F, Indole-Diterpenes from the Mangrove-Derived Endophytic Fungus *Mucor irregularis* QEN-189. *J Nat Prod*, 2016. 79(8): p. 2066-74.
95. Gao, S.-S., et al., Rhizovarins A-F, Indole-Diterpenes from the Mangrove-Derived Endophytic Fungus *Mucor irregularis* QEN-189. *Journal of Natural Products*, 2016. 79(8): p. 2066-2074.
96. Zhukova, N.V., Lipids and fatty acids of nudibranch mollusks: potential sources of bioactive compounds. *Mar Drugs*, 2014. 12(8): p. 4578-92.

97. Kumar, M.S. and K.M. Adki, Marine natural products for multi-targeted cancer treatment: A future insight. *Biomed Pharmacother*, 2018. 105: p. 233-245.
98. Isbilen, O., N. Rizaner, and E. Volkan, Anti-proliferative and cytotoxic activities of *Allium autumnale* P. H. Davis (Amaryllidaceae) on human breast cancer cell lines MCF-7 and MDA-MB-231. *BMC complementary and alternative medicine*, 2018. 18(1): p. 30-30.
99. Mettu, R., et al., Stereoselective synthesis of-triacetyl-D-erythro-sphingosine and N,O,O-triacetyl sphingonine from a common chiral intermediate derived from D-mannitol. Vol. vi. 2012. 421.
100. Ivanisevic, J., et al., Lysophospholipids in the Mediterranean Sponge *Oscarella tuberculata*: Seasonal Variability and Putative Biological Role. Vol. 37. 2011. 537-45.
101. Khalil, Z.G., et al., Shornephine A: structure, chemical stability, and P-glycoprotein inhibitory properties of a rare diketomorpholine from an Australian marine-derived *Aspergillus* sp. *J Org Chem*, 2014. 79(18): p. 8700-5.
102. Ma, Y.-M., et al., Structural Diversity and Biological Activities of Indole Diketopiperazine Alkaloids from Fungi. *Journal of Agricultural and Food Chemistry*, 2016. 64(35): p. 6659-6671.
103. Shaala, L.A., et al., Bioactive 2(1H)-Pyrazinones and Diketopiperazine Alkaloids from a Tunicate-Derived Actinomycete *Streptomyces* sp. *Molecules*, 2016. 21(9).
104. Mioso, R., et al., Cytotoxic Compounds Derived from Marine Sponges. A Review (2010-2012). *Molecules*, 2017. 22(2).
105. Casalme, L.O., et al., Total synthesis and biological activity of dolastatin 16. *Org Biomol Chem*, 2017. 15(5): p. 1140-1150.
106. Nakashima, Y., et al., Metagenomic Analysis of the Sponge *Discodermia* Reveals the Production of the Cyanobacterial Natural Product Kasumigamide by 'Entotheonella'. *PLoS One*, 2016. 11(10): p. e0164468.
107. Gogineni, V. and M.T. Hamann, Marine natural product peptides with therapeutic potential: Chemistry, biosynthesis, and pharmacology. *Biochim Biophys Acta Gen Subj*, 2018. 1862(1): p. 81-196.
108. Lindel, T., et al., Structure–Activity Relationship of Inhibition of Fish Feeding by Sponge-derived and Synthetic Pyrrole–Imidazole Alkaloids. *Journal of Chemical Ecology*, 2000. 26(6): p. 1477-1496.
109. Song, X., et al., Molecular Targets of Active Anticancer Compounds Derived from Marine Sources. *Marine drugs*, 2018. 16(5): p. 175.
110. Pennings, S.C., et al., Unpalatable Compounds in the Marine Gastropod *Dolabella auricularia*: Distribution and Effect of Diet. *Journal of Chemical Ecology*, 1999. 25(4): p. 735-755.
111. Kamio, M., et al., How to produce a chemical defense: structural elucidation and anatomical distribution of aplysioviolin and phycoerythrobilin in the sea hare *Aplysia californica*. *Chem Biodivers*, 2010. 7(5): p. 1183-97.
112. Rudiger, W., [On the defensive dyes in *Aplysia* species. I. Aplysioviolin, a new bile pigment]. *Hoppe Seylers Z Physiol Chem*, 1967. 348(2): p. 129-38.
113. Buznikov, G.A., T.A. Slotkin, and J.M. Lauder, Sea urchin embryos and larvae as biosensors for neurotoxicants. *Curr Protoc Toxicol*, 2003. Chapter 1: p. Unit1.6.
114. Zhukova, N.V., Lipid classes and fatty acid composition of the tropical nudibranch mollusks *Chromodoris* sp. and *Phyllidia coelestis*. *Lipids*, 2007. 42(12): p. 1169-75.
115. Eser, P.O., et al., Marine- and plant-derived ω -3 fatty acids differentially regulate prostate cancer cell proliferation. *Molecular and clinical oncology*, 2013. 1(3): p. 444-452.

116. Levina, E.V., et al., Trofosides A and B and other cytostatic steroid-derived compounds from the far east starfish *Trofodiscus* über. *Russian Journal of Bioorganic Chemistry*, 2007. 33(3): p. 334-340.
117. Eser, P.O., et al., Marine- and plant-derived omega-3 fatty acids differentially regulate prostate cancer cell proliferation. *Mol Clin Oncol*, 2013. 1(3): p. 444-452.
118. Pacheco, B.S., et al., Cytotoxic Activity of Fatty Acids From Antarctic Macroalgae on the Growth of Human Breast Cancer Cells. *Front Bioeng Biotechnol*, 2018. 6: p. 185.
119. Fang, E.F., et al., Trichosanthin inhibits breast cancer cell proliferation in both cell lines and nude mice by promotion of apoptosis. *PloS one*, 2012. 7(9): p. e41592-e41592.
120. Juin, C., et al., UPLC-MSE profiling of Phytoplankton metabolites: application to the identification of pigments and structural analysis of metabolites in *Porphyridium purpureum*. *Marine drugs*, 2015. 13(4): p. 2541-2558.
121. Baudelet, P.H., et al., Antiproliferative activity of *Cyanophora paradoxa* pigments in melanoma, breast and lung cancer cells. *Mar Drugs*, 2013. 11(11): p. 4390-406.
122. Herranz-López, M., M. Losada-Echeberria, and E. Barrajon-Catalán, The Multitarget Activity of Natural Extracts on Cancer: Synergy and Xenohormesis. *Medicines*, 2019. 6(1).
123. Molinski, T.F., et al., Drug development from marine natural products. *Nature Reviews Drug Discovery*, 2008. 8: p. 69.
124. Dobretsov, S., et al., Screening for Anti-Cancer Compounds in Marine Organisms in Oman. *Sultan Qaboos Univ Med J*, 2016. 16(2): p. e168-74.
125. Fernando, I.P.S., et al., Apoptotic and antiproliferative effects of Stigmast-5-en-3-ol from *Dendronephthya gigantea* on human leukemia HL-60 and human breast cancer MCF-7 cells. *Toxicology in Vitro*, 2018. 52: p. 297-305.
126. Shaltiel, I.A., et al., The same, only different - DNA damage checkpoints and their reversal throughout the cell cycle. *J Cell Sci*, 2015. 128(4): p. 607-20.
127. Mukhtar, E., V.M. Adhami, and H. Mukhtar, Targeting microtubules by natural agents for cancer therapy. *Mol Cancer Ther*, 2014. 13(2): p. 275-84.
128. Brown, J.S., et al., Targeting DNA Repair in Cancer: Beyond PARP Inhibitors. *Cancer Discov*, 2017. 7(1): p. 20-37.
129. Uckun, F.M., et al., Spongistatins as tubulin targeting agents. *Curr Pharm Des*, 2001. 7(13): p. 1291-6.
130. Natsume, T., et al., Tumor-specific antivascular effect of TZT-1027 (Soblidotin) elucidated by magnetic resonance imaging and confocal laser scanning microscopy. *Cancer Sci*, 2007. 98(4): p. 598-604.
131. Ahn, M.Y., et al., A natural histone deacetylase inhibitor, Psammaplin A, induces cell cycle arrest and apoptosis in human endometrial cancer cells. *Gynecol Oncol*, 2008. 108(1): p. 27-33.
132. Kaminsky, V.O. and B. Zhivotovsky, Free radicals in cross talk between autophagy and apoptosis. *Antioxid Redox Signal*, 2014. 21(1): p. 86-102.
133. Houtgraaf, J.H., J. Versmissen, and W.J. van der Giessen, A concise review of DNA damage checkpoints and repair in mammalian cells. *Cardiovasc Revasc Med*, 2006. 7(3): p. 165-72.
134. Taylor, R.C., S.P. Cullen, and S.J. Martin, Apoptosis: controlled demolition at the cellular level. *Nature Reviews Molecular Cell Biology*, 2008. 9: p. 231.
135. Perez-Sanchez, A., et al., Rosemary (*Rosmarinus officinalis*) extract causes ROS-induced necrotic cell death and inhibits tumor growth *in vivo*. *Sci Rep*, 2019. 9(1): p. 808.

136. Kitanaka, C. and Y. Kuchino, Caspase-independent programmed cell death with necrotic morphology. *Cell Death Differ*, 1999. 6(6): p. 508-15.
137. Garcia-Belinchon, M., et al., An Early and Robust Activation of Caspases Heads Cells for a Regulated Form of Necrotic-like Cell Death. *J Biol Chem*, 2015. 290(34): p. 20841-55.
138. Higuchi, M., et al., Regulation of reactive oxygen species-induced apoptosis and necrosis by caspase 3-like proteases. *Oncogene*, 1998. 17(21): p. 2753-60.
139. Mahassni, S.H. and R.M. Al-Reemi, Apoptosis and necrosis of human breast cancer cells by an aqueous extract of garden cress (*Lepidium sativum*) seeds. *Saudi J Biol Sci*, 2013. 20(2): p. 131-9.
140. Nikolettou, V., et al., Crosstalk between apoptosis, necrosis and autophagy. *Biochim Biophys Acta*, 2013. 1833(12): p. 3448-3459.
141. Arakawa, S., et al., Identification of a novel compound that inhibits both mitochondria-mediated necrosis and apoptosis. *Biochemical and Biophysical Research Communications*, 2015. 467(4): p. 1006-1011.
142. Kepp, O., et al., Cell death assays for drug discovery. *Nat Rev Drug Discov*, 2011. 10(3): p. 221-37.
143. Qu, X., et al., Autophagy gene-dependent clearance of apoptotic cells during embryonic development. *Cell*, 2007. 128(5): p. 931-46.
144. Shimizu, S., et al., Role of Bcl-2 family proteins in a non-apoptotic programmed cell death dependent on autophagy genes. *Nat Cell Biol*, 2004. 6(12): p. 1221-8.
145. Vitale, I., et al., Mitotic catastrophe: a mechanism for avoiding genomic instability. *Nat Rev Mol Cell Biol*, 2011. 12(6): p. 385-92.
146. Xiao, B., L. Ma, and D. Merlin, Nanoparticle-mediated co-delivery of chemotherapeutic agent and siRNA for combination cancer therapy. *Expert Opin Drug Deliv*, 2017. 14(1): p. 65-73.
147. Hengartner, M.O., The biochemistry of apoptosis. *Nature*, 2000. 407(6805): p. 770-6.
148. Harada, S., S. Tsubotani, and H. Ono, Cephem compounds. 1984.
149. Ruiz-Torres, V., et al., An Updated Review on Marine Anticancer Compounds: The Use of Virtual Screening for the Discovery of Small-Molecule Cancer Drugs. *Molecules*, 2017. 22(7).
150. Beedessee, G., et al., Cytotoxic activities of hexane, ethyl acetate and butanol extracts of marine sponges from Mauritian Waters on human cancer cell lines. *Environ Toxicol Pharmacol*, 2012. 34(2): p. 397-408.
151. Kocarnik, J.M., S. Shiovitz, and A.I. Phipps, Molecular phenotypes of colorectal cancer and potential clinical applications. *Gastroenterology report*, 2015. 3(4): p. 269-276.
152. Grasso, S., et al., HGUE-C-1 is an atypical and novel colon carcinoma cell line. *BMC cancer*, 2015. 15: p. 240-240.
153. Roma, C., et al., BRAF V600E mutation in metastatic colorectal cancer: Methods of detection and correlation with clinical and pathologic features. *Cancer biology & therapy*, 2016. 17(8): p. 840-848.
154. Ahmed, D., et al., Epigenetic and genetic features of 24 colon cancer cell lines. *Oncogenesis*, 2013. 2(9): p. e71-e71.
155. Chan, F.K.-M., K. Moriwaki, and M.J. De Rosa, Detection of Necrosis by Release of Lactate Dehydrogenase (LDH) Activity. *Methods in molecular biology (Clifton, N.J.)*, 2013. 979: p. 65-70.



© 2019 by the authors; licensee MDPI, Basel, Switzerland. This article is an open access article distributed under the terms and conditions of the Creative Commons Attribution (CC-BY) license (<http://creativecommons.org/licenses/by/4.0/>).

Supplementary information

1. MMP analysis using Mitotracker dyes

ROS accumulation is a process resulting from a decrease in antioxidant defences or an indicator of the apoptosis process associated with mitochondrial dysfunction [1]. We studied the effect of marine extracts in mitochondrial alterations through the changes in the mitochondrial membrane potential (MMP) using the ratio between MitoTracker®Red (MitoRed) and the total mitochondrial content using MitoTracker®Green (MitoGreen) both fluorescence probes (Supplementary Figure 7). The effect of marine extracts, at different concentrations, on MMP was measured after exposing HGUE-C-1, HT-29 and SW480 cells to marine extracts for 24 h. In general, marine extracts decreased the mean red fluorescence respect to green, indicative of decreased MMP in a dose manner dependent way (Supplementary Figure 8). The strongest extract was PS which was able to decrease in a 45, 47 and 41% of MMP in HGUE-C-1, HT-29 and SW480 cells, respectively, at 100 µg/mL respect to the untreated cells (Supplementary Figure 7 B). The second most active was CR extract due to reduce in a 30, 32 and 14% of MMP in HGUE-C-1, HT-29 and SW480 cells, respectively, at 100 µg/mL (Supplementary Figure 7 A). NB was the next, producing a 26, 22 and 24% of reduction in MMP in HGUE-C-1, HT-29 and SW480 cells, respectively, at 100 µg/mL (Supplementary Figure 7 D). Finally, NA extract induced a 28, 17 and 24% of loss of MMP in HGUE-C-1, HT-29 and SW480 cells, respectively, at 100 µg/mL (Supplementary Figure 7 C).

We found all doses of marine extracts increased ROS levels and loss of MMP. Our results indicate that marine extracts could be disrupting the mitochondrial homeostasis, increasing ROS accumulation and perturbing MMP in a dose-dependent manner.

2. Analytical characterization of marine invertebrates

2.1. *Carotalcyon* sp. (CR)

Twenty-one compounds have been detected in the soft coral belonging to *Carotalcyon* sp (Table 3 and Supplementary Figure 9 A and Supplementary Figure 10 A). Among them, 12 have been characterized for the first time in a soft coral. The major compounds detected in soft coral comprised six fatty acids (peaks 13-18) and one diterpene (peak 12) in negative ionization mode while one fatty acid ($[M-H]^+$ at m/z 482.3610) was the predominant compound amount those identified in positive ionization mode. Among fatty acids, stearic acid (m/z 283.2620), heptadecenoic acid (m/z 267.2330), 2-hydroxyeicosanoic acid (m/z 327.2897), hexadecanoic acid (m/z 255.2317), 9-octadecenoic acid (m/z 281.2462) and tetracosapentaenoic acid (m/z 357.2772) have been previously described in different genus soft coral [2, 3].

Additionally, the diterpene spongian-16-one, which was found in soft coral *Carotalcyon* sp and the nudibranchs *Phyllidia varicosa* and *Dolabella auricularia*, has been identified for the first time in marine gastropoda *Aplysilla* sp. [4].

Apart from these major compounds, two isomers of the fatty acid octenoic acid, -hydroxy-, methyl ester (peaks 1 and 2) have been identified in soft coral for the first time. This compound with [M – H]⁻ ion at m/z 171 has been previously reported in marine green alga [5]. Peaks 3 and 5 (m/z 449.1448) have been characterized as isomers of asebotin. This dihydrochalcone has been early detected in some species of sea grass [6]. Peak 4 that eluted at RT 25.66 with molecular formula C₁₀H₁₇O was characterized as terpineol, a terpene reported in some marine species [7] but not in soft coral. Apart from that terpene, several terpenes derivatives have also been identified in the soft coral under study (peaks 8, 10 and 11). Peak 8 (m/z 439.3304) has been characterized as actinoranone which has reported to come from marine-derived actinomycetes and presented significant cancer cell cytotoxicity against HCT-116 human colon carcinoma [8]. Peak 10 (m/z 265.1461) and 11 (m/z 429.2977) were identified in the extract as dendronephthol C and deoxoscalarin, respectively. Dendronephthol C was early isolated from the soft coral *Dendronephthya* sp. by Elkhayat et al. [9]. Moreover, the *in vitro* cytotoxic activity against the murine lymphoma L5187Y cancer cell line was reported by the same author [10]. Likewise, deoxoscalarin was previously reported in the marine kingdom, more specifically, in marine sponges and gorgonian [9].

On its behalf, peak 6 (m/z 353.2311) was identified as sinulariaoid D which could be a potential cytotoxic compound against human cancer cell lines i.e. HepG2, HepG2/ADM, MCF-7, and MCF-7/ADM as its homologous sinulariaoid B is and which has been characterized in the soft coral *Sinularia* sp. by Ling-Fang et al. [11]. Moreover peak 7 (m/z 363.2502) eluted at RT 26.7 was identified as the antibacterial compound as pyrrolo[1,2-c]pyrimidine-4-carboxylic acid, 1-amino-3,5,6,7-tetrahydro-3-pentyl-, 4-[(aminoiminomethyl)amino]butyl ester (Sch 575948), previously isolated from marine sponges [12]. Peak 9 with molecular formula [M – H]⁻ C₁₄H₂₃O₄ was characterized as oxalic acid, allyl nonyl ester, compound with antimicrobial properties previously detected in sponges [13].

Additionally, three compounds were characterized in positive ionization mode. Among them, peak 2 (m/z 482.3610) was the main compound presented in the soft coral and characterized as 1-O-hexadecyl-sn-glycero-3-phosphocholine (lyso-PAF) previously identified in marine sponges [14] but not in soft coral. Contrarily, peak 1 (m/z 259.1768) characterized as scabralin A was early extracted and isolated from soft corals of the genus *Sinularia* and which exhibited moderate cytotoxicity toward MCF-7, WiDr, Daoy and HEp 2 carcinoma cells lines [15]. Lastly, a polyoxygenated marine steroid was characterized in soft coral in positive ionization mode as punicinol D, an active compound isolated from a gorgonian octocorals that inhibits proliferation and induce cytotoxicity to A549 cells *in vitro* [16].

2.2. *Pseudocholochirus violaceus* (PS)

Twenty-four compounds were characterized in the holothurian PS extract in both, negative and positive ionization mode (Table 4 and Supplementary Figure 9 B and Supplementary Figure 10 B). Despite all of them have been previously described in the marine kingdom, 21 were characterized for the first time in a holothurian.

Four alkaloids were characterized in this matrix. Compounds showed [M – H]⁻ ion at m/z 280.1221 (peak 1), 262.1113 (peak 2) and 262.1105 (peak 3) were characterized as N-[(2E)-3-(2-Amino-1H-imidazol-5-yl)-2-propen-1-yl]-1H-indole-2-carboxamide and 2 isomers of the alkaloid acanthomine A, respectively. All of them have been previously reported in the marine ecosystems. Specifically, N-[(2E)-3-(2-Amino-1H-imidazol-5-yl)-2-propen-1-yl]-1H-indole-2-carboxamide has been reported as analogue of the alkaloid oroidin which presented antibacterial activity against different Gram-positive bacterial strains [17]. On its behalf, acanthomine A has been isolated from marine sponges and showed a cytotoxic effect against mammalian cancer cells [18]. Finally, compound with [M + H]⁺ ion at m/z 146.0598 was characterized as 1H-Indole-3-carbaldehyde, an alkaloid derivative that has been previously isolated from marine sponges [19].

Furthermore, five terpenes derivatives have been detected in PS extract. In this regard, compounds 4 (m/z 651.2298) and 11 (m/z 445.1491) have been characterized as juncenolide D and lopholide. Juncenolide D and Lopholide is the first time that they are reported in a holothurian but not in other marine species [20, 21]. Interestingly, juncenolide D was reported to exhibit different levels of growth inhibition activity against A549 and MG63 cells *in vitro* [22]. Additionally, 3 tricyclic sesquiterpenes (peaks 6, 7 and 9) were characterized as acetyl-methoxydeacetyldihydrobotrydial isomers (m/z 383.2072), secondary metabolites from marine microorganisms [23].

Compound 5 (m/z 290.1416) presented a molecular formula C₁₆H₂₀NO₄. It was characterized as syn-3-isopropyl-6-(4-methoxybenzyl)-4-methylmorpholine-2,5-dione. Despite it is the first time in which this morpholine derivative has been characterized in holothurian. This secondary metabolite has been previously isolated from the ragged sea hare *Bursatella leachii*, a marine gastropod mollusk from the Mediterranean Sea [24]. Likewise, the polyketide Gracilioether A (peak 8, m/z 353.1972) has been characterized in holothurian for the first time. This marine natural product was earlier isolated from the marine sponge *Plakinastrella mammillaris* and *Agelas gracilis* [25, 26] and has been described as antimalarial metabolite [27] and some analogues have shown potential anti-inflammatory activity [28].

Peak 12 with molecular formula C₃₅H₃₃N₄O₇ and m/z at 621.2349 was characterized as phthalascidin. It is structurally related to the marine natural product trabectedin, also known as ecteinascidin 743 (Et-743) or Yondelis®, which was the first anticancer marine derived drug that has been approved by the European Union for the treatment of advanced or metastatic soft tissue sarcoma [29]. Moreover, four fatty acids were detected in the holothuroid extract under study (peaks 14-17) i.e. eicosapentaenoic acid (m/z 301.2173), arachidonic acid (m/z 303.2328), stearic acid (m/z 283.2643) and

hexadecanoic acid (m/z 255.2330), respectively. All of them have been previously characterized in holothurian [30].

Regarding compounds detected in positive ionization mode, peak 1 (m/z 146.0598) was characterized as 3-formylindole, an alkaloid previously isolated from the symbiotic marine bacterium *Bacillus pumilus* [31, 32]. On their behalf, compounds 2 and 3 detected in positive ionization mode, yielded a [M + H]⁺ ion at m/z 274.2730 and 302.3039, respectively. They were identified as 2-amino-1,3-hexadecanediol and 2-amino-1,3-octadecanediol, respectively. These two glycosphingolipids have been previously characterized in marine organisms different from holothurian [33]. Finally, the analysis in positive ionization mode allowed the tentative characterization of four carotenoids (peaks 4-7) in the holothurian. In fact, Bandaranayake et al. showed different species of holothurians as a good source of carotenoids, among other secondary metabolites [34]. Two isomers of astaxanthin (m/z 597.3906) and two isomers of canthaxanthin (m/z 565.4040) were detected. Both, astaxanthin and canthaxanthin, are a well-known marine, red, cyclic C40 carotenoids which have been described as one of the most important carotenoids on the nutraceutical global market due to their antioxidant properties [35].

2.3. *Phyllidia varicosa* (NA)

HPLC-ESI-TOF-MS analysis revealed the presence of twenty-five compounds, including, both, negative and positive ionization mode (Table 5 and Supplementary Figure 9 C and Supplementary Figure 10 C). Regarding those compounds detected in negative ionization mode, peak 1 (m/z 255.0874) was characterized as phenyl β-D-galactopyranoside which has been earlier reported in the sea worm *Chaetopterus variopedatus* as anti-HIV-1 activity [36]. Peak 2 (m/z 241.0710), with molecular formula C₁₁H₁₃O₆ was characterized as tetillapyrone, a hydroxypyran-2-one previously described in marine sponges [37].

Compounds 4 and 5 yielded a [M – H]⁻ ion at m/z 420.2293 corresponding to the molecular formula C₂₅H₃₀N₃O₃. They were identified as isomers of ketopremarineosin A which is a prodiginine analogue isolated from the marine *Streptomyces* sp. [38]. On its behalf, peak eluted at RT 27.19 (peak 6) has been characterized as 2-furantridecanoic acid, 2,5-dihydro-2-hydroxy-3,4-dimethyl-5-oxo-, methyl ester, a secondary metabolite of marine-derived microorganisms [39]. According to the normalized area, the main compound from this extract was peak 8 (m/z 619.2926) which was characterized for the first time in nudibranchs [40], as ethyl pheophorbide A. Two of the most abundant compounds in *Phyllidia varicosa* were compound 7 and 9 (m/z 540.3331) which presented a molecular formula C₃₂H₄₆N₆O. They were characterized as isomers of the analogue palmerolide A, a marine macrolide previously isolated from tunicates which has displayed potent cytotoxicity toward melanoma [41, 42].

Nudibranchs constitute a source of lipid bioactive compounds offering a variety of nutraceutical and pharmaceutical applications [43]. In this context, three terpenes (peaks 3, 10 and 15) were identified for the first time in this extract. Following with the most abundant compounds from *Phyllidia varicosa*, compound 10, with molecular formula C₃₂H₄₈N₃O₈, was identified as rhizovarin D, an indole-diterpene previously isolated from a fungus isolated from the marine mangrove plant *Rhizophora stylosa* [44]. Compound 3 (m/z 167.1067) was characterized as geranic acid. This terpenoid was earlier described in the marine mollusc *Actinocyclus papillatus* [45] while compound 15 showed a [M – H]⁻ ion at m/z 303.2329 and it was characterized as spongian-16-one. The latest diterpene was previously characterized in nudibranchs as a diet-derived natural product that helps to defend them against predation [46].

Moreover, twelve fatty acids i.e. two isomers of eicopentanoic acid (peaks 11 and 12), tetradecanoic acid (peak 13), 9-hexadecenoic acid (peak 14), 9,12-octadecadienoic acid (peak 16), pentadecanoic acid (peak 17), stearic acid (peak 18), two isomers of hexadecanoic acid (peaks 19 and 22), two isomers of docosatetraenoic acid (peaks 20 and 21) and 9-octadecenoic acid (peak 23) were characterized in this extract on the basis of their exact mass and previous data available focused on bioactive compounds from nudibranch [43].

Additionally, two compounds were identified in positive ionization mode. Peak 1 yielded a [M – H]⁺ ion at m/z 302.3049. This compound was characterized as sphinganine, a sphingolipid from marine organisms [47]. Peak 2 (m/z 482.3604) with molecular formula C₂₄H₅₃NO₆P has been assigned to the phospholipid 1-O-hexadecyl-sn-glycero-3-phosphocholine earlier isolated from marine sponges [48].

2.4. *Dolabella auricularia* (NB)

A total of thirty-one metabolites were identified in this extract (Table 6 and Supplementary Figure 9 D and Supplementary Figure 10 D). Among them, ten have also been characterized in *Phyllidia varicosa* i.e. phenyl β-D-galactopyranoside (peak 3), palmerolide A derivative (peak 14), eicosapentanoic acid (peak 16), two isomers of spongian-16-one (peaks 21 and 23), 9,12-octadecadienoic acid (peak 24), stearic acid (peak 25), docosatetraenoic acid (peak 26), hexadecanoic acid (peak 27) and 9-octadecenoic acid (peak 28). Most of the afore-mentioned compounds (peaks 16, 23, 24, 27 and 28) represented the major compounds in *Dolabella auricularia* (see table 3). Together with these major compounds, peaks 9 (m/z 352.9135) and 15 (m/z 464.3186) were also representative in the current extract. Peak 9 was putatively characterized as 4,5-dibromo-N-(2,2-dimethoxyethyl)-1H-pyrrole-2-carboxamide, a pyrrole-containing alkaloid which has been previously described in the marine kingdom as a compound responsible for the chemical defence of sponges [49]. It has been demonstrated that some sponge-eating nudibranch are capable to concentrate these chemicals in their body that serve as own defense for other predators [50]. On its behalf, compound 15 was identified as N-[2-(3,4-dihydroxyphenyl)ethyl]-7,10,13,16,19-

docosapentaenamide, a fatty acid previously described in opisthobranch molluscs which include nudibranch [51].

Apart from these major metabolites, other minor metabolites have been detected. Among them, peak 1 eluted at RT 6.09 (m/z 218.0820) was identified as 2,5-morpholinedione, 3-methyl-6-(phenylmethyl). It has been previously identified as a metabolite of a marine-derived *Aspergillus* sp. [52]. Peak 2 with molecular formula C₁₅H₁₉N₂O₃ has been reported in other marine organisms as a diketopiperazine named piperazinedione, 3-[(4-hydroxyphenyl)methyl]-6-(2-methylpropyl) [53]. Moreover, two piperazinyl-derived indoles (peaks 5 and 7) which have been recently isolated from a marine opisthobranch mollusc have been detected in *Dolabella auricularia* [54]. Peaks 4 and 6 that showed a [M – H]⁻ ion at m/z 454.1905 were characterized as isomers of latrunculol A. These macrolides have been described for the first time in nudibranchs but they were recently isolated from marine sponges [55]. On its behalf, peak 8, with a [M – H]⁻ ion at m/z 785.3622, has been identified as kasumigamide a tetrapeptide early isolated from marine sponges [56]. Peak 10 with a molecular formula C₃₅H₅₃O₈ was characterized as agosterol E3, a sterol primary isolated from several species of marine sponges and which has shown to present the potential to reverse multidrug resistance in tumor cells. Whilst another sponge-derived compound was characterized in *Dolabella auricularia* as carbamic acid, [(1R)-1-[[[(acetylamino)methyl]thio]methyl]-2-[[[(1S)-1-[(acetyloxy)methyl]-2-phenylethyl]amino]-2-oxoethyl]methyl-, 1,1-dimethylethyl ester (peak 12), peak 13 (m/z 599.2904) has been identified as aplysioviolin, a bioactive metabolite early characterized in nudibranch *Dolabella auricularia* [57]. Peak 18 presented a [M – H]⁻ ion at m/z 597.4049 with a molecular formula C₃₃H₅₇O₉. Its derived-steroid structure made possible to characterize it as trofoside A, a compound previously isolated from starfish [58]. Moreover, six fatty acids typically found in nudibranch species have been detected in negative ionization mode in this matrix. They have been identified as linolenic acid (peak 17), tetradecanoic acid (peak 19), docosahexaenoic acid (peak 20), palmitoleic acid (peak 22) and eicosadienoic acid (peak 29) [43, 59].

Apart from the abovementioned compounds, other two compounds were characterized in positive ionization mode for the first time in NB. In this regard, peak 1 (m/z 436.2688) with a molecular formula C₂₄H₃₈NO₆ was identified as purpurogumantatin, previously isolated from a marine-derived *Penicillium purpurogenum* which has demonstrated to inhibit human cancer K562, HL-60, HeLa, BGC-823 and MCF-7 cells *in vitro* [60]. Peak 2 which presented a [M – H]⁺ ion at m/z 535.2694, was characterized as pyropheophorbide A, a phytoplankton pigment early identified by UPLC-MS [61].

References for supplementary information:

1. Handy, D.E. and J. Loscalzo, Redox regulation of mitochondrial function. *Antioxid Redox Signal*, 2012. 16(11): p. 1323-67.
2. Imbs, A.B., O.A. Demina, and D.A. Demidkova, Lipid class and fatty acid composition of the boreal soft coral *Gersemia rubiformis*. *Lipids*, 2006. 41(7): p. 721-5.
3. Imbs, A.B., et al., Application of fatty acids for chemotaxonomy of reef-building corals. *Lipids*, 2007. 42(11): p. 1035-46.
4. Molinski, T.F. and D.J. Faulkner, 6.alpha.,7.alpha.,17.beta.-Trihydroxy-15.beta.,17-oxidospongian-16-one 7-butyrate: a new diterpene lactone from an Australian *Aplysilla* species. *The Journal of Organic Chemistry*, 1986. 51(7): p. 1144-1146.
5. S. E. Abou-ElWafa, G., et al., ChemInform Abstract: Three New Unsaturated Fatty Acids from the Marine Green Alga *Ulva fasciata* Delile. Vol. 41. 2010.
6. A Hamdy, A.-H., et al., Bioactive Phenolic Compounds from the Egyptian Red Sea Seagrass *Thalassodendron ciliatum*. Vol. 67. 2012. 291-6.
7. Vidal, N.P., et al., Farmed and wild sea bass (*Dicentrarchus labrax*) volatile metabolites: a comparative study by SPME-GC/MS. *J Sci Food Agric*, 2016. 96(4): p. 1181-93.
8. Nam, S.J., et al., Actinoranone, a cytotoxic meroterpenoid of unprecedented structure from a marine adapted *Streptomyces* sp. *Org Lett*, 2013. 15(21): p. 5400-3.
9. Elkhayat, E., et al., Dendronephthols A–C, new sesquiterpenoids from the Red Sea soft coral *Dendronephthya* sp. Vol. 70. 2014. 3822–3825.
10. Elkhayat, E.S., et al., Dendronephthols A–C, new sesquiterpenoids from the Red Sea soft coral *Dendronephthya* sp. *Tetrahedron*, 2014. 70(24): p. 3822-3825.
11. Lei, L.-F., et al., Novel cytotoxic nine-membered macrocyclic polysulfur cembranoid lactones from the soft coral *Sinularia* sp. *Tetrahedron*, 2014. 70(38): p. 6851-6858.
12. Yang, S.-W., et al., A new sterol sulfate, Sch 572423, from a marine sponge, *Topsentia* sp. Vol. 13. 2003. 1791-4.
13. Selvin, J., et al., Optimization and production of novel antimicrobial agents from sponge associated marine actinomycetes *Nocardiopsis dassonvillei* MAD08. *Appl Microbiol Biotechnol*, 2009. 83(3): p. 435-45.
14. Ivanisevic, J., et al., Lysophospholipids in the Mediterranean sponge *Oscarella tuberculata*: seasonal variability and putative biological role. *J Chem Ecol*, 2011. 37(5): p. 537-45.
15. Su, J.H., et al., Bioactive cadinane-type compounds from the soft coral *Sinularia scabra*. *Arch Pharm Res*, 2012. 35(5): p. 779-84.
16. Moritz, M.I., et al., Polyoxygenated steroids from the octocoral *Leptogorgia punicea* and *in vitro* evaluation of their cytotoxic activity. *Mar Drugs*, 2014. 12(12): p. 5864-80.
17. Zidar, N., et al., Antimicrobial activity of the marine alkaloids, clathrodin and oroidin, and their synthetic analogues. *Mar Drugs*, 2014. 12(2): p. 940-63.
18. Ibrahim, S.R. and G.A. Mohamed, Ingenine E, a new cytotoxic beta-carboline alkaloid from the Indonesian sponge *Acanthostrongylophora ingens*. *J Asian Nat Prod Res*, 2017. 19(5): p. 504-509.
19. Mokhlesi, A., et al., New 2-Methoxy Acetylenic Acids and Pyrazole Alkaloids from the Marine Sponge *Cinachyrella* sp. *Mar Drugs*, 2017. 15(11).
20. Sanchez, M.C., et al., Cembrane diterpenes from the gorgonian *Lophogorgia peruana*. *J Nat Prod*, 2006. 69(12): p. 1749-55.
21. Shen, Y.C., et al., New briaranes from the Taiwanese gorgonian *Junceella juncea*. *J Nat Prod*, 2003. 66(2): p. 302-5.

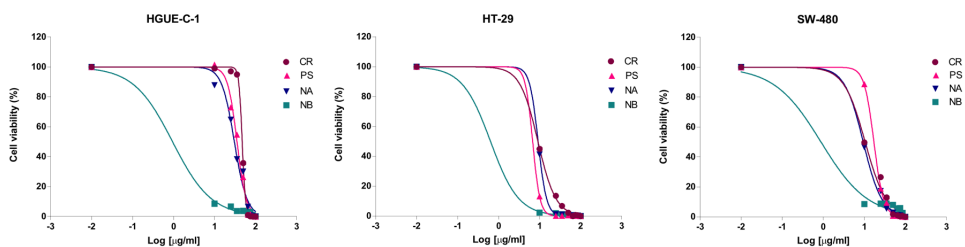
22. Li, C., et al., Bioactive (3Z,5E)-11,20-epoxybriara-3,5-dien-7,18-olide diterpenoids from the South China Sea gorgonian *Dichotella gemmacea*. *Mar Drugs*, 2011. 9(8): p. 1403-18.
23. Krohn, K., et al., Biologically active metabolites from fungi, 19: new isocoumarins and highly substituted benzoic acids from the endophytic fungus, *Scytalidium* sp. *Nat Prod Res*, 2004. 18(3): p. 277-85.
24. Suntornchashwej, S., et al., Hectochlorin and morpholine derivatives from the Thai sea hare, *Bursatella leachii*. *J Nat Prod*, 2005. 68(6): p. 951-5.
25. Festa, C., et al., Plakilactones from the marine sponge *Plakinastrella mamillaris*. Discovery of a new class of marine ligands of peroxisome proliferator-activated receptor gamma. *J Med Chem*, 2012. 55(19): p. 8303-17.
26. Ueoka, R., et al., Gracilioethers A-C, antimalarial metabolites from the marine sponge *Agelas gracilis*. *J Org Chem*, 2009. 74(11): p. 4203-7.
27. Ueoka, R., et al., Gracilioethers A-C, Antimalarial Metabolites from the Marine Sponge *Agelas gracilis*. *The Journal of Organic Chemistry*, 2009. 74(11): p. 4203-4207.
28. Festa, C., et al., Oxygenated polyketides from *Plakinastrella mamillaris* as a new chemotype of PXR agonists. *Mar Drugs*, 2013. 11(7): p. 2314-27.
29. Martinez, E.J., et al., Phthalascidin, a synthetic antitumor agent with potency and mode of action comparable to ecteinascidin 743. *Proc Natl Acad Sci U S A*, 1999. 96(7): p. 3496-501.
30. Zhang, X., et al., The sea cucumber genome provides insights into morphological evolution and visceral regeneration. *PLoS biology*, 2017. 15(10): p. e2003790-e2003790.
31. Martinez-Luis, S., et al., Antitrypanosomal alkaloids from the marine bacterium *Bacillus pumilus*. *Molecules*, 2012. 17(9): p. 11146-55.
32. Leon-Palmero, E., et al., Diversity and antimicrobial potential in sea anemone and holothurian microbiomes. *PLoS One*, 2018. 13(5): p. e0196178.
33. Kimura, K., et al., Structural elucidation of the neutral glycosphingolipids, mono-, di-, tri- and tetraglycosylceramides from the marine crab *Erimacrus isenbeckii*. *J Oleo Sci*, 2014. 63(3): p. 269-80.
34. Bandaranayake, W.M. and A.D. Rocher, Role of secondary metabolites and pigments in the epidermal tissues, ripe ovaries, viscera, gut contents and diet of the sea cucumber *Holothuria atra*. *Marine Biology*, 1999. 133(1): p. 163-169.
35. Henke, N.A., et al., Production of the Marine Carotenoid Astaxanthin by Metabolically Engineered *Corynebacterium glutamicum*. *Mar Drugs*, 2016. 14(7).
36. Wang, J.H., et al., A beta-galactose-specific lectin isolated from the marine worm *Chaetopterus variopedatus* possesses anti-HIV-1 activity. *Comp Biochem Physiol C Toxicol Pharmacol*, 2006. 142(1-2): p. 111-7.
37. Watanadilok, R., et al., Tetillapyrone and nortetillapyrone, two unusual hydroxypyran-2-ones from the marine sponge *Tetilla japonica*. *J Nat Prod*, 2001. 64(8): p. 1056-8.
38. Salem, S.M., et al., Elucidation of final steps of the marine osins biosynthetic pathway through identification and characterization of the corresponding gene cluster. *J Am Chem Soc*, 2014. 136(12): p. 4565-74.
39. Chen, G., H.F. Wang, and Y.H. Pei, Secondary metabolites from marine-derived microorganisms. *J Asian Nat Prod Res*, 2014. 16(1): p. 105-22.
40. Chee, C.F., et al., Pheophorbide b ethyl ester from a *Chlorella vulgaris* dietary supplement. *Acta Crystallogr Sect E Struct Rep Online*, 2008. 64(Pt 10): p. o1986.
41. Diyabalanage, T., et al., Palmerolide A, a cytotoxic macrolide from the antarctic tunicate *Synoicum adareanum*. *J Am Chem Soc*, 2006. 128(17): p. 5630-1.

42. Noguez, J.H., et al., Palmerolide macrolides from the Antarctic tunicate *Synoicum adareanum*. *Bioorganic & Medicinal Chemistry*, 2011. 19(22): p. 6608-6614.
43. Zhukova, N.V., Lipids and fatty acids of nudibranch mollusks: potential sources of bioactive compounds. *Mar Drugs*, 2014. 12(8): p. 4578-92.
44. Gao, S.S., et al., Rhizovarins A-F, Indole-Diterpenes from the Mangrove-Derived Endophytic Fungus *Mucor irregularis* QEN-189. *J Nat Prod*, 2016. 79(8): p. 2066-74.
45. Manzo, E., et al., Structure and synthesis of a unique isonitrile lipid isolated from the marine mollusk *Actinocyclus papillatus*. *Org Lett*, 2011. 13(8): p. 1897-9.
46. Karuso, P. and P. Scheuer, Natural Products from Three Nudibranchs: *Nembrotha kubaryana*, *Hypselodoris infucata* and *Chromodoris petechialis*. *Molecules*, 2002. 7(1): p. 1.
47. Mettu, R., et al., Stereoselective synthesis of-triacetyl-D-erythro-sphingosine and N,O,O-triacetyl sphingonine from a common chiral intermediate derived from D-mannitol. Vol. vi. 2012. 421.
48. Ivanisevic, J., et al., Lysophospholipids in the Mediterranean Sponge *Oscarella tuberculata*: Seasonal Variability and Putative Biological Role. Vol. 37. 2011. 537-45.
49. Lindel, T., et al., Structure-Activity Relationship of Inhibition of Fish Feeding by Sponge-derived and Synthetic Pyrrole-Imidazole Alkaloids. *Journal of Chemical Ecology*, 2000. 26(6): p. 1477-1496.
50. Pawlik, J.R., et al., Defensive chemicals of the Spanish dancer nudibranch *Hexabranchus sanguineus* and its egg ribbons: macrolides derived from a sponge diet. *Journal of Experimental Marine Biology and Ecology*, 1988. 119(2): p. 99-109.
51. Buznikov, G.A., T.A. Slotkin, and J.M. Lauder, Sea urchin embryos and larvae as biosensors for neurotoxicants. *Curr Protoc Toxicol*, 2003. Chapter 1: p. Unit1.6.
52. Khalil, Z.G., et al., Shornephine A: structure, chemical stability, and P-glycoprotein inhibitory properties of a rare diketomorpholine from an Australian marine-derived *Aspergillus* sp. *J Org Chem*, 2014. 79(18): p. 8700-5.
53. Ma, Y.-M., et al., Structural Diversity and Biological Activities of Indole Diketopiperazine Alkaloids from Fungi. *Journal of Agricultural and Food Chemistry*, 2016. 64(35): p. 6659-6671.
54. Casalme, L.O., et al., Total synthesis and biological activity of dolastatin 16. *Org Biomol Chem*, 2017. 15(5): p. 1140-1150.
55. Mioso, R., et al., Cytotoxic Compounds Derived from Marine Sponges. A Review (2010-2012). *Molecules*, 2017. 22(2).
56. Nakashima, Y., et al., Metagenomic Analysis of the Sponge *Discodermia* Reveals the Production of the Cyanobacterial Natural Product Kasumigamide by 'Entotheonella'. *PLoS One*, 2016. 11(10): p. e0164468.
57. Pennings, S.C., et al., Unpalatable Compounds in the Marine Gastropod *Dolabella auricularia*: Distribution and Effect of Diet. *Journal of Chemical Ecology*, 1999. 25(4): p. 735-755.
58. Levina, E.V., et al., Trofosides A and B and other cytostatic steroid-derived compounds from the far east starfish *Trofodiscus über*. *Russian Journal of Bioorganic Chemistry*, 2007. 33(3): p. 334-340.
59. Zhukova, N.V., Lipid classes and fatty acid composition of the tropical nudibranch mollusks *Chromodoris* sp. and *Phyllidia coelestis*. *Lipids*, 2007. 42(12): p. 1169-75.
60. Fang, E.F., et al., Trichosanthin inhibits breast cancer cell proliferation in both cell lines and nude mice by promotion of apoptosis. *PloS one*, 2012. 7(9): p. e41592-e41592.

61. Juin, C., et al., UPLC-MSE profiling of Phytoplankton metabolites: application to the identification of pigments and structural analysis of metabolites in *Porphyridium purpureum*. *Marine drugs*, 2015. 13(4): p. 2541-2558.

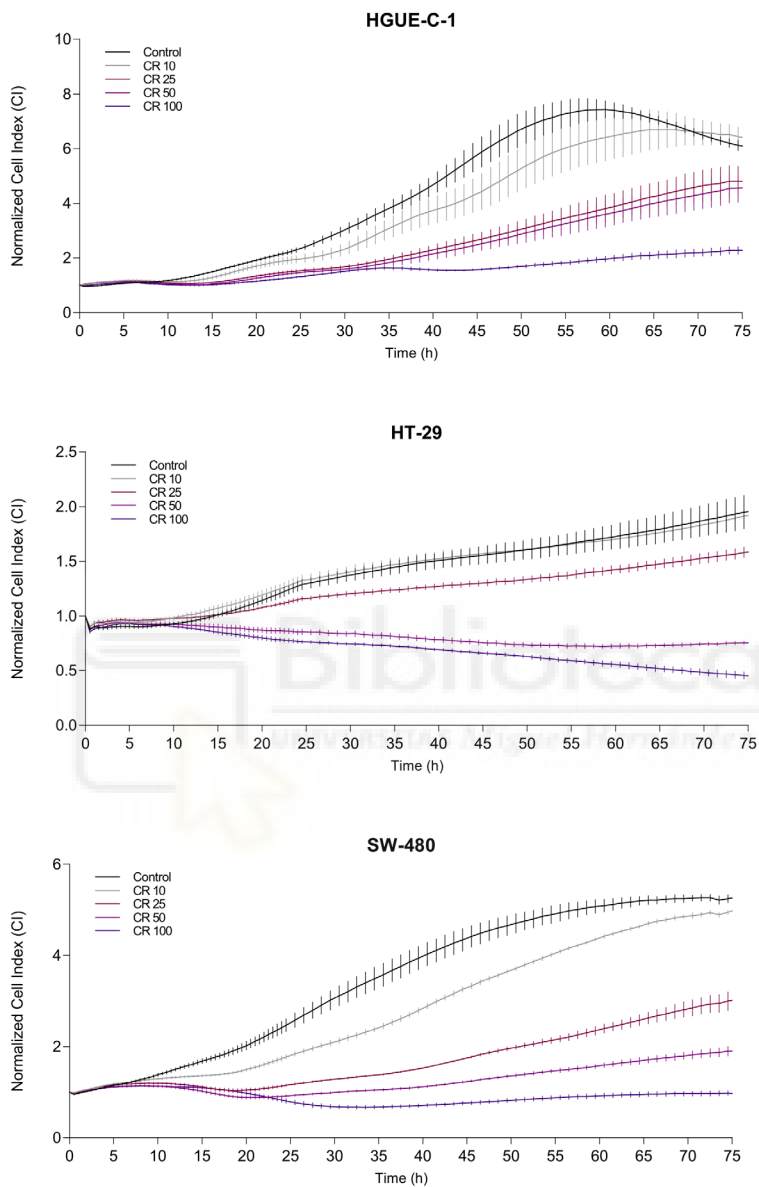


Supplementary figures and tables

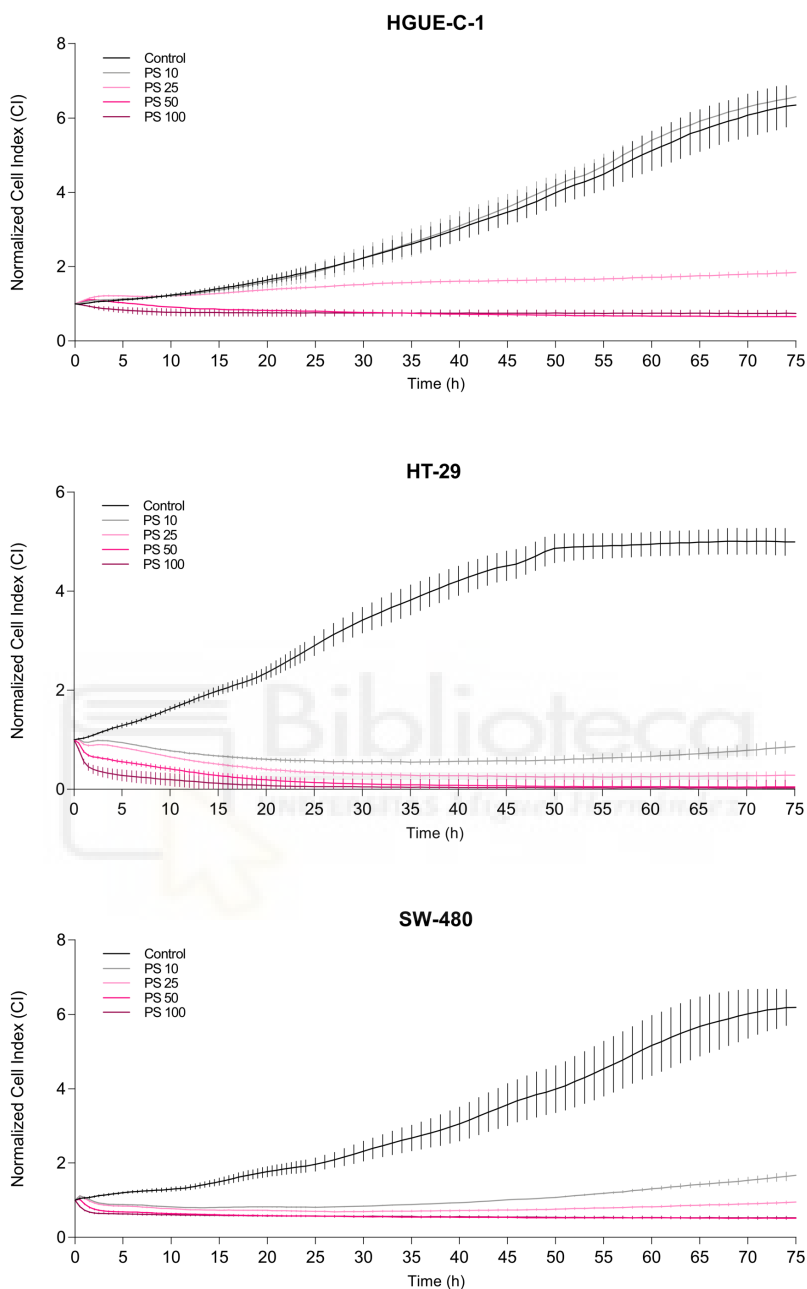


Supplementary Figure 1. Dose-response curves showing the effects of 48 h treatment with the CR, PS, NA and NB extracts on the viability of human colon carcinoma cells (HGUE-C-1, HT-29 and SW-480), as assessed using the MTT assay. The values were calculated as percentage of live cells relative to the untreated cells (Control cells plus dimethyl sulfoxide less than 0.2%, C) from three independent experiments. For dose-response assays, data points were connected by nonlinear regression lines of the sigmoidal dose-response relation. GraphPad Prism software was used to produce dose-response curves and calculate IC50 values.

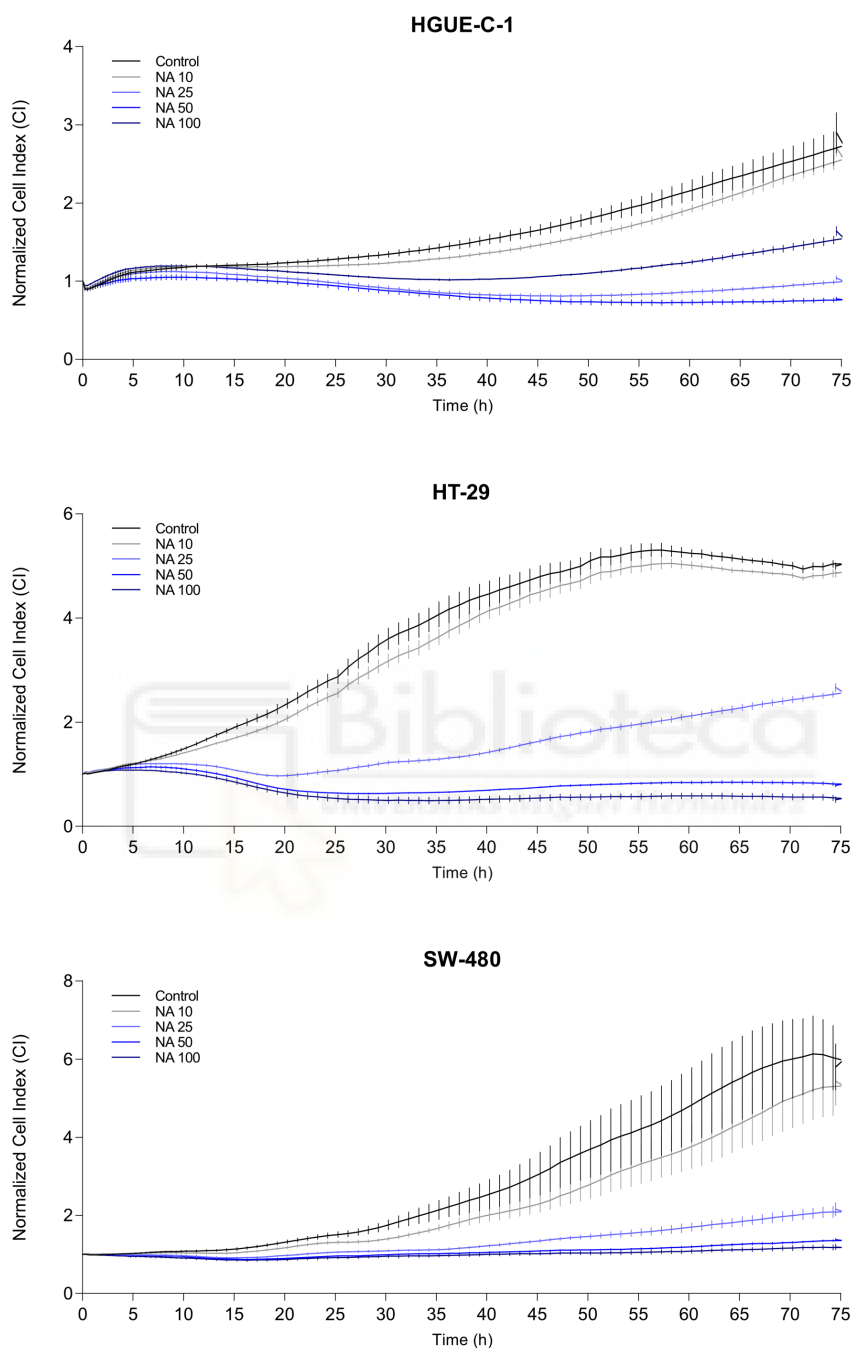




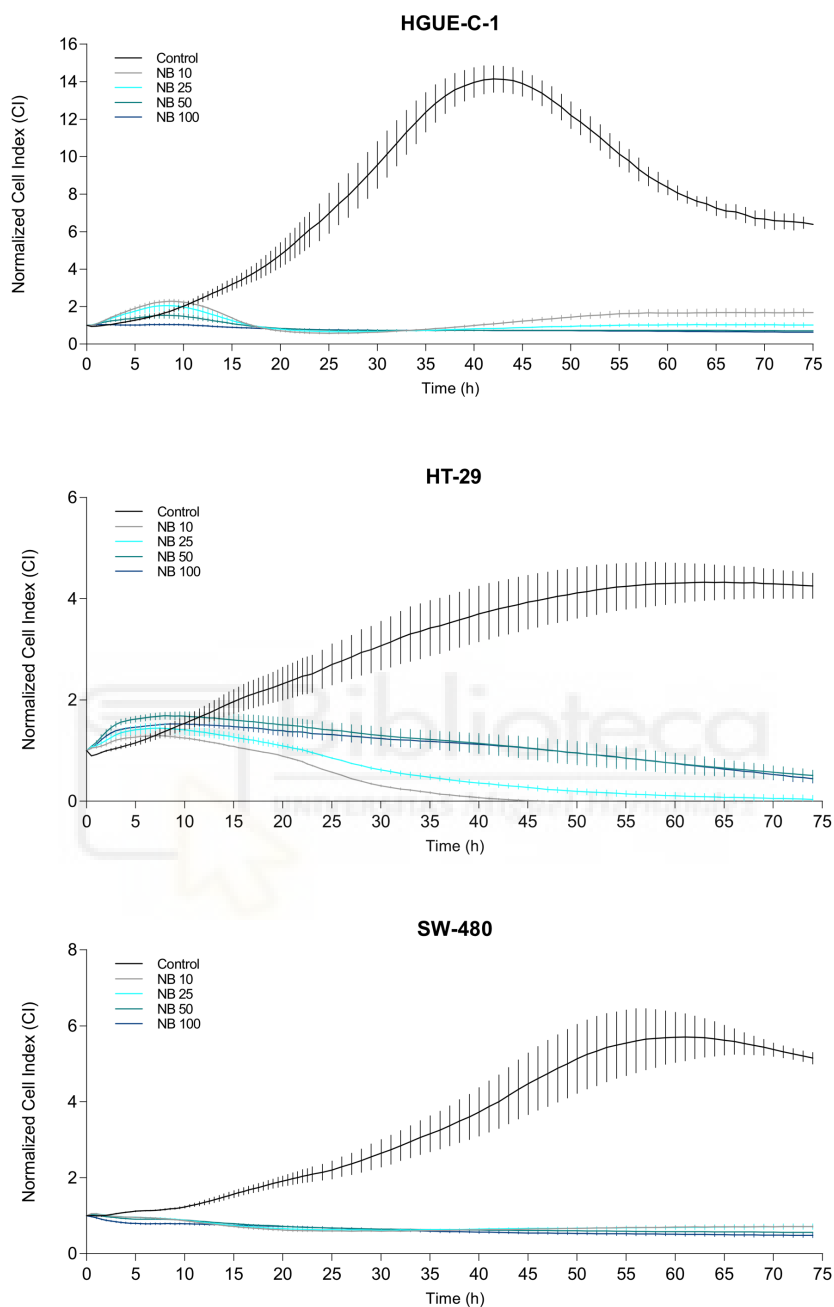
Supplementary Figure 2. Effects of treatment with 10, 25, 50 and 100 $\mu\text{g}/\text{mL}$ of the CR extract on the proliferation profiles of human colon carcinoma cells, as assessed using the Real Time Cell Analyzer System (RTCA) with E-16 plates. The data are presented as the means \pm SD of three independent experiments.



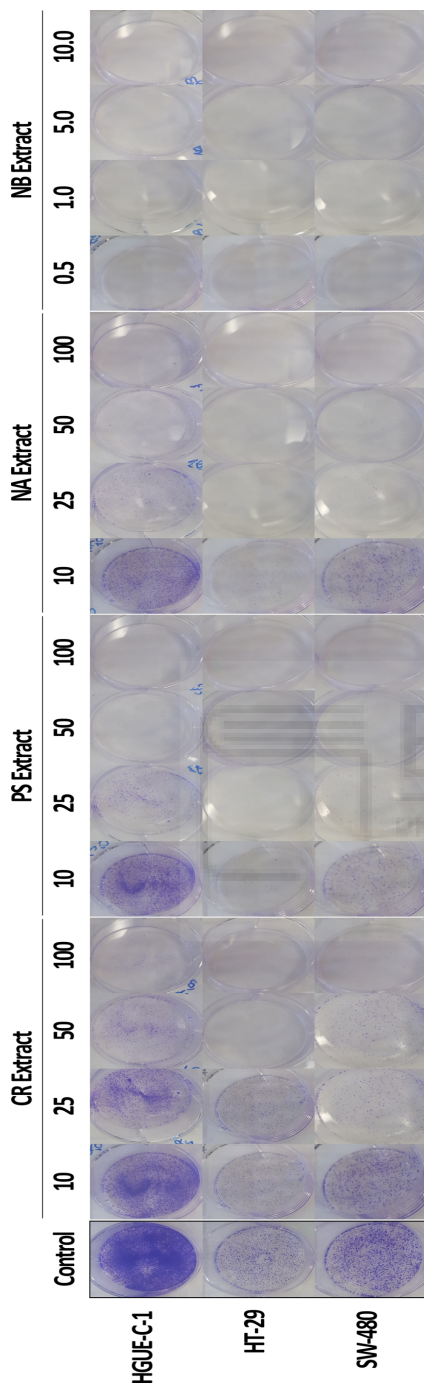
Supplementary Figure 3. Effects of treatment with 10, 25, 50 and 100 $\mu\text{g}/\text{mL}$ of the PS extract on the proliferation profiles of human colon carcinoma cells, as assessed using the Real Time Cell Analyzer System (RTCA) with E-16 plates. The data are presented as the means \pm SD of three independent experiments.



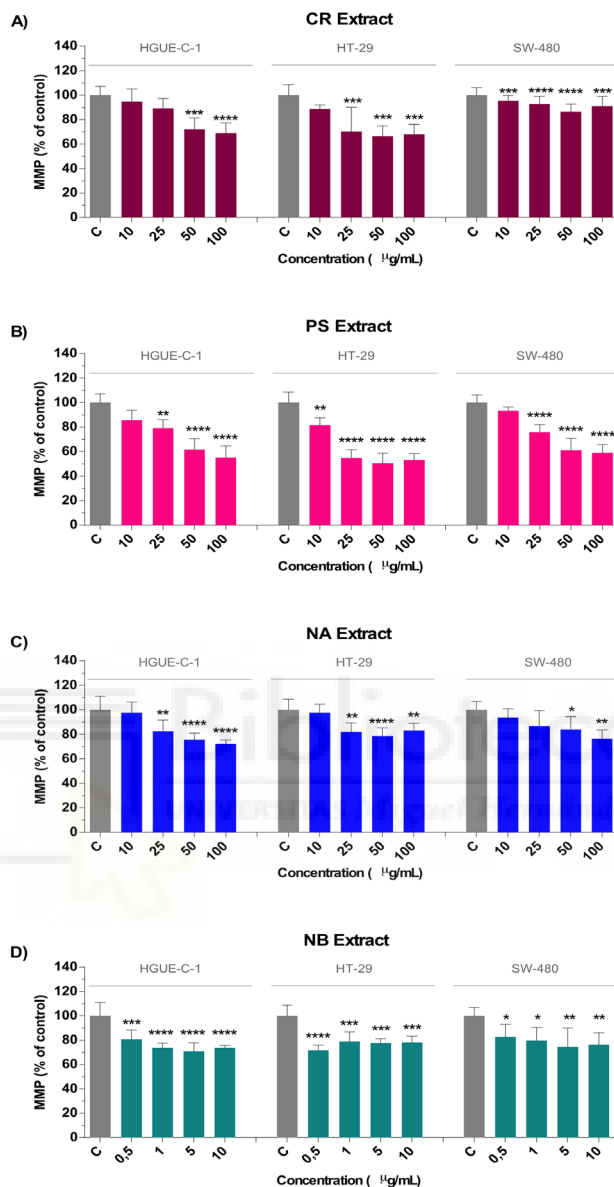
Supplementary Figure 4. Effects of treatment with 10, 25, 50 and 100 $\mu\text{g/mL}$ of the NA extract on the proliferation profiles of human colon carcinoma cells, as assessed using the Real Time Cell Analyzer System (RTCA) with E-16 plates. The data are presented as the means \pm SD of three independent experiments.



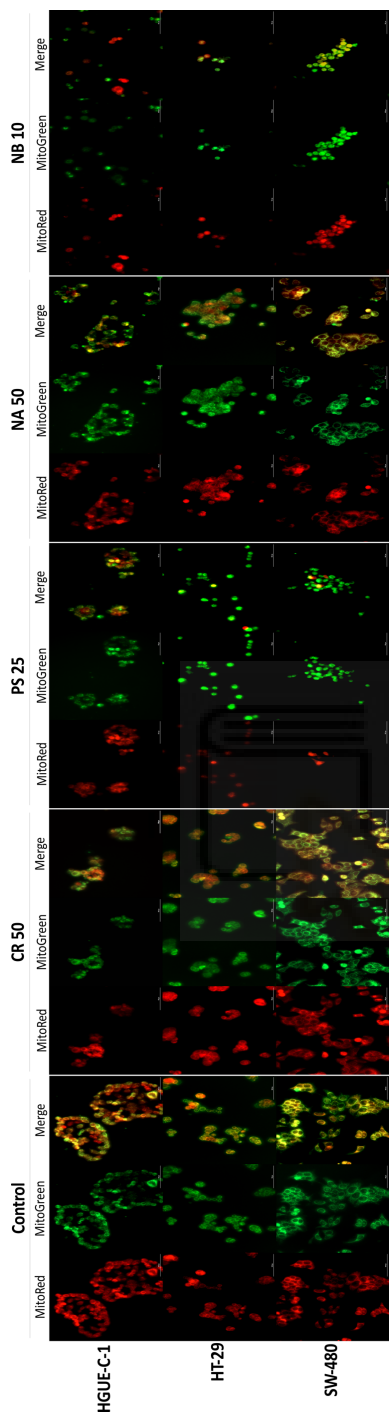
Supplementary Figure 5. Effects of treatment with 10, 25, 50 and 100 $\mu\text{g}/\text{mL}$ of the NB extract on the proliferation profiles of human colon carcinoma cells (HGUE-C-1, HT-29 and SW-480 cell lines), as assessed using the Real Time Cell Analyzer System (RTCA) with E-16 plates. The data are presented as the means \pm SD of three independent experiments.



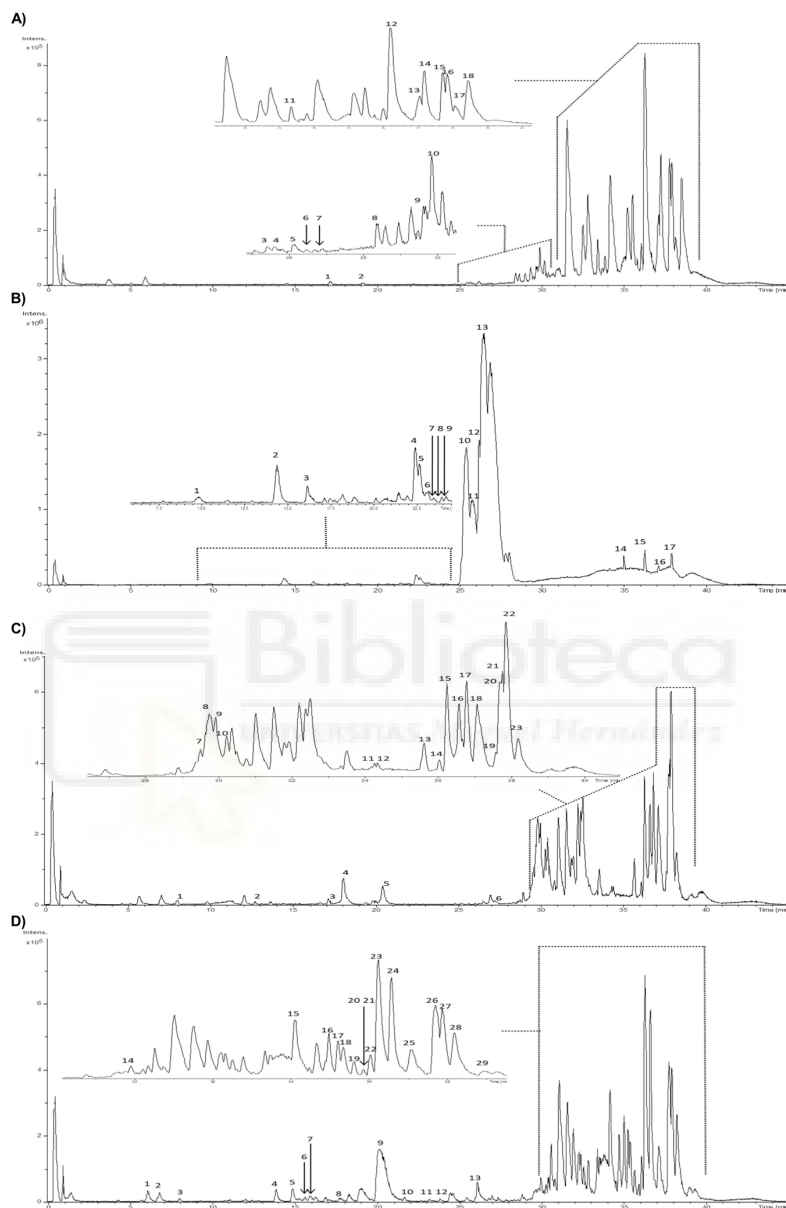
Supplementary Figure 6. Effects of marine extracts on the formation of colonies by HGUE-C-1, HT-29 and SW-480 cells. After treatment with different concentrations of the marine extracts, cells were fixed with ethanol, stained with 1.25% crystal violet



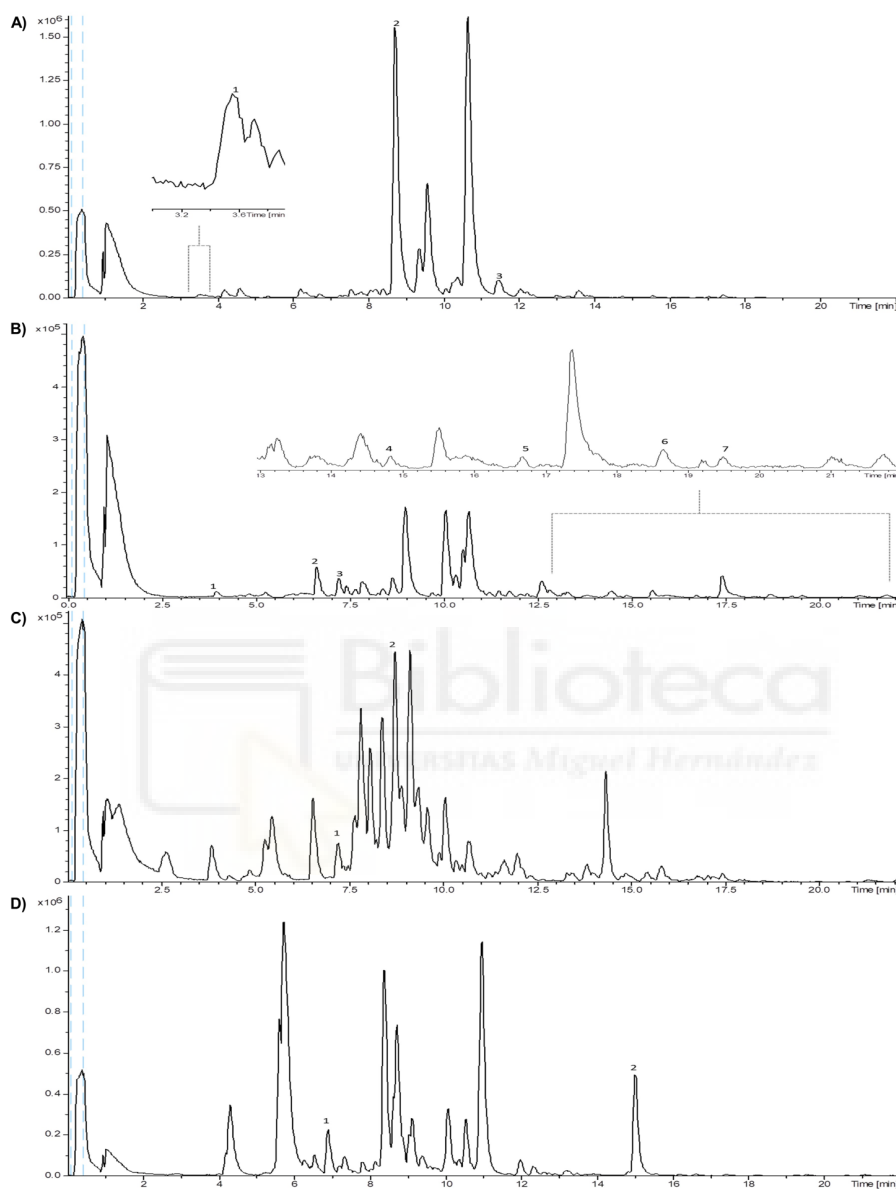
Supplementary Figure 7. Marine extracts alter the mitochondrial membrane polarization (MMP) in colon cancer cells. Depolarization of the mitochondrial Membrane was assessed by calculating the ratio of the MitoTracker Red CM-ROS and MitoTracker® green fluorescence label in HGUE, HT-29 and SW-480 cells 24 h after treatment with the CR extract (A), PS extract (B), NA extract (C) and NB extract (D) compared to untreated cells (Control cells plus dimethyl sulfoxide less than 0.2%, C). The results are presented as the percentages (mean \pm SD) from three independent experiments. p-values were calculated and compared to the same untreated cell line using ANOVAs. *p-value < 0.05, ** p-value < 0.01, *** p-value < 0.001 and **** p-value < 0.0001.



Supplementary Figure 8. Marine extracts cause mitochondrial membrane depolarization (MMD) in colon cancer cells. The decreased mitochondrial membrane polarization in HGUE-C-1, HT29 and SW480 cells is presented as a decrease in the red fluorescence (MitoTracker® Red CMXRos (Texas red)) of cells treated with different concentrations of the marine extracts a



Supplementary Figure 9. Base peak chromatograms (BPCs) of (A) *Carotalcyon sp.* (soft coral, CR), (B) *Pseudocholochirus violaceus* (holothurian, PS), (C) *Phyllidia varicosa* (nudibranch, NA), and (D) *Dolabella auricularia* (nudibranch, NB) recorded using HPLC-ESI-TOF-MS in negative ionization mode.



Supplementary Figure 10. Base peak chromatogram (BPCs) of (A) *Carotalcyon* sp. (soft coral, CR), (B) *Pseudocholochirus violaceus* (holothurian, PS), (C) *Phyllidia varicosa* (nudibranch, NA), and (D) *Dolabella auricularia* (nudibranch, NB) recorded using HPLC-ESI-TOF-MS in positive ionization mode.

Supplementary Table 1. Yield rate (%) with solid of complete marine extracts

Code	Organism	Yield (% w/w)
P	Soft Coral	7.73
D		4.45
L		2.15
C		3.10
N		3.83
SH		1.29
Si		8.07
Cy		2.92
X		3.18
Py		5.06
Eu		1.73
CR		1.35
A		Anemone
W	Hard Coral	1.83
E		ND
F		ND
Du		ND
NA	Nudibranch	2.44
NB		2.71
PS	Hotothurian	4.52

(ND, Not determined)

Supplementary Table 2. IC₅₀ values from MTT assay of complete extracts cytotoxic effect in 3 different colon cancer cell lines.

Code	HGUE-C-1			HT-29			SW-480		
	24 h	48 h	72 h	24 h	48 h	72 h	24 h	48 h	72 h
P	ND	ND	ND	ND	344.0 ± 127.9	198.0 ± 42.8	123.5 ± 18.5	276.0 ± 54.2	157.3 ± 19.9
D	66.4 ± 6.4	ND	ND	ND	174.4 ± 15.5	99.9 ± 20.3	ND	ND	356.0 ± 159.5
L	125.7 ± 22.2	101.4 ± 11.9	134.1 ± 33.8	261.3 ± 78.3	79.9 ± 15.2	46.9 ± 1.8	274.9 ± 81.4	88.0 ± 7.4	96.9 ± 6.2
C	ND	210.3 ± 61.1	160.0 ± 45.6	210.1 ± 82.9	119.6 ± 110.2	158.9 ± 30.7	90.6 ± 10.4	42.4 ± 2.6	81.1 ± 5.4
N	ND	464.8 ± 279.1	ND	267.3 ± 100.9	128.2 ± 112.8	138.2 ± 14.4	141.9 ± 20.6	30.9 ± 2.6	107.7 ± 17.6
SII	197.2 ± 92.2	231.0 ± 76.2	ND	320.1 ± 119.4	163.6 ± 121.4	114.6 ± 7.3	ND	ND	ND
Si	ND	86.0 ± 1.3	108.8 ± 7.1	202.8 ± 30.6	75.5 ± 13.5	62.6 ± 1.2	204.7 ± 59.9	106.7 ± 9.3	102.4 ± 5.0
Cy	ND	ND	ND	ND	ND	ND	ND	ND	ND
X	278.0 ± 163.5	ND	ND	24.9 ± 6.1	16.5 ± 11.8	18.0 ± 0.9	ND	ND	181.6 ± 28.1
Py	ND	ND	ND	439.1 ± 339.2	133.7 ± 124.4	148.8 ± 27.0	ND	ND	ND
Eu	ND	198.2 ± 55.5	ND	ND	182.4 ± 144.6	139.0 ± 36.2	145.5 ± 14.6	73.3 ± 5.5	212.7 ± 48.2
CR	250.9 ± 92.1	82.0 ± 5.9	58.1 ± 3.4	15.0 ± 4.4	9.4 ± 1.4	10.6 ± 1.0	105.0 ± 10.9	27.6 ± 2.8	14.8 ± 1.6
A	ND	ND	ND	ND	ND	ND	276.1 ± 179.4	174.8 ± 41.8	177.9 ± 76.8
W	ND	ND	ND	ND	ND	ND	ND	328.1 ± 153.8	245.9 ± 69.2
E	293.8 ± 133.3	ND	177.1 ± 59.8	136.1 ± 11.6	74.3 ± 14.1	41.3 ± 2.1	ND	73.0 ± 21.9	ND
F	ND	190.7 ± 58.2	ND	ND	ND	179.5 ± 32.2	175.8 ± 33.7	168.3 ± 24.3	190.3 ± 33.6
Du	ND	ND	ND	ND	214.5 ± 197.8	239.8 ± 103.3	ND	ND	305.7 ± 135.0
NA	146.0 ± 29.0	137.3 ± 2.9	78.8 ± 3.4	13.0 ± 2.7	10.0 ± 0.7	9.3 ± 1.0	57.2 ± 6.9	13.6 ± 1.5	13.0 ± 2.0
NB	11.4 ± 3.4	0.3 ± 0.3	0.1 ± 0.2	5.0 ± 3.6	0.1 ± 0.1	0.1 ± 0.1	54.3 ± 24.2	0.6 ± 0.4	0.2 ± 0.1
PS	37.5 ± 3.0	37.4 ± 1.3	48.0 ± 1.8	3.3 ± 1.1	0.7 ± 0.4	2.1 ± 0.7	24.3 ± 2.0	18.6 ± 1.2	16.9 ± 0.6

ND, Not Determined

**New mammalian Target of
Rapamycin (mTOR) Modulators
Derived from Natural Product
Databases and Marine Extracts by
Using Molecular Docking Techniques**

**Doctoral Student:
Verónica Ruiz Torres**

Article

New Mammalian Target of Rapamycin (mTOR) Modulators Derived from Natural Product Databases and Marine Extracts by Using Molecular Docking Techniques

Verónica Ruiz-Torres ¹, Maria Losada-Echeberría ¹, Maria Herranz-López ¹, Enrique Barrajon-Catalán ¹, Vicente Galiano ², Vicente Micol ^{1,3} and José Antonio Encinar ^{1,*}

¹ Institute of Research, Development and Innovation in Biotechnology of Elche (IDiBE) and Molecular and Cell Biology Institute (IBMC), Miguel Hernández University (UMH), Elche, 03202 Alicante, Spain;

² Physics and Computer Architecture Department, Miguel Hernández University (UMH), Elche, Spain; vgaliano@umh.es

³ CIBER, Fisiopatología de la Obesidad y la Nutrición, CIBERobn, Instituto de Salud Carlos III, 07122 Palma de Mallorca, Spain (CB12/03/30038)

* Correspondence: jant.encinar@umh.es; Tel.: +34-96-65-84-53; Fax: +34-96-665-87-58

Mar Drugs. 2018 Oct 15;16(10). pii: E385. doi: 10.3390/md16100385.

Received: 24 September 2018; Accepted: 12 October 2018; Published: date

Abstract: Mammalian target of rapamycin (mTOR) is a PI3K-related serine/threonine protein kinase that functions as a master regulator of cellular growth and metabolism, in response to nutrient and hormonal stimuli. mTOR functions in two distinct complexes—mTORC1 is sensitive to rapamycin, while, mTORC2 is insensitive to this drug. Deregulation of mTOR's enzymatic activity has roles in cancer, obesity, and aging. Rapamycin and its chemical derivatives are the only drugs that inhibit the hyperactivity of mTOR, but numerous side effects have been described due to its therapeutic use. The purpose of this study was to identify new compounds of natural origin that can lead to drugs with fewer side effects. We have used computational techniques (molecular docking and calculated ADMET parameters) that have enabled the selection of candidate compounds, derived from marine natural products, SuperNatural II, and ZINC natural products, for inhibitors targeting, both, the ATP and the rapamycin binding sites of mTOR. We have shown experimental evidence of the inhibitory activity of eleven selected compounds against mTOR. We have also discovered the inhibitory activity of a new marine extract against this enzyme. The results have been discussed concerning the necessity to identify new molecules for therapeutic use, especially against aging, and with fewer side effects.

Keywords: mTOR kinase; marine natural products; natural products; inhibitors; aging; obesity; cancer; virtual screening; molecular docking; calculated ADMET



1. Introduction

The mammalian target of rapamycin (mTOR) is a highly conserved phosphoinositide 3-kinase (PI3K-like) Ser/Thr protein kinase (UniProt P42345), which plays an important role in the center of numerous cellular signaling pathways that control the organization of the cell's cytoskeleton, autophagy, metabolism, survival and proliferation, and integrates the growth factor-activated and nutrient-sensing pathways [1]. It is known that mTOR binds to different regulatory subunits and forms two types of protein complexes. First, mTORC1, which is sensitive to rapamycin and is a macrolide antibiotic produced by *Streptomyces hygroscopicus* that forms a complex with the immunophilin FK506 binding protein-12 (FKBP12) (Figure 1), which binds to the FKBP12-rapamycin binding (FRB) domain of mTOR [2] and inhibits its kinase activity [3]. Second, mTORC2, in which mTOR forms a protein complex insensitive to rapamycin [4]. In addition to mTOR, the mTORC1 complex contains the following proteins—regulatory-associated protein of mTOR (RAPTOR), proline-rich Akt substrate 40 kDa (PRAS40), mammalian lethal with Sec13 protein 8 (mLST8), and DEP domain containing mTOR-interacting protein (DEPTOR) [3].

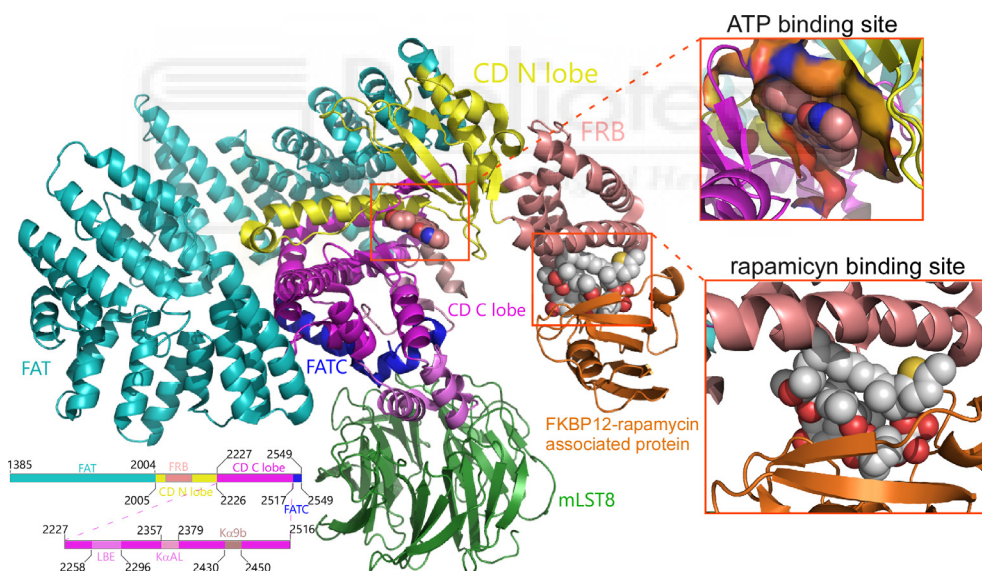


Figure 1. Secondary structure of the mTOR (residues 1376–2549)-SEC13 protein 8 (or mLST8)-FK506-binding protein 12 (or FKBP12)-ATP-rapamycin complex. mTOR presents different colors, indicating its structural domains [2]. mLST8 is colored green, Kc9b is colored orange, and ATP and rapamycin are shown as spheres. CD is the catalytic domain. The ATP and rapamycin binding sites were expanded in the boxes to the right. The figure was constructed using the structural information of the PDBs numbered as 4JSN, 4JSP, 4JSV, 4JSX, 4JT5, 4JT6, 5WBU, 5WBY, 1FAP, 1NSG, 2FAP, 3FAP, 4FAP, 5GPG, 4DRH, 4DRI, and 4DRJ, and PyMol 2.0 software was used.

In the plasma membrane, several receptors (GPCR, G protein-coupled receptor; IGF-R, insulin-like growth factor receptor; IR, insulin receptor) capture the signal transmitted by growth factors and chemokines, which act as positive inputs of the mTORC1 complex, directed mainly through two signaling pathways—PI3K/Akt [5] and Ras/Raf/MEK/ERK [6]. Additionally, nutrients such as glucose or amino acids and the cellular energy status (high ATP:AMP ratio) are inputs positive to the mTORC1 complex [7]. Low cellular energy levels are sensed by AMPK, which sequentially phosphorylates the tuberous sclerosis complex 2 (TSC2) and activates it, leading to the inhibition of the mTORC1 activity [8]. In poorly vascularized tumors, hypoxia conditions are predominant. Therefore, the complete oxidation of glucose to CO₂, to achieve ATP and reduce power (NADH and FADH₂), is impossible. Under these conditions of the lack of O₂, glucose undergoes partial oxidation until pyruvate (glycolysis) in the cellular cytoplasm and the NADH generated is re-oxidized, giving its electrons to pyruvate that becomes lactate (Warburg effect) [9]. These conditions of acidity [10] and hypoxia [11] impede the activity of mTORC1. On the other hand, several extracellular signals [insulin, epidermal growth factor (EGF), vascular endothelial growth factor (VEGF), sphingosine 1-phosphate (S1P), and lysophosphatidic acid] stimulate phospholipase D, which converts phosphatidyl choline (PC) into phosphatidic acid (PA) [12]. PA species with unsaturated fatty acid chains can dissociate DEPTOR from mTORC1 and, thus, increase its activity [13].

An active mTORC1 complex controls protein biosynthesis because it directly phosphorylates two components of the biosynthetic machinery—p70 ribosomal S6 kinase 1 (S6K1-Thr³⁸⁹) and the translation inhibitor eukaryotic translation initiation factor 4E-binding protein 1 (4E-BP1) [14,15]. Only when 4E-BP1 has been phosphorylated, can it be bound to eIF4E. As a result, this protein can be part of the eIF4F complex, which is required for the initiation of a cap-dependent mRNA translation [14]. mTORC1 also controls both membrane lipid biosynthesis, especially through two transcription factors of lipogenic genes, namely, SREBP 1/2 and PPAR- γ , and the genes of the glycolytic pathway [7]. By contrast, mTORC1 is a negative regulator of autophagy because it directly phosphorylates and suppresses some components of the ULK1/Atg13/FIP200 complex, which must remain active to initiate the process of autophagy [16]. In vascularized tumors, mTORC1 plays an important role as a central mediator of signal transducer and activation of transcription 3 (STAT3), hypoxia-inducible factor 1 α (HIF-1 α), vascular endothelial growth factor A (VEGF-A), and angiogenesis, under hypoxia, through several signaling mechanisms [17].

The biology of the mTORC2 complex (DEPTOR, SIN1, RICTOR, mLST8, and PROTOR) is less known but its activity is controlled by the PI3K/Akt and WNT receptors [18] signaling pathways. mTORC2 regulates the organization of the actin in the cytoskeleton, through various effectors, such as paxillin, Rho GTPases, or PKC- α . Additionally, mTORC2 controls diverse cellular processes, such as metabolism, survival, apoptosis, and growth, through the phosphorylation of various effectors; particularly, it directly phosphorylates two other protein kinases, Akt-Ser⁴⁷³ and serum- and glucocorticoid-induced protein kinase 1 (SGK1) [7].

It was described that the deregulation of the signaling pathways, both upstream and downstream of the mTORC1/mTORC2 is implicated in various diseases, such as aging, autoimmune disorders, neurodegenerative diseases, diabetes mellitus type II, obesity, and cancer [19]. Several epidemiological studies have related obesity to a high incidence of gastrointestinal cancers (esophageal, gastric, pancreatic, and colorectal) [20]. The mTOR signaling pathway plays an indispensable role in the regulation of adipose tissue functions, such as adipogenesis, thermogenesis, or lipid metabolism. Therefore, its modulation is important in the control of obesity, which is generated in circumstances of an abundance of nutrients [21].

Currently, different pharmacological options have been developed to inhibit mTOR, producing three generations of mTORC1 inhibitors, and their therapeutic efficacy and side effects are different in each case [22]. Both rapamycin and its chemical derivatives belong to the first generation of mTORC1 inhibitors. Despite being approved for the treatment of different types of cancer, they only cause stabilization of the disease, and not a tumor regression. That is, they behave as cytostatic and not as cytotoxic [22]. In addition, its continued clinical use causes numerous adverse effects, including suppression of the immune system, renal, dermatological, and hematological toxicity, and reduction of male fertility. Thus, in the current abundant clinical trials with rapalogs, their combination is sought, in lower doses, with other chemotherapy or radiotherapy agents to improve outcomes and overcome resistance [23]. The second generation of the mTOR inhibitors inhibits the catalytic kinase domain as ATP-competitive inhibitors and, therefore, controls the activity of both mTORC1 and mTORC2. Due to the structural similarities of the catalytic domain within the protein kinase superfamily [24], ATP-competitive inhibitors also block other kinases [25]. Additionally, various resistant mutations that interfere with drug-binding in the mTOR, have been described in both rapalogs and kinase inhibitors [26]. A third, new-generation of mTOR inhibitors is in experimental development to eliminate the resistance, and they consist of a bivalent drug that can bind simultaneously to the catalytic and regulator sites of the mTOR [26].

Considering the above-mentioned perspectives, the development of drugs targeted to mTOR, in gastrointestinal cancers associated with obesity or anti-aging, is an open field. Given the abundant structural information on the catalytic and regulator domains of mTOR, we have carried out an *in silico* study, to identify new potential inhibitors. We have used molecular docking techniques to select candidates among the compounds contained in the databases of marine natural products [27], Super Natural II [28], and ZINC natural products [29]. The compounds that showed the best binding scores were subsequently filtered using criteria from pharmacodynamics, pharmacokinetics, and toxicity properties. In a later step, we grouped the compounds with a structural similarity greater than or equal to 70%, to choose candidates to test *in vitro* that are representative of each cluster. We have tested the cytotoxic and inhibitory capacity of some compounds designed against the rapamycin binding site of the mTOR.

2. Results

2.1. Analysis of Compounds Docked to ATP and the Rapamycin Binding Sites of the mTOR Catalytic Domain

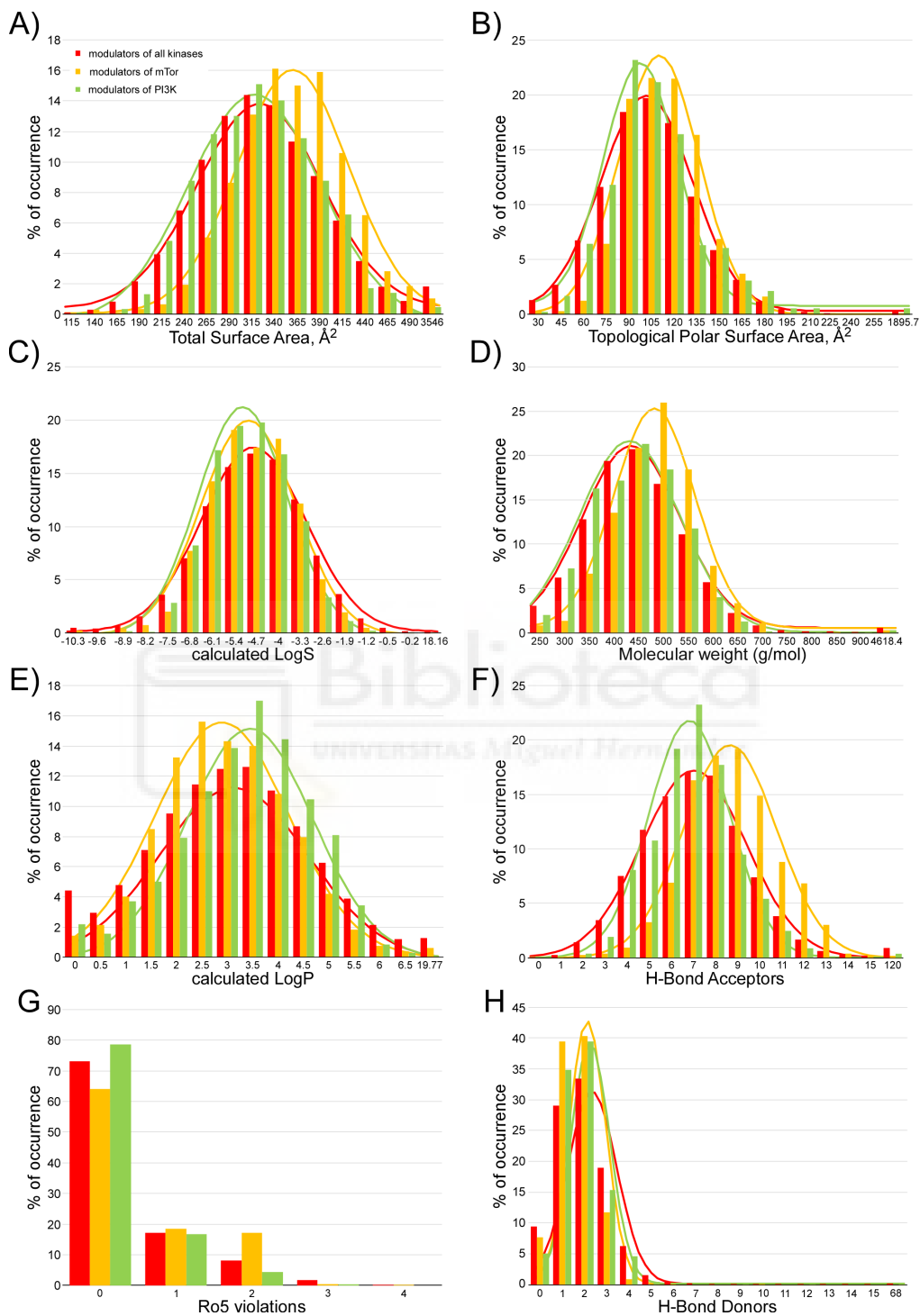
The molecular docking experiments aim to make a first selection of compounds with a low Gibbs free energy variation value (ΔG , kcal/mol), and then of potentially higher affinity, starting from a library of 484,527 compounds (including 14,442 from Marine Natural Products [27], 144,766 from ZINC natural products [29], and 325,319 from Super Natural II [28]). We have used all the structures available, thus far, to carry out the molecular docking at both of the ATP binding site (4JSN, 4JSP, 4JSV, 4JSX, 4JT5, 4JT6, 5WBU, 5WBY) and rapamycin (1FAP, 1NSG, 2FAP, 3FAP, 4FAP, 5GPG, 4DRH, 4DRI, 4DRJ) binding site. The data calculated after the molecular docking, presents, for each compound, up to twenty poses of that compound, bound to each of the explored binding site (ATP or rapamycin binding sites, see Figure 1) for all of the above-mentioned structures; likewise, ΔG was calculated. For each compound, we chose the pose with the lowest ΔG against each structure and expressed the values as the means and standard deviation. The calculated K_D ($K_D = \exp^{\Delta G/RT}$) for compounds with $\Delta G \leq -11$ kcal/mol is in the subnanomolar range that was used as a threshold to filter the docking results [30–32]. When the results obtained for the rapamycin binding site were analyzed, 4.8% (692 compounds) of the marine natural product database had an average ΔG value less than or equal to -11 kcal/mol. More than 10% (33,635 compounds) of the Super Natural II had a $\Delta G \leq -11$ kcal/mol, and only 0.098% (142 compounds) of the ZINC natural product database met that condition. Only 0.25% (820 compounds) of the Super Natural II had a $\Delta G \leq -13$ kcal/mol. Analysis of the molecular docking data on the ATP binding site revealed a low number of compounds with a $\Delta G \leq -11$ kcal/mol, only twenty-three from the marine natural product database and a hundred and seven from the Super Natural II database. The average $\Delta G \pm SD$ values for these compounds can be found in the supplementary material (Supplementary Tables S1–S5). Although we filtered the complete chemical library, considering the molecular docking data, we only discarded 89.4% of the compounds. Obviously, additional filters are needed until an approachable number of candidate compounds are obtained to be tested *in vitro*. The existence of a suitable ADMET (absorption, distribution, metabolism, excretion, and toxicity) profile for the initially selected compounds, will constitute the second filter, before proposing the compound candidates as the mTOR inhibitors.

We analyzed different parameters of the ADMET profile of compounds that bind to different protein kinases—in many cases, drugs for clinical use—and for which experimental data were recorded in the bindingDB [33]. At the time of preparing Figure 2, the search terms ‘protein kinase’, ‘mTOR kinase’, and ‘PI3K’ generated 125,289, 4258, and 2883 results, respectively, in the bindingDB database (<https://www.bindingdb.org/bind/as.jsp>). The 3D chemical structure of these compounds was downloaded from the bindingDB; for each, the fourteen parameters

represented in Figure 2, were calculated. As shown in Figure 2, thirteen of the fourteen analyzed parameters showed a Gaussian distribution at a frequency where 80%–90% of the values of these parameters varied by the total surface area (A), topological polar surface area (B), calculated LogS (C), molecular weight (D), calculated logP (E), hydrogen-bond acceptors (F), violations of Lipinski's rule of five (G), hydrogen-bond donors (H), drug likeness (I), drug score (J), calculated Caco-2 permeability (K), calculated rat acute toxicity (L), calculated *Tetrahytnema pyriformis* toxicity (M), and calculated fish toxicity (N). The extreme values of these Gaussian distributions will be used as a screening filter for candidate compounds against the mTOR kinase activity. Only compounds that present the fourteen analyzed parameters, with values included between the extreme values of the Gaussian distributions, were selected after the application of this second filter. The minimum and maximum values of the fourteen parameters analyzed were as follows: 140 to 490 for the total surface area, 30 to 195 for the topological polar surface area, -13 to 0.2 for the calculated LogS, 250 to 750 for the molecular weight, -1 to 6.5 for the calculated logP, 0 to 13 for hydrogen-bond acceptors, 0 to 7 for hydrogen-bond donors, -10 to 10 for drug likeness, 0.05 to 0.8 for drug score, -0.16 to 1.8 for the calculated Caco-2 permeability (LogPapp, cm/s), 2 to 3.15 for the calculated rat acute toxicity (LD50, mol/kg), 0.1 to 1.1 for the calculated *Tetrahytnema pyriformis* toxicity (pIGC50, µg/L), and 0.8 to 2 for the calculated fish toxicity (pLC50 mg/L). Up to two violations of Lipinski's rules were admitted. After selecting only those compounds whose physicochemical and toxicological parameters mentioned above were within the limit values, the number of candidate compounds for mTOR inhibitors was considerably reduced. Only fifty-one compounds (6 from the marine natural product database [27] and 45 from the Super Natural II database [28]) were selected as candidates for inhibitors whose target was the ATP binding site of the mTOR (see Supplementary Table S6). The number of candidates, for inhibitors against the rapamycin binding site, was also significantly reduced, although their number was higher—445 (137 from the marine natural product database [27], 99 from ZINC natural products [29], and 209 from the Super Natural II database [28]) (see Supplementary Table S7).

Among the compounds proposed as candidates for mTOR inhibitors, high structural diversity was evident, judging by the high number of clusters in which they could be grouped—twenty-six compounds that targeted the ATP binding site and a hundred and six that targeted the rapamycin binding site (see Supplementary Tables S6 and S7). Figure 3 shows the Gibbs free energy variations calculated for the compounds docked to mTOR, against both the ATP and rapamycin binding sites, and are included in Supplementary Tables S6 and S7; in all cases, ΔG values were ≤ -11 kcal/mol. Figure 3A shows the calculated Gibbs free energy variations for the forty compounds approved by the FDA as antineoplastic drugs, after molecular docking experiments against the ATP binding site of both mTOR and PI3K, which is a protein kinase highly related to the mTOR. From these data, two important conclusions were obtained. First, all of the compounds had an almost identical affinity to the ATP binding site of both protein kinases. Second, its affinity was relatively low (about -9 kcal/mol)

compared with that of the candidate compounds included in Figure 3B, with ΔG values ≤ -11 kcal/mol. As shown in Figure 3B, among the compound candidates for mTOR inhibitors, we could distinguish both compounds whose ΔG were practically the same as that of the mTOR and PI3K, and compounds that differed by up to two kcal/mol, of which we would have expected high specificity in the inhibition of both protein kinases. In a recent article [34], it was shown that the compound “9m” showed low nanomolar activity against mTOR ($IC_{50} = 7$ nM) and greater selectivity over the related PIKK family kinases. The authors proposed a binding mode of compound “9m” with the ATP binding site of mTOR. On the other hand, Figure 3C shows the Gibbs free energy variations of compounds docked to the rapamycin binding site; these compounds have been described in the literature as modulators of mTOR and have been obtained from the bindingDB database [33] (4259 compounds, of which the 56 with minor ΔG are shown in the panel (C)). Here, we could distinguish two groups, a group of compounds with a ΔG over -12 kcal/mol and another group with ΔG over -18 kcal/mol. The latter group included rapamycin and its chemical derivatives. The compounds selected as candidates for mTOR inhibitors (Figure 3D–K) have ΔG values that varied between -15 and -11 kcal/mol. Most of the compounds included in the databases, such as Super Natural II, ZINC natural products, and, especially, marine natural products, were not commercially available in adequate quantities and at an affordable price to carry out *in vitro* experiments. In fact, commercial availability was the “third selective filter” of compound candidates for mTOR inhibitors. The definition of clusters of compounds, with up to 70% identity in their structure, was a strategy that enabled the use of at least one representative compound of each cluster to test their inhibitory activity. We have not found examples in the literature of compounds, other than rapamycin or their chemical derivatives, that target the rapamycin binding site to inhibit the enzymatic activity of mTOR. Thus, it seemed conceptually innovative to target this regulatory site with non-rapamycin compounds. Additionally, the observation of its crystalline structure had revealed that its cavity was much larger than that of the ATP binding site. This would explain the greater number of candidate inhibitor compounds that we have found against the regulatory site of the mTOR. Consequently, we selected eleven commercially available compounds (see Figure 4) to test their *in vitro* inhibitory activity on mTOR kinase activity; each of these belonged to different clusters (except for cluster 7) with numerous compounds, of which we chose two compounds.



Cont.

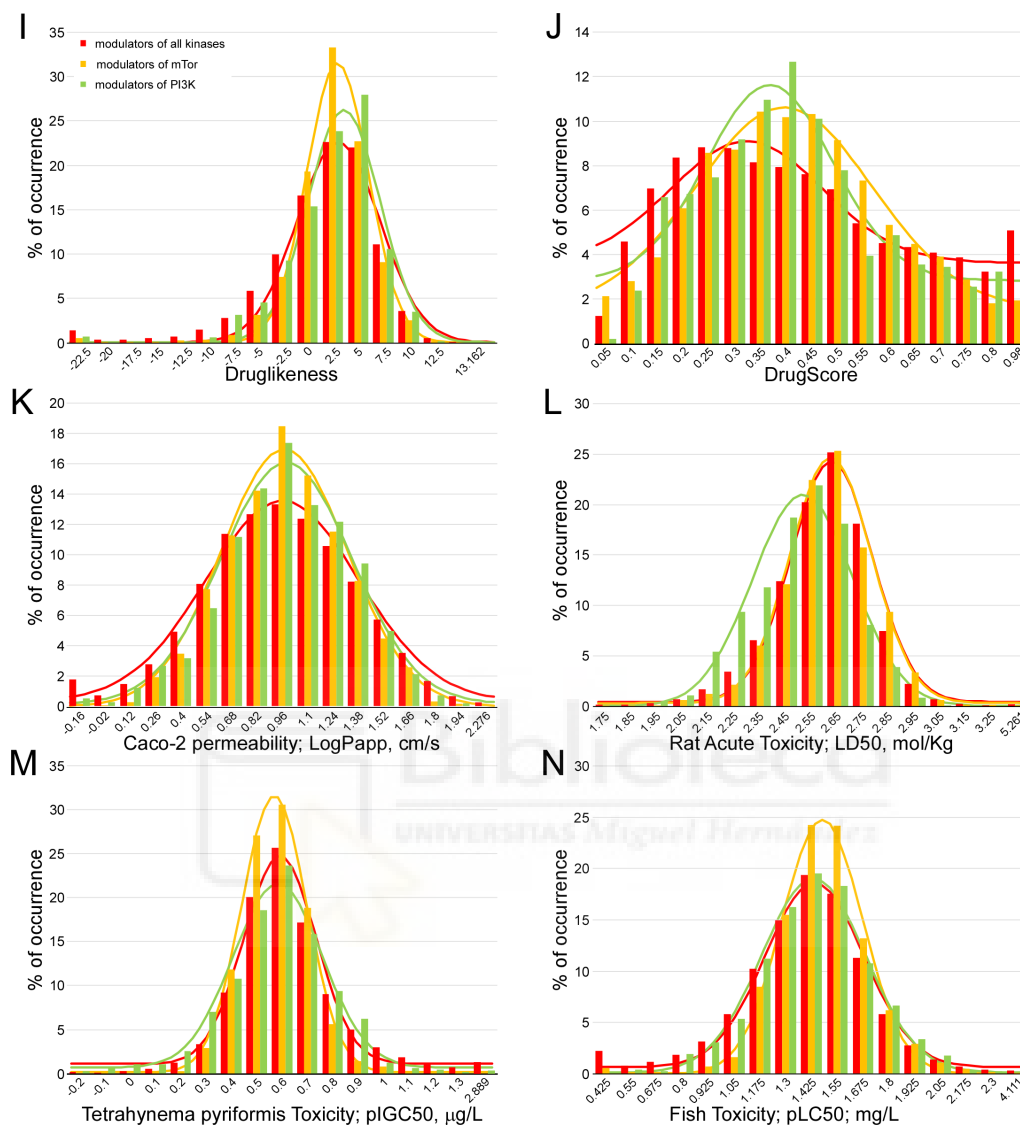


Figure 2. Analysis of the physicochemical and toxicological parameters of compounds that bind to all protein kinases, mTOR and PI3K from the bindingDB (<https://www.bindingdb.org/>) [33]. Gaussian distribution of the frequency of the calculated values for different parameters: Total surface area (A), topological polar surface area (B), calculated LogS (C), molecular weight (D), calculated logP (E), hydrogen-bond acceptors (F), violations of Lipinski's rule of five (G), hydrogen-bond donors (H), drug-likeness (I), drug-score (J), Caco-2 permeability (K), rat acute toxicity (L), *Tetrahynema pyriformis* toxicity (M), and fish toxicity (N).

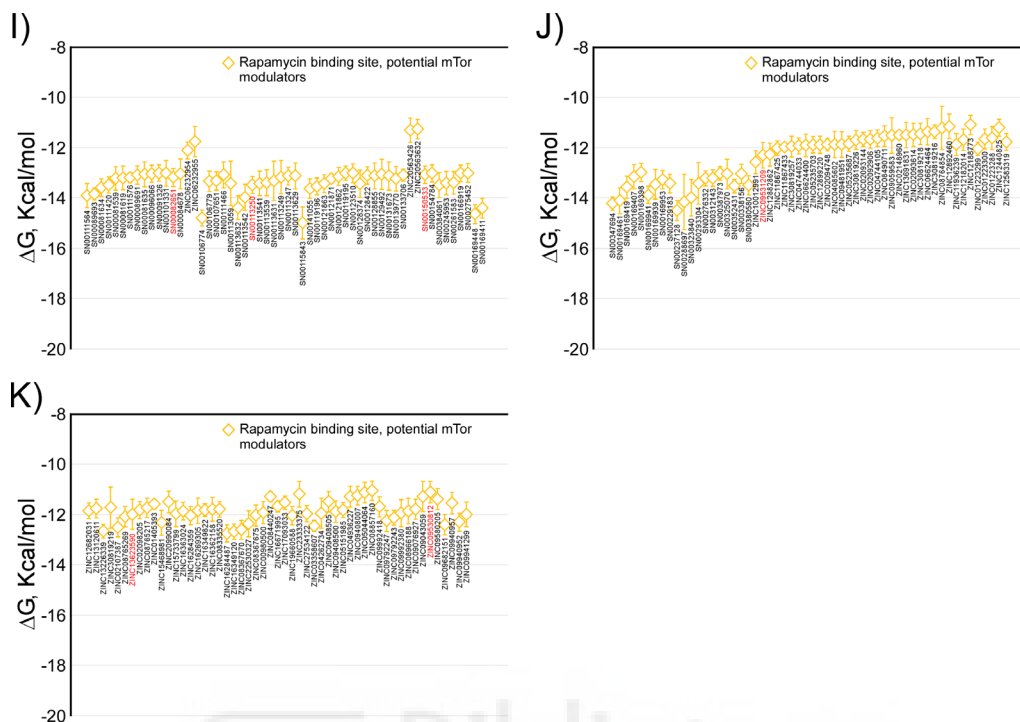


Figure 3. Comparison of the calculated Gibbs free energy variation (ΔG) for the selected inhibitor candidate compounds, against the ATP and rapamycin binding sites of the mTOR kinase. **Panel A** shows the calculated ΔG values for forty compounds approved by the FDA, for clinical use against various types of cancer against the ATP binding site. **Panel (B)** shows the ΔG values of the selected inhibitor candidate compounds against the ATP binding site of mTOR, and the same selected compounds against PI3K. **Panel (C)** shows the calculated ΔG values for fifty-six compounds registered in the bindingDB as mTOR kinase modulators. **Panels (D–K)** show the ΔG values of the selected inhibitor candidate compounds, against the rapamycin binding site of the mTOR. The common name (**A**), CAS number (for marine natural product compounds), Super Natural II, bindingDB (**C**), or ZINC names for all compounds, is indicated below each value, in black, except for the eleven compounds experimentally tested in this study (red color).

The Gibbs free energy variation (ΔG) is a representative value of the number and intensity of the atomic interactions, between the receptor (mTOR) and the docked compound [31]. The molecular docking of a protein target and the small ligand compounds predict the best interaction mode for a defined binding site. AutoDock/Vina, uses in its scoring function, the AMBER force field, which computes the terms of the contributions of van der Waals interactions, hydrogen bonding, electrostatic interactions, conformational entropy, and desolvation [30–32]. Figure 5 shows the molecular interactions between the amino acids of the rapamycin binding site and the inhibitor docked compounds. Details of the atoms involved in each type of interaction can be found in Supplementary Figure S1. In the interaction of each of the

eleven compounds and the amino acids of the rapamycin binding site, hydrophobic interactions were predominant. In addition, most of the compounds that are able to establish hydrogen bonds and, in some cases, saline bridges, (SN00082651, ZINC13623590) were detected (Supplementary Figure S1).

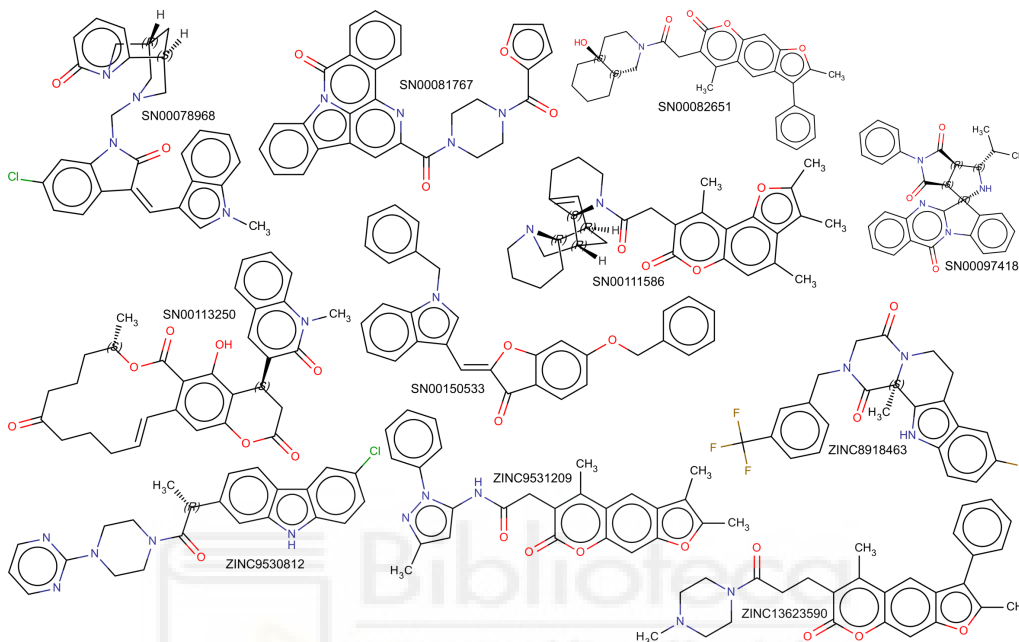
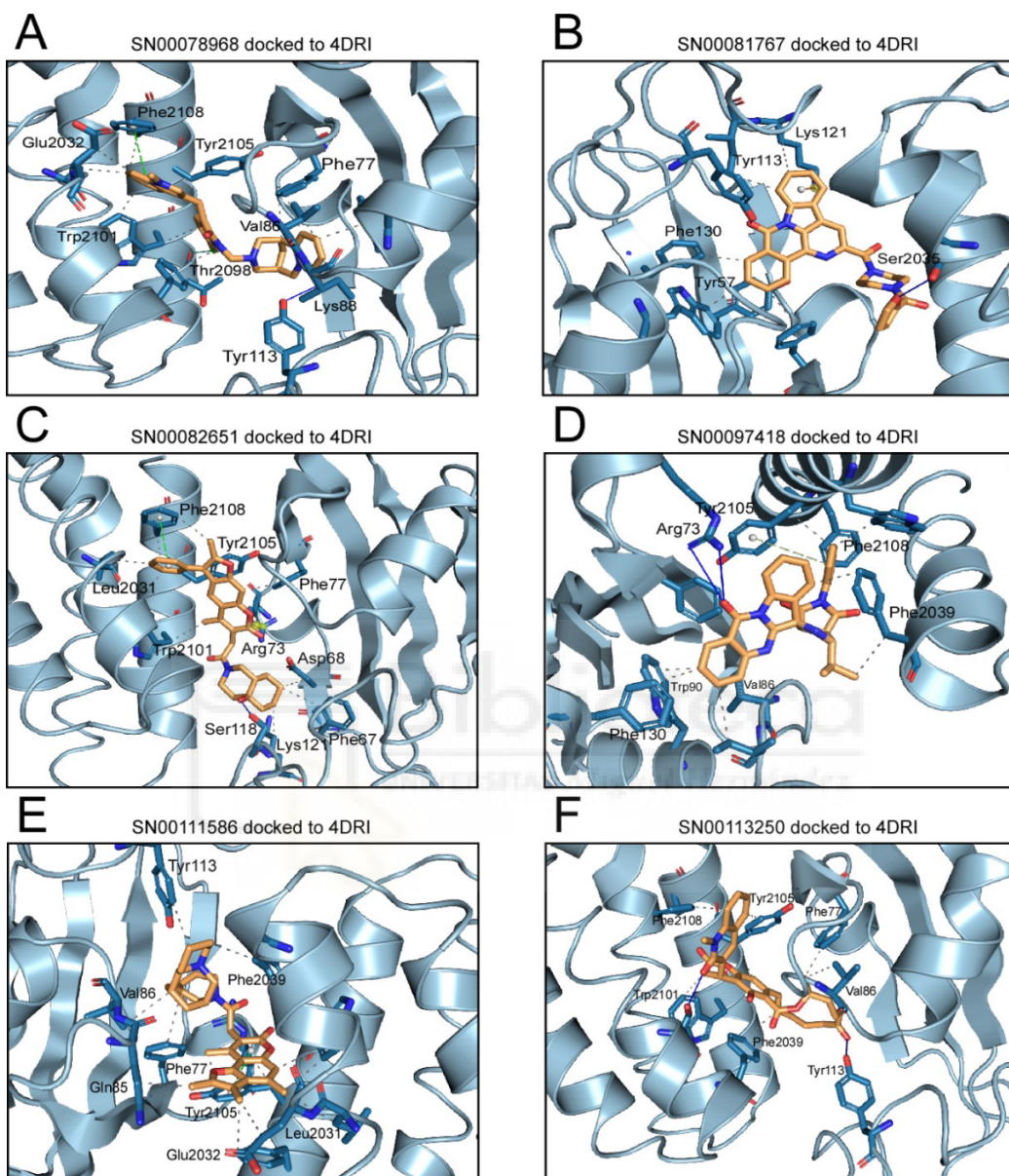


Figure 4. Molecular structure of compounds selected against the allosteric rapamycin binding site of mTOR, and tested experimentally. The name assigned to each compound by the Super Natural II [28] or ZINC database [29], in each case, is close to each structure.



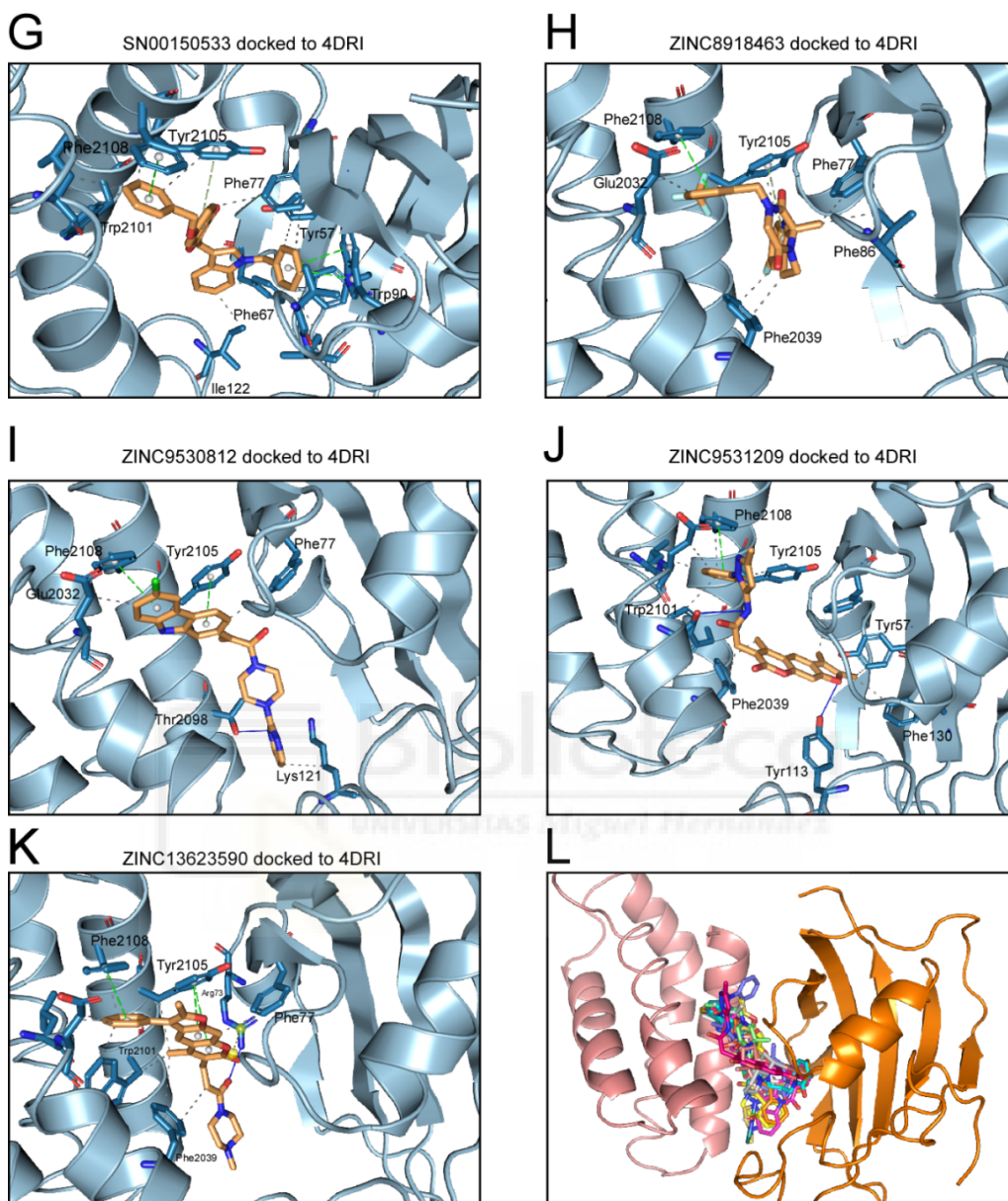


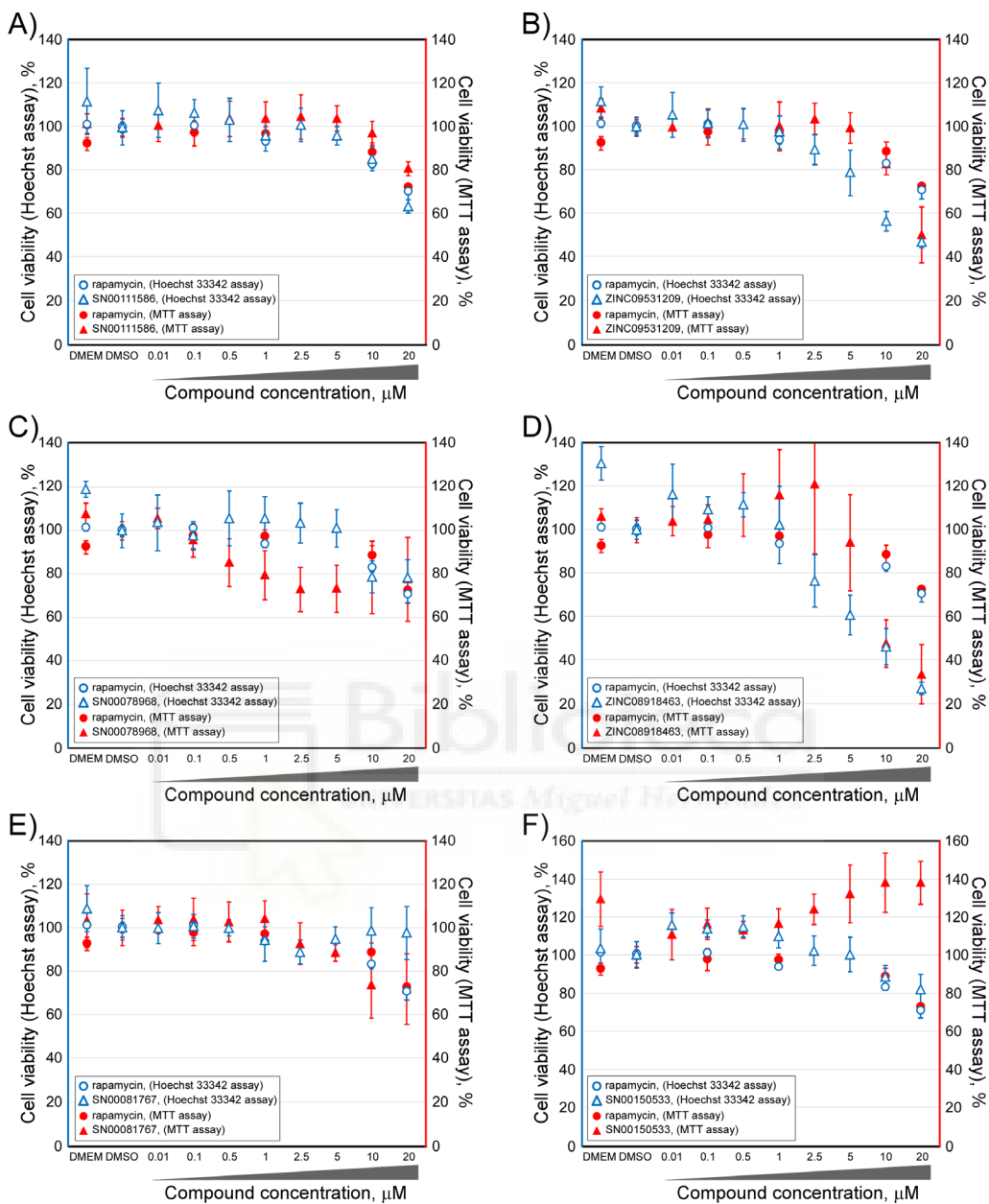
Figure 5. Molecular docking analysis for the 11 selected compounds against the allosteric rapamycin binding site of mTOR, showing the interacting residues of the binding site and each type of molecular interaction. Each panel of this figure has been prepared using the 4DRI structure of mTOR. For each compound docked to the protein, the pose with the lowest ΔG value has been shown. The interactions have been detected with the FLIP algorithm [35]. In each panel the compound analyzed is indicated. Panel L shows the best pose superimposed for each of the eleven inhibitor compounds. The full details of the molecular interactions are shown as supplementary information.

2.2. Determination of the Cell Viability of HCT116 Cells after Treatment with Selected Inhibitor Candidate Compounds

Cellular cytotoxicity induced by the selected experimental compounds was evaluated by both the MTT cell viability assay and by counting the Hoechst-stained nuclei of the HCT116 human colon cancer cell line [36]. For the MTT cell viability assay (Figure 6), HCT116 cells were treated with a range of concentrations of each compound (0–20 μM). In parallel, treatments with equivalent amounts of the corresponding compound solvent DMSO were performed up to a maximum final concentration of 0.5% *v/v*. After 24 h, cell viability was determined by MTT as described in the “Materials and Methods” section [30]. Additionally, and to confirm that the compounds were not cytotoxic, a cell count was performed by taking microphotographs of the Hoechst-stained cells at 4x, using the DAPI imaging filter cube [37] (see also Figure 6). As shown in Figure 6, HCT116 cells were sensitive to all compounds, including rapamycin, at a concentration of 20 μM . At this concentration, cell viability, followed by both techniques, was decreased by 20% to 80%, depending on each tested compound. If we observed the cell viability data in the presence of concentrations no greater than 10 μM , we can establish four groups of compounds. For the compound SN00078968, the maximum non-toxic concentration was 0.1 μM , that for compound SN00097418 was 1 μM , that for the compounds ZINC09531209, ZINC08918463, SN00081767, ZINC13623590, and ZINC09530812 was 5 μM , and, finally, that for the compounds SN00111586, SN00150533, SN00082651, and SN00113250, concentrations higher than 10 μM could not be used. Keeping in mind these maximum values of concentrations, for each compound that showed no cytotoxicity, they were then tested as potential mTOR inhibitors.

2.3. Determination of the Inhibitory Activity of the Selected Compounds against mTOR

Anti Phospho-mTOR (Ser2448) (D9C2) Rabbit mAb detects P-Ser2848 in mTOR. mTOR was phosphorylated at Ser2448 via the PI3K/Akt signaling pathway [38], and was autophosphorylated at Ser2481 [39]. Therefore, P-Ser2481 could be considered a marker of the autokinase activity of mTOR. Proteolysis of poly (ADP-ribose) polymerase (PARP), by caspase, into an 89-kD fragment was utilized as a marker for apoptosis [40,41]. As shown in Figure 7, while PARP cleavage was clearly detected in HCT116 cells treated with 10 μM rapamycin, which induced caspase-mediated apoptosis, only slight PARP cleavage was seen in the same cells treated with lower concentrations (see Figure 7A). As shown in Figure 7, the eleven compounds evaluated showed an inhibitory activity of mTOR, at the doses tested. The inhibition varied between 20% and 40%, with respect to the control, depending on each tested compound and dosage. All the compounds showed a percentage of inhibition, at the tested dose, representing approximately half of the percentage of inhibition that was achieved with the same dose of rapamycin.



Cont.

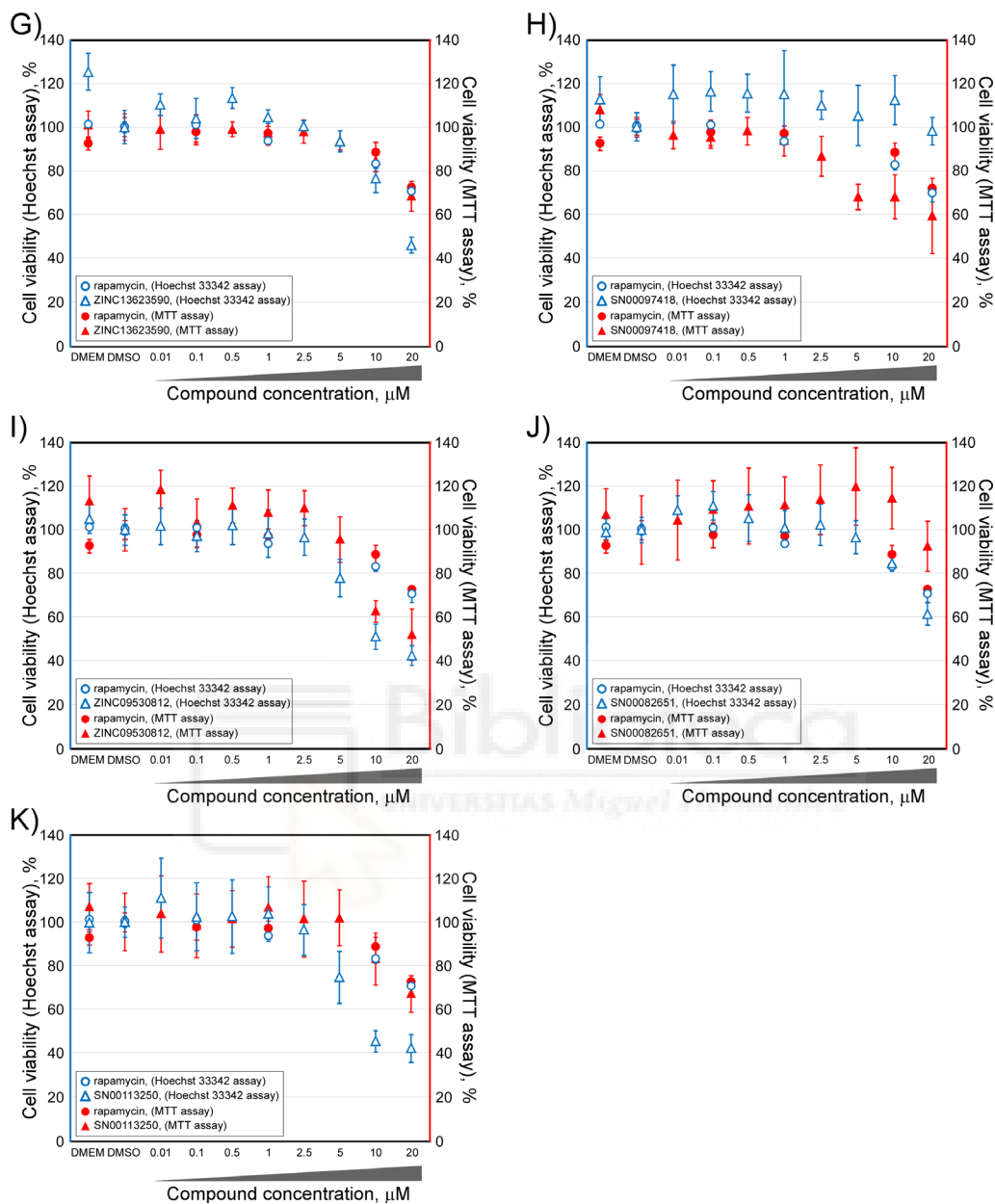


Figure 6. Viability of HCT116 cells after treatment with selected inhibitor candidate compounds, against the mTOR rapamycin binding site, as measured by both the MTT assay (symbols in red color) and counting Hoechst stained-nuclei (symbols in blue color). Each compound was always compared with rapamycin in parallel experiments. Each panel included a legend with the compounds analyzed and methodology followed (MTT or Hoechst stained-nuclei). The values were normalized with respect to media cultured only (DMEM).

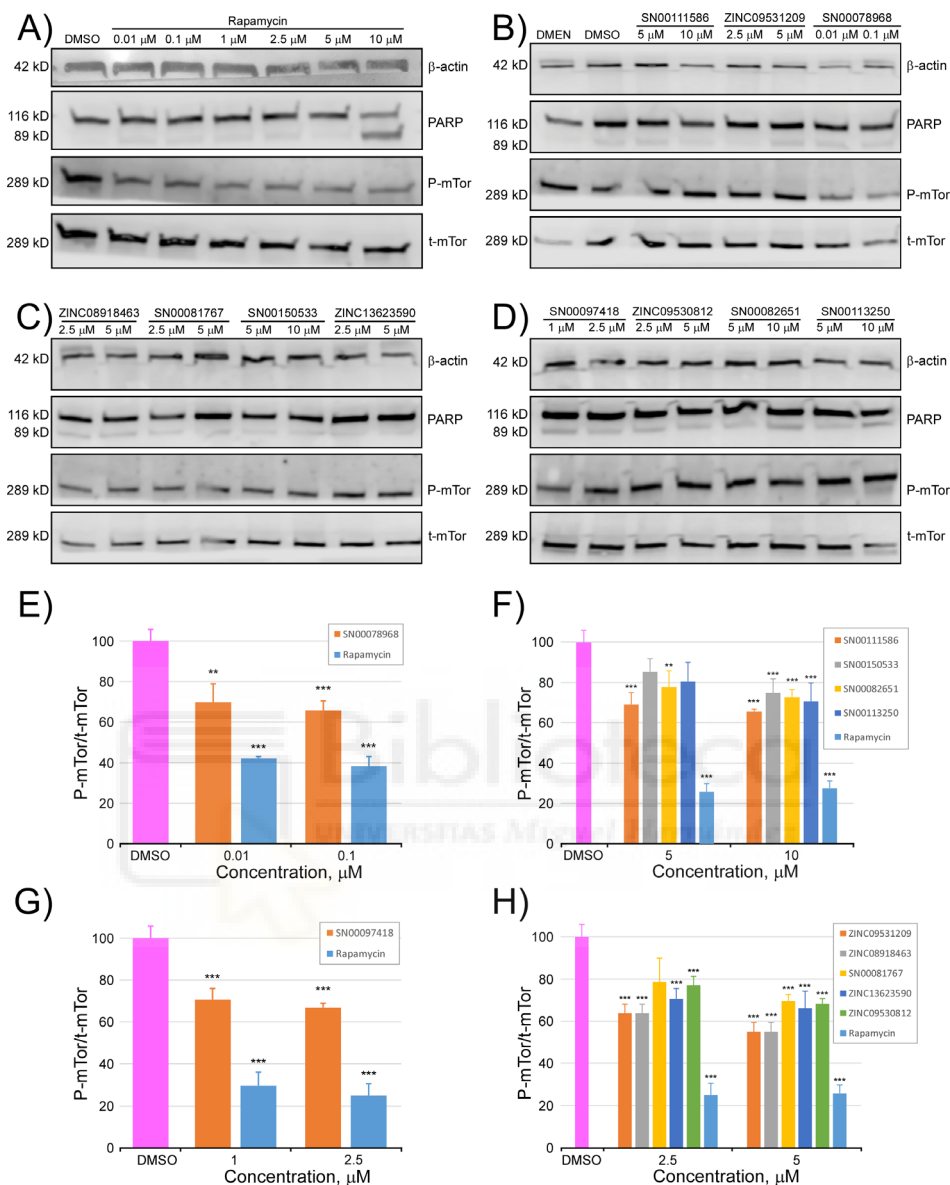


Figure 7. Inhibitory activity of selected compounds against the rapamycin binding site of mTOR. After incubation with different doses of all tested compounds and rapamycin or control medium (DMEM) and the compound vehicle (DMSO), for 24 h, HCT116 cells were lysed and subjected to Western blot analysis of total mTOR (t-mTor) and phosphorylated mTOR (p-mTOR) antibodies (**Panels (A–D)**). Image quantification analysis of the Western blots presented as the ratio of p-mTOR/t-mTOR, in percentage, with respect to the control (DMSO) for the (**E–H**) panels. Levels of PARP (116 KDa) and cleaved-PARP (89 KDa) were detected by Western blotting. β -Actin was used as a loading control. The experiment was repeated four times with similar results. ** $p < 0.01$, *** $p < 0.001$ indicate significant differences compared with the control (DMSO).

2.4. Modulating Effect of Three Marine Extracts on the Activity of mTOR

In addition to the strategy presented thus far in our study, based on the use of mTOR structural information to target to its ATP or rapamycin binding sites with small molecules of known structure, we also used three marine extracts to check the modulatory activity of mTOR (Figure 8). As shown in Figure 8A, the viability in HCT116 cells did not decrease more than 10%, at concentrations of the extracts that did not exceed 10 $\mu\text{g/mL}$ (CR extract), 1 $\mu\text{g/mL}$ (PS extract), and 5 $\mu\text{g/mL}$ (NA extract). Therefore, those maximum concentrations were used to determine their effect on the activity of mTOR. Considering the absence of the 89-kDa fragment of PARP in the blots presented in panel B (CR and PS extracts) and panel E (NA extract), none of the three marine extracts, used at the indicated doses, induced apoptosis. Surprisingly, two of the marine extracts (CR and PS extracts, panels 8C and 8D, respectively) dramatically activated the mTOR activity, increasing the p-mTOR/t-mTOR ratio by more than 50%, with respect to the control. By contrast, the NA extract (Figure 8F) showed an inhibitory effect on the mTOR activity of a similar magnitude (40% decrease with respect to the control), to that described above, for the compounds selected based on molecular docking and ADMET profiling experiments.



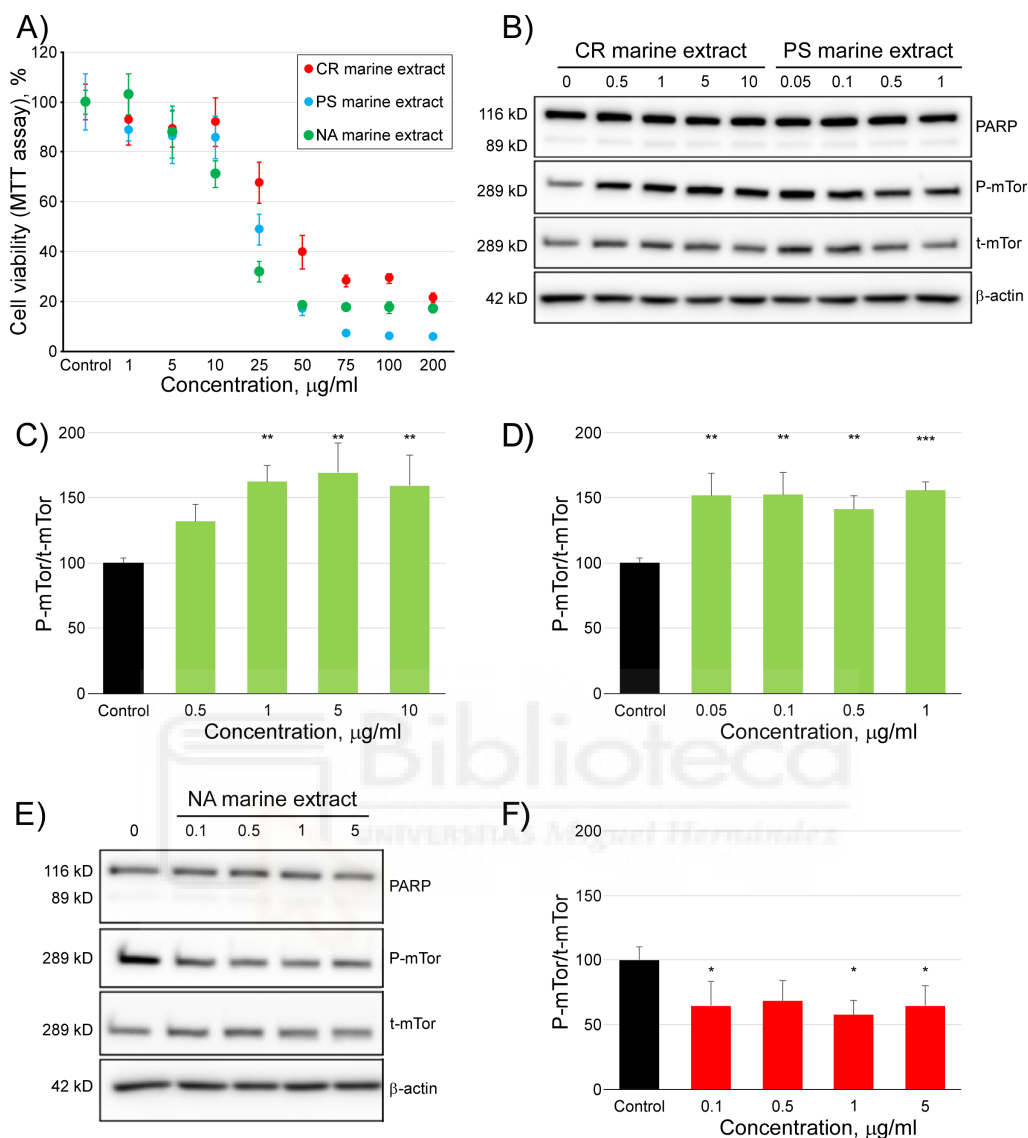


Figure 8. Analysis of the modulatory activity of three marine extracts on the activity of mTOR. **Panel (A)** shows the viability of HCT116 cells, after treatment with marine extracts against mTOR, followed by the MTT assay. After incubation with different doses of all the tested marine extracts or control [compound vehicle (DMSO)] for 24 h, HCT116 cells were lysed and subjected to the Western blot analysis of total mTOR (t-mTOR) and phosphorylated mTOR (p-mTOR) antibodies (**Panels B,E**). Image quantification analysis of the Western blots presented as the ratio p-mTOR/t-mTOR, in percentage, with respect to the control for the (**Panels C,D,F**). The levels of PARP (116 KDa) and cleaved-PARP (89 KDa) were also detected by Western blotting. β -actin was used as a loading control. The experiment was repeated four times with similar results. * $p < 0.05$, ** $p < 0.01$, and *** $p < 0.001$ indicate significant differences compared with the control.

3. Discussion

Kinase proteins play a predominant regulatory role in cell biology because they can reversibly modify the activity of a protein, by increasing or decreasing its activity, which may involve the alteration of other biological activities. Additionally, the same kinases can be phosphorylated at different amino acids, and, in some cases, can be stimulators, while others can behave as inhibitors [24]. In the cell, protein kinases exist in the basal state and are only activated, when necessary, by very varied stimuli. Given their involvement in multiple functions of cell biology, the deregulation of their activity leads to important pathologies, such as cancer, aging, and inflammatory disorders. Thus, kinase proteins have become important pharmacological targets, and the development of inhibitory drugs is an important scientific and medical activity against human disease. Additionally, the constant appearance of mutations generates resistance to inhibitory drugs, representing a scientific challenge of the first order because of the health implications that this entails.

The resolved structure from the X-ray diffraction data of the catalytic domain of the protein kinases showed the existence of an N-ter lobe and another C-ter that formed a cleft which served as a binding site for ATP and Mg^{2+} . Most kinase inhibitor drugs have this cavity as a target, and this supposes a problem of specificity when it is necessary to selectively modify the enzymatic activity of a particular protein kinase and probably contributes to the development of side effects. To support this assertion, we have carried out molecular docking experiments against the ATP binding site of the catalytic domain of 12 protein kinase and have found the best docking for forty drugs approved by the FDA, for use as antineoplastic drugs. Supplementary Figure S6 show the calculated ΔG (affinity) of the binding of these drugs to the ATP binding site. These values show that there are no significant differences for any of the molecules tested, with respect to their affinity for the ATP binding site in the twelve analyzed kinases. Thus, in our opinion, it would be more effective, from a therapeutic point of view, to develop inhibitors that target unique binding sites of each protein kinase. These regulatory sites, in many cases, have not yet been described. However, in the case of mTOR, the rapamycin binding site is known and allows specific inhibition of the mTORC1 complex, not the mTORC2 complex, which is insensitive to this drug.

Aiming to identify protein kinase targets that are different from the ATP binding site, we had, in our favor, that many kinases present modular domains (SH2, SH3) of temporary binding to other proteins or to themselves, especially, different sites of interaction with other proteins, that are involved in the formation of active complexes (this is the case of mTORC1 and mTORC2) or in the transmission of information in signaling cascades. In principle, the breakdown of any of these protein-protein interactions might be of therapeutic interest [42,43]. Although, in this work, we presented candidate compounds for mTOR inhibitors, targeted on the ATP binding site (Figure 3B and Supplementary Table S6), consistent with these ideas, we have only tested, *in vitro*, the inhibitory activity of those designed against the rapamycin binding allosteric site (Figure 3D–K and Supplementary Table S7).

In this study, we have presented up to a hundred and thirty-seven compounds of marine origin as candidates for inhibitors targeted to the rapamycin binding site. However, we could not test them all experimentally because of their lack of commercial availability. Although our group is making efforts to offer the scientific community information on the structures of marine natural compounds [27] (with more than 14,000 compounds) and there are also commercial databases available, such as MarinLit (<http://pubs.rsc.org/marinlit>) with more than 28,000 compounds in 2016, experimentation with pure compounds or enriched extracts is not easy. In our case, collaboration with the private sector allows access to the marine extracts of various species, for which we must characterize their molecular composition and determine their possible biological effects. This is the case of the three marine extracts presented in this study that has enabled the discovery of two extracts with activating capacity and one with inhibitory capacity on the mTOR protein kinase. Marine environments are largely unexplored in their biodiversity, however, undoubtedly, they harbor a huge source of potentially bioactive compounds that will allow the development of new products of interest in the pharmaceutical, food, cosmeceutical, and chemical industries. Despite these difficulties, eight marine natural products have been approved by the FDA as drugs, five of them against cancer, and twelve currently in different phases of clinical trials [27,44].

The computer-aided drug design methods accumulate a long experience in the development of small molecules with therapeutic action and reduce costs compared with high-throughput experimental screening approaches alone [45]. The experimental data that we showed in this study were consistent with this statement. In our case, we have explored a chemical library of 484,527 compounds and have proposed 491 compounds (51 against the ATP binding site and 445 against the rapamycin binding site) as candidate compounds inhibitors of mTOR. Among these candidates, we chose eleven to test their *in vitro* activity, and all of them showed the inhibitory capacity of mTOR. In our opinion, much of this success was due to the strict definition of the suitable filters to select the candidate compounds. In particular, developing a filter based on the statistical behavior of the calculated physico-chemical and toxicological parameters (ADMET profile, see Figure 2), for compounds registered in the bindingDB database [33] as protein kinase modulators, has made the difference between success and failure.

In our study we presented compounds capable of reducing *in vitro* the activity of mTOR by 20% and 40% (Figure 7), while rapamycin reached 60%, at similar concentrations and in the same cellular system tested. We wondered about the possibility of these compounds being potential candidates for further preclinical studies. mTORC1 is rapamycin sensitive and acts as a major checkpoint that coordinates the balance between cell growth and autophagy [46]. The control of mTOR activity has interest in cancer [1], obesity [21], and aging [46,47]. At the time of writing this manuscript the search term 'rapamycin' generated 1972 results in the National Institutes of Health clinical trials database (<http://clinicaltrials.gov>). These data are indicative of the clinical interest in this drug and anticipates abundant scientific

information on its desirable and adverse effects. However, available clinical trials indicate that the blocking of mTORC1 with rapalogs shows considerable adverse effects. In addition, mTORC1 is ubiquitously expressed, reducing its effectiveness to focused therapies [22]. The use of rapalogs has demonstrated the existence of abundant side effects—dermatological, metabolic, renal, hematological, and respiratory toxicities, among others [48,49]. Trials in preclinical cancer models are promising but their clinical use does not generate the expected results [50]. Several reasons may explain the limitations of targeting mTORC1 in cancer therapy—resistant mutations of mTOR, activation of alternate proliferative signaling pathways, and intratumoral heterogeneity of mTOR activity, among others [22].

Given this scenario, the answer to the previous question is necessarily affirmative. In the same sense and in relation to the association between the hyperactivation of mTOR and aging, the development of new molecules that partially inhibit this kinase has an interest not only in basic science but also as possible therapeutic applications. The exhaustion of stem cells in their tissues of origin is considered the primary cause of aging. This is understood as the functional decline of cells/organs or the accumulation of damage, and is induced by various mechanisms, including the increased expression of inhibitory factors of the cell cycle or DNA damage, among others [51]. There is still much to learn about the molecular mechanisms that lead to aging, but the implication of changes in different signaling pathways with aging, is known and includes TGF- β , p38 MAPK, JAK/STAT, Delta/Notch, PI3K, and, of course mTOR, which represents a point of interconnection between these ways [47]. Various evidence has maintained that like caloric restriction, without reaching malnutrition, inhibition of mTORC1 can have similar beneficial effects on several pathologies related to age in rodents, and in some cases, humans [47]. The existing scientific evidence shows that inhibition of mTORC1 with rapamycin is currently the only pharmacological treatment that increases lifespan in all model organisms studied—invertebrates, yeasts or rodents [52]. Progress on this matter allows us to be optimistic about the possibilities of finding the mechanisms to delay human aging. Nevertheless, precautions must be taken because many side effects are associated with the use of rapalogs, thus, research on this direction should be promoted in the discovery of new mTOR inhibitors.

Finally, although the main purpose of our study was focused on finding mTOR inhibitors, we have also found two marine extracts with *in vitro* activating activity of this kinase (Figure 8B–D). In the literature, few chemical activators of mTOR have been described [53,54]. Oxidized low-density lipoprotein inhibits mTOR and induces autophagy and apoptosis in vascular endothelial cells, which play very critical roles in cardiovascular homeostasis [54]. CR and PS extracts increase the activity of mTOR in a proportion similar to compound 3BDO [54] and do not induce apoptosis. Our laboratory studies the characterization of its chemical composition and its effects on different cell types (manuscript in preparation).

4. Materials and Methods

4.1. Protein Structures of Human mTOR and PI3K Proteins and Chemical Libraries for Molecular Docking

By now, various crystal structures of the mTOR protein (UniProt P42345) have been resolved and deposited in the Protein Data Bank. This has enabled the exploration of both the ATP binding site (4JSN, 4JSP, 4JSV, 4JSX, 4JT5, 4JT6, 5WBU, 5WBY) and rapamycin binding site (1FAP, 1NSG, 2FAP, 3FAP, 4FAP, 5GPG, 4DRH, 4DRI, 4DRJ), in molecular docking experiments, in which we use all available structures. The virtual screening of ligands is more reliable if the flexibility of the receptor protein is considered. Thus, we have used multiple crystallographic receptor conformations to perform the molecular docking experiments [55]. The molecular docking experiments on the catalytic site of PI3K (UniProt P48736) have been carried out on the twenty-four (1E8Y, 6AUD, 4ANV, 3L54, 4WWO, 4ANW, 4HVB, 1E8Z, 3ENE, 4WWP, 3LJ3, 4GB9, 5G55, 4FUL, 5JHB, 2CHX, 2V4L, 3R7Q, 3T8M, 3ZVV, 5JHA, 3APC, 3APD, and 3ML9) resolved structures from X-ray data available in the Protein Data Bank.

Molecular docking experiments allow virtual screening of potentially modulating ligands of a given target because they prioritize certain compounds to be experimentally tested. Therefore, in these experiments, they require mining of long collections of chemical compounds. We have used a library of marine natural products (14,442 compounds) [27], ZINC natural products (144,766 compounds) [29] (<http://zinc.docking.org/browse/catalogs/natural-products>), and the SuperNatural II database (325,319 compounds) [28]. The 3D structures in the sdf format of all compounds tested are available at <http://docking.umh.es/downloaddb> (Chemical libraries: 2 for Super Natural II, 7 for marine natural products, and 8 for ZINC natural products) [30–32]. Mol2 files were converted to the pdbqt format, using the Python script “prepare_ligand4.py”, included into the AutodockTools-1.5.7.rc1 [56].

4.2. Molecular Docking Procedure

Before starting the molecular docking procedure, all structures of both the mTOR and the PI3K (see above for the PDB code) were submitted to geometric optimization, using the repair function of the FoldX algorithm [57]. To perform docking with AutoDock/Vina software v1.1.2 [58], the receptor and ligand structures were transformed to the pdbqt file format, which included atomic charges, atom-type definitions, and for the ligands, the topological information (rotatable bonds) [31,32]. A grid with dimensions of $23 \times 23 \times 23$ points was centered to the co-crystallized ligands to ensure the coverage of the binding site of the structure. AutoDock/Vina was set up on a Linux cluster at lusitania2.cenits.es Linux cluster (Research, Technological Innovation and Supercomputing Center of Extremadura [CenitS]). AutoDock/Vina generated a conformer docked to the binding site in the protein, for each tested ligand, and calculated the Gibbs free energy variation of the binding process. Compounds with

lower ΔG (kcal/mol) outperformed a first screening filter, as potential candidates for inhibitors [31,32].

4.3. Calculation of the Pharmacokinetic Parameters and Potential Toxicity Properties of the Inhibitor Candidates

Physicochemical parameters for the best docked compounds were calculated, as described previously [31,32], using DataWarrior v4.7.2 software (Allschwil, Switzerland) [59]. The ADMET (absorption, distribution, metabolism, excretion, and toxicity) properties were calculated using the admetSAR [60] web application and the DataWarrior v4.7.2 [59].

4.4. Chemical Compounds against mTOR Kinase Activity

The compounds with the SuperNatural II IDs SN00097418, SN00078968, SN00082651, SN00111586, SN00081767, SN00150533, SN00113250; and ZINC database IDs ZINC09531209, ZINC13623590, ZINC08918463, ZINC09530812 were purchased from the chemical supplier MolPort (supplier references MolPort-005-910-351, MolPort-000-853-506, MolPort-006-316-888, MolPort-000-849-049, MolPort-002-535-101, MolPort-002-649-206, MolPort-028-854-639, MolPort-000-853-173, MolPort-002-672-346, MolPort-002-523-849, MolPort-005-913-128, respectively), at <https://www.molport.com/>.

4.5. Preparation of Marine Extracts

Based on observations of inter and intra-specific competition in experimental aquariums and searches on bibliographic bases, four species of marine invertebrates were chosen for their potential as producers of compounds with anticancer potential. The selected species were composed of one soft coral (CR from *Carotalcyon* sp.), one nudibranch (NA from *Phyllidia varicosa*), and one holothurian (PS from *Pseudocholochirus violaceus*), and were obtained from the distributor company of marine species, Todo Pez S.L., Alicante, Spain.

4.6. Cell Culture and Treatment

Rapamycin and MTT were purchased from Sigma-Aldrich, St. Louis, MO, USA. High-glucose Dulbecco's Modified Eagle's Medium, penicillin-streptomycin, fetal bovine serum and 0.05x trypsin/ethylene diamine tetra acetic acid was purchased from Invitrogen Life Technologies (Carlsbad, CA, USA).

The human colorectal carcinoma cell line HCT116 was purchased from the American Type Culture Collection (ATCC, MN, USA) and was maintained in Dulbecco's modified Eagle's medium (DMEM), supplemented with 10% heat inactivated fetal bovine serum (FBS), 100 U/mL of penicillin and 100 g/mL of

streptomycin. Cells were incubated at 37 °C, in a humidified atmosphere, containing 5%/95% of CO₂/air.

4.7. Cytotoxicity Assays

Cells were plated in 96-multiwell culture plates, at a density of 5×10^3 cells/well. After 24 h of incubation with the crude extract, MTT was added at a final concentration of 0.5 mg/mL and was incubated for 3 h. Next, the medium was removed, and the formazan crystals were dissolved in DMSO. Absorbance was measured at 490 nm, subtracted at 670 nm in a microplate reader (SPECTROstar Omega, BMG Labtech, Germany). OD values were expressed in percentages relative to the control group, consisting of untreated cells. Cell viability was calculated by the formula: $100 \times (\text{treated-cell absorbance} / \text{control-cell absorbance})$. All experiments were performed in triplicate, and the results were shown as the means with SD, calculated from three different experiments.

4.8. Quantification of the Total mTOR and Phosphor-mTOR Levels

After treatment, the cells were lysed with a lysis buffer—radioimmunoprecipitation assay buffer (RIPA Buffer) (BioRad Laboratories Inc.), for 60 min at −20 °C. The lysate was centrifuged at 13,200 rpm for 20 min; the protein concentration in the supernatant was spectrophotometrically determined using the Thermo Scientific Pierce Kit (BCA Protein assay kit), at 562 nm. Protein samples were diluted with the loading buffer (0.5 M Tris HCl at pH 6.8, 10% glycerol, 10% w/v SDS, 5% β₂-mercaptoethanol, 0.05% w/v bromophenol blue) and then were boiled for 5 min. Proteins (30 μg/lane) and prestained standards (Thermo Fisher Scientific, Waltham, MA, USA) were loaded onto 4%–15% SDS precast polyacrylamide gels (BioRad Laboratories Inc.).

After electrophoresis, the resolved proteins were transferred from the gel to nitrocellulose membranes. A blotting buffer (20 mM Tris/150 mM glycine, pH 8, 20% v/v methanol) was used for the gel and for membrane saturation and blotting. The transblotted membranes were washed thrice with Tris buffered saline (TBS), containing 0.05% Tween 20 (TBST). After blocking with TBS containing 5% non-fat milk, for 60 min, the membranes were incubated with the appropriate primary antibodies (PARP Antibody #9542, Phospho-mTOR (Ser2448) (D9C2) XP Rabbit mAb #5536 and mTOR Antibody #2972) (Cell Signaling Technology Inc. Beverly, MA, USA) at 1:1000 dilution (with the exception of anti-β-actin antibody (Sigma-Aldrich, St. Louis, MO, USA), at 1:4000) in TBST–5% low fat milk at 4 °C overnight. The membranes were washed three times with TBST (15 min each) and then were incubated with the secondary antibody anti-human PARP, Phospho-mTOR and mTOR 1:2000, horseradish peroxidase (HRP)-conjugate (Cell Signaling Technology Inc.), for 3 h. The bands were visualized by enhanced chemiluminescence (Licor; Lincoln, NE, USA).

4.9. Statistical Analysis

Values are represented as the mean \pm standard deviation (SD). The values were subjected to statistical analysis (one-way ANOVA, and Tukey's test for multiple comparisons/non-parametric approaches). The differences were considered to be statistically significant at $p < 0.05$. All analyses were performed using the Graph Pad Prism 6 (GraphPad Software, Inc., La Jolla, CA, USA). * $p < 0.05$, ** $p < 0.01$, and *** $p < 0.001$ on the bars, indicate statistically significant differences, compared to the control, unless otherwise stated. All cellular measurements were performed in four-fold, unless otherwise specified.

Supplementary Materials: The following are available online at www.mdpi.com/xxx/s1. Supplementary Table S1: Physicochemical and toxicological parameters calculated for the selected compounds against the ATP binding site of mTOR based on molecular docking analysis. Supplementary Table S2: Physicochemical and toxicological parameters calculated for the selected compounds against the rapamycin binding site of mTOR based on molecular docking analysis. Supplementary Table S3: Molecular docking analysis for potential inhibitor compounds (candidate molecules) at the rapamycin binding site of mTOR kinase selected among Marine Natural Products. Supplementary Table S4: Molecular docking analysis for potential inhibitor compounds (candidate molecules) at the rapamycin binding site of mTOR kinase selected among Super Natural II database. Supplementary Table S5: Molecular docking analysis for potential inhibitor compounds (candidate molecules) at the rapamycin binding site of mTOR kinase selected among ZINC database natural products. Supplementary Table S6: Molecular docking analysis for potential inhibitor compounds (candidate molecules) at the ATP binding site of mTOR kinase selected among Marine Natural Products. Supplementary Table S7: Molecular docking analysis for potential inhibitor compounds (candidate molecules) at the ATP binding site of mTOR kinase selected among Super Natural II database. Supplementary Figure S1: Detailed description of the molecular interactions between the inhibitor compound and the rapamycin binding site in mTOR. Supplementary Figure S2: Comparison of the Gibbs free energy variation (ΔG , kcal/mol) for 40 compounds approved by the FDA for clinical use against various types of cancer, obtained by molecular docking experiments against the ATP binding site of 12 protein kinases.

Author Contributions: V.M., M.H.-L., E.B.-C., and J.A.E. conceived and designed the experiments and J.A.E. wrote the paper; V.R.-T., M.L.-E., E.B.-C. and M.H.-L. conducted the *in vitro* experiments; V.G. and J.A.E. conducted the *in silico* molecular docking experiments and other computational approaches; V.M. and J.A.E. have been responsible for funding acquisition. All authors contributed to the general discussion of the manuscript. All authors contributed toward data analysis, drafting and revising the paper and agree to be accountable for all aspects of the work.

Funding: This work was supported by AGL2011-29857-C03-03 and IDI-20120751 grants (Spanish Ministry of Science and Innovation), projects AGL2015-67995-C3-1-R, AGL2015-67995-C3-2-R and AGL2015-67995-C3-3-R from the Spanish Ministry of Economy and Competitiveness (MINECO); and PROMETEO/2012/007, PROMETEO/2016/006, ACOMP/2013/093, ACIF/2010/162, ACIF/2015/158 and ACIF/2016/230 grants from Generalitat Valenciana and CIBER (CB12/03/30038, Fisiopatología de la Obesidad y la Nutrición, CIBERobn, Instituto de Salud Carlos III).

Acknowledgments: We are grateful to Research, Technological Innovation and the Supercomputing Center of Extremadura (CenitS) for allowing us to use their supercomputing facilities (LUSITANIA II). We also thank the company “TodoPez, S.L., Alicante, Spain” the generous provision of marine extracts.

Conflicts of Interest: The authors declare no conflict of interest.

References

1. Chiarini, F.; Evangelisti, C.; McCubrey, J.A.; Martelli, A.M. Current treatment strategies for inhibiting mTOR in cancer. *Trends Pharmacol. Sci.* **2015**, *36*, 124–135. doi:10.1016/j.tips.2014.11.004.
2. Yang, H.; Rudge, D.G.; Koos, J.D.; Vaidialingam, B.; Yang, H.J.; Pavletich, N.P. mTOR kinase structure, mechanism and regulation. *Nature* **2013**, *497*, 217–223. doi:10.1038/nature12122.
3. Hara, K.; Maruki, Y.; Long, X.; Yoshino, K.-I.; Oshiro, N.; Hidayat, S.; Tokunaga, C.; Avruch, J.; Yonezawa, K. Raptor, a Binding Partner of Target of Rapamycin (TOR), Mediates TOR Action. *Cell* **2002**, *110*, 177–189. doi:10.1016/S0092-8674(02)00833-4.
4. Sarbassov, D.D.; Guertin, D.A.; Ali, S.M.; Sabatini, D.M. Phosphorylation and regulation of Akt/PKB by the rictor-mTOR complex. *Science* **2005**, *307*, 1098–1101. doi:10.1126/science.1106148.
5. Ieranò, C.; Santagata, S.; Napolitano, M.; Guardia, F.; Grimaldi, A.; Antignani, E.; Botti, G.; Consales, C.; Riccio, A.; Nanayakkara, M.; et al. CXCR4 and CXCR7 transduce through mTOR in human renal cancer cells. *Cell Death Dis.* **2014**, *5*, e1310. doi:10.1038/cddis.2014.269.
6. McCubrey, J.A.; Steelman, L.S.; Chappell, W.H.; Abrams, S.L.; Wong, E.W.; Chang, F.; Lehmann, B.; Terrian, D.M.; Milella, M.; Tafuri, A.; et al. Roles of the Raf/MEK/ERK pathway in cell growth, malignant transformation and drug resistance. *Biochim. Biophys. Acta* **2007**, *1773*, 1263–1284. doi:10.1016/j.bbamcr.2006.10.001.
7. Laplante, M.; Sabatini, D.M. mTOR Signaling in Growth Control and Disease. *Cell* **2012**, *149*, 274–293. doi:10.1016/j.cell.2012.03.017.
8. Inoki, K.; Ouyang, H.; Zhu, T.; Lindvall, C.; Wang, Y.; Zhang, X.; Yang, Q.; Bennett, C.; Harada, Y.; Stankunas, K.; et al. TSC2 integrates Wnt and energy signals via a coordinated phosphorylation by AMPK and GSK3 to regulate cell growth. *Cell* **2006**, *126*, 955–968. doi:10.1016/j.cell.2006.06.055.
9. Anastasiou, D. Tumour microenvironment factors shaping the cancer metabolism landscape. *Br. J. Cancer* **2016**, *116*, 277. doi:10.1038/bjc.2016.412.
10. Balgi, A.D.; Diering, G.H.; Donohue, E.; Lam, K.K.; Fonseca, B.D.; Zimmerman, C.; Numata, M.; Roberge, M. Regulation of mTORC1 signaling by pH. *PLoS ONE* **2011**, *6*, e21549. doi:10.1371/journal.pone.0021549.
11. Arsham, A.M.; Howell, J.J.; Simon, M.C. A novel hypoxia-inducible factor-independent hypoxic response regulating mammalian target of rapamycin and its targets. *J. Biol. Chem.* **2003**, *278*, 29655–29660. doi:10.1074/jbc.M212770200.
12. Cho, J.H.; Han, J.S. Phospholipase D and Its Essential Role in Cancer. *Mol. Cells* **2017**, *40*, 805–813. doi:10.14348/molcells.2017.0241.
13. Yoon, M.S.; Rosenberger, C.L.; Wu, C.; Truong, N.; Sweedler, J.V.; Chen, J. Rapid mitogenic regulation of the mTORC1 inhibitor, DEPTOR, by phosphatidic acid. *Mol. Cell* **2015**, *58*, 549–556. doi:10.1016/j.molcel.2015.03.028.

14. Thoreen, C.C.; Chantranupong, L.; Keys, H.R.; Wang, T.; Gray, N.S.; Sabatini, D.M. A unifying model for mTORC1-mediated regulation of mRNA translation. *Nature* **2012**, *485*, 109. doi:10.1038/nature11083.
15. Yuan, H.X.; Xiong, Y.; Guan, K.L. Nutrient sensing, metabolism, and cell growth control. *Mol. Cell* **2013**, *49*, 379–387. doi:10.1016/j.molcel.2013.01.019.
16. Hosokawa, N.; Hara, T.; Kaizuka, T.; Kishi, C.; Takamura, A.; Miura, Y.; Iemura, S.; Natsume, T.; Takehana, K.; Yamada, N.; et al. Nutrient-dependent mTORC1 association with the ULK1-Atg13-FIP200 complex required for autophagy. *Mol. Biol. Cell* **2009**, *20*, 1981–1991. doi:10.1091/mbc.E08-12-1248.
17. Dodd, K.M.; Yang, J.; Shen, M.H.; Sampson, J.R.; Tee, A.R. mTORC1 drives HIF-1 α and VEGF-A signalling via multiple mechanisms involving 4E-BP1, S6K1 and STAT3. *Oncogene* **2014**, *34*, 2239. doi:10.1038/onc.2014.164.
18. Shimobayashi, M.; Hall, M.N. Making new contacts: The mTOR network in metabolism and signalling crosstalk. *Nat. Rev. Mol. Cell Biol.* **2014**, *15*, 155. doi:10.1038/nrm3757.
19. Cornu, M.; Albert, V.; Hall, M.N. mTOR in aging, metabolism, and cancer. *Curr. Opin. Genet. Dev.* **2013**, *23*, 53–62. doi:10.1016/j.gde.2012.12.005.
20. Vucenik, I.; Stains, J.P. Obesity and cancer risk: Evidence, mechanisms, and recommendations. *Ann. N. Y. Acad. Sci.* **2012**, *1271*, 37–43. doi:10.1111/j.1749-6632.2012.06750.x.
21. Cai, H.; Dong, L.Q.; Liu, F. Recent Advances in Adipose mTOR Signaling and Function: Therapeutic Prospects. *Trends Pharmacol. Sci.* **2016**, *37*, 303–317. doi:10.1016/j.tips.2015.11.011.
22. Faes, S.; Demartines, N.; Dormond, O. Resistance to mTORC1 Inhibitors in Cancer Therapy: From Kinase Mutations to Intratumoral Heterogeneity of Kinase Activity. *Oxid. Med. Cell. Longev.* **2017**, *2017*, 1726078. doi:10.1155/2017/1726078.
23. Malley, C.O.; Pidgeon, G.P. The mTOR pathway in obesity driven gastrointestinal cancers: Potential targets and clinical trials. *BBA Clin.* **2016**, *5*, 29–40. doi:10.1016/j.bbacli.2015.11.003.
24. Roskoski, R., Jr. A historical overview of protein kinases and their targeted small molecule inhibitors. *Pharmacol. Res.* **2015**, *100*, 1–23. doi:10.1016/j.phrs.2015.07.010.
25. Benjamin, D.; Colombi, M.; Moroni, C.; Hall, M.N. Rapamycin passes the torch: A new generation of mTOR inhibitors. *Nat. Rev. Drug Discov.* **2011**, *10*, 868. doi:10.1038/nrd3531.
26. Rodrik-Outmezguine, V.S.; Okaniwa, M.; Yao, Z.; Novotny, C.J.; McWhirter, C.; Banaji, A.; Won, H.; Wong, W.; Berger, M.; de Stanchina, E.; et al. Overcoming mTOR resistance mutations with a new-generation mTOR inhibitor. *Nature* **2016**, *534*, 272–276. doi:10.1038/nature17963.
27. Ruiz-Torres, V.; Encinar, J.A.; Herranz-Lopez, M.; Perez-Sanchez, A.; Galiano, V.; Barrajon-Catalan, E.; Micol, V. An Updated Review on Marine Anticancer Compounds: The Use of Virtual Screening for the Discovery of Small-Molecule Cancer Drugs. *Molecules* **2017**, *22*. doi:10.3390/molecules22071037.
28. Banerjee, P.; Erehman, J.; Gohlke, B.O.; Wilhelm, T.; Preissner, R.; Dunkel, M. Super Natural II—a database of natural products. *Nucleic Acids Res.* **2015**, *43*, D935–D939. doi:10.1093/nar/gku886.
29. Sterling, T.; Irwin, J.J. ZINC 15—Ligand Discovery for Everyone. *J. Chem. Inf. Model.* **2015**, *55*, 2324–2337. doi:10.1021/acs.jcim.5b00559.
30. Bello-Perez, M.; Falco, A.; Galiano, V.; Coll, J.; Perez, L.; Encinar, J.A. Discovery of nonnucleoside inhibitors of polymerase from infectious pancreatic necrosis virus (IPNV). *Drug Des. Dev. Ther.* **2018**, *12*, 2337–2359. doi:10.2147/DDDT.S171087.

31. Encinar, J.A.; Fernandez-Ballester, G.; Galiano-Ibarra, V.; Micol, V. *In silico* approach for the discovery of new PPARgamma modulators among plant-derived polyphenols. *Drug Des. Dev. Ther.* **2015**, *9*, 5877–5895. doi:10.2147/DDDT.S93449.
32. Galiano, V.; Garcia-Valtanen, P.; Micol, V.; Encinar, J.A. Looking for inhibitors of the dengue virus NS5 RNA-dependent RNA-polymerase using a molecular docking approach. *Drug Des. Dev. Ther.* **2016**, *10*, 3163–3181. doi:10.2147/DDDT.S117369.
33. Gilson, M.K.; Liu, T.; Baitaluk, M.; Nicola, G.; Hwang, L.; Chong, J. BindingDB in 2015: A public database for medicinal chemistry, computational chemistry and systems pharmacology. *Nucleic Acids Res.* **2016**, *44*, D1045–D1053. doi:10.1093/nar/gkv1072.
34. Guo, Q.; Yu, C.; Zhang, C.; Li, Y.; Wang, T.; Huang, Z.; Wang, X.; Zhou, W.; Li, Y.; Qin, Z.; et al. Highly Selective, Potent, and Oral mTOR Inhibitor for Treatment of Cancer as Autophagy Inducer. *J. Med. Chem.* **2018**, *61*, 881–904. doi:10.1021/acs.jmedchem.7b01402.
35. Salentin, S.; Schreiber, S.; Haupt, V.J.; Adasme, M.F.; Schroeder, M. PLIP: Fully automated protein-ligand interaction profiler. *Nucleic Acids Res.* **2015**, *43*, W443–W447. doi:10.1093/nar/gkv315.
36. Rajput, A.; Dominguez San Martin, I.; Rose, R.; Beko, A.; Levea, C.; Sharratt, E.; Mazurchuk, R.; Hoffman, R.M.; Brattain, M.G.; Wang, J. Characterization of HCT116 human colon cancer cells in an orthotopic model. *J. Surg. Res.* **2008**, *147*, 276–281. doi:10.1016/j.jss.2007.04.021.
37. Cádiz-Gurrea, M.d.l.L.; Olivares-Vicente, M.; Herranz-López, M.; Arraez-Roman, D.; Fernández-Arroyo, S.; Micol, V.; Segura-Carretero, A. Bioassay-guided purification of Lippia citriodora polyphenols with AMPK modulatory activity. *J. Funct. Foods* **2018**, *46*, 514–520. doi:10.1016/j.jff.2018.05.026.
38. Nave, B.T.; Ouwens, M.; Withers, D.J.; Alessi, D.R.; Shepherd, P.R. Mammalian target of rapamycin is a direct target for protein kinase B: Identification of a convergence point for opposing effects of insulin and amino-acid deficiency on protein translation. *Biochem. J.* **1999**, *344 Pt 2*, 427–431.
39. Peterson, R.T.; Beal, P.A.; Comb, M.J.; Schreiber, S.L. FKBP12-rapamycin-associated protein (FRAP) autophosphorylates at serine 2481 under translationally repressive conditions. *J. Biol. Chem.* **2000**, *275*, 7416–7423.
40. Edinger, A.L.; Thompson, C.B. Death by design: Apoptosis, necrosis and autophagy. *Curr. Opin. Cell Biol.* **2004**, *16*, 663–669. doi:10.1016/j.ceb.2004.09.011.
41. Nicholson, D.W. Caspase structure, proteolytic substrates, and function during apoptotic cell death. *Cell Death Differ.* **1999**, *6*, 1028. doi:10.1038/sj.cdd.4400598.
42. Jin, L.; Wang, W.; Fang, G. Targeting protein-protein interaction by small molecules. *Annu. Rev. Pharmacol. Toxicol.* **2014**, *54*, 435–456. doi:10.1146/annurev-pharmtox-011613-140028.
43. Ivanov, A.A.; Khuri, F.R.; Fu, H. Targeting protein-protein interactions as an anticancer strategy. *Trends Pharmacol. Sci.* **2013**, *34*, 393–400. doi:10.1016/j.tips.2013.04.007.
44. Pereira, F.; Aires-de-Sousa, J. Computational Methodologies in the Exploration of Marine Natural Product Leads. *Mar. Drugs* **2018**, *16*. doi:10.3390/md16070236.
45. Nantasenamat, C.; Prachayasittikul, V. Maximizing computational tools for successful drug discovery. *Expert Opin. Drug Discov.* **2015**, *10*, 321–329. doi:10.1517/17460441.2015.1016497.
46. Kapahi, P.; Chen, D.; Rogers, A.N.; Katewa, S.D.; Li, P.W.; Thomas, E.L.; Kockel, L. With TOR, less is more: A key role for the conserved nutrient-sensing TOR pathway in aging. *Cell Metab.* **2010**, *11*, 453–465. doi:10.1016/j.cmet.2010.05.001.
47. Johnson, S.C.; Rabinovitch, P.S.; Kaeberlein, M. mTOR is a key modulator of ageing and age-related disease. *Nature* **2013**, *493*, 338. doi:10.1038/nature11861.

48. Sadowski, K.; Kotulska, K.; Jozwiak, S. Management of side effects of mTOR inhibitors in tuberous sclerosis patients. *Pharmacol. Rep.* **2016**, *68*, 536–542. doi:10.1016/j.pharep.2016.01.005.
49. Pallet, N.; Legendre, C. Adverse events associated with mTOR inhibitors. *Expert Opin. Drug Saf.* **2013**, *12*, 177–186. doi:10.1517/14740338.2013.752814.
50. Li, J.; Kim, S.G.; Blenis, J. Rapamycin: One drug, many effects. *Cell Metab.* **2014**, *19*, 373–379. doi:10.1016/j.cmet.2014.01.001.
51. Neves, J.; Sousa-Victor, P.; Jasper, H. Rejuvenating Strategies for Stem Cell-Based Therapies in Aging. *Cell Stem Cell* **2017**, *20*, 161–175. doi:10.1016/j.stem.2017.01.008.
52. Weichhart, T. mTOR as Regulator of Lifespan, Aging, and Cellular Senescence: A Mini-Review. *Gerontology* **2018**, *64*, 127–134. doi:10.1159/000484629.
53. Ge, D.; Han, L.; Huang, S.; Peng, N.; Wang, P.; Jiang, Z.; Zhao, J.; Su, L.; Zhang, S.; Zhang, Y.; et al. Identification of a novel MTOR activator and discovery of a competing endogenous RNA regulating autophagy in vascular endothelial cells. *Autophagy* **2014**, *10*, 957–971. doi:10.4161/auto.28363.
54. Peng, N.; Meng, N.; Wang, S.; Zhao, F.; Zhao, J.; Su, L.; Zhang, S.; Zhang, Y.; Zhao, B.; Miao, J. An activator of mTOR inhibits oxLDL-induced autophagy and apoptosis in vascular endothelial cells and restricts atherosclerosis in apolipoprotein E^{-/-} mice. *Sci. Rep.* **2014**, *4*, 5519. doi:10.1038/srep05519.
55. Bottegoni, G.; Rocchia, W.; Rueda, M.; Abagyan, R.; Cavalli, A. Systematic exploitation of multiple receptor conformations for virtual ligand screening. *PLoS ONE* **2011**, *6*, e18845. doi:10.1371/journal.pone.0018845.
56. Morris, G.M.; Huey, R.; Lindstrom, W.; Sanner, M.F.; Belew, R.K.; Goodsell, D.S.; Olson, A.J. AutoDock4 and AutoDockTools4: Automated docking with selective receptor flexibility. *J. Comput. Chem.* **2009**, *30*, 2785–2791. doi:10.1002/jcc.21256.
57. Schymkowitz, J.; Borg, J.; Stricher, F.; Nys, R.; Rousseau, F.; Serrano, L. The FoldX web server: An online force field. *Nucleic Acids Res.* **2005**, *33*, W382–W388. doi:10.1093/nar/gki387.
58. Trott, O.; Olson, A.J. AutoDock Vina: Improving the speed and accuracy of docking with a new scoring function, efficient optimization, and multithreading. *J. Comput. Chem.* **2010**, *31*, 455–461. doi:10.1002/jcc.21334.
59. Sander, T.; Freyss, J.; von Korff, M.; Rufener, C. DataWarrior: An open-source program for chemistry aware data visualization and analysis. *J. Chem. Inf. Model.* **2015**, *55*, 460–473. doi:10.1021/ci500588j.
60. Cheng, F.; Li, W.; Zhou, Y.; Shen, J.; Wu, Z.; Liu, G.; Lee, P.W.; Tang, Y. admetSAR: A comprehensive source and free tool for assessment of chemical ADMET properties. *J. Chem. Inf. Model.* **2012**, *52*, 3099–3105. doi:10.1021/ci300367a.



© 2018 by the authors. Licensee MDPI, Basel, Switzerland. This article is an open access article distributed under the terms and conditions of the Creative Commons Attribution (CC BY) license (<http://creativecommons.org/licenses/by/4.0/>).

Supplementary figures and tables

Supplementary Table S1: Molecular docking analysis for potential inhibitor compounds (candidate molecules) at the **rapamycin binding site** of **mTOR** kinase selected among **Marine Natural Products** [1].

Marine natural products	ΔG , mean \pm S.D.	Marine natural products	ΔG , mean \pm S.D.	Marine natural products	ΔG , mean \pm S.D.
40663-80-7	-13.89 \pm 0.65	184348-39-8	-12.46 \pm 0.59	115267-16-8	-12.06 \pm 0.71
681260-42-4	-13.74 \pm 0.53	55945-74-9	-12.45 \pm 0.31	114820-24-5	-12.04 \pm 0.60
139975-57-8	-13.72 \pm 0.60	116-30-3	-12.42 \pm 0.26	121038-34-4	-12.04 \pm 1.57
104196-68-1	-13.71 \pm 0.64	126622-64-8	-12.41 \pm 0.23	114820-28-9	-12.02 \pm 0.32
133625-26-0	-13.70 \pm 0.43	147362-37-6	-12.40 \pm 0.78	639512-19-9	-12.02 \pm 0.45
681260-09-3	-13.69 \pm 0.44	16891-85-3	-12.40 \pm 0.83	64687-85-0	-12.02 \pm 0.64
178115-90-7	-13.66 \pm 0.79	120314-15-0	-12.38 \pm 0.47	890041-67-5	-12.02 \pm 0.46
135340-00-0	-13.57 \pm 0.40	120409-36-1	-12.38 \pm 0.47	29953-50-2	-12.00 \pm 0.69
112663-92-0	-13.50 \pm 0.73	131204-29-0	-12.38 \pm 0.41	36011-19-5	-12.00 \pm 0.38
152845-74-4	-13.43 \pm 0.50	524067-24-1	-12.38 \pm 0.47	93426-90-5	-12.00 \pm 1.56
162465-80-7	-13.39 \pm 0.58	160796-24-7	-12.37 \pm 0.46	175673-58-2	-11.99 \pm 0.25
211686-51-0	-13.39 \pm 0.32	75598-52-6	-12.37 \pm 0.53	150079-95-1	-11.98 \pm 0.38
159736-39-7	-13.38 \pm 0.57	50335-03-0	-12.35 \pm 0.52	798557-98-9	-11.98 \pm 0.33
139975-58-9	-13.32 \pm 0.41	70022-71-8	-12.35 \pm 0.30	79858-77-8	-11.98 \pm 0.71
94354-98-0	-13.30 \pm 0.15	122780-90-9	-12.33 \pm 0.36	864685-94-9	-11.98 \pm 0.39
14729-29-4	-13.18 \pm 0.73	65745-47-3	-12.33 \pm 0.36	173792-58-0	-11.96 \pm 0.68
214899-21-5	-13.12 \pm 0.77	149064-34-6	-12.32 \pm 0.63	849215-95-8	-11.95 \pm 0.64
116477-23-7	-13.02 \pm 0.53	179733-14-3	-12.32 \pm 0.36	191-24-2	-11.94 \pm 0.64
133613-77-1	-13.01 \pm 0.60	212502-88-0	-12.31 \pm 0.46	156953-91-2	-11.93 \pm 0.91
79067-75-7	-13.01 \pm 0.69	117631-50-2	-12.28 \pm 0.81	72509-61-6	-11.93 \pm 0.73
135340-01-1	-13.00 \pm 0.32	184885-91-4	-12.28 \pm 0.47	76915-24-7	-11.93 \pm 0.42
119212-28-1	-12.94 \pm 0.47	188111-70-8	-12.28 \pm 0.69	81657-79-6	-11.93 \pm 0.39
149764-32-9	-12.92 \pm 0.86	3148-09-2	-12.28 \pm 0.60	120154-96-3	-11.92 \pm 0.32
134458-00-7	-12.90 \pm 0.48	345642-84-4	-12.28 \pm 0.52	78111-17-8	-11.92 \pm 0.26
179733-15-4	-12.90 \pm 0.49	74608-63-2	-12.28 \pm 0.42	325690-73-1	-11.90 \pm 0.94
214767-82-5	-12.89 \pm 0.48	81657-78-5	-12.28 \pm 0.37	6853-99-2	-11.90 \pm 0.52
156953-87-6	-12.88 \pm 0.95	848656-06-4	-12.27 \pm 0.63	119539-75-2	-11.89 \pm 0.49
50335-04-1	-12.88 \pm 0.23	120963-61-3	-12.26 \pm 0.53	12794-85-3	-11.88 \pm 0.38
55544-35-9	-12.88 \pm 0.34	862892-28-2	-12.25 \pm 0.54	139594-87-9	-11.88 \pm 0.39
105418-77-7	-12.84 \pm 0.34	221163-30-0	-12.23 \pm 0.34	191212-38-1	-11.88 \pm 0.27
125282-13-5	-12.82 \pm 0.52	52645-09-7	-12.23 \pm 0.47	221367-90-4	-11.88 \pm 0.46
125302-26-3	-12.82 \pm 0.52	126297-39-0	-12.22 \pm 1.16	863116-48-7	-11.88 \pm 0.41
133056-09-4	-12.79 \pm 0.90	6758-71-0	-12.22 \pm 0.35	186593-86-2	-11.87 \pm 0.35
144587-58-6	-12.77 \pm 0.39	114820-30-3	-12.21 \pm 0.31	28097-03-2	-11.87 \pm 0.50
155944-26-6	-12.74 \pm 0.35	114820-25-6	-12.19 \pm 0.40	67463-79-0	-11.87 \pm 0.52

524067-25-2	-12.72±0.95	233607-72-2	-12.19±0.62	858950-48-8	-11.87±0.39
133056-07-2	-12.71±0.50	83481-23-6	-12.17±0.33	129033-05-2	-11.86±1.13
65773-98-0	-12.70±0.11	123048-14-6	-12.16±0.25	84773-08-0	-11.85±0.88
80375-18-4	-12.65±0.54	88840-01-1	-12.16±0.36	141266-06-0	-11.84±0.41
1008752-06-4	-12.64±0.69	123000-07-7	-12.14±0.24	140429-37-4	-11.83±0.32
823808-55-5	-12.63±0.19	171674-92-3	-12.14±0.83	150050-13-8	-11.83±0.54
123303-94-6	-12.62±0.29	88840-02-2	-12.14±0.24	168569-18-4	-11.82±0.33
123303-95-7	-12.62±0.30	88903-69-9	-12.14±0.24	185801-42-7	-11.81±0.51
50-76-0	-12.62±1.02	64726-84-7	-12.12±0.55	104759-19-5	-11.80±0.30
64421-20-1	-12.62±0.61	148371-08-8	-12.10±0.44	105305-54-2	-11.80±0.60
128229-64-1	-12.61±0.34	155645-51-5	-12.10±0.43	159813-67-9	-11.80±0.34
144587-57-5	-12.58±0.47	158734-27-1	-12.10±0.42	191212-36-9	-11.80±0.24
154466-37-2	-12.57±1.07	124689-65-2	-12.09±0.60	87164-33-8	-11.80±0.28
107900-75-4	-12.56±0.91	147362-39-8	-12.09±0.30	168482-38-0	-11.79±0.14
212502-87-9	-12.56±0.56	186593-83-9	-12.08±0.48	211239-56-4	-11.79±0.37
6377-18-0	-12.55±0.24	706784-72-7	-12.08±0.33	114820-26-7	-11.78±0.38
127687-08-5	-12.47±0.23	708255-98-5	-12.08±0.87	156953-85-4	-11.78±0.53
240480-95-9	-12.47±0.45	35906-51-5	-12.07±0.26	87532-26-1	-11.78±0.13
168569-15-1	-12.46±0.60	5035-30-3	-12.07±0.21	82915-89-7	-11.77±0.51
858950-44-4	-11.77±0.58	149764-34-1	-11.59±0.45	81275-81-2	-11.48±0.32
108195-61-5	-11.76±0.26	134887-25-5	-11.58±0.37	866403-74-9	-11.48±0.34
149764-33-0	-11.76±0.50	140447-22-9	-11.58±0.41	272118-06-6	-11.47±1.02
329050-20-6	-11.75±0.23	140715-87-3	-11.58±0.33	66536-82-1	-11.47±0.57
78798-08-0	-11.75±0.52	151606-24-5	-11.58±0.26	73538-57-5	-11.47±0.25
80860-53-3	-11.75±0.29	151606-43-8	-11.58±1.18	866403-73-8	-11.47±0.36
116229-58-4	-11.74±1.21	191212-37-0	-11.57±0.22	87532-32-9	-11.47±0.33
80928-52-5	-11.73±1.11	329050-23-9	-11.57±0.49	121250-35-9	-11.46±0.52
172854-78-3	-11.72±0.54	865369-07-9	-11.57±0.55	136024-80-1	-11.46±0.85
209169-58-4	-11.72±0.58	93474-14-7	-11.57±0.12	184679-29-6	-11.46±0.89
749216-47-5	-11.72±0.27	112455-84-2	-11.56±0.47	2061-64-5	-11.46±0.19
149444-92-8	-11.70±0.49	145163-96-8	-11.56±0.34	329050-22-8	-11.45±0.42
156310-18-8	-11.70±0.77	263764-04-1	-11.56±0.26	472-70-8	-11.45±0.37
81720-10-7	-11.70±0.22	27065-95-8	-11.55±0.26	64907-26-2	-11.45±0.52
852872-92-5	-11.70±0.44	51744-55-9	-11.55±0.41	7488-99-5	-11.45±0.46
159334-35-7	-11.69±0.49	640734-87-8	-11.55±0.33	78798-30-8	-11.45±0.73
175702-36-0	-11.69±0.34	123853-69-0	-11.54±0.48	84582-62-7	-11.45±0.26
199600-36-7	-11.68±0.37	220503-29-7	-11.54±0.23	114836-87-2	-11.44±0.61
452934-96-2	-11.68±0.55	224577-34-8	-11.54±0.50	134981-78-5	-11.43±0.37
4936-10-1	-11.68±0.28	171784-09-1	-11.53±0.36	518-06-9	-11.43±0.28
50676-98-7	-11.68±0.27	17608-76-3	-11.53±0.31	78173-92-9	-11.43±0.69
61897-90-3	-11.68±0.23	211358-70-2	-11.53±0.35	78340-85-9	-11.43±0.34
65556-58-3	-11.68±0.33	432-68-8	-11.53±0.44	79849-37-9	-11.43±0.23

91097-16-4	-11.68±0.63	52238-31-0	-11.53±0.27	870095-34-4	-11.43±0.26
2122-98-7	-11.67±0.46	53402-18-9	-11.53±0.26	96391-64-9	-11.43±0.12
78111-14-5	-11.67±0.23	74984-66-0	-11.53±0.14	105118-23-8	-11.42±0.41
94705-97-2	-11.67±0.67	84323-27-3	-11.53±0.22	114995-72-1	-11.42±0.62
140715-85-1	-11.66±0.34	85199-91-3	-11.53±0.49	123941-58-2	-11.42±0.27
147716-81-2	-11.66±1.64	863548-84-9	-11.53±0.39	17991-67-2	-11.42±0.41
890041-68-6	-11.66±0.42	126622-63-7	-11.52±0.38	208927-15-5	-11.42±0.43
104758-18-1	-11.64±0.52	159518-76-0	-11.52±0.56	77617-71-1	-11.42±0.23
152110-09-3	-11.64±0.28	16910-32-0	-11.52±0.42	77739-71-0	-11.42±0.69
2465-11-4	-11.64±0.35	445430-63-7	-11.52±0.56	79781-66-1	-11.42±0.24
88840-00-0	-11.64±0.51	514-78-3	-11.52±0.16	115268-43-4	-11.41±0.32
140852-71-7	-11.63±0.36	676339-97-2	-11.52±0.17	122540-31-2	-11.41±0.21
152213-67-7	-11.63±0.20	139933-46-3	-11.51±0.50	1406-16-2	-11.41±0.40
6673-66-1	-11.63±0.19	14984-66-8	-11.51±0.42	224577-31-5	-11.41±0.57
865308-60-7	-11.63±0.28	171370-52-8	-11.51±0.24	160472-96-8	-11.40±1.67
1403-36-7	-11.62±0.91	174630-11-6	-11.51±0.68	176328-50-0	-11.40±0.55
152186-77-1	-11.62±0.40	224577-33-7	-11.51±0.56	210761-24-3	-11.40±0.41
159934-15-3	-11.62±0.36	116237-60-6	-11.50±0.55	874383-70-7	-11.40±0.39
19698-66-9	-11.62±0.26	151247-69-7	-11.50±0.25	88095-77-6	-11.40±0.64
199600-37-8	-11.62±0.41	172854-77-2	-11.50±0.48	88357-79-3	-11.40±0.39
4626-00-0	-11.62±0.62	61897-89-0	-11.50±0.32	95189-16-5	-11.40±0.17
141968-27-6	-11.60±0.66	78306-12-4	-11.50±0.48	122970-13-2	-11.39±0.26
174063-81-1	-11.60±0.40	84821-12-5	-11.50±0.37	12794-84-2	-11.39±0.43
188111-69-5	-11.60±0.55	858950-46-6	-11.50±0.60	154563-79-8	-11.39±0.34
23518-98-1	-11.60±0.26	150050-12-7	-11.49±0.64	28380-31-6	-11.39±0.34
37976-88-8	-11.60±0.23	217449-19-9	-11.49±0.34	103614-76-2	-11.38±0.98
452934-97-3	-11.60±0.36	153212-84-1	-11.48±0.75	113831-00-8	-11.38±0.33
487016-98-8	-11.60±0.32	210761-25-4	-11.48±0.44	123641-95-2	-11.38±0.38
52212-86-9	-11.60±0.61	244066-05-5	-11.48±0.32	135213-04-6	-11.38±0.40
53755-09-2	-11.60±0.47	306971-11-9	-11.48±0.27	156953-93-4	-11.38±0.96
70214-98-1	-11.60±0.78	66212-51-9	-11.48±0.31	209167-28-2	-11.38±0.32
393828-32-5	-11.38±0.40	25747-44-8	-11.29±0.41	50364-22-2	-11.23±0.48
63693-18-5	-11.38±0.31	101527-89-3	-11.28±0.45	51446-63-0	-11.23±0.32
77658-95-8	-11.38±0.42	132438-14-3	-11.28±0.41	52423-28-6	-11.23±0.73
133805-03-5	-11.37±0.37	149764-31-8	-11.28±0.48	874193-61-0	-11.23±0.46
14050-62-5	-11.37±0.35	151232-83-6	-11.28±0.32	122540-32-3	-11.22±0.20
37933-92-9	-11.37±0.38	219832-37-8	-11.28±0.63	184885-90-3	-11.22±0.65
452934-95-1	-11.37±0.46	487016-96-6	-11.28±0.78	208708-22-9	-11.22±0.23
66648-53-1	-11.37±0.35	674819-46-6	-11.28±0.23	222960-90-9	-11.22±0.53
74185-04-9	-11.37±0.26	69081-88-5	-11.28±0.34	2497-74-7	-11.22±0.49
80680-43-9	-11.37±0.46	80442-84-8	-11.28±0.18	432-70-2	-11.22±0.96
103005-20-5	-11.36±0.73	823815-00-5	-11.28±0.42	102778-12-1	-11.21±0.41

134887-27-7	-11.36±0.56	85733-69-3	-11.28±0.25	120881-21-2	-11.21±0.64
219832-35-6	-11.36±0.36	858950-34-2	-11.28±0.43	144686-42-0	-11.21±0.22
22453-06-1	-11.36±0.31	858950-40-0	-11.28±0.28	174024-97-6	-11.21±0.23
24041-68-7	-11.36±0.26	858950-55-7	-11.28±0.31	193816-71-6	-11.21±0.40
78518-73-7	-11.35±0.36	86363-50-0	-11.28±0.33	23637-31-2	-11.21±0.33
79234-80-3	-11.35±0.71	108943-00-6	-11.27±0.47	110012-18-5	-11.20±0.16
823815-01-6	-11.35±0.45	122795-54-4	-11.27±0.35	163136-05-8	-11.20±0.33
852872-93-6	-11.35±0.52	137415-10-2	-11.27±0.40	272458-31-8	-11.20±0.17
114550-75-3	-11.34±0.37	149444-91-7	-11.27±0.99	356566-82-0	-11.20±0.27
127-22-0	-11.34±0.30	151484-78-5	-11.27±0.17	454476-89-2	-11.20±0.39
163136-04-7	-11.34±0.44	153723-34-3	-11.27±0.83	50364-21-1	-11.20±0.18
290353-68-3	-11.34±0.19	2130-17-8	-11.27±0.69	54369-11-8	-11.20±0.40
127687-07-4	-11.33±0.34	23983-43-9	-11.27±0.28	73538-56-4	-11.20±0.22
134887-26-6	-11.33±0.52	306971-07-3	-11.27±0.33	79-63-0	-11.20±0.41
144-68-3	-11.33±0.32	78370-84-0	-11.27±0.25	85733-68-2	-11.20±0.23
159934-14-2	-11.33±0.35	84323-29-5	-11.27±0.36	101509-61-9	-11.19±0.41
174232-38-3	-11.33±0.26	96157-95-8	-11.27±0.23	110012-19-6	-11.19±0.25
263764-05-2	-11.33±0.20	105377-92-2	-11.26±0.26	124417-91-0	-11.19±0.11
31272-50-1	-11.33±0.29	120853-13-6	-11.26±0.30	147641-71-2	-11.19±0.31
364344-14-9	-11.33±0.73	134887-31-3	-11.26±0.59	148839-03-6	-11.19±0.43
524067-26-3	-11.33±0.59	139083-13-9	-11.26±0.41	199600-38-9	-11.19±0.52
84711-17-1	-11.33±0.34	159518-77-1	-11.26±0.32	283176-13-6	-11.19±0.32
858950-52-4	-11.33±0.60	184885-07-2	-11.26±0.34	107503-09-3	-11.18±0.42
154563-80-1	-11.32±0.30	194856-36-5	-11.26±0.22	133161-20-3	-11.18±0.36
188558-50-1	-11.32±0.16	205750-25-0	-11.26±0.52	156953-89-8	-11.18±0.99
35115-60-7	-11.32±0.53	208708-24-1	-11.26±0.19	260062-88-2	-11.18±0.24
471-53-4	-11.32±0.24	481-17-4	-11.25±0.39	40071-60-1	-11.18±0.33
74185-11-8	-11.32±0.60	571176-94-8	-11.25±0.23	40600-59-7	-11.18±0.28
116237-58-2	-11.31±0.69	61949-67-5	-11.25±0.39	7542-45-2	-11.18±0.28
194427-76-4	-11.31±0.41	63121-06-2	-11.25±0.39	782491-78-5	-11.18±0.15
106009-90-9	-11.30±0.46	70214-92-5	-11.25±0.60	78285-84-4	-11.18±0.41
124508-52-7	-11.30±0.40	85249-28-1	-11.25±0.35	78285-85-5	-11.18±0.23
179730-36-0	-11.30±0.31	118964-36-6	-11.24±0.32	80925-08-2	-11.18±0.41
209167-27-1	-11.30±0.32	148439-45-6	-11.24±0.65	82660-61-5	-11.18±0.30
256505-53-0	-11.30±0.42	26605-16-3	-11.24±0.39	862200-49-5	-11.18±0.19
37976-89-9	-11.30±0.28	114820-27-8	-11.23±0.34	11052-32-7	-11.17±0.95
445430-65-9	-11.30±0.36	115982-22-4	-11.23±0.31	12626-18-5	-11.17±0.42
852469-37-5	-11.30±0.40	124417-90-9	-11.23±0.29	126-29-4	-11.17±0.32
90077-71-7	-11.30±0.51	176704-07-7	-11.23±0.35	127709-45-9	-11.17±0.47
125329-09-1	-11.29±0.46	195063-95-7	-11.23±0.42	135824-74-7	-11.17±0.22
164081-03-2	-11.29±0.33	20780-37-4	-11.23±0.39	137443-15-3	-11.17±0.42
169564-96-9	-11.29±0.50	233607-69-7	-11.23±0.45	143621-75-4	-11.17±0.39

175170-89-5	-11.29±0.32	40772-12-1	-11.23±0.18	144686-41-9	-11.17±0.50
184885-89-0	-11.17±0.65	112570-87-3	-11.10±0.33	85798-19-2	-11.07±0.45
20829-55-4	-11.17±0.24	115178-50-2	-11.10±0.28	88191-06-4	-11.07±0.45
481-18-5	-11.17±0.48	116179-22-7	-11.10±0.32	94935-97-4	-11.07±0.06
63109-17-1	-11.17±0.34	118574-73-5	-11.10±0.18	95043-18-8	-11.07±0.15
648883-30-1	-11.17±0.18	121379-48-4	-11.10±0.55	112693-24-0	-11.06±0.15
78183-29-6	-11.17±0.26	125640-31-5	-11.10±0.41	114571-91-4	-11.06±0.34
85249-29-2	-11.17±0.48	157459-24-0	-11.10±0.38	116972-93-1	-11.06±0.27
85798-13-6	-11.17±0.29	184885-92-5	-11.10±0.35	123158-95-2	-11.06±0.25
866403-71-6	-11.17±0.35	218916-92-8	-11.10±0.50	137529-91-0	-11.06±0.53
86748-29-0	-11.17±0.30	264618-21-5	-11.10±0.31	154071-70-2	-11.06±0.42
870095-33-3	-11.17±0.50	325690-71-9	-11.10±0.73	166038-28-4	-11.06±0.36
96363-06-3	-11.17±0.23	52043-01-3	-11.10±0.21	173681-52-2	-11.06±0.44
114820-29-0	-11.16±0.32	706784-74-9	-11.10±0.52	173693-48-6	-11.06±0.52
153585-64-9	-11.16±0.37	757976-67-3	-11.10±0.36	516-85-8	-11.05±0.34
351198-08-8	-11.15±0.46	77680-78-5	-11.10±0.45	62335-06-2	-11.05±0.31
57539-70-5	-11.15±0.55	866025-62-9	-11.10±0.14	6673-68-3	-11.05±0.38
65527-04-0	-11.15±0.21	92355-85-6	-11.10±0.52	79217-17-7	-11.05±1.00
65527-05-1	-11.15±0.21	96157-96-9	-11.10±0.26	80442-78-0	-11.05±0.36
75246-76-3	-11.15±0.26	103190-14-3	-11.09±0.21	80442-79-1	-11.05±0.36
782491-79-6	-11.15±0.22	122970-14-3	-11.09±0.49	81296-42-6	-11.05±0.56
84323-28-4	-11.15±0.12	139220-18-1	-11.09±0.35	82915-90-0	-11.05±0.52
85733-79-5	-11.15±0.26	147395-97-9	-11.09±0.31	126060-09-1	-11.04±0.30
858950-38-6	-11.15±0.24	157207-88-0	-11.09±0.25	131467-00-0	-11.04±0.34
147641-74-5	-11.14±0.37	164991-65-5	-11.09±0.37	131565-70-3	-11.04±0.25
151345-08-3	-11.14±0.31	171784-10-4	-11.09±0.19	14270-73-6	-11.04±0.75
151890-81-2	-11.14±0.27	199600-39-0	-11.09±0.62	145163-97-9	-11.04±0.22
2034-72-2	-11.14±0.32	244303-77-3	-11.09±0.54	151890-80-1	-11.04±0.42
129239-13-0	-11.13±1.14	105239-70-1	-11.08±0.27	199165-88-3	-11.04±0.34
157078-48-3	-11.13±1.90	131487-01-9	-11.08±0.36	89955-50-0	-11.04±0.41
174630-08-1	-11.13±0.75	145038-56-8	-11.08±0.23	128129-56-6	-11.03±0.44
17757-07-2	-11.13±0.38	145940-74-5	-11.08±0.44	132410-40-3	-11.03±0.40
200942-18-3	-11.13±0.39	148472-99-5	-11.08±0.64	137415-08-8	-11.03±0.41
26047-31-4	-11.13±0.32	184584-40-5	-11.08±0.41	145680-52-0	-11.03±0.35
2643-02-9	-11.13±0.34	306971-06-2	-11.08±0.19	158758-41-9	-11.03±0.36
315209-08-6	-11.13±0.31	33886-74-7	-11.08±0.12	28949-66-8	-11.03±0.37
508193-31-5	-11.13±0.38	400710-54-5	-11.08±0.40	385815-30-5	-11.03±0.33
50909-86-9	-11.13±0.44	489446-57-3	-11.08±0.79	60492-18-4	-11.03±0.36
70214-99-2	-11.13±0.76	52043-00-2	-11.08±0.38	71103-05-4	-11.03±0.44
75179-58-7	-11.13±0.34	6891-35-6	-11.08±0.23	851610-86-1	-11.03±0.50
79664-61-2	-11.13±0.23	74185-09-4	-11.08±0.18	85735-14-4	-11.03±0.19
81855-46-1	-11.13±0.77	84897-09-6	-11.08±0.40	866403-75-0	-11.03±0.38

82660-62-6	-11.13±0.33	86047-14-5	-11.08±0.22	874221-89-3	-11.03±0.39
851606-66-1	-11.13±0.20	106463-75-6	-11.07±0.19	94806-02-7	-11.03±0.06
119147-12-5	-11.12±0.29	116331-46-5	-11.07±0.49	94806-03-8	-11.03±0.40
211358-65-5	-11.12±0.43	14325-03-2	-11.07±0.28	94806-05-0	-11.03±0.23
306971-12-0	-11.12±0.32	153723-35-4	-11.07±0.71	96253-60-0	-11.03±0.32
38-26-6	-11.12±0.62	225662-09-9	-11.07±0.35	102679-93-6	-11.02±0.45
474779-75-4	-11.12±0.51	308098-61-5	-11.07±0.34	117857-72-4	-11.02±0.47
74185-13-0	-11.12±0.45	356566-84-2	-11.07±0.27	124392-06-9	-11.02±0.65
85733-78-4	-11.12±0.30	47922-48-5	-11.07±0.22	132410-38-9	-11.02±0.13
85798-12-5	-11.12±0.24	61897-88-9	-11.07±0.45	144436-06-6	-11.02±0.49
12771-72-1	-11.11±0.39	74185-10-7	-11.07±0.62	151890-89-0	-11.02±0.57
219774-74-0	-11.11±0.52	81575-78-2	-11.07±0.27	174024-98-7	-11.02±0.23
256377-68-1	-11.11±0.52	847613-59-6	-11.07±0.42	306967-75-9	-11.02±0.63
465-95-2	-11.02±0.39	16250-61-6	-11.01±0.37	32450-26-3	-11.00±0.19
474417-54-4	-11.02±0.28	169626-35-1	-11.01±0.39	326794-17-6	-11.00±0.39
494862-71-4	-11.02±0.41	201213-05-0	-11.01±0.27	37926-43-5	-11.00±0.32
564-16-9	-11.02±0.16	201800-59-1	-11.01±0.34	4030-92-6	-11.00±0.30
631913-68-3	-11.02±0.25	20780-41-0	-11.01±0.36	4657-58-3	-11.00±0.14
64825-79-2	-11.02±0.52	244157-96-8	-11.01±0.58	474-70-4	-11.00±0.47
69081-87-4	-11.02±0.19	100667-75-2	-11.00±0.29	58497-29-3	-11.00±0.28
69819-82-5	-11.02±0.25	105645-77-0	-11.00±0.34	58514-32-2	-11.00±0.47
82471-15-6	-11.02±0.79	120416-68-4	-11.00±0.44	62014-96-4	-11.00±0.42
86783-84-8	-11.02±0.25	122540-27-6	-11.00±0.26	745828-23-3	-11.00±0.34
125282-11-3	-11.01±0.40	134887-29-9	-11.00±0.66	81306-61-8	-11.00±0.32
13963-13-8	-11.01±0.25	145038-57-9	-11.00±0.24	851610-88-3	-11.00±0.24
145163-99-1	-11.01±0.48	148149-82-0	-11.00±0.44	86748-30-3	-11.00±0.19
14660-91-4	-11.01±0.40	211486-15-6	-11.00±0.40	95189-17-6	-11.00±0.26
156953-95-6	-11.01±0.73	306971-10-8	-11.00±0.22		

Supplementary Table S2: Molecular docking analysis for potential inhibitor compounds (candidate molecules) at the **rapamycin binding site** of **mTOR** kinase selected among **Super Natural II** database [2].

Super Natural II	ΔG , mean \pm S.D.	Super Natural II	ΔG , mean \pm S.D.	Super Natural II	ΔG , mean \pm S.D.
SN00128384	-15.98 \pm 1.07	SN00169417	-14.46 \pm 0.44	SN00167982	-14.02 \pm 0.8
SN00169366	-15.97 \pm 0.74	SN00136698	-14.44 \pm 1.24	SN00286831	-14.02 \pm 0.71
SN00130058	-15.57 \pm 0.89	SN00167934	-14.43 \pm 0.28	SN00371872	-14.02 \pm 0.55
SN00169369	-15.57 \pm 0.53	SN00393875	-14.43 \pm 0.5	SN00111395	-14.01 \pm 0.4
SN00367917	-15.42 \pm 0.36	SN00081740	-14.42 \pm 0.4	SN00323840	-14.01 \pm 0.73
SN00169470	-15.38 \pm 0.2	SN00169362	-14.4 \pm 0.51	SN00136695	-14 \pm 0.8
SN00387839	-15.34 \pm 0.81	SN00169411	-14.4 \pm 0.39	SN00169439	-13.99 \pm 0.84
SN00130898	-15.17 \pm 0.37	SN00169416	-14.4 \pm 0.38	SN00321411	-13.98 \pm 0.28
SN00168000	-15.13 \pm 0.52	SN00113632	-14.38 \pm 0.47	SN00113542	-13.97 \pm 0.52
SN00335277	-15.12 \pm 0.36	SN00170378	-14.38 \pm 0.72	SN00169459	-13.97 \pm 0.46
SN00164826	-15.1 \pm 0.43	SN00395571	-14.38 \pm 0.3	SN00169460	-13.97 \pm 0.35
SN00383686	-15.07 \pm 0.92	SN00130963	-14.34 \pm 0.92	SN00275124	-13.97 \pm 0.53
SN00074793	-15.02 \pm 0.94	SN00274542	-14.34 \pm 0.65	SN00239003	-13.96 \pm 0.66
SN00115843	-14.99 \pm 0.64	SN00248218	-14.33 \pm 0.37	SN00386116	-13.96 \pm 0.4
SN00169375	-14.99 \pm 0.49	SN00343570	-14.33 \pm 0.35	SN00254348	-13.94 \pm 0.52
SN00376086	-14.97 \pm 0.24	SN00354912	-14.33 \pm 0.46	SN00260096	-13.94 \pm 0.61
SN00304654	-14.96 \pm 1	SN00167953	-14.32 \pm 0.37	SN00288290	-13.94 \pm 0.4
SN00330635	-14.96 \pm 0.96	SN00169428	-14.3 \pm 0.71	SN00059271	-13.93 \pm 0.55
SN00169424	-14.92 \pm 0.45	SN00348164	-14.27 \pm 0.45	SN00080936	-13.93 \pm 0.42
SN00290152	-14.9 \pm 1.07	SN00111460	-14.24 \pm 0.76	SN00169443	-13.93 \pm 0.47
SN00169633	-14.88 \pm 1.07	SN00347694	-14.24 \pm 0.27	SN00169469	-13.93 \pm 1.21
SN00232174	-14.88 \pm 0.31	SN00089681	-14.23 \pm 0.32	SN00243072	-13.93 \pm 0.45
SN00082747	-14.87 \pm 0.71	SN00169452	-14.23 \pm 0.68	SN00269626	-13.93 \pm 0.59
SN00330261	-14.86 \pm 0.99	SN00238877	-14.23 \pm 0.49	SN00344654	-13.93 \pm 0.55
SN00106774	-14.8 \pm 0.32	SN00307850	-14.22 \pm 0.61	SN00130239	-13.92 \pm 0.8
SN00169373	-14.79 \pm 0.84	SN00129404	-14.21 \pm 0.45	SN00169368	-13.92 \pm 0.61
SN00169438	-14.79 \pm 0.46	SN00169361	-14.21 \pm 0.71	SN00172800	-13.92 \pm 0.6
SN00172785	-14.79 \pm 0.83	SN00277812	-14.2 \pm 0.32	SN00081043	-13.91 \pm 0.72
SN00167918	-14.74 \pm 0.86	SN00167950	-14.19 \pm 0.59	SN00113230	-13.91 \pm 0.54
SN00264474	-14.73 \pm 0.94	SN00167970	-14.19 \pm 0.76	SN00129111	-13.91 \pm 0.42
SN00169425	-14.7 \pm 0.7	SN00111397	-14.18 \pm 0.49	SN00111564	-13.9 \pm 0.48
SN00037382	-14.69 \pm 0.8	SN00268217	-14.18 \pm 0.52	SN00130855	-13.9 \pm 0.36
SN00125316	-14.69 \pm 0.37	SN00288697	-14.18 \pm 1.1	SN00169941	-13.9 \pm 0.34
SN00119553	-14.67 \pm 0.25	SN00097689	-14.17 \pm 0.48	SN00341689	-13.9 \pm 1.05
SN00167887	-14.64 \pm 0.84	SN00169387	-14.17 \pm 0.74	SN00167811	-13.89 \pm 0.16
SN00394378	-14.64 \pm 0.33	SN00263404	-14.17 \pm 0.79	SN00169405	-13.89 \pm 0.52

SN00169448	-14.63±0.38	SN00111571	-14.16±0.58	SN00253506	-13.89±0.54
SN00137074	-14.62±1.4	SN00169406	-14.14±0.57	SN00322991	-13.89±0.5
SN00376674	-14.61±0.54	SN00323189	-14.14±0.75	SN00169384	-13.88±0.47
SN00169451	-14.6±0.79	SN00137008	-14.13±0.61	SN00267944	-13.88±0.54
SN00066079	-14.59±0.79	SN00169461	-14.13±0.52	SN00337878	-13.88±0.63
SN00238129	-14.59±0.51	SN00111415	-14.12±0.28	SN00082502	-13.87±0.99
SN00169370	-14.58±0.44	SN00169635	-14.09±1.14	SN00322705	-13.87±0.74
SN00282638	-14.57±0.3	SN00297098	-14.09±0.63	SN00097229	-13.86±0.25
SN00172758	-14.52±0.76	SN00307022	-14.09±0.35	SN00167973	-13.86±0.64
SN00239538	-14.52±0.41	SN00111437	-14.08±0.37	SN00169367	-13.86±0.84
SN00237128	-14.51±0.4	SN00379780	-14.07±0.79	SN00172770	-13.86±0.5
SN00123829	-14.49±0.61	SN00167990	-14.06±0.95	SN00173925	-13.86±0.38
SN00228019	-14.49±0.69	SN00253708	-14.06±0.6	SN00264249	-13.86±1.67
SN00169371	-14.48±0.22	SN00167965	-14.04±0.68	SN00350405	-13.86±0.49
SN00169617	-14.48±0.82	SN00340494	-14.04±0.14	SN00397406	-13.86±0.21
SN00301026	-14.48±0.18	SN00169383	-14.03±0.66	SN00089693	-13.84±0.24
SN00081734	-14.47±0.29	SN00174849	-14.03±0.61	SN00169363	-13.84±0.97
SN00169427	-14.47±0.32	SN00378076	-14.03±0.69	SN00169429	-13.84±0.26
SN00297928	-13.84±0.57	SN00237456	-13.64±0.56	SN00101954	-13.51±0.33
SN00169942	-13.83±0.29	SN00384384	-13.64±0.37	SN00170384	-13.51±0.35
SN00167979	-13.82±0.49	SN00100399	-13.63±0.87	SN00240611	-13.51±0.36
SN00214272	-13.82±0.56	SN00125315	-13.63±0.23	SN00241069	-13.51±0.89
SN00391214	-13.82±0.39	SN00136711	-13.63±0.47	SN00242230	-13.51±0.48
SN00397355	-13.82±0.85	SN00169381	-13.63±1.12	SN00247481	-13.51±0.18
SN00128376	-13.81±0.36	SN00236890	-13.63±0.66	SN00260522	-13.51±0.66
SN00318192	-13.81±0.54	SN00137143	-13.62±0.74	SN00352768	-13.51±0.33
SN00128796	-13.8±0.54	SN00141055	-13.62±0.38	SN00369562	-13.51±0.51
SN00214050	-13.8±0.46	SN00169437	-13.62±0.37	SN00380580	-13.51±0.38
SN00359062	-13.8±0.8	SN00170401	-13.62±0.38	SN00106727	-13.5±0.85
SN00114308	-13.79±0.28	SN00174908	-13.62±0.59	SN00114309	-13.5±0.25
SN00135616	-13.79±0.36	SN00081767	-13.61±0.53	SN00142234	-13.5±0.53
SN00227072	-13.79±0.5	SN00164496	-13.61±0.66	SN00300506	-13.5±0.47
SN00270743	-13.79±0.35	SN00169440	-13.61±0.55	SN00323388	-13.5±0.37
SN00081067	-13.78±0.67	SN00268935	-13.61±1.2	SN00326320	-13.5±1.02
SN00294655	-13.78±0.59	SN00383086	-13.61±0.28	SN00380662	-13.5±0.6
SN00078114	-13.77±0.48	SN00097956	-13.6±0.43	SN00389675	-13.5±0.29
SN00116397	-13.77±0.6	SN00169430	-13.6±0.73	SN00139953	-13.49±0.79
SN00081079	-13.76±0.74	SN00169938	-13.6±0.39	SN00169374	-13.49±0.26
SN00169357	-13.76±0.76	SN00170390	-13.6±0.58	SN00176546	-13.49±0.65
SN00239757	-13.76±0.34	SN00172791	-13.6±0.49	SN00226829	-13.49±0.69
SN00097206	-13.74±0.36	SN00296952	-13.6±0.33	SN00354803	-13.49±0.33
SN00169457	-13.74±0.61	SN00310110	-13.6±0.52	SN00111420	-13.48±0.32

SN00316971	-13.74±0.72	SN00081634	-13.59±0.35	SN00113250	-13.48±0.34
SN00344013	-13.74±0.63	SN00169419	-13.59±0.45	SN00169939	-13.48±0.59
SN00091350	-13.73±0.51	SN00233069	-13.59±0.26	SN00172771	-13.48±0.36
SN00078117	-13.72±0.61	SN00097418	-13.58±0.32	SN00172824	-13.48±0.44
SN00272690	-13.72±0.19	SN00226941	-13.58±0.4	SN00175908	-13.48±0.91
SN00327455	-13.72±1.26	SN00349017	-13.58±0.34	SN00384061	-13.48±0.49
SN00113232	-13.71±0.83	SN00057684	-13.57±0.55	SN00133377	-13.47±0.56
SN00246695	-13.71±0.67	SN00176544	-13.57±0.45	SN00164139	-13.47±0.64
SN00364759	-13.71±0.44	SN00296040	-13.57±0.57	SN00170398	-13.47±0.44
SN00379189	-13.71±0.38	SN00058537	-13.56±0.48	SN00170692	-13.47±0.46
SN00098044	-13.7±0.4	SN00084674	-13.56±0.31	SN00233772	-13.47±0.36
SN00118874	-13.7±0.46	SN00139965	-13.56±0.37	SN00111703	-13.46±0.4
SN00168374	-13.7±0.39	SN00171845	-13.56±0.27	SN00167708	-13.46±0.62
SN00169376	-13.7±0.6	SN00173958	-13.56±0.53	SN00236102	-13.46±0.35
SN00256709	-13.7±0.69	SN00226062	-13.56±0.66	SN00297135	-13.46±0.33
SN00173918	-13.69±0.44	SN00392830	-13.56±0.7	SN00128374	-13.44±0.54
SN00296190	-13.69±0.46	SN00427143	-13.56±0.35	SN00167932	-13.44±0.59
SN00368224	-13.69±0.37	SN00097225	-13.54±0.43	SN00229183	-13.44±0.37
SN00078115	-13.68±0.63	SN00119196	-13.54±0.33	SN00249152	-13.44±0.34
SN00281885	-13.68±0.64	SN00246166	-13.54±1.12	SN00261527	-13.44±0.93
SN00337460	-13.68±0.32	SN00250332	-13.54±0.26	SN00293304	-13.44±0.83
SN00170394	-13.67±0.44	SN00352431	-13.54±0.27	SN00323402	-13.44±0.68
SN00281856	-13.67±1.06	SN00123863	-13.53±0.5	SN00364809	-13.44±0.33
SN00288395	-13.67±0.29	SN00278770	-13.53±0.42	SN00097411	-13.43±0.32
SN00261089	-13.66±0.66	SN00365186	-13.53±0.32	SN00106730	-13.43±0.97
SN00401354	-13.66±0.55	SN00172789	-13.52±0.47	SN00121863	-13.43±0.36
SN00167810	-13.64±0.39	SN00173913	-13.52±0.42	SN00159020	-13.43±0.62
SN00169372	-13.64±0.66	SN00259728	-13.52±0.43	SN00169385	-13.43±0.81
SN00169426	-13.64±0.46	SN00284649	-13.52±0.19	SN00169412	-13.43±0.75
SN00225970	-13.64±0.64	SN00304457	-13.52±0.53	SN00173175	-13.43±0.26
SN00319849	-13.43±0.52	SN00168388	-13.36±0.51	SN00239708	-13.3±0.46
SN00113059	-13.42±0.88	SN00265184	-13.36±0.55	SN00245140	-13.3±0.22
SN00113541	-13.42±0.49	SN00290515	-13.36±0.37	SN00151101	-13.29±0.52
SN00380133	-13.42±0.26	SN00136713	-13.34±0.49	SN00168356	-13.29±0.45
SN00113761	-13.41±0.48	SN00139973	-13.34±0.27	SN00169409	-13.29±0.3
SN00120909	-13.41±0.33	SN00141013	-13.34±0.74	SN00169953	-13.29±0.36
SN00167456	-13.41±0.33	SN00170395	-13.34±0.5	SN00172578	-13.29±0.39
SN00167948	-13.41±0.54	SN00172352	-13.34±0.45	SN00173029	-13.29±0.29
SN00169396	-13.41±1.1	SN00173144	-13.34±1.32	SN00257182	-13.29±0.71
SN00169410	-13.41±0.92	SN00174834	-13.34±0.69	SN00298985	-13.29±0.51
SN00172830	-13.41±0.44	SN00270457	-13.34±0.4	SN00371902	-13.29±0.68
SN00173921	-13.41±0.61	SN00295429	-13.34±0.51	SN00399954	-13.29±0.34

SN00245953	-13.41±0.47	SN00105976	-13.33±0.69	SN00078665	-13.28±0.36
SN00261587	-13.41±1.22	SN00106779	-13.33±0.4	SN00098043	-13.28±0.91
SN00295246	-13.41±0.48	SN00169433	-13.33±0.67	SN00108027	-13.28±0.16
SN00337526	-13.41±0.78	SN00313656	-13.33±0.34	SN00126281	-13.28±0.66
SN00341502	-13.41±0.24	SN00337147	-13.33±0.43	SN00139966	-13.28±0.57
SN00084682	-13.4±0.63	SN00381153	-13.33±0.42	SN00168359	-13.28±0.64
SN00097687	-13.4±0.34	SN00381225	-13.33±0.27	SN00169364	-13.28±0.9
SN00113539	-13.4±0.51	SN00097227	-13.32±0.69	SN00171132	-13.28±0.54
SN00139951	-13.4±0.73	SN00107651	-13.32±0.37	SN00173907	-13.28±0.5
SN00167956	-13.4±0.89	SN00113631	-13.32±0.78	SN00249525	-13.28±0.42
SN00172575	-13.4±0.41	SN00132224	-13.32±0.26	SN00262135	-13.28±0.4
SN00172786	-13.4±0.55	SN00134172	-13.32±0.68	SN00080974	-13.27±0.42
SN00173928	-13.4±0.74	SN00162890	-13.32±0.22	SN00151510	-13.27±1.07
SN00173971	-13.4±0.49	SN00167812	-13.32±0.3	SN00172798	-13.27±0.59
SN00176973	-13.4±0.37	SN00171706	-13.32±1.05	SN00172807	-13.27±0.49
SN00258951	-13.4±0.42	SN00172273	-13.32±0.59	SN00173960	-13.27±0.65
SN00082617	-13.39±1.14	SN00174876	-13.32±0.41	SN00174895	-13.27±0.45
SN00126280	-13.39±0.56	SN00224043	-13.32±0.32	SN00176984	-13.27±0.53
SN00169386	-13.39±0.77	SN00224821	-13.32±0.35	SN00270246	-13.27±0.63
SN00170255	-13.39±0.72	SN00236253	-13.32±0.36	SN00277065	-13.27±0.92
SN00172793	-13.39±1.11	SN00290973	-13.32±0.65	SN00393370	-13.27±0.29
SN00172855	-13.39±0.5	SN00295732	-13.32±0.4	SN00004671	-13.26±0.31
SN00243155	-13.39±0.47	SN00129447	-13.31±0.49	SN00058256	-13.26±0.61
SN00261583	-13.39±0.45	SN00130378	-13.31±0.44	SN00078968	-13.26±0.24
SN00051604	-13.38±0.51	SN00135095	-13.31±0.93	SN00128800	-13.26±0.29
SN00059871	-13.38±0.44	SN00167809	-13.31±0.38	SN00167706	-13.26±0.98
SN00111609	-13.38±0.34	SN00169358	-13.31±0.39	SN00169651	-13.26±0.55
SN00111702	-13.38±0.41	SN00170382	-13.31±0.63	SN00172689	-13.26±0.31
SN00169360	-13.38±0.83	SN00173892	-13.31±0.72	SN00174921	-13.26±0.47
SN00169467	-13.38±0.68	SN00261952	-13.31±0.43	SN00257818	-13.26±0.42
SN00169652	-13.38±0.9	SN00371690	-13.31±0.93	SN00259282	-13.26±1.25
SN00170403	-13.38±0.41	SN00383457	-13.31±0.45	SN00358372	-13.26±0.48
SN00170408	-13.38±0.3	SN00074337	-13.3±0.87	SN00385666	-13.26±0.68
SN00012590	-13.37±0.33	SN00108001	-13.3±0.59	SN00051582	-13.24±0.42
SN00143594	-13.37±0.59	SN00129403	-13.3±0.49	SN00056789	-13.24±0.71
SN00167111	-13.37±0.69	SN00136704	-13.3±0.42	SN00111674	-13.24±0.39
SN00263628	-13.37±0.36	SN00146412	-13.3±0.51	SN00111676	-13.24±0.33
SN00277690	-13.37±0.49	SN00164493	-13.3±0.54	SN00170396	-13.24±0.52
SN00336143	-13.37±0.59	SN00168380	-13.3±0.4	SN00174886	-13.24±0.27
SN00355930	-13.37±0.22	SN00169394	-13.3±0.64	SN00276332	-13.24±0.3
SN00381519	-13.37±0.7	SN00225740	-13.3±0.33	SN00366405	-13.24±0.38
SN00142239	-13.36±0.47	SN00228121	-13.3±0.88	SN00080896	-13.23±0.17

SN00084702	-13.23±0.31	SN00008387	-13.19±0.36	SN00176547	-13.14±0.7
SN00106729	-13.23±0.64	SN00059442	-13.19±0.53	SN00237320	-13.14±0.38
SN00121871	-13.23±0.19	SN00111576	-13.19±0.2	SN00318097	-13.14±0.58
SN00128073	-13.23±0.24	SN00111663	-13.19±0.25	SN00322232	-13.14±0.49
SN00132837	-13.23±0.41	SN00114250	-13.19±0.49	SN00346826	-13.14±0.34
SN00139770	-13.23±0.49	SN00168445	-13.19±0.46	SN00362478	-13.14±0.84
SN00170400	-13.23±0.77	SN00173909	-13.19±0.25	SN00391697	-13.14±0.57
SN00173927	-13.23±0.41	SN00236462	-13.19±0.37	SN00111675	-13.13±0.4
SN00177126	-13.23±0.57	SN00396821	-13.19±0.64	SN00114045	-13.13±0.34
SN00239403	-13.23±0.26	SN00015562	-13.18±0.48	SN00114929	-13.13±0.6
SN00260416	-13.23±0.19	SN00082651	-13.18±0.36	SN00121449	-13.13±0.34
SN00312143	-13.23±0.33	SN00109705	-13.18±0.72	SN00128075	-13.13±0.13
SN00390239	-13.23±0.35	SN00111711	-13.18±0.37	SN00132230	-13.13±0.56
SN00081539	-13.22±0.47	SN00128385	-13.18±0.74	SN00141410	-13.13±0.42
SN00106712	-13.22±0.88	SN00169407	-13.18±0.48	SN00169379	-13.13±0.57
SN00106728	-13.22±0.72	SN00173926	-13.18±0.58	SN00169401	-13.13±0.78
SN00107343	-13.22±0.47	SN00282816	-13.18±0.58	SN00172576	-13.13±0.89
SN00113504	-13.22±0.75	SN00360740	-13.18±0.26	SN00173575	-13.13±0.62
SN00126645	-13.22±0.69	SN00362382	-13.18±0.36	SN00252317	-13.13±0.3
SN00168033	-13.22±0.58	SN00366650	-13.18±0.28	SN00275296	-13.13±0.52
SN00168449	-13.22±0.5	SN00379911	-13.18±0.48	SN00051581	-13.12±0.41
SN00171123	-13.22±0.49	SN00059388	-13.17±0.65	SN00080933	-13.12±0.32
SN00171712	-13.22±0.53	SN00080939	-13.17±0.28	SN00099712	-13.12±0.67
SN00172586	-13.22±0.89	SN00108028	-13.17±0.33	SN00099739	-13.12±0.57
SN00172805	-13.22±0.67	SN00111586	-13.17±0.56	SN00113247	-13.12±0.36
SN00239126	-13.22±0.85	SN00113249	-13.17±0.66	SN00113629	-13.12±0.52
SN00245060	-13.22±0.76	SN00126282	-13.17±0.74	SN00114348	-13.12±0.37
SN00327269	-13.22±0.38	SN00167479	-13.17±0.6	SN00123349	-13.12±0.29
SN00111652	-13.21±0.44	SN00172134	-13.17±0.98	SN00128855	-13.12±0.52
SN00113218	-13.21±0.44	SN00173917	-13.17±0.55	SN00131673	-13.12±0.56
SN00114971	-13.21±0.54	SN00296536	-13.17±0.44	SN00141017	-13.12±0.37
SN00141018	-13.21±0.36	SN00300438	-13.17±0.53	SN00161478	-13.12±0.25
SN00157973	-13.21±0.97	SN00351762	-13.17±0.37	SN00258210	-13.12±0.38
SN00172772	-13.21±0.23	SN00005498	-13.16±0.63	SN00266522	-13.12±0.81
SN00253892	-13.21±0.83	SN00082503	-13.16±0.29	SN00273506	-13.12±0.5
SN00266324	-13.21±0.34	SN00122833	-13.16±0.54	SN00331477	-13.12±0.36
SN00298123	-13.21±0.74	SN00126328	-13.16±0.42	SN00347599	-13.12±0.37
SN00346715	-13.21±0.57	SN00133950	-13.16±0.93	SN00352443	-13.12±0.49
SN00062444	-13.2±0.4	SN00139969	-13.16±0.48	SN00012599	-13.11±0.78
SN00080932	-13.2±0.48	SN00172291	-13.16±0.35	SN00020195	-13.11±0.24
SN00081619	-13.2±0.47	SN00331859	-13.16±0.41	SN00037381	-13.11±0.28
SN00083037	-13.2±0.44	SN00368459	-13.16±1.37	SN00098042	-13.11±0.37

SN00097226	-13.2±0.6	SN00391702	-13.16±0.66	SN00108118	-13.11±0.7
SN00097526	-13.2±0.36	SN00427137	-13.16±0.46	SN00108496	-13.11±0.44
SN00111701	-13.2±0.55	SN00052444	-13.14±0.32	SN00168436	-13.11±0.69
SN00129322	-13.2±0.55	SN00106930	-13.14±0.43	SN00178201	-13.11±0.41
SN00142238	-13.2±0.5	SN00121862	-13.14±0.36	SN00298711	-13.11±0.3
SN00167993	-13.2±1.14	SN00128072	-13.14±0.33	SN00310178	-13.11±0.41
SN00169365	-13.2±0.64	SN00136712	-13.14±0.25	SN00356104	-13.11±0.92
SN00169441	-13.2±0.38	SN00170253	-13.14±0.4	SN00357461	-13.11±0.58
SN00171707	-13.2±0.32	SN00172787	-13.14±0.52	SN00358384	-13.11±0.33
SN00176530	-13.2±0.86	SN00172818	-13.14±0.37	SN00397632	-13.11±0.66
SN00299625	-13.2±0.39	SN00173914	-13.14±0.67	SN00083218	-13.1±0.42
SN00345686	-13.2±0.51	SN00173916	-13.14±0.78	SN00084750	-13.1±0.82
SN00106967	-13.1±0.46	SN00141487	-13.07±0.29	SN00111617	-13.03±0.47
SN00107978	-13.1±0.34	SN00168463	-13.07±0.51	SN00111712	-13.03±0.42
SN00109757	-13.1±0.94	SN00172784	-13.07±0.45	SN00157950	-13.03±1.02
SN00114567	-13.1±0.58	SN00231454	-13.07±0.45	SN00162428	-13.03±0.97
SN00115698	-13.1±0.44	SN00238169	-13.07±0.4	SN00169445	-13.03±0.46
SN00118873	-13.1±0.45	SN00246480	-13.07±0.28	SN00169450	-13.03±0.51
SN00118966	-13.1±0.46	SN00302481	-13.07±0.69	SN00169465	-13.03±0.4
SN00128422	-13.1±0.35	SN00305691	-13.07±0.86	SN00172587	-13.03±0.72
SN00129448	-13.1±0.56	SN00352327	-13.07±0.34	SN00246352	-13.03±0.36
SN00167927	-13.1±0.5	SN00051583	-13.06±0.63	SN00264331	-13.03±0.52
SN00167983	-13.1±1.06	SN00077583	-13.06±0.8	SN00341572	-13.03±0.42
SN00169456	-13.1±0.32	SN00081635	-13.06±0.5	SN00350731	-13.03±0.28
SN00169466	-13.1±0.56	SN00111618	-13.06±0.42	SN00350939	-13.03±0.31
SN00171097	-13.1±0.5	SN00111625	-13.06±0.43	SN00380271	-13.03±0.51
SN00172799	-13.1±0.49	SN00113229	-13.06±0.38	SN00427145	-13.03±0.78
SN00173922	-13.1±0.67	SN00115081	-13.06±0.43	SN00091501	-13.02±0.36
SN00174844	-13.1±0.43	SN00129492	-13.06±0.6	SN00107402	-13.02±0.41
SN00174852	-13.1±0.32	SN00133970	-13.06±0.32	SN00111673	-13.02±0.63
SN00311638	-13.1±0.97	SN00136710	-13.06±0.3	SN00119083	-13.02±0.39
SN00334224	-13.1±0.44	SN00167494	-13.06±0.88	SN00123510	-13.02±0.37
SN00008385	-13.09±0.3	SN00171122	-13.06±0.34	SN00154784	-13.02±0.34
SN00012601	-13.09±0.83	SN00172354	-13.06±0.42	SN00155161	-13.02±0.59
SN00089691	-13.09±0.36	SN00172612	-13.06±0.5	SN00166919	-13.02±0.33
SN00097688	-13.09±0.53	SN00245319	-13.06±0.25	SN00167949	-13.02±0.87
SN00099738	-13.09±0.55	SN00247179	-13.06±0.62	SN00169454	-13.02±0.64
SN00131056	-13.09±0.63	SN00289906	-13.06±0.49	SN00170399	-13.02±0.54
SN00133706	-13.09±0.24	SN00297321	-13.06±0.43	SN00172802	-13.02±0.58
SN00158885	-13.09±0.7	SN00304569	-13.06±0.5	SN00173042	-13.02±0.48
SN00173298	-13.09±0.48	SN00325070	-13.06±0.59	SN00244833	-13.02±0.62
SN00281717	-13.09±0.53	SN00338156	-13.06±0.38	SN00265480	-13.02±0.22

SN00307932	-13.09±0.51	SN00343402	-13.06±0.45	SN00276132	-13.02±0.66
SN00314913	-13.09±0.49	SN00366096	-13.06±0.69	SN00281219	-13.02±1
SN00080956	-13.08±0.2	SN00084678	-13.04±0.6	SN00329349	-13.02±0.59
SN00111466	-13.08±0.52	SN00096066	-13.04±0.34	SN00350549	-13.02±0.6
SN00111704	-13.08±0.44	SN00101586	-13.04±0.42	SN00052010	-13.01±0.45
SN00128074	-13.08±0.24	SN00105422	-13.04±0.59	SN00084069	-13.01±0.47
SN00133957	-13.08±0.4	SN00136682	-13.04±0.63	SN00091326	-13.01±0.33
SN00139931	-13.08±0.25	SN00139955	-13.04±0.32	SN00101331	-13.01±0.51
SN00150533	-13.08±0.35	SN00139974	-13.04±0.25	SN00107344	-13.01±0.23
SN00167116	-13.08±0.34	SN00167952	-13.04±0.67	SN00113839	-13.01±0.36
SN00167486	-13.08±0.38	SN00170407	-13.04±0.53	SN00114306	-13.01±0.33
SN00167575	-13.08±0.35	SN00171701	-13.04±0.55	SN00119195	-13.01±0.28
SN00174857	-13.08±0.55	SN00172788	-13.04±0.3	SN00169944	-13.01±0.28
SN00234930	-13.08±0.39	SN00283611	-13.04±0.64	SN00170380	-13.01±0.58
SN00259653	-13.08±0.41	SN00297425	-13.04±0.6	SN00252020	-13.01±0.79
SN00338890	-13.08±0.45	SN00345704	-13.04±0.58	SN00275452	-13.01±0.37
SN00355392	-13.08±0.27	SN00348816	-13.04±0.38	SN00319706	-13.01±0.34
SN00362462	-13.08±0.59	SN00387973	-13.04±0.27	SN00381395	-13.01±0.29
SN00369721	-13.08±0.59	SN00007650	-13.03±0.36	SN00015950	-13±0.45
SN00051603	-13.07±0.52	SN00035917	-13.03±0.42	SN00059694	-13±0.47
SN00081562	-13.07±0.3	SN00038957	-13.03±0.68	SN00111665	-13±0.29
SN00108034	-13.07±0.56	SN00083606	-13.03±0.42	SN00113215	-13±0.54
SN00111540	-13.07±0.28	SN00091357	-13.03±0.42	SN00113217	-13±0.72
SN00132319	-13.07±0.51	SN00109120	-13.03±0.31	SN00121452	-13±0.23
SN00166673	-13±0.41	SN00173915	-13±0.75	SN00280962	-13±0.72
SN00169398	-13±0.36	SN00238003	-13±0.35	SN00292426	-13±0.75
SN00350231	-13±0.5	SN00352197	-13±0.31	SN00390671	-13±0.58
SN00427228	-13±0.61				

Supplementary Table S3: Molecular docking analysis for potential inhibitor compounds (candidate molecules) at the rapamycin binding site of mTOR kinase selected among ZINC database natural products [5].

ZINC database	ΔG , mean±S.D.	ZINC database	ΔG , mean±S.D.	ZINC database	ΔG , mean±S.D.
ZINC20807902	-13.04±0.47	ZINC04085602	-11.89±0.52	ZINC30819228	-11.48±0.18
ZINC02141237	-12.88±0.27	ZINC06624334	-11.89±0.49	ZINC09682151	-11.48±0.4
ZINC20807905	-12.84±0.24	ZINC09481951	-11.89±0.51	ZINC16671995	-11.47±0.22
ZINC08335520	-12.68±0.31	ZINC09792243	-11.88±0.29	ZINC30819218	-11.47±0.42
ZINC16284487	-12.61±0.34	ZINC14458042	-11.87±0.28	ZINC15468981	-11.44±0.49
ZINC10012991	-12.59±0.45	ZINC05235687	-11.86±0.31	ZINC02095105	-11.44±0.4
ZINC13120611	-12.59±0.37	ZINC08367675	-11.86±0.42	ZINC02103315	-11.44±0.65

ZINC16349120	-12.54±0.3	ZINC15725220	-11.84±0.57	ZINC24504925	-11.44±0.34
ZINC30819219	-12.44±0.81	ZINC09941299	-11.84±0.49	ZINC03331795	-11.44±0.34
ZINC00754174	-12.43±0.35	ZINC15725460	-11.82±0.81	ZINC04262734	-11.43±0.59
ZINC02928797	-12.39±0.76	ZINC09408505	-11.82±0.4	ZINC30819216	-11.38±0.28
ZINC27534122	-12.38±0.31	ZINC12949356	-11.81±0.53	ZINC06624464	-11.38±0.53
ZINC08918463	-12.37±0.25	ZINC09992471	-11.81±0.31	ZINC15725194	-11.37±0.47
ZINC14458178	-12.36±0.27	ZINC13642830	-11.8±0.59	ZINC20970245	-11.36±0.31
ZINC20938915	-12.34±0.47	ZINC15733799	-11.8±0.51	ZINC09530812	-11.33±0.43
ZINC09580205	-12.34±0.41	ZINC09577184	-11.8±0.51	ZINC20563426	-11.31±0.48
ZINC02928802	-12.33±0.56	ZINC09992380	-11.8±0.53	ZINC20563632	-11.27±0.39
ZINC09531209	-12.32±0.51	ZINC12583319	-11.79±0.34	ZINC13595929	-11.26±0.35
ZINC08367670	-12.3±0.37	ZINC16284359	-11.79±0.37	ZINC05151985	-11.23±0.29
ZINC12882862	-12.29±0.46	ZINC06624637	-11.77±0.4	ZINC08764854	-11.23±0.86
ZINC19879437	-12.28±0.36	ZINC13623590	-11.76±0.59	ZINC09076927	-11.23±0.39
ZINC01405393	-12.26±0.18	ZINC16269305	-11.76±0.49	ZINC00980500	-11.23±0.44
ZINC09940957	-12.23±0.42	ZINC30819248	-11.76±0.44	ZINC12440825	-11.22±0.34
ZINC15725210	-12.21±0.63	ZINC06232955	-11.76±0.6	ZINC06623908	-11.22±0.71
ZINC09992418	-12.19±0.39	ZINC09408500	-11.76±0.42	ZINC04936227	-11.19±0.41
ZINC00626315	-12.18±0.23	ZINC16349822	-11.73±0.25	ZINC12892460	-11.17±0.49
ZINC09224560	-12.18±0.48	ZINC16362158	-11.73±0.47	ZINC19660588	-11.14±0.36
ZINC15725066	-12.17±0.67	ZINC08966188	-11.73±0.5	ZINC12188773	-11.11±0.39
ZINC06232954	-12.11±0.33	ZINC11865630	-11.72±0.22	ZINC09408007	-11.08±0.36
ZINC00754173	-12.1±0.46	ZINC30819226	-11.71±0.37	ZINC04074031	-11.07±0.27
ZINC15725068	-12.09±0.28	ZINC12182014	-11.7±0.43	ZINC09043059	-11.06±0.59
ZINC09792247	-12.07±0.42	ZINC12682031	-11.7±0.3	ZINC06624359	-11.03±0.64
ZINC01223299	-12.06±0.27	ZINC15725231	-11.69±0.62	ZINC12753676	-11.02±0.33
ZINC11867425	-12.04±0.29	ZINC02093144	-11.69±0.28	ZINC05044064	-11±0.41
ZINC02107387	-12.02±0.37	ZINC20691520	-11.68±0.25	ZINC02094748	-11.89±0.25
ZINC11867433	-12±0.16	ZINC02092906	-11.68±0.35	ZINC03358607	-11.89±0.21
ZINC20938919	-11.99±0.36	ZINC01223300	-11.67±0.4	ZINC02148960	-11.51±0.17
ZINC16363024	-11.98±0.35	ZINC02098205	-11.67±0.34	ZINC02093614	-11.5±0.46
ZINC17093033	-11.98±0.27	ZINC13226339	-11.66±0.26		
ZINC22530327	-11.97±0.51	ZINC04744105	-11.64±0.33		
ZINC30819257	-11.97±0.42	ZINC01223288	-11.63±0.46		
ZINC12896272	-11.94±0.58	ZINC08857160	-11.63±0.38		
ZINC04744033	-11.94±0.31	ZINC30819259	-11.62±0.26		
ZINC08765269	-11.93±0.4	ZINC06623842	-11.61±0.42		
ZINC09940952	-11.93±0.36	ZINC08440247	-11.61±0.2		
ZINC06624400	-11.92±0.45	ZINC08490711	-11.56±0.41		
ZINC15725282	-11.91±0.56	ZINC13642449	-11.54±0.3		
ZINC12899220	-11.9±0.34	ZINC14458006	-11.54±0.36		
ZINC20990084	-11.9±0.42	ZINC04085605	-11.53±0.36		

ZINC2333375	-11.9±0.5	ZINC08765217	-11.53±0.38
ZINC05235703	-11.9±0.33	ZINC09059583	-11.53±0.71
ZINC11936239	-11.89±0.44	ZINC13691831	-11.51±0.51

Supplementary Table S4: Molecular docking analysis for potential inhibitor compounds (candidate molecules) at the **ATP binding site** of **mTOR kinase** selected among **Marine Natural Products** [1].

Marine natural products	ΔG , mean±S.D.	Marine natural products	ΔG , mean±S.D.	Marine natural products	ΔG , mean±S.D.
101383-39-5	-12.20±0.30	133625-26-0	-11.58±0.85	156953-93-4	-11.66±0.56
112088-56-9	-11.18±1.19	133805-03-5	-11.38±0.27	159736-39-7	-12.18±0.90
114571-91-4	-11.50±0.43	135340-01-1	-12.06±0.88	162465-80-7	-12.50±0.73
115982-22-4	-11.80±0.70	135824-74-7	-11.02±0.44	117694-96-9	-11.06±0.39
120154-96-3	-12.16±0.87	140429-37-4	-12.44±1.01	191-24-2	-12.26±0.27
121071-11-2	-11.02±0.38	103614-76-2	-11.04±0.29	206535-31-1	-11.02±0.39
122780-90-9	-11.54±0.49	152845-74-4	-11.08±0.39	214899-21-5	-11.06±0.67
128229-64-1	-11.94±0.53	156953-87-6	-11.02±0.79		

Supplementary Table S5: Molecular docking analysis for potential inhibitor compounds (candidate molecules) at the **ATP binding site** of **mTOR kinase** selected among **Super Natural II** database [2].

Super Natural II	ΔG , mean±S.D.	Super Natural II	ΔG , mean±S.D.	Super Natural II	ΔG , mean±S.D.
SN00003459	-11.62±0.54	SN00126328	-11.40±0.90	SN00167993	-11.34±0.65
SN00005498	-11.42±0.69	SN00128374	-11.60±0.81	SN00168000	-11.66±0.25
SN00008379	-11.02±0.90	SN00128376	-11.40±0.75	SN00168004	-11.28±0.46
SN00008447	-11.00±1.01	SN00128384	-12.92±0.92	SN00111460	-11.46±0.72
SN00008773	-11.02±0.68	SN00128385	-11.82±0.98	SN00111466	-11.14±0.68
SN00017897	-11.10±0.83	SN00128827	-11.00±1.20	SN00111540	-11.00±0.45
SN00051580	-11.04±1.03	SN00129403	-11.38±0.66	SN00111542	-11.52±1.00
SN00051581	-11.12±0.84	SN00129404	-11.00±0.54	SN00111571	-11.26±0.95
SN00051582	-11.18±0.66	SN00129405	-12.60±1.56	SN00115210	-11.00±0.26
SN00051602	-11.04±0.81	SN00129448	-11.04±0.68	SN00116397	-11.34±0.27
SN00051604	-11.18±0.69	SN00130058	-12.98±0.41	SN00120425	-12.02±0.41
SN00052444	-11.10±1.10	SN00130855	-12.00±0.52	SN00123829	-11.82±1.09
SN00052930	-11.26±1.18	SN00130898	-12.62±0.69	SN00124057	-11.28±0.79
SN00058602	-11.42±0.90	SN00130963	-12.28±1.27	SN00125316	-11.60±0.51
SN00059432	-11.36±0.98	SN00131034	-11.28±1.66	SN00167932	-12.04±0.48
SN00061688	-11.56±1.13	SN00131673	-11.20±0.85	SN00167942	-11.32±0.67
SN00062324	-11.02±0.67	SN00132839	-11.14±1.04	SN00167952	-11.88±0.40

SN00062444	-11.30±1.12	SN00132840	-11.48±1.04	SN00167960	-11.14±0.77
SN00066079	-12.06±0.61	SN00133377	-11.52±0.24	SN00167965	-12.80±0.25
SN00074337	-11.30±0.80	SN00136688	-11.20±0.39	SN00167970	-12.08±0.41
SN00074793	-11.98±0.93	SN00136695	-11.34±0.38	SN00167976	-11.36±0.83
SN00076726	-11.10±0.73	SN00136914	-11.16±0.40	SN00167979	-12.04±0.21
SN00080936	-11.36±0.73	SN00137005	-11.06±0.74	SN00167982	-11.84±1.41
SN00080939	-11.16±0.72	SN00137007	-11.10±0.35	SN00167989	-11.28±0.91
SN00081043	-11.42±0.68	SN00137008	-11.14±0.66	SN00167990	-12.04±0.33
SN00081067	-11.34±0.69	SN00137009	-11.08±0.11	SN00111420	-11.12±0.31
SN00081079	-11.42±0.66	SN00137074	-11.84±0.48	SN00111437	-11.28±0.79
SN00081767	-11.36±0.84	SN00137076	-11.22±0.13	SN00167912	-11.56±0.53
SN00084682	-11.76±0.55	SN00142234	-11.82±0.93	SN00167918	-11.88±1.56
SN00086012	-11.06±0.77	SN00142238	-11.46±1.18		
SN00097206	-11.46±0.60	SN00151101	-11.42±0.66		
SN00097225	-11.06±0.65	SN00156840	-11.06±0.53		
SN00097229	-11.52±0.59	SN00162099	-11.06±0.93		
SN00106712	-11.68±0.24	SN00164826	-11.94±0.63		
SN00106774	-12.18±0.46	SN00166271	-11.14±0.34		
SN00108027	-11.78±0.89	SN00167115	-11.48±0.58		
SN00108028	-11.82±0.73	SN00167116	-11.12±0.52		
SN00108060	-11.44±0.94	SN00167892	-11.52±0.48		
SN00111397	-11.24±0.90	SN00167901	-11.38±0.54		

Supplementary Table S6: Physicochemical and toxicological parameters calculated for the selected compounds against the ATP binding site of mTOR based on molecular docking analysis. Each cluster groups compounds with structures with up to 70% structural similarity. Compounds whose name is CAS format belong to the Marine Natural Products database [1], while those compounds whose name begins with SN belong to the Super Natural II database [2].

Compound	Cluster 70% ^a	^a Total Surface Area, Å ²	^a TPSA, Å ²	cLogS ^a	MW ^a	cLogP ^a	HBA ^a	HBD ^a	Ro5 violations ^a	Druglikeness ^a	DrugScore ^a	RAT (LD50, mol/kg) ^b	Caco-2 Permeability (LogPapp, cm/s) ^b	TPT (pIC50, μg/L) ^b	FT (pLC50, mg/L) ^b
114571-91-4	1	383.9	107.5	-7.281	595.3	2.965	8	2	1	0.405	0.07853	2.631	0.375	0.700	1.023
135824-74-7	1	383.9	107.5	-7.281	595.3	2.965	8	2	1	0.405	0.07853	2.631	0.375	0.700	1.023
117694-96-9	2	265.3	71.5	-6.325	385.4	3.277	6	1	0	5.488	0.50169	2.801	1.532	0.362	1.373
133805-03-5	3	237.0	118.2	-5.447	357.3	2.762	7	5	0	1.524	0.55632	2.597	0.231	0.153	1.289
135340-01-1	4	295.1	79.8	-6.055	427.5	2.877	6	2	0	1.910	0.47490	2.447	1.255	0.457	2.280
140429-37-4	5	305.1	99.5	-6.743	441.5	3.159	7	4	0	5.165	0.44521	2.529	0.358	0.393	1.398

SN0023047 1	5	298.2	126.0	-	469.5	3.376	9	4	0	3.943	0.43415	2.460	0.296	0.476	1.369
SN0000549 8	6	379.7	74.7	-	501.6	5.017	6	1	2	5.821	0.37008	2.614	0.551	0.349	1.542
SN0011139 7	6	410.6	93.1	-	550.7	4.249	7	0	1	3.575	0.50267	2.773	0.865	0.565	0.616
SN0011142 0	6	385.8	93.1	-	522.6	3.470	7	0	1	4.179	0.60912	2.797	0.852	0.464	0.608
SN0011143 7	6	399.6	93.1	-	536.6	3.924	7	0	1	3.105	0.54974	2.741	0.801	0.515	0.595
SN0011157 1	6	400.1	93.1	-	536.6	3.809	7	0	1	3.894	0.55219	2.776	0.765	0.523	0.609
SN0000837 9	7	340.7	69.7	-	497.4	4.111	6	1	0	-0.857	0.09979	2.372	0.842	0.568	1.499
SN0000844 7	7	353.8	81.8	-	500.5	3.851	7	2	1	-5.039	0.07583	2.357	0.826	0.542	1.640
SN0000877 3	7	356.0	93.5	-	504.5	3.846	7	1	1	-5.138	0.07311	2.468	0.910	0.615	1.510
SN0001789 7	8	370.5	143.2	-	498.6	3.385	9	2	0	-2.767	0.20633	2.473	1.010	0.573	1.371
SN0005860 2	9	300.9	79.8	-	417.4	5.889	6	2	1	1.766	0.26763	2.550	1.174	0.800	1.147
SN0006607 9	10	344.0	95.9	-	494.5	4.970	7	1	0	2.751	0.10182	2.414	1.065	0.489	1.307
SN0007479 3	11	330.0	117.4	-	470.4	3.216	8	1	0	2.407	0.20231	2.569	1.040	0.554	1.029
SN0007672 6	12	274.5	53.4	-	390.4	5.649	5	0	1	1.289	0.22060	2.543	1.562	0.334	1.264
SN0008093 6	13	358.6	58.4	-	486.6	5.899	6	0	1	6.806	0.12842	2.578	1.105	0.347	1.249
SN0008093 9	13	334.1	58.4	-	458.5	5.211	6	0	1	6.920	0.26864	2.390	0.997	0.359	1.394
SN0008104 3	13	349.5	58.4	-	493.0	5.817	6	0	1	6.906	0.21352	2.396	0.882	0.642	1.262
SN0008106 7	13	340.4	58.4	-	476.5	5.312	6	0	1	5.580	0.24749	2.432	0.951	0.626	1.147
SN0008107 9	13	340.4	58.4	-	476.5	5.312	6	0	1	5.580	0.24749	2.427	0.802	0.525	1.246
SN0008176 7	13	341.5	88.7	-	476.5	4.405	8	0	0	6.606	0.32421	2.254	0.707	0.259	1.403
SN0009720 6	13	374.3	58.4	-	498.6	5.895	6	0	1	8.099	0.22226	2.500	0.698	0.394	1.241
SN0009722 5	13	347.8	58.4	-	472.5	5.134	6	0	1	7.810	0.28342	2.367	0.635	0.261	1.548
SN0009722 9	13	368.1	76.9	-	516.6	5.246	8	0	2	7.543	0.23433	2.212	0.728	0.280	1.238
SN0011146 0	13	363.5	58.4	-	526.5	6.060	6	0	2	-0.270	0.13727	2.545	0.878	0.603	1.249
SN0011154 0	13	412.6	95.4	-	576.6	5.106	10	0	2	7.487	0.21189	2.322	1.013	0.368	1.041
SN0010677 4	14	390.6	105.0	-	537.6	3.764	7	1	1	2.570	0.48702	2.602	1.259	0.541	0.857
SN0011521 0	15	396.3	102.9	-	531.6	3.437	9	1	1	3.193	0.58891	2.439	0.796	0.415	1.075
SN0012837 4	16	306.7	97.2	-	442.4	4.691	6	1	0	-0.534	0.05304	2.754	1.225	0.809	0.662
SN0013167 3	17	265.1	70.1	-	374.4	3.937	4	0	0	-0.838	0.07709	2.363	1.453	0.523	1.022
SN0016946 1	18	416.2	72.7	-	574.9	5.997	4	4	2	1.528	0.21055	2.736	0.857	0.371	1.760
SN0017248 8	19	440.1	98.0	-	628.9	6.073	5	4	2	-0.001	0.07404	3.020	0.985	0.897	0.778
SN0022955 8	19	391.1	113.0	-	546.6	3.637	8	1	1	-0.318	0.24032	2.675	0.675	0.430	0.935
SN0029046 8	19	381.1	103.8	-	530.6	3.849	7	1	1	-0.551	0.29535	2.638	1.111	0.418	1.064

SN0029545 7	19	381.1	103.8	-	530.6	3.849	7	1	1	-0.551	0.29535	2.638	1.111	0.418	1.064
SN0017395 5	20	457.1	180.3	-	637.7	2.417	11	3	2	-6.958	0.07667	2.692	0.642	0.759	0.826
SN0031802 1	20	373.3	116.2	-	510.6	1.914	8	2	1	3.904	0.54231	2.663	0.611	0.436	1.216
SN0023998 7	21	354.5	49.4	-	460.6	5.739	4	0	1	-1.562	0.20369	2.537	1.116	0.905	0.581
SN0024672 9	21	354.5	49.4	-	460.6	5.852	4	0	1	1.712	0.31481	2.657	1.063	0.714	0.623
SN0024595 3	22	411.7	77.5	-	578.7	5.110	8	1	2	1.983	0.22382	2.643	1.180	0.699	1.276
SN0035239 3	22	383.7	97.6	-	548.6	5.531	8	2	2	-1.773	0.12085	2.598	0.627	0.691	1.433
SN0038406 1	22	383.7	97.6	-	548.6	5.531	8	2	2	-1.773	0.12085	2.598	0.627	0.691	1.433
SN0035206 3	23	343.5	49.4	-	446.6	5.582	4	0	1	0.443	0.30148	2.575	1.000	0.640	0.895
SN0036461 6	24	345.7	161.7	-6.66	527.5	3.197	10	4	1	2.464	0.22028	2.587	0.782	0.605	1.125
SN0038308 6	25	382.3	59.1	-	616.8	2.008	8	0	1	-1.202	0.35389	2.896	0.838	0.532	0.885
SN0040427 3	26	333.9	32.9	-	505.3	5.320	4	0	2	-1.033	0.05322	2.619	0.780	0.923	0.681

Abbreviations: Topological polar surface area (TPSA); molecular weight (MW); the calculated logarithm (base 10) of the solubility measured in mol/liter (cLogS); calculated logarithm of partition coefficient between n-octanol and water (cLogP); number of hydrogen bond donors (HBD); number of hydrogen bond acceptors (HBA); violation of Lipinski's rules (Ro5 violations), FT, Fish Toxicity; TPT, *Tetrahymena Pyriformis* Toxicity; RAT, Rat Acute Toxicity. LD50 is the amount of a compound, given all at once, which causes the death of 50% (one half) of a group of test rats.

^a These parameters were calculated using the DATAWARRIOR software v4.7.2 [3].

^b These parameters were calculated using the <http://lmmd.ecust.edu.cn:8000/predict/> site [4].

Supplementary Table S7: Physicochemical and toxicological parameters calculated for the selected compounds against the rapamycin binding site of mTOR based on molecular docking analysis. Each cluster groups compounds with structures with up to 70% structural similarity. Compounds whose name is CAS format belong to the Marine Natural Products database[1], compounds whose name begins with SN belong to the Super Natural II database[2], and compounds whose name begins with ZINC belong to the ZINC natural products [5]. Text in **bold** only for compounds tested *in vitro* in these paper.

Compound	Cluster 70% ^a	^a Total Surface Area, Å ²	^a TPSA, Å ²	cLog S ^a	MW ^a	cLog P ^a	HBA ^a	HBD ^a	Ro5 violations ^a	Druglikeness ^a	DrugScore ^a	RAT (LD50, mol/kg) ^b	Caco-2 Permeability (LogPapp, cm/s) ^b	TPT (pIC50, µg/L) ^b	FT (pLC50, mg/L) ^b
1008752-06-4	1	430.3	92.7	5.365	580.8	5.397	7	3	2	-2.153	0.13911	2.891	0.595	0.363	1.377
107900-75-4	1	430.3	92.7	5.365	580.8	5.397	7	3	2	-2.153	0.13911	2.891	0.595	0.363	1.377
116477-23-7	1	423.5	54.5	5.170	552.8	6.395	5	3	2	-1.962	0.13214	2.818	0.627	0.377	1.513

117631-50-2	1	423.9	72.5	5.66 1	564. 8	5.743	6	2	2	-2.153	0.12867	2.956	0.958	0.338	1.346
154466-37-2	1	425.3	75.6	5.48 5	564. 8	6.198	6	3	2	-2.232	0.12269	2.885	0.689	0.361	1.347
162465-80-7	1	422.5	54.9	5.96 3	550. 8	6.477	5	2	2	-1.687	0.14789	2.834	0.700	0.537	1.470
148439-45-6	1	315.1	51.4	4.39 8	456. 6	2.838	6	1	0	2.906	0.39595	2.936	1.452	0.477	1.127
SN00383086	1	382.3	59.1	1.62 2	616. 8	2.008	8	0	1	-1.202	0.35389	2.896	0.838	0.532	0.885
112693-24-0	2	291.7	31.9	4.57 5	347. 5	5.340	3	1	1	-4.613	0.21355	2.429	0.612	0.713	1.152
113831-00-8	3	276.4	118. 9	5.50 9	423. 4	2.025	7	1	0	-2.627	0.30705	2.566	0.819	0.555	1.412
151247-69-7	3	284.9	115. 0	5.23 8	425. 5	1.457	7	1	0	-1.649	0.35257	2.580	0.836	0.446	1.317
114571-91-4	4	383.9	107. 5	7.28 1	595. 3	2.965	8	2	1	0.405	0.07853	2.631	0.375	0.700	1.023
135824-74-7	4	383.9	107. 5	7.28 1	595. 3	2.965	8	2	1	0.405	0.07853	2.631	0.375	0.700	1.023
120314-15-0	4	340.0	72.9	4.92 0	493. 6	3.634	6	0	0	1.365	0.46583	2.671	1.050	0.418	0.751
120409-36-1	4	340.0	72.9	4.92 0	493. 6	3.634	6	0	0	1.365	0.46583	2.671	1.050	0.418	0.751
123853-69-0	4	341.9	90.0	4.66 0	509. 6	3.273	7	0	1	1.028	0.22449	2.642	1.129	0.458	0.753
164991-65-5	4	318.9	79.4	4.50 0	481. 6	3.071	6	1	0	2.770	0.27517	2.797	0.952	0.455	0.911
93426-90-5	4	338.0	72.9	5.00 8	495. 7	3.981	6	0	0	0.691	0.19654	2.671	1.161	0.464	0.700
123641-95-2	4	397.7	139. 8	1.86 3	566. 6	1.652	11	1	2	1.909	0.35392	2.825	0.771	0.428	1.124
631913-68-3	4	418.1	163. 5	2.17 6	591. 6	0.720	12	1	2	-2.454	0.19530	2.694	0.787	0.518	0.981
79664-61-2	4	427.4	128. 8	2.07 8	594. 7	1.984	11	0	2	0.216	0.27573	2.706	0.892	0.453	1.136
SN00111586	4	384.8	75.7	3.81 2	516. 7	4.127	6	1	1	1.523	0.49715	2.775	1.148	0.482	0.554
184348-39-8	4	365.9	103. 8	4.19 3	508. 7	2.819	7	2	1	4.554	0.58861	2.723	0.398	0.292	1.478
SN00108034	4	402.2	83.9	5.43 5	551. 1	5.209	6	1	2	-0.734	0.18048	2.742	0.829	0.723	0.888
SN00108118	4	446.4	83.9	5.94 4	601. 2	6.260	6	1	2	-0.483	0.16585	2.811	0.841	0.801	0.813

114995-72-1	5	404.0	94.5	4.86 9	514. 7	4.080	7	2	1	-5.750	0.14400	2.928	0.251	0.664	0.732
115267-16-8	5	404.0	94.5	4.86 9	514. 7	4.080	7	2	1	-5.750	0.14400	2.928	0.251	0.664	0.732
115268-43-4	5	411.7	97.8	4.86 9	514. 7	4.135	7	2	1	-4.611	0.08640	2.625	0.834	0.745	1.151
173792-58-0	5	395.3	68.1	5.56 9	507. 7	5.931	5	1	2	1.638	0.29615	2.668	0.844	0.732	0.982
118574-73-5	6	326.6	40.5	5.77 2	414. 7	6.297	2	2	1	-1.174	0.21439	2.937	1.626	0.933	0.618
145163-99-1	6	326.6	40.5	5.77 2	414. 7	6.297	2	2	1	-1.174	0.21439	2.937	1.626	0.933	0.618
465-95-2	6	338.1	60.7	5.74 7	458. 7	5.562	3	3	1	-4.206	0.18522	2.377	1.218	1.057	0.985
17991-67-2	6	345.3	94.8	5.33 0	486. 7	4.533	5	3	0	-1.702	0.25439	2.377	1.154	0.951	0.699
471-53-4	6	341.0	74.6	5.78 0	470. 7	5.356	4	2	1	-2.356	0.20001	2.377	1.154	0.951	0.699
564-16-9	6	337.0	57.5	6.12 8	456. 7	6.064	3	2	1	-3.051	0.16620	2.390	1.544	0.959	0.815
74984-66-0	6	337.9	57.5	6.11 1	456. 7	6.002	3	2	1	-3.658	0.16499	2.390	1.544	0.959	0.815
119212-28-1	7	419.4	108. 6	6.04 8	556. 7	4.654	7	2	1	-2.651	0.11378	2.869	1.117	0.596	0.669
345642-84-4	7	398.0	119. 5	5.02 8	530. 7	4.139	7	4	1	0.505	0.36350	2.976	0.742	0.496	1.044
52645-09-7	7	398.0	119. 5	5.02 8	530. 7	4.139	7	4	1	0.505	0.36350	2.976	0.742	0.496	1.044
55945-74-9	7	398.0	119. 5	5.02 8	530. 7	4.139	7	4	1	1.039	0.38925	2.976	0.742	0.496	1.044
65773-98-0	7	396.9	116. 3	5.07 9	528. 6	4.108	7	3	1	-4.951	0.22532	2.976	0.742	0.496	1.044
122795-54-4	7	265.3	71.5	6.32 5	385. 4	3.277	6	1	0	5.488	0.50169	2.801	1.532	0.362	1.373
12626-18-5	7	420.4	102. 7	4.32 8	579. 7	4.703	10	1	1	0.388	0.07198	2.962	1.117	0.634	0.639
12771-72-1	7	353.7	113. 7	3.46 4	511. 6	2.606	10	2	1	0.324	0.10920	2.913	0.889	0.621	0.782
SN00239708	7	408.1	39.3	6.63 9	614. 8	4.937	6	0	1	0.278	0.12456	2.985	1.298	0.748	0.847
SN00250332	7	431.2	49.7	7.60 8	616. 8	6.110	6	1	2	0.986	0.17249	2.934	0.958	0.584	1.173
SN00257182	7	445.8	103. 5	6.38 3	670. 8	2.785	9	2	1	4.064	0.15131	2.973	0.999	0.550	0.821

SN00278770	7	408.1	39.3	6.63 9	614. 8	4.937	6	0	1	0.278	0.12456	2.985	1.298	0.748	0.847
SN00288395	7	415.3	60.7	7.48 0	602. 8	3.829	6	2	1	1.984	0.27340	2.794	0.483	0.462	1.546
SN00348164	7	445.8	103. 5	6.38 3	670. 8	2.785	9	2	1	4.064	0.15131	2.973	0.999	0.550	0.821
SN00352327	7	436.3	70.0	7.20 9	632. 8	5.088	7	2	2	0.001	0.17800	2.929	0.973	0.507	1.462
140715-85-1	7	303.8	114. 3	3.50 7	445. 5	0.684	9	3	0	6.959	0.74762	2.453	0.150	0.409	1.413
140715-87-3	7	324.0	123. 6	3.31 8	475. 5	0.701	10	3	0	7.536	0.71976	2.434	0.391	0.556	1.248
140852-71-7	7	303.8	114. 3	3.50 7	445. 5	0.684	9	3	0	6.959	0.74762	2.453	0.150	0.409	1.413
159518-77-1	7	317.6	139. 3	5.45 4	492. 6	3.889	7	3	0	5.697	0.46213	2.664	1.379	0.582	1.442
524067-24-1	7	372.9	126. 4	2.89 9	587. 5	2.229	10	4	1	3.578	0.56994	2.658	0.863	0.719	1.458
524067-25-2	7	354.3	126. 4	2.06 5	508. 6	1.504	10	4	1	5.368	0.70633	2.739	0.901	0.510	1.554
524067-26-3	7	351.7	119. 6	2.88 5	509. 6	1.903	10	3	1	3.772	0.67337	2.631	1.103	0.539	1.615
61897-88-9	7	311.9	108. 8	4.00 5	460. 4	0.597	10	0	0	0.340	0.19817	2.484	1.072	0.583	0.974
61897-89-0	7	273.0	91.3	3.94 1	402. 4	0.997	8	1	0	4.316	0.75625	2.489	0.867	0.378	1.148
61897-90-3	7	301.9	99.6	3.86 1	444. 4	1.307	9	0	0	3.727	0.42741	2.445	0.990	0.421	0.989
61949-67-5	7	278.2	102. 8	3.71 9	418. 4	0.337	9	1	0	2.257	0.72972	2.538	0.860	0.522	1.178
66212-51-9	7	273.0	91.3	3.94 1	402. 4	0.997	8	1	0	4.316	0.75625	2.489	0.867	0.378	1.148
SN00037381	7	459.8	122. 9	6.47 2	664. 8	2.633	10	4	1	5.511	0.31784	2.553	0.451	0.451	1.579
SN00037382	7	459.8	122. 9	6.47 2	664. 8	2.633	10	4	1	5.511	0.31784	2.553	0.451	0.451	1.579
SN00091501	7	346.7	78.5	5.54 9	471. 6	3.448	6	2	0	-0.716	0.32793	2.358	0.610	0.517	1.274
SN00097411	7	345.8	82.1	5.98 7	490. 6	3.559	7	1	0	3.197	0.43069	2.638	1.183	0.643	1.231
SN00097418	7	332.0	82.1	5.71 7	476. 5	3.105	7	1	0	2.776	0.47292	2.628	1.460	0.622	1.317
SN00097526	7	354.3	91.3	5.73 5	506. 6	3.035	8	1	1	2.849	0.44733	2.512	1.512	0.655	0.907

SN00097687	7	356.5	82.1	6.40 5	504. 6	3.792	7	1	1	2.776	0.22923	2.602	1.540	0.678	1.227
SN00097688	7	356.5	82.1	6.40 5	504. 6	3.792	7	1	1	2.776	0.22923	2.602	1.540	0.678	1.227
SN00097689	7	356.5	82.1	6.40 5	504. 6	3.792	7	1	1	2.776	0.22923	2.602	1.540	0.678	1.227
SN00097956	7	354.3	91.3	5.73 5	506. 6	3.035	8	1	1	2.849	0.44733	2.540	1.390	0.598	0.951
SN00098042	7	356.5	82.1	6.40 5	504. 6	3.792	7	1	1	2.776	0.13754	2.602	1.540	0.678	1.227
SN00098043	7	356.5	82.1	6.40 5	504. 6	3.792	7	1	1	2.776	0.13754	2.602	1.540	0.678	1.227
SN00098044	7	356.5	82.1	6.40 5	504. 6	3.792	7	1	1	2.776	0.13754	2.602	1.540	0.678	1.227
SN00109120	7	362.1	97.0	6.12 4	530. 0	3.287	8	2	1	-2.718	0.17234	2.371	0.493	0.626	1.044
SN00109705	7	361.2	91.7	7.41 0	517. 6	3.395	7	2	1	5.690	0.21499	2.353	0.986	0.362	1.323
SN00109757	7	364.3	91.7	7.80 2	538. 0	3.657	7	2	1	5.735	0.19700	2.308	0.936	0.620	1.195
SN00111609	7	368.0	91.3	6.00 5	520. 6	3.489	8	1	1	3.257	0.40710	2.565	1.138	0.625	0.958
SN00111617	7	387.2	111. 2	6.32 9	547. 6	3.263	9	2	1	3.942	0.08144	2.529	0.838	0.689	1.213
SN00111618	7	387.2	111. 2	6.32 9	547. 6	3.263	9	2	1	3.942	0.08144	2.529	0.838	0.689	1.213
SN00111625	7	372.0	108. 4	6.01 7	534. 6	3.091	9	1	1	2.706	0.24045	2.520	1.277	0.644	0.808
SN00111652	7	370.3	82.1	6.67 5	518. 6	4.247	7	1	1	3.197	0.20655	2.643	1.267	0.683	1.168
SN00111663	7	369.9	119. 4	6.00 0	534. 6	0.981	9	2	1	3.154	0.43051	2.484	0.524	0.602	1.233
SN00111665	7	369.9	119. 4	6.00 0	534. 6	0.981	9	2	1	3.154	0.43051	2.484	0.524	0.602	1.233
SN00111673	7	375.8	99.2	6.67 1	532. 6	3.430	8	1	1	3.037	0.21774	2.555	1.189	0.679	1.063
SN00111674	7	375.8	99.2	6.67 1	532. 6	3.430	8	1	1	3.037	0.21774	2.555	1.189	0.679	1.063
SN00111675	7	375.8	99.2	6.67 1	532. 6	3.430	8	1	1	3.037	0.21774	2.555	1.189	0.679	1.063
SN00111676	7	375.8	99.2	6.67 1	532. 6	3.430	8	1	1	3.037	0.21774	2.555	1.189	0.679	1.063
SN00111701	7	362.0	99.2	6.40 1	518. 6	2.976	8	1	1	2.622	0.23609	2.507	1.442	0.668	1.076

SN00111702	7	362.0	99.2	6.40 1	518. 6	2.976	8	1	1	2.622	0.23609	2.507	1.442	0.668	1.076
SN00111703	7	362.0	99.2	6.40 1	518. 6	2.976	8	1	1	2.622	0.23609	2.507	1.442	0.668	1.076
SN00111704	7	362.0	99.2	6.40 1	518. 6	2.976	8	1	1	2.622	0.23609	2.507	1.442	0.668	1.076
SN00111711	7	373.5	111. 2	6.05 9	533. 6	2.808	9	2	1	3.553	0.08907	2.462	1.116	0.707	1.259
SN00111712	7	373.5	111. 2	6.05 9	533. 6	2.808	9	2	1	3.553	0.08907	2.462	1.116	0.707	1.259
SN00226829	7	454.3	122. 9	6.77 7	684. 7	2.802	10	4	1	-1.525	0.17598	2.667	0.558	0.691	1.400
SN00226941	7	472.1	122. 9	6.81 6	678. 8	2.977	10	4	1	5.455	0.29582	2.563	0.509	0.493	1.622
SN00233772	7	467.9	122. 9	6.93 3	670. 8	2.989	10	4	1	0.402	0.23603	2.593	0.254	0.467	1.483
SN00243155	7	472.1	122. 9	6.81 6	678. 8	2.977	10	4	1	5.455	0.29582	2.563	0.509	0.493	1.622
SN00253708	7	466.2	122. 9	6.78 6	682. 8	2.734	10	4	1	4.171	0.29753	2.568	0.313	0.687	1.365
SN00260522	7	459.8	122. 9	6.47 2	664. 8	2.633	10	4	1	5.511	0.31784	2.553	0.451	0.451	1.579
SN00261089	7	472.1	122. 9	6.81 6	678. 8	2.977	10	4	1	5.455	0.17749	2.645	0.492	0.501	1.649
SN00261527	7	484.4	122. 9	7.16 0	692. 8	3.321	10	4	1	5.455	0.16587	2.666	0.469	0.517	1.617
SN00267944	7	454.7	124. 6	6.69 1	630. 7	3.465	10	4	1	5.435	0.30801	2.573	0.182	0.514	1.448
SN00290152	7	394.5	55.9	7.26 4	614. 8	5.315	6	1	2	3.065	0.08223	2.563	1.329	0.690	1.193
SN00297098	7	466.2	122. 9	6.78 6	682. 8	2.734	10	4	1	4.171	0.29753	2.568	0.313	0.687	1.365
SN00304654	7	466.2	122. 9	6.78 6	682. 8	2.734	10	4	1	4.171	0.29753	2.568	0.313	0.687	1.365
SN00305691	7	394.5	55.9	7.26 4	614. 8	5.315	6	1	2	3.065	0.13706	2.563	1.329	0.690	1.193
SN00310110	7	484.4	122. 9	7.16 0	692. 8	3.321	10	4	1	5.455	0.27645	2.572	0.495	0.519	1.589
SN00318192	7	472.1	122. 9	6.81 6	678. 8	2.977	10	4	1	5.455	0.29582	2.611	0.558	0.502	1.544
SN00322991	7	472.1	122. 9	6.81 6	678. 8	2.977	10	4	1	5.455	0.29582	2.563	0.509	0.493	1.622
SN00323189	7	482.0	105. 3	5.74 8	692. 8	3.139	10	2	1	5.337	0.33501	2.738	0.596	0.530	1.492

SN00327455	7	482.0	105.3	5.748	692.8	3.139	10	2	1	5.337	0.33501	2.738	0.596	0.530	1.492
SN00330261	7	466.2	122.9	6.786	682.8	2.734	10	4	1	4.171	0.29753	2.568	0.313	0.687	1.365
SN00331859	7	455.8	151.1	6.482	670.8	2.499	10	4	1	7.229	0.31746	2.442	0.518	0.498	1.601
SN00340494	7	437.4	67.3	6.513	650.8	4.010	7	1	1	2.712	0.16918	3.037	0.995	0.455	0.952
SN00341689	7	484.4	122.9	7.160	692.8	3.321	10	4	1	5.455	0.27645	2.572	0.495	0.519	1.589
SN00344654	7	484.4	122.9	7.160	692.8	3.321	10	4	1	5.455	0.27645	2.627	0.551	0.527	1.509
SN00350405	7	466.2	122.9	6.786	682.8	2.734	10	4	1	4.171	0.29753	2.568	0.313	0.687	1.365
SN00354912	7	472.5	122.9	7.100	700.7	2.834	10	4	1	4.171	0.28254	2.568	0.313	0.687	1.365
SN00356104	7	472.5	122.9	7.100	700.7	2.834	10	4	1	4.171	0.28254	2.568	0.313	0.687	1.365
SN00371872	7	466.2	122.9	6.786	682.8	2.734	10	4	1	4.171	0.29753	2.568	0.313	0.687	1.365
SN00379189	7	475.3	122.9	7.208	699.2	3.239	10	4	1	5.544	0.27544	2.484	0.392	0.743	1.307
SN00379780	7	475.3	122.9	7.208	699.2	3.239	10	4	1	5.544	0.27544	2.484	0.392	0.743	1.307
SN00383686	7	472.5	122.9	7.100	700.7	2.834	10	4	1	4.171	0.28254	2.568	0.313	0.687	1.365
SN00390671	7	424.6	122.9	5.816	614.7	1.914	10	4	1	2.821	0.37313	2.619	0.588	0.541	1.310
SN00393875	7	472.5	122.9	7.100	700.7	2.834	10	4	1	4.171	0.28254	2.568	0.313	0.687	1.365
169626-35-1	7	261.4	77.6	3.702	358.4	1.846	6	2	0	6.152	0.80604	2.742	0.688	0.302	1.809
749216-47-5	7	261.9	85.5	2.575	384.4	1.057	7	2	0	3.167	0.83799	2.948	1.359	0.667	1.225
SN00004671	7	375.1	108.0	5.783	520.0	2.782	8	3	1	6.406	0.09708	2.336	0.483	0.583	1.241
SN00007650	7	342.3	78.5	6.276	485.5	3.725	6	2	0	-3.519	0.07754	2.454	0.864	0.597	1.427
SN00008385	7	335.0	79.0	4.726	459.5	2.838	7	1	0	4.798	0.21584	2.361	0.629	0.514	1.175
SN00008387	7	358.1	79.0	5.190	509.5	3.585	7	1	1	-1.052	0.10926	2.437	0.705	0.565	1.184
SN00015950	7	331.2	78.5	6.240	461.5	3.520	6	2	0	5.002	0.16079	2.338	0.812	0.546	1.441

SN00132224	7	326.1	80.8	6.82 2	473. 5	3.829	6	0	0	3.149	0.08388	2.299	1.330	0.563	0.592
SN00133950	7	351.3	80.8	7.30 2	499. 5	4.293	6	0	0	3.149	0.07232	2.299	1.330	0.563	0.592
SN00134172	7	351.3	80.8	7.30 2	499. 5	4.293	6	0	0	3.149	0.07232	2.299	1.330	0.563	0.592
SN00141410	7	289.7	57.7	5.93 1	408. 5	3.206	5	0	0	4.079	0.11164	2.244	1.607	0.627	0.896
SN00259728	7	364.8	75.6	5.02 3	463. 6	5.156	5	2	1	-1.969	0.24622	3.009	0.398	0.602	0.828
SN00319706	7	483.3	156. 9	4.93 4	627. 7	2.851	11	5	2	5.612	0.42236	2.420	0.463	0.542	1.186
ZINC0891846 3	7	272.4	34.1	4.16 1	445. 4	2.311	5	1	0	-1.751	0.39121	2.822	0.561	0.463	1.409
ZINC1359592 9	7	305.5	38.3	4.14 9	430. 6	1.848	5	2	0	2.709	0.68469	3.003	0.990	0.407	1.113
ZINC0062631 5	7	326.2	34.0	3.98 1	420. 6	5.889	4	1	1	-0.420	0.33662	2.586	0.935	0.539	1.426
ZINC0075417 3	7	340.0	34.0	4.25 1	434. 6	6.231	4	1	1	-0.628	0.29247	2.569	0.977	0.542	1.359
ZINC0075417 4	7	340.0	34.0	4.25 1	434. 6	6.231	4	1	1	-0.628	0.29247	2.569	0.977	0.542	1.359
122540-32-3	8	350.5	83.8	4.19 5	402. 5	5.102	5	2	1	-8.705	0.27481	2.168	0.599	0.415	1.770
133805-03-5	9	237.0	118. 2	5.44 7	357. 3	2.762	7	5	0	1.524	0.55632	2.597	0.231	0.153	1.289
135213-04-6	10	367.1	98.8	3.42 8	488. 6	1.889	8	2	0	7.247	0.68595	2.201	0.194	0.305	1.680
135340-00-0	11	296.5	79.3	5.75 2	429. 5	2.940	6	2	0	3.173	0.51873	2.621	0.744	0.645	1.484
SN00281717	11	359.2	117. 1	7.14 2	522. 5	2.432	8	2	1	1.650	0.35101	2.380	0.525	0.823	0.930
139083-13-9	12	311.6	90.6	7.57 4	471. 3	4.608	6	4	0	2.392	0.32460	2.439	0.146	0.727	1.180
140429-37-4	12	305.1	99.5	6.74 3	441. 5	3.159	7	4	0	5.165	0.44521	2.529	0.358	0.393	1.398
139220-18-1	13	460.5	123. 0	3.96 4	555. 8	6.141	7	1	2	1.381	0.19497	2.558	0.691	0.455	1.005
139594-87-9	14	481.4	139. 6	5.41 1	616. 8	4.944	9	3	1	-4.121	0.16102	2.928	0.216	0.650	1.222
6758-71-0	14	334.4	55.8	5.62 7	468. 7	4.759	4	1	0	-4.133	0.12760	3.003	1.068	0.894	0.603
SN00162890	14	331.9	93.1	4.93 4	496. 6	2.795	6	2	0	2.689	0.52676	2.488	0.865	0.203	0.970

SN00344013	14	333.4	114.4	4.47 1	526.6	0.753	9	0	1	-2.992	0.30107	2.609	1.085	0.609	0.507
148149-82-0	14	261.3	46.5	3.86 2	318.5	5.247	3	1	1	-6.927	0.18013	2.399	1.376	0.472	1.012
152110-09-3	14	322.3	71.1	5.38 6	460.6	4.051	6	0	0	-5.411	0.24523	2.291	0.891	1.118	0.656
152186-77-1	14	322.3	71.1	5.38 6	460.6	4.051	6	0	0	-5.411	0.24523	2.291	0.891	1.118	0.656
79849-37-9	14	349.0	91.3	5.57 7	516.7	3.229	7	1	1	-4.368	0.13884	2.988	0.825	1.135	0.965
858950-34-2	14	387.8	117.6	5.58 8	574.7	2.862	9	1	1	-4.453	0.12579	2.988	0.825	1.135	0.965
SN00083037	14	326.4	43.4	6.52 5	454.7	5.890	3	0	1	-3.184	0.16147	2.154	1.365	0.856	0.545
SN00352197	14	327.5	46.5	6.40 6	456.7	5.774	3	1	1	-6.034	0.09630	2.106	1.319	0.918	1.474
199165-88-3	14	287.7	66.8	4.41 9	402.6	3.580	4	2	0	-7.188	0.32673	2.303	0.714	0.902	0.814
32450-26-3	14	348.8	89.9	4.82 6	472.6	3.643	6	1	0	1.980	0.51450	2.162	1.249	1.007	0.626
71103-05-4	14	307.0	63.6	5.14 8	426.6	4.422	4	1	0	-5.599	0.25703	2.679	1.350	0.818	0.511
674819-46-6	14	306.2	29.5	5.88 0	398.6	6.124	2	1	1	0.171	0.27502	2.196	1.495	1.052	0.514
SN00329349	14	356.9	77.3	3.55 6	484.6	3.799	6	0	0	0.250	0.48306	3.036	1.602	0.710	0.573
141266-06-0	15	324.9	57.6	4.61 4	435.6	4.780	4	1	0	1.649	0.48008	2.762	0.942	0.581	0.707
14270-73-6	16	351.3	88.1	4.09 9	470.5	2.818	7	2	0	-1.719	0.23766	2.071	0.727	0.527	1.371
14325-03-2	17	435.2	127.1	6.47 3	562.7	5.155	8	4	2	-2.052	0.15939	2.566	0.379	0.550	1.158
151484-78-5	17	364.1	89.8	5.69 9	466.6	4.429	6	3	0	0.654	0.36172	2.556	0.716	0.603	1.421
147395-97-9	18	353.7	114.5	4.05 5	488.5	2.491	11	1	1	5.147	0.63320	2.527	0.994	0.488	1.145
149764-31-8	19	468.0	153.2	6.51 5	694.9	4.562	9	2	1	-5.327	0.12965	2.423	0.382	1.008	0.851
149764-33-0	19	429.4	101.4	7.19 1	614.9	6.178	6	2	2	-3.517	0.10502	2.444	0.350	0.963	0.897
149764-34-1	20	487.4	144.0	6.07 9	678.9	6.146	8	2	2	-5.888	0.10773	2.339	0.496	1.154	0.526
151890-81-2	21	404.5	79.2	6.00 0	530.8	5.914	5	3	2	-5.397	0.14435	3.009	0.146	0.985	0.950

211358-65-5	21	408.7	99.4	5.55 0	546. 8	5.090	6	4	2	-4.456	0.17391	3.009	0.146	0.985	0.950
329050-20-6	21	361.1	66.8	5.63 6	474. 7	5.581	4	2	1	-2.383	0.19528	2.790	1.180	0.724	0.855
74185-11-8	21	404.5	79.2	6.00 0	530. 8	5.914	5	3	2	-5.397	0.14435	3.009	0.146	0.985	0.950
78518-73-7	21	362.2	69.9	5.58 5	476. 7	5.426	4	3	1	-1.348	0.22409	2.824	1.025	0.790	0.879
86748-29-0	21	362.2	69.9	5.58 5	476. 7	5.438	4	3	1	-1.201	0.22832	2.824	1.025	0.790	0.879
86748-30-3	21	365.7	87.0	5.20 1	490. 7	4.888	5	3	0	-1.002	0.26835	2.790	1.180	0.724	0.855
86783-84-8	21	362.2	69.9	5.58 5	476. 7	5.426	4	3	1	-1.348	0.22409	2.824	1.025	0.790	0.879
16250-61-6	21	326.9	53.0	5.36 8	428. 7	5.346	3	2	1	-0.784	0.16705	2.422	1.486	0.833	0.817
208708-22-9	21	275.3	66.8	4.26 9	388. 5	3.512	4	2	0	-1.655	0.39531	2.120	1.191	0.890	0.555
208708-24-1	21	271.3	49.7	4.61 7	374. 6	4.220	3	2	0	-2.866	0.32192	2.094	1.216	0.914	0.736
233607-69-7	21	358.7	65.0	5.58 1	488. 7	5.173	5	1	1	-2.045	0.21150	2.440	1.043	1.005	0.712
86363-50-0	21	322.8	38.7	5.72 5	426. 6	6.281	3	1	1	-2.047	0.11516	2.813	1.339	0.731	0.807
191212-37-0	21	370.7	76.0	5.62 0	490. 7	4.937	5	2	0	-3.905	0.19923	2.942	1.248	0.992	0.538
205750-25-0	21	359.6	61.8	5.86 7	488. 7	4.646	5	0	0	-3.580	0.20256	2.530	1.268	0.625	1.141
452934-96-2	21	370.7	76.0	5.62 0	490. 7	4.937	5	2	0	-3.641	0.20037	2.653	1.226	0.965	0.528
487016-98-8	21	360.7	65.0	5.81 6	490. 7	4.503	5	1	0	-2.378	0.21953	2.797	1.249	0.645	1.471
858950-55-7	21	318.6	76.0	5.26 2	460. 7	3.735	5	2	0	-1.393	0.18554	3.033	0.927	0.842	1.488
2061-64-5	21	324.4	38.7	5.98 9	428. 7	6.386	3	1	1	-2.464	0.10498	2.941	1.343	0.931	1.229
256377-68-1	21	323.1	38.7	6.35 3	442. 7	6.317	3	1	1	-2.926	0.09584	2.883	1.424	0.910	1.147
40071-60-1	21	324.4	38.7	5.98 9	428. 7	6.386	3	1	1	-2.464	0.10498	2.941	1.343	0.931	1.229
75179-58-7	21	299.6	38.7	5.55 9	400. 6	5.713	3	1	1	-0.530	0.16459	2.941	1.343	0.931	1.229
263764-04-1	21	331.9	70.1	5.09 2	442. 6	4.296	4	2	0	-0.157	0.29991	2.749	1.472	1.025	0.974

263764-05-2	21	333.0	70.1	5.32 0	444. 7	4.548	4	2	0	-6.898	0.19018	2.919	1.316	1.175	0.757
94806-03-8	21	326.8	49.8	5.49 1	426. 6	5.148	3	1	1	-1.438	0.20531	2.765	1.795	1.096	0.756
SN00231454	21	394.4	90.4	5.18 6	563. 7	4.484	7	1	1	-3.449	0.10274	3.007	1.213	0.994	0.656
SN00298985	21	394.4	90.4	5.18 6	563. 7	4.484	7	1	1	-3.449	0.10274	3.007	1.213	0.994	0.656
155645-51-5	22	487.8	120. 0	5.83 9	604. 7	5.090	9	2	2	4.157	0.29143	2.616	0.380	0.473	1.086
186593-86-2	22	478.9	143. 6	5.50 0	627. 1	4.154	10	3	1	1.973	0.19434	2.668	0.692	0.675	1.053
244157-96-8	22	430.4	145. 3	3.78 8	566. 1	2.805	10	4	1	5.786	0.55061	2.631	0.480	0.592	1.203
157207-88-0	23	296.3	31.1	3.93 2	351. 5	5.019	3	2	1	-3.380	0.18748	2.445	0.347	0.622	1.346
158758-41-9	24	317.3	108. 4	6.57 4	430. 5	3.104	6	3	0	-1.559	0.09817	2.463	1.210	0.491	1.507
159934-14-2	25	365.0	35.8	5.15 4	466. 8	6.006	3	1	1	3.202	0.36296	2.770	1.036	0.611	0.815
159934-15-3	25	371.6	61.7	5.79 8	480. 7	5.797	4	2	1	0.560	0.27362	2.746	0.690	0.463	0.989
454476-89-2	25	336.7	38.1	6.18 4	426. 7	5.895	2	2	1	-1.196	0.20928	2.570	0.795	0.698	0.864
640734-87-8	25	346.8	29.3	5.59 4	438. 7	5.873	2	1	1	-0.545	0.25131	2.759	0.971	0.560	0.655
175170-89-5	26	263.9	116. 2	6.89 9	366. 4	2.813	7	4	0	1.292	0.43869	2.447	0.654	0.317	1.843
94935-97-4	26	290.2	93.5	6.85 9	394. 4	3.387	7	3	0	2.735	0.44898	2.596	1.214	0.389	1.529
188558-50-1	27	315.9	115. 6	4.37 8	404. 5	3.191	8	4	0	-1.700	0.23369	2.469	0.945	0.410	1.546
20829-55-4	28	278.8	89.8	4.14 0	372. 4	1.917	6	4	0	4.423	0.75414	2.416	0.344	0.091	1.984
244066-05-5	28	337.9	78.9	4.91 3	440. 5	3.185	6	3	0	1.452	0.53518	2.834	0.452	0.461	1.334
2122-98-7	29	362.3	136. 3	6.62 0	496. 6	5.280	9	2	1	-2.986	0.16488	2.652	0.687	0.896	0.808
2497-74-7	29	337.5	136. 3	6.19 0	468. 6	4.901	9	2	0	-3.146	0.19497	2.665	0.604	0.824	0.873
2643-02-9	29	366.5	156. 5	6.17 0	512. 6	4.457	10	3	1	-2.057	0.16436	2.669	0.589	0.822	0.849
6891-35-6	29	337.5	136. 3	6.19 0	468. 6	4.901	9	2	0	-2.772	0.11896	2.665	0.604	0.824	0.873

220503-29-7	30	262.2	109.1	4.806	389.4	0.196	8	1	0	4.726	0.68721	2.624	0.510	0.508	1.462
221367-90-4	31	447.0	114.9	6.297	580.7	6.321	8	4	2	-1.327	0.14177	2.688	0.290	0.643	1.129
474779-75-4	32	284.3	40.0	6.287	476.2	3.417	4	1	0	3.641	0.34513	2.893	0.822	0.917	1.328
50909-86-9	33	309.8	64.9	6.010	407.5	4.415	5	2	0	4.183	0.45231	2.653	0.931	0.385	1.548
639512-19-9	34	396.0	104.2	6.676	530.6	6.296	8	0	2	-4.603	0.07506	2.281	1.188	0.925	0.990
65527-04-0	35	339.4	57.5	6.375	458.7	6.168	3	2	1	-2.039	0.16802	2.836	1.318	0.984	1.494
65527-05-1	35	339.4	57.5	6.375	458.7	6.168	3	2	1	-2.039	0.16802	2.836	1.318	0.984	1.494
80442-78-0	36	319.7	79.2	5.211	462.7	3.591	5	3	0	-2.102	0.17479	3.016	0.758	0.904	1.551
80442-79-1	36	319.7	79.2	5.211	462.7	3.591	5	3	0	-2.102	0.17479	3.016	0.758	0.904	1.551
80442-84-8	36	387.1	91.3	6.031	546.7	4.560	7	1	1	-2.106	0.11510	2.917	0.754	1.135	0.910
858950-46-6	36	339.0	83.5	5.491	516.7	3.147	7	1	1	-2.553	0.14999	2.623	0.970	1.106	0.891
858950-48-8	36	339.0	83.5	5.491	516.7	3.147	7	1	1	-2.553	0.14999	2.861	0.974	1.078	1.007
86047-14-5	37	220.5	63.2	3.617	313.3	1.398	5	0	0	2.172	0.80186	2.331	1.503	0.210	1.746
866403-75-0	38	293.9	76.0	4.812	426.6	3.782	5	2	0	0.304	0.27639	2.694	0.965	1.142	0.864
SN00005498	39	379.7	74.7	5.727	501.6	5.017	6	1	2	5.821	0.37008	2.614	0.551	0.349	1.542
SN00012590	39	329.7	49.7	5.164	427.6	5.474	4	0	1	-1.131	0.16053	2.719	0.873	0.544	1.720
SN00012599	39	341.2	61.8	5.591	442.6	5.415	5	1	1	-0.424	0.27549	2.403	0.718	0.475	1.862
SN00012601	39	339.0	61.8	5.562	454.5	5.179	5	1	1	4.075	0.40158	2.513	1.018	0.553	1.486
SN00105976	39	480.3	123.5	5.465	632.8	5.414	10	2	2	2.577	0.17477	2.447	0.339	0.384	1.810
SN00052010	39	408.7	83.8	6.623	523.7	4.525	7	1	1	2.228	0.32009	2.654	0.817	0.496	1.170
SN00078665	39	388.9	57.9	5.136	526.1	4.647	6	0	1	5.174	0.41259	2.642	0.950	0.659	1.187
SN00078968	39	375.1	57.9	5.131	512.0	4.391	6	0	1	5.212	0.44120	2.631	0.938	0.656	1.154

SN00015562	40	379.7	71.8	5.62 4	478. 6	3.875	6	2	0	1.776	0.25753	2.516	0.536	0.479	1.587
ZINC1275367 6	40	280.6	69.0	4.02 8	423. 5	1.863	8	2	0	-1.617	0.33768	2.592	0.922	0.570	1.402
SN00056789	41	333.1	51.5	5.70 7	451. 5	4.774	5	0	0	-1.075	0.09591	2.680	1.308	0.570	0.605
SN00057684	41	341.5	51.5	5.37 5	461. 5	4.664	5	0	0	2.723	0.15679	2.703	1.318	0.524	0.681
SN00059271	41	364.1	51.5	5.95 0	487. 6	5.028	5	0	1	2.810	0.12834	2.683	1.144	0.467	0.817
SN00059388	41	331.1	51.5	5.25 1	447. 5	4.224	5	0	0	2.570	0.17371	2.684	1.386	0.594	0.638
SN00059442	41	330.3	51.5	5.59 7	451. 5	4.702	5	0	0	1.283	0.14044	2.600	1.036	0.500	0.770
SN00058256	41	344.1	51.5	5.86 7	465. 6	5.044	5	0	1	-1.048	0.08761	2.682	1.233	0.570	0.642
SN00066079	42	344.0	95.9	8.87 6	494. 5	4.970	7	1	0	2.751	0.10182	2.414	1.065	0.489	1.307
SN00074793	43	330.0	117. 4	6.42 8	470. 4	3.216	8	1	0	2.407	0.20231	2.569	1.040	0.554	1.029
SN00080932	44	375.2	67.7	7.22 3	520. 6	5.192	7	0	2	5.874	0.22899	2.574	0.909	0.478	1.114
SN00080933	44	375.2	67.7	7.22 3	520. 6	5.192	7	0	2	5.874	0.22899	2.574	0.909	0.478	1.114
SN00080974	44	368.8	67.7	6.90 9	502. 6	5.092	7	0	2	7.214	0.24880	2.538	1.021	0.368	1.203
SN00080956	44	359.4	73.2	7.56 2	475. 5	5.554	6	1	1	1.410	0.20749	2.369	0.618	0.177	1.485
SN00097226	44	370.1	99.2	7.38 0	497. 6	4.745	7	2	0	5.274	0.25494	2.791	0.573	0.486	1.365
SN00097227	44	370.1	99.2	7.38 0	497. 6	4.745	7	2	0	5.274	0.25494	2.791	0.573	0.486	1.365
SN00080936	45	358.6	58.4	7.46 3	486. 6	5.899	6	0	1	6.806	0.12842	2.578	1.105	0.347	1.249
SN00080939	45	334.1	58.4	6.77 5	458. 5	5.211	6	0	1	6.920	0.26864	2.390	0.997	0.359	1.394
SN00081043	45	349.5	58.4	7.51 1	493. 0	5.817	6	0	1	6.906	0.21352	2.396	0.882	0.642	1.262
SN00081067	45	340.4	58.4	7.08 9	476. 5	5.312	6	0	1	5.580	0.24749	2.432	0.951	0.626	1.147
SN00081079	45	340.4	58.4	7.08 9	476. 5	5.312	6	0	1	5.580	0.24749	2.427	0.802	0.525	1.246
SN00097206	45	374.3	58.4	6.77 0	498. 6	5.895	6	0	1	8.099	0.22226	2.500	0.698	0.394	1.241

SN00097225	45	347.8	58.4	6.25 3	472. 5	5.134	6	0	1	7.810	0.28342	2.367	0.635	0.261	1.548
SN00097229	45	368.1	76.9	6.96 4	516. 6	5.246	8	0	2	7.543	0.23433	2.212	0.728	0.280	1.238
SN00111460	45	363.5	58.4	7.55 3	526. 5	6.060	6	0	2	-0.270	0.13727	2.545	0.878	0.603	1.249
SN00111540	45	412.6	95.4	7.00 0	576. 6	5.106	10	0	2	7.487	0.21189	2.322	1.013	0.368	1.041
SN00081767	45	341.5	88.7	6.06 4	476. 5	4.405	8	0	0	6.606	0.32421	2.254	0.707	0.259	1.403
SN00081539	46	354.9	93.1	2.60 7	472. 5	2.567	7	0	0	4.907	0.72448	2.600	0.633	0.414	0.873
SN00081619	46	375.4	93.1	2.87 4	508. 6	3.029	7	0	1	4.504	0.65160	2.766	0.911	0.458	0.536
SN00081634	46	363.1	93.1	2.81 3	488. 6	3.434	7	0	0	3.522	0.65593	2.758	0.785	0.539	0.596
SN00081635	46	355.5	93.1	2.64 4	470. 5	2.302	7	0	0	3.212	0.72119	2.523	0.442	0.513	0.859
SN00081734	46	380.1	93.1	3.43 9	514. 6	3.825	7	0	1	-0.875	0.37958	2.768	0.688	0.493	0.591
SN00081740	46	366.4	93.1	3.16 9	500. 6	3.370	7	0	1	-0.847	0.41618	2.759	0.798	0.497	0.502
SN00089681	46	355.9	93.1	3.04 5	486. 6	2.930	7	0	0	-0.522	0.46789	2.770	0.756	0.483	0.528
SN00089691	46	352.6	93.1	2.68 9	474. 6	2.994	7	0	0	3.840	0.70030	2.758	0.785	0.539	0.596
SN00089693	46	369.7	93.1	3.31 5	500. 6	3.384	7	0	1	-0.551	0.43240	2.776	0.657	0.486	0.618
SN00091326	46	360.0	113. 3	2.82 6	486. 5	2.377	8	1	0	4.716	0.70299	2.556	0.512	0.537	1.030
SN00101331	46	399.7	102. 3	3.20 0	528. 6	2.861	8	0	1	3.746	0.36931	2.637	0.766	0.462	0.976
SN00111395	46	396.8	93.1	3.37 6	536. 6	3.794	7	0	1	4.651	0.56237	2.794	1.013	0.532	0.517
SN00111397	46	410.6	93.1	3.64 6	550. 7	4.249	7	0	1	3.575	0.50267	2.773	0.865	0.565	0.616
SN00111415	46	386.4	93.1	3.25 2	522. 6	3.354	7	0	1	4.971	0.60749	2.798	0.916	0.485	0.526
SN00111420	46	385.8	93.1	2.99 8	522. 6	3.470	7	0	1	4.179	0.60912	2.797	0.852	0.464	0.608
SN00111437	46	399.6	93.1	3.26 8	536. 6	3.924	7	0	1	3.105	0.54974	2.741	0.801	0.515	0.595
SN00111564	46	389.1	93.1	3.14 4	522. 6	3.484	7	0	1	3.429	0.59823	2.746	0.761	0.514	0.624

SN00111571	46	400.1	93.1	3.52 2	536. 6	3.809	7	0	1	3.894	0.55219	2.776	0.765	0.523	0.609
SN00111576	46	390.8	102. 3	3.61 7	532. 6	3.285	8	0	1	-3.334	0.24130	2.675	0.708	0.659	0.752
SN00096066	46	332.7	46.6	4.29 6	434. 5	4.359	4	0	0	2.150	0.55207	2.731	1.296	0.467	0.915
SN00082651	47	357.7	83.9	3.79 4	486. 6	3.323	6	1	0	1.613	0.57553	3.064	1.020	0.475	0.649
SN00084678	47	408.4	83.9	5.84 4	540. 7	5.341	6	1	2	0.973	0.06315	2.988	0.900	0.580	0.794
ZINC0623295 4	47	300.1	79.6	4.92 1	423. 5	2.425	6	1	0	-9.721	0.18853	2.879	1.053	0.424	0.968
ZINC0623295 5	47	300.1	79.6	4.92 1	423. 5	2.425	6	1	0	-9.721	0.18853	2.879	1.053	0.424	0.968
SN00106774	48	390.6	105. 0	4.43 1	537. 6	3.764	7	1	1	2.570	0.48702	2.602	1.259	0.541	0.857
SN00106779	49	459.2	125. 3	4.89 3	602. 8	4.934	8	3	1	0.984	0.30645	3.026	0.844	0.628	1.026
SN00107651	50	368.4	129. 6	5.79 3	499. 6	2.290	7	1	0	3.826	0.30194	2.562	0.906	0.619	1.170
SN00111466	51	391.6	78.2	8.68 0	536. 6	6.346	7	1	2	2.765	0.07514	2.323	0.981	0.312	1.237
SN00113059	52	457.6	99.5	5.55 2	622. 8	5.373	8	2	2	7.117	0.28495	2.899	0.966	0.495	1.313
SN00113247	53	408.4	119. 3	5.32 8	530. 6	5.712	8	1	2	-7.121	0.16622	2.979	1.147	0.734	0.621
SN00113249	53	408.4	119. 3	5.32 8	530. 6	5.712	8	1	2	-7.121	0.16622	2.979	1.147	0.734	0.621
SN00113250	53	408.4	119. 3	5.32 8	530. 6	5.712	8	1	2	-7.121	0.16622	2.979	1.147	0.734	0.621
SN00113539	53	422.1	119. 3	5.83 8	556. 6	6.357	8	1	2	-6.227	0.13126	2.855	1.083	0.654	0.694
SN00113541	53	422.1	119. 3	5.83 8	556. 6	6.357	8	1	2	-6.227	0.13126	2.855	1.083	0.654	0.694
SN00113542	53	422.1	119. 3	5.83 8	556. 6	6.357	8	1	2	-6.227	0.13126	2.855	1.083	0.654	0.694
SN00113629	53	399.0	110. 2	6.99 9	541. 6	5.929	8	1	2	-6.172	0.12393	2.952	1.148	0.710	0.616
SN00113631	53	399.0	110. 2	6.99 9	541. 6	5.929	8	1	2	-6.172	0.12393	2.952	1.148	0.710	0.616
SN00113632	53	399.0	110. 2	6.99 9	541. 6	5.929	8	1	2	-6.172	0.12393	2.952	1.148	0.710	0.616
SN00115843	54	465.9	91.9	5.65 3	621. 7	5.451	9	0	2	7.268	0.27690	2.625	0.682	0.517	0.891

SN00119195	55	310.6	54.5	6.16 7	443. 5	4.259	4	0	0	2.541	0.08980	2.680	1.774	0.670	0.620
SN00119196	55	310.6	54.5	6.16 7	443. 5	4.259	4	0	0	2.541	0.08980	2.680	1.774	0.670	0.620
SN00121862	55	292.9	37.4	6.24 5	415. 5	4.857	3	0	0	3.062	0.08600	2.573	1.819	0.666	0.669
SN00121863	55	292.9	37.4	6.24 5	415. 5	4.857	3	0	0	3.062	0.08600	2.573	1.819	0.666	0.669
SN00121871	55	306.6	37.4	6.51 5	429. 5	5.312	3	0	1	2.614	0.07443	2.538	1.689	0.773	0.601
SN00141055	55	326.2	37.4	7.35 6	500. 4	5.591	3	0	2	-2.405	0.11959	2.213	1.674	1.096	0.541
SN00123510	56	348.9	77.3	6.36 8	462. 5	5.223	6	0	1	-1.770	0.20038	2.331	1.493	0.719	1.727
SN00128374	57	306.7	97.2	7.29 1	442. 4	4.691	6	1	0	-0.534	0.05304	2.754	1.225	0.809	0.662
SN00128422	58	325.3	45.2	8.48 5	458. 0	6.384	4	1	1	4.426	0.14961	2.842	0.846	0.718	1.199
SN00128855	59	412.6	112. 9	7.24 9	564. 0	5.145	7	2	2	2.941	0.09264	2.610	0.743	0.823	0.724
SN00129492	60	447.7	123. 5	6.90 0	596. 6	5.410	10	2	2	4.973	0.24397	2.069	0.778	0.676	0.951
SN00131673	61	265.1	70.1	8.24 7	374. 4	3.937	4	0	0	-0.838	0.07709	2.363	1.453	0.523	1.022
SN00133706	62	384.5	47.1	5.35 1	514. 6	4.131	6	0	1	4.249	0.15674	2.189	1.579	0.494	1.063
SN00139770	62	419.1	47.1	6.95 7	564. 7	5.325	6	0	2	4.249	0.05624	2.189	1.579	0.494	1.063
ZINC2056342 6	62	314.2	67.6	5.22 7	429. 5	3.398	7	1	0	3.814	0.55587	2.465	1.112	0.488	1.330
ZINC2056363 2	62	317.4	67.6	4.71 1	441. 5	2.978	7	1	0	0.579	0.50642	2.564	0.733	0.429	1.273
SN00150533	63	352.8	40.5	6.46 1	457. 5	6.196	4	0	1	2.201	0.28254	2.664	1.292	0.746	0.556
SN00154784	64	334.1	92.4	3.67 1	446. 5	3.255	6	2	0	1.668	0.63141	3.007	1.058	0.535	0.726
SN00166919	65	427.6	66.5	6.34 0	592. 7	5.386	8	0	2	1.987	0.19885	2.686	1.287	0.700	1.224
SN00245953	65	411.7	77.5	6.02 6	578. 7	5.110	8	1	2	1.983	0.22382	2.643	1.180	0.699	1.276
SN00261583	65	382.8	83.4	8.24 3	534. 6	6.481	7	3	2	4.848	0.17121	2.452	0.731	0.392	1.772
SN00275452	65	424.0	77.5	5.83 3	592. 7	5.304	8	1	2	1.983	0.21756	2.643	1.180	0.699	1.276

SN00384061	65	383.7	97.6	6.86 7	548. 6	5.531	8	2	2	-1.773	0.12085	2.598	0.627	0.691	1.433
SN00169398	66	464.2	84.8	7.14 8	620. 0	6.391	5	5	2	4.395	0.19609	2.949	0.947	0.384	1.544
SN00169407	66	477.4	84.8	7.43 6	644. 0	6.434	5	5	2	3.161	0.18158	2.923	1.039	0.484	1.362
SN00169411	66	446.8	93.0	6.79 2	606. 9	6.399	5	5	2	4.019	0.20645	2.846	0.627	0.531	1.438
SN00169419	66	460.0	93.0	7.08 0	630. 9	6.441	5	5	2	2.785	0.18828	2.809	0.670	0.594	1.246
SN00169448	66	426.7	72.7	6.81 8	576. 9	6.290	4	4	2	4.019	0.22051	2.841	0.946	0.421	1.657
SN00169461	66	416.2	72.7	6.90 4	574. 9	5.997	4	4	2	1.528	0.21055	2.736	0.857	0.371	1.760
SN00347694	66	446.1	45.2	7.21 3	669. 0	6.388	5	1	2	-2.782	0.05839	3.031	0.879	0.385	0.983
SN00169939	67	418.4	43.1	8.93 8	592. 9	6.337	3	2	2	-7.573	0.06144	2.697	1.395	0.907	0.519
SN00169941	67	416.5	43.1	8.86 7	590. 9	6.500	3	2	2	-7.107	0.06046	2.697	1.395	0.907	0.519
SN00169953	67	390.3	29.1	8.05 3	539. 8	5.950	3	2	2	-6.866	0.07400	2.689	1.295	0.786	0.673
SN00229183	68	360.3	49.0	5.77 4	486. 7	5.049	4	3	1	1.338	0.33755	2.709	0.703	0.657	1.354
SN00237128	69	482.3	61.1	4.97 8	690. 9	4.561	8	4	1	5.164	0.32946	2.872	1.055	0.701	1.245
SN00288697	69	482.3	61.1	4.97 8	690. 9	4.561	8	4	1	5.164	0.32946	2.872	1.055	0.701	1.245
SN00299304	69	482.3	61.1	4.97 8	690. 9	4.561	8	4	1	5.164	0.26357	2.926	1.013	0.660	1.385
SN00323840	69	482.3	61.1	4.97 8	690. 9	4.561	8	4	1	5.164	0.32946	2.872	1.055	0.701	1.245
SN00276332	70	429.7	77.5	6.71 9	570. 7	6.479	8	0	2	2.512	0.12816	2.486	1.108	0.440	0.929
SN00312143	70	429.7	77.5	6.87 4	570. 7	6.368	8	0	2	2.512	0.12790	2.454	1.013	0.423	0.978
SN00387973	70	403.2	77.5	6.40 7	544. 6	6.070	8	0	2	2.512	0.14849	2.491	1.000	0.468	0.952
SN00325070	71	377.2	161. 3	3.70 2	568. 5	1.579	10	2	1	-0.035	0.25653	2.889	0.824	1.164	0.751
SN00338156	72	334.7	152. 0	5.07 2	546. 5	2.960	10	4	1	1.574	0.09404	3.052	0.491	0.918	1.056
SN00352431	72	334.7	152. 0	5.07 2	546. 5	2.960	10	4	1	1.574	0.09404	3.052	0.491	0.918	1.056

SN00380580	73	442.0	69.7	5.73 4	606. 7	5.307	8	0	2	5.407	0.13743	3.039	1.623	0.707	0.530
ZINC1001299 1	74	322.2	34.1	8.13 1	442. 5	5.612	4	0	1	-2.835	0.15476	2.479	1.129	0.563	1.134
ZINC0209290 6	75	291.6	56.5	6.29 6	403. 5	5.846	5	1	1	-5.535	0.10473	2.442	0.757	0.400	0.680
ZINC0209314 4	75	279.8	56.5	6.23 6	411. 4	5.360	5	1	1	-6.875	0.11313	2.538	0.706	0.548	0.606
ZINC0209474 8	75	291.6	56.5	6.29 6	403. 5	5.846	5	1	1	-5.535	0.10473	2.442	0.757	0.400	0.680
ZINC0214896 0	75	293.1	56.5	6.11 1	403. 5	5.918	5	1	1	-5.699	0.10627	2.452	0.832	0.438	0.703
ZINC0474403 3	75	285.7	56.5	5.81 2	407. 4	4.858	5	1	0	-6.841	0.13206	2.683	0.823	0.573	0.612
ZINC0474410 5	75	273.5	56.5	5.46 8	393. 4	4.514	5	1	0	-6.841	0.15005	2.683	0.823	0.573	0.612
ZINC0523568 7	75	301.0	56.5	5.85 0	421. 5	5.399	5	1	1	-6.875	0.11757	2.607	0.745	0.585	0.818
ZINC0523570 3	75	291.6	56.5	5.84 2	403. 5	5.101	5	1	1	-5.501	0.12723	2.534	0.797	0.348	0.674
ZINC0662440 0	75	271.9	73.6	5.77 1	418. 4	4.135	7	2	0	-5.501	0.14581	2.359	0.239	0.363	0.896
ZINC0662446 4	75	246.6	56.5	6.27 6	401. 4	4.075	7	2	0	-5.501	0.13897	2.639	0.028	0.514	1.137
ZINC0849071 1	75	259.6	73.6	5.42 7	404. 4	3.791	7	2	0	-5.501	0.16352	2.359	0.239	0.363	0.896
ZINC0876485 4	75	263.5	56.5	5.86 3	400. 4	2.765	6	2	0	-5.388	0.16434	2.491	0.558	0.465	0.780
ZINC0905958 3	75	258.9	56.5	6.62 0	415. 4	4.419	7	2	0	-5.501	0.12486	2.639	0.028	0.514	1.137
ZINC0948195 1	75	286.7	69.4	6.04 4	412. 4	5.020	6	1	1	-5.275	0.12364	2.380	0.839	0.451	0.691
ZINC1186742 5	75	314.6	56.5	6.89 6	437. 5	5.729	5	1	1	-3.023	0.09875	2.560	0.709	0.311	0.696
ZINC1186743 3	75	294.8	56.5	6.23 4	423. 9	5.363	5	1	1	-5.360	0.11158	2.650	0.865	0.700	0.584
ZINC1289246 0	75	298.3	84.8	7.08 3	444. 5	4.121	6	1	0	-2.487	0.12711	2.515	0.553	0.664	1.060
ZINC1289922 0	75	285.7	73.6	6.04 1	432. 5	4.589	7	2	0	-5.535	0.12863	2.501	0.299	0.343	1.088
ZINC1369183 1	75	296.8	84.8	7.15 7	444. 5	4.011	6	1	0	-2.447	0.12829	2.492	0.635	0.746	0.890
ZINC0408560 2	75	290.0	56.5	5.35 4	425. 5	4.228	6	2	0	-5.050	0.15346	3.008	0.262	0.602	1.078

ZINC1288286 2	75	302.2	56.5	5.69 8	439. 6	4.572	6	2	0	-5.050	0.13511	3.008	0.262	0.602	1.078
ZINC0209361 4	75	319.4	56.5	6.18 4	431. 5	6.111	5	1	1	-6.278	0.09804	2.623	0.770	0.583	0.669
ZINC3081921 6	75	291.9	56.5	5.49 5	403. 5	5.154	5	1	1	-5.535	0.13359	2.523	0.700	0.327	0.795
ZINC3081921 8	75	291.9	56.5	5.49 5	403. 5	5.154	5	1	1	-5.535	0.13359	2.523	0.700	0.327	0.795
ZINC3081922 6	75	288.9	56.5	5.94 5	395. 5	5.347	5	1	1	-9.883	0.12068	2.710	0.639	0.522	0.695
ZINC3081925 7	75	301.2	56.5	6.28 9	409. 5	5.691	5	1	1	-9.883	0.10630	2.710	0.639	0.522	0.695
ZINC0953120 9	75	313.3	74.3	5.96 6	441. 5	4.622	7	1	0	-1.621	0.14820	2.320	0.915	0.544	1.059
ZINC1193623 9	76	335.0	50.8	5.59 9	435. 5	3.036	5	2	0	1.803	0.49740	2.629	0.692	0.251	1.429
ZINC1218201 4	77	291.1	77.4	4.76 1	418. 5	1.516	8	1	0	3.053	0.64827	2.216	1.034	0.348	1.474
ZINC1218877 3	78	313.3	68.9	5.10 2	429. 5	2.206	7	1	0	0.849	0.51730	2.768	0.646	0.486	1.420
ZINC0122328 8	79	279.8	81.3	6.73 0	404. 5	2.277	6	1	0	-1.202	0.30182	2.525	1.266	0.588	1.311
ZINC0122329 9	79	290.8	81.3	7.10 8	418. 5	2.602	6	1	0	-1.080	0.28736	2.526	1.429	0.648	1.159
ZINC0122330 0	79	290.8	81.3	7.10 8	418. 5	2.602	6	1	0	-1.080	0.28736	2.526	1.429	0.648	1.159
ZINC1244082 5	80	345.9	65.6	4.22 9	450. 5	3.061	7	0	0	-0.800	0.25491	2.621	1.269	0.576	1.282
ZINC1258331 9	81	330.6	70.4	7.97 1	428. 6	6.401	4	1	1	-0.474	0.11093	2.454	0.697	0.793	1.304
ZINC1268203 1	82	311.2	56.5	6.10 5	414. 5	4.234	6	0	0	2.588	0.44008	2.758	1.160	0.408	1.426
ZINC1312061 1	83	329.5	57.0	5.99 1	440. 5	5.690	6	1	1	-1.666	0.20523	2.562	1.536	0.492	1.140
ZINC1322633 9	84	312.9	78.0	5.00 5	447. 5	2.637	8	2	0	3.333	0.58229	2.541	0.866	0.428	1.353
ZINC0876521 7	85	277.5	72.3	4.34 8	406. 5	1.410	7	2	0	-4.206	0.21833	2.687	0.878	0.406	1.279
ZINC0876526 9	85	305.3	88.1	4.61 8	420. 5	3.842	7	2	0	-3.241	0.18812	2.815	0.760	0.416	1.315
ZINC1362359 0	85	322.2	56.5	5.05 0	444. 5	3.000	6	0	0	-3.061	0.18200	2.747	1.201	0.603	1.018
ZINC3081921 9	85	301.6	56.5	5.41 1	415. 5	5.230	5	0	1	-5.535	0.13172	2.546	0.912	0.401	0.919

ZINC0209820 5	85	311.6	102.6	4.89 2	424.5	0.239	7	0	0	-7.577	0.19536	2.404	0.881	0.442	0.671
ZINC0210738 7	85	312.7	102.6	5.43 6	438.5	2.190	7	1	0	-5.870	0.17063	2.568	0.888	0.372	0.747
ZINC0140539 3	86	311.6	94.2	7.56 4	438.5	4.891	5	1	0	-3.837	0.06303	2.602	0.832	0.631	1.251
ZINC1546898 1	87	294.6	38.9	6.12 1	396.5	0.589	5	1	0	0.501	0.44605	2.564	1.182	0.770	1.099
ZINC1573379 9	88	301.0	51.2	5.02 3	437.6	3.303	5	1	0	-3.434	0.29836	2.539	0.243	0.461	1.469
ZINC2099008 4	88	294.6	51.2	5.02 8	437.6	3.595	5	1	0	-0.574	0.38422	2.595	0.680	0.499	1.345
ZINC1626930 5	89	322.3	57.0	6.46 7	436.5	5.284	6	1	1	2.165	0.09747	2.335	1.294	0.519	1.087
ZINC1628435 9	89	334.8	57.0	6.65 0	450.5	5.784	6	1	1	1.903	0.08442	2.371	1.320	0.547	1.011
ZINC1634982 2	89	310.0	57.0	6.12 3	422.5	4.941	6	1	0	2.165	0.11062	2.319	1.230	0.465	1.115
ZINC1636215 8	89	322.3	57.0	6.46 7	436.5	5.284	6	1	1	2.165	0.07310	2.410	1.248	0.514	1.127
ZINC1636302 4	89	310.0	57.0	6.12 3	422.5	4.941	6	1	0	2.165	0.08297	2.398	1.183	0.462	1.151
ZINC0833552 0	90	298.5	47.8	6.68 7	406.5	5.710	5	1	1	2.213	0.09231	2.417	1.567	0.694	1.307
ZINC0836767 0	90	289.4	47.8	6.73 5	412.9	5.628	5	1	1	2.274	0.09257	2.399	1.535	0.952	1.120
ZINC0836767 5	90	296.3	57.0	6.01 7	408.5	4.952	6	1	0	2.240	0.11476	2.431	1.718	0.482	1.163
ZINC1628448 7	90	304.8	47.8	7.47 1	447.3	6.234	5	1	1	2.251	0.07486	2.399	1.535	0.952	1.120
ZINC1634912 0	90	286.3	47.8	6.34 3	392.5	5.366	5	1	1	2.213	0.10390	2.413	1.521	0.625	1.372
ZINC2253032 7	90	334.8	57.0	6.74 7	450.5	6.031	6	1	1	1.768	0.07959	2.420	1.656	0.705	0.898
ZINC0098050 0	90	302.0	79.9	6.54 4	437.5	5.204	6	2	1	2.575	0.09937	2.405	1.125	0.599	1.510
ZINC0844024 7	91	318.1	84.6	6.94 8	421.5	4.324	6	1	0	3.655	0.11433	2.198	1.319	0.584	0.884
ZINC1667199 5	91	321.3	84.6	7.34 0	441.9	4.586	6	1	0	3.697	0.10337	2.153	1.368	0.844	0.865
ZINC1709303 3	92	305.8	47.8	5.47 7	422.5	5.110	5	1	1	1.337	0.31333	2.511	1.327	0.642	1.073
ZINC1966058 8	93	296.0	67.6	5.57 8	419.5	3.213	7	1	0	1.874	0.50779	2.578	1.008	0.649	1.358

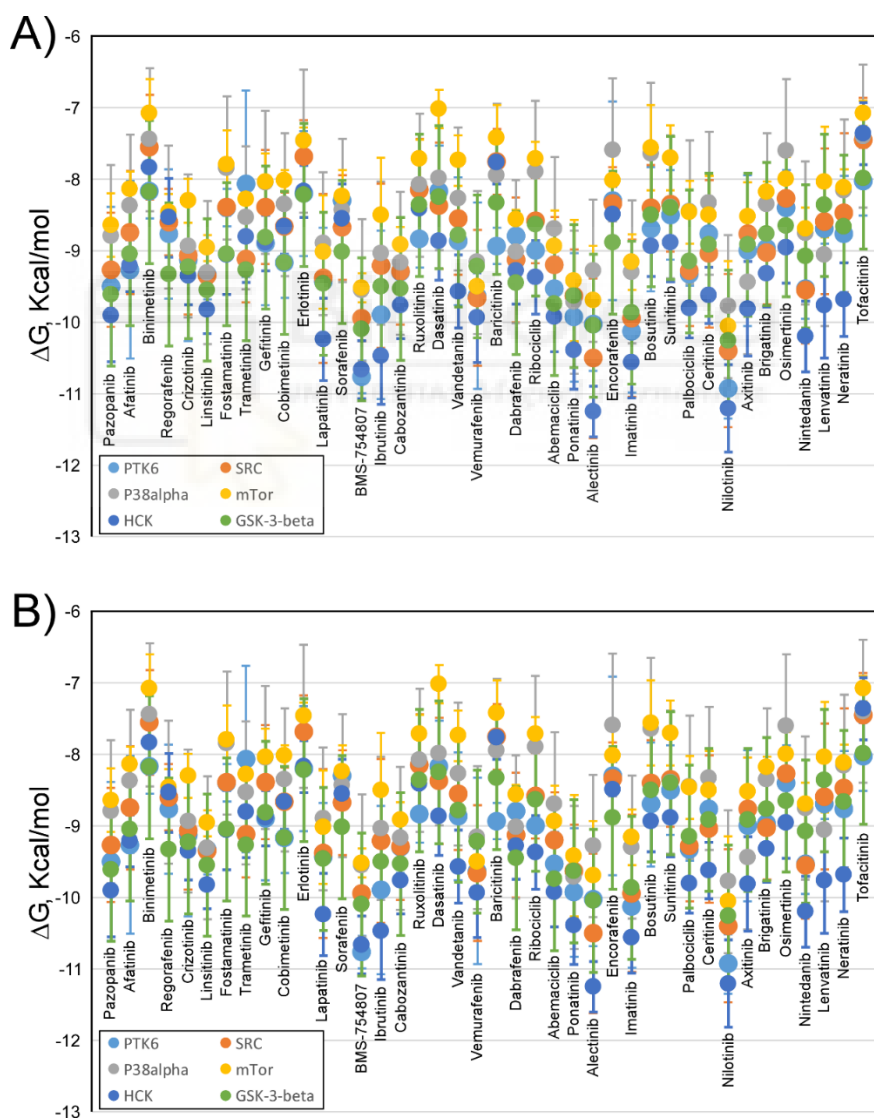
ZINC23333375	94	273.5	43.1	6.719	404.4	4.926	4	1	0	-5.096	0.19351	2.523	1.387	0.726	1.050
ZINC27534122	95	293.2	71.5	6.887	439.5	3.197	7	1	0	-0.631	0.29648	2.400	0.458	0.427	1.136
ZINC03358607	96	340.0	72.8	6.743	449.6	5.733	5	0	1	-0.998	0.19883	2.551	0.016	0.523	1.356
ZINC04262734	97	310.5	77.3	4.938	414.5	4.434	6	0	0	2.097	0.30555	2.480	0.876	0.887	0.682
ZINC04936227	98	317.5	34.9	5.960	426.6	2.529	5	1	0	2.300	0.49984	2.608	0.991	0.573	1.302
ZINC05151985	98	331.2	47.8	6.001	426.6	4.650	5	1	0	2.300	0.40995	2.640	0.870	0.642	1.294
ZINC09408007	98	331.3	34.9	6.369	440.6	3.100	5	1	0	2.554	0.45284	2.665	0.898	0.669	1.224
ZINC09408500	98	331.0	34.9	6.577	440.6	2.930	5	1	0	2.300	0.26450	2.640	0.870	0.642	1.294
ZINC09408505	98	343.5	47.8	6.345	440.6	4.994	5	1	0	2.300	0.21672	2.640	0.870	0.642	1.294
ZINC05044064	99	320.8	73.2	5.984	422.6	5.999	5	1	1	-1.102	0.17314	2.567	1.392	0.730	1.080
ZINC08857160	100	315.7	71.6	7.840	449.3	6.391	6	0	1	3.181	0.25543	2.381	1.485	0.840	1.279
ZINC08966188	101	286.5	60.4	5.624	443.5	3.778	7	2	0	-4.305	0.25185	2.498	0.860	0.538	1.212
ZINC09076927	101	290.9	87.0	4.434	428.5	2.377	9	1	0	0.389	0.53742	2.625	1.318	0.511	1.300
ZINC09792243	101	293.2	60.4	5.397	443.5	3.692	7	1	0	-2.425	0.28166	2.683	1.020	0.527	1.224
ZINC09792247	101	293.2	60.4	5.397	443.5	3.692	7	1	0	-2.425	0.28166	2.683	1.020	0.527	1.224
ZINC09992380	101	300.0	60.4	5.053	449.5	3.638	7	1	0	-5.508	0.27596	2.705	0.675	0.509	1.354
ZINC09992418	101	300.0	60.4	5.053	449.5	3.638	7	1	0	-5.508	0.27596	2.705	0.675	0.509	1.354
ZINC09043059	102	286.1	85.4	6.152	447.4	0.536	5	0	0	-1.527	0.30017	2.436	1.394	0.907	0.908
ZINC09530812	103	265.2	30.3	5.035	419.9	1.801	6	1	0	2.293	0.61268	2.811	0.592	0.724	1.257
ZINC09580205	104	343.1	49.2	6.000	445.5	5.627	5	0	1	1.033	0.18478	2.220	1.288	0.400	1.427
ZINC09682151	105	313.0	54.7	5.395	436.5	4.443	6	1	0	3.625	0.47600	2.459	1.109	0.436	1.290
ZINC09940952	106	332.7	59.2	7.283	441.9	5.003	5	0	1	4.098	0.33862	2.390	1.562	0.856	1.250

ZINC0994095 7	106	341.8	59.2	-	435.5	5.085	5	0	1	4.050	0.33850	2.547	1.651	0.556	1.268
ZINC099412 99	106	337.4	59.2	-	439.5	4.914	5	0	0	2.535	0.34261	2.565	1.496	0.752	1.309

Abbreviations: Topological polar surface area (TPSA); molecular weight (MW); the calculated logarithm (base 10) of the solubility measured in mol/liter (cLogS); calculated logarithm of partition coefficient between n-octanol and water (cLogP); number of hydrogen bond donors (HBD); number of hydrogen bond acceptors (HBA); violation of Lipinski’s rules (Ro5 violations), FT, Fish Toxicity; TPT, *Tetrahymena Pyriformis* Toxicity; RAT, Rat Acute Toxicity. LD50 is the amount of a compound, given all at once, which causes the death of 50% (one half) of a group of test rats.

^a These parameters were calculated using the DATAWARRIOR software v4.7.2 [3].

^b These parameters were calculated using the <http://lmm.d.ecust.edu.cn:8000/predict/> site[4].



Supplementary Figure S1. Comparison of the Gibbs free energy variation (ΔG , Kcal/mol) for 40 compounds approved by the FDA for clinical use against various types of cancer, obtained by molecular docking experiments against the ATP binding site of 12 protein kinases (see below for both the UniProt and PDB code of each protein). The data has been distributed in two panels (**A** and **B**) to facilitate comparison.



List of PDB codes of the structures used in the molecular docking experiments for the different protein kinases analyzed. The results of ΔG included in **Supplementary Figure S1** result from averaging the values obtained in molecular docking experiments with all the structures listed in the next tables for each protein. For each PDB entry, the experimental method (X-ray diffraction data only), the resolution A, and the position of the amino acids of the resolved structure are included.

Protein: PTK6, UniProt code: Q13882

PDB entry	Method	Resolution (Å)	Positions
5D7V	X-ray	2.33	185-446
5DA3	X-ray	1.7	185-446
5H2U	X-ray	2.24	185-446

Protein: SRC, UniProt code: P12931

PDB entry	Method	Resolution (Å)	Positions
2H8H	X-ray	2.2	2-536
1YOJ	X-ray	1.95	254-536
1YOL	X-ray	2.3	254-536
1YOM	X-ray	2.9	254-536
4MXO	X-ray	2.1	254-536
4MXX	X-ray	2.6	254-536
4MXY	X-ray	2.58	254-536
4MXZ	X-ray	2.58	254-536
2BDF	X-ray	2.1	258-536
2BDJ	X-ray	2.5	258-536
1YI6	X-ray	2	261-536
1FMK	X-ray	1.5	86-536
1KSW	X-ray	2.8	86-536
1Y57	X-ray	1.91	86-536
2SRC	X-ray	1.5	86-536
4K11	X-ray	2.3	87-534

Protein: mTor, UniProt code: P42345

PDB entry	Method	Resolution (Å)	Positions
4JSN	X-ray	3.2	1376-2549
4JSP	X-ray	3.3	1376-2549
4JSV	X-ray	3.5	1376-2549
4JSX	X-ray	3.5	1376-2549
4JT5	X-ray	3.45	1376-2549
4JT6	X-ray	3.6	1376-2549
5WBU	X-ray	3.42	1376-2549
5WBV	X-ray	3.1	1376-2549

Protein: CHK2, UniProt code: O96017

PDB entry	Method	Resolution (Å)	Positions
2CN5	X-ray	2.25	210-531
2CN8	X-ray	2.7	210-531
2W0J	X-ray	2.05	210-531
2W7X	X-ray	2.07	210-531
2WTC	X-ray	3	210-531
2WTD	X-ray	2.75	210-531
2WTI	X-ray	2.5	210-531
2WTJ	X-ray	2.1	210-531
2XBJ	X-ray	2.3	210-531
2XK9	X-ray	2.35	210-531
2XM8	X-ray	3.4	210-531

Protein: HCK, UniProt code: P08631

PDB entry	Method	Resolution (Å)	Positions
5H0B	X-ray	1.65	81-526
5H0H	X-ray	1.72	81-526
5H0G	X-ray	1.8	81-526
5H09	X-ray	1.95	81-526
2HK5	X-ray	2	247-514
1QCF	X-ray	2	81-526
5H0E	X-ray	2.1	81-526
2COT	X-ray	2.15	81-526
3VS3	X-ray	2.17	81-526

2XM9	X-ray	2.5	210-531	3VRZ	X-ray	2.22	81-526
2YCF	X-ray	1.77	210-530	2COI	X-ray	2.3	81-526
2YCQ	X-ray	2.05	210-531	3VS6	X-ray	2.37	81-526
2YCR	X-ray	2.2	210-531	3VS1	X-ray	2.46	81-526
2YCS	X-ray	2.35	210-531	3VRY	X-ray	2.48	81-526
2YIQ	X-ray	1.89	210-531	1AD5	X-ray	2.6	79-526
2YIR	X-ray	2.1	210-531	3VS2	X-ray	2.61	81-526
2YIT	X-ray	2.2	210-531	3VS4	X-ray	2.75	81-526
3I6U	X-ray	3	84-502	2C00	X-ray	2.85	81-526
3I6W	X-ray	3.25	70-512	3VS5	X-ray	2.85	81-526
4A9R	X-ray	2.85	210-531	4LUD	X-ray	2.85	81-526
4A9S	X-ray	2.66	210-531	3VS0	X-ray	2.93	81-526
4A9T	X-ray	2.7	210-531	2HCK	X-ray	3	79-526
4A9U	X-ray	2.48	210-531	3VS7	X-ray	3	81-526
4BDA	X-ray	2.6	210-531	4LUE	X-ray	3.04	81-526
4BDB	X-ray	2.5	210-531				
4BDC	X-ray	3	210-531				
4BDD	X-ray	2.67	210-531				
4BDE	X-ray	2.55	210-531				
4BDF	X-ray	2.7	210-531				
4BDG	X-ray	2.84	210-531				
4BDH	X-ray	2.7	210-531				
4BDI	X-ray	2.32	210-531				
4BDJ	X-ray	3.01	210-531				
4BDK	X-ray	3.3	210-531				

Protein: FYN, UniProt code: P06241

PDB entry	Method	Resolution (Å)	Positions
2DQ7	X-ray	2.8	261-537

Protein: AKT1, UniProt code: P31749

PDB entry	Method	Resolution (Å)	Positions
6CCY	X-ray	2.18	144-466
3CQU	X-ray	2.2	144-480
3CQW	X-ray	2	144-480
3MV5	X-ray	2.47	144-480
3MVH	X-ray	2.01	144-480
3OCB	X-ray	2.7	144-480
3OW4	X-ray	2.6	144-480
3QKK	X-ray	2.3	144-480
3QKL	X-ray	1.9	144-480
3QKM	X-ray	2.2	144-480
4EKK	X-ray	2.8	144-480
4EKL	X-ray	2	144-480
4GV1	X-ray	1.49	144-480
3O96	X-ray	2.7	2-443
4EJN	X-ray	2.19	2-446

Protein: AKT2, UniProt code: P31751

PDB entry	Method	Resolution (Å)	Positions
1GZK	X-ray	2.3	146-460
1GZN	X-ray	2.5	146-480
1GZO	X-ray	2.75	146-460
1MRV	X-ray	2.8	143-481
1MRY	X-ray	2.8	143-481
1O6K	X-ray	1.7	146-481
1O6L	X-ray	1.6	146-467
2JDO	X-ray	1.8	146-467
2JDR	X-ray	2.3	146-467

2UW9	X-ray	2.1	146-467
2X39	X-ray	1.93	146-467
2XH5	X-ray	2.72	146-479
3D0E	X-ray	2	146-480
3E87	X-ray	2.3	146-480
3E88	X-ray	2.5	146-480
3E8D	X-ray	2.7	146-480

Protein: P38 alpha, UniProt code: Q16539

PDB entry	Method	Resolution (Å)	Positions
2FST	X-ray	1.45	2-360
3LFF	X-ray	1.5	2-360
3OEF	X-ray	1.6	1-360
5WJJ	X-ray	1.6	1-360
3ZS5	X-ray	1.6	2-360
4EHV	X-ray	1.6	2-360
4GEO	X-ray	1.66	2-360
3FMK	X-ray	1.7	1-360
3ROC	X-ray	1.7	1-360
5XYY	X-ray	1.7	1-360
2FSL	X-ray	1.7	2-360
2QD9	X-ray	1.7	2-360
3K3I	X-ray	1.7	5-352
2RG6	X-ray	1.72	2-360
2GFS	X-ray	1.75	2-360
2ZAZ	X-ray	1.8	1-360
3FL4	X-ray	1.8	1-360
3FLY	X-ray	1.8	1-360
3GC7	X-ray	1.8	1-360
3KQ7	X-ray	1.8	1-360
5MTX	X-ray	1.8	1-360
1WBS	X-ray	1.8	2-360
2NPQ	X-ray	1.8	2-360
3HUC	X-ray	1.8	2-360
4AA0	X-ray	1.8	2-360
3S3I	X-ray	1.8	4-352
2FSO	X-ray	1.83	2-360

5KCV	X-ray	2.7	2-446
------	-------	-----	-------

Protein: GSK-3 beta, UniProt code: P49841

PDB entry	Method	Resolution (Å)	Positions
1J1B	X-ray	1.8	1-420
1Q5K	X-ray	1.94	7-420
4AFJ	X-ray	1.98	27-393
4PTE	X-ray	2.03	1-420
4NM3	X-ray	2.1	1-383
1J1C	X-ray	2.1	1-420
1Q41	X-ray	2.1	2-420
3DU8	X-ray	2.2	1-420
1Q3D	X-ray	2.2	2-420
5K5N	X-ray	2.2	28-384
4ACC	X-ray	2.21	1-420
3SAY	X-ray	2.23	1-420
1R0E	X-ray	2.25	35-420
4NM5	X-ray	2.3	13-383
4NM7	X-ray	2.3	13-383
1Q3W	X-ray	2.3	2-420
3I4B	X-ray	2.3	7-420
4I71	X-ray	2.31	1-420
2JLD	X-ray	2.35	1-420
4PTG	X-ray	2.36	1-420
3ZRK	X-ray	2.37	23-393
1PYX	X-ray	2.4	1-420
5KPK	X-ray	2.4	1-420
3GB2	X-ray	2.4	34-383
3F7Z	X-ray	2.4	35-383
1O9U	X-ray	2.4	35-384
5HLP	X-ray	2.45	1-420
3ZRL	X-ray	2.48	23-393
3ZRM	X-ray	2.49	23-393
4NM0	X-ray	2.5	1-383
5F94	X-ray	2.51	36-385
5F95	X-ray	2.52	36-385
4ACD	X-ray	2.6	1-420

5N68	X-ray	1.85	1-360	4ACG	X-ray	2.6	1-420
4F9Y	X-ray	1.85	2-360	4ACH	X-ray	2.6	1-420
2FSM	X-ray	1.86	2-360	5KPL	X-ray	2.6	1-420
4E5A	X-ray	1.87	1-360	6B8J	X-ray	2.6	1-420
3HL7	X-ray	1.88	1-360	1GNG	X-ray	2.6	27-393
3NNW	X-ray	1.89	1-354	4DIT	X-ray	2.6	27-393
3MPT	X-ray	1.89	1-360	3F88	X-ray	2.6	35-383
3ZSG	X-ray	1.89	2-360	3ZDI	X-ray	2.64	35-384
3D83	X-ray	1.9	1-360	5KPM	X-ray	2.69	1-420
3FLN	X-ray	1.9	1-360	1I09	X-ray	2.7	1-420
3FLQ	X-ray	1.9	1-360	4J1R	X-ray	2.7	1-420
3FMH	X-ray	1.9	1-360	3Q3B	X-ray	2.7	2-420
3FMN	X-ray	1.9	1-360	3SD0	X-ray	2.7	35-384
3ZYA	X-ray	1.9	1-360	4PTC	X-ray	2.71	1-420
5ML5	X-ray	1.9	1-360	1Q4L	X-ray	2.77	2-420
5N67	X-ray	1.9	1-360	4B7T	X-ray	2.77	35-384
4DLI	X-ray	1.91	2-360	1UV5	X-ray	2.8	35-384
2Y8O	X-ray	1.95	1-360	1H8F	X-ray	2.8	35-386
3HLL	X-ray	1.95	1-360	2OW3	X-ray	2.8	35-386
3HV6	X-ray	1.95	2-360	5T31	X-ray	2.85	1-420
3CTQ	X-ray	1.95	5-352	3L1S	X-ray	2.9	7-420
4KIN	X-ray	1.97	2-360	3PUP	X-ray	2.99	1-420
1R3C	X-ray	2	1-360	5HLN	X-ray	3.1	1-420
1ZYJ	X-ray	2	1-360	4IQ6	X-ray	3.12	1-420
1ZZ2	X-ray	2	1-360	3M1S	X-ray	3.13	1-420
2I0H	X-ray	2	1-360	5OY4	X-ray	3.2	1-420
3E92	X-ray	2	1-360	2O5K	X-ray	3.2	29-393

Protein: IGF-1R, UniProt code: P08069

PDB entry	Method	Resolution (Å)	Positions
1P4O	X-ray	1.5	974-1294
3LW0	X-ray	1.79	983-1286
5FXS	X-ray	1.9	980-1286
2OJ9	X-ray	2	982-1286
3I81	X-ray	2.08	982-1286
1JQH	X-ray	2.1	979-1286
3O23	X-ray	2.1	982-1286

Protein: IGF-1R, UniProt code: P08069

PDB entry	Method	Resolution (Å)	Positions
4CFE	X-ray	3.02	1-552
4CFF	X-ray	3.92	1-552
4ZHX	X-ray	2.99	2-552
5ISO	X-ray	2.63	1-552
6B1U	X-ray	2.77	2-552
6B2E	X-ray	3.8	2-552

4D2R	X-ray	2.1	985-1286
1K3A	X-ray	2.1	988-1286
3NW7	X-ray	2.11	982-1286
3NW5	X-ray	2.14	982-1286
3NW6	X-ray	2.2	982-1286
5HZN	X-ray	2.2	983-1286
5FXQ	X-ray	2.3	980-1286
3D94	X-ray	2.3	986-1286
5FXR	X-ray	2.4	980-1286
2ZM3	X-ray	2.5	981-1286
1M7N	X-ray	2.7	974-1294
3F5P	X-ray	2.9	981-1286
3QQU	X-ray	2.9	988-1286
3LVP	X-ray	3	951-1286

References

1. Ruiz-Torres, V.; Encinar, J.A.; Herranz-Lopez, M.; Perez-Sanchez, A.; Galiano, V.; Barrajon-Catalan, E.; Micol, V. An updated review on marine anticancer compounds: The use of virtual screening for the discovery of small-molecule cancer drugs. *Molecules* 2017, 22.
2. Banerjee, P.; Erehman, J.; Gohlke, B.O.; Wilhelm, T.; Preissner, R.; Dunkel, M. Super natural ii--a database of natural products. *Nucleic Acids Res* 2015, 43, D935-939.
3. Sander, T.; Freyss, J.; von Korff, M.; Rufener, C. Datawarrior: An open-source program for chemistry aware data visualization and analysis. *J Chem Inf Model* 2015, 55, 460-473.
4. Cheng, F.; Li, W.; Zhou, Y.; Shen, J.; Wu, Z.; Liu, G.; Lee, P.W.; Tang, Y. Admetsar: A comprehensive source and free tool for assessment of chemical admet properties. *J Chem Inf Model* 2012, 52, 3099-3105.
5. Sterling, T.; Irwin, J.J. Zinc 15--ligand discovery for everyone. *J Chem Inf Model* 2015, 55, 2324-2337.



**A Nudibranch Marine Extract
Chemosensitizes Selectively
Colorectal Cancer Cells inducing
Endoplasmic Reticulum Stress
mediated by ROS**

**Doctoral Student:
Verónica Ruiz Torres**

Article

A Nudibranch Marine Extract Chemosensitizes Selectively Colorectal Cancer Cells by inducing Endoplasmic Reticulum Stress mediated by ROS.

Verónica Ruiz-Torres¹, Nicholas Forsythe², Almudena Pérez-Sánchez¹, Sandra Van Schaeybroeck², Enrique Barrajón-Catalán^{1,*,#} and Vicente Micol^{1,3,#}.

¹ Instituto de Investigación, Desarrollo e Innovación en Biotecnología Sanitaria de Elche (IDiBE), Universitat Miguel Hernández; 03202, Elche, Spain.

² Drug Resistance Group, Centre for Cancer Research and Cell Biology, School of Medicine, Dentistry and Biomedical Science, Queen's University Belfast, Belfast, United Kingdom.

³ CIBER, Fisiopatología de la Obesidad y la Nutrición, CIBERobn, Instituto de Salud Carlos III, Palma de Mallorca 07122, Spain (CB12/03/30038).

* Correspondence: e.barrajon@umh.es; Tel.: +34-965-222-586

Both authors share senior co-authorship.

Under process of publishing

Abstract: Marine compounds suppose an unexplored source of potential drugs against cancer. The present study shows the antiproliferative effect of the nudibranch extract (*Dolabella auricularia*, NB) in the colon cancer cell models and postulates how colon cancer cell growth and malignancy can be declined through the modification of one of the most potent resistance mechanisms presented by tumor cells and that differentiates them from non-tumor cells, the stress balance. NB extract augmented the accumulation of reactive oxygen species (ROS) and increased endoplasmic reticulum stress (ERS) via unfolded protein response stimulation. Stress scavengers, N-acetylcysteine (NAC) and 4-phenylbutyric acid (4-PBA) diminished stress induced by NB. Results showed that NB extract increased ER stress through ROS overproduction in superinvasive colon cancer cells, decreasing their resistance threshold, and producing a non-return level of ERS, causing DNA damage, cell cycle arrest, and therefore avoiding their hyperproliferative capacity and subsequent migration and invasion. On the contrary, NB extract presented a lower effect on non-tumor human colon cells, suggesting that its effect can be selective and related to stress balance homeostasis.

Keywords: marine compounds, marine invertebrate, nudibranch, antiproliferative, colon cancer, cell cycle arrest, apoptosis, cell death, oxidative stress, Endoplasmic Reticulum Stress.



1. Introduction

Oceans cover 70% of the planet's surface and represent more than 90% of the habitats where the planet's life forms. The marine ecosystem is a hostile environment in which species, mostly sessile or with low movement capabilities, compete to survive and protect themselves by developing defensive chemical weapons (or secondary metabolites). Bioactive marine compounds, due to their diversity and complexity, have attracted current research in many areas and especially have turned out to be a new potential source of anticancer compounds. In fact, by the end of 2017, seven marine substances were approved by the FDA as drugs, and 4 of them especially to treat cancer (cytarabine as Cytosar-U®, eribulin mesylate as Halaven®, brentuximab vedotin as Adcetris® and trabectedine as Yondelis®) [1]. The antitumor capacity of marine compounds recorded in scientific studies shows that their activity is capable of affecting various cancer hallmarks through different metabolic pathways [1, 2].

Cancer is a worldwide cause of death, colorectal cancer is presented as the third most common cancer in men and the second in women [3], but the first when both sexes are considered together. Cancer is known as a heterogeneous disease, which is characterized by a rapidly proliferating and surviving cells as a result of alterations in genes, metabolism and tumor microenvironment. This study is focused on the changed metabolic scenario that is present in cancer cells compared to that one in normal cells. Cancer cells have important redox deregulation resulting in persistent intracellular high levels of reactive oxygen species (ROS) defined in many studies to be tumor-promoting agents [4]. The ability of tumor cells to survive to high oxidative stress level is based on an improved antioxidant defense system [5]. Kumari S. *et al.* indicated an overactivation in the nicotinamide adenine dinucleotide phosphate (NADPH) and glutathione (GSH) antioxidant enzymes, cofactors such as nicotinamide adenine dinucleotide (NADH) and flavin adenine dinucleotide (FADH) and also overexpression of the transcription factor Nrf2 in cancer cells to contribute in balancing oxidative stress. Furthermore, they explained how these antioxidant enzymes can facilitate multiple mechanisms to trigger the spread of metastatic cancer cells [6]. Piskounova *et al.* [7] demonstrated that metastatic cells show stronger antioxidant power than non-metastatic ones that allow them to survive to a high level of oxidative stress.

Endoplasmic Reticulum (ER) is a specific organelle that plays an important role in synthesizing and folding proteins in a continuous proliferating context, as in the case of the cancer cells. Changes in cellular environment such as oxidative stress generation, DNA damage or other factors can induce accumulation of improperly folded proteins leading the ERS. In this situation, the first survival adaptation displayed by cells is the called unfolded protein response (UPR), which promotes the reestablishment of ER homeostasis. When misfolded proteins are accumulated by a deficiency of the UPR or an excessive ERS, cell death pathways are initiated [8].

ERS and oxidative stress are linked and are the result of altered cellular metabolism in many different cancers [9]. In the last years, the interest of the scientific

community has increased towards the development of therapies aimed at treating the altered metabolism of tumor cells. The high-stress levels of tumor cells, that differentiates them from non-tumor cells, makes them more vulnerable to metabolic modulators agents, which induce cell death more easily [10]. Therefore, targeting ROS and ERS pathways and their relation with the mechanisms involved in cancer development are new potential strategies to prevent cancer.

In the present study, the antiproliferative effect of the nudibranch extract (*Dolabella auricularia*) was investigated in a clinically relevant colon cancer cell model and compared with non-tumoral human colon cells. The relationship between this antiproliferative activity and the increase in ROS and ERS was also studied, with especial interest in the proteins and mechanisms involved in these effects. The results confirm the putative relevance of *D. auricularia* extract in the development of new treatments for colon cancer management and contribute to explaining how the oxidative status is linked with proliferation and metastasis.

2. Results

In a previous study, twenty species of marine invertebrates were selected for their behavior of competence in experimental aquariums by the marine species distributor company of TODO PEZ S.L. Extracts of chosen species were produced and screened for their antiproliferative activity in a panel of human colon cancer cell lines (HGUE-C-1, HT-29 and SW-480). From those extracts which reported the strongest activity, the nudibranch *Dolabella auricularia* (NB) was the most potent (**Figure 1 f**). NB extract showed a potent antiproliferative effect inducing an imbalance in oxidative homeostasis, increasing the intracellular oxygen species (ROS), generating DNA damage, mitochondrial depolarization and cell cycle arrest in G2/M phase. In the present study, we have focused on investigating the mechanism involved in the antiproliferative effect of NB and its relationship with the induction of oxidative stress and its antimetastatic effect in the highly aggressive and metastatic HCT-116 human colon cancer cell line [11, 12] and in new superinvasive cell lines derived from it. The effects on these tumoral cell models were compared with non-tumoral colon CCD-18Co human cells.

2.1. NB extract inhibits the proliferation of adenocarcinoma cell lines and was less cytotoxic in fibroblast colon cell line

To investigate the cytotoxic effect of NB extract, HCT-116 and CCD-18Co were treated with different concentrations for 24 h and cell viability was tested by MTT assay. Observations under the microscope showed a significant change in the morphology of cells. NB treated cells displayed a condensed nucleus typical of a pknosis phenomenon and expanded cytoplasm respect to untreated cells as well as membrane blebbing and membrane protrusions well characterized in apoptosis (**Figure 1 g**). NB suppressed

colon cancer cell proliferation of HCT-116 and normal CCD-18Co in a dose-dependent manner (**Figure 1 a, b and c**), but showing different concentration ranges. The IC_{50} values were $1.01 \pm 0.19 \mu\text{g/mL}$ in HCT-116 and $15.04 \pm 1.38 \mu\text{g/mL}$ in normal colon cell line CCD-18Co (15 times higher than in the cancer cell line). Despite the fact that the cytotoxic effect of NB is shown in both cell lines, NB extract was able to reduce more strongly cell viability in colon cancer cell line than in normal cells.

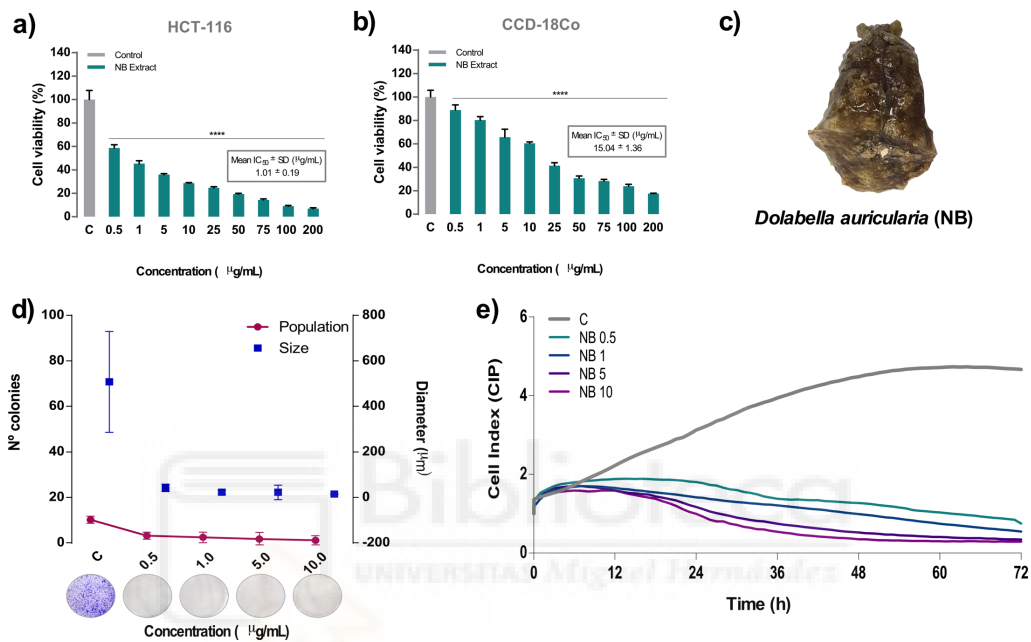


Figure 1. Effect of *Dolabella auricularia* extract (NB) on the proliferation of colon cancer and normal cell lines. Cytotoxicity of different concentrations of NB extract for 24 h was tested by MTT assay in HCT-116 (**a**) and CCD-18Co (**b**) cells. Control (C) are cells plus DMSO (extract vehicle) at less than 0.2% (v:v). Results represent the mean \pm SD from three independent experiments ($n=6$ for each experiment). **c**) Photograph of *Dolabella auricularia* invertebrate specimen. **d**) Cell survival ability of HCT-116 was measured by clonogenic assay. After NB treatment at indicated doses, colonies were labeled with Hoechst 33342 to measure size and number of colonies. Data are represented as the mean \pm SD from three independent experiments ($n=6$ for each experiment). p -values were calculated and compared to the untreated cell line using ANOVAs. * p -value < 0.05, ** p -value < 0.01, *** p -value < 0.001 and **** p -value < 0.0001. **e**) HCT-116 cell proliferation as cell index (CIP) of HCT-116 was measured by Real-Time Cell Analyzer using E-Plates for 72 h. Mean kinetic curves are shown ($n=3$).

The antiproliferative activity of NB was then further characterized in tumoral HCT-116 cells using the colony formation (clonogenic) assay and real-time cell analyzer system (RTCA). The clonogenic assay provides information about the ability of cancer cells to survive and to form a colony from a clone after a treatment exposition [13] and the RTCA assay monitors cellular processes such as proliferation, migration, and invasion in a real-time, avoiding labor-intensive label-based endpoint assays [14] which are translated to a cell index. NB extract was able to lessen the number of colonies compared to the untreated cells and, in addition, was capable to reduce the average size in a dose-dependent manner (**Figure 1 d**). NB extract, at the lowest concentration tested of 0.5 $\mu\text{g/mL}$ decreased a 92% the size of colonies respect to control cells (from 507.9 μm to 42.3 μm), and a 69% the number of cells in the colony. This effect was increased at higher concentrations of the extract. Using the RTCA technique, Cell Index of Proliferation (CIP) of HCT-116 was registered as a kinetic cellular profile (**Figure 1 e**). The kinetics of untreated cells showed an exponential phase until 60 h and a stable rate of growth until 72 h. When cells were treated with NB this exponential phase was not registered, and the CI plummeted at the lowest dose of 0.5 $\mu\text{g/mL}$. All of these results show that NB extract inhibited the proliferation of colon cancer cells in a dose-dependent manner.

2.2. NB extract increases intracellular ROS and activated ERS related proteins in colon cancer cell line.

NB extract increased the intracellular ROS level, in a dose- and in a time-dependent manner in HCT-116 cell line (**Figure 2a and 2b**) confirming the results previously obtained in other colon cancer cell lines (Ruiz-Torres V. et al. 2019, Marine invertebrate extracts induce colon cancer cell death via ROS-mediated DNA oxidative damage and mitochondrial impairment). The ROS level increased up to a 2.3 fold at 5 $\mu\text{g/mL}$ of NB compared to untreated HCT-116 cells. On the contrary, only a modest increase in ROS level was observed in normal cell line CCD-18Co that showed statistically significant differences compared to the control at the highest concentration tested of the extract. (**Figure 2 e and f**).

To elucidate if ERS was implicated in the NB effect, the expression of several ERS proteins (**Figure 2 c and d**) was measured. NB extract promoted the upregulation of GRP78, ATF4 and CHOP at 10 and 25 $\mu\text{g/mL}$ in colon cancer cell lines (**Figure 2 c**). The variation of the effect of NB extract with the time at 10 $\mu\text{g/mL}$ in ERS markers was investigated (**Figure 2 d**). GRP78 and ATF6 were slightly activated during the first 3 h and after that, the expression of these proteins was inhibited. This early response is related to the first attempt of the cell to resist to NB treatment [15]. On the other hand, some ERS markers were strongly activated in a short time (1-3 h of treatment) and persisted up to 24 h, such as phospho-IRE1 α , phospho-JNK, phospho-eIF2 α , ATF4 and CHOP.

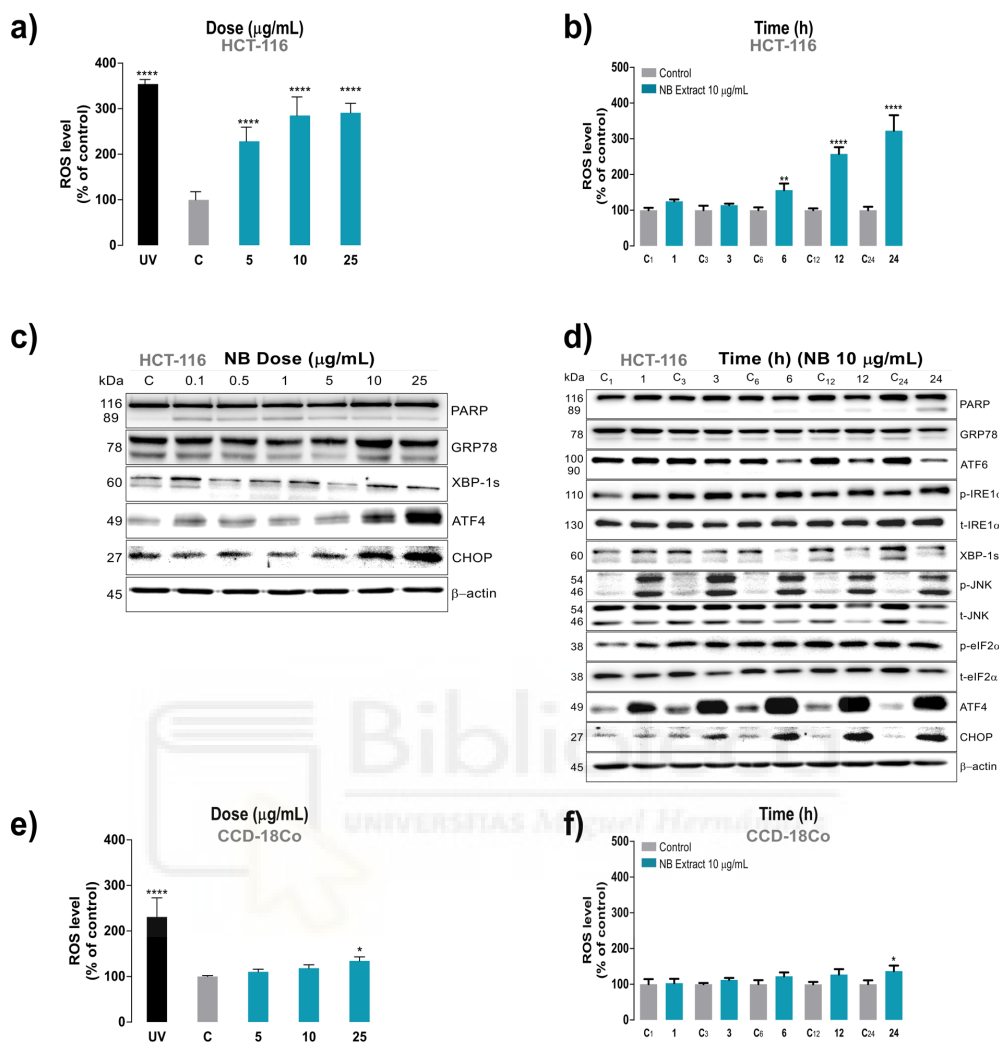


Figure 2. Effect of *Dolabella auricularia* extract (NB) on ROS generation and concomitant ERS in colon cells. Intracellular ROS levels were measured in HCT-116 and CCD-18Co using dichloro-dihydro-fluorescein diacetate (H₂DCF-DA) fluorescence probe after NB treatment in a dose- (a and e) and time-dependent manner (b and f). Data were compared to control (untreated cells plus DMSO less than 0.2%) and were represented as the mean ± SD from three independent experiment (n=6 for each experiment). *p*-values were calculated and compared to the untreated cell line using ANOVAs. **p*-value < 0.05, ***p*-value < 0.01, *** *p*-value < 0.001 and **** *p*-value < 0.0001. The ability of NB extract to modulate ERS-related proteins (PARP, GRP78, ATF6, phospho-IRE1α, total-IRE1α, XBP-1s, phospho-JNK, total-JNK, phospho-eIF2α, total-eIF2α, ATF4, CHOP) in HCT-116 cells was analyzed by Western blot (c, dose- and d, time-dependent). β-actin was used as a loading control.

2.3. NB extract induces strong G2/M phase arrest and cell death as a consequence of ERS in colon cancer cell lines.

We investigated the effect of NB extract in the cell cycle phases on HCT-116 colon cancer cell line and normal colon cell line CCD-18Co. The most remarkable effect of NB was its ability to arrest tumor cells in G2/M phase. As shown in **Figure 3 a**, NB extract at the lowest dose tested of 1.0 $\mu\text{g}/\text{mL}$ drastically arrested tumor cells in G2/M phase, increasing from $45.05 \pm 1.33\%$ in untreated cells to $89.12 \pm 0.52\%$ in treated HCT-116 cells. In CCD-18Co cells the effect was significantly weaker (**Figure 3 b**), i.e. the G2/M phase arrest was produced in a lower percentage and more gradually, reaching a $33.49 \pm 3.6\%$ at 10 $\mu\text{g}/\text{mL}$ or $43.67 \pm 1.99\%$ at 25 $\mu\text{g}/\text{mL}$ respected to a $18.91 \pm 2.72\%$ in untreated CCD-18Co cells. Furthermore, NB treatment caused an increase in the proportion of cells in subG1 phase from 0.9 ± 0.2 in untreated HCT-116 cells to $4.35 \pm 0.12\%$ in HCT-116 cells treated with NB extract at 25 $\mu\text{g}/\text{mL}$.

2.3.1. Study of the relation of ERS and G2/M cell arrest induced by NB extract with caspase-dependent apoptosis in colon cancer cells.

We investigated whether ERS induced by NB treatment and the subsequent cell cycle arrest was related to caspase-dependent apoptosis in HCT-116 colon cancer cell lines. For this study, the cell-permeable caspase inhibitor that blocks the activity of caspase proteases and inhibits apoptosis, z-VAD-fmk (z-VAD) was used.

The relationship between apoptosis and activation of ERS markers was analyzed by Western blot (**Figure 3 b**). When caspases were inhibited, cell death by NB was decreased (less intense excision band in PARP), indicating a dependence of caspases in the cell death processes. The strong activation of ERS markers such as phospho-IRE1 α , phospho-JNK (at 24 and 48 h) and the nuclear transcription factors ATF4 and CHOP (higher at 24 h) remained activated despite the inhibition of caspases.

Apoptosis produced by NB extract at 10 $\mu\text{g}/\text{mL}$ after 24 and 48 h in HCT-116 cells was examined in depth through Annexin V/7-ADD assay (**figure 3 d**). First of all, apoptosis level was increased from 24 to 48 hours after the treatment with NB (from 4.1% in the control to 12.0% after 24 h of NB treatment and from 9.1% in the control to 26.3% after 48 h of NB treatment). When caspases were inhibited with z-VAD, apoptosis was reduced from 12.0% to 8.6% (NB for 24 h) and from 26.3% to 15.6% (NB for 48 h). These results show a 3 to 10% of caspases-dependent cell death after NB treatment.

It was found that caspases 3/7 and 8 were involved in the process of apoptosis produced by NB at 24 and 48 h and their effect was inhibited in the presence of z-VAD (**Figure 3 c**) in HCT-116. Furthermore, the type of apoptosis (intrinsic or caspase 9-dependent and extrinsic or caspase 8-dependent) was analyzed through gene silencing by using specific siRNAs (**figure 3 f**). NB induced cell death through PARP excision at 24 and 48 h. Only when C8 (extrinsic apoptosis) was silenced after 24 h of NB treatment, PARP cleavage was completely inhibited. At 48 h, PARP cleavage was reduced when C8 and C9 were silenced but was not completely inhibited. The activation of phospho-

IRE1 α and phospho-JNK proteins induced by NB at 24 h were reduced when C8 was silenced (when PARP cleavage was inhibited), however, ATF4 and CHOP were highly activated.

The arrest in G2/M produced by NB after 24 h of treatment, was reduced very slightly when caspases were inhibited (**Figure 3 c**). This would be indicating that ERS and G2/M arrest are independent of apoptosis.

2.3.2. Study of the effect of NB extract cell treatment in non-dependent caspase cell death

Previous results (section 2.3.1) showed that activation of early apoptosis (phosphatidylserine (PhS) externalization) and PARP cleavage was induced after NB treatment. When caspases were inhibited by using z-VAD, these markers were reduced, but still, activation remained, indicating an additional putative non-caspase dependent cell death. Therefore, the presence of necrosis, necroptosis, and autophagy was analyzed in HCT-116 after NB treatment for 24 h.

Necrosis produced by NB after 24 h was studied through the lactate dehydrogenase (LDH) assay. The measurement of LDH in HCT-116 supernatants showed that NB did not increase LDH % compared to negative and positive control after NB treatment (**figure 4 a**), so necrosis was discarded to take place among the putative cell death mechanisms.

Necroptosis is programmed cell death independent of caspases activity [17, 18] that can exposures PhS. For this reason, necroptosis was considered as a possible mechanism of NB-induced cell death. Cells were pretreated with the necroptotic inhibitors necrostatin-1 (nec-1, an RPK1 inhibitor [19]) at 40 μ M and necrosulfonamide (nsa, an MLKL inhibitor [20]) at 0.5 μ M both for 1 h and z-VAD for 6 h and then treated with NB extract (10 μ g/mL). Annexin V assay showed an increase in the apoptotic proportion of HCT-116 from $2.53 \pm 0.65\%$ in control to $12.70 \pm 1.36\%$ with NB extract. Statistically, significant differences were found only in the condition of z-VAD were early apoptotic population decreased to $6.96 \pm 0.88\%$ (**Figure 4 b**) suggesting that no necroptosis implication on the cell death mechanism. These results were confirmed after the G2/M phase analysis (**Figure 4 c**), which not only showed that the effect of NB in G2/M arrest cell population was non-dependent on necroptosis but also that the main mechanism of G2/M arrest was not caspases-dependent as only a low, but significant change is obtained in the presence of z-VAD.

In a previously published work of our group [21], a nudibranch extract from *Phyllidia varicose* inhibited p-mTOR (molecular target of rapamycin) related to autophagy. mTOR appears to be deregulated in many cancers and its associated with cell proliferation and cancer progression [22]. According to these previous data, NB extract could be inhibiting mTOR target and inducing autophagy. If autophagy were a direct effect of NB treatment, by inhibiting it with chloroquine (chlo, autophagic inhibitor) it could be expected a decrease in cell death. However, results showed that not influence on chlo treatment were found and confirm that the strongest decrease in

cell death was obtained after using caspase inhibitor z-VAD (from $10.97 \pm 0.62\%$ to $6.02 \pm 1.06\%$ in HCT-116) (**Figure 4 d**).

The results of cell cycle revealed that G2/M was not dependent on autophagy because this parameter did not vary in percentage in the presence of the caspases inhibitor (z-VAD) and autophagy inhibitor (chlo) (**Figure 4 e**).

2.4. Is ERS the cause or the consequence of oxidative stress in the effect of NB extract?

To test whether oxidative stress was the main trigger of the NB effect in colon cancer cells, the ROS scavenger N-acetyl cysteine (NAC, 5 mM) and the ERS inhibitor 4-phenylbutyric acid (4-PBA, 5 mM, [23]) were added to cells for 2 h before the treatment with NB extract (10 μ g/mL). As ER and oxidative stress are intricately connected [24, 25], and to clarify which one of the events, i.e. ROS or ER took place before in the effect of NB, both inhibitors were combined. Whether ROS or ERS was the direct effect of NB by inhibiting with NAC or 4-PBA, a reduction in the expression of ER-related proteins should be observed as well as a reduction in ROS, G2/M arrest, DNA damage, and early apoptosis. If the NB effect is due to the sum of both effects (ROS and ERS), a reduction of these parameters should be observed in the combination of both inhibitors (**Figure 5**).

Figure 5 shows the expression of ERS-related proteins after NB treatment of colon cancer and non-tumor cells, which have been pretreated with ROS or ERS inhibitors or its combination. In colon cancer cell line HCT-116, the ROS scavenger NAC was the only inhibitor, which was able to reduce cell death (less PARP cleavage). NAC also reduced the expression of phospho-JNK and overall the transcription factors ATF4 and CHOP, suggesting that ROS were directly related to this ERS markers. Although 4-PBA inhibitor was not able to avoid cell death (cleavage of PARP was not reduced), this compound was able to inhibit phospho-IRE1 α and phospho-JNK. Finally, the combination of both inhibitors was able to reduce phospho-IRE1 α and phospho-JNK. In normal colon cell line CCD-18Co, NB did not show a patent cleavage of PARP (cell death) and ERS-related proteins activation. These results indicate that ROS were the main inductors of ERS.

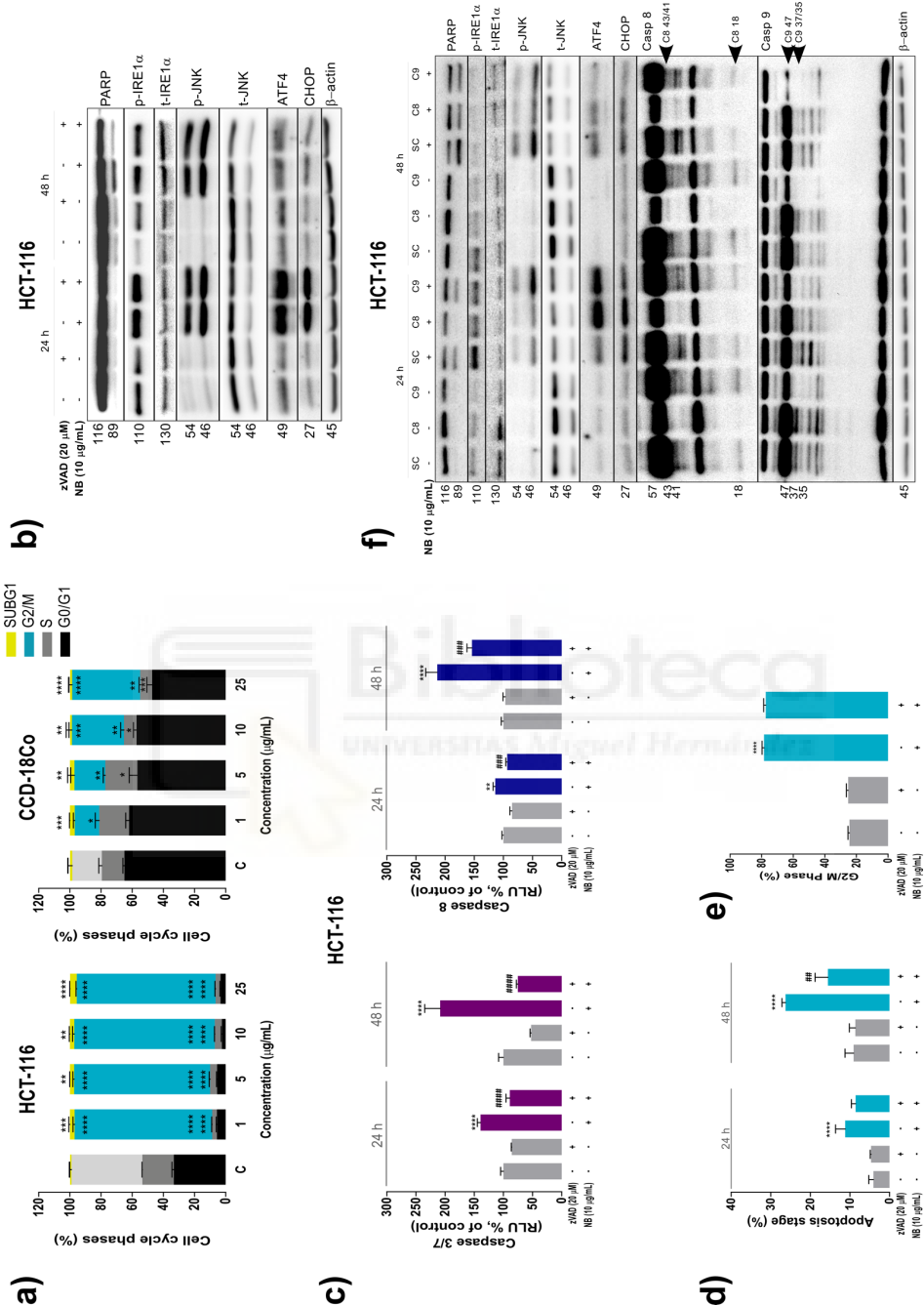


Figure 3. The relation between ERS, cell cycle modulation and caspase-dependent apoptosis cell death in colon cancer cells treated with *Dolabella auricularia* extract (NB). Effect of increasing concentrations of NB extract (1, 5, 10, 25 $\mu\text{g}/\text{mL}$) on the cell cycle of HCT-116 and CCD-18Co for 24 h (a), caspases 3/7 and 8 (c), apoptosis (d) and G2/M phase (e). Data were presented as the mean \pm SD from three independent experiments (n=3 for each experiment). *p*-values were calculated and compared to the untreated cell line (*) and NB condition (#) using ANOVAs. * or # *p*-value < 0.05, ** or ## *p*-value < 0.01, *** or ### *p*-value < 0.001 and **** or #### *p*-value < 0.0001. b) HCT-116 cells were pretreated with the pan-caspase inhibitor, zVAD (20 μM), for 2 h prior to the addition of NB extract at 10 $\mu\text{g}/\text{mL}$ for 24 h. Dependence of NB extract to modulate ERS-related proteins and its relation to apoptosis way was analyzed by Western blot. f) Caspase 8 and 9 in HCT-116 were silenced with siRNA and treated with NB extract at 10 $\mu\text{g}/\text{mL}$ for 24 h. ERS related proteins (PARP, phospho-IRE1a, total-IRE1a, phospho-JNK, total-JNK, ATF4, CHOP, caspase 8 and 9) were analyzed by Western blot. β -actin was used as a loading control.

Figure 5 b shows the contribution of the inhibition of ROS and/or ERS on the induction of apoptosis in HCT-116 and CCD-18Co colon cells treated with NB extract. Results show that both inhibitors reduced early apoptosis, however, 4-PBA avoid apoptosis more effectively than NAC. By contrast, NB was not able to induce a significant apoptotic effect in normal cell line CCD-18Co. **Figure 5 c** displays the contribution of ERS and ROS in the ability of NB to arrest G2/M cells. In this case, only 4-PBA and its combination with NAC reduced G2/M induced by NB in HCT-116. On the other hand, NB did not exert the same effect in the normal colon cell line. **Figure 5 d**, represents the DNA damage caused by NB in HCT-116 and CCD-18Co cells that partially inhibited by NAC, 4-PBA and its combination. Finally, **Figure 5 e** shows the effect of both inhibitors in ROS generation. The treatment with the ROS scavenger NAC leads to a reduction in ROS after NB treatment of 2.9-fold in HCT-116, while 4-PBA reduced ROS in 1.9-fold in HCT-116. The combination of NAC and 4-PBA obtained the highest ROS decrease of 3.3-fold in HCT-116. In the normal cell line CCD-18Co, ROS were not increased significantly at 10 $\mu\text{g}/\text{mL}$ of NB. NAC was more efficient to decrease the intracellular ROS generation than 4-PBA, however, the combination of both compounds scavenged more ROS than both inhibitors separately, indicating the existence of both stress phenomena after treatment with NB. Whether ERS was the direct cause of ROS, G2/M arrest, DNA damage, and early apoptosis, it would be expected that 4-PBA reduced these markers in a greater way than NAC. However, we found that NAC showed the higher capacity to inhibit PARP excision, ERS markers and DNA damage, meanwhile 4-PBA inhibited more apoptosis and the combination of both inhibitors showed G2/M phase arrest especially in the cancer cell line. DNA damage was reduced slightly with NAC, 4-PBA and its combination.

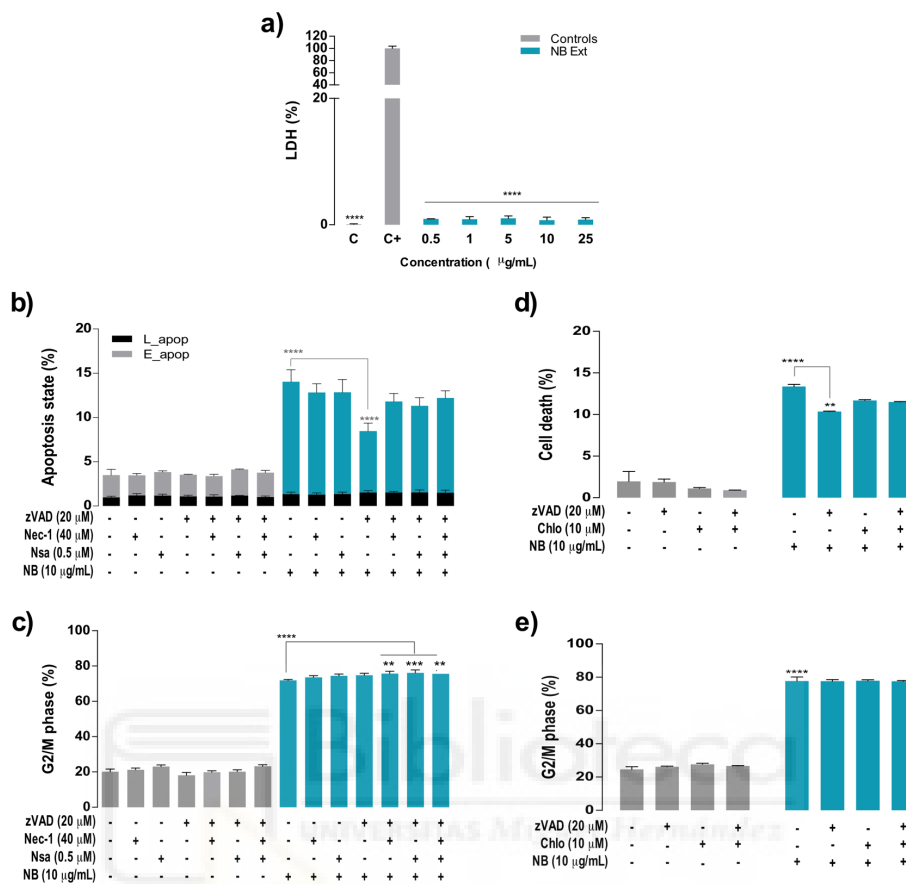


Figure 4. Effect of NB extract on non-dependent caspase cell death (necrosis, necroptosis, and autophagy) in colon cancer HCT-116 cells. HCT-116 cells were treated with NB extract at 0.5, 1, 5, 10 and 25 $\mu\text{g/mL}$ for 24 h. Lactate dehydrogenase enzyme (LDH), was determined as necrosis indicator (a). Data were compared to a positive control (lysis control, 100% of LDH, C+) and to the negative control (untreated cells plus dimethyl sulfoxide less than 0.2%, C-). (b) and (c) show the contribution of NB extract in the necroptosis cell death. HCT-116 cells were pretreated with the necroptosis inhibitors Necrostatin 1 (Nec-1) (40 μM) and Necrosulfonamide (Nsa) (0.5 μM), and the pan-caspase inhibitor, Z-VAD (20 μM), 2 h prior to the addition of NB extract at 10 $\mu\text{g/mL}$ for 24 h. Cell death (b) and G2/M phase (c) was measured using Propidium iodide (PI) through flow cytometry. (d) and (e) show the contribution of NB extract in the autophagy cell death. HCT-116 cells were pretreated with the autophagy inhibitor chloroquine (chlo) (10 μM) 2 h prior to the addition of NB extract at 10 $\mu\text{g/mL}$ for 24 h. Cell death (d) and G2/M (e) was measured using Propidium iodide (PI) through flow cytometry. Data were represented as mean \pm SD from three independent experiments (n=3 for each experiment). *p*-values were calculated and compared to the untreated cell line (*) and NB condition (#) using ANOVAs. * or # *p*-value < 0.05, ** or ## *p*-value < 0.01, *** or ### *p*-value < 0.001 and **** or #### *p*-value < 0.0001.

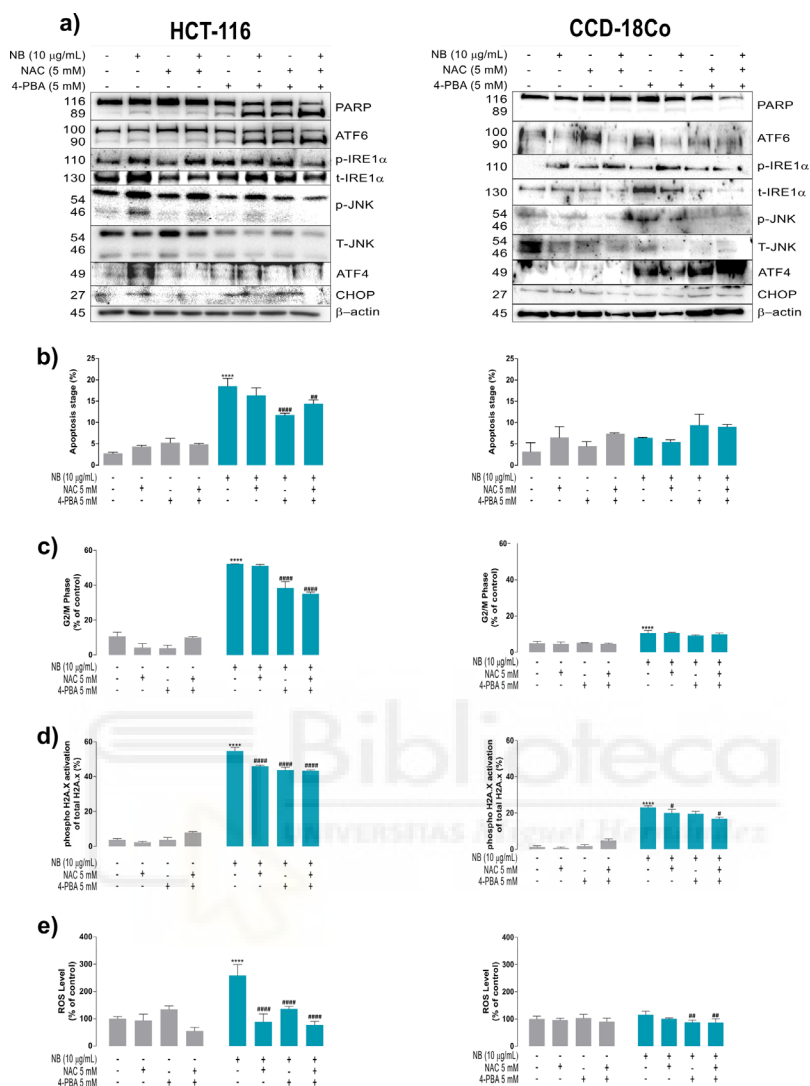


Figure 5. The relation between ROS and ERS induced by NB extract in colon cancer and colon normal cell lines. HCT-116 (left) and CCD-18Co (right) were pre-treated with ROS scavenger N-acetyl-cysteine (NAC, 5 mM) and ERS inhibitor 4-Phenylbutric acid (4-PBA, 5 mM) for 2 h prior to the NB treatment at 10 µg/mL. Ability of NB extract to modulate ERS-related proteins (PARP, phospho-IRE1α, total-IRE1α, phospho-JNK, total-JNK, ATF4 and CHOP) were analyzed by Western blot (a). β-actin was used as a loading control. The experiment was repeated twice. Apoptosis (b), G2/M phase (c), and phosphorylation of H2A γ (as DNA damage indicator) (d) were measured using the Muse® Cell Analyzer according to the manufacturer's instructions. ROS levels were measured using dichloro-dihydro-fluorescein diacetate (H₂DCF-DA) fluorescence label (e). Data were represented as mean \pm SD from three independent experiments (n=3 for each experiment). *p*-values were calculated and compared to the control (untreated cells plus dimethyl sulfoxide less than 0.2%, C) (*) and NB condition (#) using ANOVAs. * or # *p*-value < 0.05, ** or ## *p*-value < 0.01, *** or ### *p*-value < 0.001 and **** or #### *p*-value < 0.0001.

2.5. NB extract suppresses the proliferation, migration, and invasion of HCT-116-superinvasive-populations concomitantly to ERS and ROS generation.

To test the NB effect in differentiated malignant cells, we obtained highly superinvasive populations from the superinvasive HCT-116 cell line. The isolation was performed through serial selection using Boyden chambers starting with parental (P) cell lines and was repeated four times to obtain I4 superinvasive HCT-116 cells (I4) and the superinvasive I9 HCT-116 cells (I9) (Figure 6a).

First, we tested if superinvasive HCT-116 populations showed a different rate of proliferation (**Figure 6 b**), migration (**Figure 6 c**) and invasion (**Figure 6 d**) compared to parental cell line using RTCA technique. Data showed the I4 and I9 superinvasive populations presented the highest cell index of proliferation (CIP), a higher capacity of migration (CIM) and invasiveness (CII). At 48 h, I4 showed an increase of 1.3-fold in CIP, 1.6-fold in CIM and a 1.7-fold in CII respect to the P. At the same time I9 showed a 1.4-fold in CIP, an increase of 2.1-fold in CIM and 2.2-fold in CII respect to the parental cell line.

The basal level of ERS related-protein of superinvasive HCT-116 populations was checked by Western blot (**Figure 6 f**). The results showed that there were intrinsic activated ERS markers such as phospho-JNK, ATF4 and CHOP, and slightly diminished GRP78 and ATF6. Additionally, we checked the oxidative stress level (**Figure 6 e**) of superinvasive HCT-116 populations I4 and I9 and P and were compared to the normal colon cell line CCD-18Co. The normal colon cell line showed the lowest oxidative stress level and compared to this, P increased a 1.2-fold in intracellular ROS content, I4 in a 1.3-fold and I9 in a 1.9-fold.

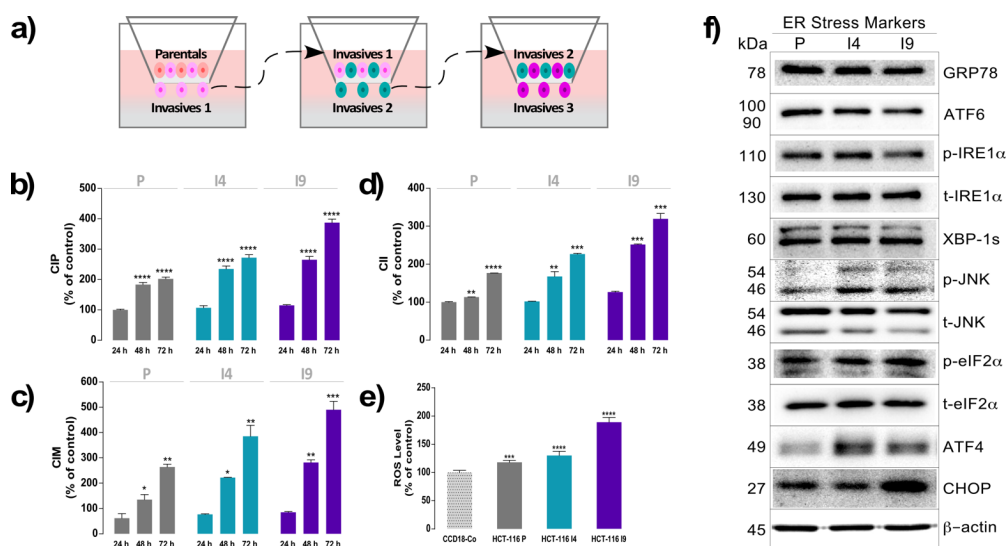


Figure 6. Isolation and characterization of superinvasive populations of HCT-116 cell lines. a) Schematic representation of the invasive isolation process of invasive 4 (I4) and invasive 9 (I9) cell lines. Real-Time Cell Analyzer (RTCA) Dual-Plate instrument (Roche Diagnostics GmbH, Germany) was used to registered basal proliferation cell index (CIP) using E-Plate (b), migration cell index (CIM) using CIM-Plate (c) and invasion cell index (CII) using CIM-Plate coated with Matrigel (d) of superinvasive populations of HCT-116. e) ROS levels were measured using dichloro-dihydro-fluorescein diacetate (H₂DCF-DA) fluorescence label. Data were represented as mean \pm SD from three independent experiments (n=3 for each experiment). *p*-values were calculated and compared to the control (untreated cells plus dimethyl sulfoxide less than 0.2%, C) using ANOVAs. **p*-value < 0.05, ** *p*-value < 0.01, *** *p*-value < 0.001 and **** *p*-value < 0.0001. f) ERS related proteins basal levels in superinvasive HCT-116 populations were studied using Western blot. β -actin was used as a loading control. The experiment was repeated twice.

NB also inhibited proliferation, migration and invasion rates of superinvasive HCT-116 populations assessed by RTCA technique (Figure 7 a). The increased proliferation rate in superinvasive populations I4 and I9 was slightly reduced when NB was added at 0.001 μ g/mL in a 14.4% in P, 16.8% in I4 and 44.8% in I9. The reduction was considerable at 0.01 μ g/mL reaching the 44.6% in P, 65.7% in I4 and 89.6% in I9, and was slightly reduced (compared to 0.01 μ g/mL) at 0.1 and 0.5 μ g/mL.

NB was also able to reduce the CIM of more differentiated HCT-116 populations I4 and I9 and P (Figure 7 b). At 0.001 μ g/mL of NB extract CIM of P was reduced a 36.4%, 39.6% of I4 and a 54.8% of I9. The effect of NB in the migration CI was more intense at 0.01 μ g/mL which produced a reduction of 61.9% in P, 67.3% in I4 and 73.1% in I9 and was stronger in a dose-dependent manner at 0.1 and 0.5 μ g/mL, reaching a 117.8% of reduction of CIM in I4 and 141.6% of I9 at 0.5 μ g/mL.

Invasive cell index (CII) was also decreased by NB extract (**Figure 7 c**). At 0.001 $\mu\text{g/mL}$, CII suffered inhibition of 45.0% in P, a 98.4% in I4 and a 104.1% in I9. At 0.01 $\mu\text{g/mL}$, the effect of NB was more potent, reaching a reduction in 49.5% in P, 105.3% in I4 and 183.3% in I9. At higher concentrations of NB, the inhibition of CII was increased. Invasive HCT-116 P, I4 and I9 cells were photographed and represented in **Figure 7 d**. At 0.5 $\mu\text{g/mL}$, the inhibition of invasive cells was nearly complete. Western blot showed interestingly that NB produced higher cell death the more invasive stage was presented. ERS markers as phospho-JNK, ATF4 and CHOP were strongly activated in superinvasive cell lines after NB extract (**Figure 7 e**).

In order to know whether the induction of ER and oxidative stresses produced by NB in the superinvasive cells, was the direct cause of its effect on the decrease of the invasion rate, the inhibitors of ERS, 4-PBA, and the ROS scavenger, NAC, as well as their combination, were used. The results are shown in **Figure 7 f and g**. On the one hand, Western blot (**Figure 7 f**) displays the effect of NB inducing PARP cleavage (inducing cell death), activating ER-related proteins such as phospho-IRE1 α , phospho-JNK and transcription factors ATF4 and CHOP. When NAC was used, the activation of ER-related proteins by NB was significantly reduced, whereas 4-PBA and its combination with NAC did not exert the same effect. On the other hand, the ability of NB to inhibit the invasiveness of superinvasive populations was also studied (**Figure 7 g**). NB at 10 $\mu\text{g/mL}$ produced a drastic reduction of CII in P, I4 and I9 cells. By reducing the ROS with NAC, the CII was recovered by 18.6% in P, 59.3% in I4 and 82.4% in I9. When ERS was inhibited by 4-PBA, the invasion rate was recovered by 48.9% in P, 95.2% in I4 and 85.0% in I9. The combination of NAC and 4-PBA reversed the inhibitory effect of NB extract in invasion by 49.3% in P, 83.6% in I4 and 122.6% in I9.

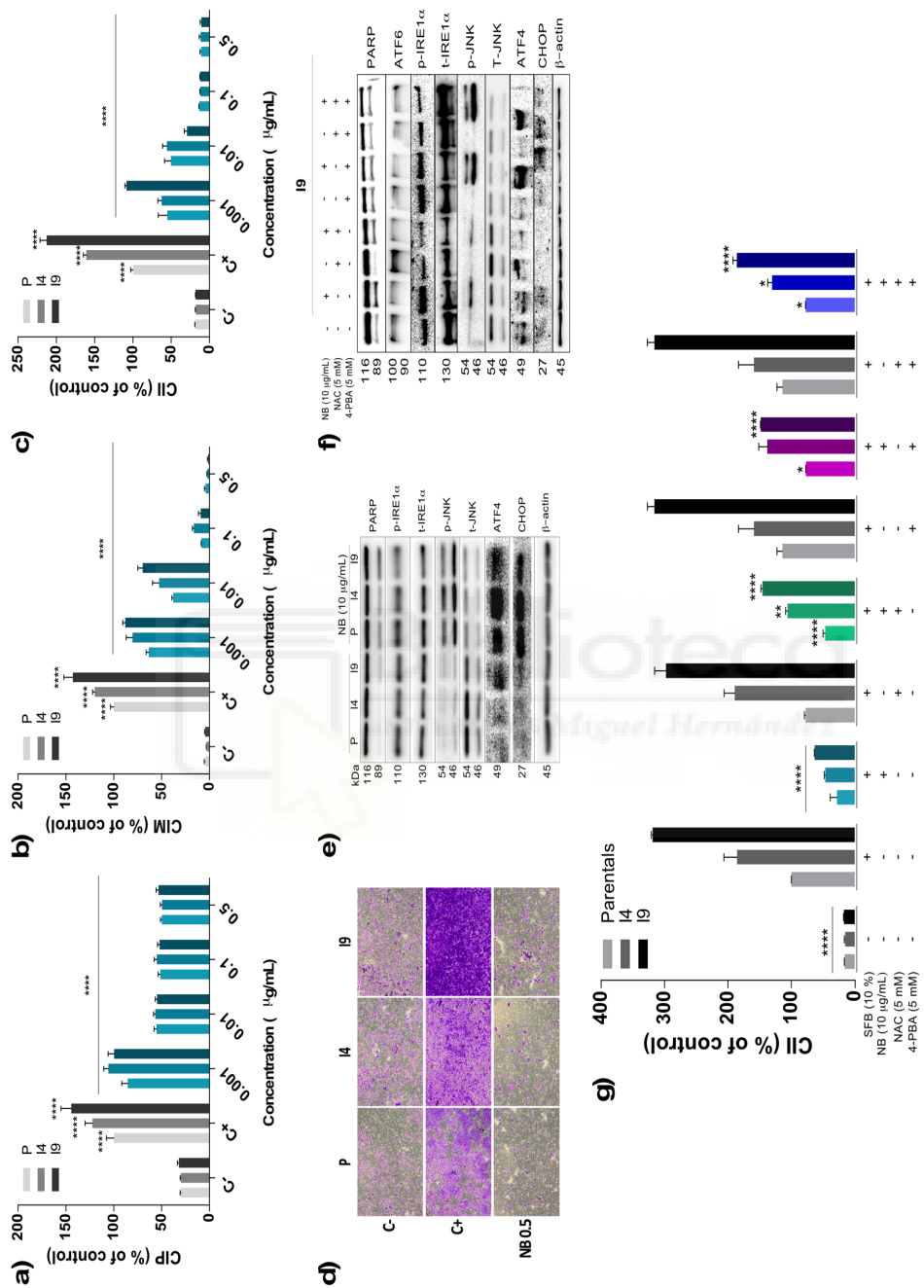


Figure 7. Effect of NB in superinvasive populations of HCT-116 cell lines. P, I4 and I9 cell lines were seeded in E-Plate for cell index of proliferation (CIP) (a), CIM-Plate for cell index of migration (CIM) (b) and CIM-Plate coated with Matrigel for cell index of invasion (CII) (c) and changes induced by NB treatment were measured. Cell index was compared to the negative control (untreated cells in media without FBS, C) and positive controls (untreated cells cultured in media with FBS 10%, C+). (d) Representative images (4X) of P, I4 and I9 invasive population stained with crystal violet in transwell insert are shown. Untreated cells were in control negative (C-, 0% SFB, 0% invasion), control positive (C+, 10% SFB, 100% invasion) and NB treated superinvasive cells (0.5 µg/mL) for 48 h. (e) Effect of NB extract in ERS-related proteins (PARP, phospho-IRE1α, total-IRE1α, phospho-JNK, total-JNK, ATF4 and CHOP) from superinvasive populations were analyzed by Western blot. β-actin was used as a loading control. The experiment was repeated twice. (f) P, I4 and I9 cell lines were pre-treated with ROS scavenger N-acetyl-cysteine (NAC, 5 mM) and ERS inhibitor 4-Phenylbutric acid (4-PBA, 5 mM) for 2 h prior to the NB treatment at 10 µg/mL. CII was measured by RTCA system and ability of NB extract to modulate ERS-related proteins (PARP, phospho-IRE1α, total-IRE1α, phospho-JNK, total-JNK, ATF4 and CHOP). (g) The relation between ROS and ERS was measured by Western blot. Data were represented as mean ± SD from three independent experiments. *p*-values were calculated and compared to the same untreated cell line (Control cells plus dimethyl sulfoxide less than 0.2%, C) using ANOVAs. **p*-value < 0.05, ** *p*-value < 0.01, *** *p*-value < 0.001 and **** *p*-value < 0.0001.

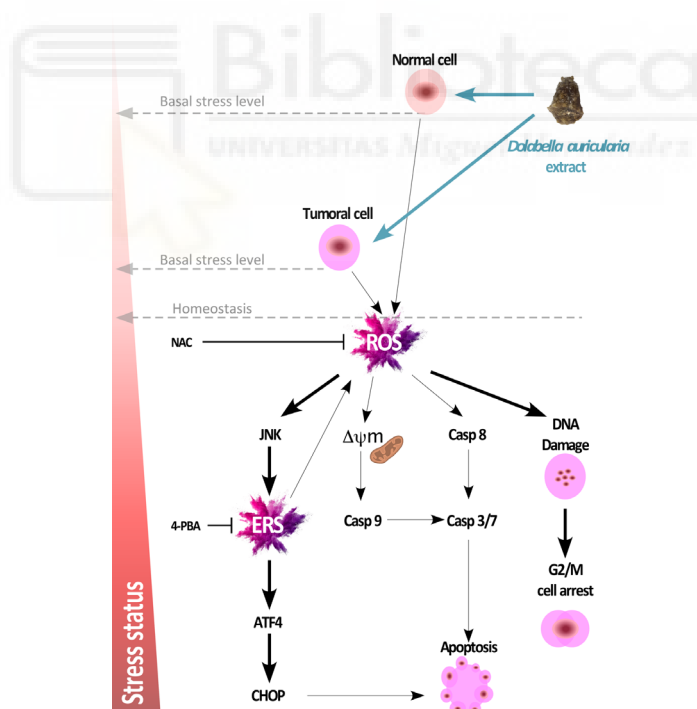


Figure 8. Schematic diagram of NB extract effect increasing oxidative and ERS in colon cancer cells and normal colon cells.

3. Discussion and conclusion

Our results demonstrated that a marine extract (NB) from the nudibranch *Dolabella auricularia* exerted selective antiproliferative effects between tumor (HCT-116 and SW-620) and normal colon cell lines. NB was able to promote lower cytotoxicity in normal colon cell line CCD-18Co under similar conditions. These results suggested the existence of a specific metabolic environment, which differentiates tumor cells from normal colon cells that make them more sensitive to the marine extract NB. Nudibranchs are known to have the ability to accumulate metabolites in its skin, to protect them from predation [26]. Pyropheophorbide a, a chlorophyll-related compound is one of the main compounds in *Dolabella auricularia* extract (result obtained from the previous work of our group). This compound was first identified in the edible red seaweed *Grateloupia elliptica* and was found to show strong anticancer activity in U87MG glioblastoma cells through the cell cycle arrest and late apoptosis and DNA degradation [27]. Some of the major compounds of the NB extract were not studied in the area of cancer, however, they are known to belong to the family of terpenes, fatty acids or steroids and many of these marine types of compounds are attracting the attention of scientists for having potential antitumor activity [1].

When cells were treated with NB, a ROS increase was observed in accordance with the early ERS markers activation after a short time of exposition and those processes play an important role in the antiproliferative effect. Different cell alterations can disturb the protein homeostasis leading to the aggregation of unfolded proteins in the ER [28]. When a cell detects the accumulation of toxic unfolded proteins within the ER lumen, it tries to adapt and to restore cell homeostasis in a survival reaction known as the unfolded protein response (UPR) [29]. Among UPR strategies are the increase of chaperones (such as GRP78) and the activation of enzymes to limit the overload of unfolded proteins (inositol-requiring enzyme 1 α (IRE1 α), protein kinase RNA (PKR)-like kinase (PERK) and activating transcription factor 6 (ATF6)), and also the reduction of the protein transit through the ER, and the increase of the ER volume to stimulate the membrane lipids leading to the endoplasmic reticulum-associated protein degradation (ERAD) [29]. After chronic ERS, the IRE1 α , PERK, and ATF6 promote the activation of transcription factors to activate cell death machinery leading apoptosis, autophagy or necrosis [30]. After 3 h of treatment of tumor cells with NB extract, molecular ERS markers related to the adaptative response such as GRP8, ATF6 or XBP1 were activated. High activation of phospho-JNK and the transcription factors ATF4 and CHOP were also observed after NB treatment. There are many studies that correlate oxidative stress with direct damage in DNA structure and protein due to an oxidation and nitration process, which induces ER stress [31, 32]. There are consistent studies about ERS induction by ROS (for example in radiotherapy or chemotherapy), which upregulates UPR genes strongly, including XBP1, GRP78, ATF4 and CHOP in lymphocytes [33, 34]. In fact, transgenic mice which presented overexpressed antioxidant enzymes (superoxide dismutase genes) showed downregulated ATF4 and CHOP levels compared to wild type [35]. On the other hand, phospho-JNK is a protein

kinase that is activated by stress and plays a main role, triggering apoptosis and autophagy. H-Y Li et. al. [36] demonstrated the direct cause-effect of ROS activating phospho-JNK and the impact in G2/M cell cycle arrest of human osteosarcoma cells by celastrol (a natural triterpenoid from a traditional Chinese medicine). These studies would support that NB extract would be inducing DNA and protein damage which would lead G2/M phase arrest and UPR and activation of ERS related proteins.

Many studies describe a direct relationship between ERS and the type of cell death such as apoptosis, autophagy and even necrosis [30, 36-38]. Our data show a direct relationship between the increase in ERS and cell apoptotic cell death and a direct connection to caspase 8. NB treatment was associated with activation of caspases and increased apoptosis, however, it was the arrest in G2/M the most remarkable effect after the treatment of colon cancer cells with NB extract. Excessive intracellular ROS were produced in colon cancer cells after NB treatment, which could disturb homeostasis by interfering with the protein folding process, damaging lipids and DNA through an oxidation or nitration process [31]. It is known that ROS induce checkpoint kinase 1 activation and G2/M arrest in colon cancer cells through the activation of ATM when DNA damage is not repaired. The G2 checkpoint would prevent cells with damaged DNA entering mitosis and would lead to repair it and proliferate or stopping the proliferation [39].

The ROS/ERS pathway was the main altered pathway by NB extract. Herein, we studied whether ROS initiated ERS cascade or was ERS, which subsequently induced ROS and triggers the following cellular events. Although we diminished ROS and ERS with NAC and 4-PBA we could not demonstrate which one was the cause or the effect of the other one. Our data show that NB strongly activated ATF4, CHOP, and phospho-JNK and this could be downregulated in a significant way with the ROS scavenger NAC or the ERS inhibitor 4-PBA. However, these inhibitors did not avoid DNA damage, as well as G2/M cell arrest. These results would lead us to think that ROS are the main cause of DNA and proteins damage and this triggers ERS, which, in turn, increases ROS in a higher extent [24, 25, 40]. Our hypothesis is that NB could be generating such amount of ROS and damage or different kind of reactive species that could not be eliminated with the inhibitors used.

Our data clearly demonstrated that NB induced intracellular ROS accumulation and ERS in colon cancer cell lines. This elevated stress levels, induced by NB, were quite different when cancer and normal cells were compared since colon cancer cells were more vulnerable to NB extract. This hypothesis was corroborated with increasing stress levels in the superinvasive HCT-116 populations. Many studies have reported higher levels of stress (oxidative and ERS) in tumor cells than in normal cells [41-43] and consider this condition as the source of tumor-initiating cells start the tumor progression [36]. Cancer cells isolated from blood and metastatic sites were reported to present higher levels of ROS than the primary subcutaneous tumors [7]. This fact is supported by other studies that demonstrated that cells with high levels of oxidative stress have developed an antioxidant capacity, which allows them to continue proliferating [44]. Our data showed higher ROS and ERS levels are HCT-116

populations as they increased their level of invasiveness. Interestingly, NB was able to inhibit the proliferation, migration and invasion cell index of the most invasive HCT-116 populations at lower concentrations compared to their parental clones. It has been shown that tumor cells have a higher level of ROS stress and a higher level of ERS than non-tumor cells. This is possible due to the physiological adaptative mechanisms developed which lead tumor cells to live in an overstressed state. However, when the stress is stimulated over the threshold, the fact that seems to be induced by NB extract, the homeostasis is disturbed, triggering the mechanisms that will arrest cell, the point from which there is no return. These results show evidence that compounds from *Dolabella auricularia* extract deserve further investigation as a natural sensitizing and anticancer agents.



4. Materials and Methods

4.1. Chemicals and Reagents

Organic solvents for preparing the extract, DMSO and labels such as Thiazolyl Blue Tetrazolium Bromide (MTT), Hoechst 33342 and 2',7'-Dichlorodihydrofluorescein diacetate (H₂DCF-DA), N-Acetyl-L-cysteine (NAC), 4-Phenylbutyric acid (4-PBA), Chloroquine (Chlo), Necrostatin-1 (Nec-1) and Necrosulfonamide (Nsa) were purchased from Sigma-Aldrich (Europe). z-VAD-fkm (zVAD) was obtained from (APExBIO).

4.2. Preparation of marine extract

The *Dolabella auricularia* nudibranch (NB) was provided by the distributor company of marine species TODO PEZ S.L. The fresh organisms were cut into small pieces and extracted with dichloromethane:methanol (D:M) (1:1, v:v) at 4 °C for 24 h. After that, the solution was filtered and evaporated to dryness on a rotatory vacuum evaporator and dried by speed vac, and stored at -80 °C until used. For *in vitro* culture evaluation of biological activity, NB was dissolved in DMSO at 50 mg/mL. The concentrations of DMSO used, did not affect cell viability.

4.3. Cell culture

Human colorectal carcinoma HCT-116 and SW-620 and fibroblasts from the normal colon (CCD-18Co) were purchased from the American Type Culture Collection (ATCC, MN, USA). Cell lines were chosen to present different markers which are the most commonly altered in colorectal cancer and have important implications for prognosis and clinical treatments. The cell line HCT-116 was produced by a primary tumor in Colon ascendens of a 48-Year-old male. This cell line show Microsatellite instability and has a mutation in codon 13 of the Kras proto-oncogene (G13D) and PIK3CA (H1047R) and is the wild type for BRAF, PTEN, and TP53. SW-620 cell line is an established cell line isolated from a Lymph node metastasis from a 51-year-old male. This line is Microsatellite stability and presents a mutation in KRAS oncogene (G12V) and TP53 (R273H and P3095) and is wild type in BRAF, PIK3CA and PTEN [45].

Colorectal carcinoma cell lines HCT-116 and SW-620 were maintained in Dulbecco's modified Eagle's medium (DMEM), Normal colon cell line CCD-18Co was cultured in Eagle's Minimum Essential Medium. Both media were supplemented with a 10% fetal bovine serum (FBS) and 100 U/mL penicillin and 100 g/mL streptomycin. Cells were maintained at 37 °C in a humidified atmosphere containing 5%/95% of CO₂/air.

4.4. Cell Viability Assay

HCT-116, SW-620, and CCD-18Co cells were seeded in 96-multiwell culture plates at a density of 5×10^3 cells/well. After 24 h incubation with NB extract, MTT was added (concentration of 0.5 mg/mL). After 3h of incubation, the formazan crystals were dissolved in DMSO. And absorbance was measured at 570 nm in a microplate reader (SPECTROstar Omega, BMG Labtech, Germany). Cell viability was directly proportional to the absorbance and presented as the mean \pm SD from three independent experiments. The cell viability was calculated as the percentage of untreated cells (control cells plus dimethyl sulfoxide less than 0.2%, C) and the IC₅₀ values were determined using GraphPad Prism v5.0 software (GraphPad Software, La Jolla, CA, USA).

4.5. Clonogenic or survival assay

The HCT-116 cell line was seeded in 6-well plates in triplicate at a density of 5×10^3 cells per well and treated the day after with NB extract at 0.5, 1.0, 5.0 and 10.0 μ g/m. After 24 h of treatment, fresh media was added and cells were kept in the tissue culture incubator for an additional 6 days for colony formation. Cell nucleus was a label with Hoechst 33342 and cells were fixed with 70% ethanol for 5 minutes. The number of colonies and its diameters was measured using the Cell Imaging Multi-Mode Reader Cytation 3 (BioTek, Germany). Cells were stained with 0.05% crystal violet for 10 minutes to take photos of plates.

4.6. Proliferation, migration and invasion assay by RTCA

The proliferation, migration and invasion rate was monitored in real-time using the xCELLigence system Real-Time Cell Analyzer (RTCA) (Roche Diagnostics GmbH, Germany). This system registered the impedance values of each well and transforms into a cell index value (CI).

For proliferation assay, HCT-116 cells were seeded at a density of 7.5×10^3 cells/well in an E-Plate. After 24 h, when the proliferation cell index (CI) was near the value of 1 as manufacturer's recommendations, cells were treated with NB extract at 0.5, 1, 5 and 10 μ g/mL and CI was automatically monitored for the duration of 72 h, which produced a kinetic curve.

For migration and invasion assay, HCT-116 were serum-starved 6 h prior to conducting the experiment. In the bottom chamber, NB extract at different concentrations in media culture with SFB at 10% were prepared and two controls were added (negative migration control, C-, with 0% SFB and positive migration control, C+, with 10% of SFB). CIM-Plate was allowed to equilibrate into the incubator for 1 h. 4×10^4 HCT-116 cells were seeded in each upper chamber in serum-free media. The

impedance value was monitored for 48 h and expressed as a cell index of migration (CIM).

For invasion assay, the procedure was the same as the migration assay, however, the CIM-Plate was coated with a 1:40 solution of Matrigel™ (BD Biosciences) according to the manufacturer's instruction. The impedance value was monitored for 48 h and expressed as a cell index of invasion (CII).

Superinvasive HCT-116 populations were isolated using Corning® BioCoat™ Matrigel® Invasion Chamber, 8.0 µm PET Membrane 6-well. This plate content 2 chambers separated by an insert of 8.0 µm, coated with Matrigel. The plate was prepared with DMEM with 10% FBS (chemoattractant) in the bottom chamber and DMEM without FBS in the upper chamber. 1.25×10^5 HCT-116 cells/ml were seeded in the upper chamber and allow to invade bottom chamber for 48 h. Invasive cells from the bottom chamber were collected and seeded in a 25 cm² flask to get confluence. The process was repeated for 4 times to obtain invasive subpopulation 4 (I4) and 9 times to isolate invasive 9 (I9).

4.7. ROS detection

Colon cell lines were seeded at 5×10^3 /well into 96-well plates and treated with different concentrations of NB extract. After treatment, 2',7'-Dichlorodihydrofluorescein diacetate (H₂DCF-DA, Sigma-Aldrich) (10 µM) for intracellular ROS measurement and DNA staining Hoechst 33342 (Sigma-Aldrich) (10 µg/mL) were incubated for 30 min. The fluorescent values were obtained using the Cell Imaging Multi-Mode Reader Cytation (BioTek Instruments, Inc., USA).

4.8. Flow cytometry assays (Cell cycle, Apoptosis, and DNA damage)

Colon cancer cells were seeded at 1.5×10^5 cells per well into 6-well plates and treated with NB extract at different concentrations for 24 h and then harvested and washed with PBS 1X. Cell cycle, apoptosis by Annexin V method and DNA damage by H2AX method was tested following the manufacturer's instruction by the Muse® Cell Analyzer (Merck KGaA, Darmstadt, Germany). For cell cycle analysis, cells were fixed with 70% ethanol for 1 h. DNA content was determined using propidium iodide (PI) a nuclear DNA stain.

Apoptosis was measured using Annexin V for detection of phosphatidylserine (PS) on the surface of apoptotic cells combined with 7-AAD as an indicator of cell death. The DNA damage was detected incubating cells with the phospho-specific anti-phospho-Histone H2A.X (Ser139)-Alexa Fluor®555 and an anti-Histone H2A.XPECy5 conjugated antibody to measure total levels of Histone H2A.X.

4.9. Caspases detection

For the caspase 8 and 3/7 activity, colon cancer cells were seeded at 2×10^5 cells in a 6 well plate and treated with NB extract for 24 h. Cells were lysed and the amount of protein was determined using Thermo Scientific Pierce Kit (BCA Protein assay kit), at 562 nm. An equal amount of protein was mixed with 100 μ L of the Caspase-Glu 3/7 and Caspase-Glu 8 assay kit (Promega, Madison, WI, USA) to each well. The mixture was incubated for 1 h at room temperature for 1 h in the dark. Luminescence was measured using the Cell Imaging Multi-Mode Reader Cytation (BioTek Instruments, Inc., USA).

4.10. Necrosis assay by Lactate Dehydrogenase (LDH) measurement

LDH is an intracellular enzyme that is released to the extracellular space when the membrane is broken in the necrotic death [16]. Colon cancer cells were seeded at 5×10^3 /well into 96-well plates. After 24 h, cells were treated with NB extract at the different concentration for 24 h, then the supernatant was collected and used according to the manufacturer's instruction (Roche Diagnostic Systems, Montclair, NJ, USA). The concentration of LDH was measured with a microplate reader (SPECTROstar Omega, BMG Labtech, Germany) at a wavelength of 490 nm.

4.11. Reverse transfection

HCT-116 cells were transfected with siRNA using Hiperfect (Qiagen) according to the manufacturer's reverse-transfection protocol. Scrambled control siRNA and C8 or C9 siRNA was prepared in RNase-free water (Qiagen) in 90 dishes to get a final concentration of 10 nM. Hiperfect and Optimem were added and incubated for 30 min at room temperature. Cells were seeded in the mastermix at 1.5×10^6 cells per dish. After 24 h, the culture medium was switched to a medium containing 10 μ g/mL of NB extract and incubated for a further 24 h.

4.12. Western blot analysis

Colon cell lines were lysed in a RIPA lysis buffer-radioimmunoprecipitation (RIPA Buffer) (BioRad Laboratories Inc.), for 60 min at -20 °C. The supernatant was collected after centrifugation at 13,200 rpm for 20 min. Protein concentration was determined spectrophotometrically using the Thermo Scientific Pierce Kit (BCA Protein assay kit), at 562 nm. Equal amounts of protein were prepared with 0.5 M Tris HCl at pH 6.8, 10% glycerol, 10% w/v SDS, 5% β 2-mercaptoethanol and 0.05% w/v bromophenol blue. 30 μ g/lane of protein and prestained ladder (Thermo Fisher Scientific, Waltham, MA, USA) were separated by SDS-PAGE and transferred to nitrocellulose membranes (Bio-Rad). Membranes were blocked with 5% non-fat milk in

Tris-buffered saline containing 0.05% Tween 20 (TBST) at 4 °C. Blots were incubated with primary antibodies (PARP Rabbit mAb Antibody #9532, ATF4 mAb Rabbit (D4B8) #1815, ATF-6 (D4Z8V) mAb Rabbit #65880, total-IRE1 α (14C10) mAb Rabbit #3294, phospho-JNK (Thr183/Tyr185) mAb Mouse antibody #9255, SAPK/JNK Antibody (total-JNK) pAb Rabbit #9252, CHOP (L63F7) mAb Mouse antibody #2895, BiP (C50B12) mAb Rabbit #3177, XBP-1s (D2C1F) mAb Rabbit #12782, phospho-eIF2 α (Ser51) (D9G8) mAb Rabbit #3398, total-eIF2 α (D7D3) mAb Rabbit #5324, Caspase-3 Antibody #9662, Caspase-9 #9502 from Cell Signaling Technology Inc. Beverly, MA, USA.

Caspase-8 (human) monoclonal antibody (12F5) was obtained from Enzo Life Sciences, Inc. and phospho-IRE1 α (S724) #ab124945 (Abcam) and anti- β -actin antibody was obtained from Sigma-Aldrich, St. Louis, MO, USA. After incubation with secondary antibodies for 1 to 3 h, bands of interest were obtained with ChemiDoc™ XRS+ System (Bio-Rad) with Image Lab™ software.

4.13. Determination of secondary metabolites by HPLC-ESI-TOF-MS

The dichloromethane:methanol extract from *Dolabella auricularia* was subjected to chemical analysis using Agilent 1200 series Rapid Resolution Liquid Chromatography (Agilent Technologies, CA, USA), which was comprised of a binary pump, degasser, and autosampler to identify the bioactive compounds in a previous job (Ruiz-Torres V. et al. 2019, Marine invertebrate extracts induce colon cancer cell death via ROS-mediated DNA oxidative damage and mitochondrial impairment).

4.14. Statistical analysis

Data shown are the mean \pm standard deviation (SD) of three independent assays. Statistical analysis was tested by one-way analysis of variance (ANOVA), followed by Tukey's post hoc test for multiple comparisons using GraphPad Prism 7.02. Significant differences between experimental groups were assumed at p -values < 0.05 (* p -value < 0.05 , ** p -value < 0.01 , *** p -value < 0.001 or **** p -value < 0.0001).

Acknowledgments

Authors want to thank Cristiaan Echegoyen from Todopez S.L. (<http://www.todopez.es>) for his help providing marine specimens and his comments about marine invertebrates.

Competing Interests: The authors declare no conflict of interest.

Funding

This research was funded by projects AGL2015-67995-C3-1-R, AGL2015-67995-C3-2-R and AGL2015-67995-C3-3-R from the Spanish Ministry of Economy and Competitiveness (MINECO); Project P11-CTS-7625 from Andalusian Regional Government Council of Innovation and Science; projects PROMETEO/2012/007, PROMETEO/2016/006 and VALi+D fellowship (ACIF/2015/158) from Generalitat Valenciana and CIBER (CB12/03/30038, Fisiopatología de la Obesidad y la Nutrición, CIBERobn). The author BMG gratefully acknowledges to the National Youth Guarantee System the grant for young research personnel.

References

1. Ruiz-Torres, V., et al., *An Updated Review on Marine Anticancer Compounds: The Use of Virtual Screening for the Discovery of Small-Molecule Cancer Drugs*. *Molecules*, 2017. **22**(7).
2. De Stefano, D., et al., *Cacospongionolide and scalaradial, two marine sesterterpenoids as potent apoptosis-inducing factors in human carcinoma cell lines*. *PLoS One*, 2012. **7**(4): p. e33031.
3. 2018, G., *Colorectal Cancer*. 2018.
4. Kim, J., J. Kim, and J.S. Bae, *ROS homeostasis and metabolism: a critical liaison for cancer therapy*. *Exp Mol Med*, 2016. **48**(11): p. e269.
5. Davison, C.A., et al., *Antioxidant Enzymes Mediate Survival of Breast Cancer Cells Deprived of Extracellular Matrix*. *Cancer Research*, 2013. **73**(12): p. 3704.
6. Kumari, S., et al., *Reactive Oxygen Species: A Key Constituent in Cancer Survival*. *Biomarker insights*, 2018. **13**: p. 1177271918755391-1177271918755391.
7. Piskounova, E., et al., *Oxidative stress inhibits distant metastasis by human melanoma cells*. *Nature*, 2015. **527**(7577): p. 186-91.
8. Riha, R., et al., *Stressed Out - Therapeutic Implications of ER Stress Related Cancer Research*. *Oncomedicine*, 2017. **2**: p. 156-167.
9. Gorlach, A., P. Klappa, and T. Kietzmann, *The endoplasmic reticulum: folding, calcium homeostasis, signaling, and redox control*. *Antioxid Redox Signal*, 2006. **8**(9-10): p. 1391-418.
10. Luengo, A., D.Y. Gui, and M.G. Vander Heiden, *Targeting Metabolism for Cancer Therapy*. *Cell Chem Biol*, 2017. **24**(9): p. 1161-1180.
11. de Toledo, M., et al., *Cooperative Anti-Invasive Effect of Cdc42/Rac1 Activation and ROCK Inhibition in SW620 Colorectal Cancer Cells with Elevated Blebbing Activity*. *PLOS ONE*, 2012. **7**(11): p. e48344.
12. Ahmed, D., et al., *Epigenetic and genetic features of 24 colon cancer cell lines*. *Oncogenesis*, 2013. **2**(9): p. e71-e71.
13. Pérez-Sánchez, A., et al., *Rosemary (Rosmarinus officinalis) extract causes ROS-induced necrotic cell death and inhibits tumor growth in vivo*. *Scientific Reports*, 2018. **Accepted, waiting for final publication. DOI 10.1038/s41598-018-37173-7**.
14. Limame, R., et al., *Comparative analysis of dynamic cell viability, migration and invasion assessments by novel real-time technology and classic endpoint assays*. *PLoS One*, 2012. **7**(10): p. e46536.

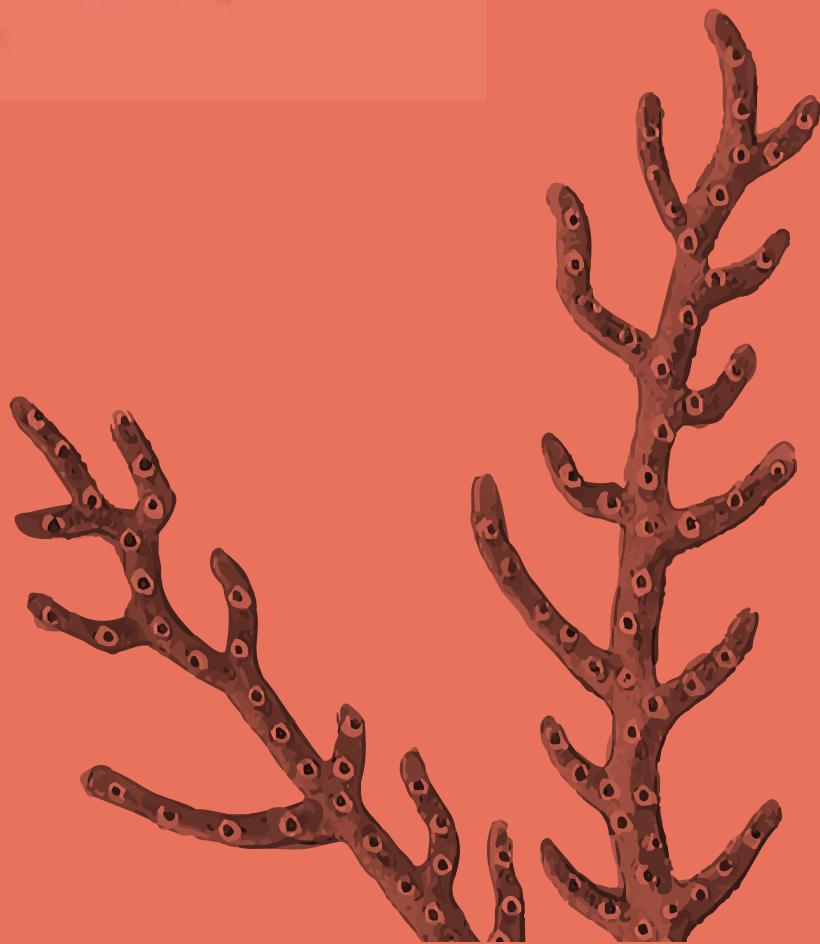
15. Walter, P. and D. Ron, *The unfolded protein response: from stress pathway to homeostatic regulation*. Science, 2011. **334**(6059): p. 1081-6.
16. Chan, F.K.-M., K. Moriwaki, and M.J. De Rosa, *Detection of necrosis by release of lactate dehydrogenase activity*. Methods in molecular biology (Clifton, N.J.), 2013. **979**: p. 65-70.
17. Sawai, H., *Characterization of TNF-induced caspase-independent necroptosis*. Leuk Res, 2014. **38**(6): p. 706-13.
18. Zargarian, S., et al., *Phosphatidylserine externalization, "necroptotic bodies" release, and phagocytosis during necroptosis*. PLoS Biol, 2017. **15**(6): p. e2002711.
19. Vandenabeele, P., et al., *Necrostatin-1 blocks both RIPK1 and IDO: consequences for the study of cell death in experimental disease models*. Cell death and differentiation, 2013. **20**(2): p. 185-187.
20. Sun, L., et al., *Mixed lineage kinase domain-like protein mediates necrosis signaling downstream of RIP3 kinase*. Cell, 2012. **148**(1-2): p. 213-27.
21. Ruiz-Torres, V., et al., *New Mammalian Target of Rapamycin (mTOR) Modulators Derived from Natural Product Databases and Marine Extracts by Using Molecular Docking Techniques*. Mar Drugs, 2018. **16**(10).
22. Populo, H., J.M. Lopes, and P. Soares, *The mTOR signalling pathway in human cancer*. Int J Mol Sci, 2012. **13**(2): p. 1886-918.
23. Sarvani, C., D. Sireesh, and K.M. Ramkumar, *Unraveling the role of ER stress inhibitors in the context of metabolic diseases*. Pharmacol Res, 2017. **119**: p. 412-421.
24. Banerjee, A., et al., *Increased reactive oxygen species levels cause ER stress and cytotoxicity in andrographolide treated colon cancer cells*. Oncotarget, 2017. **8**(16): p. 26142-26153.
25. Ozgur, R., et al., *Endoplasmic reticulum stress triggers ROS signalling, changes the redox state, and regulates the antioxidant defence of Arabidopsis thaliana*. J Exp Bot, 2014. **65**(5): p. 1377-90.
26. Cimino, G., et al., *The chemical defense of nudibranch molluscs: Structure, biosynthetic origin and defensive properties of terpenoids from the dorid nudibranch dendrodoris grandiflora*. Tetrahedron, 1985. **41**(6): p. 1093-1100.
27. Cho, M., et al., *Glioblastoma-specific anticancer activity of pheophorbide a from the edible red seaweed Grateloupia elliptica*. J Microbiol Biotechnol, 2014. **24**(3): p. 346-53.
28. Scriven, P., et al., *The unfolded protein response and cancer: a brighter future unfolding?* J Mol Med (Berl), 2007. **85**(4): p. 331-41.
29. Gardner, B.M. and P. Walter, *Unfolded proteins are Ire1-activating ligands that directly induce the unfolded protein response*. Science, 2011. **333**(6051): p. 1891-4.
30. Sano, R. and J.C. Reed, *ER stress-induced cell death mechanisms*. Biochim Biophys Acta, 2013. **1833**(12): p. 3460-3470.
31. Karpinska, A. and G. Gromadzka, *[Oxidative stress and natural antioxidant mechanisms: the role in neurodegeneration. From molecular mechanisms to therapeutic strategies]*. Postepy Hig Med Dosw (Online), 2013. **67**: p. 43-53.
32. Hasnain, S.Z., J.B. Prins, and M.A. McGuckin, *Oxidative and endoplasmic reticulum stress in beta-cell dysfunction in diabetes*. J Mol Endocrinol, 2016. **56**(2): p. R33-54.
33. Saglar, E., et al., *Assessment of ER Stress and autophagy induced by ionizing radiation in both radiotherapy patients and ex vivo irradiated samples*. J Biochem Mol Toxicol, 2014. **28**(9): p. 413-7.
34. Cai, Y., et al., *Betulinic acid chemosensitizes breast cancer by triggering ER stress-mediated apoptosis by directly targeting GRP78*. Cell Death Dis, 2018. **9**(6): p. 636.

35. Hayashi, T., et al., *Damage to the endoplasmic reticulum and activation of apoptotic machinery by oxidative stress in ischemic neurons*. J Cereb Blood Flow Metab, 2005. **25**(1): p. 41-53.
36. Li, H.Y., et al., *Celastrol induces apoptosis and autophagy via the ROS/JNK signaling pathway in human osteosarcoma cells: an in vitro and in vivo study*. Cell Death Dis, 2015. **6**: p. e1604.
37. Kim, I., W. Xu, and J.C. Reed, *Cell death and endoplasmic reticulum stress: disease relevance and therapeutic opportunities*. Nat Rev Drug Discov, 2008. **7**(12): p. 1013-30.
38. Sovolyova, N., et al., *Stressed to death - mechanisms of ER stress-induced cell death*. Biol Chem, 2014. **395**(1): p. 1-13.
39. He, L., et al., *Asperlin induces G(2)/M arrest through ROS generation and ATM pathway in human cervical carcinoma cells*. Biochem Biophys Res Commun, 2011. **409**(3): p. 489-93.
40. Zhong, F., et al., *Polypeptide from Chlamys farreri suppresses ultraviolet-B irradiation-induced apoptosis through restoring ER redox homeostasis, scavenging ROS generation, and suppressing the PERK-eIF2 α -CHOP pathway in HaCaT cells*. J Photochem Photobiol B, 2015. **151**: p. 10-6.
41. Pelicano, H., D. Carney, and P. Huang, *ROS stress in cancer cells and therapeutic implications*. Drug Resist Updat, 2004. **7**(2): p. 97-110.
42. Wang, Q., et al., *Overexpression of endoplasmic reticulum molecular chaperone GRP94 and GRP78 in human lung cancer tissues and its significance*. Cancer Detect Prev, 2005. **29**(6): p. 544-51.
43. Dejeans, N., et al., *Overexpression of GRP94 in breast cancer cells resistant to oxidative stress promotes high levels of cancer cell proliferation and migration: implications for tumor recurrence*. Free Radic Biol Med, 2012. **52**(6): p. 993-1002.
44. Gorrini, C., I.S. Harris, and T.W. Mak, *Modulation of oxidative stress as an anticancer strategy*. Nat Rev Drug Discov, 2013. **12**(12): p. 931-47.
45. Ahmed, D., et al., *Epigenetic and genetic features of 24 colon cancer cell lines*. Oncogenesis, 2013. **2**: p. e71.



© 2019 by the authors; licensee MDPI, Basel, Switzerland. This article is an open access article distributed under the terms and conditions of the Creative Commons Attribution (CC-BY) license (<http://creativecommons.org/licenses/by>)

Anexes



Doctoral Student:
Verónica Ruiz Torres

ANEXE I

Other Publications





Article

Antioxidant and Photoprotective Activity of Apigenin and Its Potassium Salt Derivative in Human Keratinocytes and Absorption in Caco-2 Cell Monolayers

Noelia Sánchez-Marzo ^{1,†}, Almudena Pérez-Sánchez ^{1,†}, Verónica Ruiz-Torres ¹, Adrián Martínez-Tébar ², Julián Castillo ³, María Herranz-López ¹ and Enrique Barrajon-Catalán ^{1,*}

¹ Instituto de Biología Molecular y Celular (IBMC) and Instituto de Investigación, Desarrollo e Innovación en Biotecnología Sanitaria de Elche (IDiBE), Universitat Miguel Hernández, 03202 Elche, Spain; n.sanchez@umh.es (N.S.-M.); almudena.perez@umh.es (A.P.-S.); vruiz@umh.es (V.R.-T.); mherranz@umh.es (M.H.-L)

² Programs of Molecular Mechanisms and Experimental Therapeutics in Oncology (ONCOBell), Catalan Institute of Oncology, Bellvitge Institute for Biomedical Research, Granvia de l'Hopitalet 199, 08908, L'Hospitalet de Llobregat, 08907 Barcelona, Spain; amartinez@idibell.cat

³ Nutrafur S.A., Camino Viejo de Pliego, km.2, 30820 Alcantarilla, Murcia, Spain; j.castillo@nutrafur.com

* Correspondence: e.barrajon@umh.es

† These authors contributed equally to this work.

Received: 4 April 2019; Accepted: 30 April 2019; Published: 30 April 2019



Abstract: Ultraviolet (UV) radiation, especially types A (UVA) and B (UVB), is one of the main causes of skin disorders, including photoaging and skin cancer. Ultraviolet radiation causes oxidative stress, inflammation, p53 induction, DNA damage, mutagenesis, and oxidation of various molecules such as lipids and proteins. In recent decades, the use of polyphenols as molecules with an antioxidant and anti-inflammatory capacity has increased. However, some of these compounds are poorly soluble, and information regarding their absorption and bioavailability is scarce. The main objective of this study was to compare the intestinal absorption and biological activity of apigenin and its more soluble potassium salt (apigenin-K) in terms of antioxidant and photoprotective capacity. Photoprotective effects against UVA and UVB radiation were studied in human keratinocytes, and antioxidant capacity was determined by different methods, including trolox equivalent antioxidant capacity (TEAC), ferric reducing antioxidant power (FRAP) and oxygen radical absorbance capacity (ORAC) assays. Finally, the intestinal absorption of both apigenins was determined using an in vitro Caco-2 cell model. Apigenin showed a slightly higher antioxidant capacity in antioxidant activity assays when compared with apigenin-K. However, no significant differences were obtained for their photoprotective capacities against UVA or UVB. Results indicated that both apigenins protected cell viability in approximately 50% at 5 J/m² of UVA and 90% at 500 J/m² of UVB radiation. Regarding intestinal absorption, both apigenins showed similar apparent permeabilities (P_{app}), 1.81 × 10⁻⁵ cm/s and 1.78 × 10⁻⁵ cm/s, respectively. Taken together, these results suggest that both apigenins may be interesting candidates for the development of oral (nutraceutical) and topical photoprotective ingredients against UVA and UVB-induced skin damage, but the increased water solubility of apigenin-K makes it the best candidate for further development.

Keywords: flavonoid; apigenin; photoprotection; UV radiation; antioxidant; keratinocytes; absorption

1. Introduction

The skin is the largest organ of the body acting as a physical and chemical barrier to protect the body against harmful external agents such as ultraviolet (UV) radiation, dehydration, temperature changes, and pathogens [1–3]. Furthermore, the skin is a sensitive organ because the nerve endings and receptors related to the sense of touch and temperature are located within the skin. UV radiation exposure is a main factor for age-related changes, including immunosuppression and allergy disorders, degenerative aging, inflammation, extracellular matrix (ECM) degeneration, DNA damage, oxidative stress, and carcinogenesis [4,5]. These effects are included in the term photoaging, which resumes the biological consequences of UV exposure, not only on skin, but also in the whole organism.

UV radiation is divided into (a) long-wave UVA (320–400 nm), (b) medium-wave UVB (280–320 nm), and (c) short-wave UVC (100–280 nm) radiation, of which UVC is absorbed by the ozone layer [4]. UVA comprises more than 90% of all solar UV radiation that reaches the Earth's surface and is considered the "aging ray" that penetrates the epidermis and dermis [6]. UVA enhances the expression of metalloproteinases (MMPs) that lead to collagen decrease and abnormal elastic fiber overgrowth, resulting in stratum corneum thickening and epidermal hyperplasia [7,8]. Moreover, UVB is a minor component of sunlight that is capable of producing direct changes on biomolecules, causing the acute effects of sunlight exposure, such as erythema (sunburn) or pigmentation (tanning). It is well established that UVB photons target DNA causing dimeric photoproducts between adjacent pyrimidine bases to form [9]. The incorrect repair of these photolesions can affect tumor suppressor genes and oncogenes, and therefore, UVB is the main radiation associated with melanoma and nonmelanoma skin cancer risk. Nonetheless, it has been suggested that UVA has mutagenic and carcinogenic actions through the generation of reactive oxygen species (ROS), which also damage DNA [10]. In addition, excessive ROS formation, not only after UVA but also following UVB overexposure, can oxidize several DNA repair proteins, compromising their efficiency [11].

In recent years, there have been a large number of studies and publications related to natural extracts and compounds that exert beneficial effects for human health [4], especially polyphenols [12]. These compounds are widely distributed in fruits, vegetables, and legumes, as well as in red wine and tea [13,14]. Polyphenols are divided into the phenolic acids, stilbenes, flavonoids, and lignans [15] (Supplementary Figure S1A). Their structural diversity is the reason why polyphenols present different biological functions, such as antitumor [15,16], anti-inflammatory [17], antimicrobial [18], antioxidant [19], and photoprotective activities [20–22]. Furthermore, prospective studies have reported that polyphenols have the ability to prevent cardiovascular diseases [23,24].

The flavonoid group represents 60% of the total natural polyphenols and can be classified into different subgroups (Supplementary Figure S1A). In recent years, flavonoids have generated great interest because they are the major group of polyphenols present in the human diet [25,26]. Pure flavonoids are quite insoluble in water, making this characteristic their main drawback when both studying their biological activity and using them on a new nutraceutical, cosmeceutical and/or pharmaceutical formulation. There are different strategies to solve this water insolubility problem. Plants usually glycosylate flavonoids to enhance their solubility or to store them in vacuoles [27,28]. Another strategy, which is especially relevant for industrial purposes, is to derivivate these compounds by obtaining salt species with an improved water solubility profile [29]. Solubility is a relevant property in drug development, but drug absorption must not be forgotten. In fact, the actual Biopharmaceutics Classification System (BCS) is based on both solubility and absorption data, allowing researchers and pharmaceutical companies to predict *in vivo* bioavailability based on *in vitro* data [30].

One of the most known and studied flavonoids is 4',5,7-trihydroxyflavone, commonly known as apigenin (Supplementary Figure S1B). This bioactive compound is found in many fruits and vegetables, such as chamomile flowers, thyme, onions, and spices [13]. Several studies have shown that this natural compound has potential anti-cancer activity [31], antioxidant and anti-inflammatory effects [32], and antimicrobial activity [33] (Supplementary Figure S1B). However, it exhibits poor solubility in water, hampering the *in vitro* dissolution rate, efficacy and oral bioavailability [34]. This situation also hinders *in vitro* studies, as most assays are developed in an aqueous environment using cell culture

assays that require the compounds to be soluble enough to be used. To avoid this situation, different apigenin salt derivatives were obtained, leading to increased solubility [30,34]. However, there have been no comparative works studying whether this salt derivatization influences biological activity except for one covering angiotensin-converting enzyme inhibitory activity from a structural point of view and comparing this activity with that of a collection of other non-salt-derived flavonoids [35].

In the present study, apigenin flavone and its more water-soluble potassium salt derivative (apigenin-K) were compared to determine their antioxidant capacity, their inhibition of UVA and UVB harmful effects on human keratinocytes, and their protection against DNA damage. In addition, the apparent permeability of both apigenins was studied in an *in vitro* model of intestinal absorption using the Caco-2 cell line.

2. Results

2.1. Antioxidant Activity

A set of antioxidant assays was carried out to determine the antioxidant potential of apigenin and apigenin-K (Table 1). The single-electron transfer-based methods Trolox equivalent antioxidant capacity (TEAC) and ferric reducing antioxidant power (FRAP) were performed. These methods are widely used in a large variety of food and biological samples [36,37]. For the TEAC assay, no significant differences were obtained. For the FRAP assay, apigenin and apigenin-K exhibited slight but significant differences (Table 1) between them. In addition, the oxygen radical absorbance capacity (ORAC) assay, based on a hydrogen atom transfer mechanism, was used to measure the capacity to eliminate peroxy radicals. Values for apigenin and apigenin-K revealed a high oxygen radical absorbance capacity for both compounds with small, but significant differences (Table 1).

Table 1. Values for different antioxidant measurements performed with apigenin and apigenin-K.

Antioxidant Assay (units)	Apigenin	Apigenin-K
TEAC ($\mu\text{mol TE}^{\text{a}}/\text{mmol}$)	2022.2 \pm 154.8	1903.6 \pm 210.5
FRAP ($\mu\text{mol Fe}^{2+}/\text{mmol}$)	113.2 \pm 12.2	88.7 \pm 14.4 ***
ORAC ($\mu\text{mol TE}^{\text{a}}/\text{mmol}$)	887.9 \pm 5.8	840.2 \pm 28.3 *

^a Trolox equivalents. Values are expressed as the means \pm SDs. * $p < 0.05$ and *** $p < 0.001$ indicate statistically significant differences between the antioxidant capacities measured for both apigenins.

The absorption spectra were compared for both apigenins, showing no differences between them and both presenting the typical flavone absorption maxima at 270 and 340 nm [38]. These absorption maxima partially match the UVA and UVB ranges.

2.2. Apigenin and Apigenin-K Protect Human Keratinocytes against UVA and UVB Radiation

Apigenin and apigenin-K were tested to determine their capacity to protect human keratinocytes from UVA- and UVB-induced damage at different radiation doses (5 or 10 J/cm² and 500 or 1000 J/m², respectively). Photoprotection percentage was calculated according to Equation (1), showed in Materials and Methods section. After cell irradiation with 5 J/cm² UVA, both apigenins showed over 50% protection when compared with control cells irradiated with the same UVA dose in the absence of compound (Figure 1A). While there were no differences between equimolar concentrations of each apigenin or between different concentrations of the same apigenin, apigenin (maroon bars) showed statistically significant differences when compared with the control (white bar). When the UVA dose was increased up to 10 J/cm², cell viability was reduced accordingly. Once again, no differences were observed between equimolar concentrations of each apigenin or between different concentrations of the same apigenin; however, significant differences were obtained for the highest concentration of each compound when compared with control cells (Figure 1A). Similar results were obtained after UVB irradiation with 500 and 1000 J/m², as both compounds exerted statistically significant photoprotection versus control cells, also with a dose-response behavior (Figure 1B).

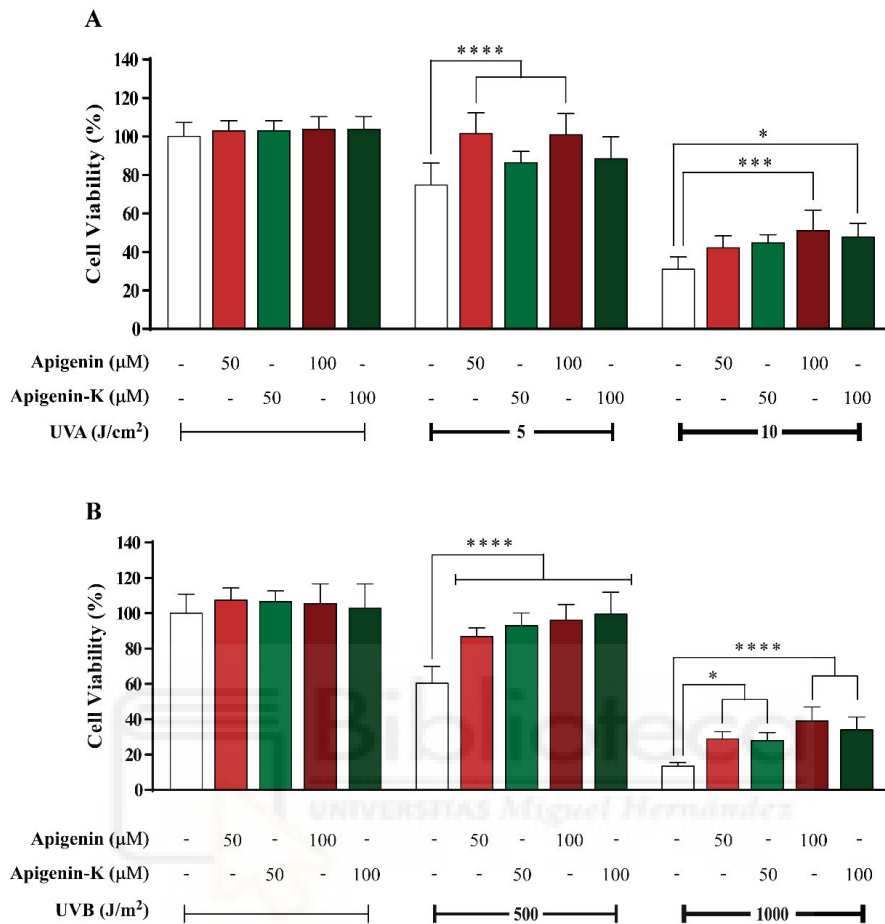


Figure 1. Human keratinocyte survival after irradiation with a 5 J/cm² or 10 J/cm² dose of UVA (A) or 500 J/m² or 1000 J/m² dose of UVB (B), in the presence of apigenin or apigenin-K (50 or 100 μM), was determined using the MTT assay after the incubation of cells for 72 h post-irradiation. The data are expressed as the means of 6 replicates ± SDs. * $p < 0.05$, *** $p < 0.001$ and **** $p < 0.0001$ indicate statistically significant differences compared with the irradiated sample in the absence of compound.

2.3. Determination of Apparent Permeability (P_{app}) Values

Caco-2 cells are a well-established in vitro model for the investigation of intestinal permeability of different compounds or drugs [34–36]. The optimum concentration of apigenin and apigenin-K was determined using the MTT assay before permeability studies to prevent monolayer damage. Figure 2 shows statistically significant cytotoxicity only at a concentration of 100 μM for both apigenins. However, a viability decrease was observed when Caco-2 cells were treated with 75 μM of each apigenin. Therefore, a final concentration of 50 μM was used in the transport experiments.

The transport across the Caco-2 cell monolayer model was monitored for a period of 120 min, as described in the Materials section, and the TEER values did not drastically change during the assay, maintaining above the level of 300–400 Ω/cm² for all monolayers. Concentration values from each timepoint were determined by HPLC and were used to obtain the bidirectional P_{app} values according to Equation (2), shown in the Materials and Methods section. Results are shown in Table 2 and Figure 3A,B. The estimated apparent permeability of both apigenins was similar in the apical (AP) to basolateral (BL) direction. Lower, but also similar, values were obtained when BL-AP transport was assayed. Moreover, the ratios of P_{app} (BL-AP) to P_{app} (AP-BL) were calculated to estimate the absorption mechanism using Equation (3) as described in Materials and Methods section (Table 2

and Figure 3C). This value tentatively indicates an active transport when is lower than 0.5, a passive diffusion transport when it is between 0.5 and 2 and an active secretion mechanism when it is higher than 2.

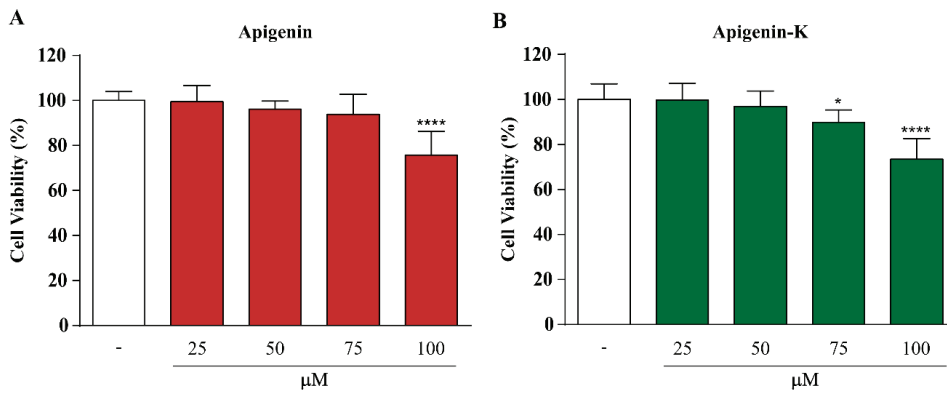


Figure 2. Cytotoxic effects of apigenin (A) and apigenin-K (B) treatment (25, 50, 75 or 100 μM) for 2 h in Caco-2 cells determined using the MTT assay. The data are expressed as the means of 6 replicates ± SDs. * $p < 0.05$ and **** $p < 0.0001$ indicate statistically significant differences compared with nontreated cells.

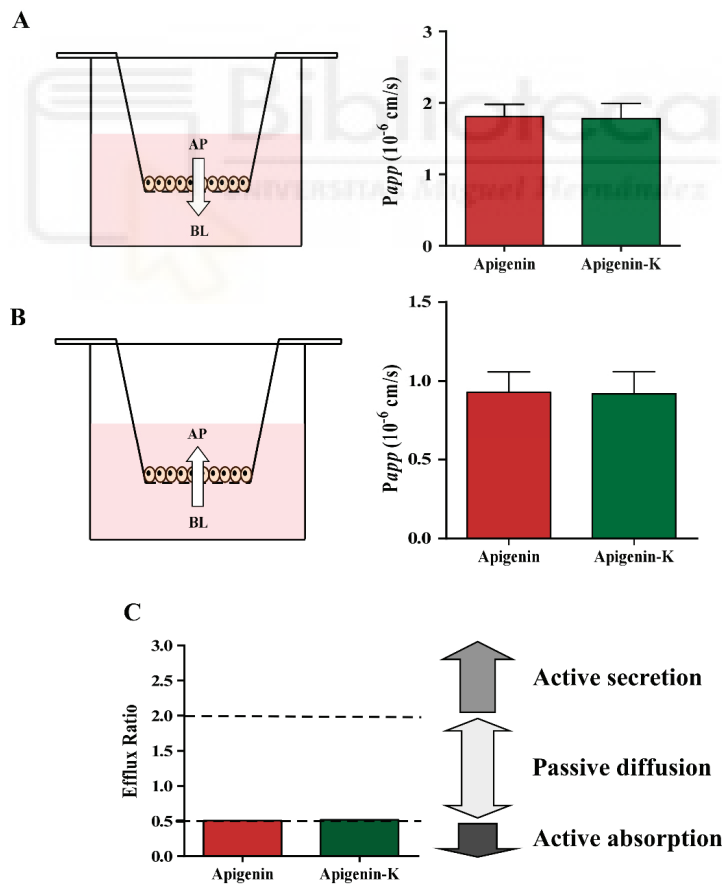


Figure 3. P_{app} values and diagram of permeation flow for both apigenins in AP-BL (A) and BL-AP (B) directions respectively. (C) Efflux ratio plot for both apigenins, showing the different transport mechanism categories.

Table 2. Apparent permeability (P_{app}) values for apigenin and apigenin-K from apical-to-basolateral (AP-BL) and basolateral-to-apical (BL-AP) compartments.

Compound	$P_{app,AP-BL}$ ($\times 10^{-5}$ cm/s)	$P_{app,BL-AP}$ ($\times 10^{-5}$ cm/s)	Efflux Ratio
Apigenin	1.81 \pm 0.17	0.93 \pm 0.13	0.51
Apigenin-K	1.78 \pm 0.21	0.92 \pm 0.14	0.52

The data are expressed as the means of 6 replicates \pm SDs.

3. Discussion

UV radiation has an array of harmful effects, and chronic exposure to sunlight is the main cause of photoaging and skin carcinogenesis. Novel approaches for skin protection have gained scientific interest in diminishing UV exposure consequences, cancer morbidity, and the costs associated with treatment. Several phytochemicals have shown substantial photoprotective and anticarcinogenic effects and have attracted considerable attention due to their low toxicity [39]. One of these promising phytochemicals is apigenin, of which high amounts are present in common fruits and plant species such as chamomile (*Chamaemelum nobile*), celery (*Apium graveolens*), onion (*Allium cepa*), thyme (*Thymus vulgaris*), and oregano (*Origanum vulgare*) [13,40].

In this work, the antioxidant and photoprotective abilities of apigenin flavone and its more soluble potassium salt, apigenin-K, were evaluated in a skin cell model. The role of oxidative stress in the consequences of UV radiation [10] has been demonstrated. For that reason, the antioxidant capacity of both apigenins was examined first. Apigenin showed a slightly stronger capacity to scavenge free radicals than apigenin-K in the TEAC, FRAP, and ORAC assays, but those results were significant only for the FRAP and ORAC assays. As apigenin-K has one less hydroxyl (–OH) group, these results are consistent with the antioxidant mechanism of polyphenols, which is based on the number of hydroxyl (–OH) groups [41]. Furthermore, the antioxidant activity of flavonoids depends upon the arrangement of the functional groups about the nuclear structure. Flavonoids vary in their chemical substitution around the heterocyclic oxygen ring, but a C₆–C₃–C₆ carbon skeleton is characteristic of all of them, comprising three rings (A, B and C), as Supplementary Figure S1B illustrates. It is generally accepted that the presence of catechol hydroxyl groups in the B ring provides the strongest antioxidant capacity exhibited by these compounds. In addition, greater antioxidant activity for flavonoids with meta-5,7-dihydroxy arrangements in the A ring has been described, as is present in apigenin [41]. Salt formation of apigenin-K may entail the loss of a hydrogen at the 7- or 4'-hydroxyl position, so the apigenin-K reduction potential should be lower [34]. Despite this, apigenin-K antioxidant activity is higher than that described for other well-known flavonoids, such as kaempferol, hesperidin, and naringenin [41,42].

The small differences between the antioxidant capacity of both apigenins exerted in the aforementioned assays were reflected in the survival increase achieved by keratinocytes exposed to UVA and UVB radiation, where the higher photoprotection of apigenin was exhibited. However, no statistically significant differences were obtained when the same concentrations of apigenin and apigenin-K were compared, suggesting that both compounds share a similar photoprotective capacity. Regarding the putative protective mechanism, some hypotheses can be deduced from the obtained data and the current state of the art. Some polyphenols have shown the ability to rapidly reach intracellular targets, so it can be postulated that apigenin and apigenin-K may be able to act as antioxidants, scavenging the ROS that originate upon UVB and UVA radiation, such as hydroxyl radicals (\cdot OH), superoxide anion radicals ($O_2^{\cdot-}$) and lipoperoxyl radicals (ROO^{\cdot}) [10]. In addition, both apigenins present an absorption spectrum that matches the UVA and UVB ranges, so both effects, antioxidant capacity and UV-absorption, contribute to reducing the harmful effects of radiation on cell viability.

Intestinal absorption of apigenin and its potassium salt derivative was estimated using the human Caco-2 cell culture model for nutraceutical purposes, and no statistically significant differences were found between the apparent permeability estimated for each compound regardless of the tested

direction (AP-BL or BL-AP). Apigenin is usually found in its glycosidic form in fruits and vegetables, but it has been elucidated that glycosides are efficiently hydrolyzed to the free flavonoids in the human intestinal tract by bacterial enzymes [43]. These enzymatic changes justify the use of aglicone forms of apigenin and apigenin-K, with improved water solubility, in an attempt to enhance absorption, and can be industrially obtained without significant costs and drawbacks.

The Caco-2 cell model is widely used due to its differentiation into polarized enterocyte-like cells with an apical and basolateral surface and the presence of active transport systems. Generally, high-absorbed drugs are found to have P_{app} values higher than 1×10^{-5} cm/s, whereas moderately absorbed drugs had P_{app} values above $(1-10) \times 10^{-6}$, and a P_{app} value lower than 1×10^{-6} is related to poorly-absorbed drugs [44]. According to these data, both apigenins present a high absorption profile, with P_{app} values above 1×10^{-5} cm/s. The values estimated in the present manuscript were similar to those reported in other studies [45–47] and higher than the values calculated for other flavonoids such as quercetin and its metabolites [48]. Fang et al. recently studied the relationship between the structure of thirty flavonoids and their apparent permeabilities in the Caco-2 cell model [47]. They discovered that substitution on the 3' carbon decreases flavonoid absorption, while substitution on the adjacent 2' or 4' carbon (as occurs in apigenin) increases absorption. Furthermore, flavones show greater permeability than their respective flavonols; for example, the apparent permeability of apigenin is 2.5-fold higher than the estimated permeability for its respective flavonol kaempferol. The calculated efflux ratios are close to 0.5, suggesting the putative participation of active transporters. However, additional assays such as utilization of the P-glycoprotein (MDR1) inhibitor verapamil in permeability studies are required [44,49] to confirm this hypothesis, as both ratios are just in the frontier between active transport and passive diffusion mechanisms. A recent work has demonstrated that apigenin and quercetin downregulate the gene expression levels of BRCP, MRP2 and MDR1 [50], the most pharmacologically relevant ABC transporters to flavonoids, which are localized on the apical side of the intestinal epithelium [51]. The function of these transporters is to efflux compounds out of the cells and into the lumen, causing the reduction of basolateral-to-apical absorption with their downregulation, which is consistent with our results. Nevertheless, the concentration-dependent behavior of apigenin in rat duodenum and jejunum, which indicated active carrier-mediated saturable mechanism in those intestinal segments [52].

Finally, according the initial objective of the study, which was the comparison between the biological activity and absorption of both compounds, it can be concluded that although some small differences in terms of antioxidant capacity have been obtained between apigenin and apigenin-K, both the photoprotective and absorption results presented no significant differences. Moreover, according to Fick's Law of diffusion (see Equation (4) in the Material and Methods section), the increased solubility of apigenin-K makes it more interesting for future studies, as higher concentrations can be obtained in the absorption phase, increasing the absorption flow and subsequent plasma concentration and biological effects. This last aspect allows the selection of apigenin-K as the best candidate for further pharmaceutical, nutraceutical, or cosmeceutical developments.

4. Materials and Methods

4.1. Chemicals and Reagents

Human keratinocyte cells (HaCaT, a spontaneously immortalized cell line) were obtained from Cell Lines Service GmbH (Eppelheim, Germany). Dulbecco's Modified Eagle's Medium (DMEM), fetal bovine serum (FBS), penicillin–streptomycin, Hank's Balanced Salt Solution (HBSS), MEM Non-Essential Amino Acids (NEAA) Solution (100×) and 1 M HEPES were obtained from Gibco (Thermo Fisher Scientific, Waltham, MA, USA). For high-performance liquid chromatography (HPLC), all chemicals were of analytical reagent grade and were used as received. For mobile phase preparation, trifluoroacetic acid (TFA) and acetonitrile were purchased from Merck (Millipore, Darmstadt, Germany) and VWR (Barcelona, Spain), respectively. Dimethyl sulfoxide (DMSO) and the remaining reagents

were purchased from Sigma-Aldrich (Steinheim, Germany). Apigenin and its monopotassium salt derivative (apigenin-K), which were 96.80% and 90.53% pure, respectively, were kindly provided by NUTRAFUR, SA—Frutarom Group (Alcantarilla, Murcia, Spain).

4.2. Cell Culture

HaCaT cells were cultured in high-glucose DMEM containing 10% heat-inactivated FBS, 0.1 mg/mL penicillin and 100 U/mL streptomycin. Caco-2 cells were grown in high-glucose DMEM and supplemented with 10% heat-inactivated FBS, 1% NEAA, 1% HEPES, 0.1 mg/mL penicillin, and 100 U/mL streptomycin. Both cell lines were trypsinized on the third day following purchaser instructions and were maintained in a humidified 5% CO₂ atmosphere at 37 °C.

4.3. Determination of Antioxidant Capacity

Three different methods were performed to determine the antioxidant capacity of both apigenins. The Trolox equivalent antioxidant capacity (TEAC) was performed, as previously reported to establish the ABTS⁺ scavenging ability of both compounds [21]. The TEAC of the samples was calculated from the standard curve of Trolox, and the results are expressed in micromoles of Trolox equivalents (TE) per millimole of compound. The ferric reducing antioxidant power (FRAP) assay was performed, as described elsewhere [37]. The reduction of a ferric-tripyridyltriazine complex was estimated, and the results are expressed in micromoles of Fe²⁺ per millimole of compound. To assay the capacity of the compounds to scavenge peroxy radicals, a validated assay of the oxygen radical absorbance capacity (ORAC) method was used [53]. The ORAC assay was carried out on a microplate reader (POLAstar Omega, BMG LabTech GmbH, Offenburg, Germany) with 495 nm excitation and 520 nm emission filters to monitor fluorescein oxidation. The results are expressed in micromoles of TE per millimole of compound.

4.4. Apigenin and Its Potassium Salt Derivative Absorption Spectra

Absorption spectra collection was performed using a microplate reader (SPECTROstar Omega, BMG LabTech GmbH, Germany). Apigenin solutions were prepared by dissolving the compounds in DMSO at a concentration of 1 µM. The results are represented by GraphPad Prism version 6.00 software using data in the range from 260 to 400 nm at 2 nm intervals [21].

4.5. Photoprotection Assay

Cells were cultured in 96-well plates and maintained in complete DMEM for 24 h. At 80–90% confluence, cells were treated with phosphate-buffered saline (PBS) containing apigenin or apigenin-K at a concentration of 50 or 100 µM, followed by treatment with UVA or UVB light emitted from a Bio-Link Crosslinker BLX-E312 (Vilber Lourmat, France) at 5 or 10 J/cm², or 500 or 1000 J/m², respectively [20]. Afterwards, the PBS was replaced with fresh medium, and the cells were incubated for 72 h. Cell viability was measured using the MTT assay. The medium was removed, and the cells were incubated with MTT for 3–5 h at 37 °C with 5% CO₂. Then, the medium was discarded, and 100 µL of DMSO per well was added to dissolve the formazan crystals. After 15 min of shaking, the absorbance was measured using a microplate reader (SPECTROstar Omega, BGM LabTech GmbH, Offenburg, Germany) at 570 nm. The photoprotection percentage was obtained using the following formula:

$$\text{Photoprotection (\%)} = 100 \times 100 - \frac{(PC - \text{sample})}{(PC - NC)} \quad (1)$$

where *PC* is the % survival in the nonirradiated control and the nontreated and nonirradiated sample and *NC* is the % survival in the irradiated control and the nontreated but irradiated sample.

4.6. Permeability Studies

The cytotoxic effects of apigenin and apigenin-K were tested using the MTT assay. Caco-2 cells were seeded in 96-well plates until cell monolayers were obtained. Then, the cells were treated with different concentrations of apigenin and apigenin-K (25, 50, 75, or 100 μM) for 2 h.

The cells were seeded into 6-well inserts with a polyethylene terephthalate (PET) membrane (pore size of 0.4 μm) (BD Falcon) at a density of 1.0×10^5 cells. Cell culture was maintained at 37 °C under 90% humidity and 5% CO_2 . The medium was replaced every 2–3 days for both the apical (AP) and basolateral (BL) chambers of the transwell filters. Cell monolayers were used 19–21 days after seeding, once confluence and differentiation were achieved. To check the integrity of each cell monolayer, the transepithelial electrical resistance (TEER) was measured before and after the experiments with an epithelial voltohmmeter (Millicell-ERS®). Permeability studies were performed by adding apigenin and apigenin-K at a concentration of 50 μM dissolved in HBSS medium (pH 7.4). The transport experiment was initiated by removing the culture medium from the AP and BL chambers. HBSS medium was prewarmed to wash the Caco-2 monolayers twice and, subsequently, to incubate the monolayers for 30 min at 37 °C. Afterwards, the test compounds were added to the apical (AP) or basolateral (BL) chambers to perform bidirectional permeability studies, while the receiving chamber contained the corresponding volume of HBSS. The six-well plate containing the cell monolayers was put into an orbital environmental shaker, which was set at a constant temperature (37 °C) and agitation rate (54 rpm) for the duration of the permeability experiments. To follow transport across the cell monolayer, several samples of 200 μL each were collected at different time points (0, 30, 60, 90, and 120 min) from the AP or BL chambers during the permeability assay. The total volume in the chamber was maintained throughout the experiment, replacing the sample volume taken with an equal volume of HBSS. Moreover, two samples of 200 μL were taken from the donor chamber at the beginning and the end of the assay, for the mass balance calculation and validation of each replicate. The samples were centrifuged for 15 min at 15,000 rpm and 4 °C. The supernatants (cytoplasmic fraction) and the pellets (cell membranes) were stored at -80 °C until analysis was performed.

Transport studies were performed from apical-to-basolateral (AP-BL) and basolateral-to-apical (BL-AP) chambers. The apparent permeability (P_{app}) values for each compound and direction can be calculated according to the following equation:

$$P_{app} = \frac{dQ}{dt} \times \frac{1}{A \times C_0 \times 60} \quad (2)$$

where P_{app} is the apparent permeability (cm/s), dQ/dt is the steady state flux, A is the diffusion area of the membrane (cm^2), C_0 is the initial compound concentration in the donor compartment (μM) and 60 is a conversion factor [54]. The dilution suffered in the receiving chamber after each sample was taken into consideration.

In addition, the efflux ratio (ER) was calculated to determine the absorption mechanism, such as the ratio of P_{app} (BL-AP) to P_{app} (AP-BL).

$$ER = \frac{P_{app} \text{ (BL-AP)}}{P_{app} \text{ (AP-BL)}} \quad (3)$$

Finally, as mentioned in the Discussion section, the diffusive flow of a substance in a medium, such as the epithelial barrier, depends on the concentration gradient of substance and the diffusion coefficient of the substance in the medium, as is expressed by Fick's First Law:

$$J = D \times \frac{dC(x)}{dx} \quad (4)$$

where J is the flow in the direction from the donor side of the barrier, D is the diffusion coefficient, x is the distance from the donor compartment, and $C(x)$ is the concentration.

4.7. Analytical Methodology

The analyses of the samples from the permeability assay were analyzed via a high-performance liquid chromatograph Agilent LC 1100 series (Agilent Technologies, Inc., Palo Alto, CA, USA) controlled by the ChemStation software and equipped with a pump, autosampler, column oven and UV-Vis diode array detector. The samples were separated on a Poroshell 120 SB-C18 column (2.7 μm , 4.6 \times 150 mm) after each 10 μL injection and were monitored at 280 nm. The mobile phases consisted of 0.1% TFA in water as mobile phase A and acetonitrile as mobile phase B, using the following multistep linear gradient: 0 min, 25% B; 5 min, 40% B; 10 min, 50% B; 15 min, 25% B; and 20 min, 25% B. The flow rate used was 0.5 mL/min and the column temperature was set at 22 $^{\circ}\text{C}$. Quantitative evaluations of the apigenin or apigenin-K concentration were performed using the corresponding calibration graph of each compound with a six-point regression curve ($r^2 > 0.999$).

4.8. Statistical Analysis

Cellular data re expressed as the means \pm SDs of six-to-ten replicates depending on the assay. One-way ANOVA and statistical comparisons of the different treatments were found using Tukey's test for the photoprotection assay. In the rest of the assays, statistically significant differences were determined by applying the Student's *t*-test. All analyses were performed in GraphPad Prism version 6.00 (GraphPad Software, San Diego, CA, USA).

Supplementary Materials: Supplementary materials can be found at <http://www.mdpi.com/1422-0067/20/9/2148/s1>. Figure S1. Polyphenol (soft green) and flavonoid (dark green) classification (A) and apigenin basic structure and main biological effects (B).

Author Contributions: Conceptualization, A.P.-S., J.C. and E.B.-C.; Funding acquisition, M.H.-L. and E.B.-C.; Investigation, N.S.-M., A.P.-S., V.R.-T. and A.M.-T.; Methodology, N.S.-M., A.P.-S. and V.R.-T.; Project administration, E.B.-C.; Supervision, M.H.-L. and E.B.-C.; Writing—original draft, N.S.-M. and A.P.-S.; Writing—review & editing, J.C., M.H.-L. and E.B.-C.

Funding: Some of the investigations described in this review have been partially or fully supported by competitive public grants from the following institutions: AGL2011-29857-C03-03 and IDI-20120751 grants (Spanish Ministry of Science and Innovation), projects AGL2015-67995-C3-1-R, AGL2015-67995-C3-2-R and AGL2015-67995-C3-3-R from the Spanish Ministry of Economy and Competitiveness (MINECO); and PROMETEO/2016/006, ACOMP/2013/093, ACIF/2015/158, APOTIP/2017/003 and APOSTD/2018/097 grants from Generalitat Valenciana and CIBER (CB12/03/30038, Fisiopatología de la Obesidad y la Nutrición, CIBERobn, Instituto de Salud Carlos III).

Acknowledgments: We thank NUTRAFUR, SL for providing us with the raw materials.

Conflicts of Interest: The authors declare no conflict of interest.

References

1. Pullar, J.M.; Carr, A.C.; Vissers, M.C.M. The roles of vitamin c in skin health. *Nutrients* **2017**, *9*, 866. [[CrossRef](#)] [[PubMed](#)]
2. Madison, K.C. Barrier function of the skin: "La raison d'être" of the epidermis. *J. Investig. Dermatol.* **2003**, *121*, 231–241. [[CrossRef](#)] [[PubMed](#)]
3. Shindo, Y.; Witt, E.; Han, D.; Epstein, W.; Packer, L. Enzymic and non-enzymic antioxidants in epidermis and dermis of human skin. *J. Investig. Dermatol.* **1994**, *102*, 122–124. [[CrossRef](#)]
4. Pérez-Sánchez, A.; Barrajón-Catalán, E.; Herranz-López, M.; Micol, V. Nutraceuticals for skin care: A comprehensive review of human clinical studies. *Nutrients* **2018**, *10*, 403. [[CrossRef](#)]
5. D'Orazio, J.; Jarrett, S.; Amaro-Ortiz, A.; Scott, T. Uv radiation and the skin. *Int. J. Mol. Sci.* **2013**, *14*, 12222–12248. [[CrossRef](#)]
6. Nichols, J.A.; Katiyar, S.K. Skin photoprotection by natural polyphenols: Anti-inflammatory, antioxidant and DNA repair mechanisms. *Arch. Dermatol. Res.* **2010**, *302*, 71–83. [[CrossRef](#)]
7. Lavker, R.M.; Gerberick, G.F.; Veres, D.; Irwin, C.J.; Kaidbey, K.H. Cumulative effects from repeated exposures to suberythemal doses of uvb and uva in human skin. *J. Am. Acad. Dermatol.* **1995**, *32*, 53–62. [[CrossRef](#)]

8. Wlaschek, M.; Heinen, G.; Poswig, A.; Schwarz, A.; Krieg, T.; Scharffetter-Kochanek, K. Uva-induced autocrine stimulation of fibroblast-derived collagenase/mmp-1 by interrelated loops of interleukin-1 and interleukin-6. *Photochem. Photobiol.* **1994**, *59*, 550–556. [[CrossRef](#)] [[PubMed](#)]
9. Ichihashi, M.; Ueda, M.; Budiayanto, A.; Bito, T.; Oka, M.; Fukunaga, M.; Tsuru, K.; Horikawa, T. UV-induced skin damage. *Toxicology* **2003**, *189*, 21–39. [[CrossRef](#)]
10. Sander, C.S.; Chang, H.; Hamm, F.; Elsner, P.; Thiele, J.J. Role of oxidative stress and the antioxidant network in cutaneous carcinogenesis. *Int. J. Dermatol.* **2004**, *43*, 326–335. [[CrossRef](#)]
11. Brem, R.; Guven, M.; Karran, P. Oxidatively-generated damage to DNA and proteins mediated by photosensitized UVA. *Free Radic. Biol. Med.* **2017**, *107*, 101–109. [[CrossRef](#)] [[PubMed](#)]
12. Sung, B.; Chung, H.Y.; Kim, N.D. Role of apigenin in cancer prevention via the induction of apoptosis and autophagy. *J. Cancer Prev.* **2016**, *21*, 216–226. [[CrossRef](#)] [[PubMed](#)]
13. Zhou, Y.; Zheng, J.; Li, Y.; Xu, D.P.; Li, S.; Chen, Y.M.; Li, H.B. Natural polyphenols for prevention and treatment of cancer. *Nutrients* **2016**, *8*, 515. [[CrossRef](#)] [[PubMed](#)]
14. Chen, X.J.; Wu, M.Y.; Li, D.H.; You, J. Apigenin inhibits glioma cell growth through promoting microRNA-16 and suppression of BCL-2 and nuclear Factor- κ B/MMP9. *Mol. Med. Rep.* **2016**, *14*, 2352–2358. [[CrossRef](#)] [[PubMed](#)]
15. Losada-Echeberria, M.; Herranz-Lopez, M.; Micol, V.; Barrajon-Catalan, E. Polyphenols as promising drugs against main breast cancer signatures. *Antioxidants* **2017**, *6*, 88. [[CrossRef](#)] [[PubMed](#)]
16. Perez-Sanchez, A.; Barrajon-Catalan, E.; Ruiz-Torres, V.; Agullo-Chazarra, L.; Herranz-Lopez, M.; Valdes, A.; Cifuentes, A.; Micol, V. Rosemary (*Rosmarinus officinalis*) extract causes ROS-induced necrotic cell death and inhibits tumor growth in vivo. *Sci. Rep.* **2019**, *9*, 808. [[CrossRef](#)]
17. Thimoteo, N.S.B.; Iryioda, T.M.V.; Alfieri, D.F.; Rego, B.E.F.; Scavuzzi, B.M.; Fatel, E.; Lozovoy, M.A.B.; Simao, A.N.C.; Dichi, I. Cranberry juice decreases disease activity in women with rheumatoid arthritis. *Nutrition* **2018**, *60*, 112–117. [[CrossRef](#)] [[PubMed](#)]
18. Alvarez-Martinez, F.J.; Barrajon-Catalan, E.; Encinar, J.A.; Rodriguez-Diaz, J.C.; Micol, V. Antimicrobial capacity of plant polyphenols against gram-positive bacteria: A comprehensive review. *Curr. Med. Chem.* **2019**. [[CrossRef](#)] [[PubMed](#)]
19. Sun, Y.; Tao, W.; Huang, H.; Ye, X.; Sun, P. Flavonoids, phenolic acids, carotenoids and antioxidant activity of fresh eating citrus fruits, using the coupled in vitro digestion and human intestinal HEPG2 cells model. *Food Chem.* **2019**, *279*, 321–327. [[CrossRef](#)]
20. Perez-Sanchez, A.; Barrajon-Catalan, E.; Caturla, N.; Castillo, J.; Benavente-Garcia, O.; Alcaraz, M.; Micol, V. Protective effects of citrus and rosemary extracts on uv-induced damage in skin cell model and human volunteers. *J. Photochem. Photobiol. B* **2014**, *136*, 12–18. [[CrossRef](#)]
21. Perez-Sanchez, A.; Barrajon-Catalan, E.; Herranz-Lopez, M.; Castillo, J.; Micol, V. Lemon balm extract (*Melissa officinalis*, L.) promotes melanogenesis and prevents uvb-induced oxidative stress and DNA damage in a skin cell model. *J. Dermatol. Sci.* **2016**, *84*, 169–177. [[CrossRef](#)]
22. Nobile, V.; Michelotti, A.; Cestone, E.; Caturla, N.; Castillo, J.; Benavente-Garcia, O.; Perez-Sanchez, A.; Micol, V. Skin photoprotective and antiageing effects of a combination of rosemary (*Rosmarinus officinalis*) and grapefruit (*Citrus paradisi*) polyphenols. *Food Nutr. Res.* **2016**, *60*, 31871. [[CrossRef](#)]
23. Mink, P.J.; Scrafford, C.G.; Barraja, L.M.; Harnack, L.; Hong, C.P.; Nettleton, J.A.; Jacobs, D.R., Jr. Flavonoid intake and cardiovascular disease mortality: A prospective study in postmenopausal women. *Am. J. Clin. Nutr.* **2007**, *85*, 895–909. [[CrossRef](#)] [[PubMed](#)]
24. Knekt, P.; Kumpulainen, J.; Jarvinen, R.; Rissanen, H.; Heliovaara, M.; Reunanen, A.; Hakulinen, T.; Aromaa, A. Flavonoid intake and risk of chronic diseases. *Am. J. Clin. Nutr.* **2002**, *76*, 560–568. [[CrossRef](#)]
25. Lefort, E.C.; Blay, J. Apigenin and its impact on gastrointestinal cancers. *Mol. Nutr. Food Res.* **2013**, *57*, 126–144. [[CrossRef](#)]
26. Formica, J.V.; Regelson, W. Review of the biology of quercetin and related bioflavonoids. *Food Chem. Toxicol.* **1995**, *33*, 1061–1080. [[CrossRef](#)]
27. Tang, D.; Chen, K.; Huang, L.; Li, J. Pharmacokinetic properties and drug interactions of apigenin, a natural flavone. *Expert Opin. Drug Metab. Toxicol.* **2017**, *13*, 323–330. [[CrossRef](#)] [[PubMed](#)]
28. Bak, M.J.; Das Gupta, S.; Wahler, J.; Suh, N. Role of dietary bioactive natural products in estrogen receptor-positive breast cancer. *Semin. Cancer Biol.* **2016**, *40–41*, 170–191. [[CrossRef](#)]

29. Salinas, J.L.; Sánchez, J.C.; Garcia, O.B.-G.; Ortega, V.V.; Gascón, J.Y.; Muñoz, F.S.; Baños, M.A.; Borrón, J.C.G.; Teruel, J.A.L. Use of Compounds Derived from 2,3-Dehydronaringenin for the Treatment of Inflammatory Processes and Pharmaceutical Composition Containing Said Derivatives. U.S. Patent Application No. 11/186,121, 20 April 2004.
30. Amidon, G.L.; Lennernas, H.; Shah, V.P.; Crison, J.R. A theoretical basis for a biopharmaceutic drug classification: The correlation of in vitro drug product dissolution and in vivo bioavailability. *Pharm. Res.* **1995**, *12*, 413–420. [[CrossRef](#)] [[PubMed](#)]
31. Madunic, J.; Madunic, I.V.; Gajski, G.; Popic, J.; Garaj-Vrhovac, V. Apigenin: A dietary flavonoid with diverse anticancer properties. *Cancer Lett.* **2018**, *413*, 11–22. [[CrossRef](#)] [[PubMed](#)]
32. Shukla, S.; Gupta, S. Apigenin: A promising molecule for cancer prevention. *Pharm. Res.* **2010**, *27*, 962–978. [[CrossRef](#)]
33. Cushnie, T.P.; Lamb, A.J. Antimicrobial activity of flavonoids. *Int. J. Antimicrob. Agents* **2005**, *26*, 343–356. [[CrossRef](#)]
34. Mascaraque, C.; Gonzalez, R.; Suarez, M.D.; Zarzuelo, A.; Sanchez de Medina, F.; Martinez-Augustin, O. Intestinal anti-inflammatory activity of apigenin k in two rat colitis models induced by trinitrobenzenesulfonic acid and dextran sulphate sodium. *Br. J. Nutr.* **2015**, *113*, 618–626. [[CrossRef](#)]
35. Guerrero, L.; Castillo, J.; Quiñones, M.; Garcia-Vallvé, S.; Arola, L.; Pujadas, G.; Muguerza, B. Inhibition of angiotensin-converting enzyme activity by flavonoids: Structure-activity relationship studies. *PLoS ONE* **2012**, *7*, e49493. [[CrossRef](#)]
36. Huang, D.; Ou, B.; Prior, R.L. The chemistry behind antioxidant capacity assays. *J. Agric. Food Chem.* **2005**, *53*, 1841–1856. [[CrossRef](#)]
37. Benzie, I.F.; Strain, J.J. The ferric reducing ability of plasma (Frap) as a measure of “antioxidant power”: The frap assay. *Anal. Biochem.* **1996**, *239*, 70–76. [[CrossRef](#)]
38. Matthäus, B. Isolation, fractionation and hplc analysis of neutral phenolic compounds in rapeseeds. *Food/Nahrung* **1998**, *42*, 75–80. [[CrossRef](#)]
39. Montes de Oca, M.K.; Pearlman, R.L.; McClees, S.F.; Strickland, R.; Afaq, F. Phytochemicals for the prevention of photocarcinogenesis. *Photochem. Photobiol.* **2017**, *93*, 956–974. [[CrossRef](#)]
40. Duke, J.A.; Beckstrom-Sternberg, S.M. *Handbook of Medicinal Mints (Aromathematics): Phytochemicals and Biological Activities*, 1st ed.; CRC Press: Boca Raton, FL, USA, 2000.
41. Rice-Evans, C.A.; Miller, N.J.; Paganga, G. Antioxidant properties of phenolic compounds. *Trends Plant Sci.* **1997**, *2*, 152–159. [[CrossRef](#)]
42. Tabart, J.; Kevers, C.; Pincemail, J.; Defraigne, J.O.; Dommès, J. Comparative antioxidant capacities of phenolic compounds measured by various tests. *Food Chem.* **2009**, *133*, 1226–1233. [[CrossRef](#)]
43. Eaton, E.A.; Walle, U.K.; Lewis, A.J.; Hudson, T.; Wilson, A.A.; Walle, T. Flavonoids, potent inhibitors of the human p-form phenolsulfotransferase. Potential role in drug metabolism and chemoprevention. *Drug Metab. Dispos.* **1996**, *24*, 232–237.
44. Wu, S.; Xu, W.; Wang, F.R.; Yang, X.W. Study of the biotransformation of tongmai formula by human intestinal flora and its intestinal permeability across the Caco-2 cell monolayer. *Molecules* **2015**, *20*, 18704–18716. [[CrossRef](#)]
45. Teng, Z.; Yuan, C.; Zhang, F.; Huan, M.; Cao, W.; Li, K.; Yang, J.; Cao, D.; Zhou, S.; Mei, Q. Intestinal absorption and first-pass metabolism of polyphenol compounds in rat and their transport dynamics in Caco-2 cells. *PLoS ONE* **2012**, *7*, e29647. [[CrossRef](#)]
46. Tian, X.J.; Yang, X.W.; Yang, X.; Wang, K. Studies of intestinal permeability of 36 flavonoids using Caco-2 cell monolayer model. *Int. J. Pharm.* **2009**, *367*, 58–64. [[CrossRef](#)]
47. Fang, Y.; Cao, W.; Xia, M.; Pan, S.; Xu, X. Study of structure and permeability relationship of flavonoids in Caco-2 cells. *Nutrients* **2017**, *9*, 1301. [[CrossRef](#)]
48. del Mar Contreras, M.; Borrás-Linares, I.; Herranz-López, M.; Micol, V.; Segura-Carretero, A. Further exploring the absorption and enterocyte metabolism of quercetin forms in the Caco-2 model using nano-LC-TOF-MS. *Electrophoresis* **2016**, *37*, 998–1006. [[CrossRef](#)]
49. Liu, L.; Guo, L.; Zhao, C.; Wu, X.; Wang, R.; Liu, C. Characterization of the intestinal absorption of seven flavonoids from the flowers of *Trollius chinensis* using the Caco-2 cell monolayer model. *PLoS ONE* **2015**, *10*, e0119263. [[CrossRef](#)]

50. Ravisankar, S.; Agah, S.; Kim, H.; Talcott, S.; Wu, C.; Awika, J. Combined cereal and pulse flavonoids show enhanced bioavailability by downregulating phase ii metabolism and abc membrane transporter function in Caco-2 model. *Food Chem.* **2019**, *279*, 88–97. [[CrossRef](#)]
51. Alvarez, A.I.; Real, R.; Perez, M.; Mendoza, G.; Prieto, J.G.; Merino, G. Modulation of the activity of abc transporters (P-glycoprotein, MRP2, BCRP) by flavonoids and drug response. *J. Pharm. Sci.* **2010**, *99*, 598–617. [[CrossRef](#)]
52. Zhang, J.; Liu, D.; Huang, Y.; Gao, Y.; Qian, S. Biopharmaceutics classification and intestinal absorption study of apigenin. *Int. J. Pharm.* **2012**, *436*, 311–317. [[CrossRef](#)]
53. Barrajon-Catalan, E.; Fernandez-Arroyo, S.; Saura, D.; Guillen, E.; Fernandez-Gutierrez, A.; Segura-Carretero, A.; Micol, V. Cistaceae aqueous extracts containing ellagitannins show antioxidant and antimicrobial capacity, and cytotoxic activity against human cancer cells. *Food Chem. Toxicol.* **2010**, *48*, 2273–2282. [[CrossRef](#)] [[PubMed](#)]
54. Lin, H.; Gebhardt, M.; Bian, S.; Kwon, K.A.; Shim, C.K.; Chung, S.J.; Kim, D.D. Enhancing effect of surfactants on fexofenadine HCL transport across the human nasal epithelial cell monolayer. *Int. J. Pharm.* **2007**, *330*, 23–31. [[CrossRef](#)] [[PubMed](#)]



© 2019 by the authors. Licensee MDPI, Basel, Switzerland. This article is an open access article distributed under the terms and conditions of the Creative Commons Attribution (CC BY) license (<http://creativecommons.org/licenses/by/4.0/>).





Communication

Intestinal Permeability Study of Clinically Relevant Formulations of Silibinin in Caco-2 Cell Monolayers

Almudena Pérez-Sánchez ^{1,†} , Elisabet Cuyàs ^{2,3,†}, Verónica Ruiz-Torres ¹,
Luz Agulló-Chazarra ¹, Sara Verdura ^{2,3} , Isabel González-Álvarez ⁴ , Marival Bermejo ⁴,
Jorge Joven ⁵, Vicente Micol ^{1,6,*} , Joaquim Bosch-Barrera ^{2,7,8,*} and Javier A. Menendez ^{2,3,*}

¹ Instituto de Biología Molecular y Celular (IBMC) and Instituto de Investigación, Desarrollo e Innovación en Biotecnología Sanitaria de Elche (IDiBE), Universidad Miguel Hernández (UMH), 03202 Elche, Spain; almudena.perez@umh.es (A.P.-S.); vruiz@umh.es (V.R.-T.); lagullo@umh.es (L.A.-C.)

² Program Against Cancer Therapeutic Resistance (ProCURE), Metabolism and Cancer Group, Catalan Institute of Oncology, 17007 Girona, Spain; ecuyas@idibgi.org (E.C.); sverdura@idibgi.org (S.V.)

³ Girona Biomedical Research Institute (IDIBGI), 17190 Girona, Spain

⁴ Pharmacokinetics and Pharmaceutical Technology Area, Engineering Department, Universidad Miguel Hernández (UMH), San Juan de Alicante, 03202 Alicante, Spain; isabel.gonzalez@umh.es (I.G.-Á.); mbermejo@umh.es (M.B.)

⁵ Unitat de Recerca Biomèdica, Hospital Universitari Sant Joan, Institut d'Investigació Sanitària Pere Virgili, Universitat Rovira i Virgili, 43201 Reus, Spain; jjoven@grupsagessa.com

⁶ CIBER, Fisiopatología de la Obesidad y la Nutrición, CIBERobn, Instituto de Salud Carlos III (CB12/03/30038), 07122 Palma de Mallorca, Spain

⁷ Department of Medical Sciences, Medical School University of Girona, 17003 Girona, Spain

⁸ Medical Oncology, Catalan Institute of Oncology (ICO), Dr. Josep Trueta University Hospital, 17007 Girona, Spain

* Correspondence: vmicol@umh.es (V.M.); jbosch@iconcologia.net (J.B.-B.); jmenendez@idibgi.org (J.A.M.)

† These authors contributed equally.

Received: 14 March 2019; Accepted: 29 March 2019; Published: 31 March 2019



Abstract: An ever-growing number of preclinical studies have investigated the tumoricidal activity of the milk thistle flavonolignan silibinin. The clinical value of silibinin as a bona fide anti-cancer therapy, however, remains uncertain with respect to its bioavailability and blood–brain barrier (BBB) permeability. To shed some light on the absorption and bioavailability of silibinin, we utilized the Caco-2 cell monolayer model of human intestinal absorption to evaluate the permeation properties of three different formulations of silibinin: silibinin-meglumine, a water-soluble form of silibinin complexed with the amino-sugar meglumine; silibinin-phosphatidylcholine, the phytolipid delivery system Siliphos; and Eurosil⁸⁵/Euromed, a milk thistle extract that is the active component of the nutraceutical Legasil with enhanced bioavailability. Our approach predicted differential mechanisms of transport and blood–brain barrier permeabilities between the silibinin formulations tested. Our assessment might provide valuable information about an idoneous silibinin formulation capable of reaching target cancer tissues and accounting for the observed clinical effects of silibinin, including a recently reported meaningful central nervous system activity against brain metastases.

Keywords: silibinin; cancer; bioavailability; blood–brain barrier

1. Introduction

Silymarin is an extract of *Silybum marianum* (milk thistle) seeds that was classified by the World Health Organization in the 1970s as an official medicine with health-promoting properties. It is a mixture of several flavonoids (e.g., taxifolin, quercetin, kaempferol, and apigenin) and seven

flavonolignans, including silychristin A, silychristin B, silydianin, silybin B, silybin A, isosilybin A, and isosilybin B [1–7]. The highest concentration of silymarin (50–70% in the extract and 20–40% in commonly used pharmaceutical preparations) corresponds to silybin or silibinin (CAS No. 22888-70-6, a 1:1 mixture of the diastereoisomers silybin A and silybin B), which is considered as the major bioactive component of silymarin [3,8,9].

Despite containing several hydrophilic ionizable groups, the overall character of silibinin is hydrophobic, with very poor solubility in water. Silibinin is soluble in polar aprotic solvents (e.g., acetone, N,N-dimethylformamide [DMF], and tetrahydrofuran [THF]), but is poorly soluble in polar protic solvents (e.g., ethanol and methanol), and is insoluble in non-polar solvents (e.g., chloroform and petroleum ether) [8]. With respect to pharmacokinetics, silibinin is quickly absorbed after oral administration and exhibits a good distribution in a variety of tissues, including liver, lung, stomach, skin, and small bowel. However, the half-life of silibinin elimination via excretion in bile and urine is very fast and oscillates between one and three hours [10]. Moreover, it has been suggested that silibinin is too large to be absorbed by simple diffusion and has poor miscibility with other lipids, thereby reducing its capacity to cross the lipid-rich outer membrane of the enterocytes of the small intestine. In addition, silibinin undergoes extensive phase II metabolism through the first liver passage after its absorption [11]. These four factors (low water solubility, rapid excretion, inefficient intestinal absorption, and elevated metabolism) significantly decrease the hematic concentration of silibinin when combined, reducing its arrival at the target organ and, consequently, limiting its therapeutic efficiency [12–14].

Numerous approaches have been pursued to overcome the low bioavailability of silibinin through the development of an enormous number (>200) of silibinin modifications [8,15–17]. These modifications can be grouped into four main categories, namely: complexation with -cyclodextrins, chemical modification to generate different derivatives with enhanced water-solubility profiles (e.g., phosphate and sulphate salts, glycol-conjugates [gluco-, manno-, galacto-, and lacto-conjugates]), incorporation into different delivery technologies (e.g., solid dispersions, floating tablets, softgel capsules, micronized/nanonized formulations, etc.), and self-microemulsifying drug delivery systems (e.g., microspheres, nanoparticles, micelles, and phytosomes). The increased absorption of some of these new formulations has confirmed the high tolerability of silibinin, with no deaths or life-threatening adverse events reported during its therapeutic use [13,18].

To shed some light on the absorption and bioavailability capabilities of different silibinin formulations with proven pre-clinical and clinical activity, we evaluated the permeation properties of three different silibinin formulations: silibinin-meglumine, a more water-soluble form of silibinin complexed with the excipient amino-sugar meglumine [19,20]; silibinin-phytosome (Siliphos), a silibinin-phosphatidylcholine (PC) complex that can be administered to humans at doses achieving micromolar concentrations with minimal or no side effects [21–23]; and Eurosil⁸⁵/Euromed, a patented extract of milk thistle ETHIS-094 that is the active component of the nutraceutical Legasil with enhanced bioavailability [24,25]. Intestinal permeability was evaluated using the Caco-2 cell monolayer model, a well-accepted model of human intestinal absorption [26–30].

2. Results

We first established the Caco-2 cell monolayer on a permeable transwell filter support and tested its integrity and reliability by measuring the transepithelial electrical resistance (TEER) as a function of time, which remained stable during the assays irrespective of the silibinin formulation assayed (Supplementary Figure S1A). We then added the silibinin formulations and sampled the apical (AP) and basolateral (BL) compartments at different time points in the assay. None of the concentrations of the different silibinins employed were toxic to the cells as measured by 3-(4,5-dimethylthiazol-2-yl)-2,5-diphenyltetrazolium bromide (MTT)-based cell viability assays (Supplementary Figure S1B).

Samples were analyzed by high-performance liquid chromatography (HPLC)–UV absorbance to quantify the amounts of silibinin crossing the cell monolayer (Figure 1A). These concentration values were employed to obtain the apparent permeability values (P_{app}). To validate the Caco-2 monolayer system, we measured the P_{app} of metoprolol, a well-transported marker by passive diffusion, across the Caco-2 monolayer from the AP to BL chamber. The P_{app} value of metoprolol was determined as 6×10^{-5} cm/s, which is expected for well-absorbed drugs [31,32]. The calculated P_{app} values for the different formulations of silibinin across the monolayer in both directions (AP–BL and BL–AP), as well as the efflux ratios (BL–AP/AP–BL), are shown in Figures 1B,C and 2A, respectively.

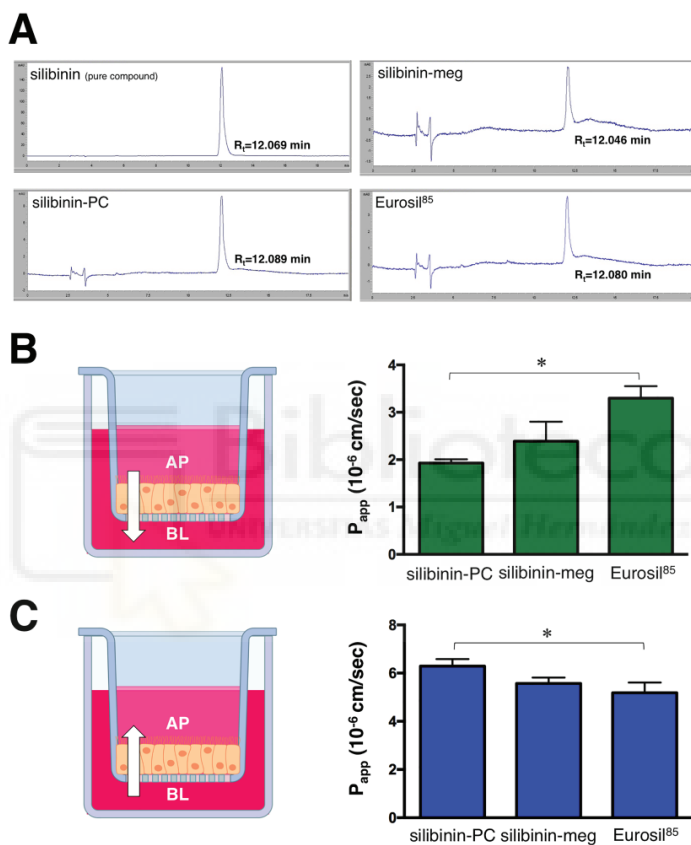


Figure 1. P_{app} values of the different formulations of silibinin. Representative HPLC elution profiles and retention times of silibinin formulations after 120 min incubation with the Caco-2 cell monolayers (A). P_{app} values in cm/s for silibinin formulations in both AP–BL (B) and BL–AP (C) directions. Each column represents the mean \pm standard deviation (SD) of P_{app} values obtained in $n = 6$ independent replicates. * One-way ANOVA $p < 0.0001$; AP: Apical; BL: Basolateral; silibinin-PC: silibinin-phosphatidylcholine; silibinin-meg: silibinin-meglumine).

The highest permeation values for the AP–BL direction were observed for the Eurosil⁸⁵/Euromed formulation (3.3×10^{-6} cm/s; Figure 1A), which was the sole formulation reaching a similar value to that observed when using a pure standard of silibinin (3.2×10^{-6} cm/s). Moreover, there was no indication of efflux or active transport according to the net efflux criterion proposed by the Food and Drug Administration guidelines, as the ratio of P_{app} BL–AP/ P_{app} AP–BL for the Eurosil⁸⁵/Euromed formulation was 1.57 (< 2), significantly lower than that obtained with silibinin-PC (Figure 2A).

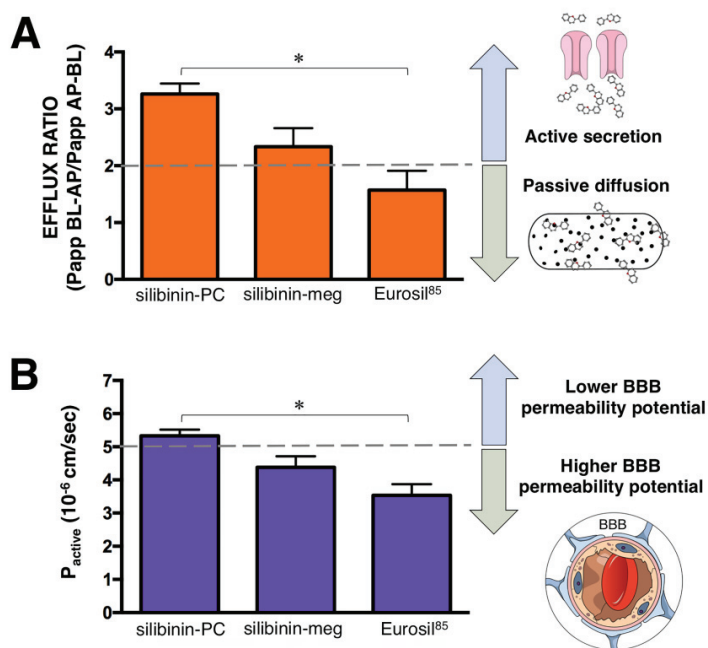


Figure 2. Transport ratios of the different formulations of silibinin. (A) Efflux ratio (P_{app} BL-AP/ P_{app} AP-BL). (B) Blood-brain barrier (BBB) permeability-related P_{active} ratio ($[P_{app}$ BL-AP - P_{app} AP-BL]/2). * One-way ANOVA $p < 0.0001$; silibinin-PC: silibinin-phosphatidylcholine; silibinin-meg: silibinin-meglumine.

Regarding the BL-AP direction, the silibinin-phosphatidylcholine complex Siliphos demonstrated the highest permeation value (6.29×10^{-6} cm/s; Figure 1B), which was similar to the value observed when using a pure standard of silibinin (6.28×10^{-6} cm/s). Moreover, this formulation showed an efflux ratio notably greater than 2 (3.3), therefore suggesting an active secretion transport (Figure 2A).

Because there exists a good correlation between the Caco-2-derived P_{active} value (i.e., $[P_{app}$ BL-AP - P_{app} AP-BL]/2) and in situ blood-brain barrier (BBB) permeation rate, the Caco-2 assay can be used to indirectly evaluate BBB potential for compounds with $P_{active} < 5 \times 10^{-6}$ cm/s. The Eurosil⁸⁵/Euromed formulation was the only one exhibiting a $P_{active} < 5$ (3.5) (Figure 2B), thereby suggesting a higher potential to permeate the BBB compared to silibinin-PC.

3. Discussion

Originally described as a remedy for the bites of poisonous snakes more than 2000 years ago, the use of silibinin-containing nutraceuticals to treat liver toxicity, including alcoholic liver disease, nonalcoholic liver disease, drug-induced liver injury, cirrhosis, viral hepatitis, and mushroom poisoning, has been well documented over the last 40 years [2,17,33]. In the last decade, numerous studies have begun to demonstrate the capacity of silibinin to exert significant tumoricidal activity against cultured cancer cells and xenografts, to enhance the efficacy of other anti-cancer therapeutic agents, to reduce the toxicity of cancer treatments, and to prevent and overcome the emergence of cancer drug resistance [34–37].

Despite this ever-growing number of preclinical studies showing the capacity of silibinin to target tumor cells, the achievement of a bona fide, clinically relevant anti-cancer activity of silibinin remains controversial in human trials [38]. This could be explained by the poor water solubility (<0.04 mg/mL) of its flavonolignan structure and subsequent low bioavailability. Not surprisingly, many methods have been developed to improve the solubility and bioavailability of silibinin. In this regard, the aim

of the present study was to compare the intestinal absorption of silibinin in different pre-clinical and clinically relevant formulations in the Caco-2 model, which expresses intestinal efflux and uptake transporters that regulate permeation of drugs from intestinal lumen to systemic circulation [26–28].

Generally, compounds with $P_{app} < 1 \times 10^{-6}$ cm/s, $P_{app} 1\text{--}10 \times 10^{-6}$ cm/s, and $P_{app} > 10 \times 10^{-6}$ cm/s can be classified as poorly (0–20%), moderately (20–70%) and well- (70–100%) absorbed compounds, respectively, in the Caco-2 model [31,32]. In our hands, all the P_{app} values of the different silibinin formulations tested were at a level of 10^{-6} cm/s, and so they can be assigned to the moderately absorbed group of compounds. The AP–BL and BL–AP trends between silibinin formulations were significantly different when comparing silibinin-PC and Eurosil⁸⁵/Euromed. Indeed, a correlation appeared to exist between the efflux mode and the reported anti-cancer effect of silibinin formulations in a clinical setting. In this respect, early studies suggested that the effect of enhanced bioavailability achieved with the phytolipid delivery system—a formulation that was initially named silipide (IdB 1016) or Siliphos—was likely related to the passage of the silibinin phosphatidylcholine complex through the gastrointestinal tract [3,39–42]. However, although high-dose oral silybin-phytosome has been shown to achieve transient high blood concentrations, low levels of silibinin and no significant anti-tumor activity were reported in prostate cancer tissue [19,20]. The results of our analysis predict the active secretion transport of the Siliphos formulation. On the other hand, when used as part of Legasil—a commercially available nutraceutical product containing the Eurosil⁸⁵/Euromed formulation—silibinin has recently been shown to exhibit significant clinical activity in cancer patients with advanced systemic disease [43–45]. Indeed, responses to Eurosil⁸⁵/Euromed-based therapy were notable in the central nervous system, where highly significant clinical and radiological improvements of brain metastases (including several complete responses) were achieved in patients with non-small cell—lung cancer [44,45]. According to our results, the silibinin formulation exhibiting the highest permeability rate (i.e., Eurosil⁸⁵/Euromed) was predicted to also exhibit a passive diffusion mechanism of transport [46,47]. Because some nutritional modalities are known to impact intestinal permeability, it might be relevant to evaluate how certain dietary approaches with proposed applications in oncology (e.g., high-fat, low-carbohydrate ketogenic diets, [48] might represent a potentially promising strategy to increase biodisponibility and the efficacy of silibinin-based anti-cancer strategies. Moreover, the Caco-2 data can be used to predict BBB permeability. For compounds that are not subject to significant levels of efflux activity in Caco-2 cells, there is a clear correlation between the P_{active} value and the permeability–surface area product (logPS) of drugs known to permeate the BBB. Considering this correlation, our findings suggest that Eurosil⁸⁵/Euromed, but not the phytolipid delivery system, could be considered a good candidate to cross the BBB.

The results presented here represent a new contribution to our rudimentary knowledge of the oral absorption and bioavailability of clinically relevant formulations of the flavonolignan silibinin. Our findings might provide valuable information to help identify the best silibinin formulation that would reach the target (cancer) tissues and would account for the clinical (anti-cancer) effects of silibinin, including the meaningful central nervous system activity against brain metastases.

4. Materials and Methods

4.1. Chemicals and Reagents

All chemicals were of analytical reagent grade and were used as received. For mobile phase preparation, trifluoroacetic acid (TFA) and acetonitrile were purchased from Merck (Millipore, Darmstadt, Germany) and VWR (Barcelona, Spain), respectively. Dimethyl sulfoxide (DMSO), metoprolol and standard compound silibinin were purchased from Sigma-Aldrich (Steinheim, Germany). Silibinin/phospholipids (Siliphos) was obtained from Indena S.p.A (Milan, Italy). Monteloeder (Elche, Alicante, Spain) provided the water-soluble milk thistle extract in its silibinin-meglumine salt, and Eurosil⁸⁵/Euromed was kindly provided by Meda Pharma S. L.

(Barcelona, Spain). Hank's Balanced Salt Solution (HBSS), Dulbecco's Modified Eagle's Medium (DMEM), fetal bovine serum (FBS), penicillin/streptomycin, MEM Non-Essential Amino Acids (NEAA) Solution (100×) and 1 M HEPES were obtained from Gibco/Thermo Fisher Scientific (Waltham, MA, USA). The human colon adenocarcinoma cell line Caco-2 was obtained from the American Type Culture Collection. Caco-2 cells were cultured in DMEM containing D-glucose (4.5 g/L) and supplemented with 10% FBS, 1% NEAA, 1% HEPES, penicillin (100 U/mL), and streptomycin (100 µg/mL) at 37 °C in a humidified atmosphere with 5% CO₂.

4.2. Cell Viability Assay

The cytotoxic effects of the different formulations of silibinin were tested and compared with those of standard silibinin using the 3-(4,5-dimethylthiazol-2-yl)-2,5-diphenyltetrazolium bromide (MTT) assay. Caco-2 cells were seeded in 96-well plates (Costar, Fisher Scientific, Pittsburgh, PA, USA) until cell monolayers were formed. Cells were treated with different concentrations of silibinin formulations (0–200 µg/mL) or standard silibinin (0–200 µM) for 2 h. The medium was removed, and cells were then incubated with MTT for 3–4 h at 37 °C and 5% CO₂. Then, the medium was removed and 100 µL of DMSO per well was added to dissolve the formazan crystal. The plates were shaken for 15 min and absorbance was measured using a microplate reader (SPECTROstar Omega, BMG LabTech GmbH, Ortenberg, Germany) at 570 nm.

4.3. Cell Culture and Permeability Studies

Caco-2 cells were seeded at a density of 1×10^5 onto Transwell 6-well inserts with a polyethylene terephthalate membrane (0.4 µm pore size; BD Falcon) and were maintained at 37 °C under 90% humidity and 5% CO₂. The medium was replaced every two to three days for both the AP and BL chambers. Cell monolayers were used 19–21 days after seeding, once confluence and differentiation were achieved. The integrity of each cell monolayer was assessed by measuring the TEER before and after the experiments with an epithelial voltammeter (Millicell-ERS). Permeability studies were performed by adding the silibinin formulations at 200 µg/mL in HBSS/0.6% DMSO (stocks were prepared at 30 mg/mL in 100% DMSO) and, in parallel, standard silibinin at different concentrations (10, 20, 50, 100, 150, 200, and 300 µmol/L).

The transport experiment was initiated by removing the culture medium from the AP and BL chambers. The Caco-2 monolayers were washed twice with pre-warmed HBSS (pH 7.4) and incubated with the same solution at 37 °C for 30 min. The test compounds were added to the AP (2.2 mL) or BL (3.2 mL) chambers, while the receiving chamber contained the corresponding volume of HBSS. The six-well plate containing the cell monolayers was placed in an orbital environmental shaker, which was maintained at a constant temperature (37 °C) and agitation rate (54 rpm) for the duration of the transport experiments.

To follow transport across the cell monolayer, several samples of 200 µL were collected at different time points (0, 30, 60, 90, and 120 min) from the AP or BL chambers during the permeability assay. The volume of the samples taken at each time point was replaced with the same volume of HBSS to maintain the total volume in the chamber throughout the experiment. Also, two samples of 200 µL were taken from the donor chamber, at the beginning and the end of the assay, for the mass balance calculation.

Transport studies were performed from apical-to-basolateral (AP–BL) and basolateral-to-apical (BL–AP) chambers. The apparent permeability (P_{app}) values for each compound were calculated according to the following equation:

$$P_{app} = \frac{dQ}{dt} \cdot \frac{1}{A \cdot C_0 \cdot 60}$$

where P_{app} is the apparent permeability (cm/s), dQ/dt is the steady-state flux, A is the diffusion area of the monolayers (cm²), C_0 is the initial concentration of the drug in the donor compartment (μM), and 60 is a conversion factor [49].

The efflux ratio was calculated to determine the absorption mechanism such as the ratio of P_{app} (BL–AP) – P_{app} (AP–BL).

4.4. Analytical Methodology

Analyses were performed using an Agilent LC 1100 series HPLC system (Agilent Technologies, Inc., Palo Alto, CA) controlled by Chemstation software, equipped with a pump, autosampler, column oven, and UV–VIS diode array detector (wavelength selected at 280 nm to detect silibinin). The samples were separated on a Poroshell 120 SB-C18 column (2.7 μm, 4.6 × 150 mm). The flow rate was 0.5 mL/min, the column temperature set at 22 °C, and the mobile phases consisted of 0.1% TFA in water as mobile phase A and acetonitrile as mobile phase B, using a gradient elution based on the following profile: 0 min, 25% B; 5 min, 40% B; 10 min, 50% B; 15 min, 25% B; 20 min, 25% B. Quantitation of the silibinin concentration was performed using a commercial standard. A calibration graph for the quantitative evaluation of silibinin was performed using a six-point regression curve ($r^2 > 0.999$).

4.5. Statistical Analysis

One-way analysis of variance and statistical comparisons of the different treatments were performed using Tukey's post-test in GraphPad Prism version 6.00 (GraphPad Software, San Diego, CA, USA).

Supplementary Materials: Supplementary materials can be found at <http://www.mdpi.com/1422-0067/20/7/1606/s1>.

Author Contributions: A.P.-S.; investigation, validation, data curation, formal analysis; writing-original draft preparation; E.C.; investigation, data curation; V.R.-T., L.A.-C., and S.V.; investigation; I.G.-Á. and M.B.; methodology, supervision; J.J.; resources; V.M.; resources, supervision; J.B.-B.; resources, conceptualization, funding acquisition; J.A.M.; conceptualization, funding acquisition, supervision, visualization, writing-original draft preparation, writing-review and editing.

Funding: Work in the Menendez laboratory was supported by the Spanish Ministry of Science and Innovation (Grant SAF2016-80639-P, Plan Nacional de I+D+I, funded by the European Regional Development Fund, Spain) and by an unrestricted research grant from the Fundació Oncolliga Girona (Lliga catalana d'ajuda al malalt de càncer, Girona). Work in the Vicente Micó laboratory was supported by Grants AGL2015-67995-C3-1-R from the Spanish Ministry of Economy and Competitiveness (MINECO); PROMETEO/2016/006, ACOMP/2013/093, ACIF/2013/064, ACIF/2015/158, APOTIP/2017/003, and APOSTD/2018/097 (Generalitat Valenciana), and CIBER (CB12/03/30038, Fisiopatología de la Obesidad y la Nutrición, CIBERobn, Instituto de Salud Carlos III, Spain). Joaquim Bosch-Barrera is the recipient of a Grant from the Health Research and Innovation Strategic Plan (SLT006/17/114; PERIS 2016-2020; Pla estratègic de recerca i innovació en salut; Departament de Salut, Generalitat de Catalunya).

Acknowledgments: The authors would like to thank Kenneth McCreath for editorial support.

Conflicts of Interest: The authors declare no conflict of interest.

Abbreviations

BBB	Blood–Brain Barrier
AP	Apical
BL	Basolateral

References

1. Abenavoli, L.; Capasso, R.; Milic, N.; Capasso, F. Milk thistle in liver diseases: Past, present, future. *Phytother. Res.* **2010**, *24*, 1423–1432. [CrossRef] [PubMed]

2. Abenavoli, L.; Izzo, A.A.; Milić, N.; Cicala, C.; Santini, A.; Capasso, R. Milk thistle (*Silybum marianum*): A concise overview on its chemistry, pharmacological, and nutraceutical uses in liver diseases. *Phytother. Res.* **2018**, *32*, 2202–2213. [[CrossRef](#)] [[PubMed](#)]
3. Bijak, M. Silybin, a Major Bioactive Component of Milk Thistle (*Silybum marianum* L. Gaernt.)—Chemistry, Bioavailability, and Metabolism. *Molecules* **2017**, *22*. [[CrossRef](#)] [[PubMed](#)]
4. Gazák, R.; Walterová, D.; Kren, V. Silybin and silymarin—new and emerging applications in medicine. *Curr. Med. Chem.* **2007**, *14*, 315–338. [[CrossRef](#)] [[PubMed](#)]
5. Kim, N.C.; Graf, T.N.; Sparacino, C.M.; Wani, M.C.; Wall, M.E. Complete isolation and characterization of silybins and isosilybins from milk thistle (*Silybum marianum*). *Org. Biomol. Chem.* **2003**, *1*, 1684–1689. [[CrossRef](#)]
6. Hackett, E.S.; Twedt, D.C.; Gustafson, D.L. Milk thistle and its derivative compounds: A review of opportunities for treatment of liver disease. *J. Vet. Intern. Med.* **2013**, *27*, 10–16. [[CrossRef](#)]
7. Lee, J.I.; Narayan, M.; Barrett, J.S. Analysis and comparison of active constituents in commercial standardized silymarin extracts by liquid chromatography-electrospray ionization mass spectrometry. *J. Chromatogr. B Analyt. Technol. Biomed. Life Sci.* **2007**, *845*, 95–103. [[CrossRef](#)]
8. Biedermann, D.; Vavříková, E.; Cvak, L.; Křen, V. Chemistry of silybin. *Nat. Prod. Rep.* **2014**, *31*, 1138–1157. [[CrossRef](#)]
9. Vargas-Mendoza, N.; Madrigal-Santillán, E.; Morales-González, A.; Esquivel-Soto, J.; Esquivel-Chirino, C.; García-Luna, Y.; González-Rubio, M.; Gayosso-de-Lucio, J.A.; Morales-González, J.A. Hepatoprotective effect of silymarin. *World J. Hepatol.* **2014**, *6*, 144–149. [[CrossRef](#)]
10. Zhao, J.; Agarwal, R. Tissue distribution of silibinin, the major active constituent of silymarin, in mice and its association with enhancement of phase II enzymes: Implications in cancer chemoprevention. *Carcinogenesis* **1999**, *20*, 2101–2108. [[CrossRef](#)]
11. Hoh, C.; Boocock, D.; Marczylo, T.; Singh, R.; Berry, D.P.; Dennison, A.R.; Hemingway, D.; Miller, A.; West, K.; Euden, S.; et al. Pilot study of oral silibinin, a putative chemopreventive agent, in colorectal cancer patients: Silibinin levels in plasma, colorectum, and liver and their pharmacodynamic consequences. *Clin. Cancer Res.* **2006**, *12*, 2944–2950. [[CrossRef](#)]
12. Saller, R.; Meier, R.; Brignoli, R. The use of silymarin in the treatment of liver diseases. *Drugs* **2001**, *61*, 2035–2063. [[CrossRef](#)]
13. Saller, R.; Melzer, J.; Reichling, J.; Brignoli, R.; Meier, R. An updated systematic review of the pharmacology of silymarin. *Forsch. Komplementmed.* **2007**, *14*, 70–80. [[CrossRef](#)] [[PubMed](#)]
14. Hawke, R.L.; Schrieber, S.J.; Soule, T.A.; Wen, Z.; Smith, P.C.; Reddy, K.R.; Wahed, A.S.; Belle, S.H.; Afdhal, N.H.; Navarro, V.J.; et al. Silymarin ascending multiple oral dosing phase I study in noncirrhotic patients with chronic hepatitis C. *J. Clin. Pharmacol.* **2010**, *50*, 434–449. [[CrossRef](#)] [[PubMed](#)]
15. Javed, S.; Kohli, K.; Ali, M. Reassessing bioavailability of silymarin. *Altern. Med. Rev.* **2011**, *16*, 239–249. [[PubMed](#)]
16. Loguercio, C.; Festi, D. Silybin and the liver: From basic research to clinical practice. *World J. Gastroenterol.* **2011**, *17*, 2288–2301. [[CrossRef](#)]
17. Federico, A.; Dallio, M.; Loguercio, C. Silymarin/Silybin and Chronic Liver Disease: A Marriage of Many Years. *Molecules* **2017**, *22*. [[CrossRef](#)]
18. Dunnick, J.K.; Singh, B.; Nyska, A.; Peckham, J.; Kissling, G.E.; Sanders, J.M. Investigating the potential for toxicity from long-term use of the herbal products, goldenseal and milk thistle. *Toxicol. Pathol.* **2011**, *39*, 398–409. [[CrossRef](#)]
19. Cufí, S.; Bonavia, R.; Vazquez-Martin, A.; Oliveras-Ferraro, C.; Corominas-Faja, B.; Cuyàs, E.; Martín-Castillo, B.; Barrajón-Catalán, E.; Visa, J.; Segura-Carretero, A.; et al. Silibinin suppresses EMT-driven erlotinib resistance by reversing the high miR-21/low miR200c signature in vivo. *Sci. Rep.* **2013**, *3*, 2459. [[CrossRef](#)] [[PubMed](#)]
20. Cufí, S.; Bonavia, R.; Vazquez-Martin, A.; Corominas-Faja, B.; Oliveras-Ferraro, C.; Cuyàs, E.; Martín-Castillo, B.; Barrajón-Catalán, E.; Visa, J.; Segura-Carretero, A.; et al. Silibinin meglumine, a water-soluble form of milk thistle silymarin, is an orally active anti-cancer agent that impedes the epithelial-to-mesenchymal transition (EMT) in EGFR-mutant non-small-cell lung carcinoma cells. *Food Chem. Toxicol.* **2013**, *60*, 360–368. [[CrossRef](#)]

21. Flaig, T.W.; Gustafson, D.L.; Su, L.J.; Zirrolli, J.A.; Crighton, F.; Harrison, G.S.; Pierson, A.S.; Agarwal, R.; Glodé, L.M. A phase I and pharmacokinetic study of silybin-phytosome in prostate cancer patients. *Investig. New Drugs* **2007**, *25*, 139–146. [[CrossRef](#)]
22. Flaig, T.W.; Glodé, M.; Gustafson, D.; van Bokhoven, A.; Tao, Y.; Wilson, S.; Su, L.J.; Li, Y.; Harrison, G.; Agarwal, R.; et al. A study of high-dose oral silybin-phytosome followed by prostatectomy in patients with localized prostate cancer. *Prostate* **2010**, *70*, 848–855. [[CrossRef](#)] [[PubMed](#)]
23. Kidd, P.; Head, K. A review of the bioavailability and clinical efficacy of milk thistle phytosome: A silybin-phosphatidylcholine complex (Siliphos). *Altern. Med. Rev.* **2005**, *10*, 193–203. [[PubMed](#)]
24. Pais, P.; D'Amato, M. In vivo efficacy study of milk thistle extract (ETHIS-094™) in STAM™ model of nonalcoholic steatohepatitis. *Drugs R. D.* **2014**, *14*, 291–299. [[CrossRef](#)] [[PubMed](#)]
25. Sorrentino, G.; Crispino, P.; Coppola, D.; De Stefano, G. Efficacy of lifestyle changes in subjects with non-alcoholic liver steatosis and metabolic syndrome may be improved with an antioxidant nutraceutical: A controlled clinical study. *Drugs R. D.* **2015**, *15*, 21–25. [[CrossRef](#)]
26. Artursson, P. Epithelial transport of drugs in cell culture. I: A model for studying the passive diffusion of drugs over intestinal absorptive (Caco-2) cells. *J. Pharm. Sci.* **1990**, *79*, 476–482. [[CrossRef](#)] [[PubMed](#)]
27. Artursson, P.; Karlsson, J. Correlation between oral drug absorption in humans and apparent drug permeability coefficients in human intestinal epithelial (Caco-2) cells. *Biochem. Biophys. Res. Commun.* **1991**, *175*, 880–885. [[CrossRef](#)]
28. Artursson, P.; Palm, K.; Luthman, K. Caco-2 monolayers in experimental and theoretical predictions of drug transport. *Adv. Drug Deliv. Rev.* **2001**, *46*, 27–43. [[CrossRef](#)]
29. Funes, L.; Laporta, O.; Cerdán-Calero, M.; Micol, V. Effects of verbascoside, a phenylpropanoid glycoside from lemon verbena, on phospholipid model membranes. *Chem. Phys. Lipids* **2010**, *163*, 190–199. [[CrossRef](#)] [[PubMed](#)]
30. Pérez-Sánchez, A.; Borrás-Linares, I.; Barrajón-Catalán, E.; Arráez-Román, D.; González-Álvarez, I.; Ibáñez, E.; Segura-Carretero, A.; Bermejo, M.; Micol, V. Evaluation of the intestinal permeability of rosemary (*Rosmarinus officinalis* L.) extract polyphenols and terpenoids in Caco-2 cell monolayers. *PLoS ONE* **2017**, *12*, e0172063. [[CrossRef](#)]
31. Yee, S. In vitro permeability across Caco-2 cells (colonic) can predict in vivo (small intestinal) absorption in man—fact or myth. *Pharm. Res.* **1997**, *14*, 763–766. [[CrossRef](#)] [[PubMed](#)]
32. Wu, S.; Xu, W.; Wang, F.R.; Yang, X.W. Study of the Biotransformation of Tongmai Formula by Human Intestinal Flora and Its Intestinal Permeability across the Caco-2 Cell Monolayer. *Molecules* **2015**, *20*, 18704–18716. [[CrossRef](#)] [[PubMed](#)]
33. Tajmohammadi, A.; Razavi, B.M.; Hosseinzadeh, H. Silybum marianum (milk thistle) and its main constituent, silymarin, as a potential therapeutic plant in metabolic syndrome: A review. *Phytother. Res.* **2018**, *32*, 1933–1949. [[CrossRef](#)] [[PubMed](#)]
34. Corominas-Faja, B.; Oliveras-Ferreros, C.; Cuyàs, E.; Segura-Carretero, A.; Joven, J.; Martín-Castillo, B.; Barrajón-Catalán, E.; Micol, V.; Bosch-Barrera, J.; Menendez, J.A. Stem cell-like ALDH(bright) cellular states in EGFR-mutant non-small cell lung cancer: A novel mechanism of acquired resistance to erlotinib targetable with the natural polyphenol silibinin. *Cell Cycle* **2013**, *12*, 3390–3404. [[CrossRef](#)] [[PubMed](#)]
35. Bosch-Barrera, J.; Menendez, J.A. Silibinin and STAT3: A natural way of targeting transcription factors for cancer therapy. *Cancer Treat. Rev.* **2015**, *41*, 540–546. [[CrossRef](#)]
36. Cuyàs, E.; Pérez-Sánchez, A.; Micol, V.; Menendez, J.A.; Bosch-Barrera, J. STAT3-targeted treatment with silibinin overcomes the acquired resistance to crizotinib in ALK-rearranged lung cancer. *Cell Cycle* **2016**, *15*, 3413–3418. [[CrossRef](#)]
37. Bosch-Barrera, J.; Queralt, B.; Menendez, J.A. Targeting STAT3 with silibinin to improve cancer therapeutics. *Cancer Treat. Rev.* **2017**, *58*, 61–69. [[CrossRef](#)]
38. Siegel, A.B.; Stebbing, J. Milk thistle: Early seeds of potential. *Lancet Oncol.* **2013**, *14*, 929–930. [[CrossRef](#)]
39. Awasthi, R.; Kulkarni, G.; Pawar, V. Phytosomes: An approach to increase the bioavailability of plant extracts. *Int. J. Pharm. Pharm. Sci.* **2011**, *3*, 1–3.
40. Gandhi, A.; Dutta, A.; Pal, A.; Bakshi, P. Recent trends of phytosomes for delivering herbal extract with improved bioavailability. *J. Pharmacogn. Phytochem.* **2012**, *1*, 6–14.

41. Barzaghi, N.; Crema, F.; Gatti, G.; Pifferi, G.; Perucca, E. Pharmacokinetic studies on IdB 1016, a silybin-phosphatidylcholine complex, in healthy human subjects. *Eur. J. Drug Metab. Pharmacokinet.* **1990**, *15*, 333–338. [[CrossRef](#)] [[PubMed](#)]
42. Morazzoni, P.; Magistretti, M.J.; Giachetti, C.; Zanolò, G. Comparative bioavailability of Silipide, a new flavanolignan complex, in rats. *Eur. J. Drug Metab. Pharmacokinet.* **1992**, *17*, 39–44. [[CrossRef](#)] [[PubMed](#)]
43. Bosch-Barrera, J.; Corominas-Faja, B.; Cuyàs, E.; Martín-Castillo, B.; Brunet, J.; Menendez, J.A. Silibinin administration improves hepatic failure due to extensive liver infiltration in a breast cancer patient. *Anticancer Res.* **2014**, *34*, 4323–4327. [[PubMed](#)]
44. Bosch-Barrera, J.; Sais, E.; Cañete, N.; Marruecos, J.; Cuyàs, E.; Izquierdo, A.; Porta, R.; Haro, M.; Brunet, J.; Pedraza, S.; et al. Response of brain metastasis from lung cancer patients to an oral nutraceutical product containing silibinin. *Oncotarget* **2016**, *7*, 32006–32014. [[CrossRef](#)] [[PubMed](#)]
45. Priego, N.; Zhu, L.; Monteiro, C.; Mulders, M.; Wasilewski, D.; Bindeman, W.; Doglio, L.; Martínez, L.; Martínez-Saez, E.; Cajal, S.R.Y.; et al. STAT3 labels a subpopulation of reactive astrocytes required for brain metastasis. *Nat. Med.* **2018**, *24*, 1024–1035. [[CrossRef](#)] [[PubMed](#)]
46. Mangas-Sanjuan, V.; González-Álvarez, I.; González-Álvarez, M.; Casabó, V.G.; Bermejo, M. Innovative in vitro method to predict rate and extent of drug delivery to the brain across the blood–brain barrier. *Mol. Pharm.* **2013**, *10*, 3822–3831. [[CrossRef](#)] [[PubMed](#)]
47. Moradi-Afrapoli, F.; Oufir, M.; Walter, F.R.; Deli, M.A.; Smiesko, M.; Zabela, V.; Butterweck, V.; Hamburger, M. Validation of UHPLC-MS/MS methods for the determination of kaempferol and its metabolite 4-hydroxyphenyl acetic acid, and application to in vitro blood–brain barrier and intestinal drug permeability studies. *J. Pharm. Biomed. Anal.* **2016**, *128*, 264–274. [[CrossRef](#)] [[PubMed](#)]
48. Nencioni, A.; Caffa, I.; Cortellino, S.; Longo, V.D. Fasting and cancer: Molecular mechanisms and clinical application. *Nat. Rev. Cancer* **2018**, *18*, 707–719. [[CrossRef](#)] [[PubMed](#)]
49. Lin, H.; Gebhardt, M.; Bian, S.; Kwon, K.A.; Shim, C.K.; Chung, S.J.; Kim, D.D. Enhancing effect of surfactants on fexofenadine.HCl transport across the human nasal epithelial cell monolayer. *Int. J. Pharm.* **2007**, *330*, 23–31. [[CrossRef](#)] [[PubMed](#)]



© 2019 by the authors. Licensee MDPI, Basel, Switzerland. This article is an open access article distributed under the terms and conditions of the Creative Commons Attribution (CC BY) license (<http://creativecommons.org/licenses/by/4.0/>).

SCIENTIFIC REPORTS

OPEN Rosemary (*Rosmarinus officinalis*) extract causes ROS-induced necrotic cell death and inhibits tumor growth *in vivo*

Received: 27 April 2018
Accepted: 29 November 2018
Published online: 28 January 2019

Almudena Pérez-Sánchez¹, Enrique Barrajón-Catalán¹, Verónica Ruiz-Torres¹, Luz Agulló-Chazarra¹, María Herranz-López¹, Alberto Valdés², Alejandro Cifuentes² & Vicente Mico^{1,3}

Colorectal cancer is the third most common diagnosed cancer globally. Although substantial advances have been obtained both in treatment and survival rates, there is still a need for new therapeutical approaches. Natural compounds are a realistic source of new bioactive compounds with anticancer activity. Among them, rosemary polyphenols have shown a vast antiproliferative capacity against colon cancer cells *in vitro* and in animal models. We have investigated the antitumor activity of a rosemary extract (RE) obtained by using supercritical fluid extraction through its capacity to inhibit various signatures of cancer progression and metastasis such as proliferation, migration, invasion and clonogenic survival. RE strongly inhibited proliferation, migration and colony formation of colon cancer cells regardless their phenotype. Treatment with RE led to a sharp increase of intracellular ROS that resulted in necrosis cell death. Nrf2 gene silencing increased RE cytotoxic effects, thus suggesting that this pathway was involved in cell survival. These *in vitro* results were in line with a reduction of tumor growth by oral administration of RE in a xenograft model of colon cancer cells using athymic nude mice. These findings indicate that targeting colon cancer cells by increasing intracellular ROS and decreasing cell survival mechanisms may suppose a therapeutic option in colon cancer through the combination of rosemary compounds and chemotherapeutic drugs.

Colorectal cancer (CRC) is the second most commonly diagnosed cancer type in females and the third in males globally, with increasing prevalence even in traditionally low-risk countries. Nevertheless, a decrease in colorectal cancer mortality rates have been noticed in a large number of countries, most probably due to reduced prevalence of risk factors, CRC screening practices and/or improved treatments¹. Several dietary components found in plant-derived foods, medicinal plants as well as their bioactive compounds have shown protective effects against a wide range of cancers, including colon cancer^{2–4}. Therefore, it seems to be of relevance to identify new bioactive food or components with an anticancer potential to prevent and/or treat human cancers^{5–7}.

Rosemary (*Rosmarinus officinalis* L.) is a bush of the Lamiaceae family that is mostly distributed in the Mediterranean area. In recent decades, experimental research has confirmed the pharmacological potential of rosemary and some of its primary compounds such as the diterpenes carnosic acid (CA) and carnosol (CAR), also expanding the range of its possible therapeutic applications. In fact, rosemary extracts have demonstrated chemoprotective effects against hepatotoxicity⁸ and gastric ulcerative lesions, and⁹ anticancer^{10–13}, antimicrobial^{14,15}, antioxidant¹⁶ and antidiabetic effects¹⁷, both *in vitro* and *in vivo*.

Recently, the antiproliferative effect of a terpenes-enriched rosemary extract (RE) obtained using supercritical fluid extraction has been demonstrated in colon cancer cell models¹³. A transcriptomic and metabolomic analysis in colon cancer cells indicated that RE treatment activated the expression of genes related to cell cycle progression and phase II antioxidant enzymes^{18,19}. The bio-guided assay fractionation of the extract revealed that CA and

¹Instituto de Biología Molecular y Celular (IBMC) and Instituto de Investigación, Desarrollo e Innovación en Biotecnología Sanitaria de Elche (IDIIBE), Universitat Miguel Hernández (UMH), 03202, Elche, Spain. ²Laboratory of Foodomics, Institute of Food Science Research (CIAL, CSIC), Nicolas Cabrera 9, 28049, Madrid, Spain. ³CIBER, Fisiopatología de la Obesidad y la Nutrición, CIBERobn, Instituto de Salud Carlos III (CB12/03/30038), 07122 Palma Sola, Spain. Almudena Pérez-Sánchez and Enrique Barrajón-Catalán contributed equally. Correspondence and requests for materials should be addressed to E.B.-C. (email: e.barrajon@umh.es)

CAR might be the main compounds responsible for such effects, but the higher activity of the complete extract compared to the fractions suggested the potential synergistic interaction between diterpenes and triterpenes. Nevertheless, the potential molecular mechanism of this antiproliferative effect and the pharmacological interactions between RE components are still unknown.

In the present report, the antiproliferative effect of RE has been deeply studied and the contribution of their different compounds to these effects through their pharmacological interaction has been characterized by synergy studies. The mechanism of the antiproliferative activity has been fully characterized by proliferation, migration, invasion and cell cycle assays in three different colon cancer cell lines. Moreover, the relationship between oxidative stress and cytotoxicity has been elucidated. Finally, we assessed the effect of RE on tumor progression *in vivo* in colon cancer mouse xenografts.

Results

Synergy studies. A previous study on the detailed composition of RE extract and the antiproliferative activity of their purified fractions in colon cancer cells revealed a putative pharmacological interaction between some of RE compounds¹³. This aspect was also pointed out by using a transcriptomic approach on some isolated compounds from RE such as CA and CAR in colon cancer cells¹⁹. Therefore, we decided to address this interaction by studying the putative synergistic effects between the major compounds in RE. We selected those compounds bearing the highest antiproliferative activities in previous studies, the diterpenes CA and CAR and the triterpenes betulinic acid (BA) and ursolic acid (UA) in single treatments or in pairwise combinations. First, individual IC₅₀ values were determined for the antiproliferative effects of these four compounds compared to RE in HT-29 cells. The results show a dose-dependent antiproliferative effect (Supplementary Fig. 1) and that the triterpenes UA and BA exhibited higher antiproliferative effect than the diterpenes CA and CAR and all isolated compounds tested showed lower IC₅₀ values than RE extract.

Further, the synergistic interactions of these four compounds were profoundly scrutinized by using six pairwise combinations at different ratios. IC₅₀ values for each combination were obtained and synergy was studied using three different methodologies: FICI value calculation, the graphic isobole method and the specialized software Compusyn. FICI values (Supplementary Table 1) showed additivity or an indifferent effect for all the combinations except for the BA-UA pair, which showed a clear antagonism behavior. Similar results were obtained using the isobole graphical method (Supplementary Figure 2), in which, no clear synergic behavior was observed for the selected ratios of the pairwise combinations of diterpenes. In contrast, antagonism was observed for the BA-UA combination. Only the Compusyn software results denoted a putative synergistic effect for different combinations between diterpenes and between di- and triterpenes, i.e. CA-CAR, CA-BA, CA-UA, CAR-UA, and CAR-BA (Supplementary Table 1). This synergistic effect was stronger in CAR-CA, CA-BA and CAR-BA combinations as shown in the polygonogram provided by the Compusyn software (Supplementary Figure 3). Again, BA-UA combination showed antagonism, as denoted in FICI calculations and isobole graphics. Taking all the synergy studies together, some pairwise combinations showed additive or synergic interactions depending on the approximation used what will be further discussed. However, the combination between the two triterpenes always brought antagonistic interaction no matter the method used.

However, no significant improvement in the antiproliferative activity was achieved when the complete extract was compared to the isolated compounds or their combinations. Therefore, for this reason, and due to its better availability, the subsequent studies were performed with the whole RE.

RE inhibits tumor cell proliferation, colony formation and migration. To illustrate the antiproliferative effects of RE, basic cytotoxicity studies previously reported^{13,19} were further extended with complementary techniques focused to study cell proliferation, colony formation and migration in the three colon cancer cellular models.

First, real-time cell proliferation was measured by RTCA as described in methods. Cells were treated with 20 and 40 µg/mL of RE for 72 h and cell growth curves were recorded by the *xCELLigence* System in real time (Fig. 1A). RE inhibited cell growth in a concentration dependent manner in all cell lines. HGUE-C-1 and SW480 cells demonstrated the highest sensitivity for RE, since a complete reduction of cell proliferation was observed already at 20 µg/mL, whereas some growth was observed for HT-29 cells at this concentration, in agreement to previous studies¹³. A cyclic growth pattern of the cell index parameter (valleys) was observed for the HGUE-C-1 and HT-29 cells, which correlated with the morphological changes of the cells during mitosis.

The clonogenic cell survival assay (colony formation assay) was employed to test whether RE was able to inhibit the ability of cancer cells to proliferate endlessly, so that retaining its reproductive capability to form a large colony or a clone (see methods section). Colorectal cancer cell lines were incubated with RE at different concentrations (20 or 40 µg/mL) for 7 days. RE suppressed the formation of colonies in the three colon cancer models in a dose-dependent manner (Fig. 1B). RE treatment at 20 and 40 µg/mL inhibited colony formation by 76.9% and 92.3%, respectively, in HGUE-C-1 cells when compared with the control; by 76.9% and 87.1%, respectively, in SW480 cells; and by 52.3% and 84.5% in HT-29 cells. Again, it was confirmed that HGUE-C-1 and SW480 cells were more sensitive to RE than HT-29 cells.

As migration capability is one of the central characteristics of metastatic cells²⁰, the inhibitory effects of RE on the migration ability of HGUE-C-1, HT-29 and SW480 cells, was evaluated by using a wound healing assay (Fig. 1C). RE treatment at 30 and 40 µg/mL significantly inhibited cell migration by 28.8 and 66.1%, respectively, in HGUE-C-1 cells, when compared with the control. In HT-29 cells, cell migration was inhibited by 22.1% and 92.5%, and in SW480 cells, RE treatment inhibited cell migration 5.6% and 76.7%, at 30 and 40 µg/mL of RE, respectively.

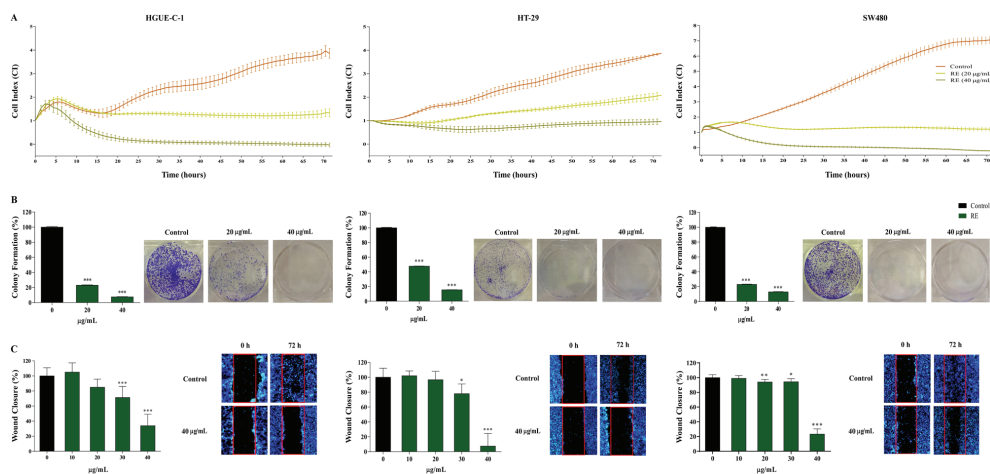


Figure 1. RE extract inhibits proliferation, migration and colony formation in human colon cancer cells. **(A)** Variation of cell index (CI) as a function of time for the three colon cancer cell lines, i.e. HGUE-C-1, HT-29 and SW480 in the absence (control) or in the presence of 20 µg/mL or 40 µg/mL of RE. Cell index was measured using the *xCELLigence* Real Time Cell Analysis System. **(B)** Inhibition of colony formation in the three colon cancer cell lines in the absence (control) or in the presence of 20 µg/mL or 40 µg/mL of RE. **(C)** Measurement of wound closure (%) by fluorescence imaging in wound healing migration assay for the three cell lines upon increasing concentrations of RE extract. Representative microscope images are also shown.

Studies on the mechanism of the antiproliferative effects of RE in colon cancer cells. *Cell cycle and apoptosis.* To illustrate the putative mechanism of cell death in the different human colon cancer cell lines treated with RE, cell cycle and apoptosis analysis, mitochondrial viability, oxidative stress and necrosis measurements were performed. Figure 2A summarizes the results of cell cycle modulation after 24 hours of exposure to RE in the three different colon cancer cell lines. Significant decreases in G0/G1 phase with a concomitant accumulation of cells in the G2/M phase was observed in SW480 cells (at 30 and 40 µg/mL RE treatments, $p < 0.05$) and in HT-29 cells (and 40 µg/mL RE treatments, $p < 0.01$). In contrast, in HGUE-C-1 cells, RE decreased G0/G1 phase with accumulation of cells in SubG1 phase, showing an increase from 2.2% in control to 15.0% at highest concentration measured ($p < 0.01$).

Then, the effect of RE on apoptosis induction was specifically evaluated by detection of Annexin V-positive cells. HGUE-C-1, HT-29 and SW480 cell lines were stained with Annexin V/7-AAD and analyzed by Muse Cell Analyzer (Fig. 2B). RE treatment for 24 h substantially increased the fraction of Annexin V/7-AAD double-positive cells in a concentration-dependent manner, suggesting either that late apoptotic or necrotic death was occurring in all the cell lines. Although both late apoptotic and necrotic cells are Annexin V and 7-AAD positive, the absence of early apoptotic cells by cell cycle analysis (Supplementary Figure 4) suggests the presence of necrosis rather than apoptosis.

The expression of up to 43 apoptosis-related proteins was measured by using RayBio Human Apoptosis Array C1 (RayBiotech, Inc. USA). In agreement to cell cycle analysis, only a few changes were observed in the three cell lines compared to the control (Supplementary Figure 5). HGUE-C-1 and SW480 cells showed a reduction in high temperature requirement A (HTRA) and survivin expression after RE treatment and an additional reduction in Bax protein was observed in SW480. No changes in these proteins were observed for HT-29 upon RE treatment. Taken together, all these results suggest that apoptosis was not the main death mechanism.

Necrosis studies. The release of the intracellular enzyme LDH due to permeabilization of the plasma membrane is a hallmark of necrosis²¹. LDH leakage assay is a simple, reliable and fast cytotoxicity assay based on the measurement of LDH activity in the extracellular medium²². RE treatment of cancer cells induced a dose-dependent release of LDH compared to the control (Fig. 2C). After 24 h of RE treatment at 40 µg/mL, HGUE-C-1 and SW480 cells exhibited the highest increase (32.6% and 20.0% of control, respectively), whereas an increase of 14.3% was observed in HT-29 cells.

The morphological observation of RE treated cells by microscopy (data not shown) also suggested a necrosis rather than apoptosis mechanism. However, as necroptosis, a mixed mechanism between necrosis and apoptosis and a caspase-independent form of regulated cell death^{23,24}, shares some morphologic features with necrosis, this option was also evaluated. To study this hypothesis, the RIP1 inhibitor necrostatin-1 (Nec-1)²⁵ was used. Pretreatment of cells with Nec-1 before RE exposure did not suppress cell death (Supplementary Figure 6A). Since autophagy has been involved as a regulator for both apoptotic and non-apoptotic cell death, the potential presence of autophagy was also evaluated. Cells were pretreated with chloroquine (CQ), a well-known autophagy

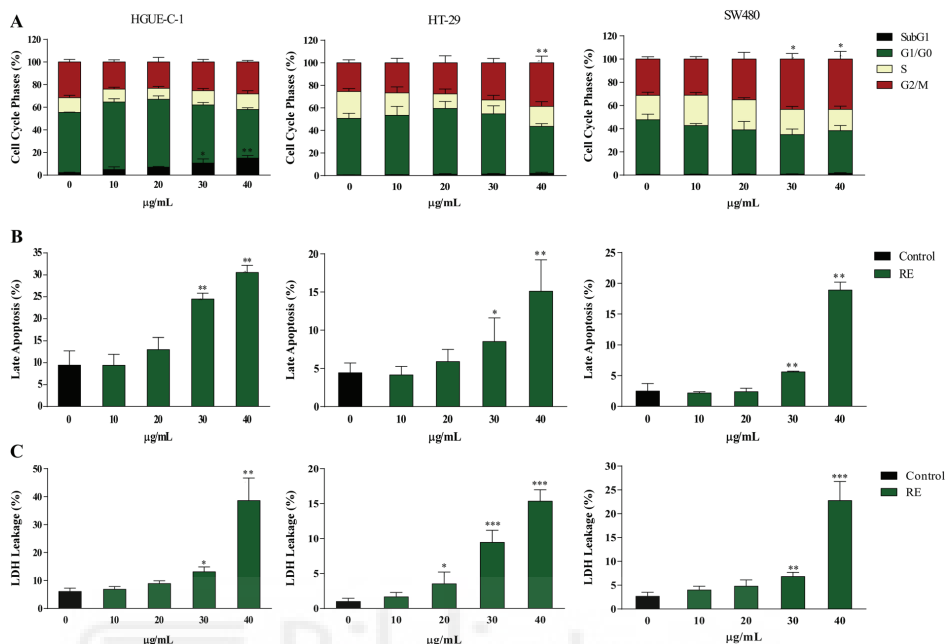


Figure 2. RE induces cell cycle arrest and cell death by necrosis in human colon cancer cells. (A) Cell cycle phases (%) analysis for the three colon cancer cell lines in the absence or in the presence of increasing concentrations of RE by Muse Cell Analyzer. (B) Measurement of late apoptosis in the three cell lines treated with the same concentrations of RE (%). (C) Plasma membrane integrity of the three cell lines treated equally and measured as LDH leakage (%).

inhibitor²⁶, but no changes were detected compared to cells treated with RE in the absence of CQ (Supplementary Figure 6B). These findings confirmed that RE inhibits colon cancer cell proliferation most probably by inducing necrosis as the major death mechanism.

Intracellular ROS generation and mitochondrial membrane potential measurements. Rosemary compounds have exhibited the capacity to regulate oxidative stress in different *in vitro* and cellular systems^{16,27}. In addition, both apoptosis and necrosis have been shown to be triggered by ROS²⁸. Therefore, we determined whether the treatment of colon cancer cells with RE could modulate intracellular ROS. ROS accumulation was evaluated in the three colorectal cancer cells using the non-polar cell-permeable probe H₂DCFDA. As shown in Fig. 3A, the treatment with RE induced an increase in fluorescence intensity for all the colorectal cancer cell lines, indicating an increase of ROS generation in a concentration-dependent manner.

Mitochondrial membrane integrity and mitochondrial viability are impaired in necrotic cell death²⁹. In addition, mitochondrial function is closely related to ROS production and control. To deepen into the effects of RE treatment on mitochondrial viability, the mitochondrial membrane potential variation was determined with the Muse Cell Analyzer, using the Muse MitoPotential kit. Figure 3B shows a dose-response enhancement in the number of cells bearing depolarized mitochondrial membranes with the increase of RE concentration that suggests a mitochondrial depolarization, which could be linked with the activation of necrosis in colorectal cancer cells. Alternatively, MitoTracker Red CMXRos and MitoTracker Green fluorescent probes were also used to examine whether mitochondrial membrane potential was injured by RE treatment in colorectal cancer cells. A decrease of the ratio between red and green fluorescence indicated a loss of mitochondrial membrane potential, as occurred when all colon cancer cells were treated with RE in a dose-dependent manner, especially in SW480 cells, (Fig. 3C,D), and corroborating the results obtained in Fig. 3B.

Nrf2 modulation by RE treatment in colorectal cancer cells. It is known that intracellular ROS generation affects the function of multiple redox-sensitive transcription factors and leads to the up-regulation of antioxidant genes. Cellular antioxidant defense mechanisms include the ROS scavenger molecules, phase II detoxification enzymes, and other detoxifying proteins^{30,31}. The transcription factor Nrf2 is a key regulator of numerous detoxifying and antioxidant genes and is activated in response to oxidative and electrophilic stress and its relationship with RE mechanism was studied by silencing it using a specific siRNA (see methods section and Supplementary Figure 7).

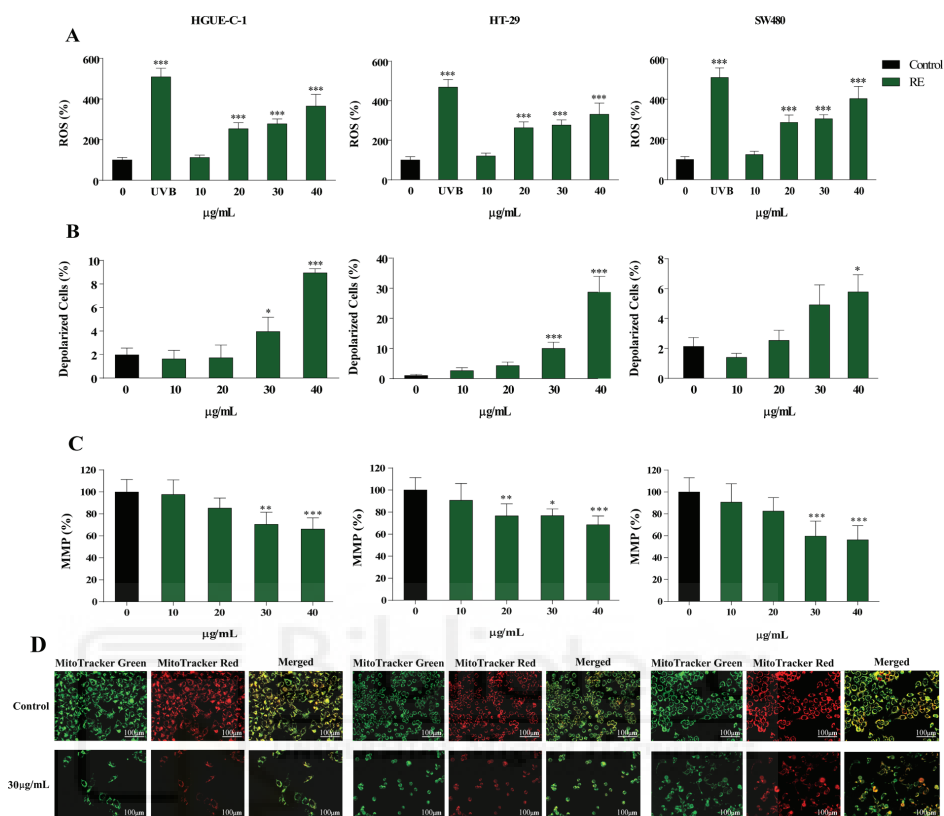


Figure 3. RE produces ROS generation and mitochondrial membrane depolarization in human colon cancer cells. (A) Measurement of intracellular ROS levels (%) of the three colon cancer cell lines after UV radiation in the absence or in the presence of 10, 20, 30 or 40 µg/mL RE, using H₂DCFDA dye. (B) Quantitation of depolarized cells (%) in the three cell lines treated with the same concentrations of RE using Muse Cell Analyzer and (C) MMP measurement (%) by using MitoTracker Green FM and MitoTracker Red CMXRos fluorescent dyes. (D) Representative fluorescence images of HGUE-C-1, HT-29 and SW480 cells, stained with MitoTracker Green and MitoTracker Red are shown.

As shown in Fig. 4, Nrf2 gene silencing in HGUE-C-1, HT-29 and SW480 cells did not modify neither viability or ROS generation in the absence of RE. Nevertheless, when cells were treated with RE, Nrf2 silencing induced a significant decrease in cell viability (Fig. 4A) concomitantly with an increase in ROS production (Fig. 4B), both in a dose-dependent way.

In vivo experiments. *Oral Acute Toxicity study.* The acute oral toxicity study of RE was performed according to the Organization for Economic Cooperation and Development (OECD) guideline 420, which specifies a limit test dose of 2000 mg/kg. After 17 days, no lethal effects or signs of toxicity were observed in any of the groups of rats treated with different doses (300 and 2000 mg/kg) of the RE. No significant differences were observed in the body weight of animals treated with RE compared to the control (Supplementary Figure 8), being this parameter one of the first critical signs of toxicity and is often the most sensible indicator of an adverse effect³². In addition, there were no significant behavioral changes, such as apathy, hyperactivity or morbidity in any of the animals when compared to the control. Normal increase in body weight was recorded for all animals with no abnormalities at necropsy on day 17th. Non-altered growth or abnormal changes were detected during the macroscopic analysis of the rat organs. For the histopathology analysis, the organs including spleen, heart, liver, lungs and kidney were examined. No pathological changes were noticed in neither the RE-treated groups nor the control group at the end of experiment (Supplementary Figure 9). Therefore, according to OECD 420 guide, the LD₅₀ of extract may be greater than 2000 mg/kg.

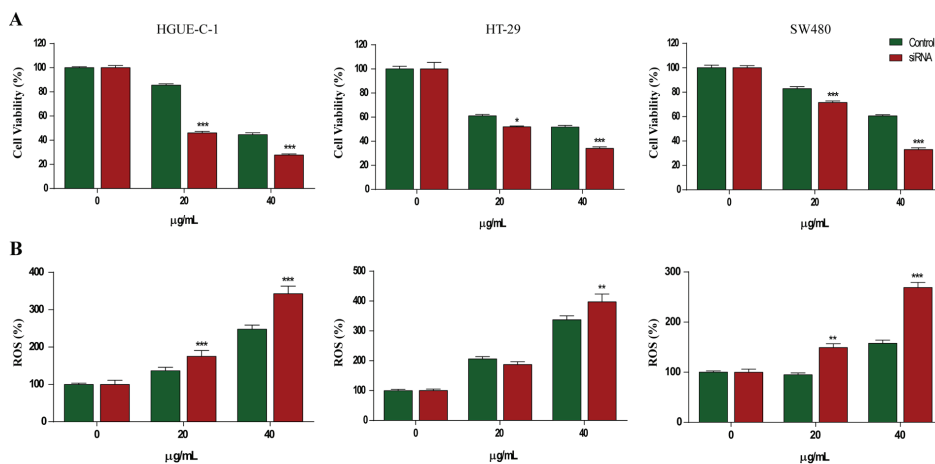


Figure 4. Nrf2 transcription factor silencing increases RE-induced cell death in colon cancer cells. (A) Measurement of cell viability (%) of the three colon cancer cell lines, i.e. HGUE-C-1, HT-29 and SW480 in the absence (control) or in the presence of 20 µg/mL or 40 µg/mL of RE, in the absence or in the presence of an Nrf2 specific siRNA. (B) Measurement of intracellular ROS levels (%) in the three cell lines treated in the same conditions as above using H₂DCFDA dye.

In vivo effects of RE on tumorigenicity of HT-29 cells in athymic mouse model. Having identified significant *in vitro* antiproliferative and necrotic activity and the putative mechanism of RE antiproliferative effects, the next step was to determine whether these results could be translated to an *in vivo* model. For this purpose, HT-29 cells were implanted in athymic nude mice and two different oral treatments with RE were assayed: a) 2 weeks pretreatment + cells inoculation + treatment; b) cells inoculation + treatment. To assess overall general health and well-being of animals during treatment, body weights were recorded once a week. RE-treatment did not cause any loss in body weight (data not shown) or change in food intake and there were no apparent signs of toxicity in animals according to the welfare list punctuation approved by the ethical committee. The average volume of tumors in control mice increased as a function of time and reached an end point of 1,000 mm³ in 35 days post-inoculation. As shown in Fig. 5, both treatments significantly reduced the measurements of tumor volume. RE treatment for 7 weeks (2 weeks pre-treatment + 5 weeks treatment) significantly reduced tumor volume by 34.1% ($p < 0.001$), whereas RE treatment after cells inoculation reduced tumor volume 27.5% ($p < 0.001$).

Discussion

This work was intended to deepen into the mechanism of our previous research that showed the antiproliferative activity of a well characterized rosemary extract in correlation to its effects on the gene expression of colon cancer cells using transcriptomic and metabolomics analysis^{13,18,19}. Our previous research characterized in detail by HPLC-ESI-QTOF-MS the composition of the RE utilized in the present work, showing that diterpenes (CA and CAR) and triterpenes (UA and BA) were the most abundant compounds¹³. This study also revealed that the antiproliferative capacity of the RE was stronger than that of their isolated fractions so cell studies on the putative synergistic effects of single compounds present in the extract should be undertaken. Therefore, in this work, potential synergistic effects among four of the most abundant compounds in the extract, two diterpenes, CA and CAR, and two triterpenes (UA and BA) were suggested. When the four terpenoids were individually considered, significant antiproliferative activity was observed for each one, in correlation with previously reported data (reviewed in¹³). The triterpenes antiproliferative activity was higher than that of diterpenes and this, in turn, a little higher than that of the whole RE. When these four compounds were studied in pairwise combinations, interesting pharmacological interactions between them were discovered although the different methods used brought some differences.

As shown by FICI and Compusyn methods, most of the pairwise combinations between di- and triterpenes showed additivity or mild synergy, which could explain the higher activity of RE when compared with individual and combined compounds. In contrast, the triterpene combination UA-BA always brought antagonism no matter the method used, indicating a putative competitive mechanism between them. Nevertheless, this antagonism did not seem to be strong enough to counterbalance the additive or synergic interaction between diterpenes and between di and triterpenes in the whole extract. Given that the isobole method is a semiquantitative and graphical approach, the results obtained through this method may be questionable³³. In contrast, FICI calculation and Compusyn software gave more consistent results between them, and their differences could be attributed to the different mathematical approach used. The polygonogram obtained by the Compusyn software (Supplementary Figure 3) summarizes the types of interactions between the main terpenes present in the extract, i.e. antagonism

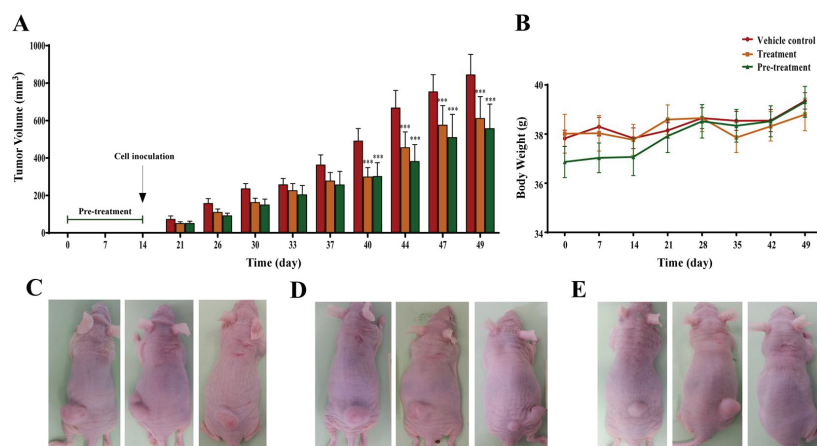


Figure 5. RE oral administration decreases tumor volume in athymic nude mice. (A) Tumor volumes (mm³) in the absence (vehicle control), pre-treatment (two weeks oral administration of RE before cell inoculation) or treatment (administration of RE after cell inoculation) groups at doses of 200 mg/kg of RE (oral administration) in a xenograft model of colon cancer cells using athymic nude mice. Animals were monitored twice a week during 35 days. (B) The body weight (g) of the animals was recorded during the assay for the three groups. Representative images of tumor formation in (C) vehicle-control, (D) treatment and (E) pre-treatment groups.

between the triterpenes BA-UA, a strong synergistic behavior between the diterpenes CAR and CA, but also synergism between diterpenes and triterpenes, i.e. CAR-UA, CAR-BA, CA-UA and CA-BA.

Therefore, these interactions may account for the strong antiproliferative capacity of whole RE. In this regard, a synergistic behavior between compounds in natural extracts has been also described not only for anticancer activity^{34,35} but also for antimicrobial³⁶ or antilipidemic³⁷ activities.

In an attempt to illustrate the mechanism of the *in vitro* antiproliferative capacity of RE, a set of assays were utilized to determine the capacity of RE to modulate several signatures of tumorigenesis such as proliferation, migration and invasion. Previous studies using the same RE showed a dose-response decrease of colon cancer cell viability¹³. RTCA experiments confirmed that the inhibition of cell proliferation was one of the effects exerted by RE, which could be complemented by a cytotoxic effect. This antiproliferative effects of RE were also confirmed in the three colon cancer cell models in a dose response manner, regardless of the different pheno and genotype of the cell line.

We next investigated whether RE is able to inhibit *in vitro* several signatures of cancer metastasis such as migration, invasion and clonogenic survival. In metastasis, cancer cells with epithelial phenotype migrate away from primary tumor crossing the basement membrane, a network of extracellular matrix, and later migrate through the stroma reaching blood or lymph vessels, where they can be carried to other organs³⁸. Once in other tissues, their invasiveness will depend on their clonogenic survival. RE severely reduced both, the cell migration in a wound-healing assay and the clonogenic survival of the three colon cancer cells in a dose-response manner, indicating that RE would not be able only to reduce tumor growth and proliferation but also their invasion and migration capabilities, which indicates a lower metastatic potential as the main hallmark of cancer.

Our cell cycle results indicate alterations of the cell cycle by RE such as late apoptosis and a decrease in G0/G1 phase with a concomitant accumulation of cells in the G2/M, especially in HT-29 and SW480 cell lines, in agreement to previously reported^{18,19,34,39}. The analysis of a panel of apoptosis-related proteins revealed that RE did not substantially change the expression of these proteins (Supplementary Figure 5). Only mild but statistically significant decrease was observed for two proapoptotic proteins (Bax and HTRA), although, with no biological relevance. A more relevant decrease was obtained for survivin in HGU-E-C-1 and SW480 cells. Survivin plays an important role in cancer development, and it has been involved in the resistance of tumor cells to both radiotherapy and chemotherapy⁴⁰. A recent meta-analysis showed that the upregulation of survivin is associated with poor prognosis in patients with colorectal cancer⁴¹. Nevertheless, these alterations in cell cycle and apoptosis proteins do not seem to justify the strong antiproliferative capacity of RE.

Further experiments using LDH leakage confirmed that necrosis was the main death mechanism (Fig. 2C), which was confirmed by morphological observation. This necrosis mechanism was also concomitant to a dose-response increase of intracellular ROS, the loss of mitochondrial potential and the activation of the Nrf2 pathway, as confirmed by Nrf2 gene silencing experiments (Fig. 4). These results confirm previous metabolomic studies that show increased expression of antioxidant enzymes and activation of Nrf2 pathway in HT-29 cells treated with CA¹⁹. These results also may offer new opportunities for alternative targeted antitumor therapies based on the combination of rosemary compounds and small Nrf2 inhibitors for certain types of cancers⁴².

Once the antiproliferative capacity as well as the inhibition of migration and invasion of colon cancer cells by RE was demonstrated *in vitro*, we examined its inhibitory role on tumor growth in a xenograft model of HT-29 colon cancer cells. The capacity of RE (200 mg/kg three times a week, p.o.) to reduce tumor size was demonstrated in a four weeks assay. Further, oral pretreatment for two weeks before cell inoculation followed by the treatment seemed to be more effective than just the treatment itself. These results confirmed those reported with other rosemary extracts and/or compounds using xenografts of SW620 or HCT116 colon cancer cells in athymic nude mice¹². Although preliminary bioavailability studies point out that diterpenes, and especially CA, show higher absorption and permeability than other rosemary compounds^{43,44}, further studies must be done to identify the potential metabolites responsible for such anticancer effects. As part of the preclinical approach, the histopathological and macroscopic analysis confirmed the absence of toxicity in an oral acute toxicity assay according OCDE 420 guidance. According to the Globally Harmonized System (GHS) of Classification and Labelling of Chemicals, RE was rated as non-classified substance at a dose of 2000 mg/kg⁴⁵, as reported for other rosemary extracts⁴⁶.

Previously reported studies in colon cancer cells postulate that rosemary compounds exert antiproliferative effects by inhibiting proliferative and survival signaling pathways such as PI3K/Akt, as well as modulating Nrf2 transcription factor pathway^{18,47}. Apoptosis and cell cycle arrest has also been proposed as part of the antiproliferative mechanism of RE^{18,48,49}. Nevertheless, our study suggest that necrosis rather than apoptosis is the mechanism to account for colon cancer cell death. In agreement to our results, a recent proteomic analysis in colon cancer cells also revealed that RE altered proteins implicated in the activation of Nrf2 transcription factor and the unfolded protein response (UPR)⁴⁸.

In this work, we have corroborated the prooxidant effects of rosemary compounds, recently reported by our group⁴⁷, as mediator of their antiproliferative effects. According to our results and those previously reported, we postulate that ROS generated by RE in colon cancer cells may be responsible for an exacerbated UPR response and endoplasmic reticulum stress (ERS) leading to the activation of Nrf2, apoptosis and autophagy as defense mechanisms. Under this scenario, autophagy may be unable to counter excessive redox imbalance and cellular stress, and cell homeostasis evolves into necrotic cell death. Targeting colon cancer cells by increasing intracellular ROS and decreasing cell survival response may increase the therapeutic potential of RE compounds as in combination to chemotherapeutic drugs.

In conclusion, we reveal that RE compounds show the *in vitro* capability to inhibit cellular proliferation, migration and invasiveness of colon cancer cells. The treatment of cancer cells with RE leads to a strong increase of intracellular ROS that results in necrosis cell death. According to our results, Nrf2 transcription factor pathway seems to be involved in cell survival upon RE treatment. These *in vitro* results were in line with a reduction of tumor growth by RE in a xenograft model of colon cancer cells in athymic nude mice. Whether similar antiproliferative mechanism takes place *in vivo* or not, requires preclinical studies to correlate the presence of rosemary metabolites with metabolic biomarkers.

Materials and Methods

Chemicals and cell culture. All chemicals, reagents and the rosemary extract obtained by supercritical fluid extraction are described in detail in the Supplementary information. Cells were grown in DMEM supplemented with 5% heat-inactivated FBS, 2 mM L-glutamine, penicillin-streptomycin (0.1 mg/mL penicillin and 100 U/mL streptomycin) at 37 °C in a humidified atmosphere with 5% CO₂. Colon adenocarcinoma HT-29 and SW480 cells were obtained from the IMIM (Institut Municipal d'Investigació Mèdica, Barcelona, Spain) and ATCC (American Type Culture Collection, LGC Promochem, UK), respectively, and HGUE-C-1 was an established cell line derived from a primary colon cancer cell line of a single primary human colon carcinoma at the Hospital General Universitario de Elche (Alicante, Spain), as described¹³. The cells were trypsinized every three days and they were seeded in 96- or 6-well plates depending on the assay¹³.

Synergy studies. The concentration that inhibited 50% of the cell growth (IC₅₀ value) of every single compound and those of their pairwise combinations were estimated by 3-(4,5-dimethylthiazol-2-yl)-2,5-diphenyltetrazolium bromide (MTT) assay as previously described¹³ (see Supplementary material for detailed methodology). The results of synergy studies were interpreted by using three different methods: fractionated inhibitory concentration index (FICI), Isobolographic method and Compusyn software⁵⁰. Further information about these methods to determine synergy is provided in the Supplementary information.

Cell cycle, apoptosis and mitochondrial membrane potential (MMP) analysis. Human colorectal cancer cell lines (15 × 10⁴ cells/well) were seeded into 6-well plates. After 24 h of culture, cells were treated with different concentrations of RE (10–40 µg/mL) for 24 h. Afterwards, the treatment, cell cycle phase pattern, apoptosis and mitochondrial membrane potential were determined by using different kits for Muse Cell Analyzer (Merck-Millipore, Darmstadt, Germany) according to the manufacturer's instructions. Additional information on these procedures is provided in Supplementary material. MMP was also evaluated by a different method using MitoTracker Red CMXRos and MitoTracker Green fluorescent probes, which is also detailed in Supplementary information.

Measurement of plasma membrane integrity. A cytotoxicity detection kit based on the extracellular detection of lactate dehydrogenase (LDH) was used to monitor cell integrity. Human colorectal cancer cell lines (5 × 10³ cells/well) were seeded into 96-well plates. Cells were treated for 24 h with RE (10–40 µg/mL), centrifuged, and 100 µL of the cell culture supernatant transferred to a clean 96-well plate. The LDH detection reagent was added and incubated for 15 min in the dark, and absorbance read at 492 nm (reference filter 600 nm). LDH leakage (% cytotoxicity) was calculated as follows:

$$\text{Cytotoxicity(\%)} = \frac{\text{exp. value} - \text{low control}}{\text{high control} - \text{low control}} \times 100$$

where *low control* represents LDH activity released from the untreated normal cells (spontaneous LDH release) and *high control* represents maximum releasable LDH activity in the cells (maximum LDH release).

Evaluation of the intracellular reactive oxygen species (ROS) generation. Intracellular ROS levels were measured using 2',7'-dichlorofluorescein diacetate (H₂DCFDA) probe (Molecular probes, Life Technologies Co., Europe). Human colorectal cancer cell lines (5×10^3 cells/well) were seeded into 96-well black plates. Cells were treated for 24 h with RE (10–40 $\mu\text{g}/\text{mL}$) and probed with 10 $\mu\text{g}/\text{mL}$ of H₂DCFDA. Fluorescence was detected by excitation at 485 nm and emission at 535 nm using a microplate reader (POLARstar Omega, BMG LabTech GmbH, Offenburg, Germany).

RNA interference assay. Cells were transfected with siRNA specific for Nrf2 by using Lipofectamine (Invitrogen, Europe) according to the manufacturer's instructions. The silencing ability of all siRNAs was determined by Dot Blot analysis (see Supplementary information for details). At 24 h post-transfection, cells were treated with the RE (20 or 40 $\mu\text{g}/\text{mL}$). After treatment cell viability, ROS level and protein expression were studied.

Wound healing assay. The ability of cells to migrate was assayed by wound healing assay. Human colorectal cancer cell lines were seeded in a 96-well plate and incubated at 37 °C. When confluent, cells were scratched with a 10- μL pipette tip, followed by washing with PBS. The cells were then treated with RE in complete medium for 72 h. Cells were stained with Hoechst 33342 reagent, and the population of cells that migrated into the scratched area was quantified by Cytation 3 Cell Imaging Multi-Mode Reader (BioTek, Germany). Quantitation of the migrated cells was measured using Image J software. Wound healing rate was assessed by calculating the wound area fraction between wound width at 0 and 72 h.

Real-Time Cell Analysis (RTCA) proliferation assay. Cell proliferation was studied using RTCA DP instrument *xCELLigence* system (Roche Diagnostics GmbH, Germany), which was placed in a humidified incubator maintained at 5% CO₂ at 37 °C. Thereafter, 7500–40000 cells (depending on cell line) were added to each well of E-plates (Roche Diagnostics GmbH, Germany) and were incubated at room temperature to allow the cells to settle. The plates were then placed in the *xCELLigence* system. After 24 h, cells were treated with RE (20 or 40 $\mu\text{g}/\text{mL}$) for 72 h. Cell growth and proliferation were monitored through the cell index (CI) values, provided by the instrument, and data analysis was performed with the supplied RTCA software.

Colony formation assay. Human colorectal cancer cell lines cells (5×10^3 cells/well) were seeded into 6-well plates. After being attached to the plate, the cells were treated at 20 or 40 $\mu\text{g}/\text{mL}$ of RE for 24 h and then cultured with fresh medium for 7 days. After that, medium was removed, and cells washed twice with PBS. The colonies were fixed with 95% ethanol for 10 min, dried and stained with 0.1% crystal violet solution for 10 min, and the plate was washed three times with water. Colonies on the plate were counted under a microscope, and each colony consisted of more than 50 cells.

In vivo experiments. An acute oral toxicity test was performed as described in Organization for Economic Cooperation and Development (OECD) 420 guideline using Fixed Dose Procedure to minimize the use of animals (see details in the Supplementary information).

In vivo antiproliferative activity of RE was determined by using male nude mice in which, xenografts of human colon cancer cells (HT-29) were established subcutaneously. Animals were randomly divided into three groups ($n = 10$ –12). In the first group, animals were treated orally with RE for two weeks before cell inoculation. In the second group, RE was administered to animals after cell inoculation, and in the last group (control), animals were treated only with the vehicle. Refer to additional information in Supplementary information.

The *in vivo* experimental protocols were approved by Ethics Committee of the Miguel Hernández University (references IBM-VMM-001-11 and UMH-IBM-VMM-02-14), according to the Spanish and European regulation and animal welfare guides.

Statistical Analysis. The data were expressed as the mean \pm standard deviation (SD) of 4–10 determinations, depending on the assay. One-way analysis of variance (ANOVA) and statistical comparisons of the different treatments were performed using Tukey's test in GraphPad Prism version 5.0 (GraphPad Software)²⁷. Data are expressed as mean \pm SD. * ($p < 0.05$), ** ($p < 0.01$) or *** ($p < 0.001$) indicate statistically significant differences compared to control unless otherwise stated.

References

- Torre, L. A. *et al.* Global cancer statistics, 2012. *CA. Cancer J. Clin.* **65**, 87–108, <https://doi.org/10.3322/caac.21262> (2015).
- Rajamanickam, S. & Agarwal, R. Natural products and colon cancer: current status and future prospects. *Drug development research* **69**, 460–471, <https://doi.org/10.1002/ddr.20276> (2008).
- Xu, G. L. *et al.* Chemical Composition, Antioxidative and Anticancer Activities of the Essential Oil: Curcuma rhizoma-Sparganii Rhizoma, a Traditional Herb Pair. *Molecules* **20**, 15781–15796, <https://doi.org/10.3390/molecules200915781> (2015).
- Balakrishna, A. & Kumar, M. H. Evaluation of Synergetic Anticancer Activity of Berberine and Curcumin on Different Models of A549, Hep-G2, MCF-7, Jurkat, and K562 Cell Lines. *BioMed research international* **2015**, 354614, <https://doi.org/10.1155/2015/354614> (2015).
- Hardman, W. E. Diet components can suppress inflammation and reduce cancer risk. *Nutrition research and practice* **8**, 233–240, <https://doi.org/10.4162/nrp.2014.8.3.233> (2014).

6. Kim, H. J., Park, S. Y., Lee, H. M., Seo, D. I. & Kim, Y. M. Antiproliferative effect of the methanol extract from the roots of Hep3B hepatocellular carcinoma cells and. *Experimental and therapeutic medicine* **9**, 1791–1796, <https://doi.org/10.3892/etm.2015.2296> (2015).
7. Menendez, J. A. *et al.* Xenohormetic and anti-aging activity of secoiridoid polyphenols present in extra virgin olive oil: A new family of gerosuppressant agents. *Cell Cycle* **12**, 555–578, <https://doi.org/10.4161/cc.23756> (2013).
8. Raskovic, A. *et al.* Antioxidant activity of rosemary (*Rosmarinus officinalis* L.) essential oil and its hepatoprotective potential. *BMC Complement Altern Med* **14**, 225, <https://doi.org/10.1186/1472-6882-14-225> (2014).
9. Dias, P. C., Foglio, M. A., Possenti, A. & de Carvalho, J. E. Antilcerogenic activity of crude hydroalcoholic extract of *Rosmarinus officinalis* L. *J. Ethnopharmacol.* **69**, 57–62 (2000).
10. Aoki, A. *et al.* Preparation of pH-sensitive anionic liposomes designed for drug delivery system (DDS) application. *Journal of oleo science* **64**, 233–242, <https://doi.org/10.5650/jos.ess14157> (2015).
11. Arai, T. *et al.* Novel local drug delivery system using thermoreversible gel in combination with polymeric microspheres or liposomes. *Anticancer Res.* **30**, 1057–1064 (2010).
12. Moore, J., Yousef, M. & Tsiani, E. Anticancer effects of rosemary (*Rosmarinus officinalis* L.) extract and rosemary extract polyphenols. *Nutrients* **8**, <https://doi.org/10.3390/nu8110731> (2016).
13. Borrás-Linares, I. *et al.* A bioguided identification of the active compounds that contribute to the antiproliferative/cytotoxic effects of rosemary extract on colon cancer cells. *Food Chem. Toxicol.* **80**, 215–222, <https://doi.org/10.1016/j.fct.2015.03.013> (2015).
14. Bozin, B., Mimica-Dukic, N., Samojlik, I. & Jovin, E. Antimicrobial and antioxidant properties of rosemary and sage (*Rosmarinus officinalis* L. and *Salvia officinalis* L., Lamiaceae) essential oils. *J. Agric. Food Chem.* **55**, 7879–7885, <https://doi.org/10.1021/jf0715323> (2007).
15. Del Campo, J., Amiot, M. J. & Nguyen-The, C. Antimicrobial effect of rosemary extracts. *J. Food Prot.* **63**, 1359–1368 (2000).
16. Perez-Fons, L., Garzon, M. T. & Micol, V. Relationship between the antioxidant capacity and effect of rosemary (*Rosmarinus officinalis* L.) polyphenols on membrane phospholipid order. *J. Agric. Food Chem.* **58**, 161–171, <https://doi.org/10.1021/jf9026487> (2010).
17. Bakirel, T., Bakirel, U., Keles, O. U., Ulgen, S. G. & Yardibi, H. *In vivo* assessment of antidiabetic and antioxidant activities of rosemary (*Rosmarinus officinalis*) in alloxan-diabetic rabbits. *J. Ethnopharmacol.* **116**, 64–73, <https://doi.org/10.1016/j.jep.2007.10.039> (2008).
18. Valdés, A. *et al.* Effect of rosemary polyphenols on human colon cancer cells: Transcriptomic profiling and functional enrichment analysis. *Genes and Nutrition* **8**, 43–60, <https://doi.org/10.1007/s12263-012-0311-9> (2013).
19. Valdes, A. *et al.* Comprehensive foodomics study on the mechanisms operating at various molecular levels in cancer cells in response to individual rosemary polyphenols. *Anal. Chem.* **86**, 9807–9815, <https://doi.org/10.1021/ac502401j> (2014).
20. Entschladen, F., Drell, T. L. 4th, Lang, K., Joseph, J. & Zaenker, K. S. Tumour-cell migration, invasion, and metastasis: navigation by neurotransmitters. *The Lancet. Oncology* **5**, 254–258, [https://doi.org/10.1016/S1470-2045\(04\)01431-7](https://doi.org/10.1016/S1470-2045(04)01431-7) (2004).
21. Chan, F. K., Moriwaki, K. & De Rosa, M. J. Detection of necrosis by release of lactate dehydrogenase activity. *Methods Mol. Biol.* **979**, 65–70, https://doi.org/10.1007/978-1-62703-290-2_7 (2013).
22. Saad, B. *et al.* Evaluation of medicinal plant hepatotoxicity in co-cultures of hepatocytes and monocytes. *Evid Based Complement Alternat Med* **3**, 93–98, <https://doi.org/10.1093/ecam/nel002> (2006).
23. Vandenneele, P., Galluzzi, L., Vanden Berghe, T. & Kroemer, G. Molecular mechanisms of necroptosis: an ordered cellular explosion. *Nature reviews. Molecular cell biology* **11**, 700–714, <https://doi.org/10.1038/nrm2970> (2010).
24. Galluzzi, L. *et al.* Molecular definitions of cell death subroutines: recommendations of the Nomenclature Committee on Cell Death 2012. *Cell Death Differ.* **19**, 107–120, <https://doi.org/10.1038/cdd.2011.96> (2012).
25. Degterev, A. *et al.* Identification of RIP1 kinase as a specific cellular target of necrostatins. *Nature chemical biology* **4**, 313–321, <https://doi.org/10.1038/nchembio.83> (2008).
26. Chen, P. *et al.* Synergistic inhibition of autophagy and neddylation pathways as a novel therapeutic approach for targeting liver cancer. *Oncotarget* **6**, 9002–9017, <https://doi.org/10.18632/oncotarget.3282> (2015).
27. Pérez-Sánchez, A. *et al.* Protective effects of citrus and rosemary extracts on UV-induced damage in skin cell model and human volunteers. *Journal of Photochemistry and Photobiology B: Biology* **136**, 12–18, <https://doi.org/10.1016/j.jphotobiol.2014.04.007> (2014).
28. Day, R. M. & Suzuki, Y. J. Cell proliferation, reactive oxygen and cellular glutathione. *Dose-response: a publication of International Hormesis Society* **3**, 425–442, <https://doi.org/10.2203/dose-response.003.03.010> (2005).
29. Golstein, P. & Kroemer, G. Cell death by necrosis: towards a molecular definition. *Trends Biochem. Sci.* **32**, 37–43, <https://doi.org/10.1016/j.tibs.2006.11.001> (2007).
30. Maher, J. M. *et al.* Oxidative and electrophilic stress induces multidrug resistance-associated protein transporters via the nuclear factor-E2-related factor-2 transcriptional pathway. *Hepatology* **46**, 1597–1610, <https://doi.org/10.1002/hep.21831> (2007).
31. Uruno, A. & Motohashi, H. The Keap1-Nrf2 system as an *in vivo* sensor for electrophiles. *Nitric Oxide* **25**, 153–160, <https://doi.org/10.1016/j.niox.2011.02.007> (2011).
32. Alemán, C. Reference database for the principal physiological indicators in three species of laboratory animal. *Lab. Anim.* **34**, 358–378, <https://doi.org/10.1258/002367700780387741> (2000).
33. Wagner, H. Synergy research: approaching a new generation of phytopharmaceuticals. *Fitoterapia* **82**, 34–37, <https://doi.org/10.1016/j.fitote.2010.11.016> (2011).
34. Einbond, L. S. *et al.* Carnosic acid inhibits the growth of ER-negative human breast cancer cells and synergizes with curcumin. *Fitoterapia* **83**, 1160–1168, <https://doi.org/10.1016/j.fitote.2012.07.006> (2012).
35. Hemalswarya, S. & Doble, M. Potential synergism of natural products in the treatment of cancer. *Phytother. Res.* **20**, 239–249, <https://doi.org/10.1002/ptr.1841> (2006).
36. Tomás-Menor, L. *et al.* The promiscuous and synergic molecular interaction of polyphenols in bactericidal activity: An opportunity to improve the performance of antibiotics? *Phytother. Res.* **29**, 466–473, <https://doi.org/10.1002/ptr.5296> (2015).
37. Herranz-Lopez, M. *et al.* Synergism of plant-derived polyphenols in adipogenesis: perspectives and implications. *Phytomedicine* **19**, 253–261, <https://doi.org/10.1016/j.phymed.2011.12.001> (2012).
38. Clark, A. G. & Vignjevic, D. M. Modes of cancer cell invasion and the role of the microenvironment. *Curr. Opin. Cell Biol.* **36**, 13–22, <https://doi.org/10.1016/j.cob.2015.06.004> (2015).
39. Visanji, J. M., Thompson, D. G. & Padfield, P. J. Induction of G2/M phase cell cycle arrest by carnosol and carnosic acid is associated with alteration of cyclin A and cyclin B1 levels. *Cancer Lett.* **237**, 130–136, <https://doi.org/10.1016/j.canlet.2005.05.045> (2006).
40. Waligorska-Stachura, J. *et al.* Survivin—prognostic tumor biomarker in human neoplasms—review. *Ginekol. Pol.* **83**, 537–540 (2012).
41. Huang, Y. J. *et al.* The prognostic value of survivin expression in patients with colorectal carcinoma: a meta-analysis. *Jpn. J. Clin. Oncol.* **43**, 988–995, <https://doi.org/10.1093/jcco/hyt103> (2013).
42. Singh, A. *et al.* Small Molecule Inhibitor of NRF2 Selectively Intervenes Therapeutic Resistance in KEAP1-Deficient NSCLC Tumors. *ACS Chem Biol* **11**, 3214–3225, <https://doi.org/10.1021/acscchembio.6b00651> (2016).
43. Perez-Sanchez, A. *et al.* Evaluation of the intestinal permeability of rosemary (*Rosmarinus officinalis* L.) extract polyphenols and terpenoids in Caco-2 cell monolayers. *PLoS ONE* **12**, e0172063, <https://doi.org/10.1371/journal.pone.0172063> (2017).
44. Fernandez-Ochoa, A. *et al.* Phenolic compounds in rosemary as potential source of bioactive compounds against colorectal cancer: *In situ* absorption and metabolism study. *J. Func Food* **33**, 202–210, <https://doi.org/10.1016/j.jff.2017.03.046> (2017).

45. Anonymous. *Globally Harmonized System of Classification and Labelling of Chemicals (GHS)*. 60 (2005).
46. Anadon, A. *et al.* Acute oral safety study of rosemary extracts in rats. *J. Food Prot.* **71**, 790–795 (2008).
47. Valdes, A., Garcia-Canas, V., Kocak, E., Simo, C. & Cifuentes, A. Foodomics study on the effects of extracellular production of hydrogen peroxide by rosemary polyphenols on the anti-proliferative activity of rosemary polyphenols against HT-29 cells. *Electrophoresis* **37**, 1795–1804, <https://doi.org/10.1002/elps.201600014> (2016).
48. Valdes, A., Artemenko, K. A., Bergquist, J., Garcia-Canas, V. & Cifuentes, A. Comprehensive Proteomic Study of the Antiproliferative Activity of a Polyphenol-Enriched Rosemary Extract on Colon Cancer Cells Using Nanoliquid Chromatography-Orbitrap MS/MS. *Journal of proteome research* **15**, 1971–1985, <https://doi.org/10.1021/acs.jproteome.6b00154> (2016).
49. Valdés, A., Sullini, G., Ibáñez, E., Cifuentes, A. & García-Cañas, V. Rosemary polyphenols induce unfolded protein response and changes in cholesterol metabolism in colon cancer cells. *Journal of Functional Foods* **15**, 429–439, <https://doi.org/10.1016/j.jff.2015.03.043> (2015).
50. Chou, T. C. Theoretical basis, experimental design, and computerized simulation of synergism and antagonism in drug combination studies. *Pharmacol. Rev.* **58**, 621–681, <https://doi.org/10.1124/pr.58.3.10> (2006).

Acknowledgements

This work was supported by projects AGL2011-29857-C03-02 and AGL2011-29857-C03-03 (Spanish Ministry of Science and Innovation); AGL2015-67995-C3-1-R (Spanish Ministry of Economy and Competitiveness (MINECO)); PROMETEO/2012/007, PROMETEO/2016/006, ACOMP/2013/093, ACIF/2013/064, ACIF/2015/158, APOTIP/2017/003 and APOSTD/2017/023 (Generalitat Valenciana), and CIBER (CB12/03/30038, Fisiopatologia de la Obesidad y la Nutricion, CIBERobn, Instituto de Salud Carlos III, Spain).

Author Contributions

A.P.S. developed all the experiments and wrote and reviewed the manuscript. E.B.C. collaborated with animal studies, reviewed the manuscript and codirected the study. V.R.T. collaborate in cellular experiments. L.M.A.C. was the responsible of synergy studies. M.H.L. reviewed the manuscript and collaborated with direction responsibilities. A.V. and A.C. provided the rosemary extract and collaborated in study design. Finally, V.M. directed the study and reviewed the manuscript.

Additional Information

Competing Interests: The authors declare no competing interests.

Publisher's note: Springer Nature remains neutral with regard to jurisdictional claims in published maps and institutional affiliations.

 **Open Access** This article is licensed under a Creative Commons Attribution 4.0 International License, which permits use, sharing, adaptation, distribution and reproduction in any medium or format, as long as you give appropriate credit to the original author(s) and the source, provide a link to the Creative Commons license, and indicate if changes were made. The images or other third party material in this article are included in the article's Creative Commons license, unless indicated otherwise in a credit line to the material. If material is not included in the article's Creative Commons license and your intended use is not permitted by statutory regulation or exceeds the permitted use, you will need to obtain permission directly from the copyright holder. To view a copy of this license, visit <http://creativecommons.org/licenses/by/4.0/>.

© The Author(s) 2019



Contents lists available at ScienceDirect

Journal of Chromatography A

journal homepage: www.elsevier.com/locate/chroma

Shotgun proteomic analysis to study the decrease of xenograft tumor growth after rosemary extract treatment



Alberto Valdés^a, Virginia García-Cañas^b, Almudena Pérez-Sánchez^c, Enrique Barrajón-Catalán^c, Verónica Ruiz-Torres^c, Konstantin A. Artemenko^d, Vicente Micol^{c,e}, Jonas Bergquist^d, Alejandro Cifuentes^{a,*}

^a Laboratory of Foodomics, Institute of Food Science Research (CIAL, CSIC), Nicolas Cabrera 9, 28049, Madrid, Spain

^b Molecular Nutrition and Metabolism, Institute of Food Science Research (CIAL, CSIC), Nicolas Cabrera 9, 28049 Madrid, Spain

^c Institute of Molecular and Cellular Biology, Miguel Hernández University, Avda. Universidad s/n, Elche 03202, Spain

^d Analytical Chemistry, Department of Chemistry-BMC, Uppsala University, Husargatan 3, 75124 Uppsala, Sweden

^e CIBER, Fisiopatología de la Obesidad y la Nutrición, CIBERobn, Instituto de Salud Carlos III (CB12/03/30038), Spain

ARTICLE INFO

Article history:

Received 16 February 2017

Received in revised form 23 March 2017

Accepted 25 March 2017

Available online 27 March 2017

Keywords:

Colon cancer

Dimethyl labeling

Mass spectrometry

Rosemary extract

Quantitative proteomics

Xenograft mice

ABSTRACT

The antiproliferative activity of Rosemary (*Rosmarinus officinalis*) has been widely studied in different *in vitro* and *in vivo* models, which demonstrate that rosemary extracts inhibit the cellular proliferation due to its ability to interact with a wide spectrum of molecular targets. However, a comprehensive proteomics study *in vivo* has not been carried out yet. In the present work, the effects of rosemary extract on xenograft tumor growth has been studied and, for the first time, a shotgun proteomic analysis based on nano-LC-MS/MS together with stable isotope dimethyl labeling (DML) has been applied to investigate the global protein changes *in vivo*. Our results show that the daily administration of a polyphenol-enriched rosemary extract reduces the progression of colorectal cancer *in vivo* with the subsequent deregulation of 74 proteins. The bioinformatic analysis of these proteins indicates that the rosemary extract mainly alters the RNA Post-Transcriptional Modification, the Protein Synthesis and the Amino Acid Metabolism functions and suggests the inactivation of the oncogene MYC. These results demonstrate the high utility of the proposed analytical methodology to determine, simultaneously, the expression levels of a large number of protein biomarkers and to generate new hypothesis about the molecular mechanisms of this extract *in vivo*.

© 2017 Elsevier B.V. All rights reserved.

1. Introduction

Rosemary (*Rosmarinus officinalis*) is an aromatic plant that belongs to the Lamiaceae family that due to its organoleptic and antioxidant characteristics has been used since ancient times for culinary purposes, as a flavoring and preservative. In addition, rosemary has also been attributed various medicinal properties, such as antimicrobial [1], anti-inflammatory [2] or antioxidant [3], as well as other beneficial effects on health, since it helps in the protection and treatment of diseases such as diabetes [4], cardiovascular diseases [5] or cancer [6]. Modern techniques of analysis have allowed the identification and quantification of the main compounds of rosemary, and the study of their effects on health. Among these effects, the anticancer activity of rosemary extract and its major

polyphenols (carnosic acid and carnosol) has been well studied *in vitro* using different cancer cell lines [7–12], as well as non-tumor lines [13]. The chemoprotective activity of rosemary and its major compounds has been linked to their ability to sequester free radicals, which could protect against oxidative damage of lipids, proteins and DNA [14]. These compounds could also induce the oxidative stress response modulated by the Nuclear Factor (Erythroid-Derived 2)-like 2 (NRF2), which regulates the expression of numerous genes involved in the antioxidant response, in detoxification processes, or in the generation of NADPH [15]. Besides to the protective effects derived from the oxidative stress response, there are also studies suggesting that these polyphenols have antiproliferative activity due to its ability to interact with a wide spectrum of molecular targets [6,16,17]. Moreover, and due to the successful results obtained using *in vitro* models, different *in vivo* studies have been carried out demonstrating that rosemary extracts inhibit the cellular proliferation in mice xenograft with colon and prostate cancer cells [18,19]. In these studies, the

* Corresponding author.

E-mail address: a.cifuentes@csic.es (A. Cifuentes).

authors specifically examined the expression of Sestrin 2, Androgen Receptor (AR), Prostate-specific antigen (PSA), CCAAT-enhancer-binding protein Homologous Protein (CHOP) and NRF2 proteins, using for the measurement the Western blot targeted approach. However, an unbiased comprehensive proteomics study should provide more information about the effects of rosemary extracts *in vivo*. Recently, the application of nano-LC–MS/MS combined with stable isotope dimethyl labeling (DML) has demonstrated to be a powerful methodology to identify important molecular changes induced by rosemary polyphenols *in vitro* [17,20]. Therefore, the aim of the present work is to study the effects of rosemary extract on xenograft tumor growth and to apply, for the first time, a DML and nano-LC–MS/MS approach to investigate the global protein changes in tumors to gain a broader knowledge of the molecular effect of this extract *in vivo*.

2. Material and methods

2.1. Chemicals

Acetonitrile (ACN), methanol (MeOH), formic acid (FA), ammonia solution, NaCl and urea were obtained from Merck (Darmstadt, Germany). Acetone, EDTA, protease inhibitor cocktail, phosphate buffered saline (PBS) solution, *n*-octyl- β -D-glucopyranoside (BOG), triethyl ammonium bicarbonate (TEAB), NaVO₄, NaF, β -glycerophosphate, Na₄P₂O₇, formaldehyde (CH₂O, 37% (v/v) in water), deuterated (CD₂O) and ¹³C-labeled formaldehyde (¹³CD₂O, 20% (v/v) in water), iodoacetamide (IAA) and dithiothreitol (DTT) were purchased from Sigma Aldrich (St. Louis, MO). Trypsin/Lys-C Mix (Mass Spec Grade V5072) was purchased from Promega (Madison, WI). Sodium cyanoborohydride (NaBH₃CN) was purchased from Fluka (Buchs, Switzerland). Ultrapure water was prepared by Milli-Q water purification system (Millipore, Bedford, MA). The rosemary extract tested along this work was obtained using supercritical fluid extraction as described elsewhere [21].

2.2. Athymic nude mice study

The *in vivo* experimental protocol was approved by Ethics Committee of the Miguel Hernández University (AGL2011-29857-C03-03), according to the Spanish and European regulation and animal welfare guides. BALB/c nude mice of 6 weeks of age were purchased from Harlan. The animals were kept in a pathogen-free housing, 12 h light/12 h dark cycle with food and water *ad libitum*. Xenografts of human colon cancer cells (HT-29) were established by subcutaneously injecting 2×10^6 cells suspended in 0.2 mL of PBS. Mice were then randomly divided into two groups. The first group, the treatment with rosemary extract was initiated two weeks prior to cell inoculation (pre-treatment), at dose of 200 mg/kg body weight administered through gavage, three times/week. The second group, animals were treated with the vehicle (10% Tween 80, 40% PEG400 and 50% PBS). Body weights were recorded once a week and tumor volumes were measured twice a week during 35 days using a Vernier caliper. Xenograft tumors were collected at the end of the study and stored at -80°C .

2.3. Protein extraction

10 mg of xenograft tumor were disrupted under liquid N₂ and dissolved in 300 μL of lysis buffer (20% (v/v) ACN, 6 M urea, 1% (m/v) BOG, 0.15 M NaCl, 1.3 mM EDTA, 1 mM Na₃VO₄, 5 mM NaF, 2.5 mM Na₄P₂O₇ and 5 mM β -Glycerophosphate in PBS) supplemented with 10 μL of protease inhibitor cocktail (Sigma Aldrich) to prevent protein degradation. The samples were incubated for 60 min at 4°C during mild agitation, sonicated for 30 min at 0°C in water bath (Elma, Singen, Germany) and then centrifuged at

10000 $\times g$ at 4°C for 15 min (Sigma, Osterode am Harz, Germany). The supernatants were collected and protein concentration was measured using Bradford protein assay (Bio-Rad laboratories, Hercules, CA).

2.4. In-solution digestion

For in-solution digestion, 20 μg of proteins were reduced with 10 μL of 45 mM DTT at 56°C for 15 min, alkylated with 10 μL of 100 mM IAA for 15 min in the dark, and digested with 1 μg of LysC/trypsin solution (5% (m/m) of total protein content) at 37°C overnight. The digests were dried in a SpeedVac system ISS110 (Thermo Scientific, Waltham, MA) to remove ACN, and water saturated ethyl-acetate was used to extract BOG according to the protocol of Yeung et al. [22]. Afterwards, the samples were dried, reconstituted in 100 μL of 1% (v/v) FA and desalted on Isolute C18 solid phase extraction columns (1 mL, 50 mg capacity, Biotage, Uppsala, Sweden) using the following schedule. The column was washed 3 times with 500 μL of 100% ACN and equilibrated 3 times with 500 μL of 1% (v/v) FA. The tryptic peptides were adsorbed to the media using three repeated cycles of loading, the column was washed using $3 \times 500 \mu\text{L}$ 1% (v/v) FA, and finally the peptides were eluted in $2 \times 150 \mu\text{L}$ of 50% (v/v) ACN (1% (v/v) FA) and dried.

2.5. Dimethyl labeling

Dimethyl labeling was performed according to Boerema et al. [23]. After desalting, tryptic peptides originated from the five vehicle-control and the five pre-treated samples were reconstituted in 140 μL of 0.1 M TEAB, and before labeling, 70 μL of each sample ($\sim 10 \mu\text{g}$ of peptides) were pooled together and used as internal control for further normalization in the downstream analysis (Fig. 1). This pooled sample ($\sim 100 \mu\text{g}/700 \mu\text{L}$) was mixed with 40 μL of 4% (v/v) CH₂O (for light (L) labeling), and samples from vehicle-control and pre-treated mice ($\sim 10 \mu\text{g}/70 \mu\text{L}$) were mixed with 4 μL of CD₂O (4%, v/v) or 4 μL ¹³CD₂O (4%, v/v), labeling them as medium (M) and heavy (H), respectively. After a brief vortexing, 40 or 4 μL of 0.6 M NaBH₃CN solution in water was added to the L and M labeled samples respectively, and 4 μL of 0.6 M NaBD₃CN was added to each pre-treated sample for H labeling. After shaking for 1 h at room temperature, the reaction was terminated by adding of 16 μL (for M and H labeled samples) or 160 μL (for L labeled samples) of 1% (v/v) ammonia solution and then of 8 μL (for M and H labeled samples) or 80 μL (for L labeled samples) of 5% (v/v) FA. Next, the pooled sample was evaporated, resuspended in 100 μL of 1% (v/v) FA, and 10 μL of this solution was added to the randomized mixtures between the M and H samples. Finally, these mixture samples were cleaned up using C18 SPE columns (as described above), dried in a SpeedVac, and redissolved in 0.1% (v/v) FA to a final concentration of 1 $\mu\text{g}/\mu\text{L}$ prior to nano-LC–MS/MS analysis.

2.6. Nano-LC–MS/MS analysis

Five- μL aliquots containing $\sim 1 \mu\text{g}$ of tryptic peptides were injected four times into a nano-LC–MS/MS system consisting of EASY-nLC II (Thermo Fisher Scientific, Bremen, Germany) coupled via nanoelectrospray ionization (ESI) ion source to Orbitrap Velos Pro™ mass spectrometer (Thermo Fisher Scientific, Bremen, Germany). The peptide separations were performed as previously described [17]. The mass spectrometer was operated in positive ion mode with unattended data-dependent acquisition mode, in which the mass spectrometer automatically switches between acquiring a high resolution survey mass spectrum in the Orbitrap (resolving power 60,000 fwhm, full width at half maximum) and consecutive low-resolution, collision-induced dissociation fragmentation of up to ten most abundant ions in the ion trap using normalized colli-

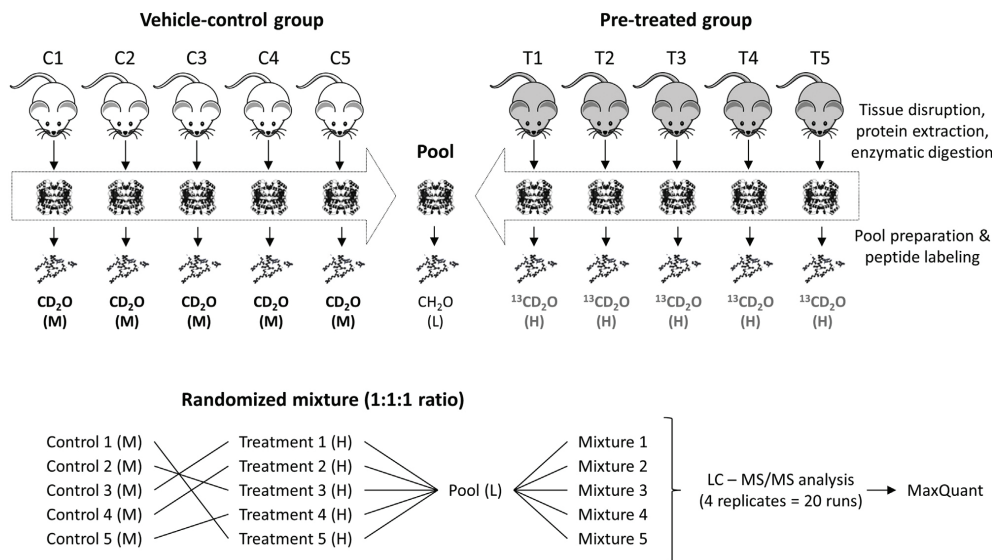


Fig. 1. Experimental design of the DML method combined with nano-LC-MS/MS analysis used in the present study. Control mice were fed for 49 days by oral gavage with an emulsion solution (40% (v/v) PEG400, 10% (v/v) Tween 80 and 50% (v/v) PBS), and pre-treated mice were fed with 200 mg/kg of rosemary extract in the same solution. Xenograft tumors were then disrupted under liquid N_2 and the proteins were extracted and digested with trypsin. 10 μ g of tryptic peptides from vehicle-control and pre-treated group were respectively labeled as “medium” and “heavy”, and another 10 μ g of each sample were pooled together and labeled as “light”. Finally, the samples were randomly mixed (1:1:1 ratio) prior to LC-MS/MS analysis.

sion energy of 35.0 eV. Ions that were once selected for acquisition were dynamically excluded for 30 s for further fragmentation. The mass spectrometry proteomics data have been deposited to the ProteomeXchange Consortium via the PRIDE [24] partner repository with the data set identifier PXD005853.

2.7. MaxQuant analysis

All MS raw files were collectively processed with MaxQuant (version 1.5.2.8) (<http://www.coxdocs.org/doku.php?id=maxquant:start>) [25], analyzing the four technical replicates as the same experiment (to increase the number of identified proteins) and applying the Andromeda search engine [26] with the following adaptations. The false discovery rate (FDR) was set to 1% for both proteins and peptides, and a minimum length of seven amino acids was specified. MaxQuant scored peptides for identification based on a search with a maximal mass deviation of precursor and fragment masses of up to 20 ppm and 0.5 Da. The Andromeda search engine was used for the MS/MS spectra search against a concatenated forward and reversed version of the Uniprot human database (downloaded on February 11, 2015, containing 89,909 entries and 245 frequently detected contaminants) for quantitative study. Enzyme specificity was set as C-terminal to Arg and Lys, also allowing cleavage at proline bonds and a maximum of two missed cleavages. Carbamidomethylation of Cys residues was set as fixed modification while oxidation of Met and protein N-acetylation were allowed as variable modifications. For dimethyl labeling, DimethylLys0 and DimethylNter0 were set as light labels, DimethylLys4 and DimethylNter4 were set as medium labels, and DimethylLys8 and DimethylNter8 were set as heavy labels. A minimum peptide ratio count of two and at least one “razor peptide” was required for quantification. After protein quantification, all the quantified ratios (M/L, H/L and H/M)

obtained from MaxQuant, were normalized by dividing the ratios with the median of the ratios.

2.8. Statistical and bioinformatics analysis

Prior to any statistical analysis, identifications flagged as reverse, potential contaminants, or proteins identified only by site modification were excluded for further analysis, and afterwards, the relative protein abundance was transformed to the \log_2 scale. The sample preparation followed in Fig. 1 enables the application of two approaches for the relative quantification of the proteins between the two conditions studied: 1) the direct comparison of the H and M labeled proteins (H/M ratio), or 2) the normalization of the H and M signals with a pooled sample (L), and the posterior comparison between them (H/L ratio vs M/L ratio). To compare both approaches, a Pearson's correlation test was performed, and the mean and the relative standard deviation (in non-logarithmic scale) were evaluated. For the Pearson's correlation test, the lists of protein ratios from each pair measurement (M/L, H/L and H/M) were shortened by excluding all proteins whose ratios were reported in less than 4 out of 5 pairs. These lists were also used to perform a Principal Component Analysis (PCA), and for those proteins quantified in 4 out of 5 labeled mixtures, the missing values were assigned as predicted by the software. When comparing the M/L and the H/L lists of proteins, a two-sample *t*-test was applied and the proteins with a *p*-value < 0.05 were considered statistically significant.

The lists of differentially expressed proteins were then uploaded and analyzed within the Panther website (<http://www.pantherdb.org/>) for protein classification, and in the bioinformatics tool Ingenuity Pathway Analysis (IPA; Qiagen, Redwood City, CA) to perform a causal upstream regulator (UR) and a functional enrichment analysis. In UR analysis, the activation state of each transcription factor is predicted based on global direction of changes in

Table 1

Tumor volumes (mm³) were monitored twice a week during 35 days. Data are expressed as the mean \pm SEM. *** ($p < 0.001$) indicates statistically significant differences compared to the vehicle-control group.

Time (days)	Vehicle-control group		Pre-treated group	
	Mean	\pm SEM	Mean	\pm SEM
0 (Cell inoculation)	0.00	0.00	0.00	0.00
7	72.07	18.33	50.57	11.79
12	157.11	25.56	90.87	14.27
16	235.25	28.18	149.24	31.42
19	256.53	33.82	203.06	50.12
23	362.46	54.27	256.18	71.98
26	490.64	66.93	301.19***	73.70
30	666.91	94.07	381.38***	90.04
33	752.96	91.95	508.98***	124.26
35	843.66	109.93	556.94***	131.20

the different experimental conditions for previously published targets of this regulator. Significance of the activation or deactivation of molecules predicted by UR analysis was tested by the Fisher's exact test, considering only the predictions with significant p -value < 0.05 , and regulation z -score > 2 or < -2 , for activation and deactivation, respectively. With the functional enrichment analysis, the biological processes and functions overrepresented in a list of differentially expressed proteins are identified. The p -value, calculated with the Fischer's exact test, reflected the likelihood that the association between a set of proteins in our data set and a related biological function is significant (p -value < 0.05).

3. Results and discussion

3.1. Effect of rosemary extract on xenograft tumor growth

Athymic nude mice were administered either with the vehicle or with the rosemary extract to determine the efficacy of rosemary extract on the progression of colon cancer *in vivo*. After 14 days of pre-treatment, xenografts with HT-29 colon cancer cells were established by subcutaneous injection and the development of tumors was observed after 7 days in both groups. After cell inoculation, the pre-treated group was administered with rosemary extract for 35 days more, whereas in the control group only vehicle was given. Body weight evolution of the animals pre-treated with rosemary extract did not present significant differences compared to the vehicle-treated animal group (data not shown) throughout the study. The mean of tumor volumes in the pre-treated group experienced less growth compared to that one corresponding to the vehicle-control group throughout the experiment. Nevertheless, statistically significant differences in the tumors size between the two groups were observed starting at day 26th after cells inoculation and were maintained until the end of the experiment. The volume of the tumors was measured at day 35, being 556.94 mm³ the average in the pre-treated group and 843.66 mm³ in the vehicle-control group, revealing a 34% reduction in tumor size in rosemary extract pre-treated mice compared to the vehicle-control group (Table 1).

These results are in good agreement with a previous *in vivo* study performed in mice xenograft with prostate cancer cells, which demonstrated that 100 mg/kg of rosemary extracts (with a 43% (m/m) of carnosic acid) decrease the tumor growth [18]. The authors of this work suggest that the decrease is caused by the upregulation of CHOP and the subsequent degradation of AR. It is critical to point out that in this study we have not targeted any specific protein but we have carried out a shotgun proteomic study to gain a broader knowledge of the proteins affected by rosemary extract treatment. These proteins will be described in the next sections.

3.2. Quantitative analysis of xenograft tumor proteome using DML method

In order to quantitatively compare the xenograft tumor proteome in vehicle-control and rosemary extract pre-treated mice, equal protein amounts of light, medium and heavy-labeled tissue lysates were mixed and analyzed with a nano-LC-MS/MS system. MS raw data files were then collectively processed with the MaxQuant software for FDR-controlled peptide and protein identification, and for dimethyl labeling-based quantification. To represent a simplified view of this complex procedure, the total ion chromatogram, the mass spectrum of the doubled charged MTDQEAIQDLWQWR peptide (which belong to the NPM1 protein), and the extracted ion chromatogram of the most abundant ions are shown in Fig. 2. This peptide was found with the three labels in all the samples, and as it is shown in Fig. 2C, the intensity of the heavy form (rosemary pre-treated mice) was lower than the light (pooled sample) and medium (vehicle-control) forms. After MaxQuant data processing, 1058 and 886 proteins were identified and quantified respectively, with a protein level FDR $< 1\%$ (see Supplemental Material Table S1 in the online version at DOI: 10.1016/j.chroma.2017.03.072). Among the quantified proteins, we considered those proteins present in 4 of the 5 mixtures and we compared the two possible quantification approaches. On the one side, the use of H/M ratios reduces the complexity of the data for protein quantification (the proteins must be found in two groups). However, as the sample preparation is independent for each pair of samples, the error in the quantification may increase. On the other side, the use of a pooled sample as a normalizer can minimize this error, and it increases the statistical power by the use of a two-sample t -test between 10 measurements (the use of H/M ratios only enables the calculation of the statistical significance using a one-sample t -test between 5 measurements). However, this last approach increases in data complexity for protein quantification because the proteins must be found in three groups. Considering all these aspects, we compared the expression levels and statistical significance of the quantified proteins (see Supplemental Material Table S2 in the online version at DOI: 10.1016/j.chroma.2017.03.072) using the Pearson's correlation test, which demonstrated a good correlation between both approaches ($r = 0.937$) (Fig. 3A). Finally, the mean and the standard deviation of the expression ratio (in non-logarithmic scale) were compared (1.003 ± 0.253 for H/M ratios and 0.971 ± 0.245 for H/L vs M/L ratios), indicating that the variation using both approaches was similar. Based on these results, and taking into account the possible reduction of the sample preparation error when using a pooled sample, and the increase of the statistical power when using the H/L and M/L ratios, we selected this last approach for further analysis.

After the selection of the quantification approach, a PCA was carried out to determine and compare the overall relation between the two conditions studied. This analysis indicated that the combination of the three principal components captured more than 66% of the variance of the data (Fig. 3B), depicting that the samples of the two groups are quite scattered. In addition to the PCA multivariate analysis, a univariate analysis using a two-sample t -test was performed to identify the differentially expressed proteins between the vehicle-control and the pre-treated mice. According to this test, 74 proteins were found significantly ($p < 0.05$) increased ($n = 17$) or decreased ($n = 57$) upon rosemary treatment. The list of significantly altered proteins and their Log₂ fold change, p -value and location is presented in Table 2.

3.3. Protein changes related to rosemary extract treatment

The significantly increased and decreased proteins in response to rosemary extract treatment were then grouped according

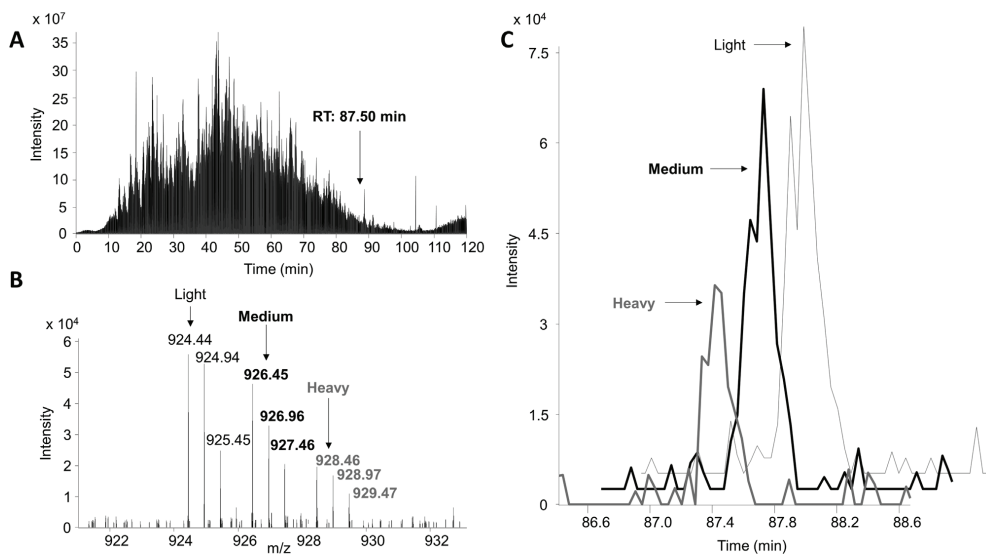


Fig. 2. Simplified representation of data processing. (A) Total ion chromatogram of a nanoLC-MS/MS run. (B) Mass spectrum at minute 87.50 from panel A. The doubled charged MTDQEAIQLWQWR peptide ($M_r = 1818.8359$ Da) was found as light, medium and heavy labeled in all the samples. (C) Extracted ion chromatogram of the m/z ranges 924.43–924.45 (light), 926.44–926.46 (medium) and 928.45–928.47 (heavy). The intensity of the heavy labeled form (from rosemary pre-treated mice) was lower than the light (from pooled sample) and the medium (from vehicle-control) forms.

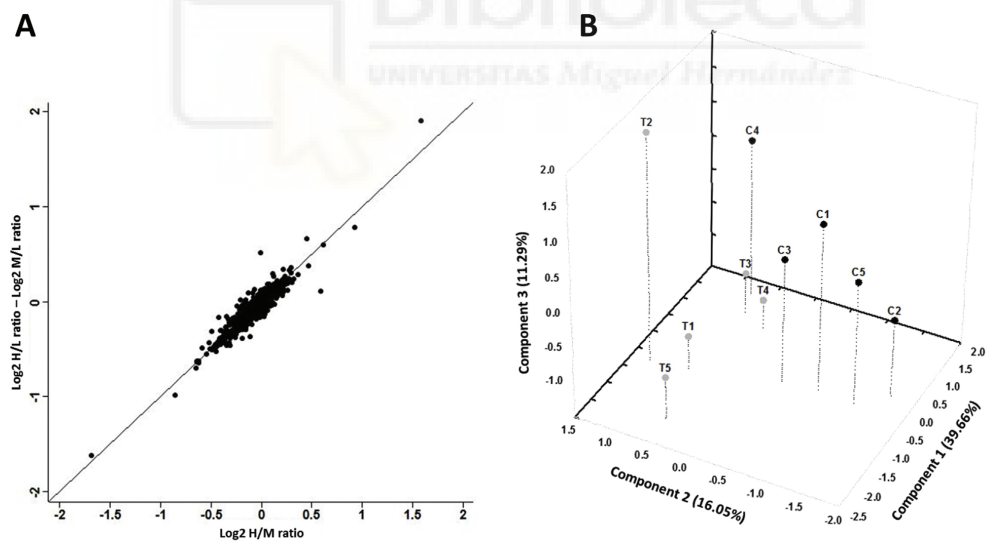


Fig. 3. (A) Scatter plot of the Log_2 H/M ratio versus Log_2 H/L ratio – Log_2 M/L ratio of the 714 proteins present in 4 out of the 5 samples of xenograft tumors. (B) Principal component analysis of xenograft tumors after rosemary extract pre-treatment during 49 days (C: vehicle-control group; T: pre-treated group).

to their class (Fig. 4). Among the different categories, a great amount of the altered proteins were related with the nucleic acid binding capacity (27%), followed by enzyme modulator proteins (10%), oxidoreductases (9%), transferases (9%), hydrolases (8%) and cytoskeletal proteins (8%). It is interesting to note that most of the proteins within the nucleic acid binding capacity category were

downregulated, suggesting an inactivation of the functions related with the transcription, translation or post-translational modifications of DNA and RNA. In addition to this protein classification, and in order to get a deeper knowledge about the molecular and cellular functions in which the proteins are involved in, a functional enrichment analysis using IPA bioinformatics tool was performed.

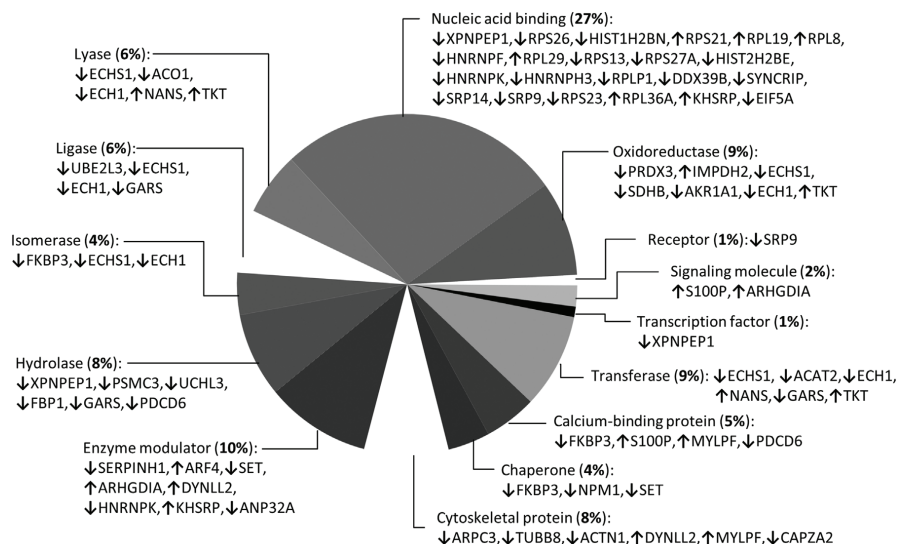


Fig. 4. PANTHER pie chart classification of the proteins found altered in xenograft tumors after rosemary extract pre-treatment.

The top ten molecular and cellular functions significantly overrepresented are shown in Table 3, and the most interesting functions and their proteins are discussed below.

3.3.1. RNA Post-Transcriptional Modification

In the case of *RNA Post-Transcriptional Modification* function, the expression of 10 out of the 11 altered proteins (NPM1, APEX1, DDX39B, HNRNPA1, HNRNPF, HNRNPH3, HNRNPK, SYNCRIP, ACO1, APRT) were decreased while only one protein (KHSRP) was increased. The Nucleophosmin 1 (NPM1) protein is a nucleolar phosphoprotein expressed at high levels in the granular region of the nucleolus and is involved in the regulation of cell growth, proliferation and transformation [27]. This protein also participates in the transport of pre-ribosomal particles and ribosome biogenesis, the regulation of DNA transcription, and the regulation of the activity and stability of p53 and ARF tumor suppressors. NPM1 is frequently overexpressed in solid tumors such as in colorectal carcinomas [28], and its exogenous expression enhanced cell migration, increased cell proliferation and correlates with poor survival [29]. On the contrary, its downregulation can induce apoptosis and suppress cell proliferation, as it has been demonstrated in acute myeloid leukemia cells treated with the dietary polyphenol epigallocatechin-3-gallate (EGCG) [30]. According to these results, our study suggests that the polyphenol enriched rosemary extract reduces the tumor progression *in vivo* as a likely consequence of the downregulation of NPM1 protein. The Apurinic-Apyrimidinic Endonuclease-1 (APEX1) protein is involved in single-strand DNA breaks and Ap sites repair, but it also stimulates the DNA-binding activity of different transcription factors involved in cancer promotion and progression [31]. As well as NPM1, APEX1 is often overexpressed in solid tumors and its expression level has been related with poor prognosis [32,33]. Moreover, the decrease of APEX1 protein can decrease the *in vitro* cell proliferation and the growth of ovarian and prostate xenograft models [34,35]. In addition, a proteomic study carried out in colon cancer cells has demonstrated that NPM1 is required for APEX1 nuclear localization and for modulating the cleansing process of rRNA [36]. This

study led us to hypothesize that the downregulation of APEX1 and NPM1 proteins observed in our study interrupts the cell cycle progression, and therefore stops the tumor growth in xenograft mice pre-treated with the rosemary extract. The DEAD-Box Helicase 39 B (DDX39B) is a protein that mediates the ATP hydrolysis during pre-mRNA splicing, and is essential for the association between small nuclear ribonucleoproteins and the pre-mRNA [37]. It has been observed that different DEAD box proteins are overexpressed in cancer cells, and DDX39B has been proposed as a potential anticancer target because its upregulation can stimulate the proliferation of human lung squamous cell carcinoma [38]. The Aconitase 1 (ACO1), also known as iron regulatory protein 1 (IRP1), is an iron-sulfur bifunctional protein that can act as a cytosolic aconitase (catalyzing the conversion of citrate to isocitrate under iron-rich conditions in the TCA cycle), or as a RNA-binding protein in iron depleted cells [39]. This dual activity has different implications in tumor cells. On the one side, the cytosolic aconitase form is involved in the generation of Acetyl-CoA (a fatty acid precursor) from cytosolic citrate under hypoxia conditions [40]. According to this study, the downregulation of ACO1 and other proteins involved in the lipid metabolism (ECH1, ECHS1 and ACAT2) suggests a readjustment of the lipid metabolism in xenograft tumors after rosemary extract treatment. On the other side, it has also been demonstrated that the overexpression of the ACO1/IRP1 RNA-binding form can suppress tumor growth in xenograft models [41]. To distinguish between the aconitase and the RNA-binding activity of IRP1, the authors performed an aconitase assay demonstrating that the aconitase activity was similar between the overexpressed IRP1 tumors and the controls. Complementarily, the authors confirmed the RNA-binding activity of IRP1 by the upregulation of Transferrin Receptor 1 (TFR1) in overexpressed IRP1 xenograft tumors (TFR1 is transcriptionally controlled by IRP1). In the present study, the expression level of TFR1 was not affected by rosemary extract treatment, but additional studies need to be assessed to evaluate whether the aconitase or the RNA-binding form is affected by the rosemary extract treatment. Other proteins found as down-regulated after rosemary extract treatment belong to the group of

Table 2
Significantly altered proteins in xenograft tumors from mice pre-treated with rosemary extract.

Protein name	Log ₂ fold change	p-value	Location
EIF5A	-0.698	1.07E-05	Cytoplasm
GOT1	-0.517	4.26E-05	Cytoplasm
HNRNPH3	-0.288	1.37E-04	Nucleus
RPL19	0.335	2.15E-04	Cytoplasm
RPS23	-0.442	0.001	Cytoplasm
HNRNPF	-0.261	0.002	Nucleus
SYNCRIP	-0.122	0.003	Nucleus
PAFAH1B2	-0.484	0.004	Cytoplasm
RPS21	0.308	0.004	Cytoplasm
RPL1	-0.369	0.004	Cytoplasm
UBE2L3	-0.451	0.005	Nucleus
CAPZ2A	-0.632	0.005	Cytoplasm
RPS26	-0.469	0.005	Cytoplasm
ANXA11	-0.330	0.006	Nucleus
PDCD6	-0.458	0.006	Cytoplasm
DYNLL2	0.289	0.007	Cytoplasm
UGP2	-0.494	0.007	Cytoplasm
ACAT2	-0.385	0.008	Cytoplasm
SRP14	-0.416	0.008	Cytoplasm
ARHGDI A	0.113	0.008	Cytoplasm
SRP9	-0.225	0.008	Cytoplasm
ARF4	0.331	0.009	Cytoplasm
RPS27A	-0.284	0.009	Cytoplasm
ADRM1	-0.980	0.010	Plasma Membrane
PSMC3	-0.283	0.010	Nucleus
OSTF1	-0.420	0.010	Nucleus
ECH1	-0.547	0.011	Cytoplasm
PHB	-0.395	0.011	Nucleus
AKR1A1	-0.502	0.011	Cytoplasm
NPM1	-0.192	0.013	Nucleus
AIMP1	0.241	0.016	Extracellular Space
HNRNPA1	-0.200	0.016	Nucleus
HIST1H2BN	-0.185	0.016	Nucleus
APEX1	-0.430	0.018	Nucleus
ANXA5	-0.430	0.019	Plasma Membrane
SET	-0.112	0.019	Nucleus
SERPINH1	-0.637	0.020	Extracellular Space
RPL36A	0.224	0.022	Cytoplasm
LAP3	0.149	0.022	Cytoplasm
TUBB8	-0.391	0.023	Cytoplasm
APRT	-0.485	0.024	Cytoplasm
PKM	-0.293	0.025	Cytoplasm
VCP	-0.187	0.027	Cytoplasm
ACO1	-0.393	0.028	Cytoplasm
ABRACL	-0.382	0.029	Other
RPS13	-0.386	0.032	Cytoplasm
GOT2	-0.153	0.032	Cytoplasm
ECHS1	-0.319	0.032	Cytoplasm
HNRNPK	-0.099	0.033	Nucleus
ACTN1	-0.278	0.033	Cytoplasm
ISOC2	-0.461	0.034	Cytoplasm
PRDX3	-0.296	0.036	Cytoplasm
HSPH1	-0.377	0.037	Cytoplasm
RPL29	0.218	0.038	Cytoplasm
UCHL3	-0.337	0.038	Cytoplasm
ARPC3	-0.308	0.038	Cytoplasm
SDHB	-0.306	0.041	Cytoplasm
GARS	-0.449	0.042	Cytoplasm
DDX39B	-0.266	0.042	Nucleus
MYLPP	1.906	0.042	Cytoplasm
NANS	0.187	0.043	Cytoplasm
SI00P	0.156	0.043	Cytoplasm
ANP32A	-0.240	0.044	Other
ANXA1	-0.354	0.044	Plasma Membrane
HIST2H2BE	-0.303	0.044	Nucleus
RPL8	0.169	0.045	Other
STMN2	0.225	0.045	Plasma Membrane
TKT	0.128	0.045	Cytoplasm
IMPDH2	0.188	0.046	Cytoplasm
FKBP3	-0.251	0.047	Nucleus
XPNPEP1	-0.284	0.049	Cytoplasm
KHSRP	0.205	0.049	Nucleus
GLO1	-0.357	0.049	Cytoplasm
FBP1	-0.335	0.049	Cytoplasm

heterogeneous ribonucleoproteins (hnRNPs): HNRNPA1, HNRNPF, HNRNPH3, HNRNPK and SYNCRIP. These RNA-binding proteins bind the single- or double-stranded RNA in cells and participate in forming ribonucleoprotein complexes. They are responsible for post-transcriptional control of RNAs and their stability, export, turnover and localization [42]. In addition, these proteins are also involved in apoptosis events, as they can control the splicing site of pro- and anti-apoptotic variants such as in Bcl-x gene [43]. For instance, the knockdown of hnRNP K shifts the splicing of the Bcl-x pre-mRNA from the anti-apoptotic Bcl-x_L isoform toward the pro-apoptotic Bcl-x_S isoform [44]. Similarly, hnRNP A1 and hnRNP F/H also enhance mRNA splicing, generating the pro-apoptotic isoform Bcl-x_S [45,46]. Due to these implications, the expression levels of these proteins have been widely studied in different tumor tissues. Specifically in colorectal cancer, hnRNP K has been found overexpressed and it is associated with poor prognosis [47], and hnRNP A1 has been suggested as a potential biomarker because its downregulation can suppress the cell proliferation *in vitro* [48]. The KH-type Splicing Regulatory Protein (KHSRP) is a single-stranded nucleic acid-binding protein involved in the mRNA decay, and was the only protein considered in the *RNA Post-Transcriptional Modification* function that was upregulated. This protein recognizes and interacts with the AU-rich element in the 3'-untranslated region of the mRNA, and enables the recruitment of the exosome and other enzymes for its degradation [49]. Some of its mRNAs targets encodes for cytokines, chemokines, transcription factors, proto-oncogenes, and cell-cycle regulators [50,51], but it can also enhance the degradation of RNA binding proteins such as hnRNP A1, hnRNP F, and hnRNP A/B [52] (as observed in our study). Moreover, a recent study has demonstrated that the phosphorylation state of KHSRP is critical for its binding capacity to the mRNA [53]. The authors also showed that the dietary polyphenol resveratrol induces the expression of KHSRP and prevents its phosphorylation, enhancing its mRNA degradation capacity. This study let us to hypothesize that the polyphenol enriched rosemary extract has similar effects, but further experimental confirmation is needed.

3.3.2. Protein Synthesis

With respect to the *Protein Synthesis* function, the expression level of 20 out of the 23 altered proteins was decreased while the expression level of 3 proteins was increased (see Table 3). Some of these proteins have already been discussed (as they are involved in the *RNA Post-Translational Modification* function), but not all. Among the downregulated proteins we found Valosin-Containing Protein (VCP), Prohibitin 1 (PHB1), Glyoxalase I (GLO1) and the Eukaryotic Translation Initiation Factor 5A (eIF5A). VCP is one of the most abundant proteins in eukaryotic cells and it can interact with different proteins involved in protein degradation, stress responses and programmed cell death [54]. Clinical studies have identified a correlation between elevated VCP expression and the progression, prognosis, and metastatic potential of colorectal carcinoma [55]. In addition, *in vitro* studies have demonstrated that downregulation of VCP resulted in the inhibition of cell proliferation, induction of apoptosis, and suppression of invasiveness of colon cancer cells, suggesting that this protein has an important role in the regulation of colon cancer [56]. PHB1 is a well-known chaperone involved in the stabilization of mitochondrial proteins [57], but it also plays a role in the regulation of proliferation and apoptosis [58]. Although the expression of this protein has been found increased in several cancers and its downregulation (as observed in our study) could prevent the cell proliferation [59], other studies suggest that PHB1 can act as a tumor suppressor [60]. Due to this controversy, deeper studies have been carried out suggesting that PHB1 activity depends on the subcellular localization of the protein: facilitating the tumorigenesis in the plasma membrane, or interacting with different tumor suppressors and reducing the proliferation

Table 3

Top ten molecular and cellular functions (IPA software) significantly overrepresented in xenograft tumors after rosemary extract pre-treatment. Fisher's exact test was used to determine the probability that the association between the genes in the data set and the functions is explained by chance.

Category	p-value ^a	Molecules ^b
RNA Post-Transcriptional Modification	4.56E-06–5.00E-02	↓ NPM1, ↓ HNRNPF, ↓ DDX39B, ↓ HNRNPA1, ↓ SYNCRIP, ↓ ACO1, ↑ KHSRP, ↓ APEX1, ↓ HNRNPH3, ↓ APRT, ↓ HNRNPK
Protein Synthesis	5.25E-06–4.67E-02	↓ NPM1, ↓ RPLP1, ↓ ADRM1, ↑ IMPDH2, ↓ CAPZA2, ↓ SYNCRIP, ↓ HNRNPK, ↓ GLO1, ↑ UCHL3, ↓ UBE2L3, ↓ DDX39B, ↓ PHB, ↓ ANXA5, ↓ ANXA1, ↓ VCP, ↓ RPL19, ↓ FBP1, ↓ ARPC3, ↑ ARHGDI A, ↓ EIF5A, ↓ XPNPEP1, ↓ ACO1, ↓ APEX1
Amino Acid Metabolism	1.15E-05–1.69E-02	↓ PKM, ↓ GOT1, ↓ GOT2
Cell-To-Cell Signaling and Interaction	1.15E-05–5.00E-02	↓ NPM1, ↓ OSTF1, ↓ ANXA5, ↓ ANXA1, ↓ PKM, ↑ ARHGDI A, ↓ HNRNPK
Cellular Movement	1.15E-05–4.26E-02	↓ NPM1, ↓ PHB, ↓ ANXA5, ↓ ANXA1, ↓ PKM, ↓ VCP, ↑ ARHGDI A, ↓ APEX1, ↓ HNRNPK, ↑ S100P
Small Molecule Biochemistry	1.15E-05–5.00E-02	↓ PAFAH1B2, ↓ SDHB, ↓ ECHS1, ↓ ACAT2, ↑ STMN2, ↑ IMPDH2, ↑ TKT, ↓ PKM, ↓ APRT, ↓ UCHL3, ↓ SET, ↓ AKR1A1, ↓ PRDX3, ↓ PHB, ↓ UGP2, ↓ HNRNPA1, ↓ ANXA1, ↓ ANXA5, ↓ VCP, ↓ FBP1, ↓ ARPC3, ↓ GOT1, ↓ NANS, ↓ ACO1, ↓ GOT2, ↓ APEX1
Cell Death and Survival	2.25E-05–4.81E-02	↓ PAFAH1B2, ↓ NPM1, ↓ SDHB, ↓ PKM, ↑ AIMP1, ↓ HNRNPK, ↓ APRT, ↓ GLO1, ↓ SET, ↓ ANXA11, ↓ PHB, ↓ RPS13, ↓ ANXA1, ↓ ANXA5, ↑ ARF4, ↓ VCP, ↑ RPL19, ↓ PDC6, ↓ APEX1, ↓ ADRM1, ↑ IMPDH2, ↓ HSPH1, ↑ RPS21, ↓ UCHL3, ↓ ANP32A, ↓ PRDX3, ↓ UBE2L3, ↓ HNRNPA1, ↓ SERPINH1, ↓ RPS27A, ↑ ARHGDI A, ↓ EIF5A, ↑ S100P
Molecular Transport	1.17E-04–5.00E-02	↓ PAFAH1B2, ↓ NPM1, ↓ SDHB, ↓ ACAT2, ↑ STMN2, ↓ PKM, ↓ APRT, ↓ SET, ↓ ANP32A, ↓ PRDX3, ↓ UGP2, ↓ PHB, ↓ DDX39B, ↓ HNRNPA1, ↓ ANXA1, ↓ ARPC3, ↓ EIF5A, ↓ GOT2, ↓ APEX1
Carbohydrate Metabolism	7.40E-04–4.18E-02	↓ PAFAH1B2, ↓ AKR1A1, ↓ UGP2, ↓ HNRNPA1, ↓ ANXA5, ↓ ANXA1, ↑ TKT, ↓ PKM, ↓ FBP1, ↓ GOT1, ↑ NANS, ↓ ACO1, ↓ GLO1
Free Radical Scavenging	1.51E-03–3.36E-02	↓ PRDX3, ↓ PHB, ↓ ANXA1, ↑ RPL29, ↓ FBP1, ↑ ARHGDI A, ↓ APEX1, ↓ HNRNPK

^a P-value calculated with the Fischer's exact test.

^b The arrows indicate an increase (↑) or decrease (↓) of the protein expression.

in the nucleus. GLO1 is a protein that belongs to the glyoxalase system and catalyzes the conversion of deleterious methylglyoxal to non-toxic D-lactate. The upregulation of GLO1 has been found in tumor tissues with high metabolic rate, where it can protect against cell damage and apoptosis [61]. In this sense, a number of studies have demonstrated that the knockdown of GLO1 using small interference RNA inhibits tumor cell proliferation and migration in murine fibrosarcoma and hepatocellular carcinoma, and it has been suggested as a potential therapeutic target against cancer [62,63]. Therefore, different drugs have been tested against GLO1 activity, such as methotrexate [64] or the food polyphenol curcumin, which has demonstrated to inhibit GLO1 activity in different cancer cell lines [65]. The eIF5A translation factor is a highly conserved protein throughout the eukaryotes that is involved in the initiation and elongation of proteins. There are two possible isoforms (eIF5A1 and eIF5A2) and both are considered as cancer biomarkers (eIF5A1 is one of the most upregulated genes in colorectal carcinomas) [66]. In addition to its role in the translation of proteins, it has been demonstrated that eIF5A controls the expression of RhoA, a cytoskeleton-regulatory protein involved in cell migration, and suggested as a marker of poor prognosis in colorectal cancer [67]. Moreover, the activity of RhoA is also controlled by the protein GDP-Dissociation Inhibitor 1 (ARHGDI A) [68], and the loss of ARHGDI A in hepatocellular carcinoma cells promotes cell migration and invasion *in vitro*, and lung metastasis formation *in vivo* [69]. Although the expression of RhoA was not altered in the present study, the expression of ARHGDI A was upregulated in our data set. This result, together with the alteration of several proteins involved in the cytoskeletal organization (ARPC3, TUBB8, ACTN1, DYNLL2, MYLPP, CAPZA2) (Fig. 4), suggest that the rose-

mary extract could also affect the migration of tumor cells. The expression levels of some ribosomal proteins were also affected by the rosemary extract treatment (RPL8, RPL29, RPL36, RPS13, RPS21, RPS23, RPS26, RPS27A, RPLP1, RPL19), but their expression did not follow a specific pattern, and IPA only considered the expression of the last two as involved in the protein synthesis function. However, different studies have demonstrated that these proteins can have extra-protein translational functions in addition to the well-known function directing the translation of mRNAs into proteins. For instance, the mRNA levels of RPLP1 have been found increased by five-fold in colorectal cancer tissues [70], and the overexpression of RPL19 can activate the Unfolded Protein Response (UPR) in breast cancer cells [71]. The authors of the last study observed an endoplasmic reticulum stress-induced cell death after UPR activation, and previous transcriptomic and proteomic studies carried out in our laboratory have demonstrated that the rosemary extract used in the present study also induces the early activation of the UPR in HT-29 colon cancer cells [20,72].

3.3.3. Amino Acid Metabolism

In the *Amino Acid Metabolism* function, three proteins were found downregulated: GOT1, GOT2 and PKM (the identifier obtained by MaxQuant software corresponds to the PKM2 isoform). The glutamic-oxaloacetic transaminase (also known as aspartate aminotransferase) is a pyridoxal phosphate-dependent enzyme that exists in cytoplasmic (GOT1) and mitochondrial (GOT2) forms. Both proteins catalyze the reversible conversion of oxaloacetate and glutamate into aspartate and alpha-ketoglutarate, but they are also involved in the generation of a proton gradient necessary for oxidative phosphorylation [73]. This last activity has been

suggested as critical in breast cancer cells, where the downregulation of GOT using siRNA reduces the *in vitro* cell proliferation. In addition, the inhibition of GOT activity using amino oxycetate also decreases the proliferation of transformed breast adenocarcinoma cells *in vitro* and *in vivo*, suggesting GOT as a novel target against breast cancer [74]. Moreover, the Pyruvate Kinase (PK) is a rate limiting-glycolytic enzyme that catalyzes the reaction between phosphoenolpyruvate and adenosine diphosphate and produces pyruvate and ATP [75]. Among the four different isoforms, the PK muscle isozyme M2 (PKM2) is expressed in tissues with anabolic functions such as cancer cells, and different studies have revealed associations between oncogenes and metabolic reprogramming [76]. In this sense, PKM2 has been demonstrated to be crucial in the Warburg effect mediated by the Myc-hnRNP cascades, and therefore it has been suggested as a target for cancer therapy [77].

3.3.4. Other proteins

Among other proteins downregulated after the rosemary extract treatment, we found two heat-stable protein inhibitors of Protein Phosphatase 2A (PP2A): SET, also known as I2PP2A, and ANP32A, also known as I1PP2A. PP2A controls cell metabolism and different biological processes such as the cell cycle, DNA replication or cell proliferation, and it is considered as a tumor suppressor that regulates critical cellular molecules like Akt, p53, c-Myc and β -catenin [78]. However, PP2A is downregulated in many solid cancers and its reactivation is considered as a strategy for human cancer treatment. According to this idea, a recent study has shown that the depletion of the PP2A inhibitor SET reduces MYC expression, decreasing the tumorigenic potential of breast cancer cells *in vitro* and *in vivo* [79]. Moreover, the PP2A inhibitor ANP32A has been isolated together with SET, and both proteins are upregulated and considered as protein biomarkers in colorectal cancer [80].

3.3.5. Upstream regulator analysis

A causal UR analysis was finally performed with IPA bioinformatics tool to obtain a broader picture of the potential transcriptional regulators activity. This analysis predicted a significant inactivation of MYC transcription factor (activation z-score = -2.419 , p -value = 2.36×10^{-9}) based on the expression of RPS23, RPLP1, PRDX3, PKM, PHB, NPM1, MYLPF, HSPH1, GOT1, GOT2, DDX39B, APEX1, and SERPINH1 proteins, but MYC also controls the expression of other proteins such as hnRNP1 (also downregulated in our study) [81]. MYC transcription factor can bind the promoters of hundreds of genes involved in cell cycle, protein synthesis and metabolism pathways [82,83], and because it is highly expressed in proliferating cells, its inhibition has been widely studied as an anticancer therapy [84]. Furthermore, several evidences suggest that the downregulation of MYC may be of importance for the antiproliferative activity of certain phenolic compounds in cancer cells [85], and a previous transcriptomic study of our group indicated that rosemary extract inactivates MYC transcription factor in leukemia cells, with a subsequent accumulation of the cells in the G2/M phase of the cell cycle [86].

4. Conclusions

In conclusion, our findings indicate that the daily administration of 200 mg/kg of a polyphenol-enriched rosemary extract reduce the progression of colorectal cancer *in vivo*, and the comprehensive shotgun proteomic approach has enabled the identification and quantification of several proteins affected by the treatment that have special relevance in cancer progression. In addition, the analysis of these proteins using bioinformatics tools displays that the rosemary extract treatment mainly alters the *RNA Post-Transcriptional Modification*, the *Protein Synthesis* and the *Amino*

Acid Metabolism functions strongly suggesting them to be responsible for the reduction of the tumor size. Moreover, these tools also reveal the inactivation of the oncogene MYC, a transcription factor that controls the expression of genes involved in protein synthesis and metabolism pathways, and its inactivation can be well explained by the downregulation of two inhibitors of PP2A, an enzyme that controls MYC activity. In summary, the shotgun protein strategy based on nano-LC–MS/MS reveals that the enriched polyphenol rosemary extract has multiple effects *in vivo*, demonstrating the high utility of this methodology to determine the expression levels of a variety of protein biomarkers and to generate a new hypothesis about the molecular mechanisms of this extract *in vivo*.

Declaration of interest

The authors declare no competing financial interest.

Acknowledgments

This work was supported by projects AGL2014-53609-P and AGL2015-67995-C3-1-R (Ministerio de Economía y Competitividad, Spain), S2013/ABI-2728 (Comunidad de Madrid), PROMETEO/2016/006 (Generalitat Valenciana) and CIBER (CB12/03/30038, Fisiopatología de la Obesidad y la Nutrición, CIBERobn, Instituto de Salud Carlos III). A.V. thanks the Ministerio de Economía y Competitividad for his FPI pre-doctoral fellowship (BES-2012-057014). The Swedish Research Council (Vetenskapsrådet), 2011-4423 and 2015-4870 to J.B. is acknowledged for financial support.

References

- [1] A.I. Hussain, F. Anwar, S.A. Chatha, A. Jabbar, S. Mahboob, P.S. Nigam, Rosmarinus officinalis essential oil: antiproliferative, antioxidant and antibacterial activities, *Braz. J. Microbiol.* 41 (2010) 1070–1078, <http://dx.doi.org/10.1590/S1517-83822010000400027>.
- [2] E. Arranz, L. Jaime, M.R. García-Risco, T. Fornari, G. Reglero, S. Santoyo, Anti-inflammatory activity of rosemary extracts obtained by supercritical carbon dioxide enriched in carnosic acid and carnosol, *Int. J. Food Sci. Technol.* 50 (2015) 674–681, <http://dx.doi.org/10.1111/ijfs.12656>.
- [3] N. Erkan, G. Ayranci, E. Ayranci, Antioxidant activities of rosemary (Rosmarinus Officinalis L.) extract, blackseed (Nigella Sativa L.) essential oil, carnosic acid, rosmarinic acid and sesamol, *Food Chem.* 110 (2008) 76–82, <http://dx.doi.org/10.1016/j.foodchem.2008.01.058>.
- [4] T. Bakirel, O. Bakirel, O.U. Keleş, S.G. Ülgen, H. Yardibi, *In vivo* assessment of antidiabetic and antioxidant activities of rosemary (Rosmarinus officinalis) in alloxan-diabetic rabbits, *J. Ethnopharmacol.* 116 (2008) 64–73, <http://dx.doi.org/10.1016/j.jep.2007.10.039>.
- [5] M.S. Afonso, A.M. de O Silva, E.B. Carvalho, D.P. Rivelli, S.B. Barros, M.M. Rogero, et al., Phenolic compounds from Rosemary (Rosmarinus officinalis L.) attenuate oxidative stress and reduce blood cholesterol concentrations in diet-induced hypercholesterolemic rats, *Nutr. Metab.* 10 (2013) 1–19, <http://dx.doi.org/10.1186/1743-7075-10-19>.
- [6] M. González-Vallinas, G. Reglero, A. Ramírez de Molina, Rosemary (Rosmarinus officinalis L.) extract as a potential complementary agent in anticancer therapy, *Nutr. Cancer* 67 (2015) 1221–1229, <http://dx.doi.org/10.3390/nu8110731>.
- [7] O. Yesil-Celiktas, C. Sevimli, E. Bedir, F. Vardar-Sukan, Inhibitory effects of rosemary extracts, carnosic acid and rosmarinic acid on the growth of various human cancer cell lines, *Plant Foods Hum. Nutr.* 65 (2010) 158–163, <http://dx.doi.org/10.1007/s1130-010-0166-4>.
- [8] C. Ibáñez, A. Valdés, V. García-Cañas, C. Simó, M. Celebier, L. Rocamora-Reverte, et al., Global Foodomics strategy to investigate the health benefits of dietary constituents, *J. Chromatogr. A* 1248 (2012) 139–153, <http://dx.doi.org/10.1016/j.chroma.2012.06.008>.
- [9] S.M. Petiwala, A.G. Puthenveetil, J.J. Johnson, Polyphenols from the Mediterranean herb rosemary (Rosmarinus officinalis) for prostate cancer, *Front. Pharmacol.* 4 (2013) 1–4, <http://dx.doi.org/10.3389/fphar.2013.00029>.
- [10] A. Valdés, V. García-Cañas, L. Rocamora-Reverte, A. Gómez-Martínez, J.A. Ferragut, A. Cifuentes, Effect of rosemary polyphenols on human colon cancer cells: transcriptomic profiling and functional enrichment analysis, *Genes Nutr.* 8 (2013) 43–60, <http://dx.doi.org/10.1002/elps.201200133>.
- [11] Y. Ishida, M. Yamasaki, C. Yukizaki, K. Nishiyama, H. Tsubouchi, A. Okayama, et al., Carnosol, rosemary ingredient, induces apoptosis in adult T-cell leukemia/lymphoma cells via glutathione depletion: proteomic approach

- using fluorescent two-dimensional differential gel electrophoresis, *Hum. Cell* 27 (2014) 68–77, <http://dx.doi.org/10.1007/s13577-013-0083-6>.
- [12] Q. Xiang, Y. Ma, J. Dong, R. Shen, Carnosic acid induces apoptosis associated with mitochondrial dysfunction and Akt inactivation in HepG2 cells, *Int. J. Food Sci. Nutr.* 66 (2015) 76–84, <http://dx.doi.org/10.3109/09637486.2014.953452>.
- [13] A. López-Jiménez, M. García-Caballero, M.A. Medina, A.R. Quesada, Anti-angiogenic properties of carnosol and carnosic acid, two major dietary compounds from rosemary, *Eur. J. Nutr.* 52 (2013) 85–95, <http://dx.doi.org/10.1007/s00394-011-0289-x>.
- [14] Q. Xiang, Q. Liu, L. Xu, Y. Qiao, Y. Wang, X. Liu, Carnosic acid protects biomolecules from free radical-mediated oxidative damage in vitro, *Food Sci. Biotechnol.* 22 (2013) 1381–1388, <http://dx.doi.org/10.1007/s10068-013-0226-2>.
- [15] T. Satoh, K. Kosaka, K. Itoh, A. Kobayashi, M. Yamamoto, Y. Shimajo, et al., Carnosic acid, a catechol-type electrophilic compound, protects neurons both in vitro and in vivo through activation of the Keap1/Nrf2 pathway via S-alkylation of targeted cysteines on Keap1, *J. Neurochem.* 104 (2008) 1116–1131, <http://dx.doi.org/10.1111/j.1471-4159.2007.05039.x>.
- [16] S.M. Petiwala, J.J. Johnson, Diterpenes from rosemary (*Rosmarinus officinalis*): defining their potential for anti-cancer activity, *Cancer Lett.* 367 (2015) 93–102, <http://dx.doi.org/10.1016/j.canlet.2015.07.005>.
- [17] A. Valdés, V. García-Cañas, K.A. Artemenko, C. Simó, J. Bergquist, A. Cifuentes, Nano-liquid chromatography-orbitrap MS-based quantitative proteomics reveals differences between the mechanisms of action of carnosic acid and carnosol in colon cancer cells, *Mol. Cell. Proteom.* 16 (2017) 8–22, <http://dx.doi.org/10.1074/mcp.M116.061481>.
- [18] S.M. Petiwala, S. Berhe, G. Li, A.G. Puthenveetil, O. Rahman, L. Nonn, et al., Rosemary (*Rosmarinus officinalis*) extract modulates CHOP/GADD153 to promote androgen receptor degradation and decreases xenograft tumor growth, *PLoS One* 9 (2014) e89772, <http://dx.doi.org/10.1371/journal.pone.0089772>.
- [19] M. Yan, G. Li, S.M. Petiwala, E. Householder, J.J. Johnson, Standardized rosemary (*Rosmarinus officinalis*) extract induces Nrf2/sestrin-2 pathway in colon cancer cells, *J. Funct. Foods* 13 (2015) 137–147, <http://dx.doi.org/10.1016/j.jff.2014.12.038>.
- [20] A. Valdés, K.A. Artemenko, J. Bergquist, V. García-Cañas, A. Cifuentes, Comprehensive proteomic study of the antiproliferative activity of a polyphenol-enriched rosemary extract on colon cancer cells using nanoliquid chromatography-orbitrap MS/MS, *J. Proteome Res.* 15 (2016) 1971–1985, <http://dx.doi.org/10.1021/acs.jproteome.6b00154>.
- [21] A. Valdés, V. García-Cañas, C. Simó, C. Ibáñez, V. Micó, J.A. Ferragut, et al., Comprehensive foodomics study on the mechanisms operating at various molecular levels in cancer cells in response to individual rosemary polyphenols, *Anal. Chem.* 86 (2014) 9807–9815, <http://dx.doi.org/10.1021/acs.jpoteome.6b00154>.
- [22] Y.G. Yeung, E.R. Stanley, Rapid detergent removal from peptide samples with ethyl acetate for mass spectrometry analysis, *Curr. Protoc. Protein Sci.* 16 (2010), <http://dx.doi.org/10.1002/0471140864.ps1612s59>, 16.12.
- [23] P.J. Boersema, R. Raijmakers, S. Lemeer, S. Mohammed, A.J. Heck, Multiplex peptide stable isotope dimethyl labeling for quantitative proteomics, *Nat. Protoc.* 4 (2009) 484–494, <http://dx.doi.org/10.1038/nprot.2009.21>.
- [24] J.A. Vizcaíno, E.W. Deutsch, R. Wang, A. Cordsas, F. Reisinger, D. Rios, et al., ProteomeXchange provides globally coordinated proteomics data submission and dissemination, *Nat. Biotechnol.* 32 (2014) 223–226, <http://dx.doi.org/10.1038/nbt.2839>.
- [25] J. Cox, M. Mann, MaxQuant enables high peptide identification rates, individualized p.b.-range mass accuracies and proteome-wide protein quantification, *Nat. Biotechnol.* 26 (2008) 1367–1372, <http://dx.doi.org/10.1038/nbt.1511>.
- [26] J. Cox, N. Neuhauser, A. Michalski, R.A. Scheltema, J.V. Olsen, M. Mann, Andromeda: a peptide search engine integrated into the MaxQuant environment, *J. Proteome Res.* 10 (2011) 1794–1805, <http://dx.doi.org/10.1021/pr101065j>.
- [27] D.M. Mitrea, C.R. Grace, M. Buljan, M.K. Yun, N.J. Pytel, J. Satumba, et al., Structural polymorphism in the N-terminal oligomerization domain of NPM1, *Proc. Natl. Acad. Sci. U. S. A.* 111 (2014) 4466–4471, <http://dx.doi.org/10.1073/pnas.1321007111>.
- [28] Y. Nozawa, N. Van Belzen, A.C. van der Made, W.N. Dinjens, F.T. Bosman, Expression of nucleophosmin/B23 in normal and neoplastic colorectal mucosa, *J. Pathol.* 178 (1996) 48–52, [http://dx.doi.org/10.1002/\(SICI\)1096-9896\(199601\)178:1<48::AID-PATH432>3.0.CO;2-Y](http://dx.doi.org/10.1002/(SICI)1096-9896(199601)178:1<48::AID-PATH432>3.0.CO;2-Y).
- [29] Y. Liu, F. Zhang, X. Zhang, L. Qi, L. Yang, H. Guo, et al., Expression of nucleophosmin/NPM1 correlates with migration and invasiveness of colon cancer cells, *J. Biomed. Sci.* 19 (2012) 53, <http://dx.doi.org/10.1186/1423-0127-19-53>.
- [30] H.T. Chi, B.T. Ly, H.A. Vu, Y. Sato, P.C. Dung, P.T. Xinh, Down-regulated expression of NPM1 in IMS-M2 cell line by (–)-epigallocatechin-3-gallate, *Asian Pac. J. Trop. Biomed.* 4 (2014) 570–574, <http://dx.doi.org/10.12980/APJB.4.2014APJB-2014-0177>.
- [31] G. Tellì, F. Quadrifoglio, C. Tiribelli, M.R. Kelley, The many functions of APE1/Ref-1: not only a DNA repair enzyme, *Antioxid. Redox. Signal.* 11 (2009) 601–619, <http://dx.doi.org/10.1089/ars.2008.2194>.
- [32] D.H. Moore, H. Michael, R. Tritt, S.H. Parsons, M.R. Kelley, Alterations in the expression of the DNA repair/redox enzyme APE/ref-1 in epithelial ovarian cancers, *Clin. Cancer Res.* 6 (2000) 602–609.
- [33] M.R. Kelley, L. Cheng, R. Foster, R. Tritt, J. Jiang, J. Broshears, et al., Elevated and altered expression of the multifunctional DNA base excision repair and redox enzyme Ape1/ref-1 in prostate cancer, *Clin. Cancer Res.* 7 (2001) 824–830.
- [34] M.L. Fishel, Y. He, A.M. Reed, H. Chin-Sinex, G.D. Hutchins, M.S. Mendonca, et al., Knockdown of the DNA repair and redox signaling protein Ape1/Ref-1 blocks ovarian cancer cell and tumor growth, *DNA Repair (Amst.)* 7 (2008) 177–186, <http://dx.doi.org/10.1016/j.dnarep.2007.09.008>.
- [35] M.L. Fishel, Y. Jiang, N.V. Rajeshkumar, G. Scandura, A.L. Sinn, Y. He, et al., Impact of APE1/Ref-1 redox inhibition on pancreatic tumor growth, *Mol. Cancer Ther.* 10 (2011) 1698–1708, <http://dx.doi.org/10.1158/1535-7163.MCT-11-0107>.
- [36] C. Vascotto, D. Fantini, M. Romanello, L. Cesaratto, M. Deganuto, A. Leonardi, et al., APE1/Ref-1 interacts with NPM1 within nucleoli and plays a role in the rRNA quality control process, *Mol. Cell. Biol.* 29 (2009) 1834–1854, <http://dx.doi.org/10.1128/MCB.01337-08>.
- [37] E.A. Gustafson, G.M. Wessel, DEAD-box helicases: posttranslational regulation and function, *Biochem. Biophys. Res. Commun.* 395 (2010) 1–6, <http://dx.doi.org/10.1016/j.bbrc.2010.02.172>.
- [38] T. Sugiyama, Y. Nagano, Y. Noguchi, DDX39, upregulated in lung squamous cell cancer, displays RNA helicase activities and promotes cancer cell growth, *Cancer Biol. Ther.* 6 (2007) 957–964, <http://dx.doi.org/10.4161/cbt.6.6.4192>.
- [39] D.J. Haile, T.A. Rouault, C.K. Tang, J. Chin, J.B. Harford, R.D. Klausner, Reciprocal control of RNA-binding and acetonate activity in the regulation of the iron-responsive element binding protein: role of the iron-sulfur cluster, *Proc. Natl. Acad. Sci. U. S. A.* 89 (1992) 7536–7540.
- [40] C.M. Metallo, Reductive glutamine metabolism by IDH1 mediates lipogenesis under hypoxia, *Nature* 481 (2012) 380–384, <http://dx.doi.org/10.1038/nature10602>.
- [41] G. Chen, C. Fillebeen, J. Wang, K. Pantopoulos, Overexpression of iron regulatory protein 1 suppresses growth of tumor xenografts, *Carcinogenesis* 28 (2007) 785–791, <http://dx.doi.org/10.1093/carcin/bgl210>.
- [42] D.J. Hogan, D.P. Riordan, A.P. Gerber, D. Herschlag, P.O. Brown, Diverse RNA-binding proteins interact with functionally related sets of RNAs, suggesting an extensive regulatory system, *PLoS Biol.* 6 (2008) e255, <http://dx.doi.org/10.1371/journal.pbio.0060255>.
- [43] T. Revil, J. Pelletier, J. Toutant, A. Cloutier, B. Chabot, Heterogeneous nuclear ribonucleoprotein K represses the production of pro-apoptotic Bcl-x(S) splice isoform, *J. Biol. Chem.* 284 (2009) 21458–21467, <http://dx.doi.org/10.1074/jbc.M109.019711>.
- [44] M.L. Hartman, M. Czyn, Anti-apoptotic proteins on guard of melanoma cell survival, *Cancer Lett.* 331 (2013) 24–34, <http://dx.doi.org/10.1016/j.canlet.2013.01.010>.
- [45] D. Garneau, T. Revil, J.F. Fiset, B. Chabot, Heterogeneous nuclear ribonucleoprotein F/H proteins modulate the alternative splicing of the apoptotic mediator Bcl-x, *J. Biol. Chem.* 280 (2005) 22641–22650, <http://dx.doi.org/10.1074/jbc.M501070200>.
- [46] Y. Wang, C.G. Cheong, T.M.T. Hall, Z.F. Wang, Engineering splicing factors with designed specificities, *Nat. Methods* 6 (2009) 825–863, <http://dx.doi.org/10.1038/nmeth.1379>.
- [47] B. Carpenter, M. McKay, S.R. Dundas, L.C. Lawrie, C. Telfer, G.I. Murray, Heterogeneous nuclear ribonucleoprotein K is over expressed, aberrantly localised and is associated with poor prognosis in colorectal cancer, *Br. J. Cancer* 95 (2006) 921–927, <http://dx.doi.org/10.1038/sj.bjc.6603349>.
- [48] Y.L. Ma, J.Y. Peng, P. Zhang, L. Huang, W.J. Liu, T.Y. Shen, et al., Heterogeneous nuclear ribonucleoprotein A1 is identified as a potential biomarker for colorectal cancer based on differential proteomics technology, *J. Proteome Res.* 8 (2009) 4525–4535, <http://dx.doi.org/10.1021/pr900365e>.
- [49] P. Briata, D. Bordo, M. Puppo, F. Corlero, M. Rossi, N. Perrone-Bizzozero, et al., Diverse roles of the nucleic acid-binding protein KHSRP in cell differentiation and disease, *WIREs RNA* 7 (2016) 227–240, <http://dx.doi.org/10.1002/wrna.1327>.
- [50] K.S. Khabar, The AU-rich transcriptome: more than interferons and cytokines, and its role in disease, *J. Interferon Cytokine Res.* 25 (2005) 1–10, <http://dx.doi.org/10.1089/jir.2005.25.1>.
- [51] W. Eberhardt, A. Doller, el-S. Akool, J. Pfeilschifter, Modulation of mRNA stability as a novel therapeutic approach, *Pharmacol. Ther.* 114 (2007) 56–73, <http://dx.doi.org/10.1016/j.pharmthera.2007.01.002>.
- [52] T. Ruggiero, M. Trabucchi, M. Ponassi, G. Corte, C. Chen, L. al-Haj, et al., Identification of a set of KSRP target transcripts upregulated by PI3K-AKT signaling, *BMC Mol. Biol.* 8 (2007) 28, <http://dx.doi.org/10.1186/1471-2199-8-28>.
- [53] F. Bollmann, J. Art, J. Henke, K. Schrick, V. Besche, M. Bros, H. Li, et al., Resveratrol post-transcriptionally regulates pro-inflammatory gene expression via regulation of KSRP RNA binding activity, *Nucleic Acids Res.* 42 (2014) 12555–12569, <http://dx.doi.org/10.1093/nar/gku1033>.
- [54] P.J. Lim, R. Danner, J. Liang, H. Doong, C. Harman, D. Srinivasan, et al., Ubiquitin and p97/VCP bind erasin, forming a complex involved in ERAD, *J. Cell Biol.* 187 (2009) 201–217, <http://dx.doi.org/10.1083/jcb.200903024>.
- [55] S. Yamamoto, Y. Tomita, Y. Hoshida, M. Sakon, M. Kameyama, S. Imaoka, et al., Expression of valosin-containing protein in colorectal carcinomas as a predictor for disease recurrence and prognosis, *Clin. Cancer Res.* 10 (2004) 651–657, <http://dx.doi.org/10.1158/1078-0432.CCR-1576-03>.
- [56] Q. Fu, Y. Jiang, D. Zhang, X. Liu, J. Guo, J. Zhao, Valosin-containing protein (VCP) promotes the growth, invasion, and metastasis of colorectal cancer through activation of STAT3 signaling, *Mol. Cell Biochem.* 418 (418) (2016) 189–198, <http://dx.doi.org/10.1007/s11010-016-2746-6>.

- [57] L.G. Nijtmans, L. de Jong, M.A. Sanz, P.J. Coates, J.A. Berden, J.W. Back, et al., Prohibitins act as a membrane-bound chaperone for the stabilization of mitochondrial proteins, *EMBO J.* 19 (2000) 2444–2451, <http://dx.doi.org/10.1093/emboj/19.11.2444>.
- [58] V. Sanchez-Quiles, E. Santamaria, V. Segura, L. Sesma, J. Prieto, F.J. Corrales, Prohibitin deficiency blocks proliferation and induces apoptosis in human hepatoma cells: molecular mechanisms and functional implications, *Proteomics* 10 (2010) 1609–1620, <http://dx.doi.org/10.1002/prot.200900757>.
- [59] A.L. Theiss, S.V. Sitarman, The role and therapeutic potential of prohibitin in disease, *Biochim. Biophys. Acta* 2011 (1813) 1137–1143, <http://dx.doi.org/10.1016/j.bbamcr.2011.01.033>.
- [60] S. Manjeshwar, D.E. Branam, M.R. Lerner, D.J. Brackett, E.R. Jupe, Tumor suppression by the prohibitin gene 3' untranslated region RNA in human breast cancer, *Cancer Res.* 63 (2003) 5251–5256.
- [61] T. Santarius, G.R. Bignell, C.D. Greenman, S. Widaa, L. Chen, C.L. Mahoney, et al., GLO1-A novel amplified gene in human cancer, *Genes. Chromosomes Cancer* 49 (2010) 711–725, <http://dx.doi.org/10.1002/gcc.20784>.
- [62] X. Hu, X. Yang, Q. He, Q. Chen, L. Yu, Glyoxalase 1 is up-regulated in hepatocellular carcinoma and is essential for HCC cell proliferation, *Biotechnol. Lett.* 36 (2014) 257–263, <http://dx.doi.org/10.1007/s10529-013-1372-6>.
- [63] Y. Wang, Y. Kuramitsu, K. Tokuda, F. Okada, B. Baron, J. Akada, et al., Proteomic analysis indicates that overexpression and nuclear translocation of lactoylglutathione lyase (GLO1) is associated with tumor progression in murine fibrosarcoma, *Electrophoresis* 35 (2014) 2195–2202, <http://dx.doi.org/10.1002/elps.201300497>.
- [64] K. Bartyik, S. Turi, F. Orosz, E. Karg, Methotrexate inhibits the glyoxalase system in vivo in children with acute lymphoid leukaemia, *Eur. J. Cancer* 40 (2004) 2287–2292, <http://dx.doi.org/10.1016/j.ejca.2004.06.024>.
- [65] T. Santel, G. Pflug, N.Y. Hemdan, A. Schäfer, M. Hollenbach, M. Buchold, et al., Curcumin inhibits glyoxalase 1—a possible link to its anti-inflammatory and anti-tumor activity, *PLoS One* 3 (2008) e3508, <http://dx.doi.org/10.1371/journal.pone.0003508>.
- [66] B. Tunca, G. Tezcan, G. Cecener, U. Egeli, A. Zorluoglu, T. Yilmazlar, et al., Overexpression of CK20, MAP3K8 and EIF5A correlates with poor prognosis in early-onset colorectal cancer patients, *J. Cancer Res. Clin. Oncol.* 139 (2013) 691–702, <http://dx.doi.org/10.1007/s00432-013-1372-x>.
- [67] K. Fujimura, S. Choi, M. Wyse, J. Strnadel, T. Wright, R. Klemke, Eukaryotic translation initiation factor 5A (EIF5A) regulates pancreatic cancer metastasis by modulating RhoA and Rho-associated kinase (ROCK) protein expression levels, *J. Biol. Chem.* 290 (2015) 29907–29919, <http://dx.doi.org/10.1074/jbc.M115.687418>.
- [68] M.A. Harding, D. Theodorescu, RhoGDI signaling provides targets for cancer therapy, *Eur. J. Cancer* 46 (2010) 1252–1259, <http://dx.doi.org/10.1016/j.ejca.2010.02.025>.
- [69] L. Liang, Q. Li, L.Y. Huang, D.W. Li, Y.W. Wang, X.X. Li, et al., Loss of ARHGDI1 expression is associated with poor prognosis in HCC and promotes invasion and metastasis of HCC cells, *Int. J. Oncol.* 45 (2014) 659–666, <http://dx.doi.org/10.3892/ijco.2014.2451>.
- [70] L. Zhang, W. Zhou, V.E. Velculescu, S.E. Kern, R.H. Hruban, S.R. Hamilton, et al., Gene expression profiles in normal and cancer cells, *Science* 276 (1997) 1268–1272.
- [71] M. Hong, H. Kim, I. Kim, Ribosomal protein L19 overexpression activates the unfolded protein response and sensitizes MCF7 breast cancer cells to endoplasmic reticulum stress-induced cell death, *Biochem. Biophys. Res. Commun.* 450 (2014) 673–678, <http://dx.doi.org/10.1016/j.bbrc.2014.06.036>.
- [72] A. Valdés, G. Sullini, E. Ibáñez, A. Cifuentes, V. García-Cañas, Rosemary polyphenols induce unfolded protein response and changes in cholesterol metabolism in colon cancer cells, *J. Funct. Foods* 15 (2015) 429–439, <http://dx.doi.org/10.1016/j.jff.2015.03.043>.
- [73] L. Lopez-Alarcon, M.L. Eboli, Oxidation of reduced cytosolic nicotinamide adenine dinucleotide by the malate-aspartate shuttle in the K-562 human leukemia cell line, *Cancer Res.* 46 (1986) 5589–5591.
- [74] J.M. Thornburg, K.K. Nelson, B.F. Clem, A.N. Lane, S. Arumugam, A. Simmons, et al., Targeting aspartate aminotransferase in breast cancer, *Breast Cancer Res.* 10 (2008) R84, <http://dx.doi.org/10.1186/bcr2154>.
- [75] B. Altenberg, K.O. Greulich, Genes of glycolysis are ubiquitously overexpressed in 24 cancer classes, *Genomics* 8 (2004) 1014–1020, <http://dx.doi.org/10.1016/j.ygeno.2004.08.010>.
- [76] R.J. DeBerardinis, J.J. Lum, G. Hatzivassiliou, C.B. Thompson, The biology of cancer: metabolic reprogramming fuels cell growth and proliferation, *Cell Metab.* 7 (2008) 11–20, <http://dx.doi.org/10.1016/j.cmet.2007.10.002>.
- [77] Q. Sun, X. Chen, J. Ma, H. Peng, F. Wang, X. Zha, et al., Mammalian target of rapamycin up-regulation of pyruvate kinase isoenzyme type M2 is critical for aerobic glycolysis and tumor growth, *Proc. Natl. Acad. Sci. U. S. A.* 108 (2011) 4129–4134, <http://dx.doi.org/10.1073/pnas.1014769108>.
- [78] P. Seshacharyulu, P. Pandey, K. Datta, S.K. Batra, Phosphatase: PP2A structural importance, regulation and its aberrant expression in cancer, *Cancer Lett.* 335 (2013) 9–18, <http://dx.doi.org/10.1016/j.canlet.2013.02.036>.
- [79] M. Janghorban, A.S. Farrell, B.L. Allen-Petersen, C. Pelz, C.J. Daniel, J. Odoet, et al., Targeting c-MYC by antagonizing PP2A inhibitors in breast cancer, *Proc. Natl. Acad. Sci. U. S. A.* 111 (2014) 9157–9162, <http://dx.doi.org/10.1073/pnas.1317630111>.
- [80] H. Shi, K.A. Hood, M.T. Hayes, R.S. Stubbs, Proteomic analysis of advanced colorectal cancer by laser capture microdissection and two-dimensional difference gel electrophoresis, *J. Proteom.* 75 (2011) 339–351, <http://dx.doi.org/10.1016/j.jpro.2011.07.025>.
- [81] C.J. David, M. Chen, M. Assanah, P. Canoll, J.L. Manley, HnRNP proteins controlled by c-Myc deregulate pyruvate kinase mRNA splicing in cancer, *Cancer Lett.* 463 (2010) 364–369, <http://dx.doi.org/10.1038/nature08697>.
- [82] C.V. Dang, A. Le, P. Gao, MYC-induced cancer cell energy metabolism and therapeutic opportunities, *Clin. Cancer Res.* 15 (2009) 6479–6483, <http://dx.doi.org/10.1158/1078-0432.CCR-09-0889>.
- [83] J. Riggelen, A. Yetil, D.W. Felsner, MYC as a regulator of ribosome biogenesis and protein synthesis, *Nat. Rev. Cancer* 10 (2010) 301–309, <http://dx.doi.org/10.1038/nrc2819>.
- [84] L. Soucek, J. Whitfield, C.P. Martins, A.J. Finch, D.J. Murphy, N.M. Sodik, et al., Modelling Myc inhibition as a cancer therapy, *Nature* 455 (2008) 679–683, <http://dx.doi.org/10.1038/nature07260>.
- [85] S. Manna, S. Mukherjee, A. Roy, S. Das, C.K. Panda, Tea polyphenols can restrict benzo[a]pyrene-induced lung carcinogenesis by altered expression of p53-associated genes and H-ras, c-myc and cyclin D1, *J. Nutr. Biochem.* 20 (2009) 337–349, <http://dx.doi.org/10.1016/j.jnutbio.2008.04.001>.
- [86] A. Valdés, C. Simó, C. Ibáñez, L. Rocamora-Revorte, J.A. Ferragut, V. García-Cañas, et al., Effect of dietary polyphenols on K562 leukemia cells: a Foodomics approach, *Electrophoresis* 33 (2012) 2314–2327, <http://dx.doi.org/10.1002/elps.201200133>.

ANEXE II

Previous Publications



AUTHORS: J. Zubcoff Vallejo, A. Forcada Almarcha, F. Gomariz Castillo, J.V. Guardiola, F. Martínez Hernández, R. Salas Gutiérrez, M. Roca Antoli, **V. Ruiz Torres**, G. F. Martín González, C. Valle Pérez, F. Giménez Casalduero, Y. Fernández Torquemada, J. Bayle Sempere, P. Sánchez Jerez. ISBN: 978-84-695-6638-1

TITLE: **Desarrollo de competencias transversales y verticales como nodos del aprendizaje conectivo**

TYPE: Book chapter (National)

YEAR: 07/2015

BOOK: Universidad de Alicante. Departamento de Ciencias del Mar y Biología Aplicada. Facultad de Ciencias. Universidad de Alicante. DISEÑO DE ACCIONES DE INVESTIGACIÓN EN DOCENCIA UNIVERSITARIA

AUTHORS: J. Zubcoff Vallejo, A. Forcada Almarcha, F. Gomariz Castillo, J.V. Guardiola, F. Martínez Hernández, R. Salas Gutiérrez, M. Roca Antoli, **V. Ruiz Torres**, G. F. Martín González, C. Valle Pérez, F. Giménez Casalduero, Y. Fernández Torquemada, J. Bayle Sempere, P. Sánchez Jerez.

TITLE: **El aprendizaje conectivo y colaborativo en los estudios de Grado en Ciencias del Mar**

TYPE: paper (National)

YEAR: 01/2015

JOURNAL: Universidad de Alicante

AUTHORS: Amani Taamalli, David Arráez-Román, Enrique Barraión-Catalán, **Verónica Ruiz-Torres**, Almudena Pérez-Sánchez, Miguel Herrero, Elena Ibañez, Vicente Micol, Mokhtar Zarrouk, Antonio Segura-Carretero, Alberto Fernández-Gutiérrez. Volumen 50, Issue 6, Páginas: 1817-1825 (junio 2012).

TITLE: **Use of advanced techniques for the extraction of phenolic compounds from Tunisian olive leaves: Phenolic composition and cytotoxicity against human breast cancer cells.**

TYPE: paper (International)

YEAR: 2012 JOURNAL: Food and Chemical Toxicology PERCENTILE: Q1

IF: 3.778 (2016)

AUTHORS: Trinidad León-Quinto, Miguel Ángel Simón, Rafael Cadenas, Jonathan Jones, **Verónica Ruíz**, Juan M. Moreno y Bernat Soria, Astrid Vargas. Pp. 316-325. 2009.

TITLE: **Un Banco de Recursos Biológicos para el Lince Ibérico y sus aplicaciones en la Conservación In situ y Ex situ.**

TYPE: Book chapter (International)

YEAR: 2009

BOOK: Un enfoque multidisciplinar. UICN. Fundación Biodiversidad. Pp. 529

ANEXE III

Conferences



AUTHORS: **Verónica Ruiz-Torres**, Enrique Barraión-Catalán, and Vicente Micol.

NAME: **A nudibranch extract interrupt colon cancer progression via ROS-mediated ER stress.**

TYPE: Poster YEAR: 2019

AREA: International. CONFERENCE Natural Products in Drug Discovery and Human Health (Lisbon)

AUTHORS Almudena Pérez-Sánchez, **Verónica Ruiz-Torres**, Enrique Barraión-Catalán, and Vicente Micol.

NAME: **A nudibranch extract interrupt colon cancer progression via ROS-mediated ER stress.**

TYPE: Poster YEAR: 2019

AREA: International. CONFERENCE: Natural Products in Drug Discovery and Human Health (Lisbon)

AUTHORS: **Verónica Ruiz-Torres**, Cristiaan Echegoyen, María Herranz-López, Enrique Barraión-Catalán, and Vicente Micol.

NAME: **The antiproliferative activity and cell death effects of four marine invertebrate extracts in colon cancer cells.**

TYPE: Poster YEAR: 2018

AREA: International. CONFERENCE: EACR (European Association for Cancer Research, EACR) (Amsterdam)

AUTHORS: **Verónica Ruiz-Torres**, Cristiaan Echegoyen, María Herranz-López, Sandra Van Schaeybröeck, Vicente Micol and Enrique Barraión-Catalán.

NAME: **Marine invertebrate extracts inhibit proliferation, migration and invasion in colon cancer cell models.**

TYPE: Poster YEAR: 2018

AREA: International. CONFERENCE: EACR (European Association for Cancer Research, EACR) (Amsterdam)

AUTHORS: Almudena Pérez-Sánchez, Enrique Barraión-Catalán, **Verónica Ruíz-Torres**, Luz Agulló-Chazarra, María Herranz-López, Vicente Micol

NAME: **Antiproliferative effects of Rosemary (*Rosmarinus officinalis*, L.) extract in colon cancer cells lines**

TYPE: Poster YEAR: 2018

AREA: International. CONFERENCE: EACR (European Association for Cancer Research, EACR) (Amsterdam)

AUTHORS: Almudena Pérez-Sánchez, Enrique Barraión-Catalán, **Verónica Ruíz-Torres**, Luz Agulló-Chazarra, María Herranz-López, Vicente Micol

NAME: **Rosemary (*Rosmarinus officinalis*, L.) extract inhibits cell proliferation and migration in colon cancer cells lines**

TYPE: Poster YEAR: 2018

AREA: International. CONFERENCE: EACR (European Association for Cancer Research, EACR) (Amsterdam)

AUTHORS: María Losada-Echeberria, **Verónica Ruiz-Torres**, María Herranz-López, Enrique Barraión-Catalán and Vicente Micol.

TITLE: **Screening of polyphenolic compounds according to their mTOR inhibitory capacity**

TYPE: Poster YEAR: 2018

AREA: International. CONFERENCE: EACR (European Association for Cancer Research, EACR) (Amsterdam)

AUTHORS: **Verónica Ruiz-Torres**, Cristiaan Echegoyen, César Alonso Garrido, Maria Herránz López, Vicente Micol Molina, Enrique Barraji3n Catalán.

NAME: **The antiproliferative effects of four marine invertebrate extracts in colon cancer cells in relation to the modulation of oxidative stress-related pathways.**

TYPE: Poster YEAR: 2017

AREA: International. CONFERENCE: Oxygen Club of California (OCC) World Congress (Berlin)

AUTHORS **Verónica Ruiz-Torres**, Almudena Pérez-Sánchez, Maria Herranz-López, Javier Castillo, Vicente Micol, Enrique Barraji3n-Catalán.

NAME: **The protective antioxidant effect of Lemon balm extract against UVB-Induce damage in a skin cell model**

TYPE: Poster YEAR: 2017

AREA: International. CONFERENCE: Oxygen Club of California (OCC) World Congress (Berlin)

AUTHORS: **Verónica Ruiz-Torres**, Cristiaan Echegoyen, Enrique Barraji3n-Catalán, Vicente Micol-Molina.

YEAR: **Screening for the antiproliferative activity of extracts of marine invertebrates on human colon cancer cell lines.**

TYPE: Poster YEAR: 2016

AREA: International. CONFERENCE: The XXVIIIth International Conference on Polyphenols (Vienna)

AUTHORS: **Verónica Ruiz-Torres**, F. Javier Martínez-Hernández, Emilio Cortés, Francisca Giménez-Casalduero, Vicente Micol-Molina.

NAME: **Competencia Interespecífica de corales de acuario.**

TYPE: Poster YEAR: 2015

AREA: National. CONFERENCE: V Congreso de la Naturaleza y II del Sureste Ibérico. (Murcia - Spain)

AUTHORS: **Verónica Ruiz-Torres**, Almudena Pérez-Sánchez, Luz María Agulló, Enrique Barraji3n-Catalán, Vicente Micol-Molina.

NAME: **The antiproliferative effects of *Rosmarinus officinalis* extract in colon cancer cells are in relation to the modulation of oxidative stress-related pathways.**

TYPE: Poster YEAR: 2015

AREA: International. CONFERENCE: OCC World Congress on Oxidants and Antioxidants in Biology. (Valencia - Spain)

AUTHORS: **Verónica Ruiz-Torres**, Almudena Pérez-Sánchez, Enrique Barraji3n-Catalán, Vicente Micol-Molina.

NAME: **Lemon balm extract and their major polyphenolic compounds reduces UVB-induced oxidative stress and DNA damage in human keratinocytes.**

TYPE: Poster YEAR: 2015

AREA: International. CONFERENCE: 7th International Conference on Polyphenols and Health. (Tours)

AUTHORS: **Verónica Ruiz-Torres**, Almudena Pérez-Sánchez, Enrique Barraión-Catalán, Nuria Caturla, Vicente Micol-Molina.

NAME: **Protective effects of a combination of citrus and rosemary extracts on UV-induced damage in human keratinocytes.**

TYPE: Poster YEAR: 2014

AREA: International. CONFERENCE: 8th International Congress of Polyphenols (Lisbon)

AUTHORS: Manuela Cerdán-Calero, Enrique Barraión-Catalán, Isabel González, María Herranz-López, **Verónica Ruiz-Torres**, Lorena Funes, Marival Bermejo, Vicente Micol-Molina

NAME: **Absorción diferencial de curcuminoides de *Curcuma longa* L. Mediante ensayos de absorción intestinal In situ.**

TYPE: Poster YEAR: 2011

AREA: National. CONFERENCE: XXXIII Congreso de la Sociedad Española de Bioquímica y Biología Molecular (Córdoba - Spain)

AUTHORS: Enrique Barraión-Catalán, María Herranz-López, Salvador Fernandez-Arroyo, Almudena Pérez-Sánchez, **Verónica Ruiz-Torres**, Raul Beltran Debón, Javier Abel Menendez, Antonio Segura- Carretero, Jorge Joven, Vicente Micol-Molina

NAME: **Synergism of *Hibiscus sabdariffa* phenolic compounds in the inhibition of programmed adipogenesis**

TYPE: Poster YEAR: 2011

AREA: International. CONFERENCE: 5th International Conference on Polyphenols and Health (Sitges, Barcelona, Spain).

